

New Methods towards the Synthesis, Characterisation and Analysis of Small Molecule Glycomimetics

By

Daniel Matthew Gill



A Thesis Submitted to the University of Birmingham

For the Degree of DOCTOR OF PHILOSOPHY

School of Pharmacy

College of Medical and Dental Sciences

The University of Birmingham

Submitted: 2nd February 2020

Defended: 5th March 2020

UNIVERSITY OF
BIRMINGHAM

University of Birmingham Research Archive

e-theses repository

This unpublished thesis/dissertation is copyright of the author and/or third parties. The intellectual property rights of the author or third parties in respect of this work are as defined by The Copyright Designs and Patents Act 1988 or as modified by any successor legislation.

Any use made of information contained in this thesis/dissertation must be in accordance with that legislation and must be properly acknowledged. Further distribution or reproduction in any format is prohibited without the permission of the copyright holder.

Preface

If someone were to of asked me when I first joined university, would you ever consider doing a PhD? I probably would have said something along the lines of "I don't know, I just got here, what's a PhD?" That was 2012, I was 18, slim, had a fascination for organic chemistry and most probably a silly haircut. The only information I knew about a PhD was that Ross from Friends (David Schwimmer) had one, and that he would never shut up about it. Needless to say, I knew very little about what a Doctor of Philosophy was, nor did I care at the time. I was more interested in trying to balance my studies with a voracious social life, whilst maintaining myself on a diet of pasta with baked beans and an excessive amount of chili flakes (thanks Mum for the chili, it really made the difference). Throughout my undergraduate studies I gradually learned more about scientific research, its importance and the impact it can have on society. I enjoyed being in the chemistry lab, learning new chemical reactions, mechanisms, procedures, analytical techniques and I enjoyed wearing a nice 'white' lab coat (that would never get washed). After a long summer of 2013, working as part of the administration department for my student halls of residence, I decided an office job was definitely not for me. Thus at the end of my second year of university, I sought to gain more experience in a chemistry research lab and was fortunate enough to encounter Alan (Dr Alan Jones) in a corridor one afternoon. He was as nice and approachable then as he is now, and he gave me a position (I think it was my enthusiasm that convinced him). However, that summer (2014) I realised I knew very little about practical organic chemistry, and was sent home on my last day because I was wearing shorts (I felt like an idiot but in my defence it was really hot outside). During that role I did learn more about what a PhD was, and considered it a kind of vocation where you work all the time, are constantly stressed and have to write a

daunting thesis at the end of it. Fast forward two years and many experiments later (successful or not) and I was adamant on taking the next steps towards a career in chemistry. So when Alan asked me to come to his office one Tuesday morning, I immediately thought "What could this be about? I haven't done anything wrong." Quite the opposite as a matter of fact, and it was in that meeting where Alan convinced me to apply for the PhD position that led to me to writing this thesis some four years later. Albeit, I didn't take much convincing, skipping away from the meeting and immediately calling my Dad to inform him of the exciting possibilities.

The past three to four years of postgraduate research have been life changing, and I have had the support of many wonderful people along the way.

First and foremost, I would like to thank my academic supervisor, Dr Alan Jones, for his mentoring and guidance throughout the years. Thank you for letting me explore my ideas and bringing me down to earth when I got ahead of myself. I would like to thank my Mum (Vinny), Dad (Alan), Sister (Stephanie) and Grandma (Jean) for their love and care throughout my whole life and my studies. Especially Grandma Jean for her cooking, and I will never forget our Sunday afternoons spent in a food coma. I would like to thank my partner, Abigail, for her patience, kindness and constant encouragement. You always know exactly what to say. I would also like to thank her parents, Caroline and Gareth, for their endless humour and caring spirit. Needless to say, I could not have made it this far without any of you.

I would like to thank my friends: Alexandro, Anna and Gabriel, Annica, Anna B, Becky and Steve, Charlotte, Connor, Dave, Danny, Marju, Issie, Jaber, Lissie, Kesar, Matt, Nick C, Nick W, Russel, Sam, Tom, Zelu and Everybody else from Manchester, Telford,

and the 3rd and 4th floor Haworth labs, for your camaraderie and help keeping me relatively stress free.

Finally, I would also like to thank Dr Allen Bowden, Dr Cecile Le Duff and Ms Bridget Tang, Dr Chi Tsang and Dr Peter Ashton, Dr Louise Male, Dr Liam Cox, Dr Hannah Batchelor, Dr Kim Roper, Dr Isolda Romero Canelon and Dr Christopher Williams for their discussions and superb technical support over the years, not forgetting the past MSci students who were great company and always kept me on my toes.

Throughout my postgraduate studies I have learned many things but this one thing I am certain of. The field of chemistry (and all of science come to mention it) is like the universe, it is constantly expanding, growing, changing and evolving. Therefore, one can never know chemistry completely, because the moment one thinks they do is the same moment they realise that they may actually know nothing about it at all. In the past 200 years, numerous scientific discoveries have been made that have changed the world and our understanding of it. This body of work you are holding (whether you choose to read it or not) doesn't come close to world changing research. However, that is not to say it is of less importance and not worth considering. On the contrary, scientific research is a marathon, not a sprint, so it is from the cumulative efforts of postgraduate researchers, like myself, that helps push scientific discovery into a new paradigm of scientific understanding.

Philosophy as a discipline underpins all science, therefore, in providing new scientific insight and novel solutions to current problems, one is advancing human philosophy. Being part of this process has shaped me into a scientist who wants to be part of the solution to world problems, and if you're not part of the solution, well, you're probably part of the precipitate.

Abstract

This thesis is made up of five individual chapters and contains the collective works of three separate investigations.

Chapter 1 discusses the current biology and chemistry associated with the bio-macromolecules: heparin and heparan sulfate. It provides the reader with a detailed knowledge of the two molecules, their differences, similarities, biological activity and efforts taken towards their synthesis. This leads directly into Chapter 2, which introduces heparin and heparan sulfate glycomimetics as novel drug targets, and discusses cases from the current literature. The end of Chapter 2 lists the aims set out by this investigation, justifications of those aims and the problems encountered early on in the synthesis and characterisation of target molecules intended for a study.

Chapter 3 describes a chiral high performance liquid chromatography investigation into the effects of sterics, and double diastereodifferentiation, in the Sharpless asymmetric dihydroxylation of alkenes. This work highlights how pre-existing point chirality from a distal stereocenter influences asymmetric induction and the overall enantioselectivity in the reaction, providing evidence towards a correct model of alkene-ligand binding.

Chapter 4 discusses the design and method development for the reagent $\text{Bu}_3\text{N}\bullet\text{SO}_3$, which is capable of synthesising lipophilic organosulfates in high yield. This methodology was applied to sulfation of simple and complex alcohols (and amines), including hormones, natural products, amino acids and biologically relevant targets.

Chapter 5 draws from the work discussed in Chapters 3 and 4, and details the synthesis of a small library of heparan sulfate glycomimetics that were computationally docked into a protein's active site, with a selection of compounds tested for biological activity.

Contents

CHAPTER 1: INTRODUCTION

1.1.	HEPARIN AND HEPARAN SULFATE-----	2
1.2.	HEPARIN AND HEPARAN SULFATE: SIMILARITIES AND DIFFERENCES-----	4
1.3.	HEPARIN: AN ANTICOAGULANT DRUG-----	5
1.4.	THE CHEMICAL AND ENZYMATIC SYNTHESIS OF H AND HS OLIGOSACCHARIDES-----	7
1.5.	HEPARIN AND HEPARAN SULFATE BINDING PROTEINS AND BINDING SITES-----	9

CHAPTER 2: HEPARIN AND HEPARAN SULFATE GLYCOMIMETICS

2.1.	GLYCOTENDRIMERS-----	14
2.2.	LINEAR GLYCOPOLYMERS-----	21
2.3.	SMALL MOLECULE H/HS-GLYCOMIMETICS-----	24
2.4.	INVESTIGATION: AIMS AND JUSTIFICATION-----	35
2.5.	INVESTIGATION: CHALLENGES AND OBSERVATIONS-----	36

CHAPTER 3: AN INVESTIGATION OF REVERSE STEREOFACIAL SELECTIVITY AND DIASTEREODIFFERENTIATION IN THE SHARPLESS ASYMMETRIC DIHYDROXYLATION

3.1.	THE OSMIUM TETROXIDE CATALYSED DIHYDROXYLATION OF ALKENES-----	48
3.2.	ASYMMETRIC INDUCTION TO ACCESS ENANTIO-ENRICHED DIOLS-----	49
3.3.	THE SHARPLESS ASYMMETRIC DIHYDROXYLATION-----	50
3.4.	STERIC HINDRANCE AND REVERSE STEREOFACIAL SELECTIVITY-----	52
3.5.	TWO MODELS OF ALKENE-LIGAND BINDING-----	53
3.6.	THE PREDICTABILITY OF THE AD ON DIENES AND POLYENES-----	55
3.7.	THE TANDEM AD WITH CONFLICTING STEREOFACIAL SELECTIVITY-----	56
3.8.	AN INVESTIGATION OF THE TANDEM AD OF DIENE 6 -----	57
3.9.	RESULTS AND DISCUSSION-----	58
3.9.1.	A cHPLC method for Stereochemical Analysis.....	58
3.9.2.	A Chemoselective Chiral Pool Synthesis.....	62
3.9.3.	A Chiral Pool Synthesis using Solketal Triflates.....	68
3.9.4.	The Tandem AD of Diene 6	71
3.9.5.	Confirming the Cause of Diastereoisomerisation.....	72

3.9.6. A Stereochemical Contradiction Due to <i>In Situ</i> Changes	75
3.9.7. Regioselectivity in the Tandem AD of Diene 6	76
3.9.8. Using Double Diastereodifferentiation for SAR analysis.....	78
3.9.9. Analysis of the Stereochemical Results	83
3.9.10. Stereofacial Selectivity: The Alkene Binding Hypothesis	86
3.10. CONCLUSION-----	89

CHAPTER 4: AN INNOVATIVE SYNTHESIS OF COMPLEX ORGANOSULFATES

4.1. ORGANOSULFATES -----	108
4.2. ORGANOSULFATES IN BIOMOLECULES -----	109
4.3. THE ENZYMATIC SYNTHESIS OF ORGANOSULFATES-----	111
4.4. THE CHEMICAL SYNTHESIS OF ORGANOSULFATES-----	112
4.4.1. Direct Sulfation.....	112
4.4.2. Dicyclohexylcarbodiimide Coupling.....	113
4.4.3. Alkyl Chlorosulfates	113
4.4.4. The Sulfitylation-Oxidation Protocol	114
4.4.5. SO ₃ -Amine Complexes	115
4.5. THE PER-SULFATION OF ALCOHOLS USING R ₃ N•SO ₃ -----	118
4.6. INCREASING THE SOLUBILITY OF ORGANOSULFATES IN ORGANIC SOLVENTS -----	119
4.7. RESULTS AND DISCUSSION -----	121
4.7.1. Finding a Reliable Sulfation Method for the Synthesis of HS-Glycomimetics 1-3	121
4.7.2. The Rational Design of SO ₃ Tributylamine Complex	126
4.7.3. The Synthesis of Bu ₃ N•SO ₃	127
4.7.4. Optimisation and Rate Studies.....	129
4.7.5. An Analysis of Steric and Electronic Parameters.....	134
4.7.6. The Persulfation of Alcohols, Amino-Acids and Biologically Relevant Substrates.	136
4.8. CONCLUSION-----	142
4.9. FURTHER AND FUTURE WORK-----	142
4.9.1. Sulfamation Made Simple: A Continuation towards the Synthesis of <i>N</i> -Sulfamates	142
4.9.2. The Sulfation of Sugars and Polysaccharides	144
4.9.3. Factors Effecting <i>in situ</i> Ion-exchange	144

CHAPTER 5: THE RATIONAL DESIGN AND SYNTHESIS OF HEPARIN AND HEPARAN SULFATE GLYCOMIMETICS

5.1. SYNTHESIS OF THE 1 ST GENERATION HS-GLYCOMIMETICS -----	160
5.1.1. The Synthesis of HS-Glycomimetics RS-1 and SR-3	160
5.1.2. The Synthesis of HS-Glycomimetics S-2 and R-2	162
5.1.3. Computational Modelling and Docking Studies	164

5.1.4. Results of Biological Assays.....	168
5.1.5. Conclusion	171
5.2. Is STEREOCHEMISTRY SIGNIFICANT TO THE BINDING OF HGF? -----	172
5.2.1. The Chiral Pool Synthesis of HS-Glycomimetic 1.....	172
5.2.2. Computational Modelling and Docking Studies	173
5.2.3. Conclusions and Considerations	174
5.3. THE 2 ND GENERATION OF HS-GLYCOMIMETICS-----	174
5.3.1. Glycomimetic Design and Synthesis.....	174
5.3.2. Synthesis.....	175
5.3.3. Computational Modelling and Docking Studies	180
5.3.4. Conclusion	181
5.4. TARGET ORIENTED SYNTHESIS -----	182
5.4.1. Ring Systems and Structural Rigidity	182
5.4.2. The Insertion of Heteroatoms	185
5.4.3. Conclusion	187
5.5. OVERALL CONCLUSIONS AND FUTURE WORK -----	187

CHAPTER 6: APPENDIX

List of Abbreviations

ABR	Antithrombin Binding Region
Ac	Acetyl
AD	Asymmetric Dihydroxylation
Akt	Serine Threonine Protein Kinase
AT	Antithrombin III
Bn	Benzyl
Bu	Butyl
CAT	Catalase
chPLC	Chiral High Performance Liquid Chromatography
CIP	Cahn-Ingold-Prelog
Da	Dalton
<i>d.r.</i>	Diastereomeric Ratio
DCC	<i>N,N</i> -Dicyclohexylcarbodiimide
DEAD	Diethyl Azodicarboxylate
DHQ	Dihydroquinine
DHQD	Dihydroquinidine
DMF	Dimethylformamide
DMSO	Dimethyl Sulfoxide
DVT	Deep Vein Thrombosis
<i>e.e</i>	Enantiomeric Excess
<i>e.r</i>	Enantiomeric Ratio
eNOS	Endothelial Nitric Oxide Synthase
Et	Ethyl
FFA	Free Fatty Acid
FGF	Fibroblast Growth Factor
FGI	Functional Group Interconversion
GAG	Glycosaminoglycan
GlcA	Glucuronic Acid
GlcN	Glucosamine
GlcNAc	<i>N</i> -Acetyl-Glucosamine
GlcNS	<i>N</i> -Sulfo-Glucosamine
GPx	Glutathione Peroxidase
H	Heparin
HGF	Hepatocyte Growth Factor
HIT	Heparin Induced Thrombocytopenia
HOMO	Highest Occupied Molecular Orbital
HRMS	High Resolution Mass Spectrometry
HS	Heparan Sulfate
HSQC	Heteronuclear Single Quantum Coherence Spectroscopy
IdoA	Iduronic Acid
IR	Infrared Spectroscopy

LMWHs	Low-Molecular-Weight Heparins
LPL	Lipoprotein Lipase
LRMS	Low Resolution Mass Spectrometry
LUMO	Lowest Unoccupied Molecular Orbital
M.P	Melting Point
MAPK	Mitogen Activated Protein Kinase
MeCN	Acetonitrile
Me	Methyl
cMET	Tyrosine Protein Kinase
Ms	Methane Sulfonyl
MW	Molecular Weight
NADPH	Nicotinamide Adenine Dinucleotide Phosphate
NaHMDS	Sodium Bis(trimethylsilyl)amide
NaOMe	Sodium Methoxide
NEH	Sodium 2-Ethylhexanoate
NMO	<i>N</i> -Methyl Morpholine- <i>N</i> -Oxide
NMR	Nuclear Magnetic Resonance Spectroscopy
NO	Nitric Oxide
NOESY	Nuclear Overhauser Effect Spectroscopy
PAPS	3'-Phosphoadenosine-5'-phosphosulfate
PDGF	Platelet Derived Growth Factor
Pr	Propyl
Py	Pyridine
ROMP	Ring Opening Metathesis Polymerisation
R_t	Retention Time
SAR	Structure Activity Relationship
S_N2	Nucleophilic Substitution (2nd Order)
S_NAr	Nucleophilic Aromatic Substitution
SOD	Superoxide Dismutase
SPR	Surface Plasmon Resonance
STs	Golgi-membrane Sulfotransferases
SULTs	Cytosolic Sulfotransferases
TBA	Tetrabutylammonium
TBDMSCl	<i>tert</i> -Butyldimethylsilyl Chloride
Tf	Trifluoromethane Sulfonyl
TFA	Trifluoroacetic Acid
THF	Tetrahydrofuran
TLC	Thin Layer Chromatography
TMS	Trimethylsilyl
Ts	<i>para</i> -Toluene Sulfonyl
UH	Unfractionated Heparin
ULMWHs	Ultra-Low-Molecular-Weight Heparins
VEGF	Vascular Endothelial Growth Factor

List of Figures

Figure 1: **A)** The general structure of H and HS, which are both synthesised as proteoglycans; **B)** The structural variances in sulfate and uronic acid functionalities present in both GAGs (obtained through post-polymerisation modifications of their respective proteoglycans); **C)** The major differences between H-GAGs and HS-proteoglycans. ----- **3**

Figure 2: **A)** The structure and nomenclature of the pentasaccharide sequence (the ABR) that binds AT and inhibits thrombin and factor Xa, cations are omitted for clarity; **B)** The structure of the ULMWH drug Fondaparinux as its administerable sodium salt. ----- **6**

Figure 3: The chemo-enzymatic synthesis of an HS-oligosaccharide using fluoros tagging to facilitate purification and structural elucidation. **i) 1)** UDP-GlcNTfa, KfiA, H₂O, 1 M Tris (pH = 7.2), 1 M MnCl₂, rt, 16 h; **2)** UDPGlcA, PmHS2, H₂O, 1.0 M Tris (pH = 7.2), 1.0 M MnCl₂, rt, 16 h, **92-93%** (2 Steps); **ii) 1)** MeOH/Et₃N/H₂O (2:1:2), rt, 12 h; **2)** Me₃N•SO₃, Na₂CO₃, H₂O, 45 °C, 16 h; **3)** 6-OST-1, 6-OST-3, PAPS, MES Buffer (pH = 7.0), 37 °C, 16 h; **4)** Sealed tube, H₂O, 128 °C, 5 h; **5)** Ac₂O, NaHCO₃, H₂O, THF, rt, 30 min, **64-65%**. Adapted from C. Cai et. al.⁵⁸ ----- **8**

Figure 4: The electrostatic and hydrogen bonding interactions between arginine (**A**) and lysine (**B**) amino-acid residues in H/HS-binding proteins, and sulfate, sulfamate and carboxylate residues presented by H/HS-GAGs. ----- **9**

Figure 5: Illustrating the mechanism of competitive binding for H- and HS-GAGs to an exogenous protein. The more homogeneously sulfated H-GAG binds less selectively to proteins, which creates a preferential binding to HS proteoglycans, creating a diffusion gradient for the mass action of proteins into the extracellular matrix and facilitates the interaction of proteins with cell surface receptors. ---- **12**

Figure 6: Illustrating a generalised structure of glycodendrimers (with increasing valence) and linear glycopolymers. Points of functionality = points where functionality or further structures can be installed. ----- **15**

Figure 7: Analogous structures of two disaccharide monomers presented in **Table 2**, Entries 2 = **A** & 3 = **B**, with a linker unit to demonstrate the point of functionalisation onto the dendritic scaffold. Inset, Minimum energy (MM2) calculations of both disaccharide functionalities, highlighting that epimerisation of GlcA(2S) to IdoA(2S) induces significant conformational changes that separate the anionic sulfate functionalities. Therefore, the spatial orientation of such groups are significant to the potent inhibition of BACE-1. ----- **17**

Figure 8: **A)** The structure of a multivalent, galactose glycodendrimer, as an H/HS-glycomimetic that inhibits L- and P-selectins.⁹¹ **B)** A fully synthetic hyper-branched polyglycerol sulfate that displayed inhibition of L- and P-selectins.⁸³ ----- **19**

Figure 9: The monomer structures of various synthetic linear anionic polymers that display biological activity toward a variety of H/HS-binding proteins. **pVS** = polyvinyl sulfonate, **pSS** = polystyrene sulfonate, **pAS** = polyanisole sulfonate, **pAMPS** = polyacrylo-2-amino methyl-2-propanesulfonate. - **21**

Figure 10: The synthesis of linear glycopolymers by ring-opening metathesis polymerisation (ROMP), demonstrating a single point change in the monomer structure (**A** to **B**) that can turn AT mediated anticoagulation on and off. Adapted from Heish Wilson et. al.¹¹¹⁻¹¹² ----- **22**

Figure 11: The monomer structure of a linear glycopolymer that displayed pM inhibition of heparinase enzyme and P-selectin. Adapted from Loka et. al.¹¹⁵ Cations omitted for clarity. ----- **23**

Figure 12: **A)** The chemical structure of Suramin, a drug used for the treatment of African sleeping sickness. **B)** The structure of a Suramin-based glycomimetic targeting FGF-2. **C)** Illustrating the proposed glycomimetic binding of FGF-2, calculated from docking studies, demonstrating a 1:1 protein-

- ligand complex that binds the H/HS-binding site and the receptor-binding site. Adapted from Manetti et. al.¹²⁴ ----- 26
- Figure 13:** The structure of a Suramin-based glycomimetic used to target Heparanase.¹²⁸ ----- 27
- Figure 14:** **A)** The structure of the potent FGF and VEGF inhibitor discovered from a small molecule H-glycomimetic library utilising the Ugi (4-component) condensation reaction. **B)** MM2 minimized energy structure. Adapted from Zhang et. al.¹²⁹ ----- 29
- Figure 15:** **A)** Structure of a di-sulfated methyl 6-azido-6-deoxy- α -D-mannopyranoside with a variable R group on the 5-position; **B)** The structure of a lead compound that displayed the best binding affinity for FGF-1 and VEGF; **C)** The structure of a H/HS glycomimetic with enhanced binding affinity for FGF-2 and VEGF; **D)** The structure of a H/HS glycomimetic with selective binding affinity for FGF-1; **E)** The structure of a H/HS glycomimetic with selective binding affinity for VEGF. Adapted from L. Liu et. al.¹³¹ **F)** Click reaction; **G)** Swern oxidation–Wittig sequence.----- 30
- Figure 16:** The rational design of small molecule H/HS glycomimetic targeting HGF, **A)** based on the structure of a parent trisaccharide; **B)** The structures of small molecule HS-glycomimetics **1**, **2**, **3** and **4** targeting the HGF/Met receptor interaction. Adapted from Raiber et. al.¹³⁴ (* = Point of chirality.) 32
- Figure 17:** Illustrating the two proposed biological pathways associated with endothelial dysfunction (inflammation) and vascular calcification. The small H/HS-glycomimetic's demonstrate anti-inflammatory activity and inhibit vascular calcification through a variety of proposed intracellular interactions, which are shown to upregulate or downregulate specific proteins and enzymes associated with oxidative damage, inflammation and calcification. Overall, the glycomimetic induce significant therapeutic effects. R = H, Me; **Green** = therapeutic effects; **Red** = Pathological effects; **?** = potentially unknown biological action. Adapted from Mahmoud et. al.^{149 & 154} ----- 34
- Figure 18:** A schematic representation for the aims of this investigation using the synthesis of HS-glycomimetics **1** and **3** for examples. *varying stereochemistry, R = Na, Me ----- 36
- Figure 19:** **A)** The 2nd generation of Sharpless ligands, PHAL, PYR and AQN **B)** The formulation recipe for ADmix based on molar equivalence (eq.) of each reagent, with the expanded structure of (DHQ)₂PHAL (used in ADmix α). ----- 51
- Figure 20:** The Sharpless mnemonic device is used to predict the stereochemical outcome of a given AD based on the size and position of an alkene's substituents. R_L = Large substituent, R_M = Medium-sized substituent and R_S = Smallest substituent. ----- 52
- Figure 21:** **A)** The Corey-Noe model- **B)** The Sharpless model of alkene-ligand binding, using styrene as the example alkene. **Blue:** Methoxyquinoline groups of DHQ/DHQD, **Red:** Alkene-OsO₄ binding region, OsO₄ is held by the ligand, **Green:** Aromatic spacer of the ligand e.g. phthalazine (Interactions are through VdW and π - π stacking).----- 54
- Figure 22:** The cHPLC chromatogram of **\pm 12** in the Phenomenex® Cellulose-1 stationary phase under optimised conditions operating in reverse phase: MeCN/H₂O 7:18, 1 mL min⁻¹. ----- 61
- Figure 23:** The observed ¹H-NMR resonance values for the o- and m- phenolic protons of **7** as a measure of acidity and relative pK_a values, with resonance structures illustrating intramolecular hydrogen bonding between the o-phenol and the methyl ester as reasoning behind the observed chemoselectivity under S_N2 conditions.⁶⁷----- 63
- Figure 24:** The cHPLC chromatograms of acetates **RR-12**, **SR-12**, **RS-12** and **SS-12** in the Phenomenex® Cellulose-1 stationary phase. **A)** Overlay of each cHPLC chromatogram displaying the proposed readout relating to tetraol **\pm 5**. HPLC Conditions: Cullulose-1®, MeCN/H₂O 7:18, 1 mL min⁻¹. ----- 70
- Figure 25:** The synthesis of **α -5** and **β -5** from the tandem AD of diene **6**; **(A & B)** The stereochemical outcomes of tetraols **α -5** and **β -5**, calculated from the cHPLC chromatograms of their corresponding

tetrakis acetates. (C) Overlay of the chPLC chromatograms demonstrating a reversed stereoselectivity from both conditions.-----	71
Figure 26: The AD of mono-alkenes related to diene 6 , caculated from the chPLC chromatograms of the product diols as their diacetate esters. A) AD of alkene 17 ; B) AD of Alkene 18 ; C) AD of Alkene 19 . Chromatograms of chiral pool derived standards are given in green.-----	73
Figure 27: A comparison of the Corey-Noe (A) and the Sharpless model (B) for the binding of alkene 19 . Experimental results support the Sharpless model to explain poor asymmetric induction due to steric interactions of the vicinal methyl ester. ^{28 & 31} -----	75
Figure 28: The stacked ¹ H-NMR spectra (in DMSO-d ₆) of the crude reaction mixtures from the tandem AD of diene 6 (pink), an Upjohn dihydroxylation of 6 (Blue) and the pure tetraol ±5 (Black). The results display intermediate diols 23 and 24 in an opposing 2:1/1:2 concentrations. -----	77
Figure 29: The proposed reinterpretation of the Corey-Noe (A) and Sharpless (B) models for the binding of alkene 12 , based on the experimental results of regioselectivity analysis in the AD. ^{21 & 38} -----	78
Figure 30: Stereochemical outcomes for the dihydroxylation of alkene S-25 with d.r values provided (From Table 6, Entries 1-3). Diols were afforded by dihydroxylation under Upjohn and AD (α & β) conditions and analysed as their corresponding tetrakis acetyl esters (12).-----	83
Figure 31: Stereochemical outcomes for the dihydroxylation of alkene R-25 with d.r values provided (Table 6, Entries 13 & 14). Diols were afforded by dihydroxylation under AD (α & β) conditions and analysed as their corresponding tetrakis acetyl esters (12). -----	85
Figure 32: Illustrating the differences in binding of S-25 and R-25 in the Corey-Noe and the Sharpless binding models as reasoning behind the observed stereofacial selectivity in the AD of alkene S-25 . It is hypothesis that double diastereodifferentiation from the distal acetal facilitates an enhanced asymmetric induction to the sterically blocked alkene. A) The Corey-Noe model suggests a disfavoured X-axis rotation of S-25 for the cause of stereofacial inversion of the resulting diol; B) The Sharpless model suggests a favoured X-axis rotation, leading to a lower energy transition state that causes stereochemical inversion of the resulting diol; C) The mode of binding for R-25 and (DHQD) ₂ PHAL, proposing a favoured diastereofacial interaction of the (<i>R</i>)-acetal. All energies were minimized using molecular force field (MM2) calculations. ^{21 & 38} -----	87
Figure 33: The generic structure of sulfate monesters and dialkylsulfates. -----	108
Figure 34: A variety of natural products, drug compounds and xenobiotic metabolites containing organosulfate motifs. Fondaparinux, Mytilipin B, Avibactam®, paracetamol sulfate, (+)-Gonyautoxin 3, Sotradecol and tyrosyl sulfate. M ⁺ represents biologically relevant cations such as Na ⁺ and K ⁺ . ²⁻⁸ --	109
Figure 35: The differences in exact mass and <i>m/z</i> of protonated organosulfate and organophosphate groups.-----	110
Figure 36: The sulfation of alcohols with R ₃ N•SO ₃ , and the commercially available amines used. -	115
Figure 37: Orbital diagrams of Me ₃ N/Et ₃ N and SO ₃ with the structure of the Lewis adduct Et ₃ N•SO ₃ . -----	116
Figure 38: A) The resonance structures of DMF; B) The structure of DMF•SO ₃ as a soft-hard Lewis adduct.-----	117
Figure 39: The structure and hybridisation of Py•SO ₃ for the rationalisation of its reactivity. -----	118
Figure 40: The proposed sulfation of alcohols with Bu ₃ N•SO ₃ . (R = Alkyl or Aryl.) -----	126
Figure 41: Ortep and space filling model of the Bu ₃ N•SO ₃ crystal structure, obtained from small molecule single crystal X-Ray diffraction. Ellipsoids drawn at the 50% probability level. (Crystal structure solved by Dr L. Male.). -----	129

- Figure 42:** **A)** The % conversion over time of BnOH to **27** at different temperatures using 2.0 eq. of Bu₃N•SO₃; **B)** The % conversion over time of different alcohol types using 2.0 eq. of Bu₃N•SO₃ at 70 °C; **C)** Time period ¹H-NMR for the synthesis of **27**, using 2.0 eq. of Bu₃N•SO₃ at 70 °C. **Black:** BnOH; **Purple:** Conversion at 0.5 h (22%); **Green:** Conversion at 1 h (47%); **Orange:** Conversion at 2.0 h (72%) and **Violet:** Conversion at 4.0 h (95%). At 6.0 h full conversion was achieved (Table 10, Entry 5). ----- **133**
- Figure 43:** The application of optimised methodology to benzylic and phenolic alcohols to analyse changes in steric and electronic factors. (Parentheses indicates reaction conversion as measured by ¹H-NMR spectroscopy.) ^aIsolated by chromatography (SiO₂). ----- **134**
- Figure 44:** **A)** The different affinities of anions for ammonium ions in organic solution. Adapted from Fritz.⁷⁷ **B)** illustrating the three in situ ion-exchange conditions for the precipitation of organosulfates as their Na⁺ salts. (For R groups, see Figure 43.) ----- **135**
- Figure 45:** **A)** The persulfation of complex alcohols. ^aIsolated as [Bu₃NH]⁺ salt. (Parentheses indicate reaction conversion as measured by ¹H-NMR spectroscopy) **B)** Ball and stick and space filling model of **33**, demonstrating its anti-periplanar conformation and intermolecular bonding interactions from the alkyl chains of [Bu₃NH]⁺. ----- **137**
- Figure 46:** The chemoselective synthesis of sulfate **34** and the synthesis of persulfate **35**. ^aIsolated as [Bu₃NH]⁺ salt. (Parentheses indicate reaction conversion as measured by ¹H-NMR spectroscopy.) ----- **138**
- Figure 47:** The chemoselective synthesis of sulfate **36** and the persulfate **37**. (Parentheses indicate reaction conversion as measured by ¹H-NMR spectroscopy.) ----- **138**
- Figure 48:** **A)** The sulfation of Fmoc protected amino esters **L-40** and **L-41**; **B)** The chiral HPLC trace (254 nm) of **L-42** and **±42**. ^ayield for the sulfation of a racemic analogue, ^bintermediate was unstable (90% pure calculated by ¹H-NMR), ^c30 °C using 5 eq. Bu₃N•SO₃. (Parentheses indicate reaction conversion as measured by ¹H-NMR spectroscopy). ----- **140**
- Figure 49:** The synthesis of **α-1** and **R-2** using Bu₃N•SO₃ (Parentheses indicate reaction conversion as measured by ¹H-NMR spectroscopy). ----- **141**
- Figure 50:** The general synthesis of *N*-sulfamates using Bu₃N•SO₃. R = alkyl, aryl & benzyl; R¹ = alkyl, aryl & benzyl; R² = amino acid side chain. ----- **143**
- Figure 51:** The selected HS-glycomimetics chosen for a computational docking study, along with relevant non-sulfated intermediates that were selected to examine the effects of sulfation to binding interaction. ----- **165**
- Figure 52:** **A)** The minimum energy docked structure of HS-glycomimetic **RS-1** into the H/HS-binding site of NK1 (HGF), Table 11, Entry 1; **B)** Zoomed in view of the docked structure; **C)** Ligplot representation of the binding interaction, displaying the vicinal amino acid residues and the hydrogen bonding of specific amino acids to **RS-1**. ----- **167**
- Figure 53:** A graphical representation of the biological results presented in **Table 12**, n = 3. ----- **169**
- Figure 54:** Resonance structures of ester **51c**, illustrating intramolecular hydrogen bonding interaction between the *o*-phenols and the methyl ester functionality. ----- **176**
- Figure 55:** The rational design for a glycomimetic containing a p-sulfate/sulfamate functionality. - **185**

List of Schemes

- Scheme 1:** Retrosynthetic analysis of HS-glycomimetics **1-3**, * = Changes in stereochemistry. -----**37**
- Scheme 2:** The synthesis of diene **6**. Conditions: i) H₂SO₄, MeOH, reflux, 12 h, **95%**; ii) Allyl bromide, K₂CO₃, TBAI, acetone, reflux, 4 h, **99%**. -----**38**
- Scheme 3:** The synthesis of **α-5**, **A**) The assigned stereochemical outcome from the original literature report by Raiber et. al.¹³⁴ **B**) The predicted stereochemical outcome from the Sharpless mnemonic device (Chapter 3). -----**38**
- Scheme 4:** The unsuccessful synthesis of **RS-1** following the literature procedure.¹³⁴ M⁺ = [Me₃NH] or H or Na. -----**39**
- Scheme 5:** A chronological history for the OsO₄ catalysed dihydroxylation of alkenes **A**) 1914, the Hofmann methodology for the synthesis of (±)-tartaric acid,¹ **B**) 1925, the Milas dihydroxylation,^{2,3} **C**) 1976, the Upjohn Dihydroxylation,⁶ **D**) 1976, the Sharpless dihydroxylation.⁷ R = H, Alkyl or Aryl; R' = CO₂R, Alkyl and Aryl. -----**49**
- Scheme 6:** **A**) The asymmetric dihydroxylation of *E*-stilbene using cinchona alkaloid derived ligand (DHQ)Ac; **B**) The structures of the ligand and its pseudoenantiomer (DHQD)Ac. Adapted from K. B. Sharpless.¹⁰ %e.e in parenthesis. Note: For (DHQD)Ac, 1*R*,2*R*-Hydrobenzoin was obtained with **85%** yield (**82%**). -----**50**
- Scheme 7:** The AD of ortho and para substituted phenyl-allyl ethers. Displaying how changes in an alkene's proximal steric environment can diminish asymmetric induction, with an example demonstrating a reversal in stereofacial selectivity for an o-nitro derivative (pink).²⁸⁻²⁹ -----**53**
- Scheme 8:** The AD of dienes **6** and **6'** for the synthesis of HS-glycomimetics. Conditions: **i**) ADmix α, ^tBuOH/H₂O (1:1), MeSO₂NH₂, 0 °C, 12h; **ii**) KOH, MeOH; **iii**) ADmix β, ^tBuOH/H₂O (1:1), MeSO₂NH₂, 0 °C, 12h; **iv**) Me₃N•SO₃, DMf, 40 °C, 12 h. Adapted from Raiber et. al.⁵¹ Cations omitted for clarity. -----**56**
- Scheme 9:** The Sharpless mnemonic's prediction for the AD of dienes **6** and **6'** using ADmix α and β. R = Me, H. -----**57**
- Scheme 10:** The tandem dihydroxylation of diene **6** by Upjohn dihydroxylation. Tetraol **±5** contains all four enantiomers generated in the reaction. Conditions: OsO₂(OH)₄, NMO, acetone/H₂O, 40 °C, 12 h, **95%**. -----**58**
- Scheme 11:** The nucleophilic substitution of functionalised Solketal derivatives.⁶¹⁻⁶⁵ -----**62**
- Scheme 12:** The alternate synthesis of **SS-14** by S_NAr of **16** with (*S*)-Solketal alkoxide. Conditions: **i**) Ph₃P, DEAD, PhMe, 90 °C, 12 h, **90%**; **ii**) NaH, DMSO, 1 h, **28%**. -----**67**
- Scheme 13:** The chiral pool synthesis of acetates (**12**) for their use as chPLC chiral standards. Conditions: **i**) (*S*)-Solketal-OTf (3.0 eq.), K₂CO₃ (2.0 eq.), MeCN, 82 °C, 12 h, **33%**; **ii**) (*R*)-Solketal-OTf (3.0 eq.), K₂CO₃ (2.0 eq.), MeCN, 82 °C, 12 h, **38%**; **iii**) (*S*)-Solketal-OTf (1.5 eq.), K₂CO₃ (2.0 eq.), MeCN, 82 °C, 12 h, **82%**; **iv**) (*R*)-Solketal-OTf (1.5 eq.), K₂CO₃ (2.0 eq.), MeCN, 82 °C, 12 h, **82%**; **v**) (*R*)-Solketal-OTf (1.5 eq.), K₂CO₃ (2.0 eq.), MeCN, 82 °C, 12 h, **40%**; **vi**) (*S*)-Solketal-OTf (1.5 eq.), K₂CO₃ (2.0 eq.), MeCN, 82 °C, 12 h, **43%**. **vii**) TFA, MeOH, 40 °C, **90-96%** **viii**) AcCl, Py, CH₂Cl₂, 0 °C, **95-99%**. -----**68**
- Scheme 14:** Chiral pool derived synthesis of alkenes (**S** & **R**)-**23**, **R**-**24**, (**S** & **R**)-**25** and **S**-**2**. -----**80**
- Scheme 15:** A general scheme for the enzymatic synthesis of organosulfates by sulfotransferase enzymes, using PAPS cofactor as the source of SO₃⁻. Cations are omitted for clarity. PAP = 3'-phosphoadenosine-5'-phosphate. -----**111**

- Scheme 16:** The syntheses of sodium dodecyl sulfate by direct sulfation methods. **A)** The structure of sodium dodecyl sulfate; **B)** The bisulfate intermediate formed during direct sulfation; **C)** The dynamic equilibrium of the unstable bisulfate intermediate with dodecanol and SO₃ (g) ----- **112**
- Scheme 17:** The DCC coupling of aliphatic alcohols and H₂SO₄. R = alkyl. Adapted from Hoiberg et. al.³⁹ ----- **113**
- Scheme 18:** The synthesis of organosulfates from alkyl chlorosulfate esters. Adapted from Simpson et. al.⁴⁰ ----- **114**
- Scheme 19:** The sulfitylation–oxidation protocol for the synthesis of organosulfates. Adapted from Huibers et. al.⁴⁴ ----- **114**
- Scheme 20:** The Parikh-Doering oxidation reaction for the sulfation of alcohols.⁵⁴ R¹ = alkyl, R² = Alkyl or H ----- **118**
- Scheme 21:** The final two steps toward synthesis of Avibactam®. **A)** Benzyl protected hydroxylamine intermediate; **B)** Organosulfate as its lipophilic TBA salt; **C)** Avibactam as its desired Na⁺ salt. **i)** 1. H₂, Pd/C, Me₃N•SO₃; Et₃N, ^tPrOH (aq.), 2. TBAOAc, CH₂Cl₂, methyl isobutyl ketone, **85%**; **ii)** NEH, EtOH/H₂O (98:2) **90%**.⁵⁷ ----- **120**
- Scheme 22:** The unsuccessful synthesis of HS-glycomimetics **1-3** following the only known literature procedure.⁶¹ R = H, Me or Na; M⁺ = [HNR₃]⁺ or Na. ----- **121**
- Scheme 23:** The isolation of organosulfate-Na⁺ salts via hydrolysis. Adapted from Deno et. al.³⁸ - **124**
- Scheme 24:** The synthesis of Bu₃N•SO₃. ----- **128**
- Scheme 25:** The general synthesis of complex organosulfates and persulfates using Bu₃N•SO₃. -- **136**
- Scheme 26:** The chemoselective 0.1 mmol scale synthesis of **39**. ^a**38** was not characterised (Parentheses indicate reaction conversion as measured by ¹H-NMR spectroscopy). ----- **139**
- Scheme 27:** The unsuccessful sulfation of α-methyl glucoside with Bu₃N•SO₃. R = [Bu₃NH]⁺ ----- **141**
- Scheme 28:** The synthesis of first generation HS-glycomimetics **α-1** and **β-3**, including four biologically relevant intermediates considered in this investigation. Conditions: **i)** K₂CO₃, K₃Fe(CN)₆, K₂OsO₂(OH)₄, ^tBuOH/H₂O, 0 °C, 12 h, **99%** for both; **ii)** Bu₃N•SO₃, MeCN, 90 °C, 8 h; **iii)** NaOH, MeOH, 70 °C, 2 h **99%** for both; **ii)** Bu₃N•SO₃, MeCN, **88%** and **86%** for **α-1** and **β-3**, respectively. ----- **161**
- Scheme 29:** The synthesis of HS-glycomimetics **S-2** and **R-2**. Conditions: **i)** 4-Bromobutylacetate, K₂CO₃, TBAI, acetone, reflux, 12 h, **90%**, **ii)** ADmix β, ^tBuOH/H₂O, 0 °C, 12 h, **99%** for both; **iii)** ADmix α, ^tBuOH/H₂O, 0 °C, 12 h, **99%** for both; **iv)** K₂CO₃, MeOH, rt, 12 h, **99%** for both; **v)** Bu₃N•SO₃, MeCN, 90 °C, 12 h, **72%** and **97%** for **R-2** and **S-2**, respectively. ----- **162**
- Scheme 30:** A chiral pool synthesis of **S-10** for the comparison of optical rotation. Conditions: **i)** 4-Bromobutylacetate, K₂CO₃, TBAI, acetone, reflux, 12 h, **90%**, **ii)** 1) NaOMe 2) TFA, MeOH, 12 h. **quant.** ----- **163**
- Scheme 31:** A chiral pool synthesis of **1**, synthesising each stereochemical combination. Conditions: **i)** 1) Bu₃N•SO₃, MeCN, 90 °C, 2) NEH, ^tBuOMe/EtOH, **49-82%**. ----- **172**
- Scheme 32:** The synthetic strategy and rational design for the second generation HS-glycomimetics, utilising previously demonstrated synthetic methods. Conditions: **i)** H₂SO₄, MeOH, reflux; **ii)** allyl bromide, K₂CO₃, TBAI, acetone, reflux; **iii)** K₂OsO₂(OH)₄, NMO, acetone/H₂O (9:1); **iv)** Bu₃N•SO₃, MeCN, 90 °C. ----- **175**
- Scheme 33:** The target oriented synthesis of tricyclic diene **57** and tetra-alkene **60**. Conditions: **i)** PhH, 200 °C, 18 h, **6%** and **5%** for **55** and **56**, respectively; **ii)** Allyl-Br, K₂CO₃, TBAI, acetone, reflux, **99%**; **iii)** Grubbs-2nd Gen., Toluene, Ar 50 °C, 1 h, **99%**. ----- **183**

Scheme 34: The target oriented synthesis of cyclic alkenes **65** and **66**. Conditions: **i)** PhH, 200 °C, 18 h, **56%** and **83%** for **61** and **62**, respectively; **ii)** Allyl-Br, K₂CO₃, TBAI, acetone, reflux, **38%** and **12%** for **63** and **66**, respectively; **iii)** Grubbs-2, PhMe, 50 °C, 1 h, **74%** and **99%** for **65** and **66**, respectively.

-----**184**

Scheme 35: The synthesis of HS-glycomimetic **71**. Conditions: **i)** HNO₃, AcOH, Ac₂O, **15%**; **ii)** Allyl-Br, K₂CO₃, TBAI, acetone, reflux, **48%**; **iii)** K₂OsO₂(OH)₄, NMO, acetone/H₂O, 9:1, 40 °C, **61%**; **iv)** H₂, Pd/C, MeOH (H-Cube), **94%**; **v)** 1) Bu₃N•SO₃, MeCN, 90 °C, 2) NEH, ^tBuOMe/ⁱPrOH, **33%**. -----**186**

List of Tables

Table 1: A selection of proteins associated with pathological roles in disease states and their protein-specific binding sequences discovered in H and HS. -----	10
Table 2: The use of single point HS-glycodendrimers for the inhibition of BACE-1. -----	16
Table 3: A comparison of hydroxyl protecting groups for the derivatization of tetraol ±2 to facilitate chPLC analysis. -----	59
Table 4: Investigating the viability of different electrophilic (<i>R</i>)-Solketal derivatives in an S _N 2 reaction with 7 . -----	64
Table 5: Double diastereodifferentiation in the AD of alkene A , using a variety of chiral ligands. ---	79
Table 6: The SAR of the AD: All stereochemical outcomes were calculated by chPLC. -----	82
Table 7: The pK _a and orbital hybridisation of amines in commercially available Lewis adducts of SO ₃ . -----	116
Table 8: The screening of reagents and conditions for the synthesis of glycomimetic ±1 . -----	123
Table 9: The relative pK _{aH} and Log P values of tertiary alkyl amines. -----	127
Table 10: The optimisation of sulfation on a model system. -----	131
Table 11: The minimum docking energies, Number of sulfate groups and hydrogen bonding interactions of selected HS-glycomimetics and non-sulfated intermediates. -----	166
Table 12: Biological data for eNOS and ROS. All data are averaged % of increase (+) or decrease (–) compared to control (FFA induced oxidatively stresses endothelial cells).-----	169
Table 13: The calculated minimum docking energies and hydrogen bonding interactions of each stereochemical combination of HS-glycomimetic 1 . -----	173
Table 14: The synthesis of a second generation HS-glycomimetics. -----	178
Table 15: Listing the minimum docking energies, hydrogen bonding interactions and number of sulfate groups of the second generation HS-glycomimetics. -----	180

Chapter 1: Introduction

1.1. Heparin and Heparan Sulfate

In biology, the extracellular matrix is a network of enzymes, fibrous proteins and proteoglycans that provide physical and biochemical support to the surrounding cells. Proteoglycans are specific glycoproteins comprising of a core membrane bound protein, such as perlecan or serglycin, a linkage region and at least one covalently linked glycosaminoglycan (GAG) chain: a large polysaccharide made of linear repeating disaccharide units (between 50-200, Figure 1, A).¹ GAGs, such as heparin (H) and heparan sulfate (HS), are structurally related polysaccharides that are involved in blood coagulation,² angiogenesis (the formation of new blood vessels),³ inflammation,⁴ and cancer cell growth (Figure 1, B).⁵ Unfractionated heparin (UH) was isolated from animal tissue in 1916 as a polydispersed mixture of GAG chains, it is the oldest discovered anticoagulant drug still clinically used.⁶⁻⁷ Anticoagulants are medicines that prevent blood clots, and the commercialisation of UH was an important milestone in medical science as a lack of effective anticoagulants, at the time, limited the advancement of medical and surgical procedures that are now common practise.⁸

HS was characterised from crude extracts of UH, and was considered a type of heparin due to the minute concentrations found (<1%). However, it was later confirmed that HS is in fact a component of cell surface proteoglycans, so it is not as easily extracted as H, and it is now widely accepted that H is a specialised non-proteoglycan form of HS (Figure 1, C).⁹⁻¹⁰ H has been extensively studied due to its commercial availability and had a market value of \$9.4bn in 2017, with over a century of research providing insight into the structure and function of both H- and HS-GAGs.¹¹ However, a comprehensive understanding of both H and HS is still incomplete.

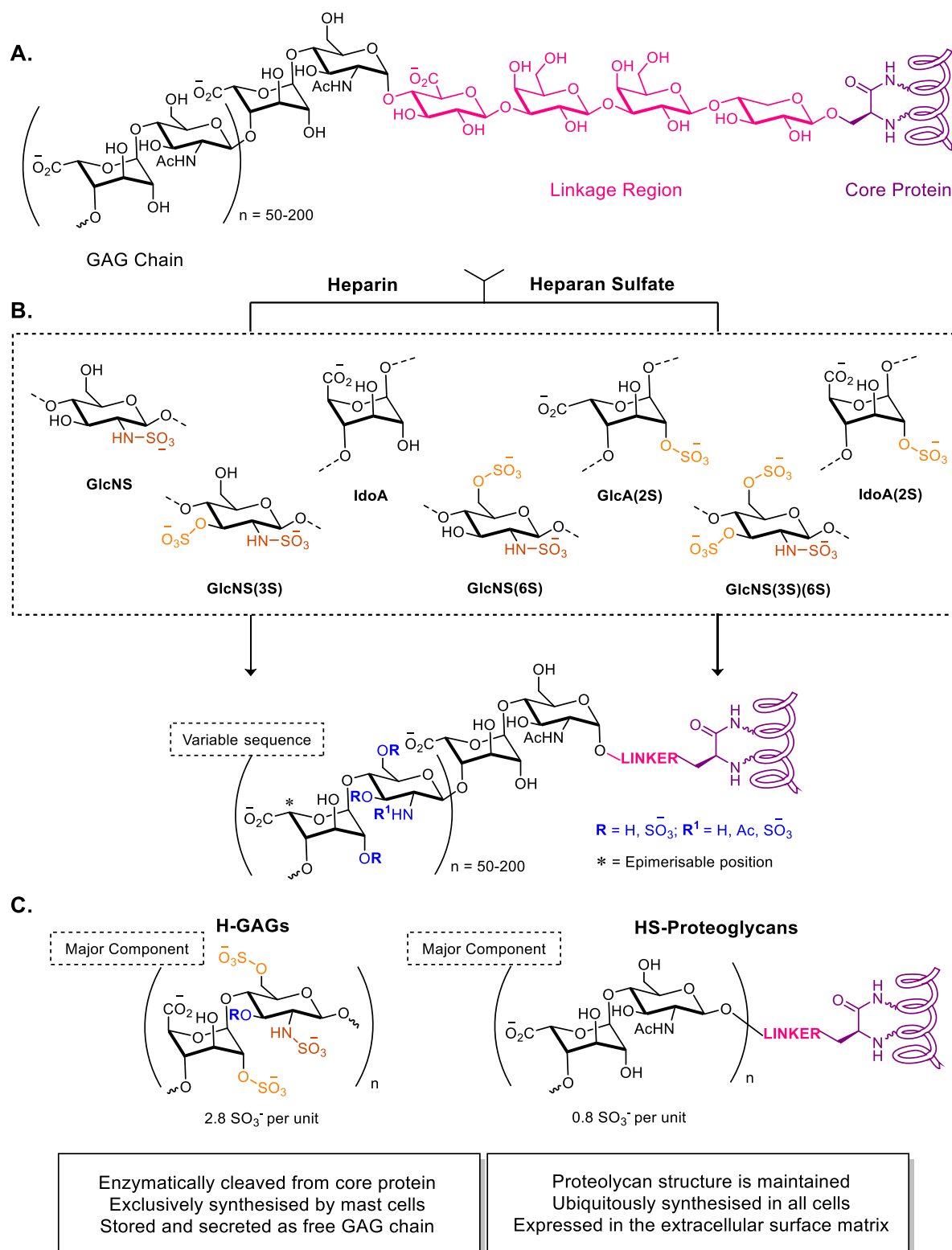


Figure 1: **A)** The general structure of H and HS, which are both synthesised as proteoglycans; **B)** The structural variances in sulfate and uronic acid functionalities present in both GAGs (obtained through post-polymerisation modifications of their respective proteoglycans); **C)** The major differences between H-GAGs and HS-proteoglycans.

1.2. Heparin and Heparan Sulfate: Similarities and Differences

H and HS are biosynthesised through an identical process, and contain identical disaccharide units of *D*-glucosamine (GlcN) and uronic acids: *D*-glucuronic acid (GlcA) and *L*-iduronic acid (IdoA, Figure 1, A). The hydroxyl groups are irregularly sulfated in multiple positions and the amino residues can be presented as free GlcN, *N*-acetyl amides (GlcNAc) or *N*-sulfamates (GlcNS) (Figure 1, B).¹²⁻¹³ This creates an abundance of structural heterogeneity that spans the GAG chains.⁹

H proteoglycans undergo exhaustive modifications that install high concentrations of sulfate groups along the GAG chain (2.8 SO₃⁻ per unit) and epimerise GlcA residues to IdoA (Figure 1, C). Consequently, H exhibits a relatively more homogeneous structure compared to HS, which consists largely of unmodified GlcNAc-GlcA (Figure 1, C). Moreover, H is exclusively biosynthesised in mast cells (specialised migratory cells found in connective tissue) and is enzymatically cleaved from its core protein before storage and secretion into the blood. Therefore, natural H is found as an unbound, polydispersed GAG (UH) which facilitated its initial discovery and subsequent clinical use.¹⁴

Conversely, HS is ubiquitously biosynthesised in all mammalian cells as a proteoglycan, and is a major component of the extracellular surface matrix (Figure 1, C). The lower concentrations of sulfate and sulfamate functionalities (0.8 SO₃⁻ per unit), and a higher concentration of the GlcA residues creates distinct biochemical properties which distinguish HS from H. These properties are complementary to its physiological position in the extracellular environment and are discussed further in Chapter 1.5.¹⁵

1.3. Heparin: An Anticoagulant Drug

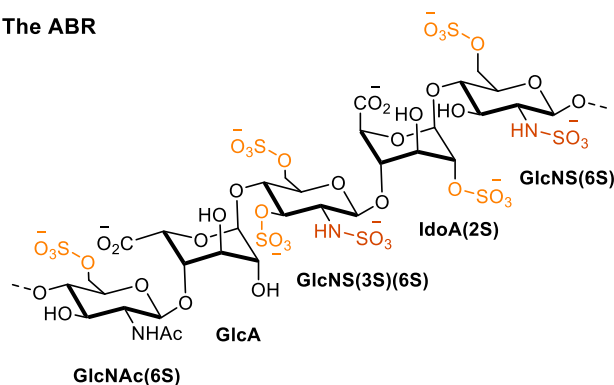
UH is commonly extracted from pig intestines, and is purified extensively before being used therapeutically as an anticoagulant, for the treatment of venous and arterial thromboembolisms (the formation of blood clots that break loose and block smaller blood vessels). H-GAGs exhibit anticoagulant activity through binding and potentiating the action of antithrombin III (AT), which blocks the prothrombinase enzymes factor Xa and thrombin (factor IIa), attenuating blood coagulation.¹⁶ However, a common side effect from the administration of UH is the risk of triggering heparin-induced thrombocytopenia (HIT), which creates abnormally low levels of blood platelets and increases the risk of accidental bleeding.¹⁷⁻¹⁸ Furthermore, UH is susceptible to contamination, which caused major fatalities in 2008.¹⁹ Therefore, aims to diminish unwanted side-effects and provide a safer drug action resulted in the introduction of low molecular weight heparins (LMWHs) as anticoagulant drugs.²⁰

LMWHs, such as enoxaparin and tanziparin, are chemically or enzymatically depolymerised formulations of UH. The additional processing generates higher purity H fragments of lower molecular weight (avg. <8000 Da), which creates a more desirable pharmacokinetic profile and greater drug bioavailability.²¹ However, the use of LMWHs does not reduce the risk of triggering HIT.¹⁷

By investigating the binding interactions of LMWH fragments and AT, it was found that a H-GAG with the unique pentasaccharide sequence: GlcNAc(6S)-GlcA-GlcNS(3S,6S)-IdoA(2S)-GlcNS(6S) (Figure 2, A) can bind AT and selectively inhibit the action of factor Xa.^{4, 20} Moreover, the same pentasaccharide domain can only inhibit thrombin if it is part of an octadecasaccharide (18 unit) sequence. Therefore, a size dependent selectivity was discovered for H induced anticoagulation, and the identification of the pentasaccharide sequence, now referred to as the Antithrombin Binding Region (ABR),

led to the development of ultra-low molecular weight heparins (ULMWHs) such as Fondaparinux (Figure 2, B).

A. The ABR



B. Fondaparinux

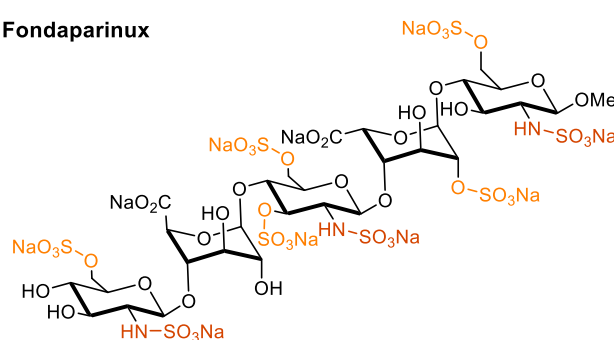


Figure 2: **A)** The structure and nomenclature of the pentasaccharide sequence (the ABR) that binds AT and inhibits thrombin and factor Xa, cations are omitted for clarity; **B)** The structure of the ULMWH drug Fondaparinux as its administerable sodium salt.

Fondaparinux, marketed as Atrixa[®], is a synthetic ULMWH designed for the treatment of deep vein thrombosis (DVT) that can selectively inhibit factor Xa and circumvent the secondary effects that trigger HIT.²² However, unlike UH it lacks a common antidote, such as protamine sulfate (a small arginine rich protein), which can counteract drug action in the event of an accidental overdose.²³ Therefore, the administration of Fondaparinux is highly regulated and is typically used for patients already expressing symptoms of HIT.

The original (chemical) synthesis of Fondaparinux was achieved in 55 steps (<1% overall yield),²⁴ which reduced the drugs cost-effectiveness compared to UH-derived anticoagulants. A variety of novel methods were developed to reduce the number of

synthetic steps, thus reducing the production costs and lowering the market price.²⁵⁻²⁹ However, tighter regulations on the manufacturing processes, and the use of advanced analytical methods to detect contaminants, have safeguarded the future use of UH-derivatives.¹⁹ Therefore, Fondaparinux is not commonly prescribed in western countries, and not at all in countries where private healthcare is implemented, such as the USA, due to the lower costs of alternative medicines.

1.4. The Chemical and Enzymatic Synthesis of H and HS Oligosaccharides

Synthetic organic chemistry has the advantage of creating structurally defined natural and unnatural oligosaccharide sequences as potential drug candidates, and guarantees a level of homogeneity not found in UH and LMWH formulations. Given the polymeric structure of H and HS, chemically defined disaccharide precursors can be subsequently combined in any order.²⁸⁻³¹ However, this method presents two challenges: Stereochemical control when forming the glycosidic bond, due to the anomeric effect and neighbouring group participation, and the regioselective protection of hydroxyl and amino groups to enable late stage sulfation, sulfamation and *N*-acetylation. Nonetheless, chemical methods directed at these challenges have provided efficient and robust synthetic routes to H- and HS-based oligosaccharides.³⁴⁻⁴¹ Furthermore, recent methodologies have been developed to introduce late stage sulfation without the need of hydroxyl protecting groups.⁴²⁻⁴⁶

The chemo-enzymatic syntheses of oligosaccharides provides more direct routes that are stereoselective, site-selective and do not require a protecting group strategy.⁴⁷⁻⁴⁸ However, enzymatic methods typically yield heterogeneously sulfated products of near-indistinguishable isomers. Therefore, the ambiguous GAG chains require complex purification and analysis, which hinders the investigation of potential drug candidates

and their structure activity relationships (SAR).⁴⁹⁻⁵⁰ To bypass this issue, and create more homogenous oligosaccharide structures, chemical synthesis has been successfully combined with enzymatic methods.⁴¹⁻⁵³

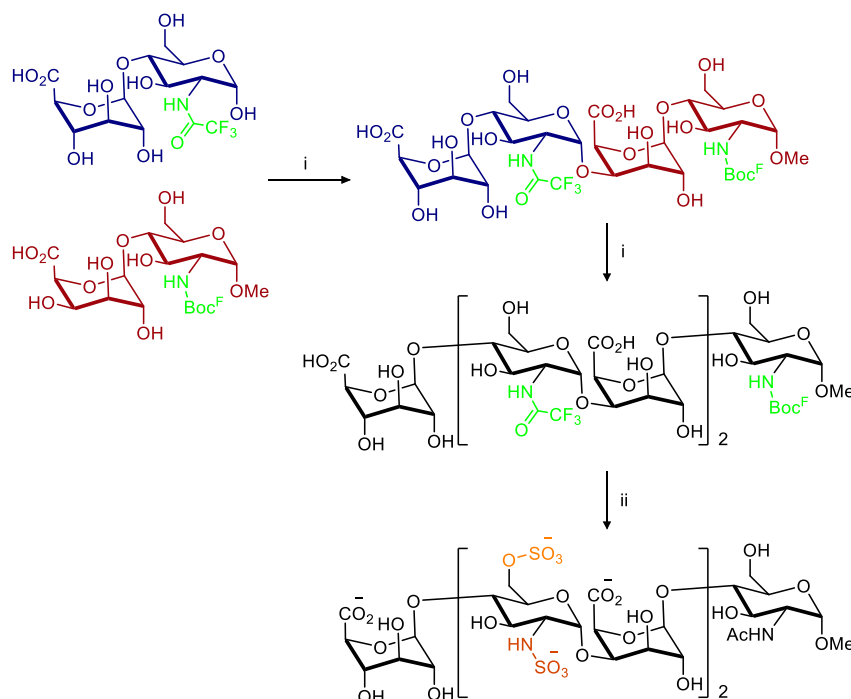


Figure 3: The chemo-enzymatic synthesis of an HS-oligosaccharide using fluororous tagging to facilitate purification and structural elucidation. **i)** **1)** UDP-GlcNTfa, KfiA, H₂O, 1 M Tris (pH = 7.2), 1 M MnCl₂, rt, 16 h; **2)** UDPGlcA, PmHS2, H₂O, 1.0 M Tris (pH = 7.2), 1.0 M MnCl₂, rt, 16 h, **92-93%** (2 Steps); **ii)** **1)** MeOH/Et₃N/H₂O (2:1:2), rt, 12 h; **2)** Me₃N•SO₃, Na₂CO₃, H₂O, 45 °C, 16 h; **3)** 6-OST-1, 6-OST-3, PAPS, MES Buffer (pH = 7.0), 37 °C, 16 h; **4)** Sealed tube, H₂O, 128 °C, 5 h; **5)** Ac₂O, NaHCO₃, H₂O, THF, rt, 30 min, **64-65%**. Adapted from C. Cai et. al.⁵⁸

Short-chain oligosaccharides containing the ABR pentasaccharide sequence (GlcNAc(6S)-GlcA-GlcNS(3S,6S)-IdoA(2S)-GlcNS(6S), Figure 2, A) have been chemo-enzymatically synthesized in 10 steps, providing a direct route to drug-like ULMWHs.⁵⁴ Furthermore, their biological activity can be attenuated by the addition of protamine, a clinical advantage over Fondaparinux.⁵⁵ H-biotin conjugates were designed to enable the accurate measurement of blood compound concentration through streptavidin based sensors, and the conjugate can be removed by dialysis in the event of an overdose.⁵² The commercialisation of a H-biotin conjugate is currently in clinical trials.⁵⁶ Moreover, the fluororous tagging of sugar monomers facilitates the straightforward purification and analysis of otherwise ambiguous oligosaccharides chains, which can

then be enzymatically sulfated and sulfonated at selected *O*- and *N*- positions (Figure 3).⁵⁷⁻⁵⁸

The chemical and enzymatic synthesis of H/HS-based oligosaccharides are well defined in the current literature. However, investigations to date have exclusively targeted the AT mediated anticoagulant cascade, providing more efficient methods to access existing anticoagulant drugs or demonstrating a novel synthetic/enzymatic methodology. Therefore, the scope of these investigations has been limited to a specific family of proteins that are no longer relevant to modern drug discovery (due to more established, cost effective treatments). However, H and HS are known to bind a variety of other endogenous proteins that are of greater clinical importance and warrant further discussion.

1.5. Heparin and Heparan Sulfate Binding Proteins and Binding Sites

H- and HS-binding proteins display cationic binding sites at their accessible surface that contain (basic) arginine and lysine amino-acid residues, which bind through electrostatic and hydrogen bonding interactions with anionic groups presented by H/HS-GAGs (Figure 4).⁵⁹

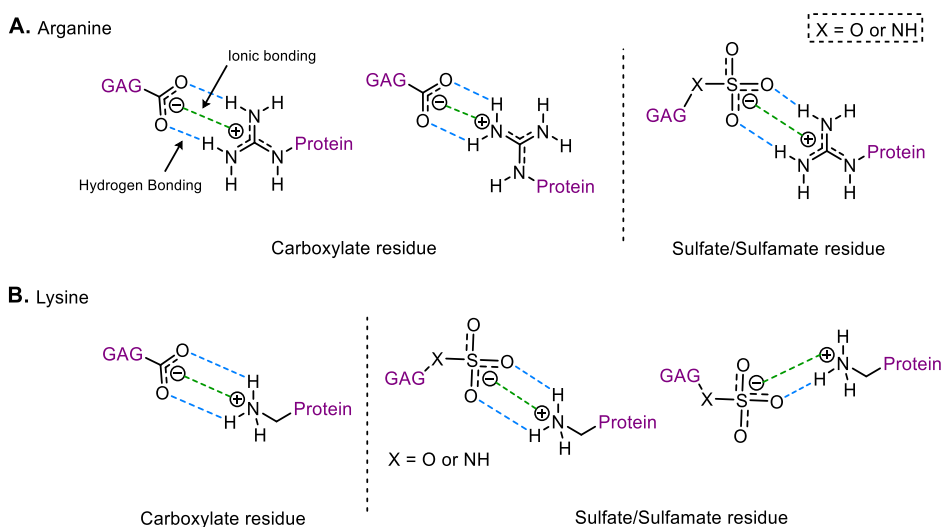


Figure 4: The electrostatic and hydrogen bonding interactions between arginine (**A**) and lysine (**B**) amino-acid residues in H/HS-binding proteins, and sulfate, sulfamate and carboxylate residues presented by H/HS-GAGs.

H and HS are known to be involved in a number of pathological roles by facilitating dysfunctional protein-receptor interactions.⁶⁰ Therefore, specific oligosaccharide sequences (like the ABR) are potential candidates for the development of novel protein inhibitors.⁵⁹ The identification of specific protein-binding sequences are important to drug discovery and the comprehensive understanding of H and HS. Therefore, from decades of research, with the aid of modern analytical techniques and assays,⁶¹⁻⁶³ a number of binding sequences have been identified (Table 1).

Table 1: A selection of proteins associated with pathological roles in disease states and their protein-specific binding sequences discovered in H and HS. **FGF** = Fibroblast Growth Factor; **PDGF** = Platelet Derived Growth Factor; **HGF** = Hepatocyte Growth Factor; **VEGF** = Vascular Endothelial Growth Factor; **LPL** = Lipoprotein Lipase (enzyme). **Green** = ubiquitously expressed disaccharide units.

Entry	Protein	GAG	Protein Binding Domain	Ref.
1	AT	H	~GlcNAc(6S)-GlcA-GlcNS(3S)(6S)- IdoA(2S)-GlcNS(6S) ~	64
2	FGF-1	H/HS	~(GlcNS(6S)-IdoA(2S)) _n ~	65
3	FGF-2	HS	~GlcA-GlcNS-GlcA-GlcNS-IdoA(2S)~	66
4	PDGF	H/HS	~(GlcNS(6S)-IdoA(2S)) _n ~	67
5	HGF	H/HS	~GlcA-GlcNS/Ac-(IdoA(2S)-GlcNS(6S)) ₂ -GlcA-GlcA-GlcNS/Ac~	68
6	VEGF	HS	~(GlcNS- IdoA(2S)-GlcNS(6S) -IdoA(2S)-GlcNS) ₂ ~	69
7	LPL	H/HS	~(IdoA(2S)-GlcNS(6S)) ₅ ~	70

Growth factors are signaling proteins involved in cellular processes such as angiogenesis, cell growth and wound healing (Table 1, Entries 2 – 6).⁷¹⁻⁷² The growth factors presented are shown to bind H/HS in characteristic regions containing GlcNS(6S)-IdoA(2S) disaccharide units (Table 1, Green), with the exception of FGF-2, as preliminary findings by Maccarana elucidated a pentasaccharide binding domain containing GlcNS-IdoA(2S) (Table 1, Entry 3).⁶⁶ A later screening of 48 synthetic

disaccharides against FGF-2 discovered three hit compounds containing GlcNS and IdoA(2S) motifs, which were characterized in their protein-bound conformation by X-ray crystallography,⁷³ confirming the findings by Maccarana.⁶⁶ This suggests that the majority of growth factors bind to a single, commonly expressed, disaccharide domain found in H/HS-GAGs.

Cytokines are a category of cell signalling proteins that have complex biological actions specific to each cytokine and its associated cell surface receptor. A variety of cytokines bind HS-proteoglycans, and have pathological roles in inflammation and autoimmune disorders.⁷¹ Moreover, cytokines and growth factors are proposed to bind with commonly expressed domains containing GlcA(2S)/IdoA(2S) and GlcNS/GlcNS(6S), thus the majority of H/HS-protein interactions can be considered nonspecific. However, H and HS are proposed to contain hidden binding domains, where non-anionic functionalities become transiently accessible to an interacting protein. This creates a specific binding conformation with the protein's accessible surface through hydrogen bonding and Van der Waals interactions.⁷⁴ Therefore, the presence of anionic functionalities are important to drive GAG-protein binding, but non-anionic groups are necessary for the binding of specific proteins and sites on the protein's surface.⁷⁴⁻⁷⁵

HS-proteoglycans have a lower concentration of sulfate functionalities (0.8 SO₃⁻ per unit, Figure 1, C), which increases structural heterogeneity in all HS-GAGs and enhances protein-specific binding at the extracellular surface. Furthermore, the enhanced hydrogen bonding and Van der Waals interactions from non-sulfated domains have been shown to account for up to 70% of the binding free energy.⁷⁵ Highly-sulfated H binds proteins predominantly through electrostatic interactions (Figure 4), thus, HS proteoglycans bind proteins with greater affinity and avidity. This highlights a highly ordered biosynthesis for H and HS-GAGs, which creates sulfate

regions for electrostatically driven protein binding in both biomolecules, but differentiates the two in favour of HS binding, which generates a diffusion gradient for the mass action of exogenous proteins into the extracellular matrix (Figure 5).⁷⁶

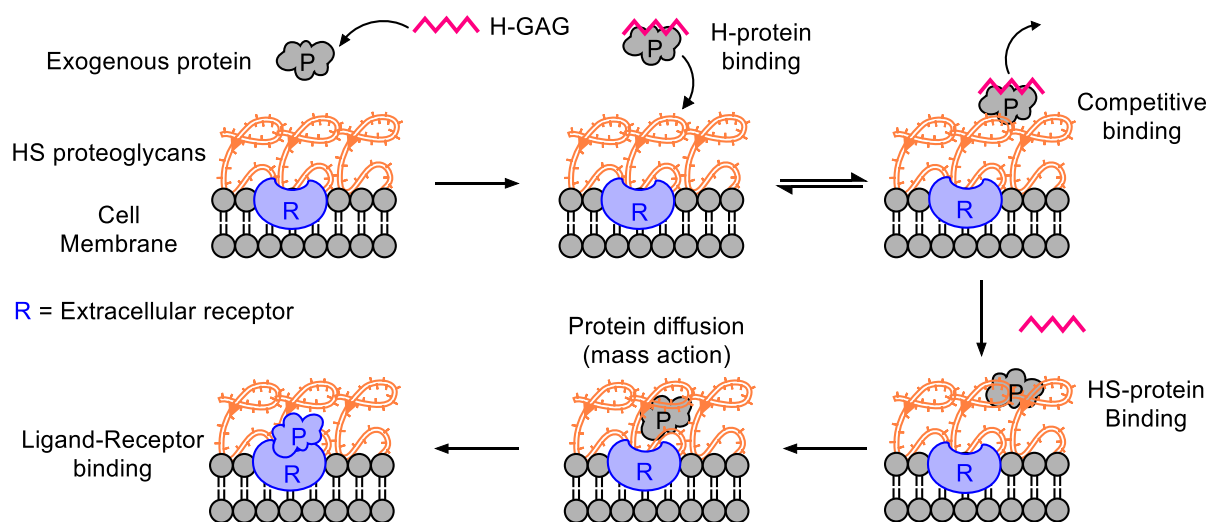


Figure 5: Illustrating the mechanism of competitive binding for H- and HS-GAGs to an exogenous protein. The more homogenously sulfated H-GAG binds less selectively to proteins, which creates a preferential binding to HS proteoglycans, creating a diffusion gradient for the mass action of proteins into the extracellular matrix and facilitates the interaction of proteins with cell surface receptors.

Overall, the structure and function of H and HS are complimentary to their physiological position. This allows them to bind proteins with varying degrees of avidity, to facilitate biochemical processes at the extracellular surface and in the greater extracellular environment. The number of H/HS-binding proteins is extensive, and exhibit similar binding domains across different families. Furthermore, the findings discussed in this chapter suggest that H and HS present numerous binding domains in a single GAG chain, and that growth factor binding sites are disaccharide specific, dependent on the presence of both anionic and non-polar functionalities.

Due to the extensive heterogeneity and structural conformations presented by H- and HS-oligosaccharides, their use as potential drug targets is limited by the complex elucidation of a specific binding interaction. Furthermore, the synthesis of structurally defined GAGs, although well established (Chapter 1.4), is still restricted by elaborate

chemical and chemo-enzymatic methods. Additionally, all natural oligosaccharides have poor physiological stability and drug-likeness,⁷⁷ thus H/HS-derivatives are not suitable as drug scaffolds for the targeting of specific proteins. However, the use of structurally related glycomimetics offer a unique solution to this problem.⁷⁸ Glycomimetics are molecular mimics of functional polysaccharides with an improved affinity for a target protein (or receptor) and drug-like pharmacokinetic properties. More information about H and HS-glycomimetics are found in the upcoming chapter.

Chapter 2: Heparin and Heparan Sulfate Glycomimetics

Glycomimetics are designed to mimic the active functionalities of carbohydrate-based biomolecules, but remove the potential drawbacks associated with oligosaccharide based structures, such as an elaborate molecular synthesis and poor target-binding efficiency.⁷⁷⁻⁷⁸ A variety of investigations into glycomimetic drug-scaffolds have been conducted over the past 10 years,⁷⁹⁻⁸⁵ and the state of the art in modern drug design has established three distinct categories: Glycodendrimers, linear glycopolymers and small molecule glycomimetics. This chapter focuses on the design and synthesis of glycomimetics targeting H/HS-binding proteins for therapeutic purposes, and discusses recent contributions from each category.

2.1. Glycodendrimers

Dendrimers are macromolecules which have repeating structures that emanate from a central point (Figure 6).⁸⁶ The use of dendrimers in nature facilitates polyvalent interactions that are essential for establishing the strong and reversible binding of biomolecules.⁸⁷ Inspired by nature, synthetic glycodendrimers are an efficient strategy to create bioactive glyco-conjugates with increased avidity for protein binding through the clustering of polyvalent groups. Therefore, the use of dendrimers as novel glycomimetics, or glycodendrimers, permits the synthesis of large homogenous structures that can mimic macromolecular polysaccharides such as H and HS.

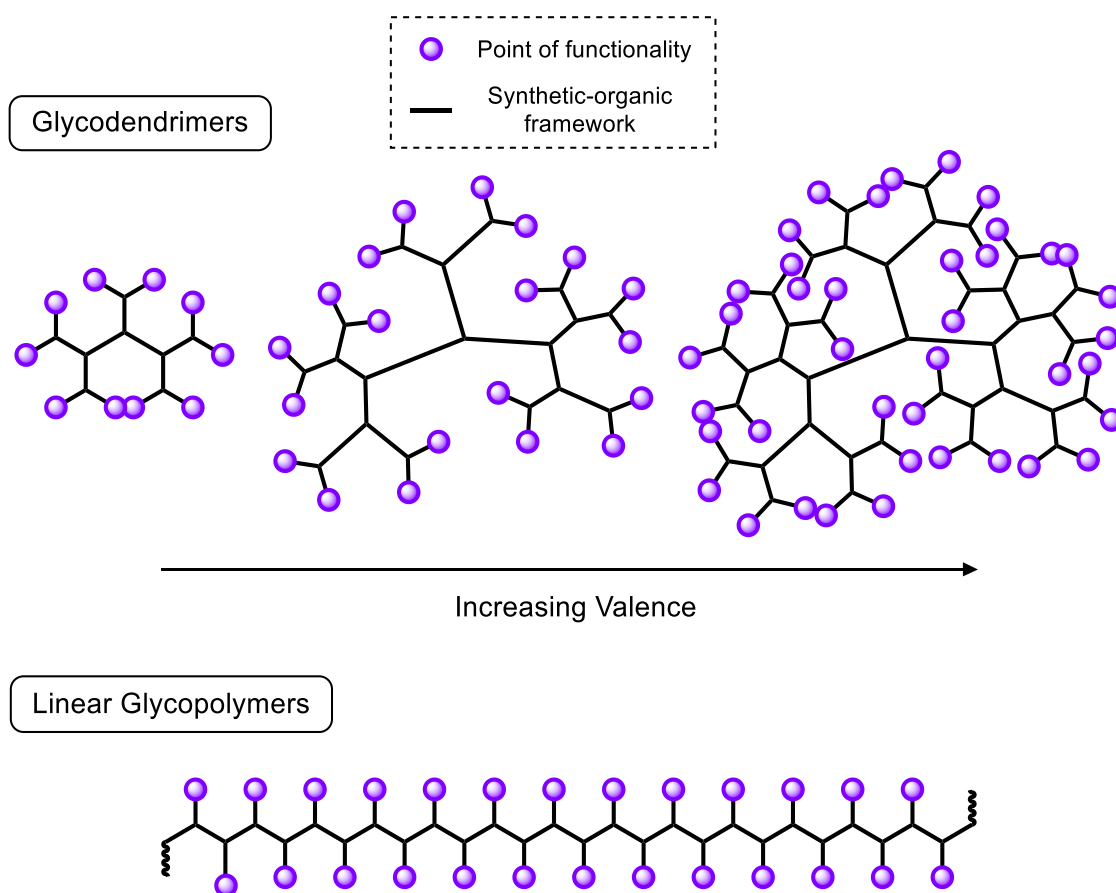
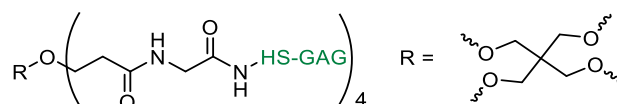


Figure 6: Illustrating a generalised structure of glycodendrimers (with increasing valence) and linear glycopolymers. Points of functionality = points where functionality or further structures can be installed.

The synthesis of single-entity glycodendrimers have been reported.⁸⁸ A variety of tetravalent dendrimers were capped with defined HS oligosaccharides, and demonstrated the ability to mimic HS by successfully inhibiting the enzyme beta-secretase 1 (BACE-1). BACE-1 is an aspartic-acid protease enzyme important for the biosynthesis of myelin sheaths in nerve cells and pathologically generates amyloid- β peptides, making it an Alzheimer's disease drug target.⁶² All of the glycodendrimers demonstrated < 0.1% the anticoagulant activity of H towards factor Xa, and they also displayed no FGF-receptor signaling through the binding of FGF-1 or FGF-2. This work showcases a successfully designed potent, protein-specific glycomimetic inhibitor (Table 2).

Table 2: The use of single point HS-glycodendrimers for the inhibition of BACE-1. ^aAverage molecular weight (MW) of H was 12 kDa. Adapted from P. C. Tyler.⁸⁸



Entry	IC ₅₀ (nM)	End-capped Oligosaccharide (HS-GAG)	MW (Da)
H (control)	0.2	Heterogeneous mixture	12000 ^a
1	760	GlcNAc(6S)	2606.8
2	13.1	GlcNAc(6S)-GlcA(2S)	3807.5
3	52.5	GlcNAc(6S)-IdoA(2S)	3807.5
4	36.9	GlcNAc(6S)-GlcA-GlcNAc(6S)-GlcA	5412.7
5	1.6	GlcNAc(6S)-GlcA(2S)-GlcNAc(6S)-GlcA(2S)	6229.1
6	1.5	GlcNS(6S)-IdoA(2S)-GlcNS(6S)-IdoA(2S)	6709.1

The epimerisation of the uronic acid unit decreased potency of the resulting glycodendrimer (IC₅₀ = 13.1 – 52.5 nM, Table 2, Entries 2 & 3, respectively). Therefore, the GlcA(2S) epimer is biologically significant to the HS-binding of BACE-1, and likely induces a conformational change in the disaccharide that potentiates the binding interaction of the glycodendrimer. However, epimerisation of the uronic acid unit is less significant when a tetrasaccharide motif is used, and both epimers present the greatest inhibition of BACE-1 (Table 2, Entries 5 & 6).⁸⁸ The removal of the 2*O*-sulfate attenuates BACE-1 inhibition by a factor of 23 (Table 2, Entry 4) and 3× greater potency was observed with the smaller disaccharide analogue (Table 2, Entry 2), thus it is a more efficient inhibitor. The monosaccharide GlcNAc(6S) analogue displayed relatively poor biological activity (IC₅₀ = 760, Table 2, Entry 1), which correlates with the proposed biological importance of the GlcA(2S) monosaccharide unit.

Overall, the results are suggestive of a disaccharide-specific binding interaction between the end-capped GAGs and BACE-1, with the presentation of a GlcA(2S) unit critical for potent inhibitory activity. The results also highlight that epimerisation of carboxylate groups, and additional sulfate functionalities, potentiate inhibition, which can be attributed to greater electrostatic interactions between the enzyme's cationic amino-acid residues and the poly-anionic glycodendrimers.

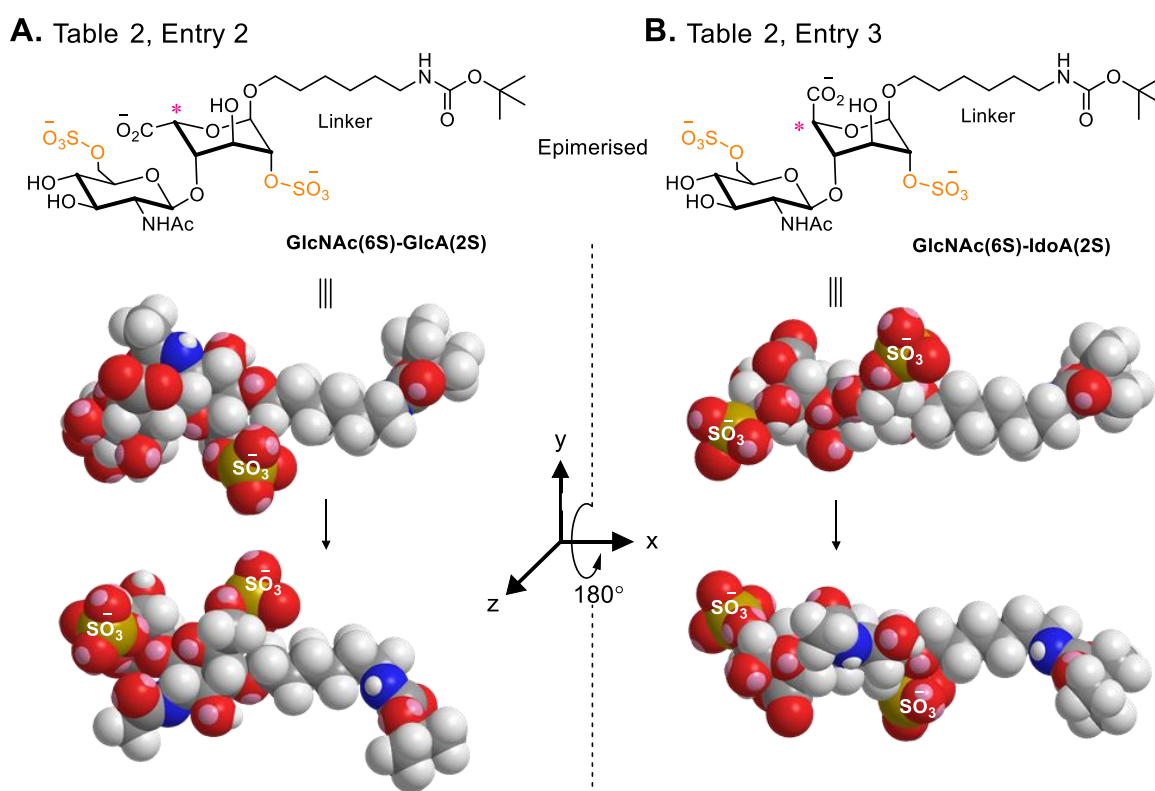


Figure 7: Analogous structures of two disaccharide monomers presented in **Table 2**, Entries 2 = **A** & 3 = **B**, with a linker unit to demonstrate the point of functionalisation onto the dendritic scaffold. Inset, Minimum energy (MM2) calculations of both disaccharide functionalities, highlighting that epimerisation of GlcA(2S) to IdoA(2S) induces significant conformational changes that separate the anionic sulfate functionalities. Therefore, the spatial orientation of such groups are significant to the potent inhibition of BACE-1.

The poor biological activity from the monosaccharide example (Table 2, Entry 1) suggests that secondary binding interactions from the clustering of distal end capped groups is minimal, thus high potency is attributed to the spatial orientation of proximal anionic groups. Minimum energy (MM2) calculations of end-capped disaccharides (Table 2, Entries 2 & 3) are in agreement with this, and demonstrate that epimerisation

of the GlcA(2S) unit to IdoA(2S) creates a major conformational change that alters the spatial orientation of sulfate groups in the monomer units (Figure 7). Additionally, the effects of epimerisation agree with the previously discussed, highly ordered biosynthesis of H and HS (See Chapter 1.5). Therefore, the epimerisation of uronic acid residues provides additional target specificity by modifying the spatial orientation of sulfate/sulfamate groups beyond their configurational positions.⁸⁹

It has been demonstrated that naturally derived H oligosaccharides (containing up to 30 disaccharide units) can be linked to synthetic poly-ethylene oxide cores, and this method was used in the synthesis of star-like glycodendrimers.⁹⁰ When the glycodendrimers were mixed with a solution containing FGF-2 it led to the formation of cylindrical micelles and eventual microfibre structures, suggesting a highly ordered FGF-2 binding interaction. The investigation by Novoa-Carballal et. al. concluded that the glycodendrimers do not affect the FGF-2 specific binding sequence of the parent H-GAGs, so the observed enhancement of FGF-2 binding was attributed to the polyvalent dendritic structures that present multiple anionic and non-polar functionalities. The H chains demonstrated enough separation to bind multiple FGF-2 proteins, forming a highly dense complex with over 35 (± 1) bound protein structures.⁹⁰ This highlights that the clustering of distal poly-anionic groups has a minimal effect on the binding interaction, thus it is proposed that the high binding affinity is attributed to proximal functionalities presented in disaccharide units.

Overall, star-like H-glycodendrimers were shown to be good at imitating natural H and HS at the structural and functional level. However, in this example, heterogeneously sulfated H-GAGs were used and the binding of FGF-2 was predictable. Furthermore, previous evidence suggests FGF-2 binds H/HS-GAGs in regions of GlcNS(6S)-IdoA(2S) disaccharide units,⁶⁶ which are abundant in naturally derived H-GAGs. Therefore, no

conclusions can be drawn as to whether the glycodendrimers targeted a specific binding interaction, but the probability is likely due to the formation of ordered microfibre structures.

An earlier investigation using a similar dendritic structure reported the use of a highly sulfated, multivalent galactose glycodendrimer as a glycomimetic inhibitor of L- and P-selectins (L = Leucocytes, P = Platelets, Figure 8, A).⁹¹ Selectins are a family of cell adhesion molecules that bind H and HS-GAGs. They are involved in chronic and acute inflammatory processes and a number of pathological diseases, so the inhibition of selectins has clinical potential.⁹²⁻⁹³

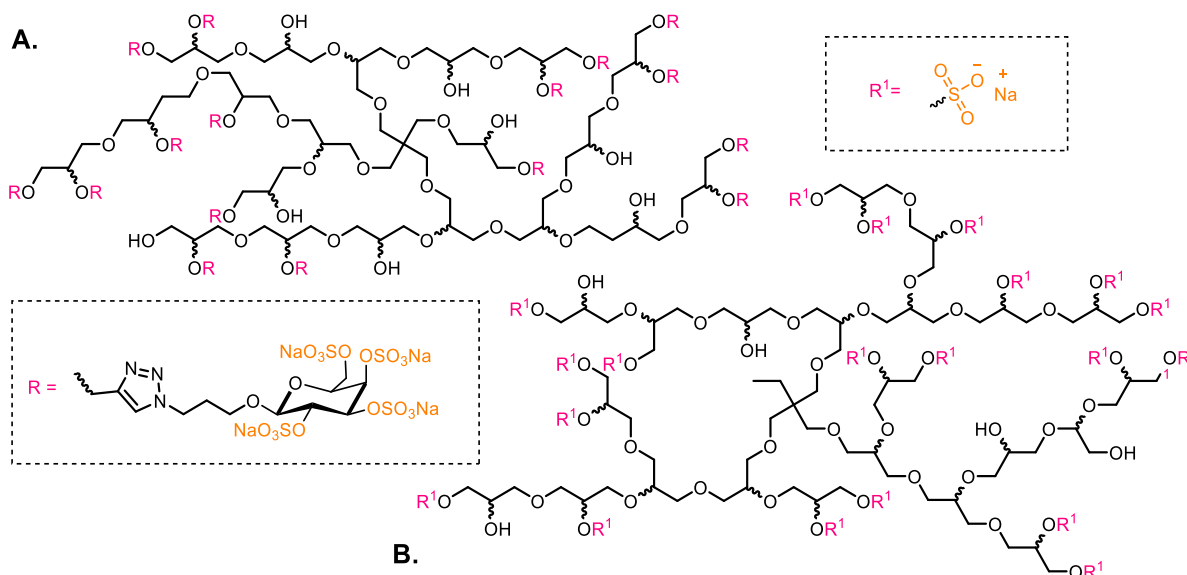


Figure 8: A) The structure of a multivalent, galactose glycodendrimer, as an H/HS-glycomimetic that inhibits L- and P-selectins.⁹¹ **B)** A fully synthetic hyper-branched polyglycerol sulfate that displayed inhibition of L- and P-selectins.⁸³

The glycodendrimer demonstrated an IC_{50} in the 1 – 7 nM range, and surface plasmon resonance (SPR) measurements were carried out alongside the inhibition studies, which accredited the potent inhibitory activity to an overabundance of anionic (sulfate) groups (Figure 8, A). This work demonstrates that a per-sulfated, homogenous glycodendrimer containing an abnormal (to H and HS) sugar monomer can successfully

inhibit selectins. It also highlights that GAG-protein binding is not dependent on specific interactions when an overabundance of anionic charge is presented. Therefore the requirement to have a specific saccharide-based carbon framework is not a prerequisite in the design of H and HS glycomimetics.

An overabundance of anionic groups have demonstrated significant biological activity using a fully synthetic, hyper-branched polyglycerol sulfate.⁹⁴⁻⁹⁵ The non-saccharide based glycodendrimers displayed good biocompatibility and successfully inhibited the action of L- and P-selectin at nM concentrations (Figure 8, B), agreeing with previous reports.⁹² Therefore, the extent of sulfation needs to be considered in the rational design of glycomimetics, to diminish non-specific binding interactions driven by an overabundance of electrostatic charge.

Overall, the finding presented so far propose that the binding-sites of selectins, growth factors and other H/HS-binding proteins are selective to a specific spatial orientation of anionic groups presented in disaccharide units. However, an overabundance of anionic charge in a glycodendrimer can outcompete protein specific interactions, thus a fully synthetic, poly-anionic glycodendrimer can be used successfully. Therefore, simpler organic frameworks can be used, but the concentration of anionic groups in the overall structure needs to be considered to warrant protein specific binding interactions.

Therapeutic biological activity has also been demonstrated by linear polymer frameworks incorporating sulfonate functionalities (Figure 9).⁹⁷⁻⁹⁹ However, the use of such molecules as therapeutic agents, to inhibit H/HS-binding proteins, is limited by their polydispersity and a lack of rational design and target specificity. Therefore, linear

anionic polymers are not considered to be glycomimetics, but for a comprehensive review of these compounds and their biological activity, see Paluck et. al.¹⁰⁰

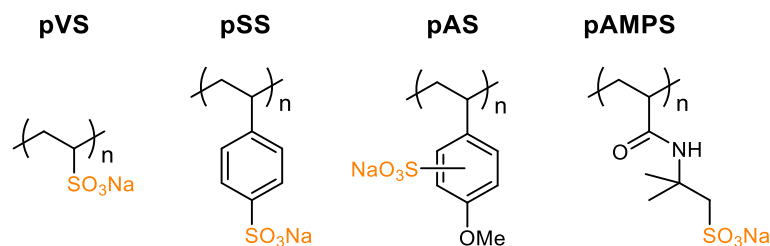


Figure 9: The monomer structures of various synthetic linear anionic polymers that display biological activity toward a variety of H/HS-binding proteins. **pVS** = polyvinyl sulfonate, **pSS** = polystyrene sulfonate, **pAS** = polyanisole sulfonate, **pAMPS** = polyacrylo-2-amino methyl-2-propanesulfonate.

2.2. Linear Glycopolymers

Linear glycopolymers (as glycomimetics) benefit from the similar advantages displayed by glycodendrimers, and can provide polyvalent sites that establish strong and reversible binding interactions of biomolecules. However, the work previously discussed (Chapter 1.6.1) highlighted that polyvalent interactions are not significant to potent inhibition or high avidity binding. Even so, linear glycopolymers are more representative of the natural biomolecules they intend to imitate, increasing the likelihood of enhanced biological activity. Oligosaccharide-containing monomers can be synthesised and readily combined in a polymerisation reaction, so the use of linear glycopolymers permits an efficient syntheses to homogenous glycomimetic designs. Furthermore, the polymers can be functionalised onto surfaces¹⁰¹⁻¹⁰² and membranes¹⁰³ for biomedical and sensing purposes, and have been demonstrated in a variety of clinical applications.¹⁰⁴⁻¹⁰⁹ The key examples relating to their use as novel H/HS-based glycomimetics are discussed in this chapter.

Linear glycopolymers containing short and well-defined H/HS-GAGs are an attractive alternative to natural H-based anticoagulants (such as Fondaparinux), and can also be used to target specific H/HS-binding proteins.

Hsieh-Wilson and co-workers have demonstrated a ring-opening metathesis polymerization (ROMP)¹¹⁰ methodology to linear glycopolymers, and generated a series of H- and HS-based glycomimetics tailored to replicate the potent activity of anticoagulant drugs, or to target specific HS-binding proteins with an attenuated anticoagulant activity (Figure 10).¹¹¹⁻¹¹¹² A single point change in their disaccharide monomer (Pink, Figure 10) switched AT mediated coagulation on and off. Their findings presented a H-glycomimetic with 100× the potency of H at inhibiting thrombin ($IC_{50} = 114 (\pm 1) \text{ pM}$, Figure 10, A).¹¹¹ Moreover, they also demonstrated that AT activity was attenuated by removing a specific 3-*O*-sulfate in their monomer unit, which was discovered to be a potent chemokine antagonist (Figure 10, B).¹¹²

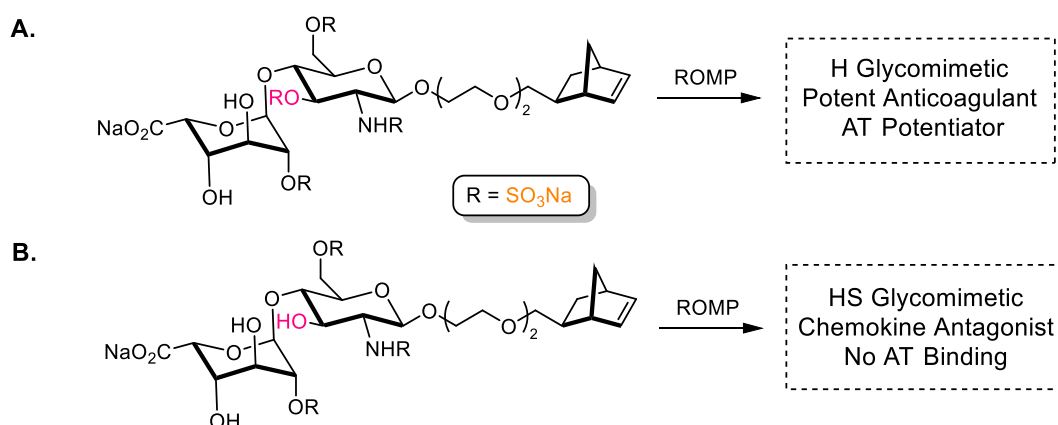


Figure 10: The synthesis of linear glycopolymers by ring-opening metathesis polymerisation (ROMP), demonstrating a single point change in the monomer structure (**A to B**) that can turn AT mediated anticoagulation on and off. Adapted from Heish Wilson et. al.¹¹¹⁻¹¹²

Chemokines are a family of cytokines that bind a specific cell surface G-protein coupled receptor, and act as chemoattractive agents that guide the migration of white blood cells to sites of infection and inflammation.¹¹³ They are associated with a variety of pathologies, so this work presents significant clinical importance in the design of novel therapeutics.^{71, 114} Furthermore, the results elegantly demonstrate that a single change in sulfation induces a conformational change in the monomer, which permits the fine modulation of biological activity in the polymer structure. Additionally, the results are

in agreement with the proposed theory that individual H/HS-binding sites are sensitive to the spatial orientation of anionic sulfate functionalities (See Chapter 1.5).

The design and synthesis of a glycomimetic heparanase inhibitor has been described.¹¹⁵ Heparanase is an enzyme that degrades HS-proteoglycans, converting them into small-chain oligosaccharide fragments. Increased heparanase activity is linked to cancer cell metastasis and pathological angiogenesis, so heparanase inhibitors are drug targets for cancer therapies. Specifically, a 12 unit glycopolymer bearing a pendant GlcNS(6S)-GlcA motif inhibited heparanase at pM concentrations (Figure 11). The glycomimetic demonstrated minimal secondary interactions with growth factors: FGF-1, FGF-2, and VEGF, which is in agreement with previous results.⁸⁸ Furthermore, the HS-glycomimetic prohibited the metastasis of carcinoma cells, which was attributed to the inhibition of P-selectin, serendipitously providing a dual action inhibitor of tumour cell growth and metastasis.

Previous reports⁹¹ suggest that the inhibition of P-selectins are ascribed to the overabundance of anionic groups present in the polymer. Therefore, regardless of the specific inhibition of heparanase, the binding of P-selectin is likely attributed to non-specific electrostatic interactions.

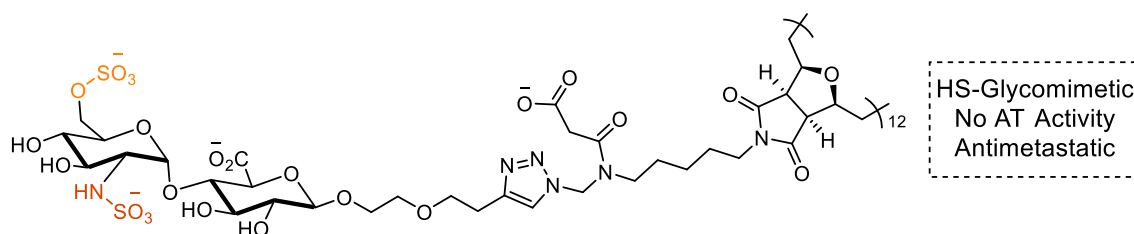


Figure 11: The monomer structure of a linear glycopolymer that displayed pM inhibition of heparinase enzyme and P-selectin. Adapted from Loka et. al.¹¹⁵ Cations omitted for clarity.

Overall, the work discussed in this chapter highlights that glycodendrimers and linear glycopolymers can be synthesised through a variety of chemical methods, and can be tuned to target specific H/HS-binding proteins.

It has been revealed that polymer based glycomimetics benefit from the polyvalence of anionic groups, which enhances protein-binding interactions. However, synthetic polymers with multiple anionic functionalities are also effective H/HS-glycomimetics that have demonstrated comparable biological activity. Therefore, it is proposed that in some cases, significant biological activity is actually attributed to the abundance of anionic charge density in the polymer structure, which has major consequences in the targeting of specific proteins using polymer-based glycomimetic scaffolds. Additionally, it has been highlighted that single point changes in the glyco-monomer can attenuate or promote specific biological activity, and that the binding sites of multiple H/HS-binding proteins are sensitive to conformational changes in the GAG. Thus, potent inhibitory activity is linked to the spatial orientation of anionic and non-polar functionalities in small monomer-like units, so H/HS-binding proteins can be targeted using small molecule glycomimetics.

2.3. Small Molecule H/HS-Glycomimetics

Small molecule glycomimetics represent a comparably niche category compared to glycodendrimers and linear glycopolymers.¹¹⁶ They do not possess multivalent groups associated with large macromolecules, so they are dissimilar to the biomolecules that they are designed to imitate. However, due to their size, they can be used to target the binding sites of multiple proteins, which, from the work discussed previously (Chapters 1.6.1 & 1.6.2) is shown to be important for high affinity protein-binding interactions that can lead to potent inhibitory activity. Therefore, small molecule glycomimetics can be rationally designed to target specific binding sites, which can

facilitate the protein's biological activity,¹¹⁷ or inhibit the interactions of endogenous H and HS, thus attenuating protein-receptor binding.¹¹⁸⁻¹¹⁹

Due to the size-dependent selectivity of H binding AT, the likelihood of AT activation is diminished using small molecule glycomimetics, so specific proteins can be targeted with little possibility of AT activation.⁴ These molecules do not require extensive chemical synthesis, permitting a higher throughput for the screening of glycomimetic compounds against drug targets.¹²¹ The molecular-weight range for a small molecule drug is approximately 350-900 Da (depending on the type of drug), but this factors in a prerequisite for the drug-molecule to be able to diffuse across a cell membrane.¹²² This limit is not applicable to small molecule glycomimetics targeting H/HS-binding proteins, as their biological activity is associated with the extracellular environment, therefore, a ability for diffusion across cell membranes is not essential to their design. Additionally, the presence of sulfate functionalities adds significant charge density and an associated drop in lipophilicity, so any potential for membrane diffusion is significantly diminished. Consequently, a more definitive term for small molecule H/HS-glycomimetics is: a glycomimetic structure designed to target the binding sites of H/HS-binding proteins. Over the years a selection of small molecule H/HS-glycomimetics have been investigated and are discussed in this chapter.

Suramin is a medication used for the treatment of African sleeping sickness.¹²³ However, Suramin (Figure 12, A) and a number of Suramin analogues have been repurposed as glycomimetics targeting FGF-2 (fibroblast growth-factor 2, Table 1) mediated angiogenesis.¹²⁴⁻¹²⁵ The glycomimetics were evaluated for their ability to inhibit FGF receptor activation, and demonstrated a wide range of inhibitory activity ($IC_{50} = 85 - 857 \mu M$).¹²⁴ Furthermore, the most potent inhibitor (Figure 12, B, $IC_{50} = 142 (\pm 18) \mu M$) completely blocked FGF induced angiogenesis, therefore all FGF-2-based receptor activation was blocked.

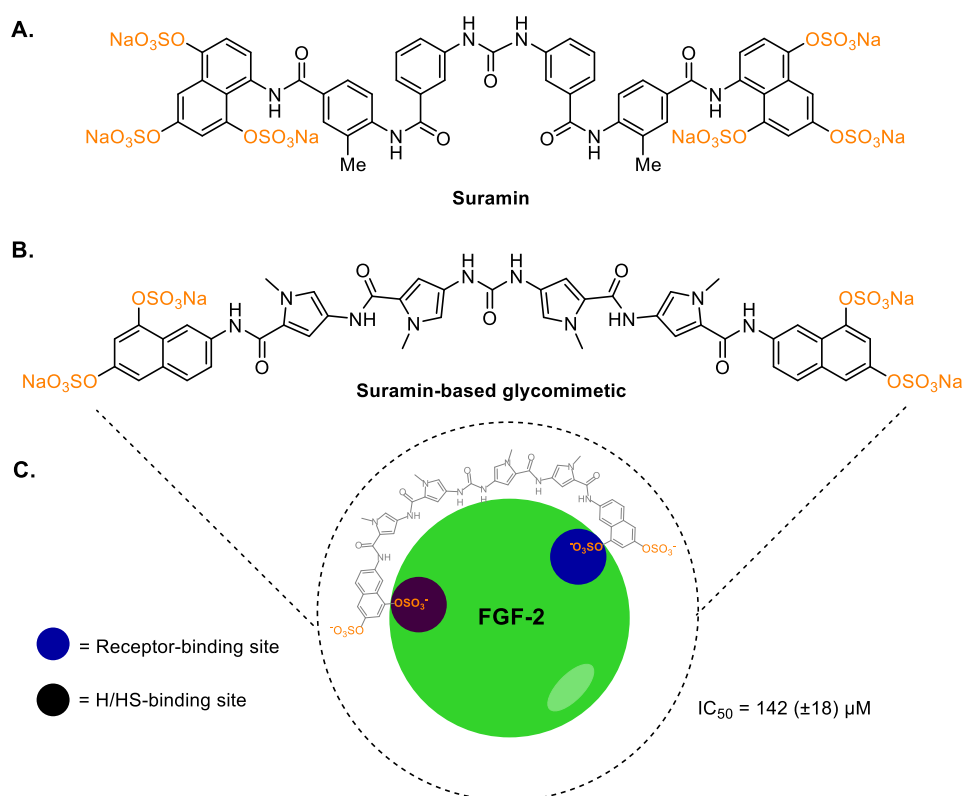


Figure 12: **A)** The chemical structure of Suramin, a drug used for the treatment of African sleeping sickness. **B)** The structure of a Suramin-based glycomimetic targeting FGF-2. **C)** Illustrating the proposed glycomimetic binding of FGF-2, calculated from docking studies, demonstrating a 1:1 protein-ligand complex that binds the H/HS-binding site and the receptor-binding site. Adapted from Manetti et. al.¹²⁴

The investigation correlated affinity data with molecular docking calculations, providing an *in silico* SAR of their Suramin-based glycomimetic. It was concluded that the glycomimetic (Figure 12, B) forms a 1:1 protein-ligand complex through a bidentate

interaction of terminal naphthylsulfonate motifs to the HS-binding site and the receptor-binding site of FGF-2 (Figure 12, C). This is the first report of a bidentate inhibitor of FGF-2, and strongly suggests that small molecule glycomimetics can inhibit the action of growth factors by blocking all potential binding sites on the protein's accessible surface. Furthermore, this correlates with the potent inhibitory activity demonstrated by glycodendrimers and linear glycopolymers.^{88, 115} However, a bidentate (chelating) interaction was not considered in previous investigations, so small molecule glycomimetics have the potential to bind both sites simultaneously or can target either site independently, giving them an advantage over previously demonstrated polymeric structures.

Suramin can also inhibit heparanase (See Chapter 1.6.2),¹²⁶⁻¹²⁷ prompting the investigation of Suramin-based heparanase inhibitors. A potent inhibitor was discovered ($IC_{50} = 2.0 (\pm 0.6) \mu M$, Figure 13, A)¹²⁸ which suggests that small molecule glycomimetics can be of similar potency to linear glycopolymers, therefore they are more efficient drug targets due to their smaller molecular weights.

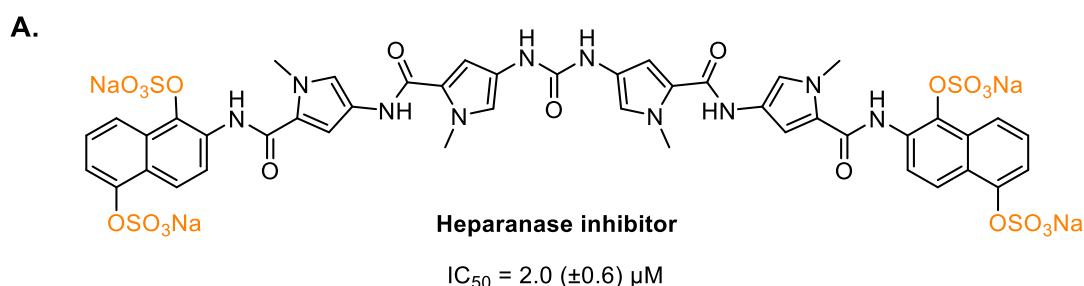


Figure 13: The structure of a Suramin-based glycomimetic used to target Heparanase.¹²⁸

The investigation concluded that an alternate hypothesis is necessary for the proposed mechanism of heparanase inhibition, which can account for the greater than expected potency demonstrated by the Suramin-based glycomimetic.¹²⁸ A new hypothesis was not proposed, however, the results previously discussed^{115, 125} suggest that the

glycomimetic (Figure 13) likely binds both the H/HS-binding site and the enzymes active site through a bidentate interaction, thus accounting for the potent inhibition of enzyme activity.¹²⁸ Overall, this work reveals a marked advantage of using small molecule glycomimetics as novel protein-receptor antagonists and enzyme inhibitors.

Zhang and co-workers demonstrated a small molecule library can be used to identify novel H-glycomimetics capable of targeting VEGF and FGF-2.¹²⁹ The library was designed to contain H-like functionalities such as carbohydrate motifs, hydroxyl groups, sulfonate functionalities and carboxylates, which were combined in an Ugi (4-component) condensation reaction (Figure 14).¹³⁰ A library of 18,720 compounds were screened against VEGF and FGF-2, and only 20 glycomimetics demonstrated significant inhibitory activity ($IC_{50} = 1.65 - 14.50 \mu M$).¹²⁹ Interestingly, 90% of the active compounds had a linear structure and presented at least 1 anionic residue. The most potent inhibitor contained 2 sulfonate groups on each side of the molecule (Figure 14, A).

It was concluded that the exact spatial location of anionic charge is not significant due to the degrees of freedom accessible to their glycomimetic (Figure 14, A), and the distance between the two anionic groups is important for potency due to the blocking of the H/HS binding site and the receptor-binding site.¹²⁹ The findings seemingly compare with previous examples.^{124, 128} However, minimum energy (MM2) calculations (Figure 14, B) highlight that flexibility in the structure is diminished by the presence of bulky aromatic groups, which restricts the anionic sulfonate groups in a sterically hindered conformation. Therefore, a bidentate binding interaction is unlikely in this case, and the high potency interaction is likely caused by additional hydrogen bonding and hydrophobic interactions from the vicinal groups.

Ugi condensation

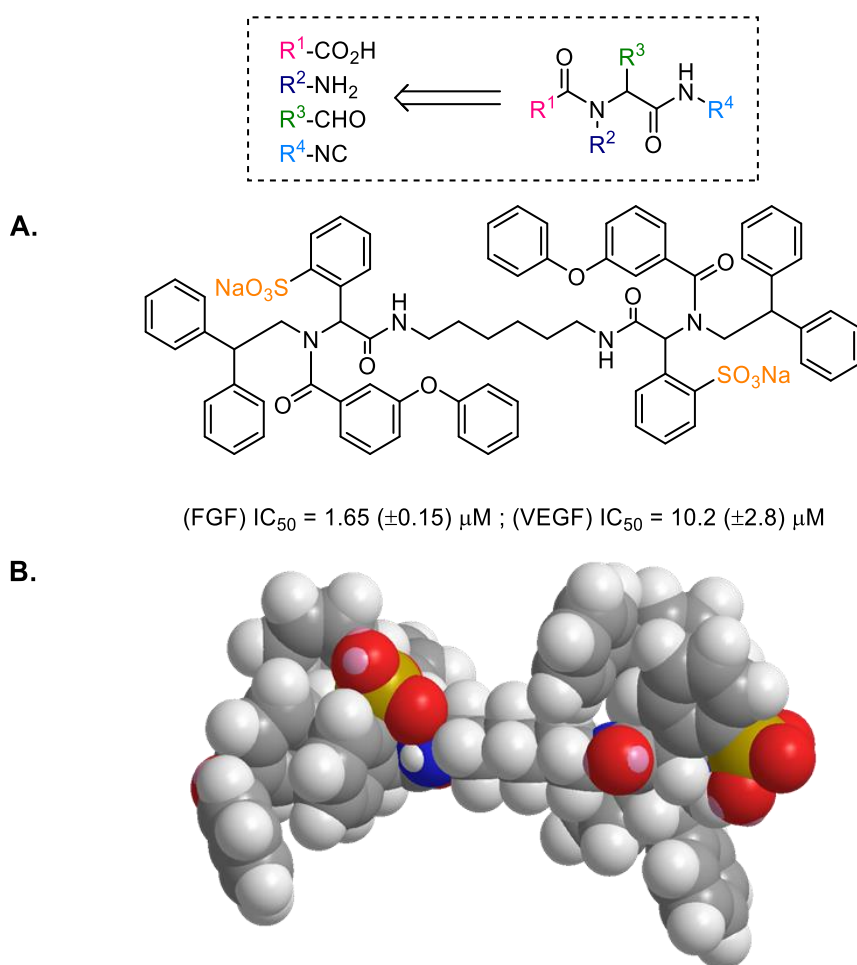


Figure 14: **A)** The structure of the potent FGF and VEGF inhibitor discovered from a small molecule H-glycomimetic library utilising the Ugi (4-component) condensation reaction. **B)** MM2 minimized energy structure. Adapted from Zhang et. al.¹²⁹

Furthermore, the H/HS-glycomimetic (Figure 14, A) demonstrated 10× less inhibitory activity towards VEGF, which correlates with the structural differences in each protein's binding site (See Table 1). Therefore, this investigation indirectly demonstrates that small molecule H/HS-glycomimetics can be designed to target protein specific binding-sites by auxiliary non-polar functionalities.

The previously discussed findings were also confirmed by varying hydrophobic functionality around a sulfated monosaccharide structure, which can be changed to selectively target the H/HS-binding sites of individual growth factors: FGF-1, FGF-2, and VEGF.¹³¹ Specifically, a di-sulfated methyl 6-azido-6-deoxy- α -D-mannopyranoside

(Figure 15, A) was screened and the most active 5-allyloxy derivative (Figure 15, B) was diversified using the Cu(I)-catalysed Huisgen azide–alkyne cycloaddition (Click reaction, Figure 15, F).¹³² The diversity was extended further by incorporating a Swern oxidation–Wittig reaction sequence (Figure 15, G),¹³³ so the investigation by Liu et. al. used a variety of hydrophobic and polar functionalities designed to probe the protein's accessible surface area in the vicinity of the H/HS-binding site.

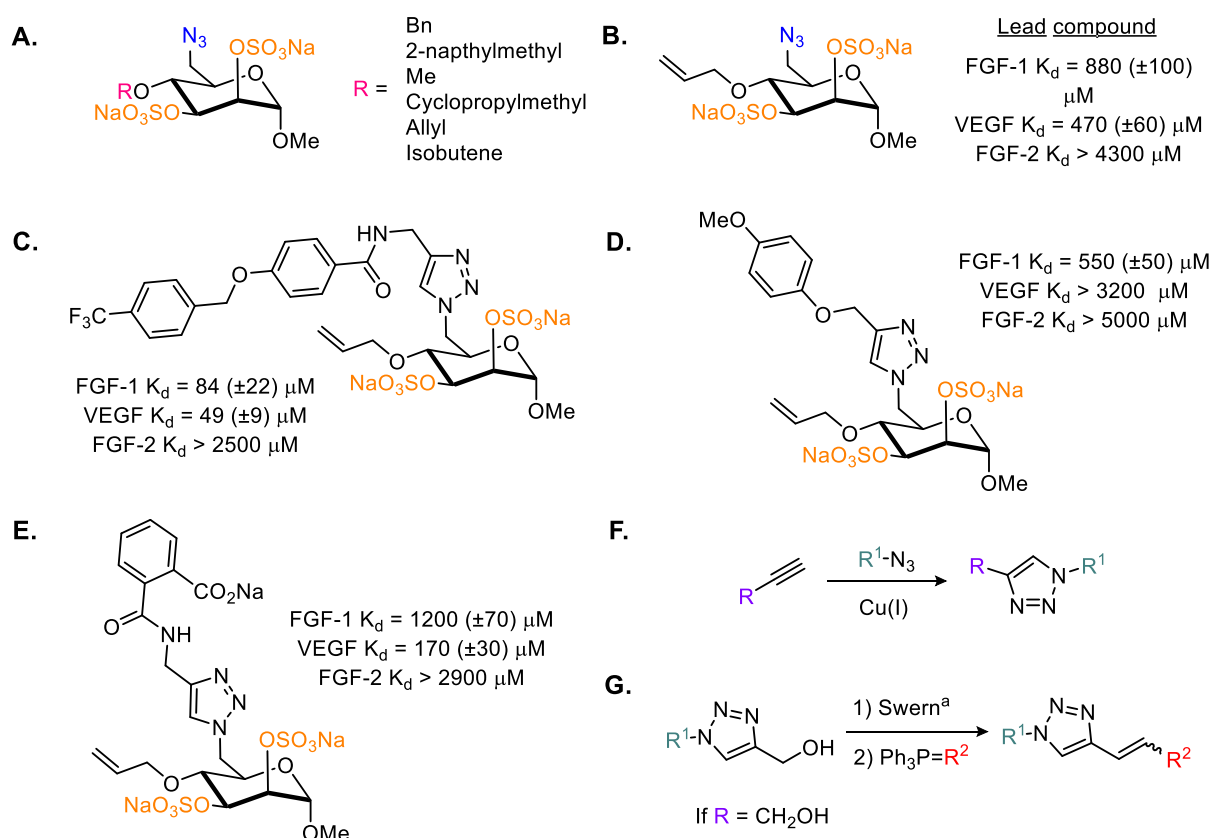


Figure 15: **A)** Structure of a di-sulfated methyl 6-azido-6-deoxy- α -D-mannopyranoside with a variable R group on the 5-position; **B)** The structure of a lead compound that displayed the best binding affinity for FGF-1 and VEGF; **C)** The structure of a H/HS glycomimetic with enhanced binding affinity for FGF-2 and VEGF; **D)** The structure of a H/HS glycomimetic with selective binding affinity for FGF-1; **E)** The structure of a H/HS glycomimetic with selective binding affinity for VEGF. Adapted from L. Liu et. al.¹³¹ **F)** Click reaction; **G)** Swern oxidation–Wittig sequence.

The binding affinities were measured using SPR affinity assays and the glycomimetics competed with immobilized H for each protein, so protein-glycomimetic binding was only detected for the H/HS-binding site. A hit compound (Figure 15, C) was identified with μM binding affinity toward FGF-1 ($K_d = 84(\pm 22) \mu\text{M}$) and VEGF ($K_d = 49(\pm 9) \mu\text{M}$),

with good selectivity over FGF-2 ($K_d > 2500 \mu\text{M}$). Furthermore, two protein specific glycomimetics were also identified for FGF-1 and VEGF (Figure 15, D & E, respectively).

The results of this investigation confirm that small molecule glycomimetics can be designed to target specific H/HS-binding proteins using additional non-polar functionalities, thus targeting the accessible surface area surrounding the H/HS-binding site. Furthermore, this investigation shows that H/HS-glycomimetics can also be diversified to target specific growth factors. However, the assay used was site specific, so no conclusion can be made regarding the glycomimetic's ability to bind the receptor-binding sites of FGF-1, FGF-2, and VEGF. Nonetheless, the specific targeting of the H/HS-binding site is significant, and has further applications in the design of novel protein inhibitors.

It has been revealed that simple, highly sulfated glycomimetics **1-4** (Figure 16) can attenuate the HGF activation of its associated (MET) receptor and inhibit cancer cell development.¹³⁴ There is strong evidence that an over-expression or dysfunction of the HGF/MET interaction contributes to the growth and metastasis of cancer cells.¹³⁵⁻¹³⁸ Furthermore, the HGF/MET-receptor interaction is facilitated by the co-binding of HS-proteoglycans.¹³⁹ However, the HS binding interaction was considered to be non-specific,¹⁴⁰ but recent evidence suggests that a core active disaccharide is responsible for inducing HGF activity.¹⁴¹⁻¹⁴² The rational design of glycomimetics **1-4** by Raiber et. al.¹³⁴ was based on a trisaccharide structure (Figure 16, A) with an internal GlcA(2S)/IdoA(S2) unit (Figure 16, left), and either two terminal GlcNS(3S) units, or a GlcNS(3S) and a GlcNS(6S) unit (Figure 16, right).

A simplified design replaced the central uronic acid unit with a benzoic acid scaffold. This was decorated with *para* substituted aliphatic chains that contained variable

sulfate functionalities designed to occupy a similar spatial orientation to the model trisaccharide (Figure 16, B).

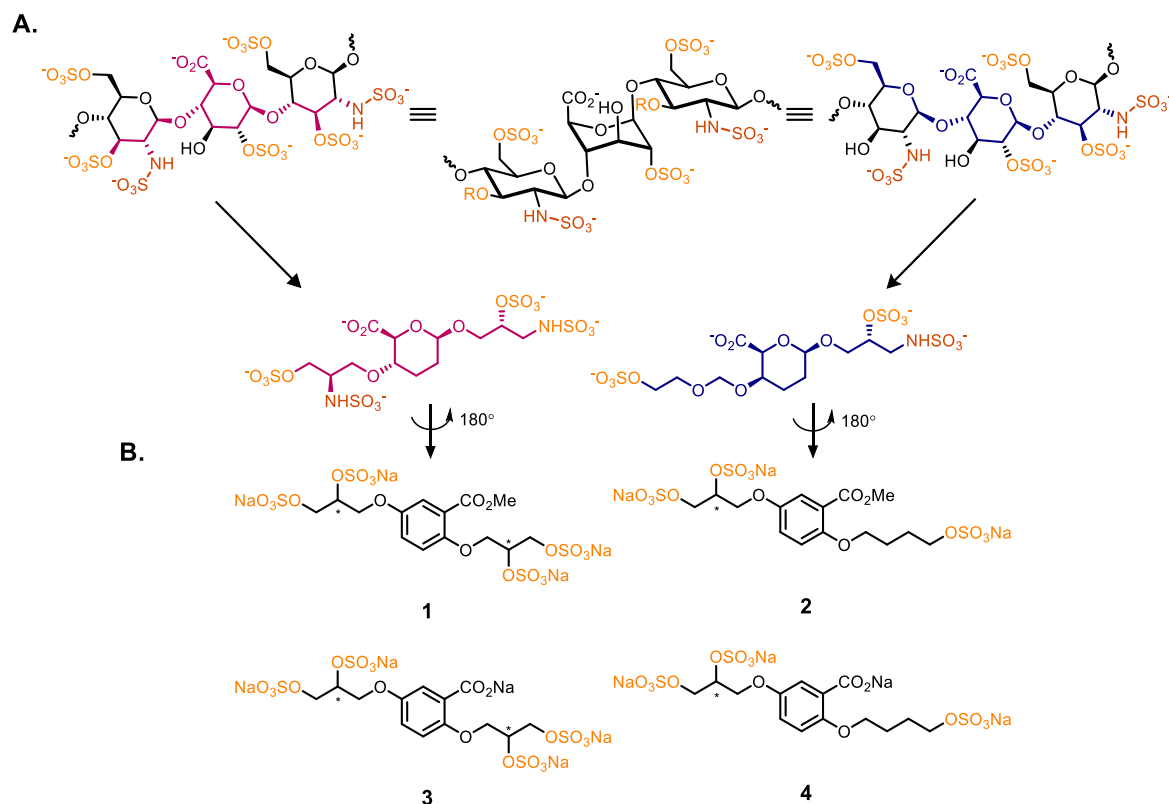


Figure 16: The rational design of small molecule H/HS glycomimetic targeting HGF, **A**) based on the structure of a parent trisaccharide; **B**) The structures of small molecule HS-glycomimetics **1**, **2**, **3** and **4** targeting the HGF/Met receptor interaction. Adapted from Raiber et. al.¹³⁴ (* = Point of chirality.)

The inhibitory activity of the HS-glycomimetics **1-4** were first determined for HGF and FGF-2 through western blot analysis.¹³⁴ Both the MET and the FGF receptor are activated by productive binding of their respective growth factors (HGF and FGF-2), which leads to the phosphorylation of an intrinsic tyrosine kinase domain and the activation of ERK mitogen-activated protein-kinase (MAPK).¹⁴³ HS-Glycomimetics **S-2** and **RS-3** (Figure 17) were found to completely inhibit HGF activity between 0.1 – 0.2 μ M concentration, demonstrating no observed FGF receptor activation. However, at lower concentrations (0.001 – 0.01 μ M) neither compound displayed HGF/MET inhibition. Nonetheless, both glycomimetics showed significant inhibition of HGF-induced cell migration,¹⁴⁴ thus a potential to prevent cancer cell metastasis.

The investigation conducted docking studies of **S-2** (Figure 17) with HGF (PDB code: 1BHT), and proposed that the active conformation adopts an exact mode of binding to the natural bound ligand (an H-type pentasaccharide), suggesting that the small molecule glycomimetics actively compete for the HS-binding site through a highly specific binding interaction. Overall, this work established that small, rationally designed organosulfates can be used to block MET receptor activation, and selectively target growth factors recruited in pathological diseases. However, no evidence was given as to whether the glycomimetics bind the HS-binding site, the receptor binding site, or both sites on the HGF's accessible surface.

Since the initial discovery of the hitherto reported H/HS-glycomimetics,¹³⁴ compounds **1-3** have been repurposed as novel anti-inflammatory agents and have demonstrated clinical potential at targeting lipid and fatty acid induced endothelial dysfunction,¹⁴⁵⁻¹⁴⁹ vascular calcification,¹⁵⁰⁻¹⁵³ and wound healing.^{148, 154-155} Subsequent investigations using the glycomimetics **SR-1**, **R-2**, **S-2** and **RS-3**,¹³⁴ have provided evidence that the restorative and anti-inflammatory effects are executed through the binding of HGF, attenuating MET receptor activation, which affects two downstream intracellular signalling pathways: Akt/eNOS/Nrf2/ARE and c-Met/Notch3/HES1 (Figure 17).

Overall, the activation of these signaling pathways has a therapeutic effect and restores endothelial cell function to baseline levels through the phosphorylation of intracellular proteins, and the upregulation/downregulation of specific genes. Therefore, considering the clinical significance of glycomimetics **1-3**, which has been verified by a number of separate investigations,¹⁴⁵⁻¹⁵⁵ a robust chemical synthesis is imperative to provide a large stock of compounds for future research into their biological activity. Moreover, no SAR analysis was considered for the binding of the

original glycomimetics to HGF. Therefore, an efficient synthesis of **1-3** is warranted with a further investigation of their SAR.

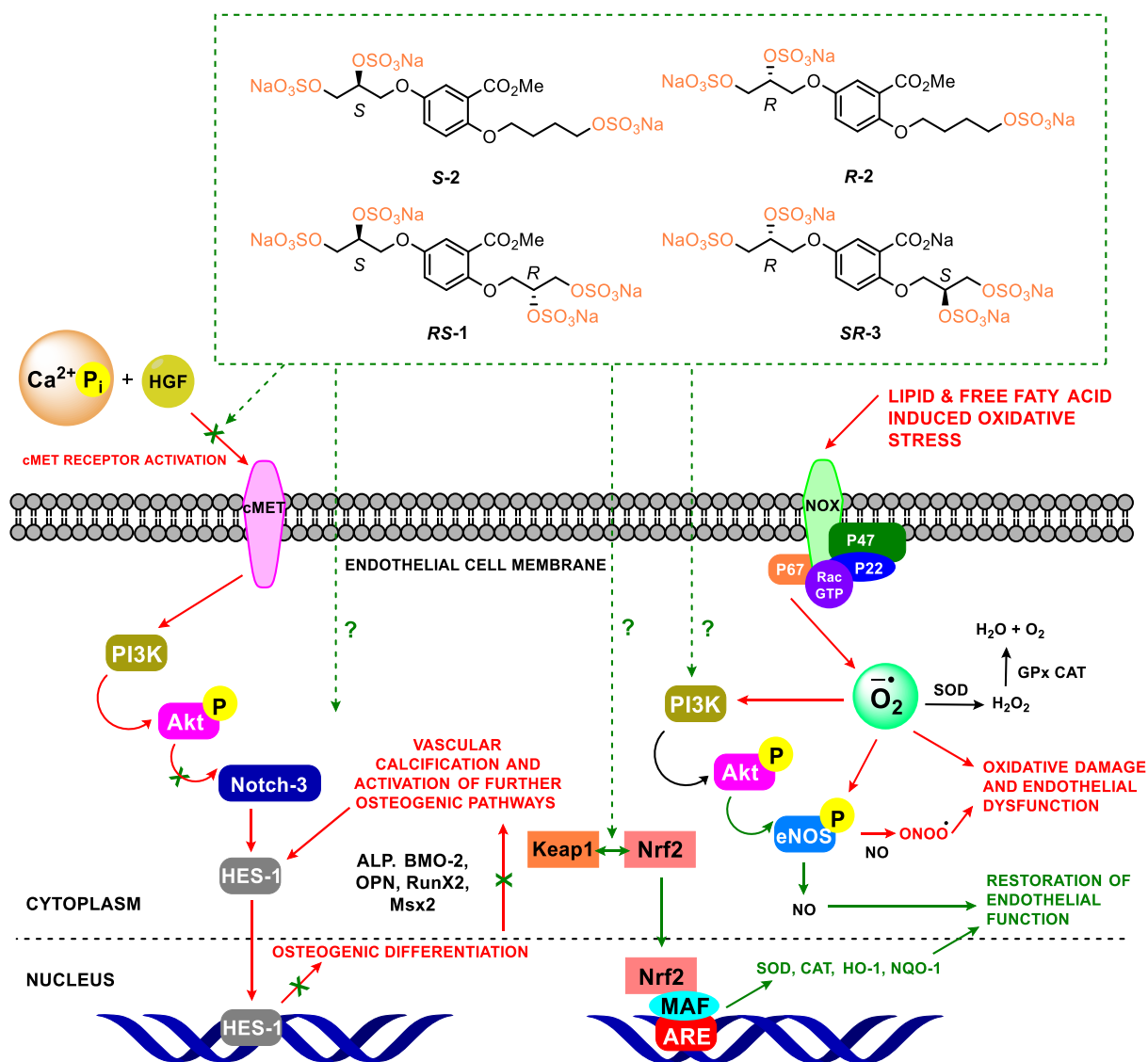


Figure 17: Illustrating the two proposed biological pathways associated with endothelial dysfunction (inflammation) and vascular calcification. The small H/HS-glycomimetics demonstrate anti-inflammatory activity and inhibit vascular calcification through a variety of proposed intracellular interactions, which are shown to upregulate or downregulate specific proteins and enzymes associated with oxidative damage, inflammation and calcification. Overall, the glycomimetic induce significant therapeutic effects. R = H, Me; **Green** = therapeutic effects; **Red** = Pathological effects; **?** = potentially unknown biological action. Adapted from Mahmoud et. al.¹⁴⁹ & 154

2.4. Investigation: Aims and Justification

The work discussed in this chapter has highlighted that H/HS-glycomimetics are capable of targeting specific binding-sites on H/HS-binding proteins. Therefore, small molecule glycomimetics are valuable tools for the study of growth factor-receptor interactions, and can be designed to inhibit them by already demonstrating therapeutic effects *in vitro*.¹⁴⁵⁻¹⁵⁵

The designs of HS-glycomimetics **1-3**, to target pathological HGF/MET-receptor interactions, have provided the foundation for an investigation aimed at elucidating and potentiating the glycomimetic inhibition of HGF through an SAR analysis.¹³⁴ Previously, it has been demonstrated that additional non-polar functionalities can enhance the protein-binding interactions of small molecule glycomimetics, and can be used to target specific binding sites, thus enhancing specific inhibitory activity.^{129, 131} Therefore, this investigation aims to utilise this methodology and:

- Create a robust chemical synthesis towards the first generation of small molecule HS-glycomimetics, providing a stock of compounds for further use and biological testing
- Examine the original glycomimetics computationally and in a binding affinity assay to gain additional evidence to support or query the results of previous investigations on HGF binding/inhibition
- Design additional generations of HS-glycomimetics and computationally model their interactions in the H/HS-binding site of HGF
- Synthesise the newly designed glycomimetic structures and quantify their HGF-binding affinities in a biological assay, thus providing an SAR profile (Figure 18)

Synthesis and characterisation of enantiopure derivatives to assess the importance of chirality to the HS-glycomimetics binding of HGF

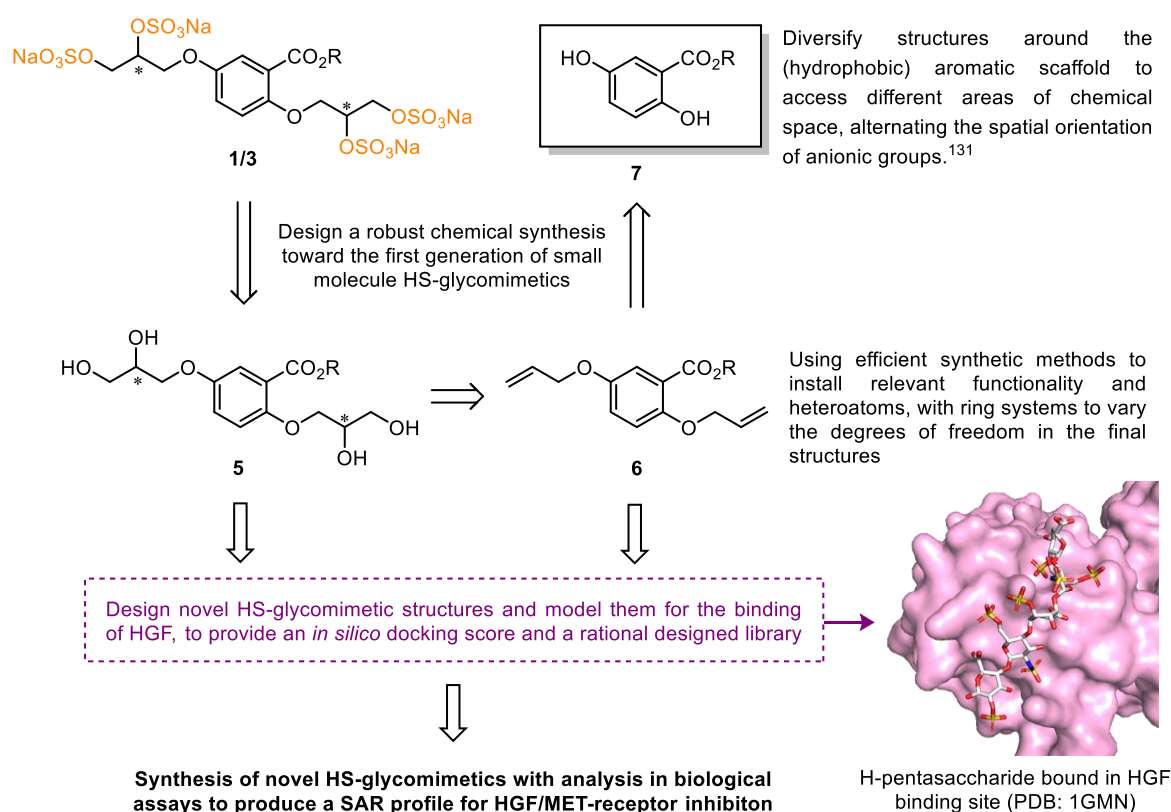
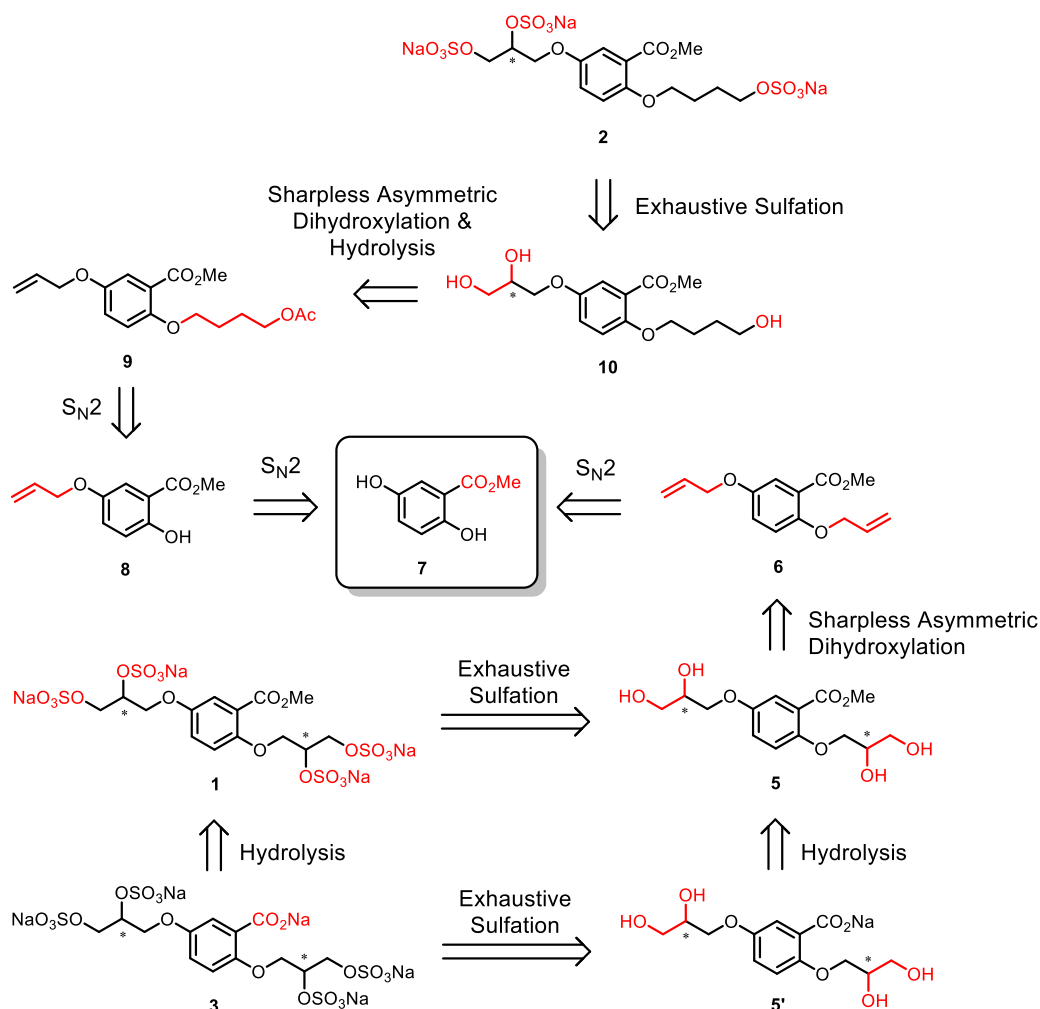


Figure 18: A schematic representation for the aims of this investigation using the synthesis of HS-glycomimetics **1** and **3** for examples. *varying stereochemistry, R = Na, Me

2.5. Investigation: Challenges and Observations

To design an efficient synthetic strategy for the first generation HS-glycomimetics **1-3**, retrosynthetic analysis was carried out with reference to the original literature procedure by Raiber et. al. (Scheme 1).¹³⁴ From the analysis, it is apparent that the first generation HS-glycomimetics do not require a complex chemical syntheses, using nucleophilic substitution (S_N2) to decorate an aromatic core scaffold (**7**). Enantioenriched 1,2-diols are installed through a single or double (tandem) Sharpless asymmetric dihydroxylation reaction, with the final per-hydroxylated intermediates sulfated directly to give the target structures, or sulfated after the hydrolysis of a specific acetate functionality. This route was optimal for the investigation, as the simple

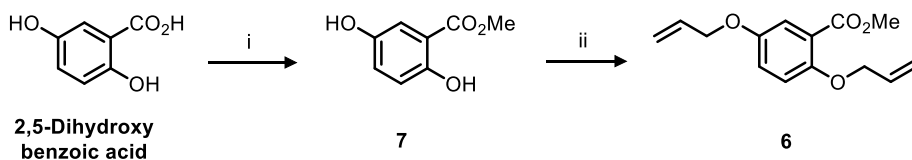
and reliable synthetic methods can also be used to access novel targets, which permits a higher throughput of compounds necessary for an SAR investigation. Furthermore, all known intermediates are reported to be achieved in moderate to excellent yields (58-92%).¹³⁴



Scheme 1: Retrosynthetic analysis of HS-glycomimetics **1-3**, * = Changes in stereochemistry.

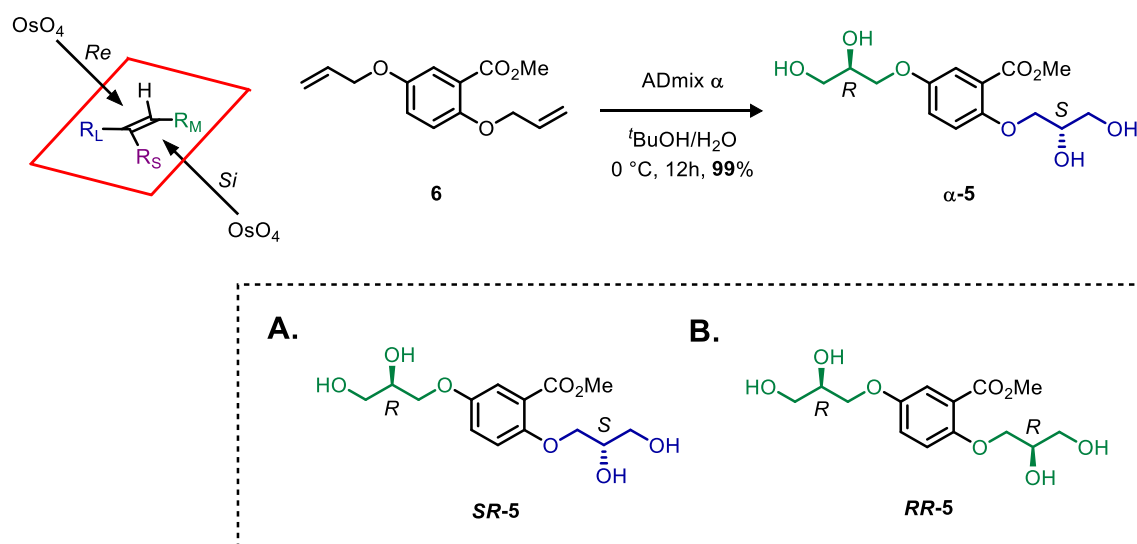
The synthesis of glycomimetic **1** requires the fewest (four) synthetic steps, therefore the synthesis toward this target was attempted first. 2,5-Dihydroxybenzoic acid was subjected to Fisher esterification in methanol, affording the desired methyl ester **7** in excellent yield (95% after recrystallization). Successive $\text{S}_{\text{N}}2$ was performed with pheolic **7** and allyl bromide, however, the literature conditions using sodium hydride (NaH) as base in dimethylformamide (DMF)¹³⁴ was replaced for potassium carbonate

(K₂CO₃) in acetone, as this provided a cleaner work up procedure and eliminated the requirement of anhydrous reaction conditions (Scheme 2). Overall, diene **6** was afforded in 99% yield.



Scheme 2: The synthesis of diene **6**. Conditions: i) H₂SO₄, MeOH, reflux, 12 h, **95%**; ii) Allyl bromide, K₂CO₃, TBAI, acetone, reflux, 4 h, **99%**.

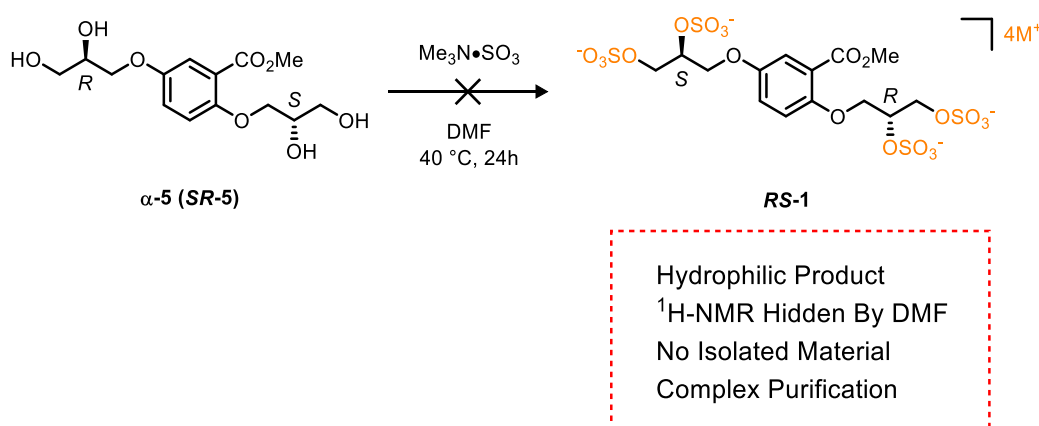
With **6** in hand, a tandem Sharpless asymmetric dihydroxylation was performed using ADmix α , affording the tetraol **α -5** in 99% yield. However, stereochemical assignment could not be established based on previous findings¹³⁴ and a closer inspection of the original literature highlighted a stereochemical abnormality, with the assignment of enantiomer **SR-5** (Scheme 3) as the major stereoisomer. The original assignments contradict the predicted stereochemical outcome of **RR-5** from the Sharpless mnemonic device (Scheme 3, B).



Scheme 3: The synthesis of **α -5**, **A**) The assigned stereochemical outcome from the original literature report by Raiber et. al.¹³⁴ **B**) The predicted stereochemical outcome from the Sharpless mnemonic device (Top left, this is discussed in Chapter 3).

The resulting stereochemistry could have implications to the biological activity of the final HS-glycomimetic **RS-1**. Therefore, this investigation sought to find the cause of this stereochemical abnormality, and measure the stereochemical outcome of the product tetraol (**α -5**) using high performance liquid chromatography on a chiral stationary phase. The full details of this investigation are discussed in Chapter 3.

The final sulfation of **α -5** (suspected to contain the enantiomer **SR-5**, Scheme 3, A), following the literature procedure, was met with significant challenges and no desired glycomimetic (**RS-1**) could be isolated (Scheme 4).¹³⁴



Scheme 4: The unsuccessful synthesis of **RS-1** following the literature procedure.¹³⁴ M⁺ = [Me₃NH] or H or Na.

Further attempts to synthesise **RS-1** using this methodology resulted in similar unsuccessful outcomes, and no crude product(s) could be isolated by liquid-liquid extraction or chromatography (SiO₂). Additional synthetic routes, using a variety of conditions and reagents, provided no worthwhile results, so this investigation sought to design a methodology for the sulfation of alcohols that permits the efficient synthesis, extraction and purification of small highly sulfated species, such as HS-glycomimetics **1-3**. The full details of this investigation are discussed in Chapter 4.

References

1. R. V. Iozzo, L. Schaefer, *Matrix Biol.*, 2015, **42**, 11 – 55
2. P. Chiodelli, A. Bugatti, C. Urbinati, M. Rusnati, *Molecules*, 2015, **20**, 6342 – 6388
3. D. Xu, J. D. Esko, *Annu. Rev. Biochem.*, 2014, **83**, 129 – 157
4. U. Lindahl, L. Kjellen, *J. Intern. Med.*, 2013, **273**, 555 – 571
5. V.H. Pomin, B. Mulloy, *Curr. Opin. Struct. Biol.*, 2015, **34**, 17 – 25
6. J. Maclean, *Am. Journ. Physiol.*, 1916, **41**, 250
7. J. Maclean, *Circulation*, 1959, **19**, 75 – 78
8. Unfractionated Heparin is the least processed form of the Heparin which is purified from the extracts of animal tissues, most commonly porcine (pig) intestines. Heparin Sodium, CAS: 9041-08-1, R. J. Linhardt, N. S. Gunay, *Semin. Thromb. Hemost.*, 1999, **25**, 5 – 16
9. J. T. Gallagher, A. Walker, *Biochem. J.*, 1985, **230**, 665 – 74
10. J.T. Gallagher, *Handbook of Experimental Pharmacology*, 2012, **207**, 347 – 360
11. <https://www.coherentmarketinsights.com/market-insight/heparin-market-2602>
12. S. R. Hanson, M. D. Best, C.-H. Wong, *Angew. Chem. Int. Ed.*, 2004, **43**, 5736 – 5763
13. E. Chapman, M. D. Best, S. R. Hanson, C.-H. Wong, *Angew. Chem. Int. Ed.*, 2004, **43**, 3526 – 3548
14. G. R. Hetzel, C. Sucker, *Nephrology Dialysis Transplantation*, 2005, **20**, 2036 – 2042
15. M. C. Z. Meneghetti, A. J. Hughes, T. R. Rudd, H. B. Nader, A. K. Powell, E. A. Yates, M. A. Lima. *J. R. Soc. Interface.*, 2015, **12**, 20150589
16. Thrombin is a small protein molecule and factor Xa is an enzyme that are both recruited in the coagulation cascade which leads to the formation of fibrin and the development of an insoluble blood clot. C. J. Pallister, M. S. Watson, *Haematology*, Scion publishing, 2010, 336 – 347
17. L. A. Linkins, *Brit. Med. J.*, 2015, **350**, 7566
18. HIT can also lead to autoimmunity and the formation of antibodies that activate platelets and lead to accelerated blood clot formation. H. Watson, S. Davidson & D. Keeling, *Br. J. Haematol.*, 2012, **159**, 528 – 540
19. A. Y. Szajek, E. Chess, K. Johansen, G. Gratzl, E. Gray, D. Keire, R. J. Linhardt, J. Liu, T. Morris, B. Mulloy, *Nat. Biotechnol.*, 2016, **34**, 625 – 630
20. A. Naggi, C. Gardini, G. Pedrinola, L. Mauri, E. Urso, A. Alekseeva, B. Casu, G. Cassin Elli, M. Guerrini, M. Iacomini, V. Baigorria, G. Torri, *J. Pharma. Biomed. Anal.*, 2016, **118**, 52 – 63,
21. D. A. Garcia, T. P. Baglin, J. I. Weitz, M. M. Samama, *Chest*, 2012, **141**, e24S – e43S
22. D. Vaidyanathan, A. Williams, J. S. Dordick, M. A. G. Koffas, R. J. Linhardt, *Bioeng. Transl. Med.*, 2017, **2**, 12 – 30

23. Protamine sulfate is commonly used for the treatment of Heparin overdose. J. M. Weiler, P. Freiman, M. D. Sharath, W. J. Metzger, J. M. Smith, H. B. Richerson, Z. K. Ballas, P. C. Halverson, D. J. Shulan, S. Matsuo, R. L. Wilson, *Journal of Allergy and Clinical Immunology*, 1985, **75**, 297 – 303
24. C. A. A. Van Boeckel, T. Beetz, J. N. Vos, A. J. M. de Jong, S. F. Van, A. elst, R. H. Van den Bosch, J. M. R. Mertens, F. A. Van der Vlugt, *J. Carbohydr. Chem.*, 1985, 293
25. F. Lin, G. Lian, Y. Zhou, *Carbohydr. Res.*, 2013, **371**, 32 – 39
26. C. H. Chang, L. S. Lico, T. Y. Huang, S. Y. Lin, C. L. Chang, S. D. Arco, *Angew. Chem. Int. Ed.*, 2014, **53**, 9876 – 9879
27. X. Dai, W. Liu, Q. hou, C. Cheng, C. Yang, S. Wang, M. Zhang, P. Tang, H. Song, D. Zhang, *J. Org. Chem.*, 2016, **81**, 162 – 184
28. T. Li, H. Ye, X. Cao, J. Wang, Y. Liu, L. Zhou, Q. Liu, W. Wang, J. Shen, W. Zhao, *ChemMedChem*, 2014, **9**, 1071 – 1080
29. A. Manikowski, E. Koziol, A. Czajkowska-Wojciechowska, *Carbohydr. Res.*, 2012, **361**, 155 – 161
30. M. Mende, C. Bednarek, M. Wawryszyn, P. Sauter, M. B. Biskup, U. Schepers, S. Brase, *Chem. Rev.*, 2016, **116**, 8193 – 8255
31. M. M. L. Zulueta, S. Y. Lin, Y. P. Hu, S. C. Hung, *Curr. Opin. Chem. Biol.*, 2013, **17**, 1023 – 1029
32. S. B. Dulaney, X. Huang, *Adv. Carbohydr. Chem. Biochem.*, 2012, **67**, 95 – 136
33. C. Gao, K. J. Edgar, *Biomacromolecules*, 2019 **20**, 608 – 617
34. S. U. Hansen, G. J. Miller, C. Cole, G. Rushton, E. Avizienyte, G. C. Jayson, J. M. Gardiner, *Nat. Commun.*, 2013, **4**, 2016 – 2020
35. G. J. Miller, S. U. Hansen, E. Avizienyte, G. Rushton, C. Cole, G. C. Jayson, J. M. Gardiner, *Chem. Sci.*, 2013, **4**, 3218 – 3222
36. S. U. Hansen, G. J. Miller, G. C. Jayson, J. M. Gardiner, *Org. Lett.*, 2013, **15**, 88 – 91
37. R. Schwörer, O. V. Zubkova, J. E. Turnbull, P. C. Tyler, *Chem. Eur. J.*, 2013, **19**, 6817 – 6823
38. G. C. Jayson, S. U. Hansen, G. J. Miller, C. L. Cole, G. Rushton, E. Avizienyte, J. M. Gardiner, *Chem. Commun.*, 2015, **51**, 13846 – 13849
39. E. Avizienyte, C. L. Cole, G. Rushton, G. J. Miller, A. Bugatti, M. Presta, J. M. Gardiner, G. C. Jayson, *PLoS ONE*, 2016, **11**, e0159739
40. S. U. Hansen, G. J. Miller, M. J. Cliff, G. C. Jayson, J. M. Gardiner, *Chem. Sci.*, 2015, **6**, 6158 – 6164
41. N. J. Pawar, L. Wang, T. Higo, C. Bhattacharya, P. K. Kancharla, F. Zhang, K. Baryal, C. Huo, J. Liu, R. J. Linhardt, X. Huang, L. C. Hsieh-Wilson, *Angew. Chem. Int. Ed.*, 2019, **58**, 2 – 9
42. H. E. Caputo, J. E. Straub, M. W. Grinstaff, *Chem. Soc. Rev.*, 2019, **48**, 2338 – 2365
43. L. S. Simpson, T. S. Widlanski, *J. Am. Chem. Soc.*, 2006, **128**, 1605 – 1610

44. S. Islam, D. M. Mate, R. Martínez, F. Jakob, U. Schwaneberg, *Biotechnology and Bioengineering*, 2018, **115**, 1106 – 1115.
45. D. Gorelik, Y. C. Lin, A. I. Briceno-Strocchia, M. S. Taylor, *J. Org. Chem.*, 2019, **84**, 900 – 908
46. T. Wang, L. Lui, J. Voglmeir, *Biochimica et Biophysica Acta*, 2020, **1868**, 140301
47. J. Liu, R. J. Linhardt, *Nat. Prod. Rep.*, 2014, **31**, 1676 – 1685
48. V. Dimakos, M. S. Taylor, *Chem. Rev.*, 2018, **118**, 11457 – 11517
49. S. Roy, A. El-Hadri, S. Richard, F. Denis, K. Holte, J. Duffner, F. Yu, Z. Galcheva-Gargova, I. Capila, B. Schultes, M. Petitou, G. V. Kaundinya, *J. Med. Chem.*, 2014, **57**, 4511 – 4520
50. Z. Wang, P.-H. Hsieh, Y. Xu, D. Thieker, E. J. En Chai, S. Xie, B. Cooley, R. J. Woods, L. Chi, and J. Liu, *J. Am. Chem. Soc.*, 2017, **139**, 5249 – 5256
51. W. Zhou, P. H. Hsieh, Y. Xu, T. R. O’Leary, X. Huang, J. Liu, *Chem. Commun.*, 2015, **51**, 11019 – 11021
52. B. Wu, N. Wei, V. Thon, M. Wei, Z. Yu, Y. Xu, X. Chen, J. Liu, P. G. Wang, T. Li, *Org. Biomol. Chem.*, 2015, **13**, 5098 – 5101
53. S. B. Dulaney, Y. Xu, P. Wang, G. Tiruchinapally, Z. Wang, J. Kathawa, M. H. El-Dakdouki, B. Yang, J. Liu, X. Huang, *J. Org. Chem.*, 2015, **80**, 12265 – 12279
54. Y. Xu, S. Masuko, M. Takieddin, H. Xu, R. Liu, J. Jing, S. A. Mousa, R. J. Linhardt, J. Liu, *Science*, 2012, **334**, 498 – 501
55. Y. Xu, C. Cai, K. Chandarajoti, P. H. Hsieh, L. Li, T. Q. Pham, E. M. Sparkenbaugh, J. Sheng, N. S. Key, R. Pawlinski, *Nat. Chem. Biol.*, 2014, **10**, 248 – 250
56. E. Esposito, I. Vlodavsky, U. Barash, G. Roscilli, F. M. Milazzo, G. Giannini, A. Naggi, *Eur. J. Med. Chem.*, 2020, 112221
57. C. Zong, A. Venot, O. Dhamale, G. J. Boon, *Org. Lett.*, 2013, **15**, 342 – 345
58. C. Cai, D. M. Dickinson, L. Li, S. Masuko, M. Suflita, V. Schultz, S. D. Nelson, U. Bhaskar, J. Liu, R. J. Linhardt, *Org. Lett.*, 2014, **16**, 2240 – 2243
59. H. E. Conrad, *Heparin-binding proteins*, 1998, Academic Press. 182 – 366
60. J. Taipale, L. Keski-Oja, *FASEB Journal*, 1997, **11**, 51 – 59
61. R. S. Boothello, A. Sarkar, V. M. Tran, T. K. N. Nguyen, N. V. Sankaranarayanan, A. Y. Mehta, A. Alabbas, S. Brown, A. Rossi, A. C. Joice, *ACS Chem. Biol.*, 2015, **10**, 1485 – 149
62. K. L. Stewart, E. Hughes, E. A. Yates, G. R. Akien, T. Y. Huang, M. A. Lima, T. R. Rudd, M. Guerrini, S. C. Hung, S. E. Radford, *J. Am. Chem. Soc.*, 2016, **138**, 8328 – 8331
63. C. Zong, R. Huang, E. Condac, Y. Chiu, W. Xiao, X. Li, W. Lu, M. Ishihara, S. Wang, A. Ramiah, *J. Am. Chem. Soc.*, 2016, **138**, 13059 – 13067
64. U. Lindahl, G. Bäckström; M. Höök; L. Thunberg; L. A. Fransson, A. Linker, *Proc. Natl. Acad. Sci.*, 1979, **76**, 3198 – 3202.
65. J. Kreuger, M. Salmivirta, L. Sturiale, G. Giménez-Gallego, U. Lindahl, *J. Biol. Chem.*, 2001, **276**, 30744 – 30752.
66. M. Maccarana, B. Casu, U. Lindahl, *J. Biol. Chem.*, 2003, **268**, 23898 – 23905

67. E. Feyzi, F. Lustig, G. Fagerm, D. Spillmann, U. Lindahl, M. Salmivirta, *J. Biol. Chem.*, 1997, **272**, 5518 – 524
68. S Ashikari, H. Habuchi, K. Kimata, *J. Biol. Chem.*, 1995, **270**, 29586 – 29593
69. C. J. Robinson, B. Mulloy, J. T. Gallagher, S. E. Stringer, *J. Biol. Chem.*, 2006, **281**, 1731 – 1740
70. D. Spillmann, A. Lookene, G. Olivecrona, *J. Biol. Chem.*, 2006, **281**, 23405 – 23413
71. J. Gallagher, *Int. J. Exp. Pathol.*, 2015, **96**, 203 – 231
72. U. Lindahl, J. P. Li, *Int. Rev. Cell. Mol. Biol.*, 2009, **267**, 105 – 159
73. Y. C. Li, I. H. Ho, C. C. Ku, Y. Q. Zhong, Y. P. Hu, Z. G. Chen, C. Y. Chen, W. C. Lin, M. M. L. Zulueta, S. C. Hung, M. G. Lin, C. C. Wang, C. D. Hsiao, *ACS Chem. Biol.*, 2014, **9**, 1712 – 1717
74. D. P. Mascotti, T. M. Lohman, *Biochem.*, 1995, **34**, 2908 – 2915
75. L. D. Thompson, M. W. Pantoliano, B. A. Springer, *Biochem.*, 1994, **33**, 3831 – 3840
76. M. Xie, J.-P. Li, *Cellular Signalling*, 2019, **54**, 115 – 121
77. R. Lever, C. P. Page, *Nat. Rev. Drug. Discov.*, 2002, **1**, 140 – 148
78. B. Ernst, J. L. Magnani, *Nat. Rev. Drug Discov.*, 2009, **8**, 661 – 677
79. E. M. Sanchez-Fernandez, J. M. Garcia Fernandez, C. O. Mellet, *Chem. Commun.*, 2016, **52**, 5497 – 5515
80. D. Rowlands, K. Sugahara, J. C. F. Kwok, *Molecules*, 2015, **20**, 3527 – 3548
81. I. Delso, J. Valero-Gonzales, E. Marca, T. Terejo, R. Hurtado-Guerrero, P. Marino, *Chem. Bio. Drug Desig.*, 2016, **87**, 163 – 170
82. P. Valverde, A. Arda, N.-C. Reichardt, J. Jimenez-Barbero, A. Gimeno, *Med. Chem. Commun.*, 2019, **10**, 1678 – 1691
83. M. Rawat, C. I. Gama, J. B. Matson, L. C. Hsieh-Wilson, *J. Am. Chem. Soc.*, 2008, **130**, 2959 – 2961
84. Y. Miura, T. Fukuda, H. Seto, Y. Hoshino, *Nat. Polym. J.*, 2016, **48**, 229 – 237
85. For a comprehensive review of glycomimetics covering a variety of diseases, pathological roles, designs and drug candidates, see: R. Hevey, *Pharmaceuticals*, 2019, **12**, 55
86. D. Astruc, E. Boisselier, C. Ornelas, *Chem. Rev.*, 2010, **110**, **4**, 1857 – 1959
87. C. Fasting, C. A. Schalley, M. Weber, O. Seitz, S. Hecht, B. Koksche, J. Darnedde, C. Graf, E.-W. Knapp, R. Haag, *Angew. Chem. Int. Ed.*, 2012, **51**, 10472 – 10498
88. P. C. Tyler, S. E. Guimond, J. E. Turnbull, O. V. Zubkova, *Angew. Chem. Int. Ed.*, 2015, **54**, 2718 – 2723
89. B. M. Sattelle, S. U. Hansen, J. Gardiner, A. Almond, *J. Am. Chem. Soc.*, 2010, **132**, 13132 – 13134
90. R. Novoa-Carballal, A. Carretero, R. Pacheco, R. L. Reis, I. Pashkuleva, *Chem. Eur. J.*, 2018, **24**, 14341. The extent of their glycodendrimer structures were calculated by isothermal titration calorimetry.
91. H. Türk, R. Haag, S. Alban, *Bioconj. Chem.*, 2004, **15**, 162

92. R. S. Cotran, V. Kumar and S. L. Robbins, *Robbins' pathologic basis of disease*, 5th Edition, W.B. Saunders, Philadelphia, 1994
93. M. M. Fuster, J. D. Esko, *Nat. Rev.*, 2005, **5**, 526 – 542
94. M. Calderón, M. A. Quadir, S. K. Sharma, R. Haag, *Adv. Mater.*, 2010, **22**, 190 – 218. For a similar report please see: S. M. Rele, W. Cui, L. Wang, S. Hou, G. Barr-Zarse, D. Tatton, Y. Gnanou, J. D. Esko, E. L. Chaikof, *J. Am. Chem. Soc.*, 2005, **127**, 10132 – 10133
95. M. Ferraro, K. Silberreis, E. Mohammadifar, F. Neumann, J. Dervede, R. Haag, *Biomacromolecules*, 2018, **19**, 4524 – 4533
96. S. Liekens, D. Leali, J. Neyts, R. Esnouf, M. Rusnati, P. Dell'Era, P. C. Maudgal, E. De Clercq, M. Presta, *Mol. Pharmacol.*, 1999, **56**, 204 – 213
97. S. Liekens, J. Neyts, B. Degreve; E. DeClercq, *Oncology Res.*, 1997, **9**, 173 – 181
98. N. Sangaj, P. Kyriakakis, D. Yang, C.-W. Chang, G. Arya, S. Varghese, *Biomacromolecules*, 2010, **11**, 3294 – 3300
99. F. El-Khadali, G. Hélyar, G. Pavon-Djavid, V. Migonney, *Biomacromolecules*, 2002, **3**, 51 – 56
100. S. J. Paluck, T. H. Nguyen, H. D. Maynard, *Biomacromolecules*, 2016, **17**, 3417 – 3440
101. L. Ma, B. H. Su, C. Cheng, Z. H. Yin, H. Qin, J. M. Zhao, S. D. Sun, C. S. J. Zhao, *J. Membr. Sci.*, 2014, **470**, 90 – 101
102. K. L. Christman, V. Vázquez-Dorbatt, E. Schopf, C. M. Kolodziej, R. C. Li, R. M. Broyer, Y. Chen, and H. D. Maynard, *J. Am. Chem. Soc.*, 2008, **130**, 16585 – 16591
103. C. Cheng, S. Sun, C. J. Zhao, *J. Mater. Chem. B*, 2014, **2**, 7649 – 767
104. Y. Miura, T. Fukuda, H. Seto, Y. Hoshino, *Polym. J.*, 2016, **48**, 229 – 237
105. Y. Miura, *Polym. J.*, 2012, **44**, 679 – 689
106. S. Salem, M. Müller, B. Torger, A. Janke, K. Eichhorn, B. Voit, D. Appelhans, *Macromol. Chem. Phys.*, 2015, **216**, 182 – 195
107. L. L. Kiessling, J. C. Grim, *Chem. Soc. Rev.*, 2013, **42**, 4476 – 4491
108. S. Richards, M. W. Jones, M. Hunaban, D. M. Haddleton, M. I. Gibson, *Angew. Chem.*, 2012, **124**, 7932 – 7936
109. G. J. Sheng, Y. Oh, S. Chang, L. C. Hsieh-Wilson, *J. Am. Chem. Soc.*, 2013, **135**, 10898 – 10901.
110. R. H. Grubbs, *Handbook of Metathesis*, Wiley-VCH, Weinheim, 2003
111. Y. I. Oh, G. J. Sheng, S. Chang, L. C. Hsieh-Wilson, *Angew. Chem. Int. Ed.*, 2013, **52**, 11796 – 11799.
112. G. J. Sheng, Y. I. Oh, S.-K. Chang, L. C. Hsieh-Wilson, *J. Am. Chem. Soc.*, 2013, **135**, 10898 – 10901
113. S. Mélik-Parsadaniantz, W. Rostène, *J. Neuroimmunol.*, 2008, **198**, 62 – 80
114. C. Gerard, B. J. Rollins, *Nat. Immunol.*, 2001, **2**, 108
115. R. S. Loka, E. T. Sletten, U. Barash, I. Vlodavsky, H. M. Nguyen, *ACS Applied Materials & Interfaces*, 2019, **11**, 244 – 254

116. P. Valverde, A. Ardá, N.-C. Reichardt, J. Jiménez-Barbero, A. Gimeno, *Med. Chem. Commun.*, 2019, **10**, 1678 – 1691
117. F. Nicotra, L. Cipolla, B. La Ferla, C. Airoidi, C. Zona, A. Orsato, N. Shaikh, L. Russo, *J. Biotechnol.*, 2009, **144**, 234 – 241
118. L. R. Prost, J. C. Grim, M. Tonelli, L. L. Kiessling, *ACS Chem. Biol.*, 2012, **7**, 1603 – 1608
119. P. A. Colinas, *Cur. Org. Chem.*, 2012, **16**, 1670
120. H. Goldner, *Advances in glycobiology offer researchers new drug leads*, 1994, **36**, 59
121. D. Lenci, R. Innocenti, A. Biagioni, G. Menchi, F. Bianchini, A. Trabocchi, *Molecules*, 2016, **21**, 1405
122. G. L. Patrick, *An Introduction to Drug Synthesis*, Oxford University press, 2015
123. H. Mehlhorn, *Encyclopedia of Parasitology: A-M*, Springer, 2016, 475
124. F. Manetti, V. Cappello, M. Botta, F. Corelli, N. Mongelli, D. Biasoli, A. L. Borgia, M. Ciomei, *Bioorg. Med. Chem.*, 1998, **6**, 947 – 958
125. L. Yadav, N. Puri, N. V. Rastogi, P. Satpute, V. Sharma, *J. Clin. Diagn. Res.*, 2015, **9**, XE01 – XE05
126. M. Nakajima, A. DeChavigny, C. E. Johnson, J. Hamada, C. A. Stein, G. L. Nicolson, *J. Biol. Chem.*, 1991, **266**, 9661 – 9666
127. L. Jia, S. Ma, *Eur. J. Med. Chem.*, 2016, **121**, 209 – 220
128. R. Rondanin, S. Fochi, R. Baruchello, T. Bernardi, P. Oliva, F. Semeraro, D. Simoni, G. Giannini, *Bioorg. Med. Chem. Lett.*, 2017, **27**, 4421 – 4425
129. J. Zhang, G. Rivers, Y. Zhu, A. Jacobson, J. Peyers, G. Grundstrom, P. Burch, S. Hussein, A. Marolewski, W. Herlihy, J. Rusche, *Bioorg. Med. Chem.*, 2001, **9**, 825 – 836
130. I. Ugi, R. Meyr, U. Fetzer, C. Steinbrückner, *Angew. Chem. Int. Ed.*, 1959, **71**, 386
131. L. Liu, C. Li, S. Cochran, S. Jimmink, V. Ferro, *ChemMedChem*, 2012, **7**, 1267 – 1275
132. H. C. Kolb, K. B. Sharpless, *Drug Discovery Today*, 2003, **8**, 1128 – 1137
133. H. Pommer, *Angew. Chem. Int. Ed.*, 1977, **89**, 437 – 443
134. E. A. Raiber, J. A. Wilkinson, F. Manetti, M. Botta, J. Deakin, J. Gallagher, M. Lyon, S. W. Ducki, *Bioorg. Med. Chem. Lett.*, 2007, **17**, 6321 – 6325
135. Z. Galzie, A. R. Kinsella, J. A. Smith, *Biochem. Cell Biol.*, 1997, **75**, 669
136. M. Lyon, J. A. Deakin, J. T. Gallagher, *J. Biol. Chem.*, 2002, **277**, 1040
137. J. A. Recio, G. Merlino, *Cancer Res.*, 2003, **63**, 1576 – 1582
138. E. Gherardi, M. E. Youles, R. N. Miguel, T. L. Blundell, L. Lamele, J. Gough, A. Bandyopadhyay, G. Hartmann, P. Jonathan, G. Butler, *Pro. Nat. Acad. Sci.*, 2003, **100**, 12039 – 12044
139. H. Sakata, S. J. Stahl, W. G. Taylor, J. M. Rosenberg, K. Sakaguchi, P. T. Wingfield, J. S. Rubin, *J. Biol. Chem.*, 1997, **272**, 9457 – 9463
140. J. A. Deakin, B. S. Blaum, J. T. Gallagher, D. Uhrin, M. Lyon, *J. Biol. Chem.*, **284**, 6311 – 6321

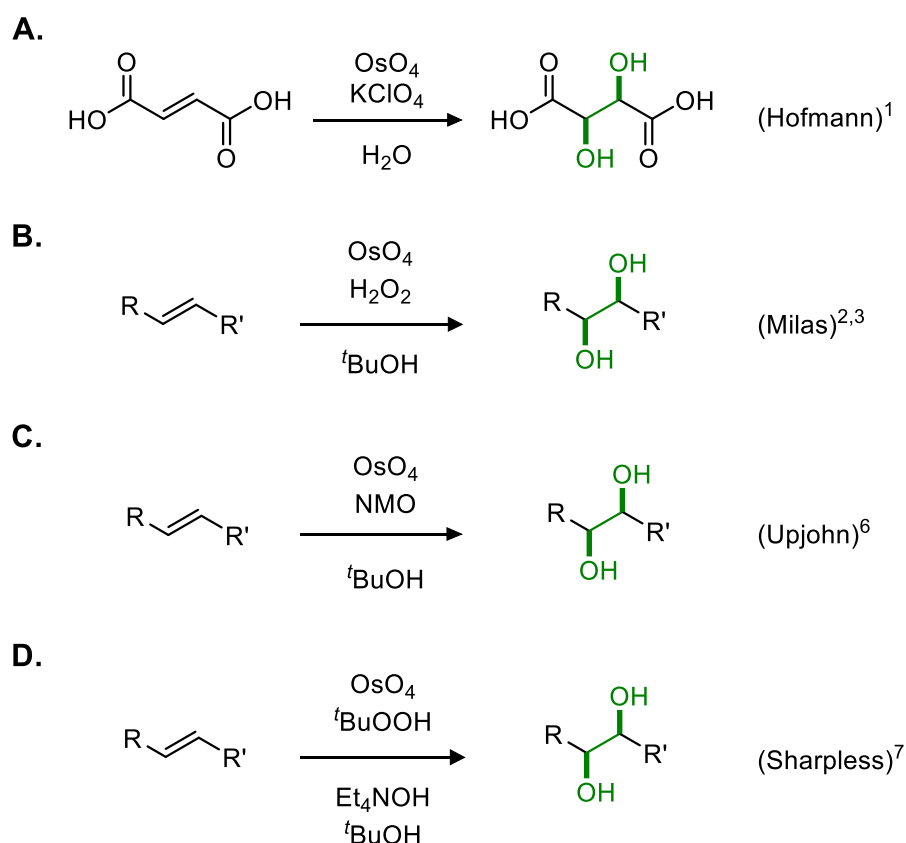
141. M. Deleheddedm, M. Lyon, R. Vidyasagar, T. J. McDonnell, D. G. Fernig, *J. Biol. Chem.*, 2002, **277**, 12456
142. K. Kato, R. Sakiyama, K. Oka, T. Nakamura, *J. Pharmacol. Pharmacother.*, 2015, **6**, 77 – 82
143. G. Pearson, F. Robinson, T. Beers Gibson, B. Xu, M. Karandikar, K. Berman, M. H. Cobb, *Endocrine Rev.*, 2001. **22**, 153 – 83
144. M. Stoker, *J. Cell. Physiol.*, 1989, **139**, 565
145. A. M. Mahmoud, F. L. Wilkinson, A. M. Jones, J. A. Wilkinson, M. Romero, J. Duarte, M. Y. Alexander, *Heart*, 2015, **101**, A41
146. F. L. Wilkinson, A. M. Mahmoud, A. M. Jones, J. A. Wilkinson, M. Romero, J. Duarte, M. Y. Alexander, *Heart*, 2016, **102**, A136
147. F. L. Wilkinson, A. M. Mahmoud, A. M. Jones, J. A. Wilkinson, M. Romero, J. Duarte, M. Y. Alexander, *Cardiovascular Research*, 2016, **101**, S65
148. A. W. W. Langford-Smith, A. Hasan, R. Weston, N. Edwards, A. M. Jones, A. J. M. Boulton, F. L. Bowling, S. T. Rashid, F. L. Wilkinson, M. Y. Alexander, *Sci. Rep.*, 2019, **9**, 2309
149. A. M. Mahmoud, F. L. Wilkinson, A. M. Jones, J. A. Wilkinson, M. Romero, J. Duarte, M. Y. Alexander, *Biochimica et Biophysica Acta (BBA) - General Subjects*, 2017, **1861**, 3311 – 3322,
150. G. P. Sidgwick, P. Walling, A. Shabbir, R. Weston, A. Schiro, F. Serracino-Inglott, A. M. Jones, M. Kamalov, M. A. Brimble, F. L. Wilkinson, M. Y. Alexander, *Heart*, 2016, **102**, A132
151. F. L. Wilkinson, G. P. Sidgwick, A. Shabbir, R. Weston, A. M. Jones, M. Y. Alexander, *Heart*, 2016, **102**, A11
152. G. P. Sidgwick, R. Weston, A. M. Jones, F. L. Wilkinson, M. Y. Alexander, *Heart*, 2017, **103**, A126
153. G. P. Sidgwick, R. Weston, A. M. Jones, F. L. Wilkinson, M. Y. Alexander, *J. Vasc. Res.*, 2017, **54**, 24
154. A. M. Mahmoud, A. M. Jones, G. P. Sidgwick, A. M. Arafat, F. L. Wilkinson, M. Y. Alexander, *Cell. Phys. Biochem.*, 2019, **53**, 323 – 336
155. R. Weston, A. W. W. Langford-Smith, A. Hasan, A. M. Jones, F. L. Wilkinson, A. Boulton, T. Rashid, M. Y. Alexander, *Diabetic Medicine*, 2017, **34**, 39 – 39

Chapter 3: An Investigation of Reverse Stereofacial Selectivity and Diastereodifferentiation in the Sharpless Asymmetric Dihydroxylation

Introduction

3.1. The Osmium Tetroxide Catalysed Dihydroxylation of Alkenes

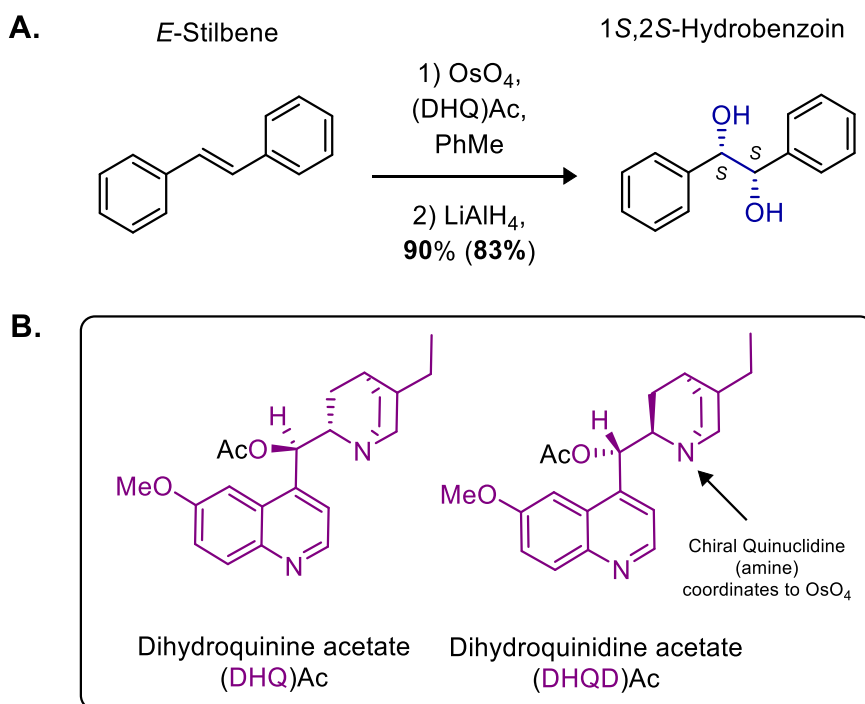
The osmium tetroxide (OsO_4) catalysed dihydroxylation of alkenes is a chemical transformation used for the synthesis of *syn*-1,2-diols. It was first reported by K. A. Hofmann¹ for the synthesis of (\pm)-tartaric acid (Scheme 5, A), initiating research into OsO_4 throughout the 20th century. Development of the Hofmann methodology established the Milas dihydroxylation² (Scheme 5, B), which requires marginally less catalytic quantities of OsO_4 that is regenerated by hydrogen peroxide as a stoichiometric co-oxidant.³ At the time, this process improved the safety and cost effectiveness of using OsO_4 , making it superior to alternate dihydroxylation methods using cheaper and less toxic reagents, such as potassium permanganate.⁴ However under the reactions highly oxidative conditions, free diols are prone to further oxidation leading to aldehyde and ketone by-products parallel to a Lemieux-Johnson oxidation.⁵ To resolve this, Van-Rheenen and co-workers developed their (Upjohn) dihydroxylation methodology⁶ with *N*-methylmorpholine-*N*-oxide (NMO, Scheme 5, C). This method permits the chemoselective synthesis of diols from alkenes under mild conditions, and with no generation of over-oxidation products. Additionally, the rate of dihydroxylation with OsO_4 accelerates in the presence of a coordinating amine ligand,⁸⁻⁹ thus the NMO serves a dual purpose as a secondary oxidant, and as an acceleratory ligand in its reduced form. Interestingly, K. B. Sharpless demonstrated an alternate dihydroxylation methodology⁷ using *tert*-butyl hydroperoxide as the oxidant (Scheme 5, D). However the Upjohn dihydroxylation method has a further advantage of a simpler work up procedure,⁶ so it is found to be a more attractive route for the preparation of *syn*-1,2-diols. Although, due to a lack of absolute stereocontrol, it was quickly surpassed by emerging asymmetric methodologies.



Scheme 5: A chronological history for the OsO₄ catalysed dihydroxylation of alkenes **A**) 1914, the Hofmann methodology for the synthesis of (±)-tartaric acid,¹ **B**) 1925, the Milas dihydroxylation,^{2,3} **C**) 1976, the Upjohn Dihydroxylation,⁶ **D**) 1976, the Sharpless dihydroxylation.⁷ R = H, Alkyl or Aryl; R' = CO₂R, Alkyl and Aryl.

3.2. Asymmetric Induction to Access Enantio-enriched Diols

Continuing with research into the OsO₄ catalysed dihydroxylation of alkenes, Sharpless and co-workers were among the first to pioneer the catalytic asymmetric dihydroxylation. Their seminal¹⁰ work investigated cinchona alkaloids derivatives: dihydroquinine acetate ((DHQ)Ac) and dihydroquinidine acetate ((DHQD)Ac) (Scheme 6, B), as OsO₄ coordinating chiral ligands. The results confirmed an ability to synthesise diols stereoselectively, but more importantly the stereochemistry of the resulting diol is directed by asymmetric induction from the ligand's point chirality. This is illustrated for the asymmetric dihydroxylation of *E*-stilbene using dihydroquinine acetate (DHQ)Ac (Scheme 6, A).¹⁰



Scheme 6: **A)** The asymmetric dihydroxylation of *E*-stilbene using cinchona alkaloid derived ligand (DHQ)Ac; **B)** The structures of the ligand and its pseudoenantiomer (DHQD)Ac. Adapted from K. B. Sharpless.¹⁰ %e.e in parenthesis. Note: For (DHQD)Ac, 1*R*,2*R*-Hydrobenzoin was obtained with **85%** yield (**82%**).

3.3. The Sharpless Asymmetric Dihydroxylation

Leading on from this discovery, work was undertaken to fully elucidate the Sharpless asymmetric dihydroxylation (AD) methodology: to confirm a reaction mechanism that is now accepted to be a [3 + 2] cycloaddition,¹¹⁻¹³ vary the reaction conditions¹⁴⁻¹⁵ and improve the ligand(s) to optimise stereoselectivity.¹⁶⁻¹⁸ This established a second generation (2nd) of ligands (PHAL, PYR and AQN, Figure 19, A) with the introduction of ADmix (α and β).¹⁹ ADmix is a purchasable pre-formulated mixture of $\text{K}_2\text{OsO}_2(\text{OH})_4$ (source of OsO_4), oxidant ($\text{K}_3\text{Fe}(\text{CN})_6$), base (K_2CO_3) and ligand ($(\text{DHQ})_2\text{PHAL}$ for ADmix α and $(\text{DHQD})_2\text{PHAL}$ for ADmix β (Figure 19, B). The commercialisation of the AD now makes the asymmetric synthesis of diols straightforward and practical, finding use in most areas of synthetic organic chemistry, such as in the synthesis of complex natural products.²⁰

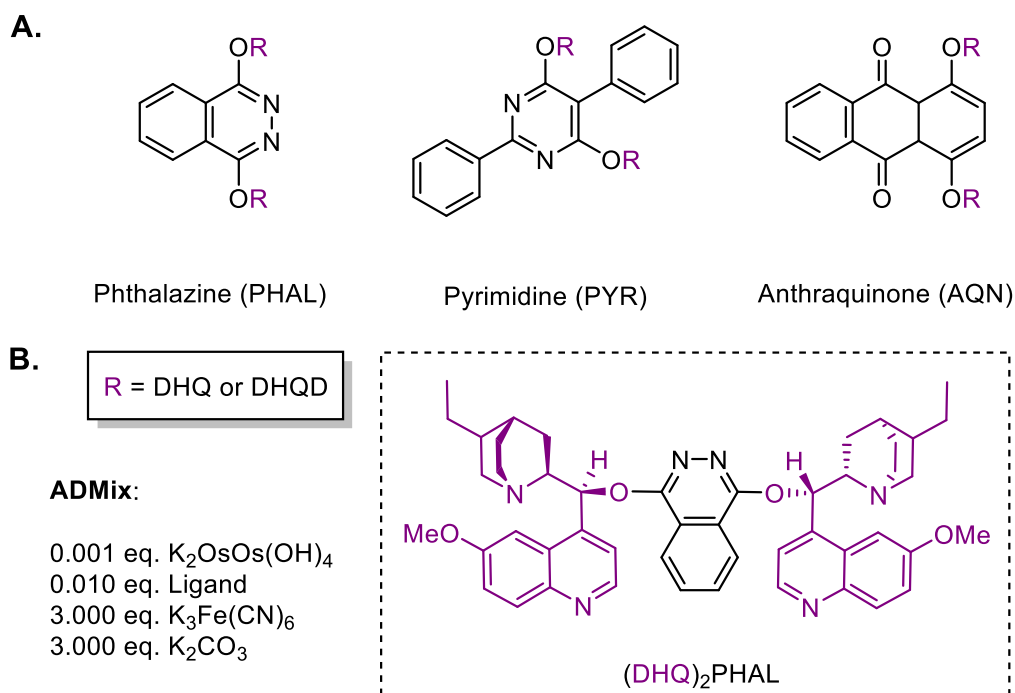


Figure 19: **A)** The 2nd generation of Sharpless ligands, PHAL, PYR and AQN **B)** The formulation recipe for ADMix based on molar equivalence (eq.) of each reagent, with the expanded structure of $(\text{DHQ})_2\text{PHAL}$ (used in ADMix a).

Through the competitive efforts of Sharpless and E. J. Corey, it was established that the 2nd generation ligands possess a 'binding pocket' that obeys enzyme-like kinetics,²¹ which commands the stereoselectivity and contributes to the observed 'ligand accelerated catalysis'.²²⁻²³ Interestingly, the use of the original alkaloids DHQ and DHQD has remained consistent throughout the development of the AD methodology. Therefore, it could be argued that nature made the AD possible, and without a natural source of chirality (*cinchona pubescens*) this Nobel Prize winning research may not have been uncovered.²⁴

A renowned feature of the AD is its mnemonic device: A semi-empirical guide designed to predict the stereochemical outcome of any given AD, based on relative sizes of an alkene's substituents and the chosen ligand.²⁵⁻²⁶ It is a map to the enantioselective synthesis of 1,2-diols, and is validated by the stereochemical outcomes of numerous AD reactions²⁷ (Figure 20).

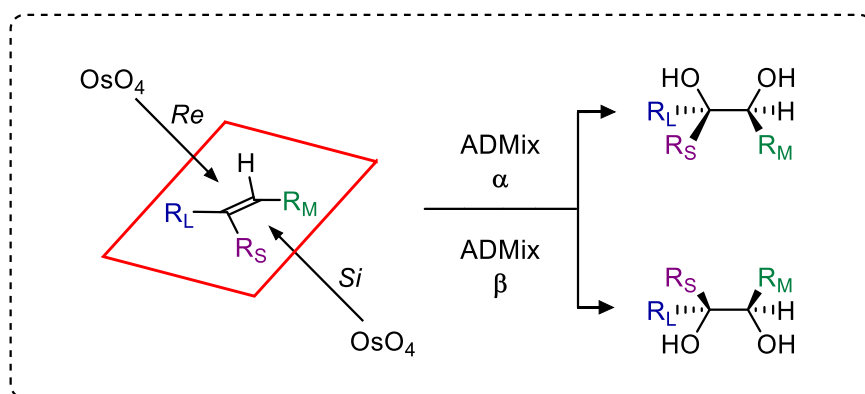
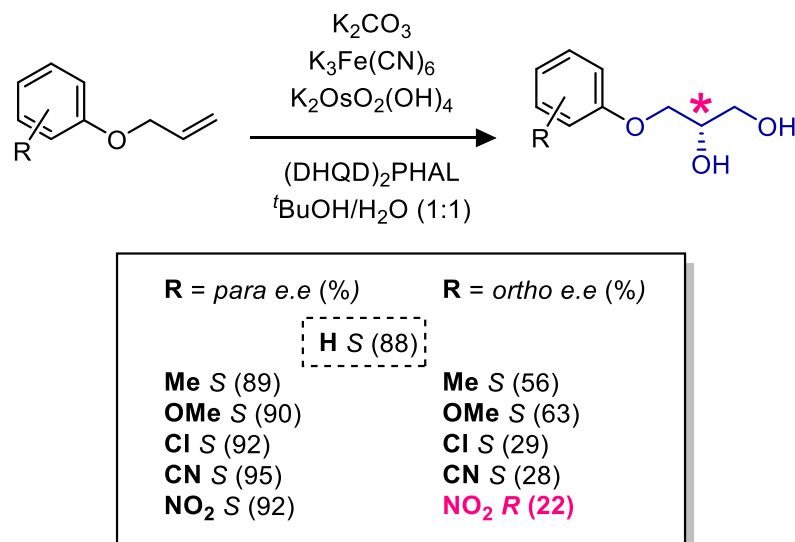


Figure 20: The Sharpless mnemonic device is used to predict the stereochemical outcome of a given AD based on the size and position of an alkene's substituents. R_L = Large substituent, R_M = Medium-sized substituent and R_S = Smallest substituent.

3.4. Steric Hindrance and Reverse Stereofacial Selectivity

In most cases the AD of alkenes proceeds in high yield and with good, predictable stereoselectivity.²⁷ However, asymmetric induction from the ligand is strongly influenced by steric hindrance in proximity to the reacting alkene and is known to diminish stereoselectivity. This is demonstrated in the AD of simple *ortho*- (*o*) and *para*- (*p*) substituted phenyl-allyl ethers (Scheme 7).²⁸ Additionally, sterically hindered alkenes can gain reversed stereoselection from an AD, synthesising diols that contradict the Sharpless mnemonic's predicted stereochemical outcome (Scheme 7).²⁹ Conversely, small and aliphatic alkenes (such as allyl chloride) are not affected by steric hindrance in an AD, but lack the sufficient size or structural differences to interact with the ligand(s) in a productive way. Therefore, asymmetric induction is weaker and diols were shown to be installed with little enantioselection. This encouraged the use of directing groups, such as *p*-methoxybenzoyl derivatives,³⁰ which are shown to be useful at promoting asymmetric induction to homoallylic alcohols and amines. However, a reacting functionality is required to install the directing group, which must be subsequently removed, thus prolonging the overall synthesis to the desired chiral diol. An improvement of specific ligands (PYR and AQN, Figure 19) finally corrected

this issue.³¹ However, the effects of proximal steric hindrance on stereoselectivity remains comparably overlooked, and no prior reports have suggested how asymmetric induction can be improved on sterically hindered alkenes.



Scheme 7: The AD of *ortho* and *para* substituted phenyl-allyl ethers. Displaying how changes in an alkene's proximal steric environment can diminish asymmetric induction, with an example demonstrating a reversal in stereofacial selectivity for an *o*-nitro derivative (pink).²⁸⁻²⁹

Interestingly, there are reports that demonstrate a reversed³²⁻³³ or identical enantioselectivity (using opposite ligands)³⁴⁻³⁵ in the AD, thus highlighting that the Sharpless mnemonic device cannot predict the correct stereochemical outcome for all alkenes. Notably, an explanation for this stereochemical inversion has not been settled, however, there are cases that capitalise on its effects, and use double diastereodifferentiation to install sequential chiral centers with an enhanced stereoselection (This is discussed further in Chapter 3.9.8).³⁶⁻³⁷

3.5. Two Models of Alkene-Ligand Binding

There are several hypotheses in the current literature to explain stereoselectivity in the AD. The most conceivable is that an alkene's largest substituents has the dominant interaction with the ligand's chiral 'binding pocket', and stabilises the transition state leading to a controlled stereofacial attack from OsO₄. Therefore, sterically hindered

structures destabilise the transition state, and directly affect asymmetric induction to the alkene. This proposes that stereoselectivity is dependent on the alkene's size and overall shape.^{25, 38} However, the competitive binding interactions of different substituents on a single alkene have been shown to invert stereoselectivity in different ligand classes.³⁹ Consequently, this means stereoselectivity is also ligand dependent, and is difficult to ascribe to a specific factor as all ligand(s) can tolerate large functionalities, such as adamantane.³⁹ Overall, divergent explanations for inhibited stereoselectivity, or reversed stereoselectivity, encouraged work on an alkene-ligand binding model,⁴⁰ and directed research into density functional theory, transition state calculations,⁴¹⁻⁴² and computational software to re-validate the mnemonic device.⁴³ This provided further tools to predict the stereochemical outcome from an AD, but did not provide a justification to the effects of steric hindrance. Overall, two major models of alkene-ligand binding were established, The Corey-Noe model (Figure 21, A) and the Sharpless model (Figure 21, B).^{21,38}

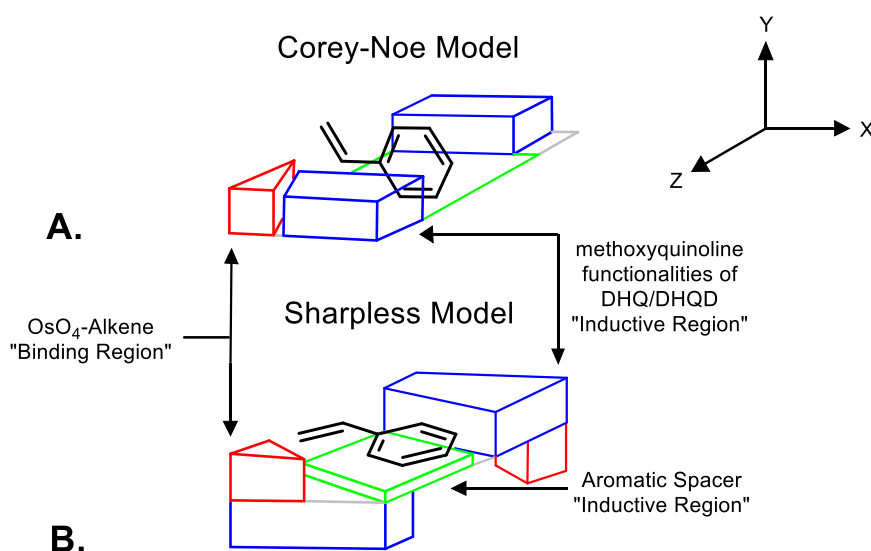


Figure 21: **A)** The Corey-Noe model- **B)** The Sharpless model of alkene-ligand binding, using styrene as the example alkene. **Blue:** Methoxyquinoline groups of DHQ/DHQD, **Red:** Alkene-OsO₄ binding region, OsO₄ is held by the ligand, **Green:** Aromatic spacer of the ligand e.g. phthalazine (Interactions are through VdW and π - π stacking).

The two binding models propose a comparably similar alkene-ligand binding pocket with two main differences: The positioning of the alkene's largest substituent changes by 90° around the X-axis, and the alkaloid components (Blue) reside in parallel or antiparallel conformation around the aromatic spacer (e.g. PHAL, Green).

Specifically, the Corey-Noe model proposes an alkene's largest substituent (for the example of styrene this is a benzene ring, Figure 21) interacts face on with two parallel methoxyquinolines (Figure 21, Blue), and edge on with the aromatic spacer (green) creating a 'U-shaped' binding pocket.²¹ The Sharpless model proposes that the methoxyquinolines are situated antiparallel (Blue), providing an edge on interaction with one methoxyquinoline group and a face on interaction with an "inductive" aromatic spacer, creating an 'L-shaped' binding pocket.³⁸ Remarkably, the dispute between the two binding models has not been settled and remains open to interpretation. Therefore, when discussing alkene-ligand binding both these models will be used to support explanations for the stereochemical results generated in this investigation.

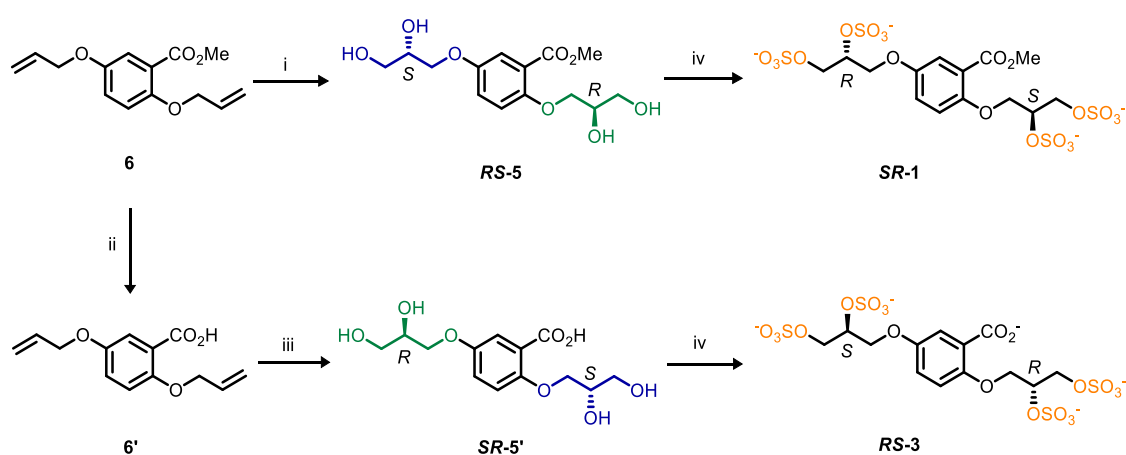
3.6. The Predictability of the AD on Dienes and Polyenes

A potential drawback to the mnemonic device is that it is designed around single AD examples, thus its validity is limited to singular dihydroxylation events ($n = 1$).²⁷ For dienes or poly-alkenes, sequential AD events ($n > 1$) are possible. Therefore, the mnemonic's stereochemical prediction is unsuitable as there is no prior predictability based on the alkene's structure, which is likely to change *in situ*. It has been demonstrated that certain hydroxyl (and amine) functionalities can irreversibly bind to the ligand and block the AD catalytic cycle.²¹ Therefore, if a diol is installed stereoselectively, it could inhibit sequential AD or block asymmetric induction to the vicinal alkene. Conversely, poly-alkenes (such as squalene) were used to investigate

chemoselectivity, and revealed that specific diols could be installed along its structure with good enantioselectivity.²⁷ The observed chemoselectivity is directed by differences in steric and electronic environments from neighbouring groups.²⁷ Therefore, for unsymmetrical, unconjugated dienes and poly-alkenes with similar steric environments, regioselectivity is unpredictable and the stereochemical predictions using the Sharpless mnemonic are not validated. Overall, each dihydroxylation of an $n > 1$ alkene is considered independently of the other, irrespective of reaction order and the different alkene environments only influence each other through sterics.

3.7. The Tandem AD with Conflicting Stereofacial Selectivity

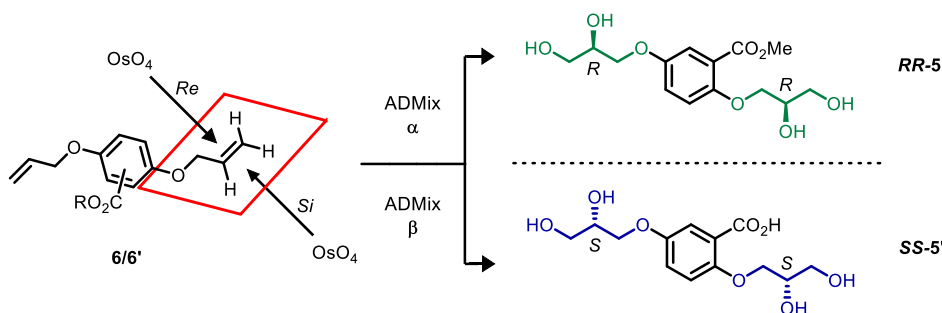
The Tandem AD ($n = 2$) of dienes finds a niche role in complex molecular synthesis, providing useful routes to polyketide structures found in a variety of natural products.⁴⁵⁻⁴⁷ Moreover, a tandem AD of dienes **6** and **6'** installs essential functionality and stereochemistry, which is essential to the structure of small, highly sulfated heparin glycomimetics.⁴⁸⁻⁵¹ (Scheme 8).



Scheme 8: The AD of dienes **6** and **6'** for the synthesis of HS-glycomimetics. Conditions: **i**) ADmix α , t BuOH/ H_2O (1:1), $MeSO_2NH_2$, $0^\circ C$, 12h; **ii**) KOH, MeOH; **iii**) ADmix β , t BuOH/ H_2O (1:1), $MeSO_2NH_2$, $0^\circ C$, 12h; **iv**) $Me_3N \cdot SO_3$, DMF, $40^\circ C$, 12 h. Adapted from Raiber et. al.⁵¹ Cations omitted for clarity.

The original report of the tandem AD⁵¹ states the stereochemical assignments of the resulting tetraols (**RS-5** & **SR-5'**) as single diastereomers (Scheme 4). Furthermore,

this assignment is conserved in all sequential reports of these glycomimetic compounds.⁴⁸⁻⁵⁰ The stereochemical assignments contradict the Sharpless mnemonic's stereochemical prediction for a tandem AD, which proposes an outcome of ***RR-5*** and ***SS-5'***, respectively (Scheme 9). Additionally, the 2-position alkene is sterically hindered by a vicinal methyl ester, therefore, based on previous results one would expect asymmetric induction to be inhibited to some extent (See Chapter 3.4). Therefore, if the original assignments are accurate the synthesis of tetraols ***RS-5*** and ***SR-5'*** are stereochemical abnormalities, and warrant further investigation into the causes of such unexpected results.



Scheme 9: The Sharpless mnemonic's prediction for the AD of dienes **6** and **6'** using ADMix α and β . R = Me, H.

3.8. An Investigation of the Tandem AD of Diene **6**

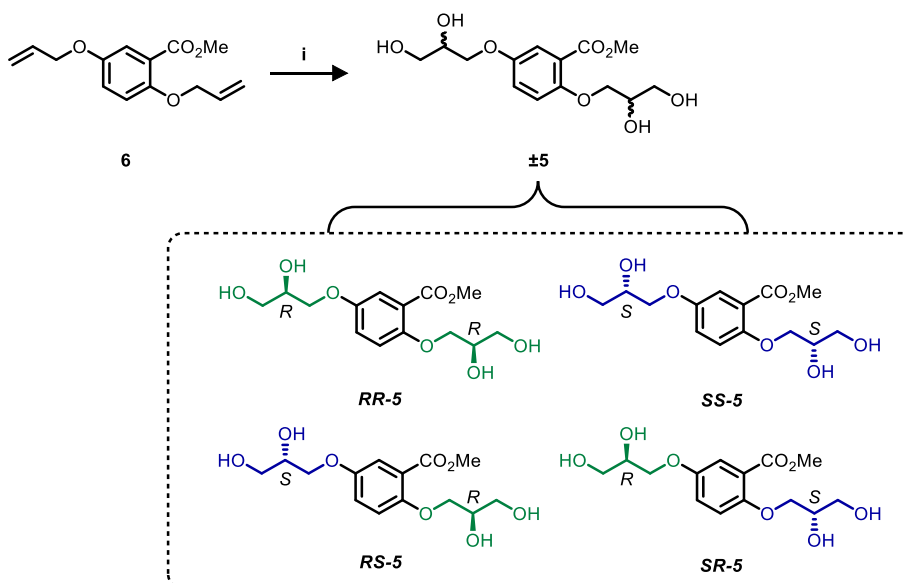
On closer inspection of the original report, it was discovered that the stereochemical configurations of the tetraols were never ascertained, and thus have remained conjectured for 12 years.⁴⁸⁻⁵¹ The true stereochemical assignments are important to a related medicinal chemistry investigation, and may have potential implications to the biological activity of their associated glycomimetics.⁵² Therefore, this investigation principally sought to improve upon previous research and assign the stereochemistry of the synthesised tetraols, using high performance liquid chromatography on a chiral stationary phase (chPLC). Further examinations of the AD provided valuable information on the factors that govern asymmetric induction and stereofacial selectivity

in the reaction. Moreover, the results provided novel insight into how these factors can be influenced to improve enantioselection in the AD of sterically blocked alkenes (*vide infra*). The details of these investigations are discussed in the upcoming chapter.

3.9. Results and Discussion

3.9.1. A chPLC method for Stereochemical Analysis

Firstly, the investigation sought to optimise a chPLC method to resolve the four stereochemical combinations that can be generated from a tandem AD of diene **6**.⁵³ The racemic standard used for the chPLC optimisation was synthesised by Upjohn dihydroxylation of **6**, affording the racemic tetraol **±5** in 95% yield (Scheme 10).

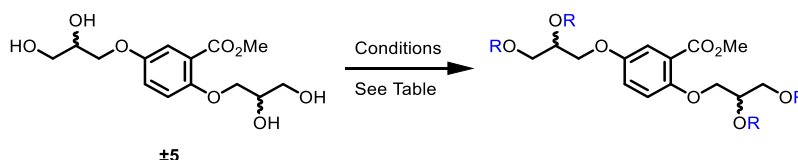


Scheme 10: The tandem dihydroxylation of diene **6** by Upjohn dihydroxylation. Tetraol **±5** contains all four enantiomers generated in the reaction. Conditions: $\text{OsO}_2(\text{OH})_4$, NMO, acetone/ H_2O , 40 °C, 12 h, **95%**.

A screening of tetraol **±5** was carried out on all chiral stationary phases provided by Phenomenex®.⁵⁴ A variety of normal and reverse phase conditions were investigated, however, **±5** was conclusively found to be a poor analyte, demonstrating no desired resolution of diastereoisomeric peaks, which was suspected to be caused by a collective polarity of the four hydroxyl groups.⁵⁵ Consequently, a derivatization of **±5** was proposed to facilitate chPLC analysis, thus a variety of protecting groups were

considered based on predicted Log P values (Table 3).⁵⁶ Modern chiral stationary phases contain hydrophobic functionalities, such as substituted aromatics or linear alkyl chains, which are functionalised onto a chiral support (e.g. cellulose and amylose sugars). Therefore, for effective resolution/chiral selection a degree of hydrophobicity is desirable from the analyte, to improve its affinity for the chiral stationary phase.⁵⁷ Overall, the calculated Log P values (Table 3) are a qualitative prediction of a compound's hydrophobicity used to deduce a suitable cHPLC derivative of **±5**.

Table 3: A comparison of hydroxyl protecting groups for the derivatization of tetraol **±5** to facilitate cHPLC analysis. Conditions: **i**) TMSCl, imidazole, DMF, RT, 4h, **0%**; **ii**) TBDMSCl, imidazole, DMF, RT, 4h, **57%**; **iii**) AcCl, pyridine, CH₂Cl₂, 0°C, 30 min, **99%**.



Entry	R	Conditions	cLog P	Compound No.
1	H	N/A	-1.2964	±5
2	Me	N/A	1.3684	N/A
3	TMS	i	7.3859	N/A
4	TBDMS	ii	12.333	±11
5	Ac	iii	2.1912	±12

By examining the predicted Log P values it became apparent why the parent tetraol **±5** was incompatible as an analyte (Table 3, Entry 1). **±5** is proposed to have a hydrophilic cLog P, thus a poor affinity for the hydrophobic chiral stationary phase.⁵⁵

The protecting groups (R) were exhaustively installed on all hydroxyl functionalities so reagents could be used in super-stoichiometric excess, thus permitting a faster synthesis and subsequent chPLC analysis. Furthermore, to determine if the installed stereocenters are susceptible to racemization under the reaction conditions, it was desirable to have removable protecting groups. Therefore, the tetrakis methyl ether (Table 3, Entry 2) was immediately considered unsuitable because it requires acidic reagents for its removal, such as boron tribromide or hydrobromic acid,⁵⁸ which may hydrolyse or decompose the parent tetraol **±5**. Conversely, the tetrakis trimethylsilyl derivative (TMS, Table 3, Entry 3) was found by experiment to be too unstable, and hydrolysed during purification creating a complex mixture of regioisomers that was not useful for chPLC analysis.

The *t*-butyl-dimethyl analogue (TBDMS, Table 3, Entry 4) was considered next because the increased steric bulk of the *t*-butyl group makes it less susceptible to hydrolysis.⁵⁸ silyl ether **±11** displayed greater stability during purification, however, it was also found to be a poor HPLC analyte, and eluted from the chiral stationary phase with no resolution of enantiomers. Furthermore, the longer reaction time (4 hours) and low isolated yield (57%) was sufficient evidence to stop the investigation of silyl protecting groups.

The use of tetrakis acetate **±12** by esterification with acetyl chloride (AcCl, Table 3, Entry 5) was predicted to have a positive Log P value making it markedly more lipophilic compared to **±5**. Furthermore, **±12** was afforded in 99% isolated yield, and displayed good stability during work up and purification. Additionally, the acyl groups are removable by basic hydrolysis (See Appendix, Chapter: 6.5). In a preliminary chPLC screening, per-acetate **±12** demonstrated good affinity for a selection of chiral stationary phases, and gave the best resolution from a Phenomenex[®] Cellulose-1

stationary phase operating in reverse phase conditions (MeCN/H₂O).⁵⁹ The cHPLC conditions were subsequently optimised with analyte **±12**, and adequate resolution of each enantiomer was obtained (Figure 22). Notably, the chiral stationary phase displayed a markedly greater affinity for one enantiomer compared to the other three, demonstrating a constructive chiral-chiral interaction that extends the retention time (R_t) by 25 minutes.

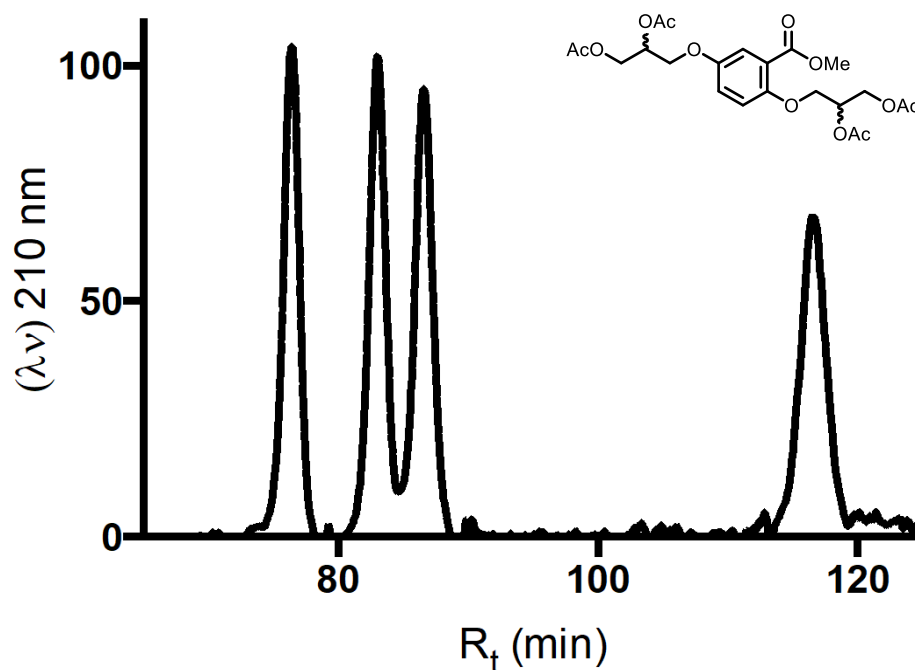
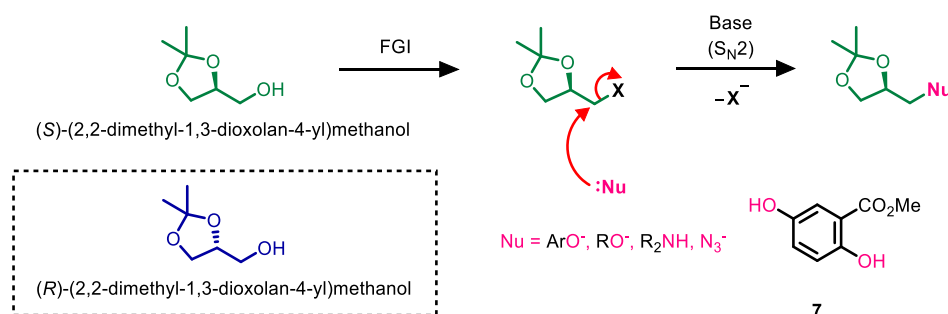


Figure 22: The cHPLC chromatogram of **±12** in the Phenomenex® Cellulose-1 stationary phase under optimised conditions operating in reverse phase: MeCN/H₂O 7:18, 1 mL min⁻¹.

3.9.2. A Chemoselective Chiral Pool Synthesis

The assignment of each peak in the ± 12 chPLC chromatogram (Figure 22) required a chiral standard for valid comparison, thus a potential synthesis of each enantiomer was investigated next.

To access each stereochemical combination, a stepwise synthetic method was envisioned that utilised (*R*)- and (*S*)-(2,2-Dimethyl-1,3-dioxolan-4-yl)methanol (Solketal, Scheme 11). Both enantiomers are available from Merck^{®60} and are known to undergo substitution at the free hydroxyl position (after functional group interconversion), leaving the acetal intact (Scheme 11).⁶¹⁻⁶⁵ Therefore, it was proposed that nucleophilic substitution (S_N2) with phenol **7** would install each asymmetric diol as the protected 2,2-dimethyl-1,3-dioxolane.



Scheme 11: The nucleophilic substitution of functionalised Solketal derivatives.⁶¹⁻⁶⁵

An enhanced chemoselectivity was observed for substitution of the *meta*- (*m*) over the *ortho*-phenol (*o*) of **7** under S_N2 conditions. Conversely, analysis of the ^1H -NMR spectra of **7** (in CDCl_3) demonstrated the *o*-phenolic proton to be deshielded, and is characterised by a singlet resonance peak at 10.34 ppm. Comparably, the *m*-phenolic proton is characterised as a singlet resonance peak at 4.66 ppm (Figure 23). Therefore, the *o*-phenolic proton is more acidic in character. Acidity is directly proportional to the stability of the corresponding anion in a given solution, thus the more acidic, stabilised *o*-phenoxide anion was suspected to be present in higher concentrations under basic

conditions.⁶⁶ However, the observed reactivity of substitution at the *m*-position is indicative of interactions from the methyl ester, which hinders the rate of substitution at the vicinal *o*-phenol. This can be purely deduced from an effect of steric hindrance, but it is likely further caused by an intramolecular hydrogen bond that stabilises the *o*-phenolic proton through resonance, thus effecting the S_N2 mechanism leading to the observed chemoselectivity (Figure 23).⁶⁷

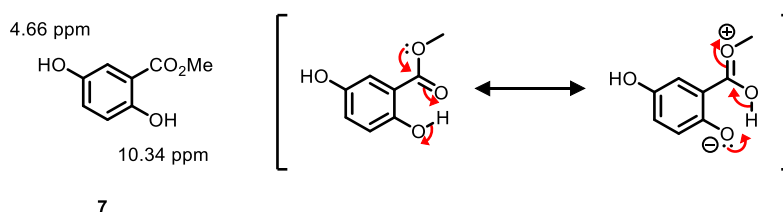
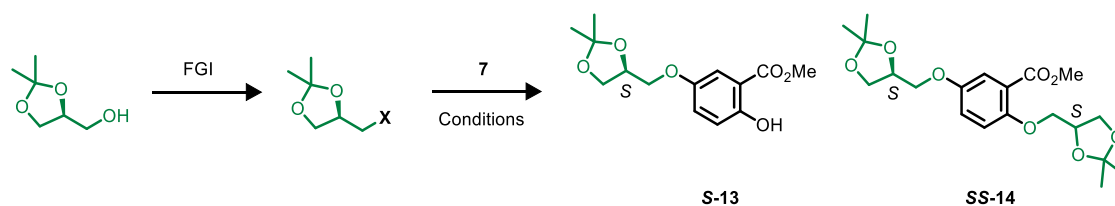


Figure 23: The observed ¹H-NMR resonance values for the *o*- and *m*- phenolic protons of **7** as a measure of acidity and relative pK_a values, with resonance structures illustrating intramolecular hydrogen bonding between the *o*-phenol and the methyl ester as reasoning behind the observed chemoselectivity under S_N2 conditions.⁶⁷

Overall, the observed nucleophilicity of **7** under S_N2 conditions gives a stepwise substitution of both reacting phenols. Therefore, the synthesis of acetal **S-13** and diacetal **SS-14** was anticipated with an electrophilic (*R*)-Solketal derivative (Table 4). Both acetals were required for the investigation, however the synthesis of **SS-14** was used to determine a viable synthetic route as substitution of the *o*-phenol was imperative.

A range of literature derived FGIs were carried out using an enantioenriched (*S*)-Solketal (98% *e.e*), and the electrophilic (*R*)-solketal derivatives were examined under a variety of S_N2 conditions with **7** (Table 4).

Table 4: Investigating the viability of different electrophilic (*R*)-Solketal derivatives in an S_N2 reaction with **7**. For all reactions the stoichiometry was 2:1 (Solketal:**7**) and all yields are as %; Conditions: **i**) K₂CO₃, TBAI, acetone, reflux; **ii**) NaH, TBAI, THF or DMF, 0 °C – RT; **iii**) K₂CO₃, DMF, 180 °C; **iv**) PPh₃, DEAD, PhMe, 90 °C, 12 h; **v**) K₂CO₃, MeCN (dry), reflux; **vi**) ^ausing a 2-fluoro-5-alkyloxy methyl benzoate derivative (**15**), NaH, DMSO, 100 °C.



Entry	FGI	Yield	X	Conditions	Yield S-13	Yield SS-14	Ref.
1	Appel Halogenation	14	Br	i	-	-	68
2	Halogenation	N/A	I	-	N/A	N/A	69
3	Tosylate	80	Ts	ii, iii	-	-	70
4	Mesylate	95	Ms	ii, iii	10*	-	70
5	Mitsunobu	N/A	[OPPh ₃] ⁺	iv	87	-	71
6	Triflate	97	Tf	v	45	29	72
7	Deprotonation	N/A	O ⁻	vi	N/A	28 ^a	73

Halogenation of (*S*)-Solketal via an Appel reaction using carbon tetrabromide afforded the (*R*)-Solketal bromide in 14% isolated yield.⁶⁸ The product was found to be a highly volatile oil that vaporised under reduced pressure, this created difficulties in its purification that likely contributed to the lack of a final material. Nonetheless, the reaction of the bromide with phenol **7** did not yield any substitution products (Table 4, Entry 1). It was speculated that the iodide derivative would be less volatile and would provide a simpler isolation.⁶⁹ However, all attempts to synthesise the alkyl iodide

did not afford any desired product⁷⁴ and the investigation of halide leaving groups was stopped.

The use of sulfonate esters was investigated next and the (*R*)-Solketal tosylate (OTs) was isolated in 80% yield.⁷⁰ The improved yield was attractive, however, similar to the bromide it did not afford any substitution products with phenol **7**, even under more forcing conditions (Table 4, Entry 3). A cause of the observed reactivity can be ascribed to steric hindrance from both the *p*-tosyl group and the 1,3-dioxolane ring. To investigate this, the mesylate (OMs) derivative was subsequently examined (Table 4, Entry 4) and was isolated in 95% yield.⁷⁰ Under forcing conditions, reaction of the (*R*)-Solketal-OMs afforded acetal **S-13** in 10% yield. The conditions were observed to be highly sensitive to water and likely hindered the reaction by unwanted hydrolysis of the OMs ester. Consequently, extra precautionary measures were taken to exclude water entirely from the reagents and the reaction vessel, however, under stringent anhydrous conditions, using a fresh bottle of anhydrous dimethylformamide (DMF), the reaction still proceeded to afford acetal **S-13** in low yield (15%). Notably, the OMs starting material was isolated (in 59% yield) from the reaction mixture, therefore, it was proposed that steric hindrance from the 1,3-dioxolane ring inhibits a productive S_N2 mechanism,⁷⁵ and the OTs and OMs esters lack sufficient bond polarisation at the electrophilic center to induce S_N2 with **7**, thus stronger electrophilic groups were investigated next.

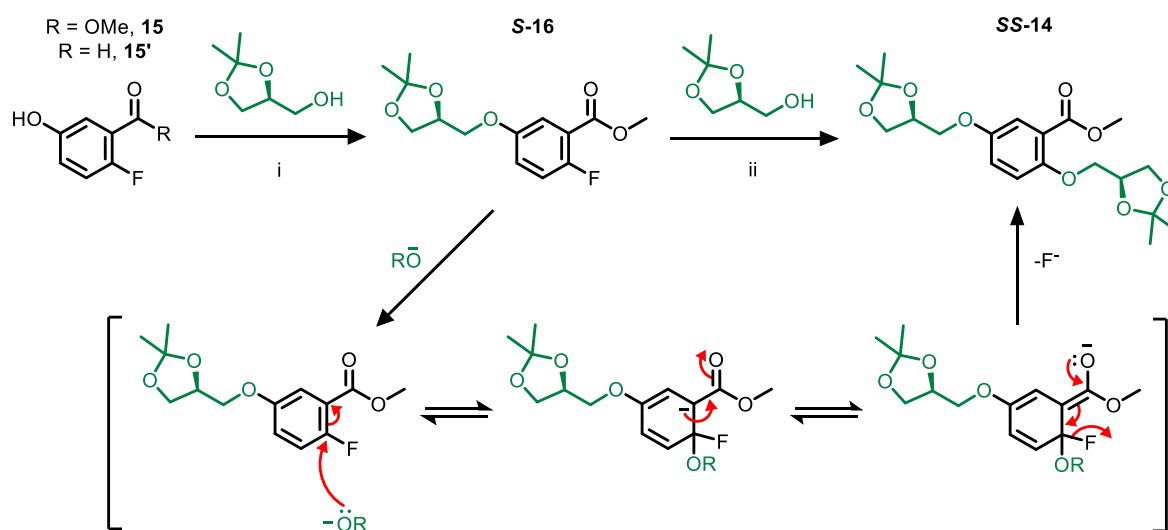
The Mitsunobu reaction was considered due to a one-pot procedure that permits no prior FGI of the (*S*)-Solketal (Table 4, Entry 5). Moreover, the highly electrophilic oxyphosphonium species was proposed to improve the S_N2 reaction, as substitution is thermodynamically driven by the resulting energy output from the P=O bond.⁷⁶ This method was found to be optimal for substitution of the *m*-phenol, giving an 87%

isolated yield of **S-13**.⁷¹ However, substitution of the *o*-phenol was never observed, again, this can be attributed to steric hindrance caused by the vicinal methyl ester. A Mitsunobu mediated S_N2 of sterically hindered phenols was successfully demonstrated using a saturated solution of reactants in an ultrasonic bath.⁷⁷ However, adapting the known procedure using **7** and (*S*)-Solketal synthesised acetal **S-13** exclusively, in 56% yield. Additionally, exchanging the starting phenol **7** for **S-13** gave no observable production of **SS-14**, and the larger concentration of by-products (triphenylphosphine oxide) complicated subsequent work up procedures and purification. A modern innovation of the Mitsunobu reaction uses a phosphine oxide nucleophilic catalyst, which significantly reduces waste and simplifies the purification of final products.⁷⁸ Unfortunately, this work was described after the initial investigation, and further use of the Mitsunobu reaction was stopped. However, the high yielding method to acetal **S-13** was a useful discovery and was kept for later use.

Trifluoromethane sulfonate (Tf) esters are known to be highly reactive intermediates,⁷² and it was anticipated that an (*R*)-Solketal-OTf would perform well under S_N2 conditions with phenol **7**. The results of an initial screening were pleasing (Table 4, Entry 6): The (*R*)-Solketal-OTf was synthesised from (*S*)-Solketal in 97% yield, and under mild S_N2 conditions afforded acetals **S-13** and **SS-14** in 45% and 29% isolated yield, respectively.

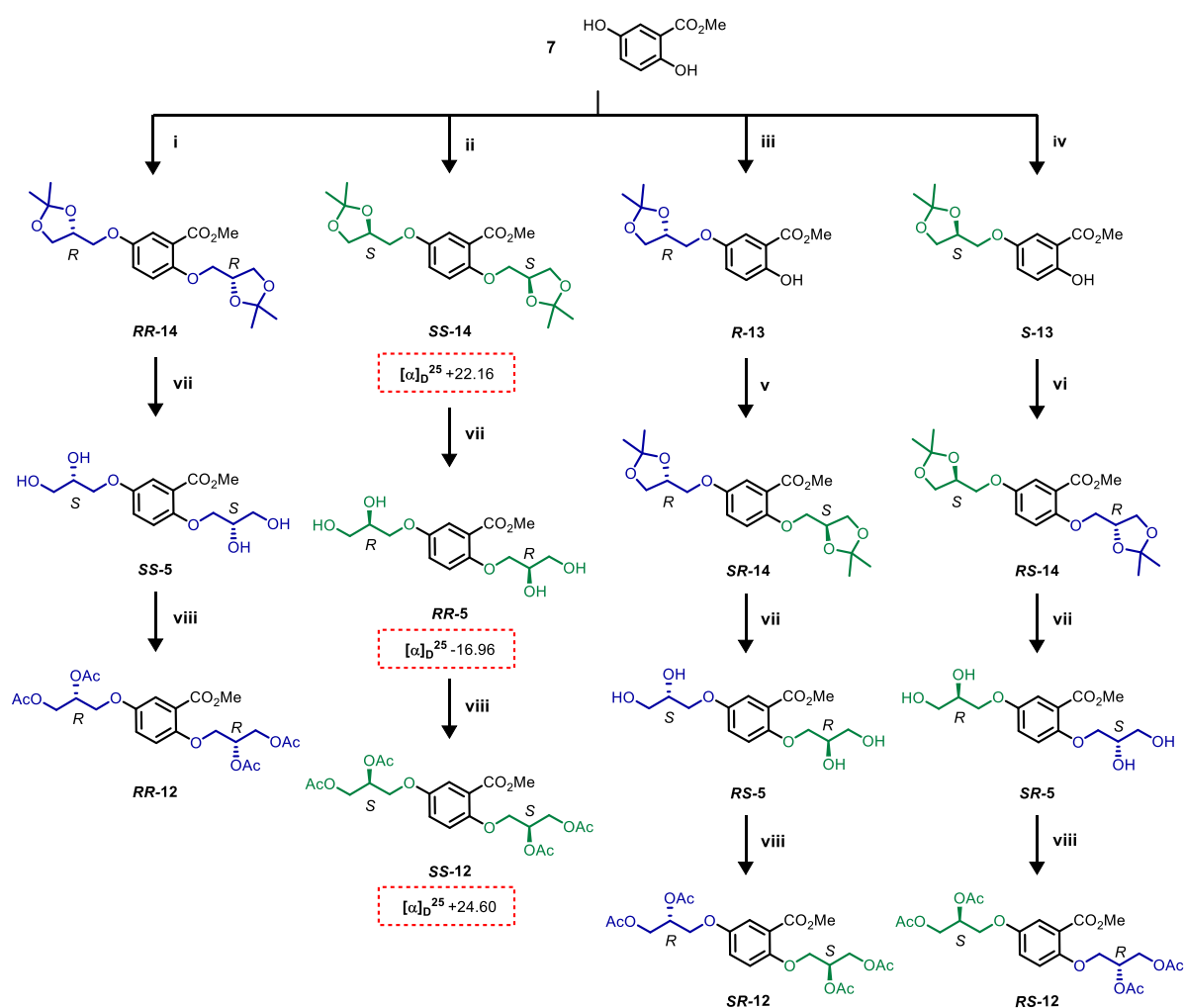
In summary, the use of Solketal-OTf esters were the chosen method for the chiral pool derived alkylation of **7** and are discussed in the next chapter. However, in the process of exploring alternate reaction pathways, the nucleophilic aromatic substitution (S_NAr) was also considered (Scheme 12). Experiments using the 2-fluoromethyl benzoate ester **16** with a (*S*)-Solketal alkoxide were carried out to examine if swapping the reactivity of both components was a viable route to access acetal **SS-14**.⁷³

The acetal **16** was obtained from phenol **15** in 90% isolated yield using the previously discussed Mitsunobu conditions (Table 4, Entry 5). The S_NAr of **16** with the (*S*)-Solketal alkoxide (generated *in situ* with NaH) afforded acetal **SS-14** in 28% yield (Table 4, Entry 7). The preliminary results of this method were promising, however, the high temperature conditions (Scheme 12) generated a major transesterification by-product that reduced the overall yield of the desired acetal **SS-14**.⁷⁹ R. Grubbs and Co-workers described a similar methodology, which stops unwanted side reaction using a *t*-butyl imine as a masked aldehyde.⁸⁰ Remarkably, S_NAr with a variety of alkoxide nucleophiles was shown to proceed in high yield. However, attempts to adapt this procedure on aldehyde **15'** (Scheme 12) did not afford any desired material, thus the reaction was not pursued further. Overall, the S_NAr approach was successfully demonstrated for the synthesis of diacetal **SS-14**, making it an interesting alternative, but significant by-products stopped any further investigation.



Scheme 12: The alternate synthesis of **SS-14** by S_NAr of **16** with (*S*)-Solketal alkoxide. Conditions: **i**) Ph_3P , DEAD, PhMe, 90 °C, 12 h, 90%; **ii**) NaH, DMSO, 100 °C, 1 h, 28%.

3.9.3. A Chiral Pool Synthesis using Solketal Triflates



Scheme 13: The chiral pool synthesis of acetates (**12**) for their use as chPLC chiral standards. Conditions: **i**) (*S*)-Solketal-OTf (3.0 eq.), K₂CO₃ (2.0 eq.), MeCN, 82 °C, 12 h, **33%**; **ii**) (*R*)-Solketal-OTf (3.0 eq.), K₂CO₃ (2.0 eq.), MeCN, 82 °C, 12 h, **38%**; **iii**) (*S*)-Solketal-OTf (1.5 eq.), K₂CO₃ (2.0 eq.), MeCN, 82 °C, 12 h, **82%**; **iv**) (*R*)-Solketal-OTf (1.5 eq.), K₂CO₃ (2.0 eq.), MeCN, 82 °C, 12 h, **82%**; **v**) (*R*)-Solketal-OTf (1.5 eq.), K₂CO₃ (2.0 eq.), MeCN, 82 °C, 12 h, **40%**; **vi**) (*S*)-Solketal-OTf (1.5 eq.), K₂CO₃ (2.0 eq.), MeCN, 82 °C, 12 h, **43%**. **vii**) TFA, MeOH, 40 °C, **90-96%** **viii**) AcCl, Py, CH₂Cl₂, 0 °C, **95-99%**.

The tandem S_N2 conditions using (*R*)- and (*S*)-Solketal-OTf, permitted a one-pot synthesis to enantiomers **RR-14** and **SS-14** in 33% and 38% yield, respectively. Using a reduced stoichiometry of both triflate esters, enantiomers **S-13** and **R-13** were afforded in 82% yield for both. Phenols **R-13** and **S-13** were subjected to further substitution afforded the enantiomers **SR-14** and **RS-14** in 40% and 43% yield, respectively (Scheme 13).

The absolute stereochemical configurations of acetals ***RR*-14**, ***SS*-14**, ***SR*-14** and ***RS*-14** were confirmed by small molecule single crystal X-ray crystallography (solved by Dr Louise Male, see Chapter 6: Appendix), and were found to be in agreement with the assigned stereochemistry of the originally purchased Solketals.⁸ Acid catalysed hydrolysis of the acetals (**14**) afforded their corresponding tetraols (**5**) in high isolated yields (90-96%). Subsequent acylation of each tetraol (**5**) to the corresponding tetrakis acetates (**12**) was achieved in high yields (95-99%) (Scheme 13).

The ¹H- and ¹³C-NMR spectra of each diastereoisomer for acetals (**14**), tetraols (**5**) and tetrakis acetates (**12**) were indistinguishable.⁸² Notably, an average melting point increase of 19 °C was demonstrated by the ***RS*-14** and ***SR*-14** enantiomers (M.P 85.5 °C), compared to the ***RR*-14** and ***SS*-14** enantiomers (M.P 66.5 °C). Contrast of the specific rotations for all examples were in agreement with the assigned stereochemistry. However, a reversal of *Laevorotary* and *Dextrorotary* rotation was witnessed twice: after the hydrolysis of **14** to the tetraols **5**, and again after subsequent acylation to **12** (Scheme 13, Red).

Interestingly, due to group priority changes around the stereocenter, the Cahn-Ingold-Prelog (CIP) rules invert the *R* and *S* assignments of each sequential intermediate in the synthesis.⁸³ Therefore, even though the configuration doesn't change, an opposite assignment is given to its product that is coincidentally in agreement with the specific rotational changes in polarised light (Scheme 13, Red).

From the cHPLC chromatograms of the enantiopure tetrakis acetates (**12**) it was possible to elucidate the chromatogram of \pm **5** (Figure 24). Due to the aforementioned group priority changes the readout of retention times (R_t) relating to the tetraols (**5**) is proposed to be in the order of: **SS-5**, **RS-5**, **SR-5** and **RR-5**. All stereochemical analysis will be presented for the CIP rules relevant to the free tetraols (and diols), and not as their corresponding acetates (**12**). This is a more direct observation of stereochemistry (See appendix).

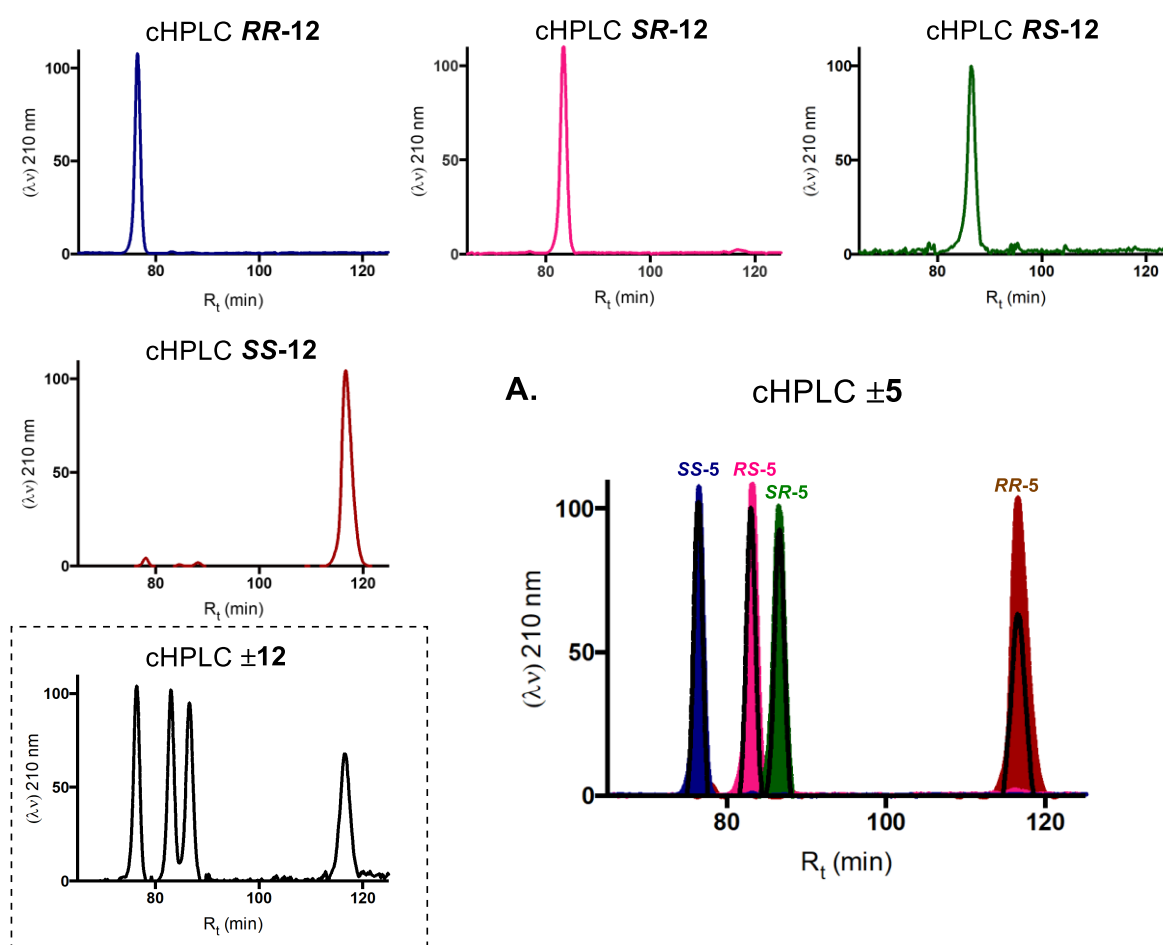


Figure 24: The cHPLC chromatograms of acetates **RR-12**, **SR-12**, **RS-12** and **SS-12** in the Phenomenex® Cellulose-1 stationary phase. **A)** Overlay of each cHPLC chromatogram displaying the proposed readout relating to tetraol \pm **5**. HPLC Conditions: Cullulose-1®, MeCN/H₂O 7:18, 1 mL min⁻¹.

3.9.4. The Tandem AD of Diene **6**

The previously reported tandem AD of diene **6** using ADMix α , and **6'** Using ADMix β , reported a stereochemical outcome of tetraols **RS-5** and **SR-5'**, respectively (See Chapter 3.7).⁵¹ A tandem AD was carried out using diene **6** following the literature procedure,¹⁹ and afforded tetraols **α -5** and **β -5** in high isolated yields (99%, Figure 25). The use of diene **6** is a more direct evaluation of the ligands (DHQ)₂PHAL and (DHQD)₂PHAL. Furthermore, dienes **6** and **6'** are closely matched in structure, thus analogous conclusions can be drawn for both based on the results of diene **6**, eliminating the requirement of a separate cHPLC investigation.⁸⁴

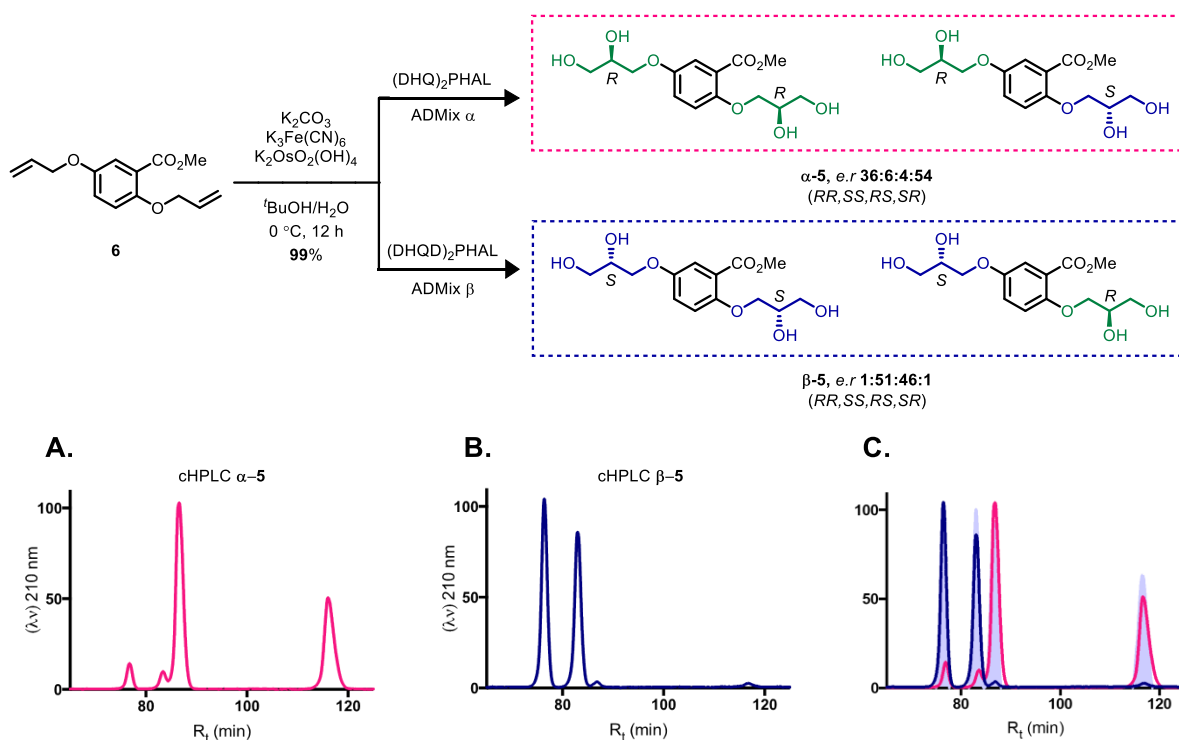


Figure 25: The synthesis of **α -5** and **β -5** from the tandem AD of diene **6**; **(A & B)** The stereochemical outcomes of tetraols **α -5** and **β -5**, calculated from the cHPLC chromatograms of their corresponding tetrakis acetates. **(C)** Overlay of the cHPLC chromatograms demonstrating a reversed stereoselectivity from both conditions.

The stereochemical analysis of tetraols **α -5** and **β -5** confirmed an opposing enantiomeric mixture is obtained under both sets of conditions (Figure 25). Therefore, the originally reported stereochemical assignments are incorrect.⁵¹ The cause of

observed stereoisomerisation is attributed to the diol synthesised at the α -position, which, is installed with poor enantioselectivity from either ligand, agreeing with previous reports.²⁸ Conversely, The diol installed at the m -position was synthesised with good enantioselectivity (*e.r* 90:10 – 2:98 (*R,S*)) and the resulting stereocenters are in accordance with the Sharpless mnemonic's prediction. Tetraol **a-5** is shown to contain enantiomer **SR-5** as the major stereoisomer, demonstrating a conflicting stereochemical inversion that is not in agreement with the Sharpless mnemonic device (This is discussed further in Chapter 3.9.6). Overall, the results of the chPLC investigation provide evidence of a previous misassignment of stereochemistry that has now been corrected.

3.9.5. Confirming the Cause of Diastereoisomerisation

It was proposed that the resultant stereochemical mixtures, found in tetraols **a-5** and **β -5**, are caused by steric hindrance from the vicinal methyl ester.²⁸⁻²⁹ To confirm this hypothesis, a study examining the different steric and electronic environments of diene **6** was designed. Alkenes **17** and **19** (Figure 26) were used as model substrates to examine the different steric environments of diene **6**, with the addition of a *para* (*p*) regioisomer **18** to assess any changes in the electronic environment. Overall, this study was used to confirm the behaviours of the two alkene environments towards the AD ligands (ADMix α and β).

All model alkenes (**17-19**) were synthesised from their corresponding methyl hydroxybenzoates ($n = 2 - 4$) using the hitherto mentioned S_N2 reaction with allyl bromide, which afforded the allyloxy benzoates in 80 – 94% isolated yields (See Chapter 6.6). The chPLC results of alkene **17** displayed good enantioselectivity under α and β conditions. Diols **a-20** and **β -20** were synthesised (*e.r* ADMix $\alpha = 93:7$ & *e.r*

ADmix $\beta = 3:97$ (*R,S*), Figure 26) and the installed stereocenters are in agreement with the previous AD results of diene **6**.

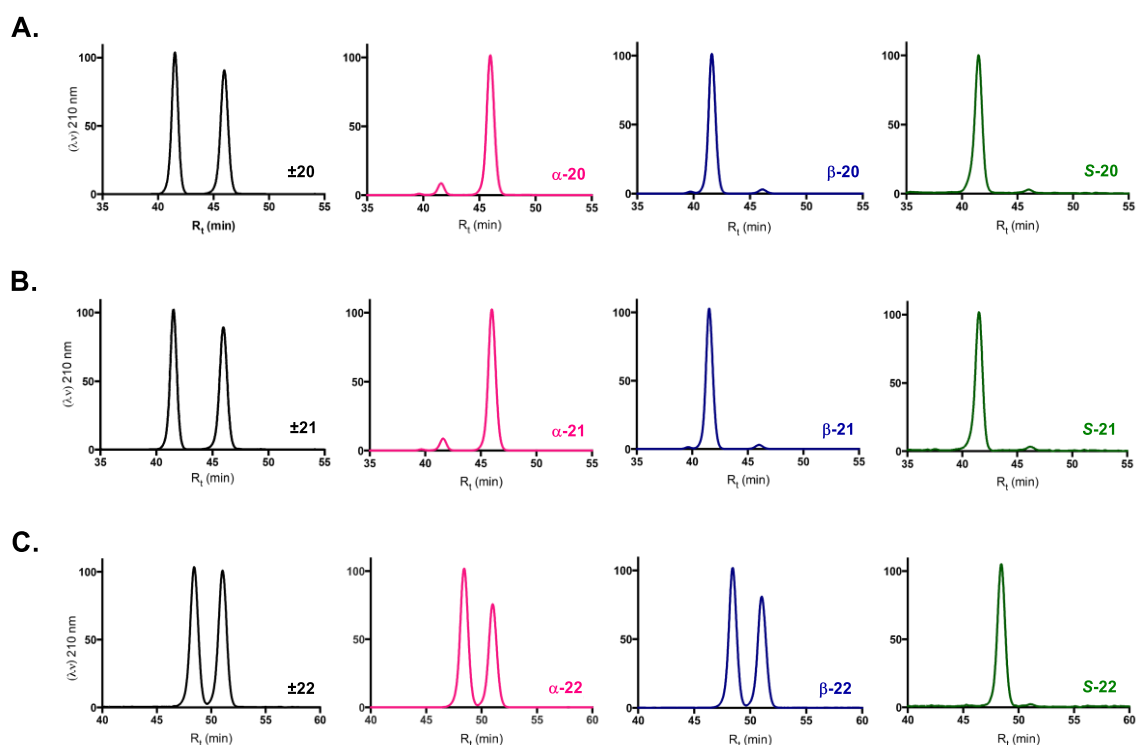
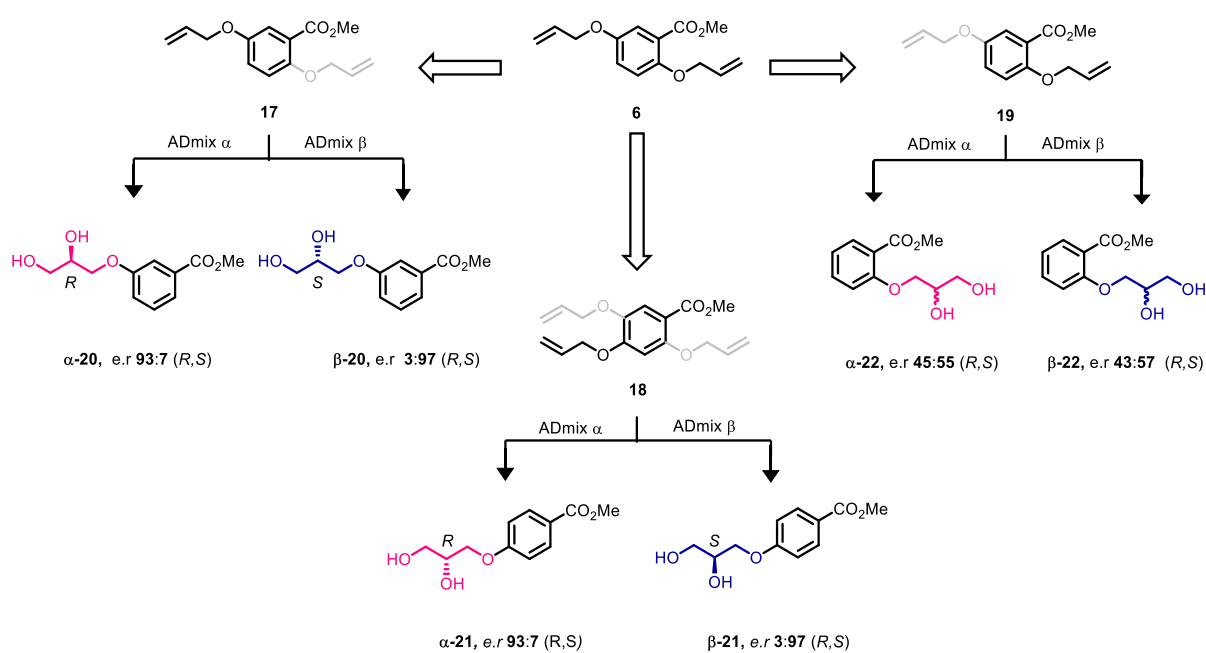


Figure 26: The AD of mono-alkenes related to diene **6**, caculated from the cHPLC chromatograms of the product diols as their diacetate esters. **A)** AD of alkene **17**; **B)** AD of Alkene **18**; **C)** AD of Alkene **19**. Chromatograms of chiral pool derived standards are given in green.

Interestingly, diols **α-21** and **β-21**, synthesised from alkene **18**, displayed matching enantioselectivity (*e.r* ADmix α = 93:7 & *e.r* ADmix β = 3:97 (*R,S*), Figure 26), therefore steric hindrance from the methyl ester has minimal effect on asymmetric induction at the *m*-alkene. Conversely, the chPLC results of diols **α-22** and **β-22**, from the AD of alkene **19**, displayed very poor enantioselectivity under α and β conditions (*e.r* ADmix α = 43:57 & *e.r* ADmix β = 45:55 (*R,S*), Figure 26). The high isolated yields (93 – 99%) and similar reaction times (within 6 h at 0 °C) for all substrates are indicative of ligand accelerated catalysis.²²⁻²³ Therefore, the lack of enantioselectivity for the AD of alkene **19** is ascribed to steric hindrance from the methyl ester, and is speculated to destabilise the transition state of the alkene-ligand complex, thus preventing successful asymmetric induction from the Sharpless ligands. Furthermore, the results from the AD of alkenes **17** and **18** confirm that changes in electronic environments are not significant to stereoselectivity in the AD.

The experimental results favour the Sharpless model of alkene-ligand binding (see Chapter 3.5), as a more prominent destabilising interaction is facilitated by an edge-on steric clash from the methyl ester, with the face of the methoxyquinoline group in the L-shaped binding pocket (Figure 27, B).³⁸ Furthermore, extrapolation of the Corey-Noe model suggests that the methyl ester can orientate outside the proposed binding pocket and away from the ligand, thus having a minimal effect on the stability of the transition state (Figure 27, A).²¹ Moreover, the effects of steric hindrance are minimal in the AD of alkene **17**, therefore, the binding pocket is highly susceptible to small changes in the local steric environment, indicating a tight fitting substituent that is explained better using the Sharpless binding model.

Overall, the results demonstrate that subtle differences in an alkene's steric environment have significant effects on asymmetric induction in the AD. Consequently,

the tandem AD of diene **6** is likely to obey similar principles observed from the related mono AD of alkenes **17-19**, thus poor enantioselectivity at the *o*-alkene is caused by steric hindrance from the vicinal methyl ester.

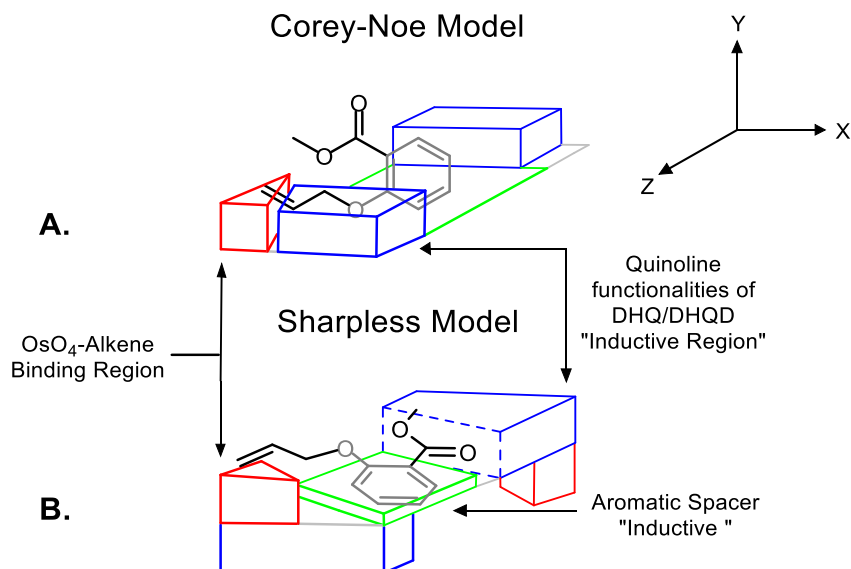


Figure 27: A comparison of the Corey-Noe (**A**) and the Sharpless model (**B**) for the binding of alkene **19**. Experimental results support the Sharpless model to explain poor asymmetric induction due to steric interactions of the vicinal methyl ester.^{28 & 31}

3.9.6. A Stereochemical Contradiction Due to *In Situ* Changes

Previously, the tandem AD of diene **6** (with ADmix α) was shown to contain enantiomer **SR-5** as the major stereoisomer (Chapter 3.9.4). Intriguingly, this result suggests that the diol was installed with an improved enantioselectivity at an otherwise sterically blocked position. Furthermore, the results oppose the Sharpless mnemonic's predicted stereochemical outcome and demonstrate reverse enantioselectivity at the *o*-alkene.

Throughout this investigation all AD reactions were carried out following an identical literature procedure, and mechanistic features of the catalytic cycle are considered identical in every reaction. Therefore, only *in situ* structural changes to diene **6** can be attributed to the observed enantioselectivity in the synthesis of **α -5**. Consequently, it was proposed that by altering the diene's structure and related activity, the AD can be

investigated further. This result could provide information on why a reverse stereofacial selectivity is achieved and how enantioselectivity could be improved in the AD of sterically hindered substrates. Additionally, the results of a structure-reactivity relationship could help to ascertain a correct alkene-ligand binding model.^{28 & 31} To examine the potential *in situ* changes of diene **6**, an analysis of regioselectivity in the tandem AD was investigated next.

3.9.7. Regioselectivity in the Tandem AD of Diene **6**

A competitive procedure was designed to examine the reaction rates of each alkene environment, in order to study any possible regioselectivity during the tandem AD of diene **6**. A standard AD procedure, using ADmix β , was carried out with 0.5 the standard reagent stoichiometry. The same methodology was applied to an Upjohn dihydroxylation that served as the control experiment. When total conversion of diene **6** was observed (by TLC) the reactions were quenched with excess sodium sulfite (Na_2SO_3) and the catalytic cycle was stopped ($\text{Os}^{\text{(viii)}}\text{O}_4$ (active form) + Na_2SO_3 + H_2O \rightarrow $\text{Os}^{\text{(vi)}}\text{H}_2\text{O}_4$ (inactive form) + Na_2SO_4). Individual ^1H -NMR experiments were performed on both reaction mixtures (in $\text{DMSO}-d_6$) to observe characteristic hydroxyl and alkene proton peaks (Figure 28).

From analysis of the ^1H -NMR spectral data, each reaction mixture contained regioisomers **23** & **24** in varying concentrations. The relative integrations of peaks **X** and **Y** demonstrated that diols **23** & **24** were synthesised in a 1:2 ratio, respectively (Figure 28, pink). Therefore, a competitive regioselectivity was confirmed and the rate of dihydroxylation at one alkene is approximately double that of the other. Elucidation of both regioisomers (**23** and **24**) was carried out by ^1H - ^1H NOESY analysis on a purified sample of diol **23**,⁸⁵ and confirmed a 2:1 preference for AD at the more sterically hindered *o*-alkene. An opposing regioselectivity was demonstrated in the

Upjohn dihydroxylation of diene **6**, which favoured dihydroxylation at the *m*-alkene in an opposing 2:1 ratio for diols **23** and **24**, respectively (Figure 28, blue).

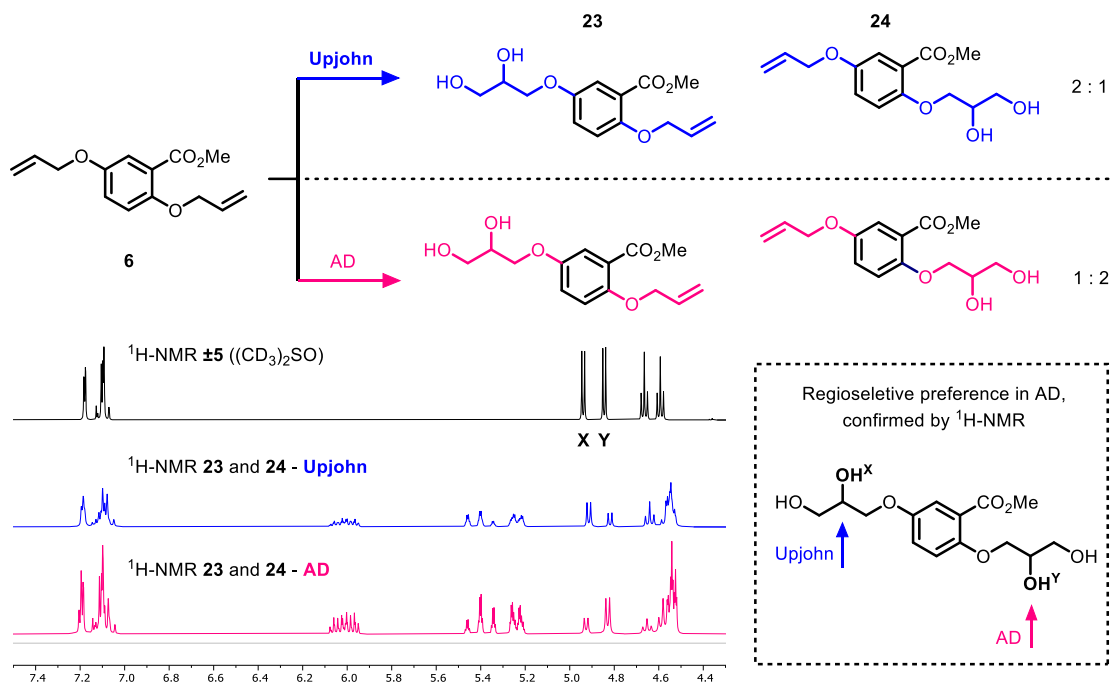


Figure 28: The stacked ¹H-NMR spectra (in DMSO-d₆) of the crude reaction mixtures from the tandem AD of diene **6** (pink) conditions: ADMix β, ^tBuOH/H₂O (1:1); Upjohn dihydroxylation of **6** (Blue) conditions: OsO₂(OH)₄, NMO, acetone/H₂O, 40 °C and the pure tetraol **±5** (Black). The results display intermediate diols **23** and **24** in opposing 2:1/1:2 concentrations.

The observed regioselectivity can be attributed to an enhanced interaction from the Sharpless ligand ((DHQD)₂PHAL, ADMix β), as it is the only definitive feature compared to the Upjohn dihydroxylation conditions.⁸⁶ The previous results from alkenes **17-19** ascribed steric hindrance from the methyl ester as the cause of poor enantioselectivity (See Chapter 3.9.5), and support the Sharpless model of alkene-ligand binding.³⁸ However, the results of the ¹H-NMR spectra contradict this hypothesis, and demonstrate preferential reactivity at the sterically hindered *o*-alkene under AD conditions. This suggests a favourable interaction between the methyl ester and the ligand, however the vicinal diol is known to be installed with poor enantioselectivity. Therefore, an observed inductive but inhibiting effect indicates a steric blocking of the binding pocket and supports the Corey-Noe binding model, with an enhanced

(inductive) interaction from parallel methoxyquinoline groups (Figure 29, A).²¹ Moreover, an extrapolation of the Sharpless binding model suggests the steric clash of the methyl ester and the methoxyquinoline groups would lead to a preferred regioselectivity at the *m*-alkene, or, an indistinguishable regioselectivity of the two alkene environments (Figure 29, B).³⁸

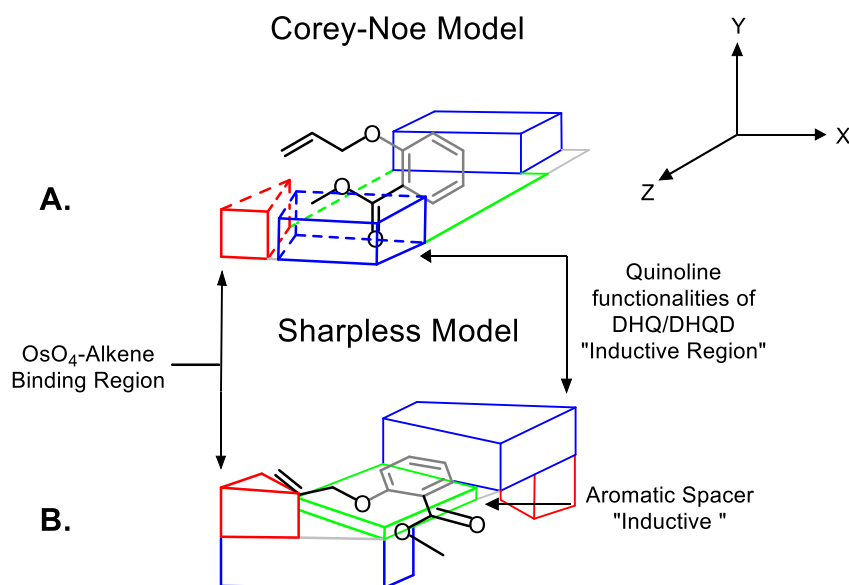


Figure 29: The proposed reinterpretation of the Corey-Noe (**A**) and Sharpless (**B**) models for the binding of alkene **12**, based on the experimental results of regioselectivity analysis in the AD.^{21 & 38}

Overall, the analysis of regioselectivity by ¹H-NMR confirms the *in situ* structural changes of diene **6** create intermediate diols **23** and **24** (in a 1:2 ratio, respectively). This indicates a preferential reactivity of the more sterically hindered alkene that is in agreement with the Corey-Noe model of alkene-ligand binding (Figure 29).²¹ However, the observed chemoselectivity correlates with poor enantioselectivity at the *o*-alkene, thus the investigation warranted further analysis of potential structure-reactivity relationships for the tandem AD of diene **6**.

3.9.8. Using Double Diastereodifferentiation for SAR analysis

Double diastereodifferentiation is best explained as a concept of "matched and mismatched" stereogenic pairs.⁸⁷ The stereochemical outcome of a reaction involving

two chiral reactants is directed by each reactant's already present stereochemistry. The two reactants can represent a 'matched' pair, and a reaction between the two proceeds with a complimentary diastereofacial selection, creating new stereocenters with high stereoselectivity. Or, they can represent a 'mismatched' pair, and a reaction between the two proceeds with clashing diastereofacial selection, creating new stereocenters with poor stereoselectivity.

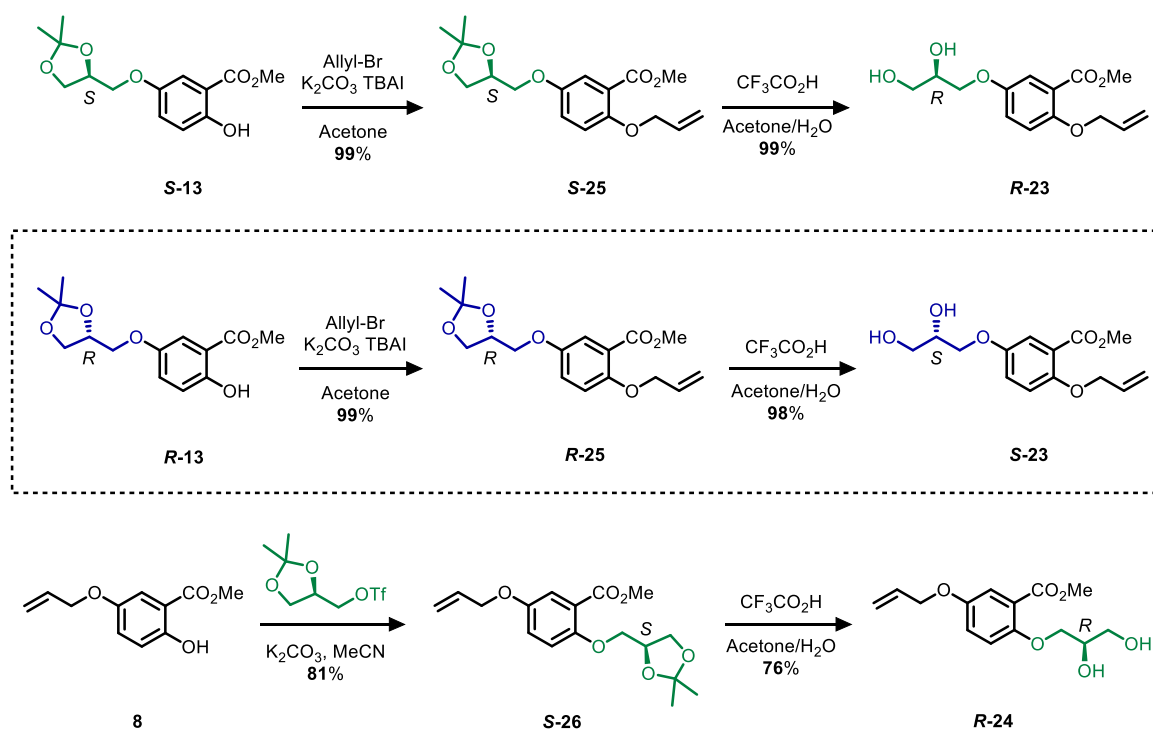
Table 5: Demonstrating double diastereodifferentiation in the AD of alkene **A** using a variety of chiral ligands. Results adapted from K. B. Sharpless.⁸⁸

Entry	Ligand	Mole % of Ligand	<i>d.r.</i> (B:C)
1	Quinuclidine	10	2.6:1
2	(DHQ) ₂ PHAL (ADmix α)	1	1:1.3
3	(DHQD) ₂ PHAL (ADmix β)	1	39:1
4	(DHQ) ₂ PYR	5	1:4.1
5	(DHQD) ₂ PYR	5	6.9:1

In catalytic systems such as the AD, double diastereodifferentiation is still achievable when a chiral reactant is replaced by a (chiral) ligand. Thus, a prerequisite for this methodology is the use of an alkene with at least one substituent that contains a stereocenter, and previous reports have used stereogenic centers 1-2 carbon bond lengths away from the reacting alkene. This is demonstrated clearly in the synthesis of (polyol) carbohydrate-precursors from the AD of alkene **A** (Table 5).⁸⁸ The results with ligand (DHQD)₂PHAL are indicative of a 'matched pair' with alkene **A**, and the

enantioselectivity is greatly enhanced for the synthesis of diol **B** (Table 5, Entry 3). Conversely, a 'mismatched' pair is observed with ligand (DHQ)₂PHAL (Table 5, Entry 2), which demonstrated poor enantioselectivity in the AD of alkene **A**. Notably, the other chiral ligands (Table 5, Entries 4 & 5) demonstrated only a marginal improvement in enantioselectivity in comparison to the racemic ligand quinuclidine.

The SAR, for diene **6** was investigated using alkenes **S-25** and **R-23** (98% *e.e.*). Alkene **S-25** was afforded in 99% yield via an S_N2 of phenol **S-13** with allyl bromide. Subsequent acidic hydrolysis of the acetal afforded **R-23** in 99% isolated yield (Scheme 14).



Scheme 14: Chiral pool derived synthesis of alkenes (**S** & **R**)-**23**, **R-24**, (**S** & **R**)-**25** and **S-2**. For exact conditions, see appendix.

The aim of this SAR study was to determine if pre-installed (point) chirality promotes asymmetric induction to the sterically hindered alkene through double diastereodifferentiation, which would explain the enhanced stereocontrol and reversed stereoselectivity observed in the synthesis of **a-5**. Furthermore, by using a distal

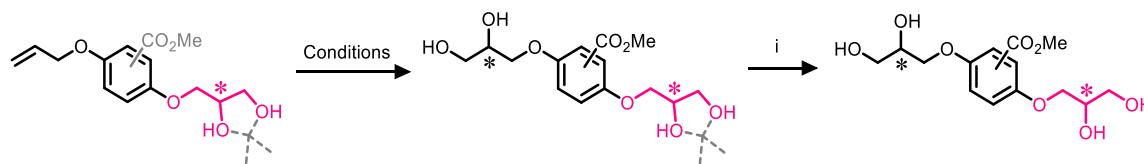
stereocenter (9 bonds from the reacting alkene) it presents a novel case for using double diastereoselection in the AD.⁸⁹ To support the results, the regioisomers **S-26** and **R-24**, and enantiomers **R-25** and **S-23**, were investigated (Scheme 14) and control experiments were performed for each alkene using Upjohn conditions.

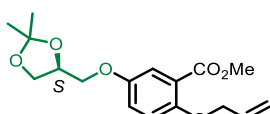
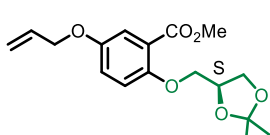
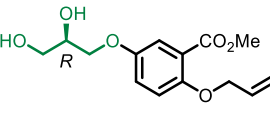
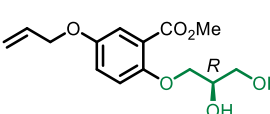
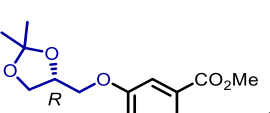
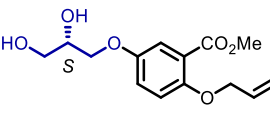
A chemoselective S_N2 of phenol **7** with allyl bromide afforded alkene **8** in 74% yield.⁹⁰ S_N2 of the *o*-phenol with (*R*)-Solketal-OTf afforded acetal **S-26** in 81% yield. Acid hydrolysis of the acetal afforded diol **R-24** in 76% yield (Scheme 14).

Overall, the results of the structure-reactivity relationship study provided a data set of 15 different stereochemical outcomes based on single point changes to the alkene's structure and point chirality (Table 6).

Table 6 can be found on the following page (82).

Table 6: The SAR of the AD: All stereochemical outcomes were calculated by chPLC. Conditions: **i**) TFA/MeOH/acetone/H₂O. All tetraols were analysed as their tetrakis acetyl esters (**12**).⁹¹



Entry	Alkene	Conditions	Enantiomeric Ratio (<i>e.r./d.r</i>)			
			<i>SS</i>	<i>RS</i>	<i>SR</i>	<i>RR</i>
1	 S-25	ADmix α	1	1	61	37
2		ADmix β	1	1	49	48
3		Upjohn	1	2	48	49
4	 S-26	ADmix α	–	6	3	91
5		ADmix β	3	95	–	2
6		Upjohn	2	47	3	48
7	 R-23	ADmix α	–	–	56	44
8		ADmix β	2	3	51	45
9		Upjohn	–	–	67	33
10	 R-24	ADmix α	–	8	3	89
11		ADmix β	2	94	–	4
12		Upjohn	–	48	–	42
13	 R-25	ADmix α	51	49	–	–
14		ADmix β	64	36	–	–
15	 S-23	Upjohn	50	50	–	–

3.9.9. Analysis of the Stereochemical Results

The stereochemical results for the AD of alkene **S-25**, using ADmix α (Table 6, Entry 1), are indicative of a 'matched' stereogenic pair between the alkene and the ligand ((DHQ)₂PHAL).⁸⁷ An *d.r* of 61:37 (**SR-5,RR-5**) was observed, demonstrating an enhanced asymmetric induction to the sterically hindered *o*-alkene. No improved enantioselectivity was observed using ADmix β (Table 6, Entry 2), and represents the 'mismatched' stereogenic pair with a similar stereochemical outcome obtained under non-asymmetric (Upjohn) conditions (Table 6, Entry 3). Additionally, the improved stereochemical outcome gained from ADmix α (Table 6, Entry 1) contradicts the Sharpless mnemonic's stereochemical prediction and all previous examples on alkenes **17-19** (Chapter 3.9.5). Remarkably, this result represents a mismatched enantioselectivity gained from a 'matched' diastereogenic pair (Figure 30).

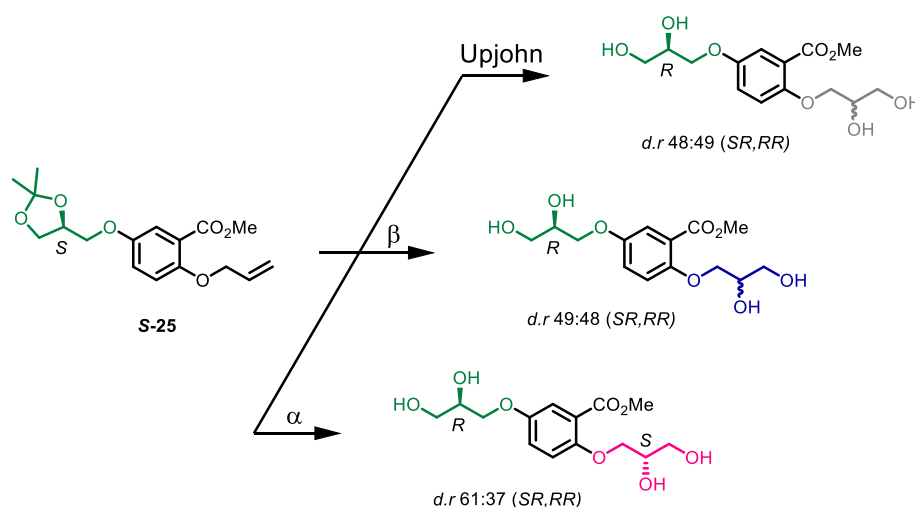


Figure 30: Stereochemical outcomes for the dihydroxylation of alkene **S-25** with *d.r.* values provided (From Table 6, Entries 1-3). Diols were afforded by dihydroxylation under Upjohn and AD (α & β) conditions and analysed as their corresponding tetrakis acetyl esters (**12**).

Changing the position of the methyl ester was examined using regioisomer **S-26**, and the stereochemical results demonstrated no 'matched' or 'mismatched' diastereogenic pairing, affording the Sharpless mnemonic's predicted enantioselectivity from both α and β ADmix (Table 6, Entries 4 & 5). From the results of the ¹H-NMR study (Chapter

3.9.7), it was found that diols **23** and **24** are intermediates during the tandem AD of diene **6**. Therefore, these intermediates were investigated with a fixed stereocenter, using enantiomers **R-23** and **R-24**, to examine if the stereochemistry of the one diol could influence enantioselectivity of the second diol, thus correlating with the unexplained results of tetraol **a-5**. However, the results from the AD of enantiomer **R-23** demonstrated no improved enantioselectivity, so no conclusion can be drawn for the stereochemical outcome of **a-5** (Table 6, Entries 7 & 8). Notably, excellent enantioselectivity was observed from the AD of enantiomer **R-24** (Table 6, Entries 10 & 11). However, the results of alkenes **S-26** and **R-24** (Table 6, Entries 4 – 6 & 10 – 11) are attributed to a superior asymmetric induction from the Sharpless ligands to the *m*-alkene (relative to the methyl ester), which consequently outweighs the influence of double diastereodifferentiation. This was also previously observed in the tandem AD of diene **6** and the AD of its related alkenes **17-19**.

Surprisingly, enantioselectivity was observed in the Upjohn dihydroxylation of alkene **R-23** (Table 6, Entry 9). This was proposed to be attributed to the free diol chelating the osmium species *in situ*,⁹² directing stereofacial selectivity in the Upjohn dihydroxylation from the already installed point chirality of the distal diol. It was anticipated that by repeating the experiment, and inverting the stereocenter to afford enantiomer **S-23**, would exhibit a similar enantioselectivity. This did not occur (Table 6, Entry 15), and the previous result was considered anomalous.

It was anticipated that alkene **R-25** would undergo a synonymous double diastereodifferentiation to its enantiomer **S-25**, with a predicted stereochemical outcome of tetraol **RS-5** using the ligand (DHQD)₂PHAL (from ADmix β). However, chPLC analysis of the resulting diol provided a further surprising result, identifying the tetraol **SS-5** as the major stereoisomer, with a *d.r* of 64:36 (**SS**/**RS**, Figure 31).

Intriguingly, this example represents a matched enantioselectivity gained from a matched diastereogenic pair, predicted by the Sharpless mnemonic device.

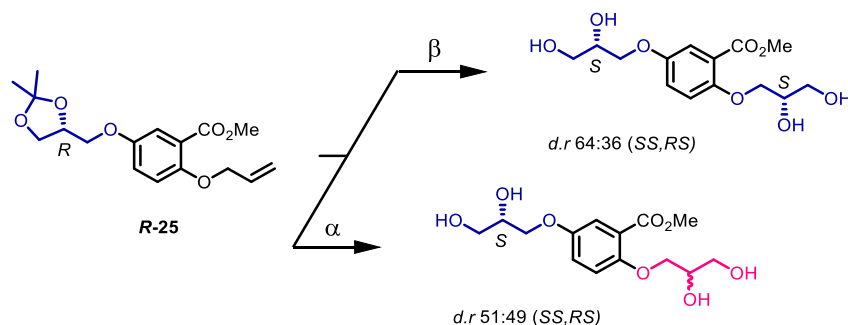


Figure 31: Stereochemical outcomes for the dihydroxylation of alkene **R-25** with *d.r.* values provided (Table 6, Entries 13 & 14). Diols were afforded by dihydroxylation under AD (α & β) conditions and analysed as their corresponding tetrakis acetyl esters (**12**).

Overall, the results of the structure-reactivity analysis did not confirm an explanation for the inverted enantioselectivity observed in the synthesis of **α -5**. However, the results demonstrate how double diastereodifferentiation can be used successfully to enhance asymmetric induction, and improve enantioselectivity, in the AD of sterically blocked alkene, using a distal stereocenter installed 9 bonds away, across an aromatic ring. Moreover, the results highlight that an identical stereofacial selectivity is operational during the AD of enantiomers **R-25** and **S-25**, using chiral ligands with opposing stereochemistry.

3.9.10. Stereofacial Selectivity: The Alkene Binding Hypothesis

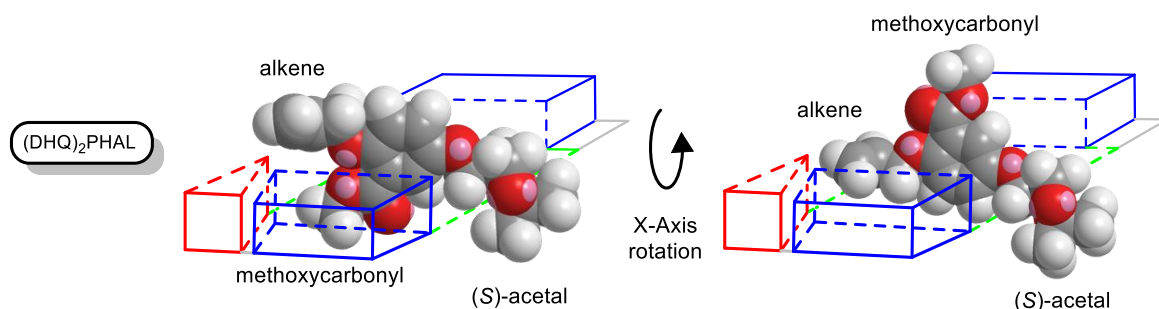
Listed below are four deductions for the AD, based on stereochemical evidence provided by this investigation, that have been used to assist in explaining the enantioselectivity observed in alkenes **S-25** and **R-25**.

- The α -alkene relative to the methyl ester approaches the OsO₄-ligand binding pocket with an identical orientation, as preferential binding was observed by ¹H-NMR analysis (Figure 28). Furthermore, a complete blocking of asymmetric induction was observed to alkene **19** using both AD ligands (Figure 26), thus an inductive effect is operational under both conditions.
- The increased sterics of the chiral acetal (2,2-dimethyl-1,3-dioxolane) enhances double diastereodifferentiation in the AD of the distal alkene, and is directly related to changes in alkene-ligand binding (Tabel 6).
- Double diastereoselective interactions outcompete steric hindrance and stabilise the transition state, which improves asymmetric induction to the reacting alkene and enhances enantioselectivity in the AD.
- Ligand accelerated catalysis is operational in all AD reactions, regardless of the stereochemical outcome. Therefore, non-asymmetric dihydroxylations have minimal effect on the resultant stereochemistry, and stereochemical rules applied to such reactions are not applicable.⁹³⁻⁹⁴

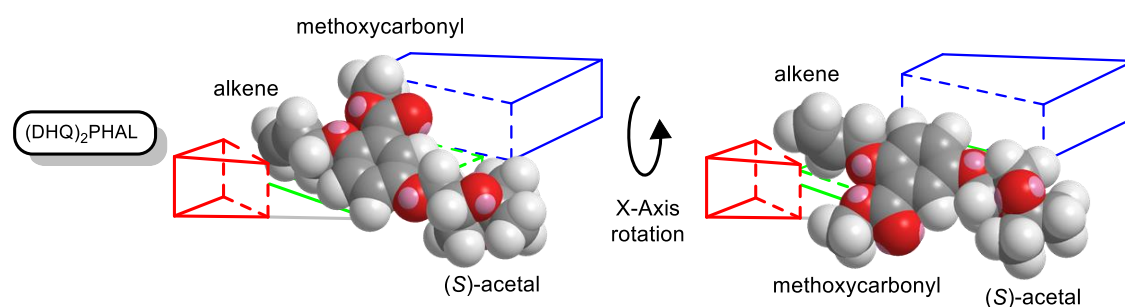
From the four deductions, it is proposed that enantiomers **S-25** and **R-25** approach the alkene-ligand binding pocket with a matching geometry, due to the observed inductive effects of the vicinal methyl ester. However, the lower energy transition state of enantiomer **S-25**, inside the (DHQ)₂PHAL binding pocket, flips the prochiral face of the reacting alkene and leads to a reversed enantioselectivity and an unpredicted

stereochemical outcome. No stereoselectivity was observed using (DHQD)₂PHAL, therefore, the lower energy transition state is facilitated by double diastereodifferentiation from the distal (*S*)-acetal group and its 'matched' diastereogenic interactions with (DHQ)₂PHAL.

A. Corey-Noe Model



B. Sharpless Model



C.

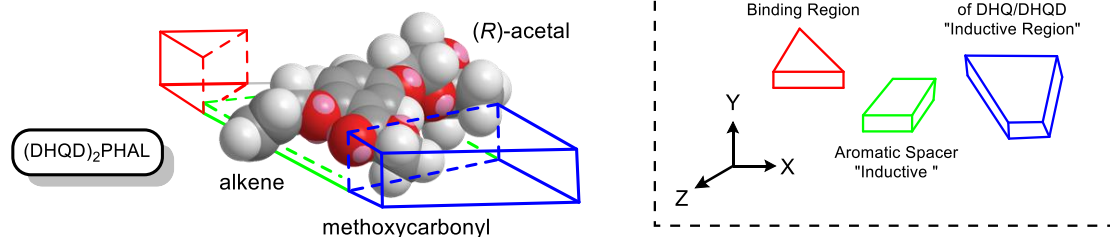


Figure 32: Illustrating the differences in binding of **S-25** and **R-25** in the Corey-Noe and the Sharpless binding models as reasoning behind the observed stereofacial selectivity in the AD of alkene **S-25**. It is hypothesis that double diastereodifferentiation from the distal acetal facilitates an enhanced asymmetric induction to the sterically blocked alkene. **A)** The Corey-Noe model suggests a disfavoured X-axis rotation of **S-25** for the cause of stereofacial inversion of the resulting diol; **B)** The Sharpless model suggests a favoured X-axis rotation, leading to a lower energy transition state that causes stereochemical inversion of the resulting diol; **C)** The mode of binding for **R-25** and (DHQD)₂PHAL, proposing a favoured diastereofacial interaction of the (*R*)-acetal. All energies were minimized using molecular force field (MM2) calculations.^{21 & 38}

Specifically, the presence of a fixed stereocenter diminishes the steric hindrance from the methyl ester in both enantiomers of alkene **25**, and in both cases it facilitates an

enhanced asymmetric induction in under both sets of AD conditions (Figure 32, B & C). However, it is hypothesised that the (*S*)-acetal inverts the alkene's (***S*-25**) stereofacial interaction with OsO₄, caused by a favoured double diastereoselective interaction with (DHQ)₂PHAL (Figure 32, A & B). This is proposed to create a more stable, lower energy transition state and installs the diol with reversed enantioselectivity. This is in similar accordance to a previous report on the AD of symmetrical divinylcarbinols.⁹⁵ Conversely, for the enantiomer ***R*-25**, it is proposed that the (*R*)-acetal has a favoured diastereofacial interaction with (DHQD)₂PHAL, and establishes a stable, lower energy transition state with no stereofacial inversion, thus the AD proceeds to install the diol with predicted enantioselectivity (Figure 32, C).

These findings strongly support the Sharpless alkene-ligand binding model³⁸ (Figure 32), which is better at justifying the observed enantioselectivity in the AD of alkenes ***S*-25** and ***R*-25**.

Extrapolation of the Sharpless model accounts for the stereofacial inversion from the alkene due to the open 'L-shape' of its proposed binding pocket, and permits rotation of the alkene around the X-axis, facilitated by the chiral acetal's diastereoselective interaction with the ligand (Figure 32, B).³⁸ Additionally, the Corey-Noe model's 'U-shape' binding pocket infers a blocked rotation of the alkene, and proposes that the alkene is sandwiched between two methoxyquinoline functionalities. Therefore, inversion of the alkene around the X-axis is highly disfavoured by this model, due to the proposed inductive effects of the methyl ester and an ordered face on interaction from the parallel methoxyquinolines (Figure 32, A).²¹

3.10. Conclusion

From the cHPLC investigation of the tandem AD on diene **6**, and related dienes **17-19**: A vicinal methyl ester functionality was demonstrated to induce preferential binding of a vicinal alkene inside the alkene-ligand 'binding pocket' (of (DHQD)₂PHAL). However, the methyl ester was shown to hinder asymmetric induction to the vicinal alkene, confirming that asymmetric induction in the AD is strongly influenced by small changes in an alkene's proximal steric environment. Overall, the previous results using the tandem AD to synthesise biologically relevant tetraols have been amended, and the exact stereochemical assignments are now confirmed.

The structure-reactivity relationship of the AD using stereo defined alkenes **23** & **24**, and **25** and **26**: demonstrated how double diastereodifferentiation in the AD can be used to improve asymmetric induction by at least +28%, to a sterically hindered alkene that was shown to be otherwise blocked of all enantioselectivity. Moreover, the novel investigation presented to show that double diastereodifferentiation can operate from a distal chiral center 9 bonds away from the reacting alkene, across an aromatic ring. Therefore, the results highlight a potential strategy for the future use of the AD, seeking to counteract poor enantioselectivity on sterically hindered alkenes.

Finally, the overall stereochemical findings from the cHPLC investigation have provided evidence in favour of the Sharpless model of alkene-ligand binding. They have uncovered a possible cause to the previously observed stereochemical inversions found throughout the relevant literature, indicating that an alkene's pro-chirality, pre-existing stereocenters and the choice of ligand (ADmix α & β , (DHQD)₂PHAL & (DHQ)₂PHAL) are inexplicably related to the stereochemical outcome. This relationship, in most cases, can be used to install target diols with a desired enantioselectivity, however in certain cases the unpredicted stereochemical result can be obtained.

In summary, the overall findings have corrected previous work relating to the synthesis of heparin sulfate glycomimetics, providing evidence to support a correct binding model for the AD of alkenes, highlighted a possible cause to previously observed cases of reversed enantioselectivity and have given a novel comprehension on how to use double diastereodifferentiation in the AD, to enhance asymmetric induction to sterically blocked alkenes. This is useful in the design of total syntheses looking to utilise the tandem AD, and can be used in future work seeking to use the AD in the synthesis of generic or medically relevant chemical structures.

For a publication on to this work, please see: *A Structure-Reactivity Relationship of the Tandem Asymmetric Dihydroxylation on a Biologically Relevant Diene: Influence of Remote Stereocenters on Diastereofacial Selectivity*, D. M. Gill, L. Male, A. M. Jones, *Eur. J. Org. Chem.*, 2019, **46**, 7568 – 7577 (found at the end of this chapter).

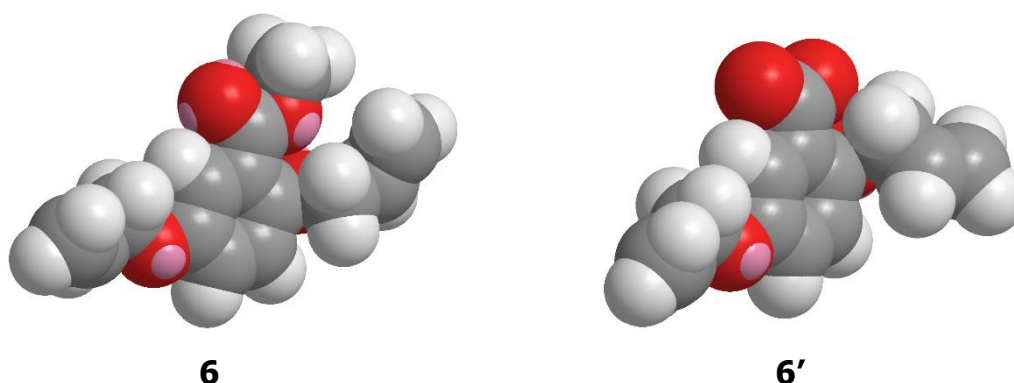
References

1. K. A. Hofmann, *Chem. Ber.*, 1914, **46**, 1667
2. N. A. Milas, E. M. Terry, *J. Am. Chem. Soc.*, 1925, **47**, 1412
3. N. A. Milas, S. Sussman, *J. Am. Chem. Soc.*, 1936, **58**, 1302
4. A. Kekulé, R. Anschütz, *Chem. Ber.*, 1880, **13**, 2150
5. R. Pappo, D. S. Allen Jr., R. U. Lemieux, W. S. Johnson, *J. Org. Chem.*, 1956, **21**, 478 – 479
6. V. Van-Rheenen, R. C. Kelly and D. Y. Cha, *Tetrahedron Lett.*, 1976, **23**, 1973 – 1976
7. K. B. Sharpless, K. Akashi, *J. Am. Chem. Soc.*, 1976, **98**, 1986 – 1987
8. R. Criegee, J. Liebig, *Ann. Chem.*, 1936, **75**, 522
9. R. Criegee, B. Marchand, H. Wannowius, *Ibid.*, 1942, **99**, 550
10. S. G. Hentges, K. B. Sharpless, *J. Am. Chem. Soc.*, 1980, **102**, 4263 – 4265
11. T. Göbel, K. B. Sharpless, *Angew. Chem. Int. Ed.*, 1993, **32**, 1329 – 1331
12. E. J. Corey, M. C. Noe, M. J. Grogan, *Tetrahedron Lett.*, 1996, **37**, 4899 – 4902
13. J. Del Monte, J. Haller, K. N. Houk, K. B. Sharpless, D. A. Singleton, T. Strassner, A. A. Thomas, *J. Am. Chem. Soc.*, 1997, **119**, 9907 – 9908
14. E. N. Jacobsen, I. Marko, W. S. Mungall, G. Schroeder, K. B. Sharpless, *J. Am. Chem. Soc.*, 1988, **110**, 1968 – 1970
15. J. S. M. Wai, I. Marko, J. S. Svendsen, M. G. Finn, E. N. Jacobsen, K. B. Sharpless, *J. Am. Chem. Soc.*, 1989, **111**, 1123 – 1125
16. K. B. Sharpless, W. Amberg, M. Beller, H. Chen, J. Hartung, Y. Kawanami, D. Lübben, E. Manoury, Y. Ogino, T. Shibata, T. Ukita, *J. Org. Chem.*, 1991, **56**, 4585
17. Y. Ogino, H. Chen, E. Manoury, T. Shibata, M. Beller, D. Lübben, K. B. Sharpless, *Tetrahedron Lett.*, 1991, **32**, 5761
18. H. Becker, S. B. King, M. Taniguchi, K. P. M. Vanhessche, K. B. Sharpless, *J. Org. Chem.*, 1995, **60**, 3940
19. K. B. Sharpless, W. Amberg, Y. L. Bennani, G. A. Crispino, J. Hartung, K.-S. Jeong, H.-L. Kwong, K. Morikawa, Z.-M. Wang, D. Xu, X.-L. Zhang, *J. Org. Chem.*, 1992, **57**, 2768 – 2771
20. M. M. Heravi, V. Zadsirjan, M. Esfandyari, T. B. Lashaki, *Tetrahedron: Asymmetry*, 2017, **28**, 987 – 1043
21. E. J. Corey, M. C. Noe, *J. Am. Chem. Soc.*, 1996, **118**, 319 – 329
22. E. N. Jacobsen, I. Markó, W. S. Mungall, G. Schröder, K. B. Sharpless, *J. Am. Chem. Soc.*, 1988, **110**, 1968
23. D. J. Berrisford, C. Bolm, K. B. Sharpless, *Angew. Chem. Int. Ed.*, 1995, **34**, 1059
24. K. B. Sharpless shared the 2001 Nobel Prize in chemistry for his work on asymmetric oxidation reactions.
25. H. C. Kolb, P. G. Anderson, K. B. Sharpless, *J. Am. Chem. Soc.*, 1994, **116**, 1278 – 1291

26. P. O. Norrby, H. C. Kolb, K. B. Sharpless, *J. Am. Chem. Soc.*, 1994, **116**, 8470 – 8478
27. H. C. Kolb, M. S. VanNieuwenhze, K. B. Sharpless, *Chem. Rev.*, 1994, **94**, 2483
28. Z.-M. Wang, X.-L. Zhang, K. B. Sharpless, *Tetrahedron Lett.*, 1993, **34**, 2267 – 2270
29. Z. A. Bredikhina, A. V. Kurenkov, O. A. Antonovich, A. V. Pashagin, A. A. Bredikhin, *Tetrahedron: Asymmetry*, 2014, **25**, 1015 – 1021
30. A. Guzman-Perez, E. J. Corey, *Tetrahedron Lett.*, 1997, **38**, 5941 – 5944
31. H. Becker, K. B. Sharpless, *Angew. Chem. Int. Ed.*, 1996, **35**, 237
32. P. Salvadori, S. Superchi, F. Minutolo, *J. Org. Chem.*, 1996, **61**, 4190 – 4191
33. D. J. Krysan, *Tetrahedron Lett.*, 1996, **37**, 1375 – 1376
34. J. M. Gardiner, S. E. Bruce, *Tetrahedron Lett.*, 1998, **39**, 1029 – 1032
35. M. Iwashima, T. Kinsho, A. B. Smith, *Tetrahedron Lett.*, 1995, **36**, 2199 – 2202
36. K. Morikawa, K. B. Sharpless, *Tetrahedron Lett.*, 1993, **34**, 5575 – 5578
37. R. A. Fernandes, P. Kumar, *Tetrahedron Lett.*, 2000, **41**, 10309 – 10312
38. H. Becker, P. T. Ho, H. C. Kolb, S. Loren, P. O. Norrby, K. B. Sharpless, *Tetrahedron Lett.*, 1994, **35**, 7315
39. K. P. M. Wanhessche, K. B. Sharpless, *J. Org. Chem.*, 1996, **61**, 7978 – 7979
40. E. J. Corey, M. C. Noe, S. Sarshar, *J. Am. Chem. Soc.*, 1993, **115**, 3828 – 3829
41. Y. D. Wu, Y. Wang, K. N. Houk, *J. Am. Chem. Soc.*, 1999, **121**, 10186 – 10192
42. P. O. Norrby, H. C. Kolb, K. B. Sharpless, *Organometallics*, 1994, **13**, 344 – 347
43. N. Moitessier, C. Henry, C. Len, Y. Chapleur, *J. Org. Chem.*, 2002, **67**, 7275 – 7282
44. C. R. Corbiel, S. Thielges, J. A. Schwartzentruber, M. Moitessier, *Angew. Chem. Int. Ed.*, 2008, **120**, 2675 – 2678
45. Y.-T. He, S. Xue, T.-S. Hu, Z.-J. Yau, *Tetrahedron Lett.*, 2005, **46**, 5393 – 5397
46. T. J. Donohoe, R. M. Harros, J. Burrows, J. Parker, *J. Am. Chem. Soc.*, 2006, **128**, 13704 – 13705
47. I. Paterson, E. A. Anderson, S. M. Dalby, J. H. Lim, P. Maltas, C. Moessner, *Chem. Commun.*, 2006, 4186 – 4188
48. A. M. Mahmood, A. M. Jones, F. J. Wilkinson, M. Romero, J. Duarte, Y. M. Alexander, *Biochimica et Biophysica Acta (BBA)*, 2017, **1861**, 3311 – 3322
49. A. M. Mahmood, A. M. Jones, G. Sidgwick, A. M. Arafat, F. L. Wilkinson, Y. M. Alexander, *Cell. Phys. Biochem.*, 2019, **53**, 323 – 336
50. A. W. W. Langford-Smith, A. Hassan, R. Weston, N. Edwards, A. M. Jones, A. J. M. Boulton, F. L. Bowling, S. T. Rashid, F. L. Wilkinson, M. Y. Alexander, *Sci. Rep.*, 2019, **9**, 2309
51. E. A. Raiber, J. A. Wilkinson, F. Manetti, M. Botta, J. Deakin, J. Gallagher, M. Lyon, S. W. Ducki, *Bioorg. Med. Chem. Lett.*, 2007, **17**, 6321 – 6325
52. W. H. Brooks, W. C. Guida, K. G. Daniel, *Curr. Top. Med. Chem.* 2011, **11**, 760 – 770
53. The synthesis of (*R*)-Mosher's acid derivatives for ¹⁹F-NMR analysis was also considered as a method for stereochemical quantification. However, it was

- proposed that the analysis of complex diastereoisomeric mixtures would be less direct than chPLC analysis.
54. The author would like to give special thanks to Dr Mark Holbrook, Dr Aidan Harrison and Phenomenex® for their HPLC screening service.
J. A. Dale, D. L. Dull, H. S. Mosher, *J. Org. Chem.*, 1969, **34**, 2543 – 2549
 55. The polarity of tetraol **±5** was found to be significant from experimentation, and the compound was considered hydrophilic in nature. All attempts failed to isolate **±5** from its crude reaction mixture using liquid-liquid extraction. This strongly corroborates with the predicted –ve Log P values (See Table 1). All work up procedures of **±5** and related tetraols were discarded and the products were dried and isolated directly using chromatography (SiO₂).
 56. cLog P values were calculated using ChemDraw® Professional 16.0
 57. G. Gübitz, *Chromatographia*, 1990, **30**, 555 – 564
 58. P. J. Kocienski, *Protecting Groups*, 3rd Edition, 2005
 59. Cellulose-1 column by Phenomenex® has a chiral selector of: Cellulose tris(3,5-dimethylphenylcarbamate)
 60. For Solketal: (*S*)-enantiomer CAS No = 22323-82-6; for (*R*)-enantiomer CAS No = 14347-78-5
 61. C. R. Harrison, P. Hodge, B. J. Hunt, E. Khoshdel, G. Richardson, *J. Org. Chem.*, 1983, **48**, 3721 – 3728
 62. W. Wu, R. Li, S. S. Malladi, H. J. Warshakoon, J. Hemamali, M. R. Kimbrell, M. W. Amolins, R. Ukani, A. Datta, A. Sunil, *J. Med. Chem.*, 2010, **53**, 3198 – 3213
 63. O. T. Ali, M. M. Sahb, J. R. Al Dulayymi, M. S. Baird, *Carbohydrate Research*, 2017, **448**, 67 – 73
 64. B. Doboszewski, E. Groaz, P. Herdeqijn, *Eur. J. Org. Chem.*, 2013, **22**, 4804 – 4815
 65. A. C. Hart, G. M. Schroeder, M. Gretchen, H. Wan, J. Grebinski, J. Ingram, J. Kempson, J. Guo, G. L. Trainor, A. V. Purandare, *ACS Med. Chem. Lett.*, 2015, **6**, 845 – 849
 66. J. Clayden, N. Greeves and S. Warren, *Organic Chemistry*, 2nd edition, Oxford University Press: New York, 2012.
 67. G. E. Dunn, T. L. Penner, *Can. J. Chem.*, 1966, **45**, 1699 – 1706
 68. B. N. Thomas, C. M. Lindermann, R. C. Corcoran, C. L. Cotant, J. E. Kirsch, P. J. Percijini, *J. Am. Chem. Soc.*, 2002, **124**, 1227 – 1233
 69. N. Martin, E. N. Thomas, *Org. Biomol. Chem.*, 2012, **10**, 7952 – 7964
 70. E. Celik, M. Maczka, N. Bergen, T. Brinkhoff, S. Schulz, J. S. Dickschat, *Org. Biomol. Chem.*, 2017, **15**, 2919 – 2922
 71. A. Bisi, A. Rampa, R. Bureisi, S. Gobbi, F. Belluti, P. Iona, E. Volati, A. Chiarini, P. Valenti, *Bio. Med. Chem.*, 2003, **11**, 1353 – 1361
 72. E. Berkowitz, S. Shen, *J. Org. Chem.*, 1996, **61**, 4666 – 4675
 73. T. F. Woiwode, C. Rose, T. J. Wandless, *J. Org. Chem.*, 1998, **63**, 9594 – 9596
 74. Y. Lui, Y. Xu, S. H. Jung, J. Chae, *Synlett*, 2012, **23**, 2663 – 2666

75. To account for steric hindrance it is simpler to view the Solketal functionality as an isobutyl analogue.⁶⁶
76. The P=O bond energy = 575 kJ mol⁻¹.⁶⁶
77. S. D. Lepore, Y. He, *J. Org. Chem.*, 2003, **68**, 8261 – 8263
78. R. H. Beddoe, K. G. Andrews, V. Magne, J. D. Cuthbertson, J. Saska, A. L. Shannon-little, S. E. Shanahan, H. F. Sneddon, R. M. Denton, *Science*, 2019, **365**, 910 – 914
79. See Appendix, Compound characterisation
80. K. M. Engle, S.-X. Lou, R. H. Grubbs, *J. Org. Chem.*, 2015, **80**, 4213 – 4220
81. See appendix, Chapter 6.3
82. See appendix: Compound characterisation
83. R. S. Cahn, C. K. Ingold, V. Prelog, *Angew. Chem. Int. Ed.*, 1966, **5**, 385 – 415
84. The standard AD of alkenes is conducted under biphasic, basic conditions. Therefore, under these conditions it was hypothesised that the carboxylic functionality of **6'** would be present as a carboxylate anion. Modelling calculations (MM2) predicted a similar steric environment from the carboxylate (**6'**) and the methyl ester (**6**) due to differences in intramolecular hydrogen bonding between the carbonyl and the methylene protons. This is illustrated below.



85. See Appendix, Chapter 6.4
86. Changes in the solvent were proposed not to effect chemoselectivity between the Upjohn and the AD conditions.
87. S. Masamune, W. Choy, J. S. Petersen, L. R. Sita, *Angew. Chem. Int. Ed.*, 1985, **24**, 1 – 30
88. K. Morikawa, K. B. Sharpless, *Tetrahedron Lett.*, 1993, **34**, 5575 – 5578
89. To the best of our knowledge, no work on diastereoselection in the AD has been performed on a substrate with a stereocenter installed >2 bonds away from the reacting alkene.
90. See Chapter 3.9.2
91. See appendix: Chiral HPLC Data and Analysis

92. N. A. Milas, J. H. Trepagnier, J. T. Nolan Jr., M. I. Iliopoulos, *J. Am. Chem. Soc.*, 1959, **81**, 4730 – 4733
93. J. K. Cha, W. J. Christ, Y. Kishi, *Tetrahedron Lett.*, 1984, **40**, 2247 – 2255
94. E. Vedejs, C. K. McClure, *J. Am. Chem. Soc.*, 1986, **108**, 1094 – 1096
95. A. Bayer, J. S. Svendsen, *Eur. J. Org. Chem.*, 2001, **9**, 1769 – 1780

Asymmetric Dihydroxylation

A Structure-Reactivity Relationship of the Tandem Asymmetric Dihydroxylation on a Biologically Relevant Diene: Influence of Remote Stereocenters on Diastereofacial Selectivity

Daniel M. Gill,^[a] Louise Male,^[b] and Alan M. Jones^{*,[a]}

Abstract: The Sharpless asymmetric dihydroxylation (AD) finds widespread use in natural product and drug molecule syntheses, in part, due to its efficiency and predictability. However, the tandem AD of dienes is much less studied, but important in complex molecular synthesis. Herein, a biologically relevant tandem AD is reported, and several anomalies are discovered with the accepted model. These include the formation of unpredicted diastereoisomers, with matched and mismatched stereo-

centers contradicting the Sharpless mnemonic device. From a structural analysis of the tandem AD, we present a strategy to improve asymmetric induction in sterically hindered alkenes using double diastereodifferentiation from a 9-bond distant stereocenter. A theoretical justification for the unpredicted stereoselectivity, accounting for the influence of steric hindrance and pre-installed chirality, is proposed.

Introduction

The Sharpless asymmetric dihydroxylation (AD) is a reliable enantioselective reaction that is used in industrial processes,^[1] natural product syntheses^[2] and drug molecule syntheses, such as, the opioid receptor antagonist (–)-Naltrexone.^[3]

The AD employs osmium tetroxide (OsO₄, typically 0.002 molar equiv.) to install a vicinal *syn*-diol.^[4a–4c] by reaction with a prochiral alkene. The Cinchona alkaloid derived ligand(s) command the diols resulting stereochemistry through asymmetric induction,^[5] with a predictable route to either accessible stereoisomer using the Sharpless mnemonic device.^[6]

In spite of this predictability, AD of sterically hindered or linear aliphatic alkenes has shown to proceed with poor stereocontrol.^[4b,7] These observations motivated the development of different ligand classes^[6a] and the use of surrogate “directing” groups to facilitate asymmetric induction.^[8] Overall, the stereochemical issues associated with linear aliphatic alkenes have been amended, however, the negative effect of steric hindrance remains comparably overlooked. Moreover, there are cases of product diols with inverted stereochemistry, in conflict with the Sharpless mnemonic.^[9,10]

Specifically, in systems where a tandem AD event is required (e.g. dienes), the Sharpless mnemonic is limited as there is evidence that stereocontrol is directed by pre-existing stereochemistry, irrespective of ligand choice.^[9b,9e,11] Therefore, the

predictability of the Sharpless mnemonic for diene systems is open to interpretation.

The AD on single alkenes has been well explored, but to the best of our knowledge the scope of the tandem AD has not been purposefully investigated.

Limited examples that employ a tandem AD in the synthesis of natural products are displayed in Figure 1.^[12]

An Investigation into the Tandem AD

During a medicinal chemistry investigation towards highly sulfated heparin glycomimetics,^[13] we encountered a biologically relevant tandem AD.^[14] We found that the reported^[14] stereochemical outcome of the resulting tetraol contradicted the Sharpless mnemonic.

Inspired by the importance of chirality in drug-receptor binding,^[15] we sought to conclusively elucidate the stereochemical outcome of the AD. Herein we describe an investigation into the tandem AD, exploring chemoselectivity, the roles of steric hindrance, and pre-installed point chirality on stereofacial selectivity (and the overall stereochemical outcome), using the biologically relevant precursor, diene **1**.

Results and Discussion

The Chiral Stationary Phase-Based High Performance Liquid Chromatography Method for Stereochemical Analysis

In order to quantify, for the first time, the stereochemical outcome of the tandem AD on diene **1**, we developed a chiral stationary phase-based high performance liquid chromatography (chPLC) method to resolve the four possible diastereoisomers.

[a] School of Pharmacy, University of Birmingham
Edgbaston, B15 2TT, United Kingdom
E-mail: A.M.Jones.2@bham.ac.uk
<https://www.jonesgroupresearch.wordpress.com>

[b] School of Chemistry, University of Birmingham
Edgbaston, B15 2TT, United Kingdom

Supporting information and ORCID(s) from the author(s) for this article are available on the WWW under <https://doi.org/10.1002/ejoc.201901474>.

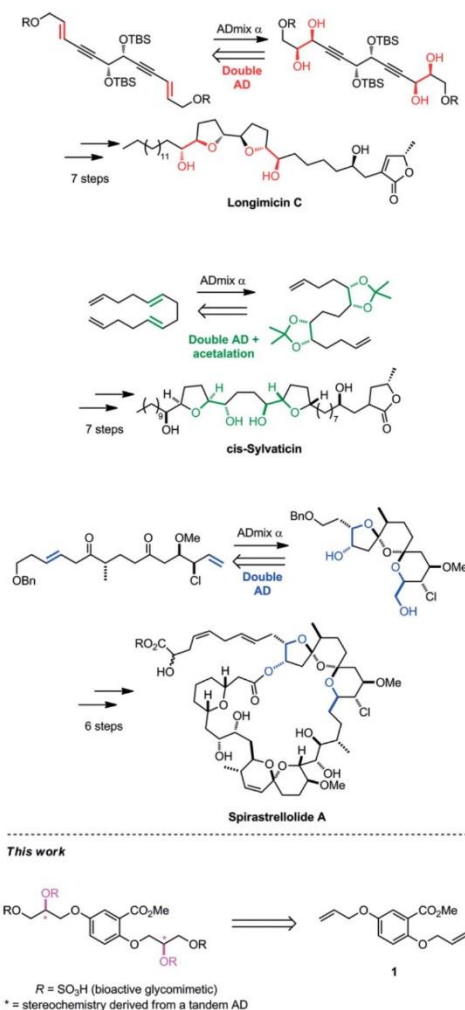
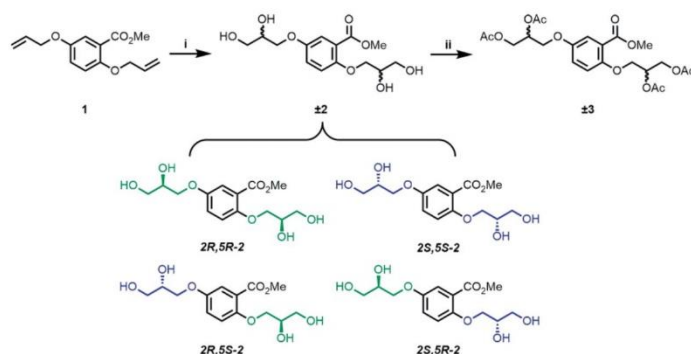


Figure 1. Examples that use a tandem AD in the synthesis of natural products: Longimicin C (red),^[12a] cis-Sylvaticin (green)^[12b] and Spirastrellolide A (blue).^[12c] This work details our investigation to uncover the stereochemical outcome of a tandem AD reaction towards a bioactive molecule.



Scheme 1. Synthesis of ± 3 for reverse phase chPLC optimisation and the four potential stereoisomers of tetraol ± 2 . Conditions: i) $\text{K}_2\text{OsO}_2(\text{OH})_4$, NMO, acetone/ H_2O (9:1), 40 °C, 12 h, 95 %; ii) AcCl , pyridine, CH_2Cl_2 , 0 °C, 0.5 h, 97 %.

mers that can be generated (**2R,5R-2**, **2S,5S-2**, **2R,5S-2** and **2S,5R-2**, Scheme 1).^[16] The racemic standard used for this analysis was synthesised by Upjohn dihydroxylation of **1** to afford tetraol ± 2 (Scheme 1).

Early in the investigation it was found that tetraol (**2**) gave poor separation with a variety of chiral stationary phases, under normal and reverse phase conditions.^[17] Therefore, derivatisation was required for chPLC analysis. A survey of protecting groups revealed the tetrakis acetate (± 3) enabled full resolution under reverse phase chPLC conditions.^[18]

Synthesis of Enantiopure Acetals as chPLC Standards

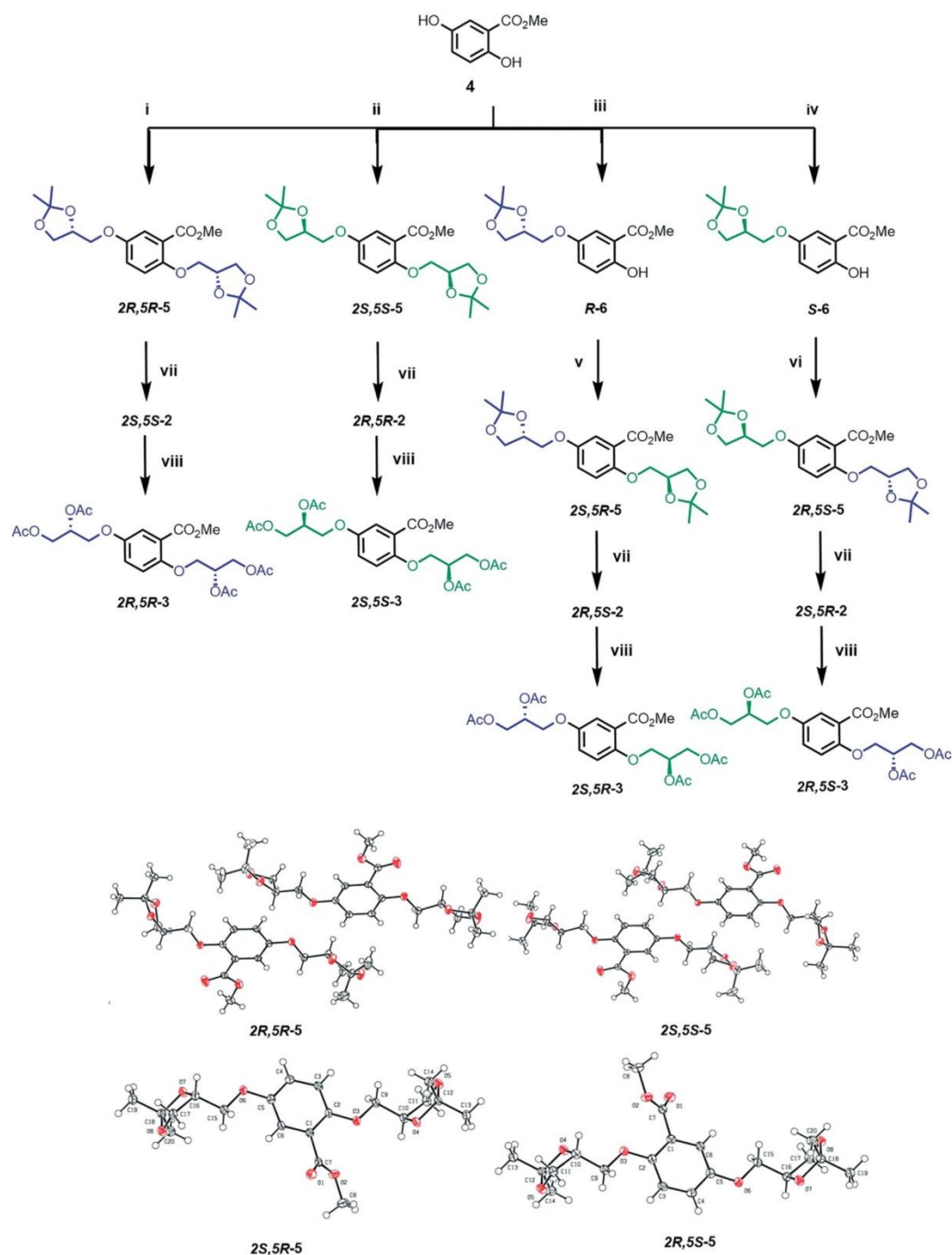
Each individual stereoisomer of **2** was elucidated by comparison to an authentic chiral standard. This was achieved through chiral pool synthesis of four enantiopure diacetals (**5**, Scheme 2) using solketal triflates (98 % e.e.). This provided a step-wise route to each stereochemical combination in moderate yield (33–40 %, after sequential recrystallization steps),^[19] with the absolute stereochemical assignments obtained from small molecule X-ray crystallography (Scheme 2, inset).^[22]

Hydrolysis of acetals **5** in trifluoroacetic acid gave each corresponding tetraols (**2**) in high yield,^[20] followed by acylation to their tetrakis acetates (**3**) for chPLC analysis.^[21]

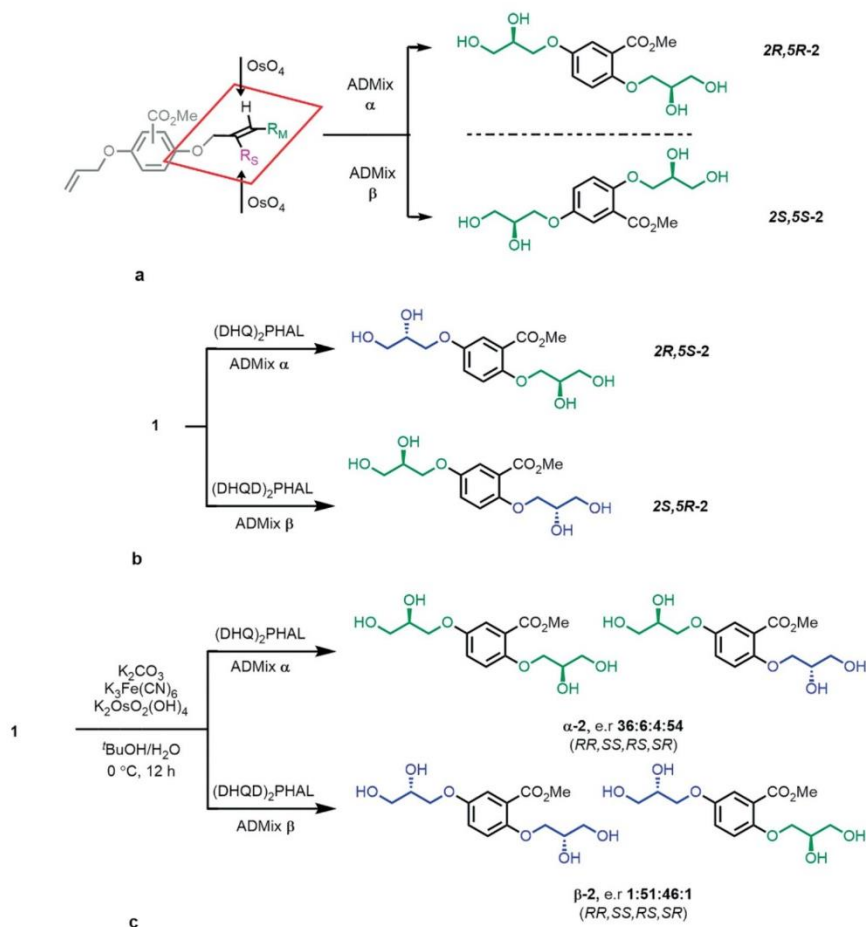
Overall, the specific retention times of each stereoisomer were revealed in the elution order of: **2R,5R-3**, **2S,5R-3**, **2R,5S-3**, **2S,5S-3**.^[23] Furthermore, the acidic hydrolysis and subsequent acylation steps did not degrade the stereochemical integrity.^[24]

A Contradicting Stereochemistry from the Tandem AD

The tandem AD of **1** using ADmix α [ligand (DHQD)₂PHAL] or β [ligand (DHQD)₂PHAL] should afford tetraols (**2**) with opposite stereochemistry.^[25] Using the Sharpless mnemonic device, ADmix α was predicted to give tetraol **2R,5R-2**, whilst ADmix β was predicted to give **2S,5S-2** (Scheme 3a).^[26] Conversely, this prediction contradicts the original assignment of a single **2R,5S-2** diastereoisomer with ADmix α (and **2S,5R-2** from ADmix β , Scheme 3b) from the identical substrate (**1**) and its hydrolysed analogue, respectively.^[13]



Scheme 2. Chiral pool synthesis of enantiopure diacetals **2*R*,5*R*-5**, **2*S*,5*S*-5**, **2*S*,5*R*-5** and **2*R*,5*S*-5** with representative single-crystal X-ray ORTEP visualisation inset (ellipsoids drawn at the 50 % probability level). Conditions: i) (*S*)-Solketal triflate (3.0 equiv.), K₂CO₃ (2.0 equiv.), MeCN, 82 °C, 12 h, **33** %; ii) (*R*)-Solketal triflate (3.0 equiv.), K₂CO₃ (2.0 equiv.), MeCN, 82 °C, 12 h, **38** %; iii) (*S*)-Solketal triflate (1.5 equiv.), K₂CO₃ (2.0 equiv.), MeCN, 82 °C, 12 h, **82** %; iv) (*R*)-Solketal triflate (1.5 equiv.), K₂CO₃ (2.0 equiv.), MeCN, 82 °C, 12 h, **82** %; v) (*S*)-Solketal triflate (1.5 equiv.), K₂CO₃ (2.0 equiv.), MeCN, 82 °C, 12 h, **40** %; vi) (*R*)-Solketal triflate (1.5 equiv.), K₂CO₃ (2.0 equiv.), MeCN, 82 °C, 12 h, **43** %. vii) TFA, MeOH, 40 °C, **90–96** %; viii) AcCl, Py, CH₂Cl₂, 0 °C **95–99** %.



Scheme 3. **a**) The predicted stereochemical outcome, from the Sharpless mnemonic of a tandem AD of diene **1** using ADMix α and β . **b**) The originally reported stereochemistry of a tandem AD of diene **1** using ADMix α and β .^[13,14] **c**) The confirmed diastereoisomers, measured by chPLC, for the tandem AD on diene **1** using ADMix α and β .

The chPLC analysis of **α -2** and **β -2** (Scheme 3c) demonstrated that a diastereoisomeric mixture was obtained in both products. Furthermore, the installation of the diol at the 2-position, *ortho* to the methyl ester, caused the reversed diastereoselectivity. The diol at the 5-position (*meta*) was installed with good stereocontrol ($> 90\%$ *e.e.*) in accordance with the Sharpless mnemonic.

We speculated that the methyl ester inhibited chiral transmission at the 2-position alkene, as this effect has been previously observed in the AD of substituted aryl allyl ethers.^[7] Additionally, ADMix α conditions gave a contradicting stereochemical inversion for **α -2**, affording **2S,5R-2** as the major diastereoisomer, which, is not in agreement with the Sharpless mnemonic nor the original assignment.^[14]

Stereochemical Analysis of a Single AD on Related Alkenes

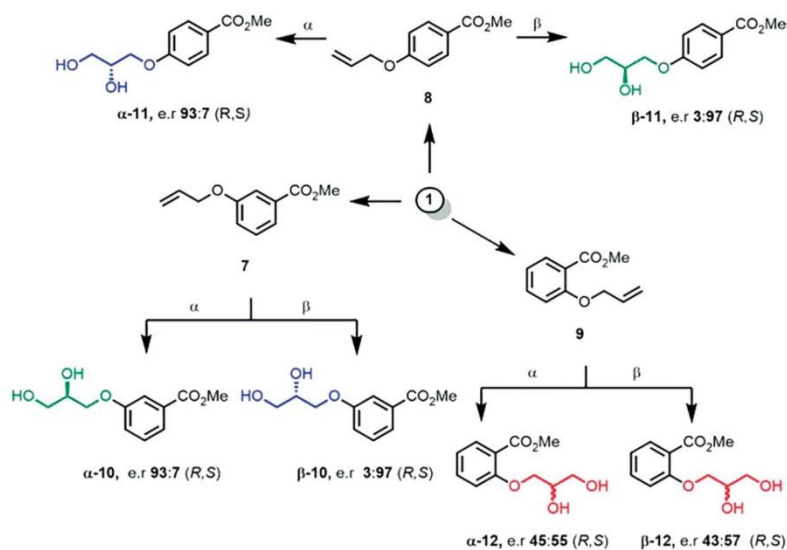
As a model study to confirm whether the *ortho* ester inhibits chiral transmission, we deconstructed diene **1** into its compo-

nent alkenes, with the addition of a *para* regioisomer to serve as a stereoelectronic comparison (**7-9**, Scheme 4).

chPLC analysis of the resulting diols **α -10** and **β -10**, from the *meta* substituted alkene **7**, displayed high enantiomeric ratios ($\alpha = 93:7$ & $\beta = 3:97$ *R/S*, Scheme 4) in accordance with previous results of **1**. The stereochemical outcome was comparable to diols **α -11** and **β -11**, from the *para* substituted alkene **8**, with a similar *e.r.* ($\alpha = 93:7$ & $\beta = 3:97$ *R/S*, Scheme 4).

For the AD of alkene **9**, we observed diols of low *e.r.* from both ADMix's ($\alpha = 43:57$ & $\beta = 45:55$ *R/S*, Scheme 4), demonstrating the consequence of the steric effects attributed to the *ortho*-methyl ester, which blocks asymmetric induction to the vicinal alkene.

All reactions^[27] were high yielding (93–99 %), within 6 h at 0°C , thus ligand accelerated catalysis was operational.^[28] Therefore, for alkene **9** (and consequently diene **1**), the lack of stereocontrol was expected to be caused by poor transition state stability of the alkene in the OsO_4 -ligand binding pocket, due to



Scheme 4. The AD of methyl allyloxy benzoate regioisomers as the deconstructed alkenes present in **1**. Conditions: $K_2OsO_2(OH)_4$, $K_3Fe(CN)_6$, K_2CO_3 , $tBuOH/H_2O$ (1:1), 0 °C, 6 h, ligand for ADMix α : (DHQD)₂PHAL and for ADMix β : (DHQD)₂PHAL. 96–99 %.

the steric hindrance of the *ortho* methyl ester.^[10a] The results of alkenes **7** and **8** further highlight that this inhibitory effect is a steric phenomenon, as there is no evidence to suggest electronic interactions, associated with the aromatic system, have an effect.

The overall results demonstrate the considerable effects of steric hindrance on stereo-control, in the AD of mono and dienes.

Examining Chemoselectivity in the Tandem AD of Diene **1**

The influence of the methyl ester on asymmetric induction, and the conflicting cHPLC result of **alpha-2** (Scheme 3c), prompted us to consider how the reaction could be manipulated with the intent of improving the *e.r.* of the vicinal (2-position) alkene. Therefore, we sought to find the cause of the stereochemical conflict and we first examined chemoselectivity in the double AD of **1**.

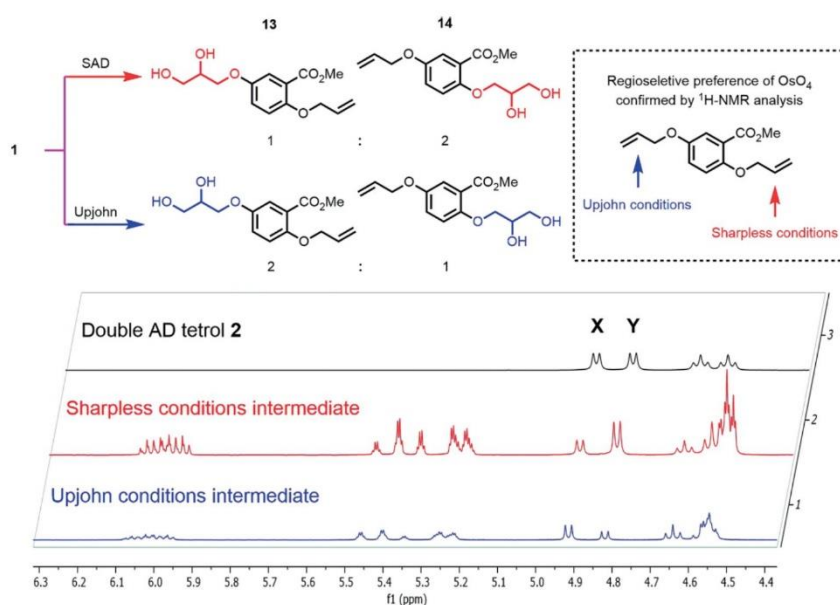


Figure 2. Regioselectivity of a dihydroxylation under AD and Upjohn conditions with the stacked 1H -NMR spectra of the crude samples from each reaction, displaying diols **13** and **14** in opposing 2:1 concentrations.

By conducting a standard AD experiment on **1** using a sub-stoichiometric equivalent of reagents, we were able to determine the relative ratios of intermediate diols.^[29] The same reaction was also carried out under Upjohn conditions, providing the control experiment. The reactions were stopped when no diene (**1**) was observed by thin layer chromatography, and ¹H NMR spectra were recorded on the crude samples (in d₆-DMSO).

From analysis of the crude products, each reaction was found to contain diols **13** and **14** (Figure 2). However, from the relative integration of peaks **X** and **Y**, it was observed that under AD conditions diol **14** had formed in a 2:1 ratio with **11** (Figure 2, red). This demonstrated that installation of a diol at the more sterically encumbered 2-alkene was preferred. Expectedly, the opposite result was found in the control experiment, which favoured installation of the diol at the 5-position alkene (Figure 2, blue).

Structural elucidation of the diols (**13** and **14**) was established by ¹H-¹H NOESY NMR spectroscopy on a purified sample of **14**, and, independently by synthesising enantiomers **R-13**, **S-13** and **R-14** (Table 1).

We have attributed this chemoselectivity to the Sharpless ligand [(DHQD)₂PHAL in ADMix β]. However, previous results from alkene **9** verified that AD on the 2-position alkene produces diols of low *e.r.* using either ADMix. Therefore, we hypothesised that the *vicinal* methyl ester has a favourable interaction with the OsO₄-ligand complex. However, regardless of this en-

hanced regioselectivity, chiral transmission from the ligand to the reacting alkene is blocked.

Unfavourable stacking interactions within the binding pocket of the OsO₄-ligand complex have been hypothesized to reduce stereoselectivity in other complex systems.^[7,10] This hypothesis is not in agreement with our results. Furthermore, it does not explain the mnemonic opposing stereochemistry of **α-2**.

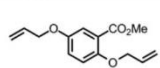
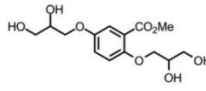
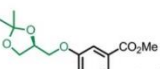
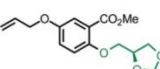
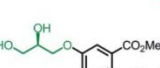
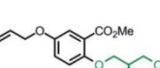

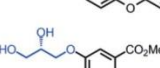
Taking into consideration the previously reported hypotheses on the AD and the results so far: the regioselectivity of the 2-position alkene and the unpredictable stereochemical outcome we have observed with **α-2**, we proposed that double diastereodifferentiation could be used to gain an improved *e.r.* at the vicinal (2-position) alkene.^[30]

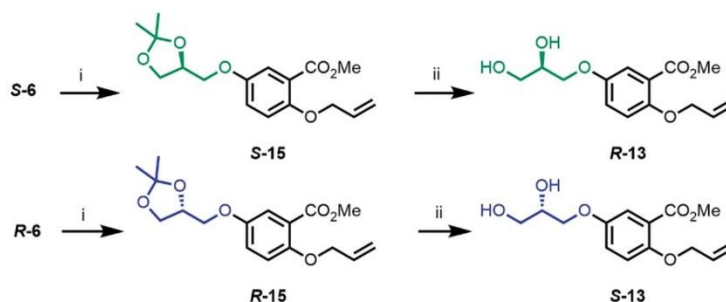
Investigating Diastereodifferentiation in the Tandem AD

Previous reports of diastereofacial selectivity in the AD use substrates with a stereogenic centre 1–2 bonds distant from the reacting alkene. This has provided stereoselective syntheses of various polyols.^[8,9a,11,31] Importantly, there are examples where a reversal of facial selectivity is observed which capitalise on double diastereodifferentiation.^[9]

We used acetal **S-6** to install a stereogenic centre of known *e.r.* (99:1) at the 5-position. Then, by installing an alkene at the 2-position it provided chiral alkene **S-13** (Scheme 5). The aim

Table 1. The stereochemical outcomes of the AD (and Upjohn dihydroxylation) of chiral alkenes for the sturcutre acitvty relationship of diene **1**. **Green** = major diastereoisomer; **Red** = minor diastereoisomer; **Blue** = low/insignificant diastereoisomeric ratios (*d.r.*).

Entry	Alkene	Conditions	Stereochemical Outcome (<i>e.r./d.r.</i>)				Product
			2 <i>S</i> ,5 <i>S</i>	2 <i>R</i> ,5 <i>S</i>	2 <i>S</i> ,5 <i>R</i>	2 <i>R</i> ,5 <i>R</i>	
1		ADMix α	6	4	54	36	
2		ADMix β	51	46	1	1	
3		OsO ₄ /NMO	25	25	25	25	
4		ADMix α	1	1	61	37	
5		ADMix β	1	1	49	48	
6		OsO ₄ /NMO	1	2	48	49	
7		ADMix α	—	6	3	91	
8		ADMix β	3	95	—	2	
9		OsO ₄ /NMO	2	47	3	48	
10		ADMix α	—	—	56	44	
11		ADMix β	2	3	51	45	
12		OsO ₄ /NMO	—	—	60	40	
13		ADMix α	—	8	3	89	
14		ADMix β	2	94	—	4	
15		OsO ₄ /NMO	—	48	—	52	
16		ADMix α	51	49	—	—	
17		ADMix β	64	36	—	—	
18		OsO ₄ /NMO	50	50	—	—	



Scheme 5. Chiral pool synthesis of chiral alkenes **S-13** and **R-13** from **S-15** and **R-15**. Conditions: i) Allyl bromide, K_2CO_3 , TBAI, acetone, 56 °C, 4 h, 95–99 %; ii) TFA, H_2O , 40 °C, 4 h, 99 %.

was to perform an AD on **S-13**, to determine if double diastereodifferentiation was achievable from a distal chiral centre, installed 9 bonds from a reacting alkene which is otherwise blocked from chiral transmission by the vicinal methyl ester.

In order to verify our hypothesis, we ran control experiments under AD and Upjohn conditions. Additionally, the use of a regioisomer **14**, unprotected diols (**S-11** and **R-11**) and opposite enantiomers **R-13** and **S-11** (Scheme 5) provided a data set of 15 different stereochemical outcomes based on point changes to the substrate. The results are summarised in Table 1.

A Structure Reactivity Relationship for the AD of Diene 1

The stereochemical results for alkene **S-15** (Table 1, entries 4–5) are representative of a matched and mismatched pair.^[30] Conditions with ADmix α gave an increase in *e.e* of +24 % to the **2S,5R-2** diastereoisomer over **2R,5R-2** (entry 4). ADmix β gave no diastereofacial selectivity (entry 5), and a comparable result was obtained under Upjohn conditions (entry 6). Interestingly, under ADmix α conditions (entry 4), the stereochemical outcome contradicts the Sharpless mnemonic and the previous results on mono-alkenes (**7** & **8**), therefore, it represents a matched pair but a mismatched stereochemical outcome.

Using the regioisomer **S-16** (entries 7–9) we probed the effects of swapping the alkene and chiral centre. No significant diastereofacial selectivity was observed, giving the predicted stereochemical outcomes for both α and β conditions (entries 7 and 8). Furthermore, with alkenes **R-13** & **R-14** (entries 10–15) we considered the effects of free diols under AD conditions. These species are formed during the tandem AD of **1**, mimicking the intermediates found in the 1H NMR spectroscopy study (Figure 2). Therefore, a previously installed chiral centre could influence the installation of the subsequent diol. However, the results from **R-13** demonstrated no significant diastereofacial selectivity under both conditions (entries 10–11). However, for **R-12**, when the diol is installed in the 2-position we observed excellent diastereoselection under AD conditions (entries 13–14). These results, and the results of alkene **S-16** (entries 7 & 8), can be attributed to chiral transmission from the Sharpless ligand(s) outweighing diastereofacial effects, as the AD of alkene **5** proceeded with good stereo-control regardless of pre-installed chiral centres (Scheme 3).

Anomalous, for **R-13**, under Upjohn conditions (entry 12) a preference for the **2S,5R-2** stereoisomer was observed. This outcome was considered to be an effect of diol chelation to OsO_4 *in situ*.^[32] Therefore, it was anticipated that the opposite enantiomer **S-13** would give the opposite diastereochemical result (**2R,5S-2**) but did not occur (entry 18).

We anticipated the results for alkene **R-15** (entries 16–17) to be similar to **S-15**, with a similar increase in the stereoisomer **2R,5S-2** gained from opposite AD conditions, using ADmix β . However, chPLC analysis provided a further unexpected result, defining **2S,5S-2** as the major product with +28 % *e.e* (entry 17). Therefore, this case represents a matched pair with a matching stereochemistry to the Sharpless mnemonic.

Considering the stereochemical outcomes from the AD of enantiomers **S-15** and **R-15**, it was non-trivial to explain the divergent results. Previous reports have revealed that selectivity can be dependent on chiral substituents, and in limited cases the use of either ADmix gave identical stereoisomers.^[9b]

Improving Diastereoselectivity in the AD

To assist the explanation for the observed diastereoselectivity, we have made deductions based on the evidence presented so far: (i) The alkene of **S-15** and **R-15** approaches the OsO_4 -ligand “binding pocket” with identical orientation to the neighbouring ester, as preferential binding of position 2 was observed by 1H -NMR spectroscopy (Figure 3). Furthermore, complete inhibition of chiral transmission was observed in alkene **7** (Scheme 3), therefore, both ligands have the same attraction to the alkene at position 2. (ii) The protected diol, as its corresponding acetal derivative, is important for diastereodifferentiation, as the free diol has no significant effect on the resulting stereochemical outcomes (Table 1, entries 10–11). (iii) Stereofacial interactions outweigh steric hindrance and directly contribute to the stereochemical outcome (results obtained with **S-15** and **R-15**). (iv). Ligand accelerated catalysis is operational in all AD reactions, regardless of the stereochemical outcome. Therefore, non-asymmetric dihydroxylations have minimal effect on the resulting diols stereochemistry and stereochemical rules applied to non-ADs’ are not applicable.^[33]

We therefore propose that alkenes **S-15** and **R-15** approach the OsO_4 -ligand “binding pocket” with the same orientation,

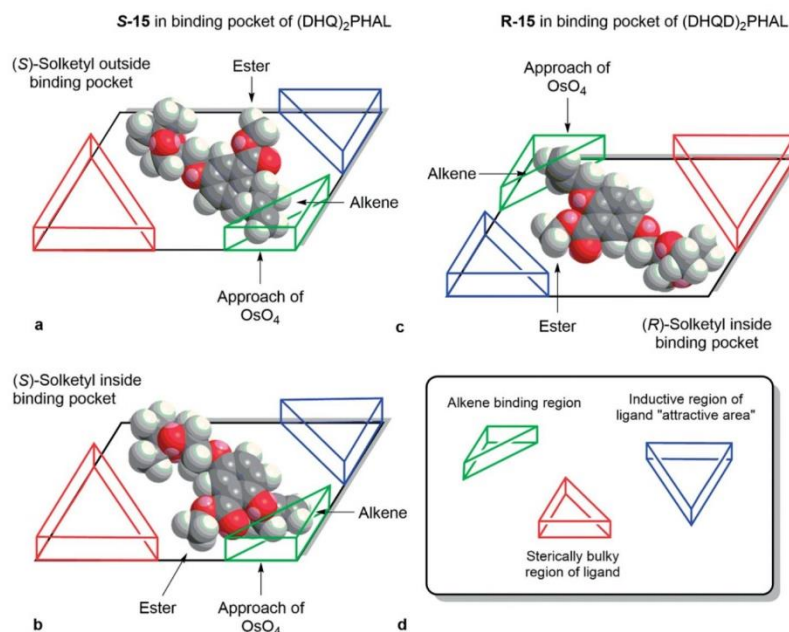


Figure 3. Demonstrating the different modes of transition state binding for **S-15** and **R-15** in the ligands (DHQ)₂PHAL and (DHQD)₂PHAL, as reasoning behind the differences in diastereofacial selectivity. For **S-15** and **R-15**, all energies were minimized using molecular force field-MM2 calculations. **a)** (*S*)-acetal functionality in **S-15** resides outside the "binding pocket" due to the orientation of approach; **b)** the proposed binding mode of **S-15** in (DHQ)₂PHAL due to interactions with the ligand, providing a lower energy transition state and preferential attack of OsO₄ to the opposite face of the alkene, generating the unpredicted diastereoisomer. **c)** The binding mode for **R-15** in (DHQD)₂PHAL, demonstrating an exact orientation of approach and a matched interaction of the (*R*)-acetal leads to a lower energy transition state with no geometric inversion, giving the predicted diastereoisomer; **d)** regions of the "OsO₄-ligand" "binding pocket" adapted from the Sharpless mnemonic.^[6]

due to the *vicinal* methyl ester. However, the transition state of **S-15** inside (DHQ)₂PHAL is opposite to **R-15** in (DHQD)₂PHAL, and, is directly related to the stereochemistry of the acetal functionality and its interactions with the Sharpless ligands.

The presence of the acetal in (*R/S*)-**13** diminishes the steric hindrance of the ester and in both cases facilitates asymmetric induction. However, the steric bulk of the (*S*)-acetal flips the geometry of **S-15**'s interaction with (DHQ)₂PHAL, leading to a lower energy transition state and the observed stereochemical inversion relative to the Sharpless mnemonic. This hypothesis is in similar accordance to a previous report on the AD of symmetrical divinylcarbinols.^[34] For enantiomer **R-15**, we hypothesise that interactions with (DHQD)₂PHAL already leads to a lower energy transition state, with no geometric inversion due to the pre-organised stereochemistry of the (*R*)-acetal, thus, giving the predicted diastereoisomer from the Sharpless mnemonic. These hypotheses are illustrated in Figure 3.

Conclusions

From the chPLC analysis of the tandem AD on diene **1** and related alkenes **5-7**: we have demonstrated that a *vicinal* (methyl ester) functionality facilitates preferential binding of a reacting alkene inside the OsO₄-ligand complex, but, inhibits chiral transmission to the product diols/tetraols. Therefore, we

have confirmed that asymmetric induction in the mono and tandem AD is strongly influenced by steric interactions. Furthermore, we have amended previous results, providing the stereochemical assignments of biologically relevant tetraols **α-2** and **β-2 en route** to the glycomimetic class of bioactive molecules.

We have shown that by using double diastereodifferentiation in an AD, we were able to improve the *e.e.* of a diol by +28 %, which was otherwise blocked from chiral transmission. Therefore, we have presented a case for diastereofacial selectivity, which can be effective when a chiral centre is installed 9 bonds distant from a reacting alkene. Moreover, we have demonstrated a potential strategy to counteract blocking of asymmetric induction from steric hindrance, gaining higher enantioselectivity on sterically blocked alkenes, for future applications in AD.

Finally, we have uncovered a potential cause to the conflicting stereochemistry gained from AD reactions in the literature, by demonstrating that a substrate's pre-installed point chirality and choice of chiral conditions [*α* or *β*, (DHQD)₂PHAL or (DHQ)₂PHAL] are intertwined. This can be capitalised on to synthesise target diols, with enhanced diastereomeric ratios or an unpredicted stereochemical result. These findings have implications in the design of total syntheses that use AD and provides a roadmap to the use of tandem AD in complex molecular synthesis.

Experimental Section

For a general description of the chemicals and analytical methods that were used within this study see the Supporting Information.

Synthesis of 2: General AD procedure: A 25 mL round-bottomed flask was charged with $K_3Fe(CN)_6$ (3.0 equiv.), K_2CO_3 (3.0 equiv.), $K_2OsO_2(OH)_4$ (0.002 equiv.), $tBuOH/H_2O$ (1:1, 10 mL) and either (DHQD)₂PHAL or (DHQD)₂PHAL (0.02 equiv.), forming a biphasic homogeneous mixture. The flask was cooled to 0 °C (ice bath) and stirred vigorously for 20 min, creating a heterogeneous orange slurry to which the alkene (1.0 equiv.) was added. The reaction mixture was stirred at 0 °C until complete consumption of starting material was observed [TLC, EtOAc/hexane (1:1), or EtOH/EtOAc (1:4)]. The reaction was quenched with neat Na_2SO_3 (12.0 equiv.) and warmed to room temperature over 1 h. The flask was charged with H_2O (5 mL) and extracted with EtOAc (3 × 20 mL). The combined organic extracts were washed with 1.0 M $HCl_{(aq)}$ (2 × 30 mL), brine (30 mL) and dried ($MgSO_4$). Filtration of the solids and removal of solvent under reduced pressure afforded the desired compound.

Methyl 5-[(R)-2,3-Dihydroxypropoxy]-2-[(S)-2,3-dihydroxypropoxy]benzoate (α-2): Adapted from general procedure 1: Methyl 2,5-bis(allyloxy)benzoate (1) (158 mg, 0.50 mmol) was added and the reaction mixture was stirred at 0 °C for 6 h with monitoring [EtOH/EtOAc (1:4), R_f = 0.20]. The solvent was removed under reduced pressure and the crude mixture was directly purified by chromatography (SiO_2 , EtOH/EtOAc, 1:4) yielding the title as a clear oil (156 mg, 99 %). $[\alpha]_D^{25}$ = -13.15 [c = 1.0, MeOH, 36:64:54 e.r./d.r (2R5R,2S5S,2R5S,2S5R)]; IR $\tilde{\nu}_{max}$ cm^{-1} 3268 w, 2939 w, 2890 w, 1699 s (C=O), 1601 w, 1499 s, 1435 w; 1H -NMR [400 MHz, $(CD_3)_2SO$] δ_H = 7.18 (d, J = 2.7 Hz, 1H, C6-H), 7.15–7.04 (m, 2H, C3-H & C4-H), 4.94 (d, J = 5.0 Hz, 1H, CH-OH), 4.84 (d, J = 5.0 Hz, 1H, CH-OH), 4.66 (t, J = 5.7 Hz, 1H, CH₂-OH), 4.59 (t, J = 5.7 Hz, 1H, CH₂-OH), 4.01–3.85 (m, 3H), 3.86–3.69 (m, 6H, Me), 3.55–3.35 (m, 4H); ^{13}C -NMR [101 MHz, $(CD_3)_2SO$] δ_C = 166.0 (CO_2Me), 152.2 (C5), 152.0 (C2), 121.0 (C1), 119.8 (C3/C4), 115.94 (C3/C4), 115.89 (C6), 71.3 (O-CH₂), 70.3 (O-CH₂), 69.9 (2C, CH-OH), 62.72 (CH₂-OH), 62.66 (CH₂-OH), 52.0 (Me); LRMS m/z (ESI+) 339.12 (100 %, $[M + Na]^+$); HRMS m/z (ESI+) $C_{14}H_{20}O_8Na$ requires 339.1056, found 339.1057 ($[M + Na]^+$).

Methyl 5-[(S)-2,3-Dihydroxypropoxy]-2-[(±)-2,3-dihydroxypropoxy]benzoate (β-2): Adapted from general procedure 1: Methyl 2,5-bis(allyloxy)benzoate (1) (158 mg, 0.50 mmol) was added and the reaction mixture was stirred at 0 °C for 6 h with monitoring [EtOH/EtOAc (1:4), R_f = 0.20]. The solvent was removed under reduced pressure and the crude mixture was directly purified by chromatography (SiO_2 , EtOH/EtOAc, 1:4) yielding the title as a clear oil (156 mg, 99 %). $[\alpha]_D^{25}$ = -7.62 [c = 1.0, MeOH, 1:51:46:2 e.r./d.r (2R5R,2S5S,2R5S,2S5R)]; IR $\tilde{\nu}_{max}$ cm^{-1} 3260 br s (O-H), 2951 w, 2874 w, 1725 (C=O), 1611 w, 1577 w, 1498 s, 1432 w; 1H -NMR [400 MHz, $(CD_3)_2SO$] δ_H = 7.18 (d, J = 2.7 Hz, 1H, C6-H), 7.13–7.07 (m, 2H, C3-H & C4-H), 4.94 (d, J = 5.0 Hz, 1H, CH-OH), 4.84 (d, J = 5.0 Hz, 1H, CH-OH), 4.66 (t, J = 5.7 Hz, 1H, CH₂-OH), 4.59 (t, J = 5.7 Hz, 1H, CH₂-OH), 4.01–3.85 (m, 3H), 3.86–3.69 (m, 6H, Me), 3.55–3.35 (m, 4H); ^{13}C -NMR [101 MHz, $(CD_3)_2SO$] δ_C = 166.1 (CO_2Me), 152.2 (C5), 152.0 (C2), 121.0 (C1), 119.8 (C3/C4), 115.95 (C3/C4), 115.91 (C6), 71.3 (O-CH₂), 70.4 (O-CH₂), 69.9 (2C, CH-OH), 62.73 (CH₂-OH), 62.67 (CH₂-OH), 52.0 (Me); LRMS m/z (ESI+) 339.12 (100 %, $[M + Na]^+$); HRMS m/z (ESI+) $C_{14}H_{20}O_8Na$ requires 339.1056, found 339.1057 ($[M + Na]^+$).

Acknowledgments

The authors thank Dr Allen Bowden and Centre for Chemical Analysis at the School of Chemistry for analytical support, Dr Liam Cox and Dr Kim Roper for helpful discussions and Phenomenex® for preliminary cHPLC screening. D. M. G. thanks the University of Birmingham for a PhD scholarship.

Keywords: Asymmetric dihydroxylation · Tandem reaction · Diastereodifferentiation · Stereofacial selectivity

- [1] For a recent review on using the AD in the total synthesis of natural products see: M. M. Heravi, V. Zadsirjan, M. Esfandiyari, T. B. Lashaki, *Tetrahedron: Asymmetry* **2017**, 28, 987–1043.
- [2] L. Ahlgren, L. Sutin, *Org. Process Res. Dev.* **1997**, 1, 425–427.
- [3] S. Dongbang, B. Pederson, J. A. Ellman, *Chem. Sci.* **2019**, 10, 535–541.
- [4] a) E. J. Corey, M. C. Noe, M. J. Grogan, *Tetrahedron Lett.* **1996**, 37, 4899–4902; b) T. Göbel, K. B. Sharpless, *Angew. Chem. Int. Ed. Engl.* **1993**, 32, 1329–1331; *Angew. Chem.* **1993**, 105, 1417; c) A. J. Del Monte, J. Haller, K. N. Houk, K. B. Sharpless, D. A. Singleton, T. Strassner, A. A. Thomas, *J. Am. Chem. Soc.* **1997**, 119, 9907–9908.
- [5] E. N. Jacobsen, I. Marko, W. S. Mungall, G. Schroeder, K. B. Sharpless, *J. Am. Chem. Soc.* **1988**, 110, 1968–1970.
- [6] The Sharpless mnemonic device is a semi-empirical tool designed to predict the stereochemical outcome of any given AD based on the alkene's substituents: a) H. C. Kolb, M. S. Van Nieuwenhze, K. B. Sharpless, *Chem. Rev.* **1994**, 94, 2483–2547. For the first report of ADmix and phalazine (PHAL)-based ligands see: b) K. B. Sharpless, W. Amberg, Y. L. Ben-nani, G. A. Crispino, J. Hartung, K.-S. Jeong, H.-L. Kwong, K. Morikawa, Z.-M. Wang, D. Xu, X.-L. Zhang, *J. Org. Chem.* **1992**, 57, 2768–2771.
- [7] Z.-M. Wang, X.-L. Zhang, K. B. Sharpless, *Tetrahedron Lett.* **1993**, 34, 2267–2270.
- [8] a) A. Guzman-Perez, E. J. Corey, *Tetrahedron Lett.* **1997**, 38, 5941–5944; b) E. J. Corey, A. G. Perez, M. C. Noe, *J. Am. Chem. Soc.* **1995**, 117, 10805–10816.
- [9] a) R. A. Fernandes, P. Kumar, *Tetrahedron Lett.* **2000**, 41, 10309–10312; b) J. M. Gardiner, S. E. Bruce, *Tetrahedron Lett.* **1998**, 39, 1029–1032; c) N. H. Ertel, B. Dayal, K. Rao, G. Salen, *Lipids* **1999**, 34, 395–405; d) P. Salvadori, S. Superchi, F. Minutolo, *J. Org. Chem.* **1996**, 61, 4190–4191; e) M. Iwashima, T. Kinsho, A. B. Smith, *Tetrahedron Lett.* **1995**, 36, 2199–2202; f) D. J. Krysan, *Tetrahedron Lett.* **1996**, 37, 1375–1376; g) Z. A. Bredikhina, A. V. Kurenkov, O. A. Antonovich, A. V. Pashagin, A. A. Bredikhin, *Tetrahedron: Asymmetry* **2014**, 25, 1015–1021.
- [10] Asymmetric induction in sterically bulky alkenes is diminished or inhibited. A possible explanation involves the relative destabilisation of the transition state, which, is alkene dependent. However, the complexity of this hypothesis makes it difficult to account for steric effects.^[a,b] Alternative hypotheses propose different alkene OsO_4 -ligand binding, as the “U-shape” like “binding pocket” of the Sharpless ligands can potentially tolerate the presence of sterically bulky substituents.^[c,d] Density functional theory,^[e] transition state calculations^[f] and computational tools to help predict the stereochemical outcome exist.^[g] However, this is limited to simple mono-alkenes a) H. C. Kolb, P. G. Andersson, K. B. Sharpless, *J. Am. Chem. Soc.* **1994**, 116, 1278–1291; b) H. Becker, P. T. Ho, H. C. Kolb, S. Loren, P. O. Norrby, K. B. Sharpless, *Tetrahedron Lett.* **1994**, 35, 7315; c) E. J. Corey, M. C. Noe, S. Sarshar, *J. Am. Chem. Soc.* **1993**, 115, 3828–3829; d) E. J. Corey, M. C. Noe, *J. Am. Chem. Soc.* **1996**, 118, 319–329; e) P. O. Norrby, H. C. Kolb, K. B. Sharpless, *Organometallics* **1994**, 13, 344–347; f) Y. D. Wu, Y. Wang, K. N. Houk, *J. Am. Chem. Soc.* **1999**, 121, 10186–10192; g) N. Moitessier, C. Henry, C. Len, Y. Chapleur, *J. Org. Chem.* **2002**, 67, 7275–7282.
- [11] K. Morikawa, K. B. Sharpless, *Tetrahedron Lett.* **1993**, 34, 5575–5578.
- [12] a) Y.-T. He, S. Xue, T.-S. Hu, Z.-J. Yau, *Tetrahedron Lett.* **2005**, 46, 5393–5397; b) T. J. Donohoe, R. M. Harros, J. Burrows, J. Parker, *J. Am. Chem. Soc.* **2006**, 128, 13704–13705; c) I. Paterson, E. A. Anderson, S. M. Dalby, J. H. Lim, P. Maltas, C. Moessner, *Chem. Commun.* **2006**, 4186–4188; d) For a report of tandem AD of 1,5-hexadiene see: M. E. Maier, S. Reuter, *Liebigs Ann./Recueil* **1997**, 2043–2046.

- [13] a) A. M. Mahmoud, A. M. Jones, F. J. Wilkinson, M. Romero, J. Duarte, Y. M. Alexander, *Biochim. Biophys. Acta Gen. Subj.* **2017**, 1861, 3311–3322; b) A. M. Mahmoud, A. M. Jones, G. Sidgwick, A. M. Arafat, F. L. Wilkinson, Y. M. Alexander, *Cell. Physiol. Biochem.* **2019**, 53, 323–336; c) A. W. W. Langford-Smith, A. Hassan, R. Weston, N. Edwards, A. M. Jones, A. J. M. Boulton, F. L. Bowling, S. T. Rashid, F. L. Wilkinson, M. Y. Alexander, *Sci. Rep.* **2019**, 9, 2309; d) D. M. Gill, L. Male, A. M. Jones, *Chem. Commun.* **2019**, 55, 4319.
- [14] E. A. Raiber, J. A. Wilkinson, F. Manetti, M. Botta, J. Deakin, J. Gallagher, M. Lyon, S. W. Ducki, *Bioorg. Med. Chem. Lett.* **2007**, 17, 6321–6325. Note: Similar compounds were reported as single diastereoisomers and not diastereoisomeric mixtures.
- [15] W. H. Brooks, W. C. Guida, K. G. Daniel, *Curr. Top. Med. Chem.* **2011**, 11, 760–770.
- [16] Mosher's acid derivatives for ^{19}F NMR spectroscopic analysis was considered. However, analysis of complex mixtures of diastereoisomers would be less a direct read out of the reaction than chPLC.
- [17] The racemic diol **±2** was screened on proprietary chiral stationary phases (Phenomenex®) under reverse phase (H_2O and acetonitrile) and normal phase (hexane and isopropyl alcohol/ethanol) conditions.
- [18] **±3** gave the best preliminary results and the conditions were optimised using 28 % acetonitrile/72 % H_2O , 1.0 mL min $^{-1}$ at 30 °C, see supplementary data for further details.
- [19] See supplementary data **2R,5R-5**, **2S,5S-5**, **2R,5S-5** and **2S,5S-5**.
- [20] See supplementary data **2R,5R-2**, **2S,5S-2**, **2R,5S-2** and **2S,5S-2**.
- [21] See supplementary data, HPLC section: **2R,5R-3**, **2S,5S-3**, **2R,5S-3** and **2S,5S-3**.
- [22] CCDC 1956970 (for **2R,5R-5**), 1956969 (for **2S,5S-5**), 1956968 (for **2S,5R-5**), and 1956967 (for **2R,5S-5**) contain the supplementary crystallographic data for this paper. These data can be obtained free of charge from The Cambridge Crystallographic Data Centre.
- [23] Upon esterification to the tetrakis acetyl esters the CIP assignments invert due to group priority changes. Therefore, the order the compounds elute are as follows: **2S,5S-2**, **2R,5S-2**, **2S,5R-2**, **2R,5R-2**.
- [24] Further evidence for this was obtained by hydrolysing and re-acetylating an enantiopure standard of acetylated diol **S12** and **S12'**. See supplementary information: hydrolysis analysis.
- [25] Ligands from the ADmix are *pseudo* enantiomers and are opposing diastereoisomers.
- [26] Based on the Sharpless mnemonic device and reference.^[4b]
- [27] See supplementary information.
- [28] See ref.^[5].
- [29] See supplementary information: regioselectivity analysis.
- [30] Double diastereo-differentiation: the stereochemical outcome of a given reaction, involving two chiral reactants, is influenced by the already present stereocenters. They can represent a "matched" pair in which there is complimentary diastereofacial selectivity, and a new stereocentre(s) is formed with high diastereoselection. They can represent a "mismatched" pair, in which the uncomplimentary diastereofacial selectivity creates a stereocentre with little to no diastereoselection. For a comprehensive review, see: S. Masamune, W. Choy, J. S. Petersen, L. R. Sita, *Angew. Chem. Int. Ed. Engl.* **1985**, 24, 1–30; *Angew. Chem.* **1985**, 97, 1.
- [31] N. Moitessier, F. Chretien, Y. Chapleur, *Tetrahedron: Asymmetry* **1997**, 8, 2889–2892.
- [32] N. A. Milas, J. H. Trepagnier, J. T. Nolan Jr., M. I. Iliopoulos, *J. Am. Chem. Soc.* **1959**, 81, 4730–4733.
- [33] a) J. K. Cha, W. J. Christ, Y. Kishi, *Tetrahedron Lett.* **1984**, 40, 2247–2255; b) E. Vedejs, C. K. McClure, *J. Am. Chem. Soc.* **1986**, 108, 1094–1096.
- [34] A. Bayer, J. S. Svendsen, *Eur. J. Org. Chem.* **2001**, 1769–1780.

Received: October 4, 2019

Chapter 4: An Innovative Synthesis of Complex Organosulfates

Introduction

4.1. Organosulfates

Organosulfates are molecules that contain a sulfate functional group covalently bonded to a carbon framework through an oxygen atom (Figure 33). Formally, all organosulfates are the esterification products of alcohols with sulfuric acid (H_2SO_4) however, with the exception of dialkylsulfates (Figure 33), the majority of organosulfates are not synthesised in this way. Dialkylsulfates are highly reactive species that are known to be useful alkylating agents, such as dimethylsulfate,¹ but dialkylsulfates are less common in nature than sulfate monoesters and find little use outside of organic synthesis. Therefore, throughout this chapter, the term *Organosulfates* will be used to exclusively describe sulfate monoesters.

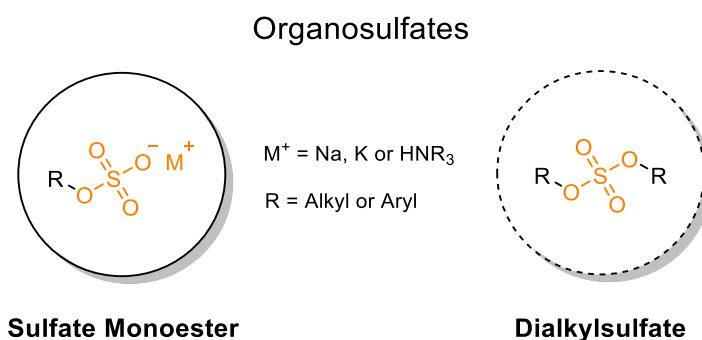


Figure 33: The generic structure of sulfate monesters and dialkylsulfates.

Organosulfates are widespread throughout nature and are found in a number of natural products and drugs. Fondaparinux (a heparin-like pentasaccharide drug used for the treatment of DVT, Chapter 1),² Mytalipin B (a marine natural product isolated from mussels and freshwater algae),³ Avibactam® (a β -lactamase inhibiting antibiotic),⁴ acetaminophen sulfate (a metabolite of paracetamol),⁵ (+)-Gonyautoxin 3 (a paralytic shellfish poison),⁶ Sotradecol® (an anionic surfactant used in the treatment of varicose veins),⁷ tyrosine sulfate (a commonly sulfated amino acid),⁸ sulfated

monoterpenes⁹ and Maitotoxin¹⁰⁻¹² are a selection of natural products and drug compounds that contain organosulfate motifs (Figure 34).

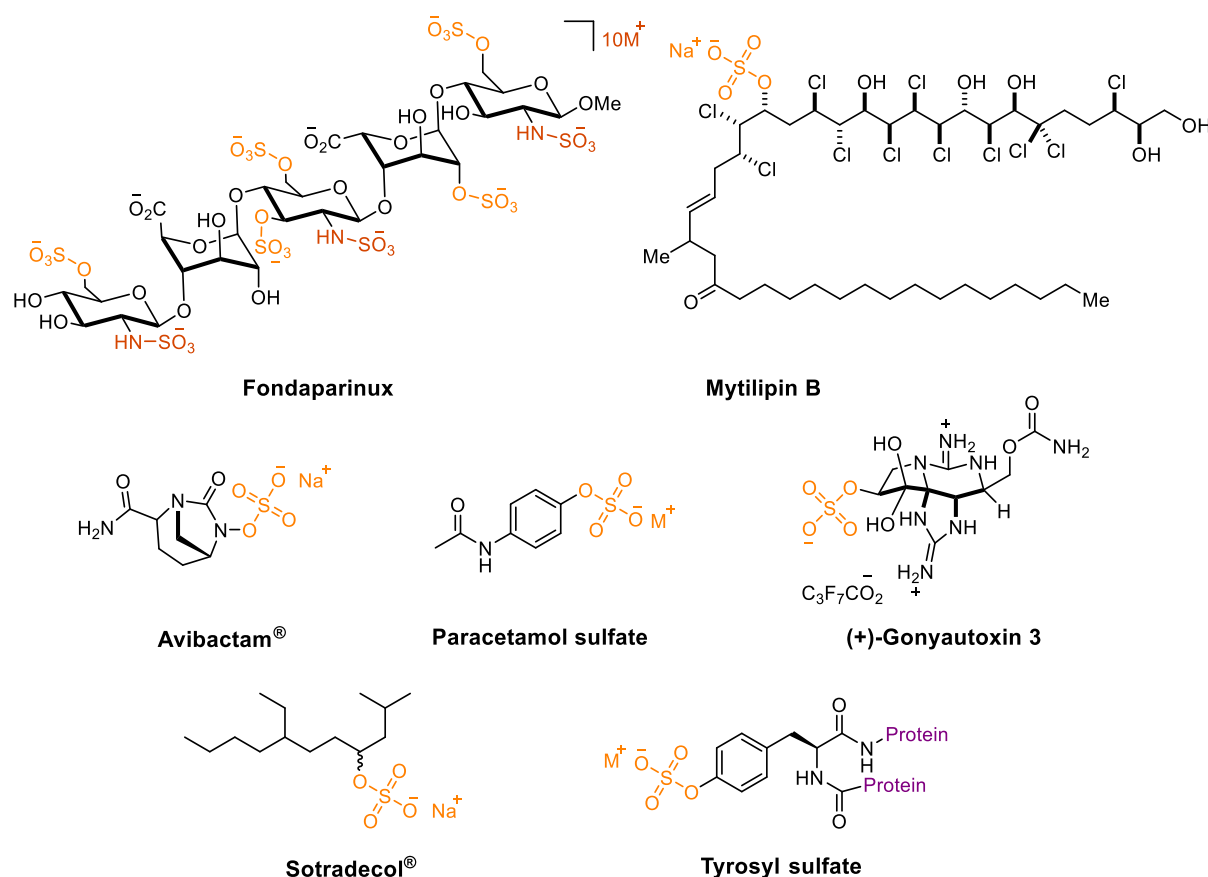


Figure 34: A variety of natural products, drug compounds and xenobiotic metabolites containing organosulfate motifs. Fondaparinux, Mytilipin B, Avibactam®, paracetamol sulfate, (+)-Gonyautoxin 3, Sotradecol and tyrosyl sulfate. M⁺ represents biologically relevant cations such as Na⁺ and K⁺.²⁻⁸

4.2. Organosulfates in Biomolecules

Biomolecules bearing organosulfate motifs have essential roles in extracellular signaling and protein-protein interactions (See Chapter 1).¹³⁻¹⁴ During the metabolism of xenobiotics and endogenous small molecules, organosulfate groups are installed to increase their solubility in the blood plasma, this enables detoxification and the elimination of metabolites from the body.¹⁵ Moreover, the activation and suppression of hormones are regulated by homeostatic sulfation pathways, which are shown to be altered in disease states.¹⁶⁻¹⁹

Sulfation is the chemical or enzymatic reaction that synthesises organosulfates from alcohols. The sulfation of amino acid residues (such as the phenol groups of tyrosine) accounts for approximately 1% of all post-translational protein modifications.²⁰ However, the resulting sulfated proteins (sulfoproteins) are comparably overlooked in favour of their more common phosphorylated analogues (phosphoproteins). This has impeded the study of sulfoprotein biology, and the 9.5×10^{-3} Da mass difference between protonated sulfate and phosphate residues²¹ strongly suggests that many sulfoproteins have been mis-assigned as phosphoproteins (Figure 35). Nonetheless, modern advances in ultra-high resolution mass spectrometry can now accurately differentiate phospho- and sulfo-proteins.²²⁻²³

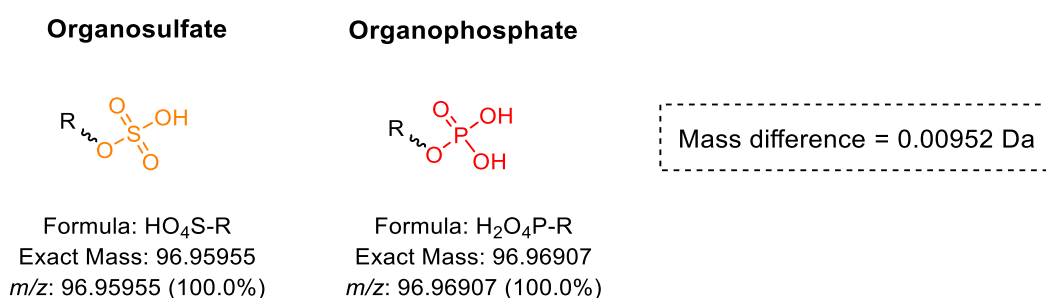


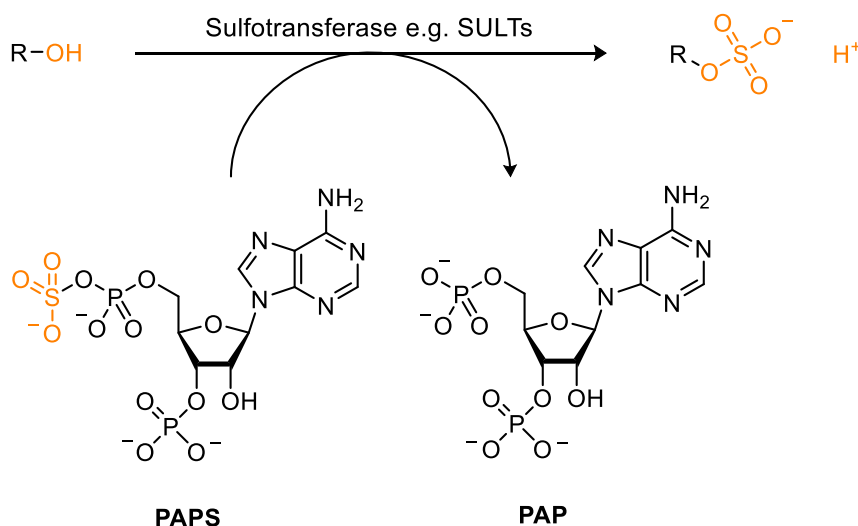
Figure 35: The differences in exact mass and *m/z* of protonated organosulfate and organophosphate groups.

Consequently, sulfoproteins may be more abundant in nature and more important to biochemical interactions than previously considered, and the incorporation of sulfated tyrosine residues into proteins is a growing area of research.²⁴⁻²⁵ Furthermore, the synthesis of drug-like molecules containing organosulfate motifs is timely to facilitate research into new therapies targeting H and HS-binding proteins (See Chapter 2).

Overall, organosulfates are central to a number of biological processes that underpin human physiology. However, a comprehensive understanding of these processes is still incomplete, so the efficient synthesis of organosulfates is essential to keep up with the growing demand from research.

4.3. The Enzymatic Synthesis of Organosulfates

In humans, the family of enzymes responsible for the sulfation of biomolecules are sulfotransferases, which catalyse the transfer of a sulfonyl moiety (SO_3^-) from a cofactor, such as 3'-phosphoadenosine-5'-phosphosulfate (PAPS), to a reacting hydroxyl group (Scheme 15).²⁶



Scheme 15: A general scheme for the enzymatic synthesis of organosulfates by sulfotransferase enzymes, using PAPS cofactor as the source of SO_3^- . Cations are omitted for clarity. PAP = 3'-phosphoadenosine-5'-phosphate.

In humans, two classes of sulfotransferases have been identified:

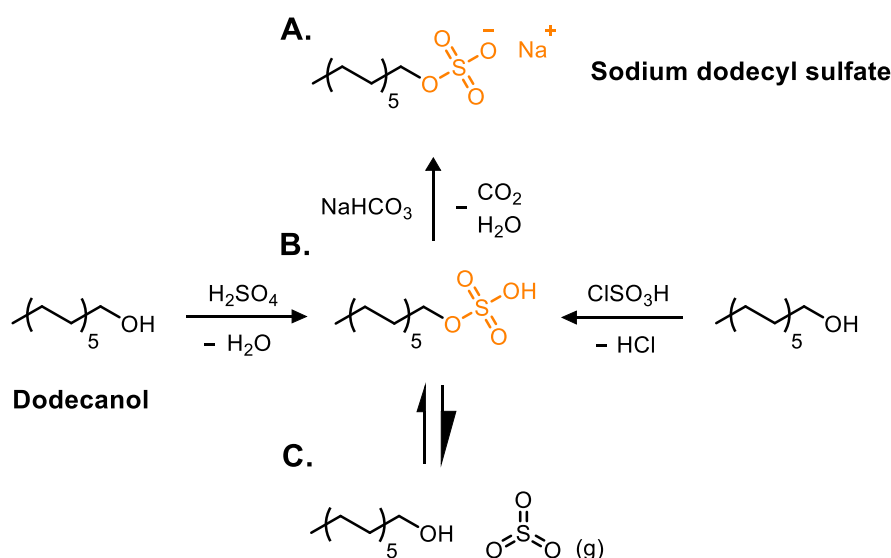
1. Golgi-membrane sulfotransferases (STs)
2. Cytosolic sulfotransferases (SULTs).

The STs sulfate large macromolecules, such as H-GAGs and proteins, whilst SULTs are shown to sulfate small molecules, steroid hormones and xenobiotics.²⁷ SULTs, also known as aryl-sulfotransferases (ArylSTs), can be used as biocatalysts for the sulfation of alcohols and phenols,²⁸⁻³⁰ and are shown to synthesise biologically relevant organosulfates with a broad substrate scope.³¹ Furthermore, ArylSTs provide efficient enzymatic routes to the synthesis of medically relevant H- and HS-GAGs.³²⁻³³ However, the majority of organosulfates are obtained through chemical methods.³⁴

4.4. The Chemical Synthesis of Organosulfates

4.4.1. Direct Sulfation

Organosulfates can be prepared directly by sulfation with sulfur trioxide ($\text{SO}_3(\text{g})$)³⁵ and by esterification with sulfuric acid or chlorosulfonic acid (ClSO_3H).³⁶ Normally a super-stoichiometric excess of reagent is employed, thus the highly acidic and exothermic conditions and are not suitable for sensitive substrates. Therefore, these methods are limited to the sulfation of simple alkyl alcohols such as sodium dodecyl sulfate (Scheme 16, A), and the direct sulfation of fatty-acid derived aliphatic alcohols is a primary manufacturing route to commercial anionic surfactants.³⁰



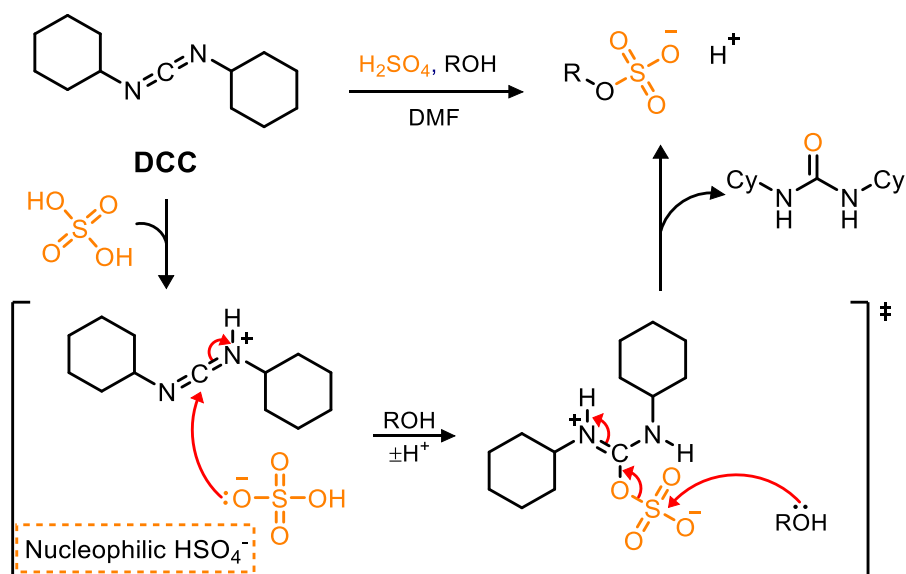
Scheme 16: The syntheses of sodium dodecyl sulfate by direct sulfation methods. **A)** The structure of sodium dodecyl sulfate; **B)** The bisulfate intermediate formed during direct sulfation; **C)** The dynamic equilibrium of the unstable bisulfate intermediate with dodecanol and $\text{SO}_3(\text{g})$.

The intermediate bisulfate ester (Scheme 16, B) is in an equilibrium which thermodynamically favours the liberation of $\text{SO}_3(\text{g})$ due to an associated increase in entropy ($+\Delta S$, Scheme 16, C). Therefore, the direct sulfation of alcohols requires an additional step (e.g. neutralisation with NaHCO_3), trapping the unstable, acidic bisulfate intermediate as a salt (Scheme 16, A). Consequently, organosulfate salts are sensitive to acidic conditions

and readily decompose into their corresponding alcohols and SO_3 (g).³⁴⁻³⁵ Moreover, optically active organosulfates are known to racemise under such acidic conditions.³⁷⁻³⁸

4.4.2. Dicyclohexylcarbodiimide Coupling

The use of dicyclohexylcarbodiimide (DCC) and H_2SO_4 is known to synthesise organosulfates at lower temperatures ($< 5^\circ\text{C}$) using a stoichiometric equivalence of acid.³⁹ This method is more tolerant of acid and oxidation sensitive substrates but is limited to sulfation of aliphatic alcohols, thus the synthesis of aryl-organosulfates are not feasible using this methodology. Nonetheless, it has a unique reaction mechanism that is proposed to involve a nucleophilic bisulfate anion, installing an SO_3^- group onto an alcohol similar to the enzymatic synthesis of organosulfates by SULTs (Scheme 17).²⁶



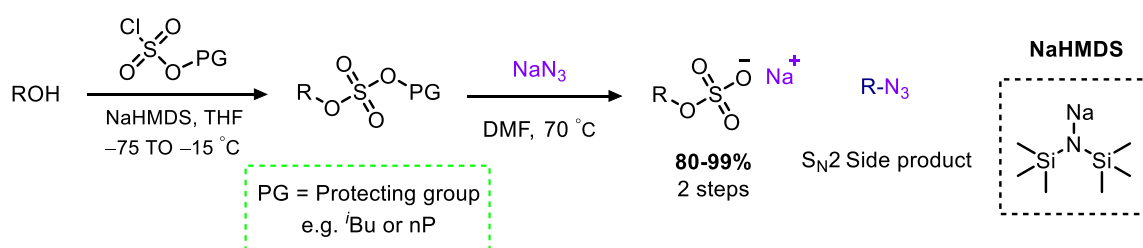
Scheme 17: The DCC coupling of aliphatic alcohols and H_2SO_4 . R = alkyl. Adapted from Hoiberg et. al.³⁹

4.4.3. Alkyl Chlorosulfates

Alkyl chlorosulfates are useful reagents toward the synthesis of organosulfates.⁴⁰⁻⁴² The dialkylsulfate intermediates are stable during purification by chromatography (SiO_2), and a separate deprotection step affords sulfate monoesters in up to 99% isolated yields (Scheme 18).⁴⁰⁻⁴¹ However, they are shown to only tolerate the synthesis of single organosulfates, and have not been demonstrated for the

persulfation of alcohols. Nonetheless, they are known to sulfate chiral alcohols without any loss of enantiopurity, a marked advantage over direct sulfation methods.³⁵⁻³⁶

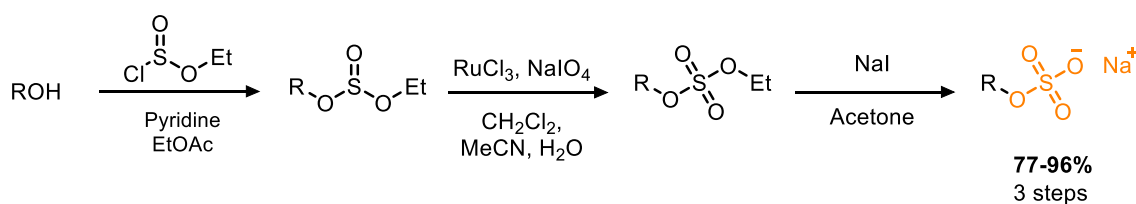
The reaction conditions require a strong base (NaHMDS), and the deprotection step, using sodium azide (NaN₃), can lead to unwanted S_N2 side products (Scheme 18).⁴⁰ Therefore, the use of protecting groups is a prerequisite for chemoselectivity and creates additional deprotection steps. Nonetheless, this methodology is an attractive route to the synthesis of sulfoproteins,⁴³ and later developments have provided a route to the chemoselective sulfation of carbohydrates.⁴⁴



Scheme 18: The synthesis of organosulfates from alkyl chlorosulfate esters. Adapted from Simpson et. al.⁴⁰

4.4.4. The Sulfitylation-Oxidation Protocol

The sulfitylation–oxidation protocol involves an initial synthesis of a protected sulfite ester (Scheme 19).⁴⁵ The protected organosulfite undergoes ruthenium catalysed oxidation to a sulfate ester (dialkylsulfate), and is subsequently deprotected to afford the sulfate monoester as its Na⁺ salt.⁴⁵ Each step proceeds in high yields (77-99%), and the methodology is shown to sulfate multiple hydroxyl functionalities on a single molecule (persulfation). However, the use of multiple reaction sequences and aqueous-based purification techniques hinders the practicality of this method.



Scheme 19: The sulfitylation–oxidation protocol for the synthesis of organosulfates. Adapted from Huibers et. al.⁴⁴

4.4.5. SO₃-Amine Complexes

The Lewis adducts of SO₃ with trimethylamine (NMe₃), triethylamine (NEt₃), dimethylformamide (DMF) and pyridine (Py), are commercially available reagents that react with alcohols to afford organosulfates as their corresponding ammonium salts (Figure 36).⁴⁶

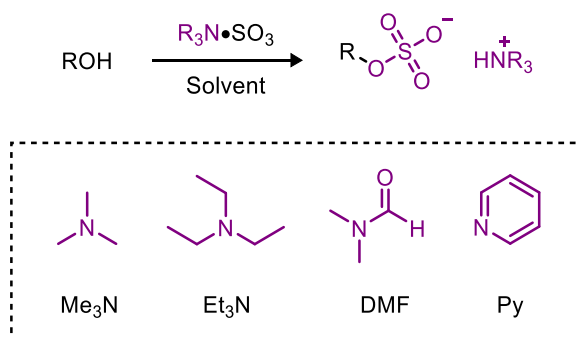


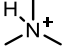
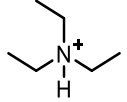
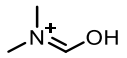
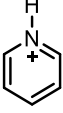
Figure 36: The sulfation of alcohols with R₃N•SO₃, and the commercially available amines used.

For a comprehensive review of chemical sulfation methods using these reagents, see Al-Horani et. al.⁴⁷ However, the prominent examples for the comprehensive preparation of organosulfates using the SO₃-amine complexes (R₃N•SO₃) include:

- A microwave assisted approach for the exhaustive (per)sulfation of phenols⁴⁸
- The triflic acid catalysed persulfation of polyols⁵⁰
- The site selective sulfation of carbohydrate residues using a catalytic borinic acid in conjunction with Me₃N•SO₃⁵¹

Lewis adducts of SO₃ with oxygen containing molecules, such as 1,4-dioxane, have also be used as sulfating agents.⁴⁶ However, these complexes are highly unstable so their use has been superseded by the more stable R₃N•SO₃ complexes.

Table 7: The pK_{aH} and orbital hybridisation of common amines and amides in commercially available Lewis adducts of SO_3 . *Obtained from The Engineering Toolbox: pK_{aH} values of amines, diamines and heterocyclic compounds.

Entry	R_3N	Structure	Conjugate Acid	N -AO Hybridisation	* pK_{aH}
1	Me_3N			sp^3	10.63
2	Et_3N			sp^3	11.01
3	DMF			sp^2	N/A
4	Py			sp^2	5.23

The reactivity of $R_3N \bullet SO_3$ are proportional to the Lewis basicity of the amine, which directly correlates to the pK_{aH} of its conjugate acid (Table 7). Me_3N and Et_3N have the highest pK_{aH} values (Table 7, Entries 1 and 2) and the nitrogen's atomic orbitals are sp^3 hybridised (Figure 38). Consequently, the electron lone pair is highly localised, and resides in a hybrid orbital with more p character (25% s, 75% p). Therefore, the electrons are further away from the atomic nucleus and are of higher energy, thus sp^3 hybridised amines are hard Lewis bases that can donate their electron pair more efficiently into the lowest unoccupied molecular orbital (LUMO) of SO_3 (Figure 37).

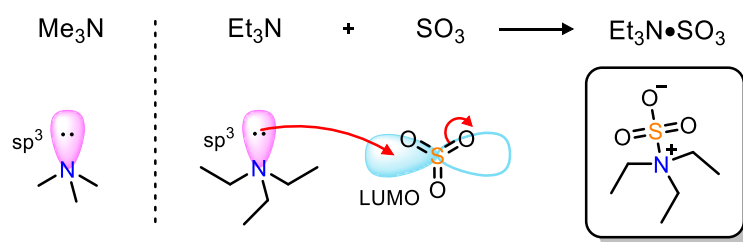


Figure 37: Orbital diagrams of Me_3N/Et_3N and SO_3 with the structure of the Lewis adduct $Et_3N \bullet SO_3$.

Hence, Me_3N and Et_3N afford stable, hard-hard Lewis adducts with SO_3 (which is a hard Lewis acid, with a sulfur oxidation state of +6). However, the inherent stability dictates reactivity, and such complexes are not efficient at sulfating phenolic alcohols.⁴⁷

The nitrogen in Dimethylformamide (DMF) is sp^2 hybridised. Consequently, the $\text{DMF}\cdot\text{SO}_3$ complex is highly reactive but the most unstable commercially available sulfating agent.⁴⁶ This can be rationalised by lone pair delocalisation into the carbonyl (Table 7, Entry 3), thus DMF cannot donate its electron pair through nitrogen (Figure 38, A) and the delocalisation of electrons makes DMF a soft Lewis base. Consequently, the poor stability and subsequent reactivity of $\text{DMF}\cdot\text{SO}_3$ can be rationalised by a disfavoured soft-hard Lewis adduct (Figure 38, B).

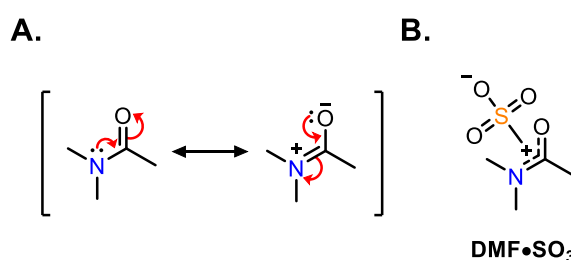


Figure 38: **A)** The resonance structures of DMF; **B)** The structure of $\text{DMF}\cdot\text{SO}_3$ as a soft-hard Lewis adduct.

$\text{Py}\cdot\text{SO}_3$ is also a highly reactive sulfating agent that is sp^2 hybridised at the nitrogen (Table 7, Entry 4). However, unlike DMF, its greater reactivity is due to a different phenomenon. The amine nitrogen is conjugated into the π -bonding aromatic system using its non-hybridized p orbital. Therefore, the electron lone pair is not delocalised into the aromatic system, but resides in a perpendicular sp^2 hybridised atomic orbital (Figure 39). The inherent sp^2 hybridisation gives the lone pair more s character (33% s, 67% p). Thus, the electrons are closer to the atomic nucleus and are of lower energy, stabilised by the +ve nuclear charge. Hence, $\text{Py}\cdot\text{SO}_3$ is a borderline soft Lewis base, so the nitrogen cannot donate its electrons as efficiently into the LUMO of SO_3 , thus

forming a stable but highly reactive Lewis adduct with SO_3 . As a result, the complex can efficiently sulfate all types of alcohol substrates, including phenols.⁴⁶⁻⁴⁹

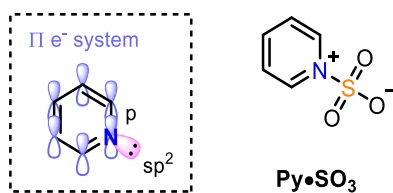
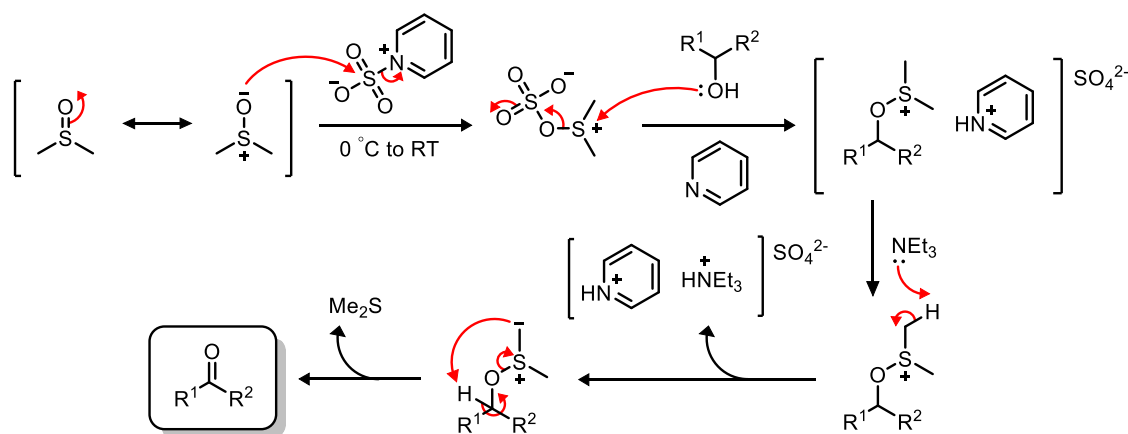


Figure 39: The structure and hybridisation of $\text{Py}\bullet\text{SO}_3$ for the rationalisation of its reactivity.

$\text{Py}\bullet\text{SO}_3$ is employed in the Parikh-Doering oxidation for the conversion of alcohols to aldehydes and ketones (Scheme 20).⁵² Furthermore, the synthesis of guanidinium sulfates, using $\text{Py}\bullet\text{SO}_3$ as the primary sulfating agent, is shown to be an efficient technique for the absolute stereochemical determination of chiral alcohols.⁵³



Scheme 20: The Parikh-Doering oxidation reaction for the sulfation of alcohols.⁵⁴ R^1 = alkyl, R^2 = Alkyl or H

4.5. The Per-Sulfation of Alcohols Using $\text{R}_3\text{N}\bullet\text{SO}_3$

Driving a persulfation reaction to completion by sulfating all possible sites on a target substrate is a synthetic challenge, due to significant anionic crowding of multiple sulfate groups. This makes the persulfation of alcohols progressively more difficult and can result in heterogeneous mixtures of semi-sulfated products. Therefore, for the persulfation of alcohols, super-stoichiometric excesses of $\text{R}_3\text{N}\bullet\text{SO}_3$ are readily employed (5-10 eq.).⁵⁴⁻⁵⁵ However, the resulting organosulfates are highly polar, which

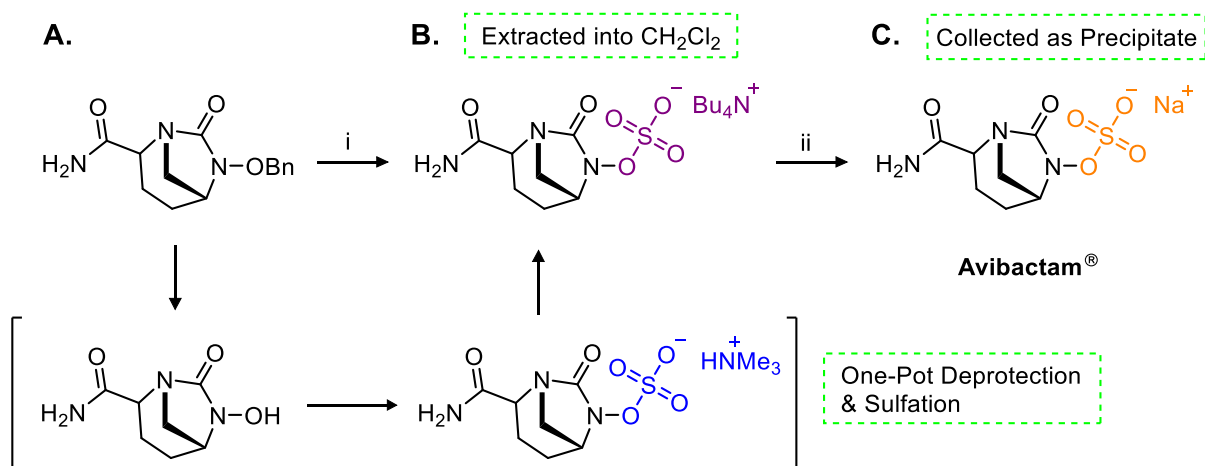
prevents effective liquid–liquid extraction and chromatography (using SiO₂) to isolate a desired persulfate from a crude reaction mixture.

A single sulfate group is polar and strongly hydrophilic, which dictates an organosulfate's overall solubility in (polar/non-polar) organic solvents.⁵⁴ Therefore, sulfation is typically the final step in a synthetic method, and further chemical modifications are limited by solvent incompatibility.⁵⁵ This effect is amplified in the synthesis of persulfates due to the multiple organosulfate motifs in a single structure, thus making aqueous-based purification techniques, such as ion-exchange chromatography, standard procedures for the final isolation of organosulfates.⁴⁸⁻⁵¹ However, aqueous-based methods cannot remove impurities as effectively as organic solvent-based purifications, which have the advantage of simply eliminating unwanted (inorganic) impurities due to the hydrophobic effect.⁵⁶ Moreover, aqueous-based purification methods limit sulfation chemistry to small-scale synthesis due to a limited loading capacity of ion-exchange chromatography columns. In summary, the persulfation of alcohols is efficiently carried out by reaction with R₃N•SO₃, but the resulting organosulfates are challenging to isolate by contemporary purification methods.

4.6. Increasing the Solubility of Organosulfates in Organic Solvents

The characteristic hydrophilic nature of organosulfates presents a challenge when designing more efficient and scalable synthetic routes. However, this problem was addressed by Ball and co-workers at AstraZeneca (UK), demonstrating a new manufacturing process for Avibactam® (Scheme 21).⁵⁷⁻⁵⁸ The team presented a one-pot deprotection and sulfation of a hydroxylamine intermediate using Me₃N•SO₃ as the sulfating agent (Scheme 21, A). This was followed by *in situ* ion-exchange with tetrabutylammonium acetate (TBAOAc), which permitted the extraction of their pure organosulfate intermediate into CH₂Cl₂ (Scheme 21, B).⁵⁷ The addition of sodium-2-

ethyl-hexanoate (NEH) into an EtOH/H₂O (98:2) solution of their organosulfate afforded Avibactam[®] in 90% yield as a pure Na⁺ salt (77% over 2 steps on a Kg scale, Scheme 21C).



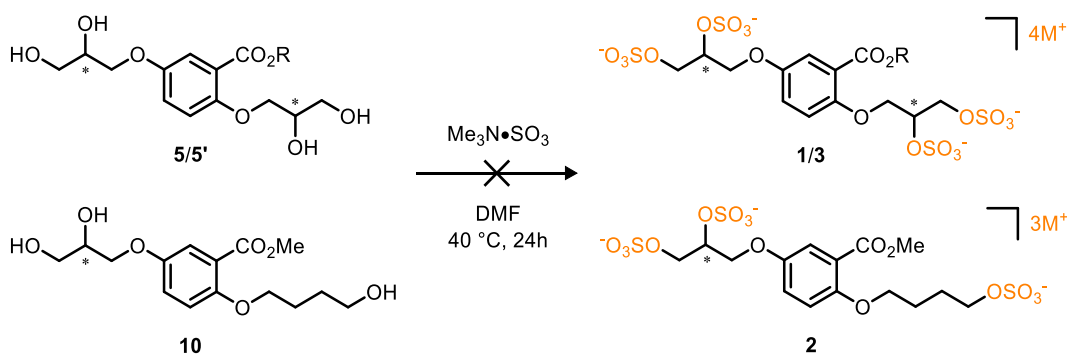
Scheme 21: The final two steps toward synthesis of Avibactam[®]. **A)** Benzyl protected hydroxylamine intermediate; **B)** Organosulfate as its lipophilic TBA salt; **C)** Avibactam as its desired Na⁺ salt. **i)** 1. H₂, Pd/C, Me₃N•SO₃; Et₃N, ^tPrOH (aq.), 2. TBAOAc, CH₂Cl₂, methyl isobutyl ketone, **85%**; **ii)** NEH, EtOH/H₂O (98:2) **90%**.⁵⁷

This process route demonstrated that the hydrophilicity of organosulfates can be diminished by increasing the alkyl chain length of the corresponding ammonium cation, which permitted efficient extraction into a non-polar organic solvent.⁵⁷⁻⁵⁸ Furthermore, the work also highlights that organosulfates can be precipitated out of organic solution by mass action,⁵⁹ affording the Na⁺ salts without requiring aqueous-based ion-exchange techniques. This methodology was applied to the sulfation of phenols, benzyl alcohols and anilines. Moreover, lipophilic alkyl ammonium salts of phenolic organosulfates were used to promote site selective C–H aryl-borylations through ion-pair electrostatic interactions.⁶⁰

4.7. Results and Discussion

4.7.1. Finding a Reliable Sulfation Method for the Synthesis of HS-Glycomimetics 1-3

The use of $R_3N\bullet SO_3$ were proposed to be the most viable reagents for the synthesis of HS-glycomimetics **1-3**. This was primarily due to their commercial availability, and effectiveness at installing multiple sulfate groups onto a single molecule.⁴⁸⁻⁵⁰ Moreover, the original report by Raiber et. al.⁶¹ used $Me_3N\bullet SO_3$ as the primary sulfating agent in the synthesis of **1-3** (Scheme 22). However, initial attempts at following the literature procedure gave poor results and afforded no persulfated material (Table 8, Entry 1).⁶¹ Repetitions of the literature method gave parallel results, and the consistently poor outcomes encouraged a screening of reagents and conditions to find a more reliable synthetic method for the necessary persulfation of polyol precursors (Table 8).



Scheme 22: The unsuccessful synthesis of HS-glycomimetics **1-3** following the only known literature procedure.⁶¹ R = H, Me or Na; M⁺ = [R₃NH]⁺ or Na.

Qualitative analysis of the aforementioned reactions by thin layer chromatography (TLC) displayed full conversion of tetraol **±5** in 24 h. However, no persulfated material (**±1**) was isolated, and it was proposed that **±5** had not reacted fully with $Me_3N\bullet SO_3$ (Table 8, Entry 1), affording a heterogeneous mixture of partly sulfated products. This was unverified by ¹H-NMR analysis because no material could be extracted from DMF, H₂O or directly isolated by chromatography (SiO₂).

To drive full conversion of **±5**, the literature procedure was adapted to use the more reactive sulfating agent, Py•SO₃ (Table 8, Entry 2). Monitoring the reaction by TLC analysis, again, highlighted that no tetraol **±5** was present in the reaction mixture. However, attempts at liquid-liquid extraction were unsuccessful and isolation of any starting material or sulfated material by chromatography (SiO₂, 100% MeOH) was unsuccessful. This was initially attributed to the significant polarity and hydrophilicity of tetraol **±5** and persulfate **±1**, thus attempts at liquid-liquid extraction were considered impractical and were stopped altogether. However, no tetraol **±5** was isolated by chromatography, which suggested that all of **±5** had been converted to a suspected persulfated intermediate, quantitatively agreeing with the TLC analysis. Overall, after multiple attempts, no organosulfate species (**±1**) could be isolated as the trimethylammonium ([Me₃NH]⁺) or pyridinium ([PyH]⁺) salts following the original literature procedure.

Changing the solvent from DMF to Py was effective, furthermore, it could be removed under reduced pressure to permit ¹H-NMR analysis of the crude reaction mixture (Table 8, Entry 3). The suspected persulfate **±1** was witnessed due to a single (singlet) peak assigned to the methyl ester (along with residual Py•SO₃ in the aromatic region). However, attempts to isolate **±1** by chromatography were also unsuccessful, thus all efforts at isolating any material by chromatography were considered impractical, and the investigation opted for a more effective isolation technique.

It was discovered that, on further inspection of the original literature report, the glycomimetics **1-3** were assigned as their bisulfate esters.⁶¹ Furthermore, all subsequent investigations testing the HS-glycomimetic's biological activity also reported **1-3** as their bisulfate esters.⁶²⁻⁷² These species are highly unstable (Chapter 4.4.1),³⁴⁻³⁵ so it is proposed that the original report disregarded this, and unsuspectingly

isolated persulfates **1-4** as their $[\text{Me}_3\text{NH}]^+$ salts (from $\text{Me}_3\text{N}\cdot\text{SO}_3$). Me_3N is toxic, and the significance this has on biological activity was not considered. Therefore, to improve upon previous work and remove ambiguity from future results, this investigation opted to synthesise all final HS-glycomimetics as their pure Na^+ salts.

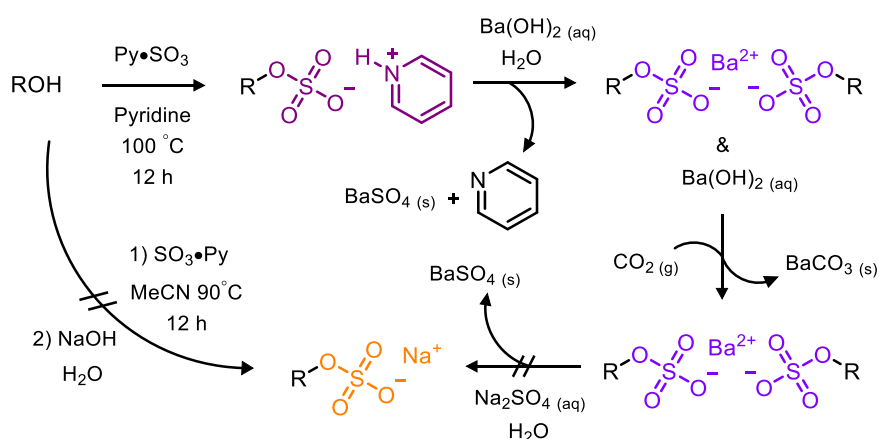
Table 8: The screening of reagents and conditions for the synthesis of glycomimetic **±1**. ^aCould not be isolated; ^bIsolated as a crude mixture of Na^+ and ammonium salts; ^cHydrolysed the methyl ester.

Entry	NR_3	Conditions	% Conversion (NMR)	Isolation method	% Yield	Ref.
1	NMe_3	DMF, 40 °C, 24 h	N/A	SiO_2 , MeOH	N/A ^a	61
2	Py	DMF, 40 °C, 24 h	N/A	SiO_2 , MeOH	N/A ^a	–
3	Py	Pyridine, 100 °C, 12 h	100	SiO_2 , MeOH	N/A ^a	61
4	Py	Pyridine, 100 °C, 12 h	100	$\text{Ba}(\text{OH})_2$ (aq.), CO_2 , Na_2SO_4	1-2 ^b	38
5	Py	Pyridine, 100 °C, 12 h	100	NaOH (aq.)	20 ^{b,c}	–
6	Py	MeCN, 90 °C, 24 h	100	NaOMe/MeOH	20 ^{b,c}	–
7	NMe_3	NEt_3 , $i\text{PrOH}$, H_2O , 40 °C, 12 h	N/A	TBAOAc, CH_2Cl_2 , NEH, EtOH/ H_2O	N/A ^a	57

A primary aim of the overall investigation is to provide an efficient and scalable synthesis of HS-glycomimetics **1-3**. Therefore, the use of ion-exchange chromatography was not warranted, as it can limit the scalability of the overall

synthesis. Consequently, this investigation opted for an *in situ* ion-exchange for the isolation of all (final) persulfated compounds.

Initial attempts to isolate **±1** as its tetrakis Na⁺ salt investigated an aqueous-based double salt exchange (Table 8, Entry 4) adapted from a procedure set by Deno et al.³⁸ Theoretically, the addition of Ba(OH)₂ (aq.) to a crude reaction mixture of **±1** hydrolysed any excess Py•SO₃, which precipitated out of solution as BaSO₄ (s) and was removed by filtration (Scheme 23). The liberated pyridine was removed under reduced pressure, affording a solution of Ba(OH)₂ and **±1** as its suspected Ba²⁺ salt. The removal of excess Ba(OH)₂ by addition of CO₂, precipitating BaCO₃ (s), affording a solution of **±1** (as its suspected Ba²⁺ salt). Final addition of Na₂SO₄ exchanged out the Ba²⁺, leaving a solution of **±1** as the intended Na⁺ salt (Scheme 23). Dehydration of the final solution afforded 1 – 2% isolated yield of crude material, and ¹H-NMR analysis confirmed the synthesis of **±1** as a mixture of its Na⁺ and [PyH]⁺ salts. Overall, this first attempts at an alternate isolation method was intricate and gave unsatisfactory results.



Scheme 23: The isolation of organosulfate-Na⁺ salts via hydrolysis. Adapted from Deno et. al.³⁸

Efforts to streamline the previous isolation method using NaOH (aq.) directly (Table 8, Entry 5) also afforded **±1** as a mixture of Na⁺ and [PyH]⁺ salts, but with an improved yield (20%) of crude isolated material (Scheme 23). Unfortunately the conditions

hydrolysed $\pm\mathbf{1}$ to give the carboxylate salt ($\pm\mathbf{3}$) as an impurity. Consequently, all aqueous based *in situ* ion-exchange procedures were stopped.

Hydrolysis of the crude intermediate using NaOMe in MeOH gave similar results (Table 8, Entry 6), affording $\pm\mathbf{1}$ as a crude mixture of Na^+ and $[\text{PyH}]^+$ salts. It was suspected that the $[\text{PyH}]^+$ intermediate was stable to basic hydrolysis, thus all attempts at isolating $\pm\mathbf{1}$ by hydrolysis with NaOH/NaOMe were halted and further routes were deliberated.

The synthesis of $\pm\mathbf{1}$ was attempted following the procedure adapted from Ball et. al. (Table 8, Entry 7).⁵⁷ It was proposed that this ion-exchange methodology would synthesise a less hydrophilic organosulfate that is soluble in organic solvents, thus facilitating a more efficient extraction, purification and ion-exchange to a desired tetrakis Na^+ salt. However, no final persulfated material ($\pm\mathbf{1}$) could be isolated.

The results of this study highlighted the complications encountered using established sulfation methods towards the synthesis of persulfates, especially small molecule HS-glycomimetics (**1-3**). However, the results also demonstrated that $\text{R}_3\text{N}\bullet\text{SO}_3$ are efficient reagents for the persulfation of alcohols. Therefore, it was concluded that the synthesis of $\pm\mathbf{1}$ was obstructed by its poor solubility in organic solvents, which prevented an effective isolation to gain either the $[\text{Me}_3\text{NH}]^+$, $[\text{PyH}]^+$ or Na^+ salts. Attempts at synthesising a more lipophilic organosulfate were unsuccessful, and the use of ion-exchange resins were also considered.⁷³ However, $\pm\mathbf{1}$ could not be isolated in all cases.

Overall, this investigation sought to design an innovative synthetic methodology, for the persulfation of alcohols, which overcomes the poor solubility of the intermediate organosulfates in organic solvents, and facilitate their efficient isolation as ammonium or biologically relevant Na^+ salts.

4.7.2. The Rational Design of SO₃ Tributylamine Complex

The investigation proposed the design of an all-in-one reagent which could be used for the sulfation of alcohols and enhance the lipophilicity of the intermediate organosulfate esters. Therefore, it was envisioned that the Lewis adduct of tributylamine (Bu₃N) and SO₃ would provide a reagent (Bu₃N•SO₃) suitable for the sulfation of alcohols, and the increased length of the alkyl chains could improve the solubility of the organosulfates in organic solvents, similar to the [Bu₄N]⁺ intermediates demonstrated by Ball et al (Figure 40).⁵⁷

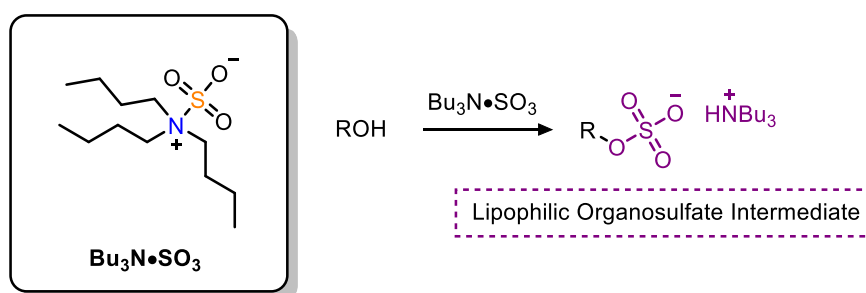


Figure 40: The proposed sulfation of alcohols with Bu₃N•SO₃. (R = Alkyl or Aryl.)

A comparison of the pK_{aH} and log P values of familiar sp³ hybridised tertiary amines were in agreement with the proposed hypothesis, and it was rationalised that the Bu₃N•SO₃ complex would be of similar reactivity, and stability (Chapter 4.4.5), to the SO₃ Lewis adducts of Et₃N and Me₃N (Table 9, Entries 1 and 2). Furthermore due to the significantly greater Log P value of the corresponding tributylammonium cation ([Bu₃NH]⁺, Table 9, Entry 4), Bu₃N•SO₃ is expected to afford lipophilic (hydrophobic) organosulfates upon reaction with hydroxyl bearing substrates.

It was anticipated that an improved lipophilicity of the intermediate organosulfate-[Bu₃NH]⁺ species would facilitate a simpler extraction and isolation by contemporary methods, such as chromatography (SiO₂). Furthermore, in similar accordance to the Ball synthesis of Avibactam[®],⁵⁷ a lipophilic organosulfate species would permit an *in situ* ion-exchange to a desired Na⁺ salts. Moreover, an enhanced solubility in organic solvents could

permit sequential chemical steps, so sulfation/persulfation would not be limited to the final step in an overall synthetic method.

Table 9: The relative pK_{aH} and Log P values of sp^3 hybridised tertiary amines

Entry	Amine	$[R_3NH]^+$	pK_{aH}	Log P
1	Me ₃ N	$[Me_3NH]^+$	10.63	0.22
2	Et ₃ N	$[Et_3NH]^+$	11.01	1.28
3	Pr ₃ N	$[Pr_3NH]^+$	10.26	2.65
4	Bu ₃ N	$[Bu_3NH]^+$	10.89	4.01

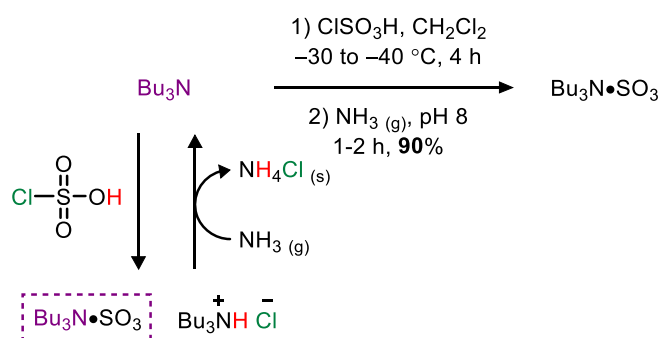
Consequently, it was expected that Bu₃N•SO₃ would streamline the synthesis of organosulfates and, more importantly, would be advantageous to the synthesis of persulfates (such as HS-glycomimetics **1-3**). Additionally, this methodology was also considered applicable to the sulfation of amino acids and further biologically relevant molecules, such as β-estradiol and cortisol. Therefore, this investigation aimed to synthesise the complex Bu₃N•SO₃, design and optimise a synthetic methodology toward the synthesis of organosulfates and persulfates, and exhibit this new methodology in the sulfation of natural products and biologically relevant compounds, including examples of original HS-glycomimetics **±1** and **R-2**.

4.7.3. The Synthesis of Bu₃N•SO₃

The only literature report pertaining to the synthesis of Bu₃N•SO₃ was a physicochemical study by Moede et. al. in 1949, whereby Bu₃N was directly reacted with SO₃ (l) in CCl₄ (0 °C).⁷⁴ However, no isolated yield or characterisation data was reported, with the exception of a melting point (94 °C).⁷⁴ Nonetheless, in 1976, Parshikov and co-workers studied Bu₃N•SO₃ for the sulfation of simple aliphatic alcohols (without spectroscopic characterisation).⁷⁵⁻⁷⁶ The results of this investigation proposed that

$\text{Bu}_3\text{N}\bullet\text{SO}_3$ reacts via an $\text{S}_{\text{N}}2$ mechanism driven by the hydrogen bonding propensity of the alcohol substrate. Mechanistically, this suggests that the reactivity of $\text{R}_3\text{N}\bullet\text{SO}_3$ are not solely dependent on the Lewis basicity of the coordinating amine and the overall stability of the Lewis adduct (See Chapter 4.4.5). Thus, $\text{Bu}_3\text{N}\bullet\text{SO}_3$ was hypothesised to be able to sulfate all alcohol types, similar to $\text{Py}\bullet\text{SO}_3$, and the sulfation of phenolic substrates was also considered by this investigation. Most importantly, no further use or development of $\text{Bu}_3\text{N}\bullet\text{SO}_3$ has been reported.

The synthesis of $\text{Bu}_3\text{N}\bullet\text{SO}_3$ was carried out by reaction of Bu_3N with ClSO_3H , affording the complex in 90% isolated yield on a 60 g scale (0.50 mol. See Appendix, Chapter 6.2). An equimolar addition of the two reagents is in 2:1 stoichiometric ratio, respectively. Therefore, the latter addition of NH_3 (g) was critical, to improve the overall yield by converting any $[\text{Bu}_3\text{NH}]\text{Cl}$ by-product back to Bu_3N for further reaction with ClSO_3H , liberating NH_3Cl (s) as a precipitate (Scheme 24). The reaction was found to be highly exothermic, so the use of lower operating temperatures (-30 to -40 °C) was favourable to the overall yield of desired product.



Scheme 24: The synthesis of $\text{Bu}_3\text{N}\bullet\text{SO}_3$.

For the first time, both ^1H and ^{13}C -NMR spectral data and the crystal structure of $\text{Bu}_3\text{N}\bullet\text{SO}_3$ were obtained (Figure 41, see Appendix for full data). Examination of the crystal structure reveals that in the solid state, $\text{Bu}_3\text{N}\bullet\text{SO}_3$ adopts a gauche conformation

within an asymmetric unit cell. This is proposed to be caused by hydrogen bonding between the methylene hydrogen atoms, α to the nitrogen, and the oxygen atoms of SO_3 . The measured N–S bond length is $1.886(\pm 3) \text{ \AA}$, which is comparable to a single covalent N–S bond length (typically: $1.73 - 1.83 \text{ \AA}$, compared to 2.06 \AA for a donor–acceptor system).⁷⁷⁻⁷⁸ Furthermore, the bond angle between oxygen atoms is $115.69(\pm 4)^\circ$, which shows that the tetra-coordinate sulfur adopts a more tetrahedral-like geometry to accommodate the addition of an electron pair into the LUMO. Additionally, this could also be attributed to steric repulsion from the methylene groups. Overall, the data suggests that the $\text{Bu}_3\text{N}\bullet\text{SO}_3$ Lewis adduct exists as a betaine in the solid state, which may have implications to its reactivity and the mechanism of sulfation.

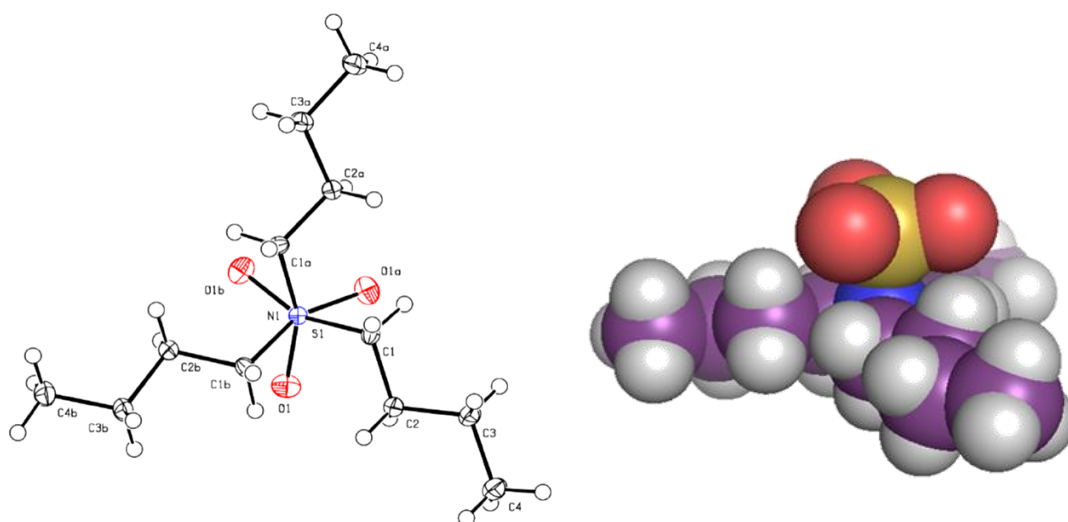


Figure 41: Ortep and space filling model of the $\text{Bu}_3\text{N}\bullet\text{SO}_3$ crystal structure, obtained from small molecule single crystal X-Ray diffraction. Ellipsoids drawn at the 50% probability level. (Crystal structure solved by Dr L. Male.).

4.7.4. Optimisation and Rate Studies

Optimisation studies of $\text{Bu}_3\text{N}\bullet\text{SO}_3$ were carried out using benzyl alcohol (BnOH) as the chromophore of BnOH made it possible to qualitatively measure sulfation by TLC. Furthermore, analysis of the crude ^1H -NMR data presented a distinct down-field shift

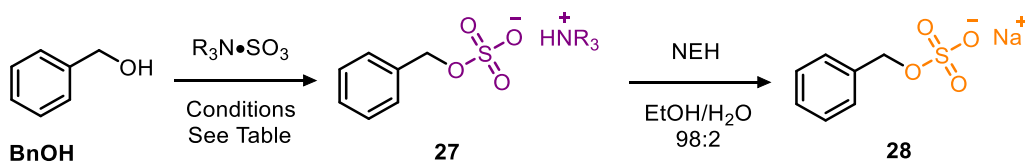
(+0.35 ppm) of the benzylic protons' signal (post sulfation). This made time course ^1H -NMR studies possible for the efficient analysis of different reaction conditions (Table 10).

The chosen solvent was Acetonitrile (MeCN), as previous reports advocate it as a compatible solvent for the sulfation of alcohols.⁴⁹ Furthermore, it has a high boiling point (82 °C) and is safe to use in a microwave reactor. Additionally, MeCN can be removed effectively under reduced pressure, giving it the advantage over alternative polar aprotic solvents, such as DMF. The *in situ* ion-exchange was also considered an essential part of the optimisation study, to determine if it was possible to isolate the resulting benzyl sulfate as its Na^+ salt (**28**). Thus the (crude) intermediate organosulfate- $[\text{Bu}_3\text{NH}]^+$ species (**27**) were subjected to ion-exchange with NEH following a procedure adapted from Ball et. al.⁵⁷ All concentrations were kept at 0.5 Mol dm^{-3} and the results of the optimisation study provided an analyses of 19 point changes to the reaction conditions, there are summarised (Table 10).

By examining the sulfation of BnOH with increasing stoichiometric equivalents of $\text{Bu}_3\text{N}\cdot\text{SO}_3$ (Table 10, Entries 1 – 4), it was discovered that 2.0 equivalents was the minimal stoichiometry for high conversions (>99%) and isolated yields (95%, Table 10, Entry 3). Less than 2.0 equivalents gave incomplete conversion to intermediate **27** within 8.0 h (Table 10, Entries 1 and 2). The effects of temperature was also investigated (Table 10, Entries 5 – 8 vs. Entry 3), and it was discovered that 90 °C (heating under reflux) using 2.0 equivalents of $\text{Bu}_3\text{N}\cdot\text{SO}_3$ gave complete conversion to **27** within 2 h. Notably, full conversion was also achieved at 30 °C (120 h, 5 days, Table 10, Entry 7) highlighting that $\text{Bu}_3\text{N}\cdot\text{SO}_3$ would be suitable for the sulfation of temperature sensitive substrates, such as proteins.⁵⁴ In order to provide a more valid assessment of the reaction conditions, the operating temperatures for the optimisation study were decreased to 70 °C. This extended

the time period for full conversion to **27**, and allowed for a more accurate assessment of reactivity based on time course $^1\text{H-NMR}$ spectra data (Figure 43, C).

Table 10: The Optimisation of sulfation on a model system. ^a**28** was not isolated; ^b**27** was isolated as the pyridinium salt; ^cadditive used during work-up; ^dmicrowave irradiation.



Entry	R ₃ N•SO ₃	Equivalence	T (°C)	t (h)	Additive	Conversion @ 0.5 h (%)	Conversion @ t (%)	Isolated yield (%)
1	Bu ₃ N	1.1	90	8.0	–	48	83	41
2	Bu ₃ N	1.5	90	4.0	–	26	69	62
3	Bu ₃ N	2.0	90	1.0	–	90	>99	95
4	Bu ₃ N	4.0	90	0.5	–	>99	>99	95
5	Bu ₃ N	2.0	70	6.0	–	22	>99	96
6	Bu ₃ N	2.0	50	8.0	–	9	60	58
7	Bu ₃ N	2.0	30	120.0	–	2	>99	96
8	Bu ₃ N	2.0	20	18.0	–	1	9	^a
9	Py	2.0	70	0.5	–	>99	>99	17 ^b
10	Py	2.0	70	0.5	TBAI ^c	>99	>99	47
11	Py	2.0	70	0.5	TBAOAc ^c	>99	>99	76
12	Me ₃ N	2.0	70	6.0	–	3	29	^a
13	Me ₃ N	2.0	70	6.0	TBAI	–	88	^a
14	Bu ₃ N	2.0	105 ^d	0.5	–	68	68	^a
15	Bu ₃ N	2.0	120 ^d	1.0	–	68	68	^a
16	Bu ₃ N	2.0	70	2.0	Na ₂ CO ₃	16	57	^a
17	Bu ₃ N	2.0	70	2.0	K ₂ CO ₃	8	8	^a
18	Bu ₃ N	2.0	70	2.0	Et ₃ N	15	34	^a
19	Bu ₃ N	2.0	70	6.0	Bu ₃ N	48	60	^a

Two commercially available complexes were also examined for comparison, $\text{Py}\bullet\text{SO}_3$ and $\text{Me}_3\text{N}\bullet\text{SO}_3$ (Table 10, Entries 9 and 12, respectively). $\text{Py}\bullet\text{SO}_3$ demonstrated a greater reactivity than $\text{Bu}_3\text{N}\bullet\text{SO}_3$, giving full conversion in 0.5 h, which is not surprising considering the different nature of the Lewis adduct (See Chapter 4.4.5). However, only 17% of the intermediate **27** (as the $[\text{PyH}]^+$ salt) could be isolated. As control experiments, the sequential exchange of the **27**- $[\text{PyH}]^+$ salt with different TBA salts facilitated the isolation of **28** in 47% and 76% yield, for TBAI and TBAOAc respectively (Table 10, Entries 10 and 11). $\text{Me}_3\text{N}\bullet\text{SO}_3$ demonstrated a 29% conversion in 6 h, but no sulfated material (**27** nor **28**) could be isolated. Surprisingly, the addition of TBAI improved the rate of conversion to 88% (Table 10, Entry 13). However, a more complex reaction mixture was unfavourable to the isolation of **28**, which highlights the benefits associated with the use of $\text{Bu}_3\text{N}\bullet\text{SO}_3$.

High conversions were achieved without microwave irradiation, contradicting other reports of sulfating agents and conditions⁴⁹ (Table 10, Entries 1 – 7 vs. 14 – 15). The addition of a hetero- or homogenous bases (Table 10, Entries 16 – 19) led to a reduced rate of conversion. Most notably, the addition of Bu_3N (Table 10, Entry 19) initially increased the rate of conversion to **27** but reduced the overall conversion to 60% after 6.0 h. This result is in conflict with other reports.⁴⁹ It was rationalised that the addition of Et_3N forms the more stable Lewis adduct $\text{Et}_3\text{N}\bullet\text{SO}_3$ *in situ*, due to its slightly greater pK_{aH} value, reducing the reactivity of the complex and the rate of conversion. This is in similar accordance to the observed reaction of Et_3N with $\text{Py}\bullet\text{SO}_3$.⁴⁶

Finally, the sulfation of different alcohol types (secondary and phenolic) was also investigated, which highlighted that a secondary alcohol (1-phenyl-ethanol) reacts slower initially, but full conversion (>99%) is achieved in a similar time to BnOH (Figure 42, B). This can be attributed to the effects of sterics in the vicinity to the reaction center. The phenolic alcohol (*p*-Guaiacol) was sulfated the slowest but demonstrated an 88%

conversion in 8.0 h. Overall, the positive results of this investigation query the previously proposed hypothesis, which suggests that the rate of sulfation is dependent on the hydrogen bonding propensity of the alcohol undergoing sulfation.⁷⁵⁻⁷⁶ It is more probable that rate is also dependent on the hardness of the (hydroxyl) nucleophile, which can account for the slower rate of conversion in the sulfation of phenols, due to electron delocalisation into the aromatic system. More importantly, the results confirmed that $\text{Bu}_3\text{N}\cdot\text{SO}_3$ can sulfate all alcohol types (Figure 42, B).

% Conversions were calculated using the following equation:

$$\frac{\text{Integral of benzylic protons post-sulfation (+0.35 ppm)}}{(\text{Integral of benzylic protons post-sulfation (+0.35 ppm)}) + (\text{Integral of benzylic protons})} \times 100$$

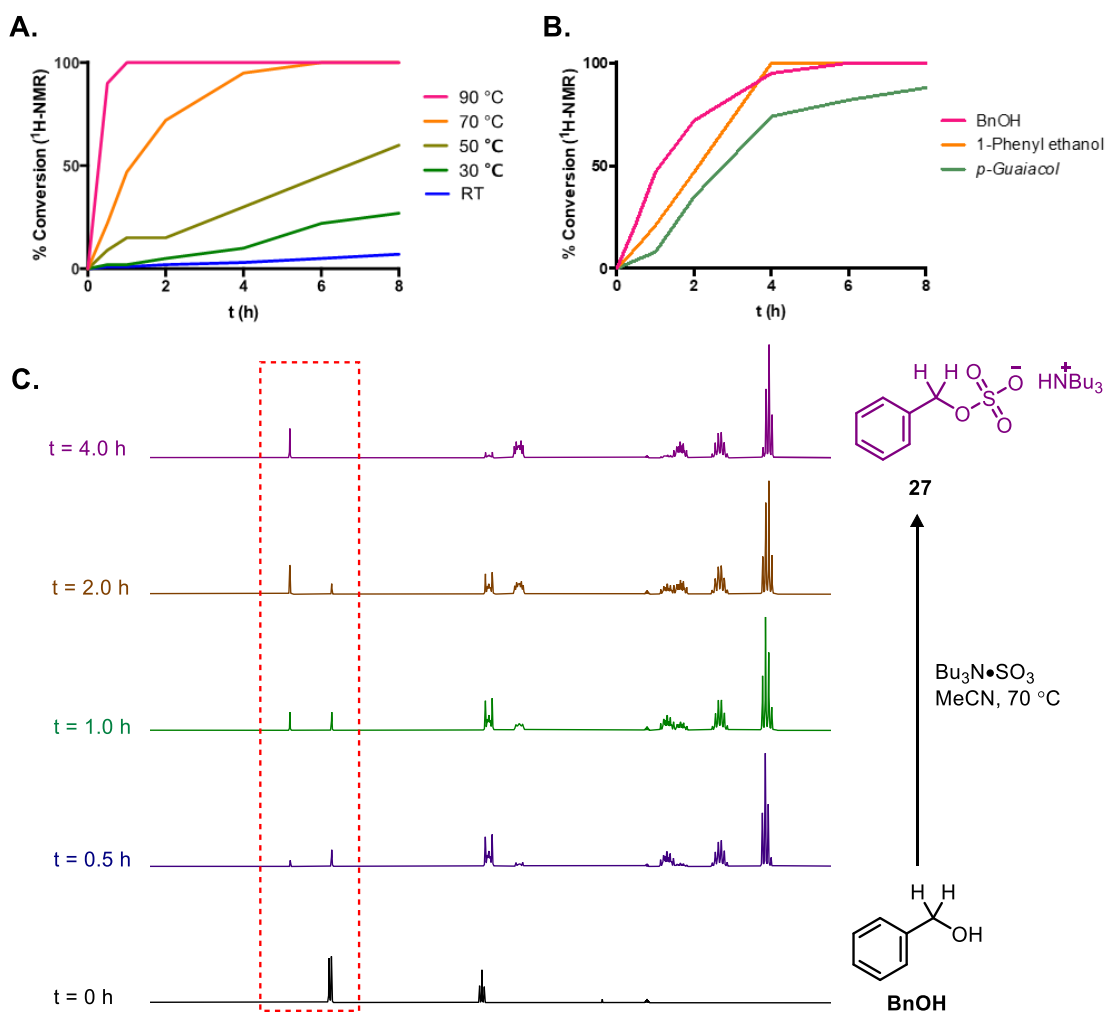


Figure 42: **A)** The % conversion over time of BnOH to **27** at different temperatures using 2.0 eq. of $\text{Bu}_3\text{N}\cdot\text{SO}_3$; **B)** The % conversion over time of different alcohol types using 2.0 eq. of $\text{Bu}_3\text{N}\cdot\text{SO}_3$ at 70 °C; **C)** Time period $^1\text{H-NMR}$ for the synthesis of **27**, using 2.0 eq. of $\text{Bu}_3\text{N}\cdot\text{SO}_3$ at 70 °C. **Black:** BnOH; **Purple:** Conversion at 0.5 h (22%); **Green:** Conversion at 1 h (47%); **Orange:** Conversion at 2.0 h (72%) and **Violet:** Conversion at 4.0 h (95%). At 6.0 h full conversion was achieved (Table 10, Entry 5).

4.7.5. An Analysis of Steric and Electronic Parameters

We applied the optimised conditions to the synthesis of substituted benzylic and phenolic sulfates. In all examples a near-quantitative conversion was observed to the corresponding organosulfate- $[\text{Bu}_3\text{NH}]^+$ intermediates (**27a-f**), independent of both steric and electronic parameters (Figure 43). However, significant differences were observed when converting the highly soluble, lipophilic intermediates into crystalline Na^+ salts (**28a-f**). This was attributed to the likely variable solubility of the Na^+ salts in organic based solvents, due to the presence of different polar groups.

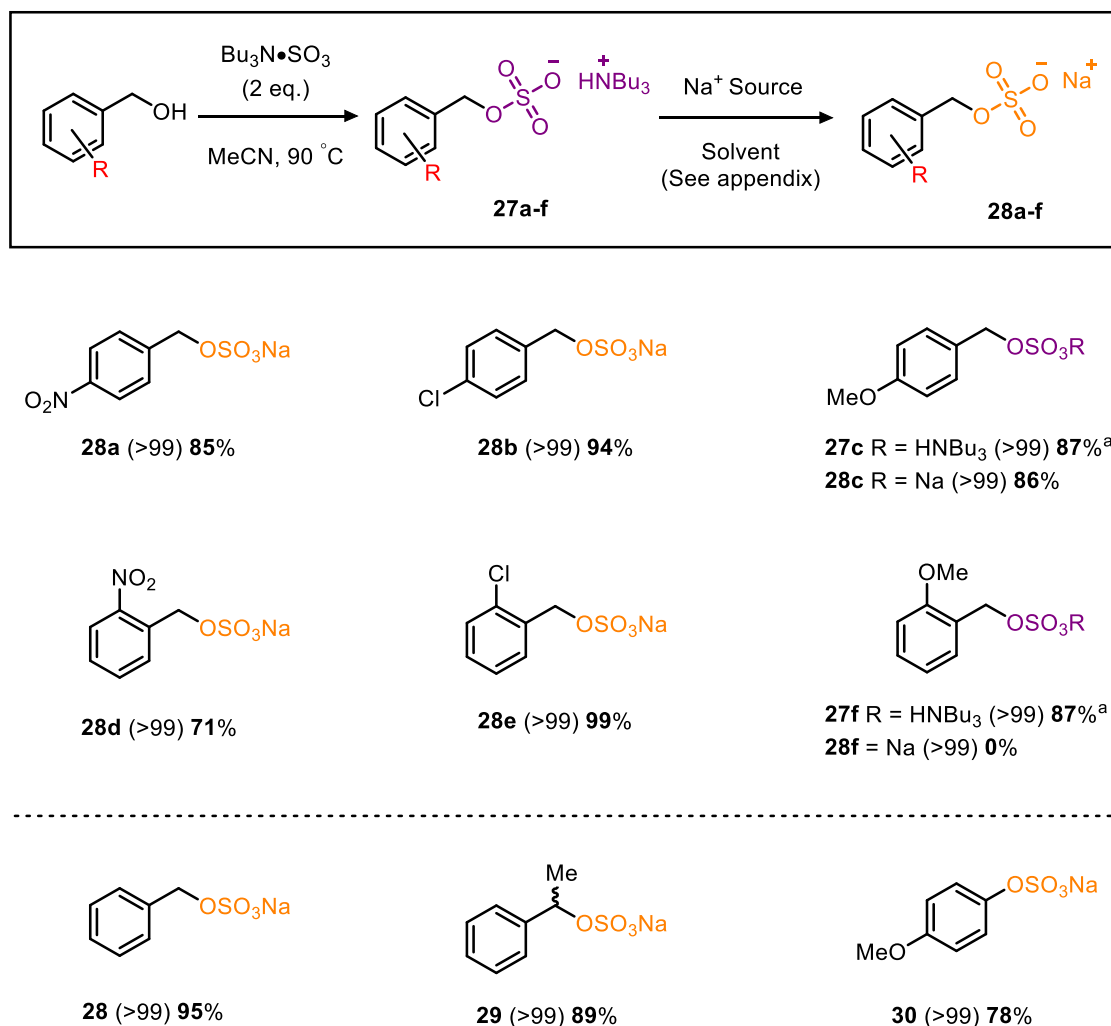


Figure 43: The application of optimised methodology to benzylic and phenolic alcohols to analyse changes in steric and electronic factors. (Parentheses indicates reaction conversion as measured by ^1H -NMR spectroscopy.) ^aIsolated by chromatography (SiO_2).

Notably, the electron withdrawing (nitro) derivatives, **28a** and **28d**, did not precipitate from the original *in situ* ion-exchange conditions. However, increasing the lipophilicity of the solvent provided an alternate set of conditions that was used by further investigations, and the Na⁺ salts were isolated in good yields (71% and 85%, respectively).

Additionally, the electron-donating (methoxy) derivatives, **28c** and **28f**, did not undergo successful ion-exchange, and a change to the more lipophilic solvent system was also unsuccessful. This was proposed to be due to the poor affinity of 2-ethylhexanoate anions for [Bu₃NH]⁺ cations *in situ*.⁷⁷ The affinity of different anions for quaternary ammonium cations is known (Figure 44, A).

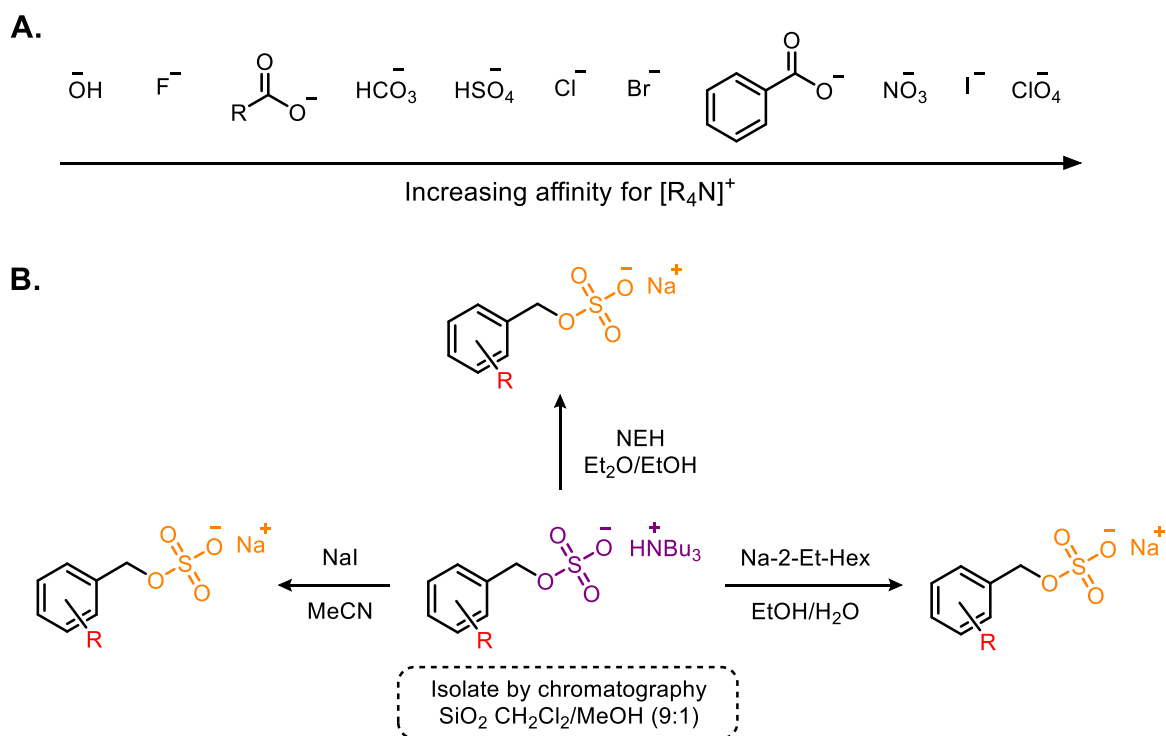


Figure 44: **A)** The different affinities of anions for ammonium ions in organic solution. Adapted from Fritz.⁷⁷ **B)** illustrating the three *in situ* ion-exchange conditions for the precipitation of organosulfates as their Na⁺ salts. (For R groups, see Figure 43.)

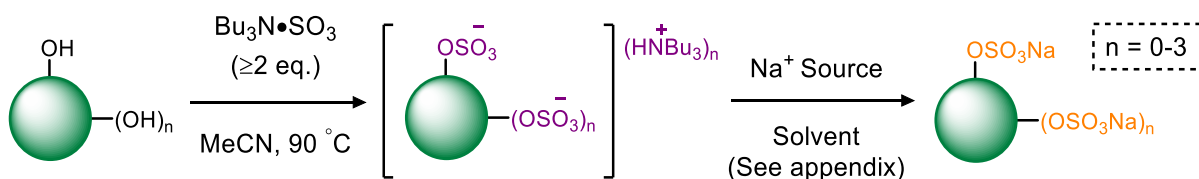
Extrapolation of the data by Fritz⁷⁷ suggested that sodium iodide (NaI) would be a better source of organically soluble Na⁺ ions, and adapting the ion-exchange condition to use NaI was successful for the isolation of sulfate **28c** as its pure Na⁺ salt, in 86% yield. Nonetheless, both **27c** and **27f** were also isolated as their [Bu₃NH]⁺ salts by

chromatography (SiO_2). This work exhibits three different *in situ* ion-exchange protocols that can be used effectively to precipitate organosulfates out of solution as their Na^+ salts (Figure 44, B). Moreover, the enhanced solubility of the $[\text{Bu}_3\text{NH}]^+$ intermediates permits an effective isolation by chromatography (SiO_2).

In short, any variances caused by changes in steric and electronic parameters are difficult to conclude with certainty. Furthermore, steric bulk adjacent to the reacting center is easily accommodated, affording sulfate **29** in 89% isolated yield. Moreover, an ion-exchange method was applied to the phenolic alcohol *p*-Guaiacol, isolating the Na^+ salt **30** in 78% yield. Therefore, the results discussed in this chapter exhibit $\text{Bu}_3\text{N}\cdot\text{SO}_3$ as a powerful reagent for the synthesis of simple organosulfates. The newly developed methodology is practical and straightforward to carry out, and the enhanced lipophilicity of the intermediate $[\text{Bu}_3\text{NH}]^+$ species allows for an efficient extraction and purification of organosulfates, with ion-exchange to their biologically relevant Na^+ salts.

4.7.6. The Persulfation of Alcohols, Amino-Acids and Biologically Relevant Substrates.

The optimised conditions were next applied to compounds containing two or more hydroxyl functionalities and hydroxyl bearing natural products (Scheme 25). Furthermore, the sulfation methodology was also applied to natural products containing different hydroxyl moieties within the same structure, to probe the selectivity profile of $\text{Bu}_3\text{N}\cdot\text{SO}_3$ and gauge any possible chemoselectivity of different hydroxyl environments.



Scheme 25: The general synthesis of complex organosulfates and persulfates using $\text{Bu}_3\text{N}\cdot\text{SO}_3$.

The sulfation of cyclohexane-1,2-diol afforded the disulfate **31** with high conversion and a 91% isolated yield (Figure 45, A). Likewise, the persulfation of glycerol was successful, and the tri-sulfate **32** was afforded as the pure Na⁺ salt (Figure 45, A). The sulfation of (±)-menthol delivered the [Bu₃NH]⁺ salt efficiently (**33**), with a 78% isolated yield after purification by chromatography (SiO₂). For **33**, all hitherto ion-exchange methods afforded no precipitate.

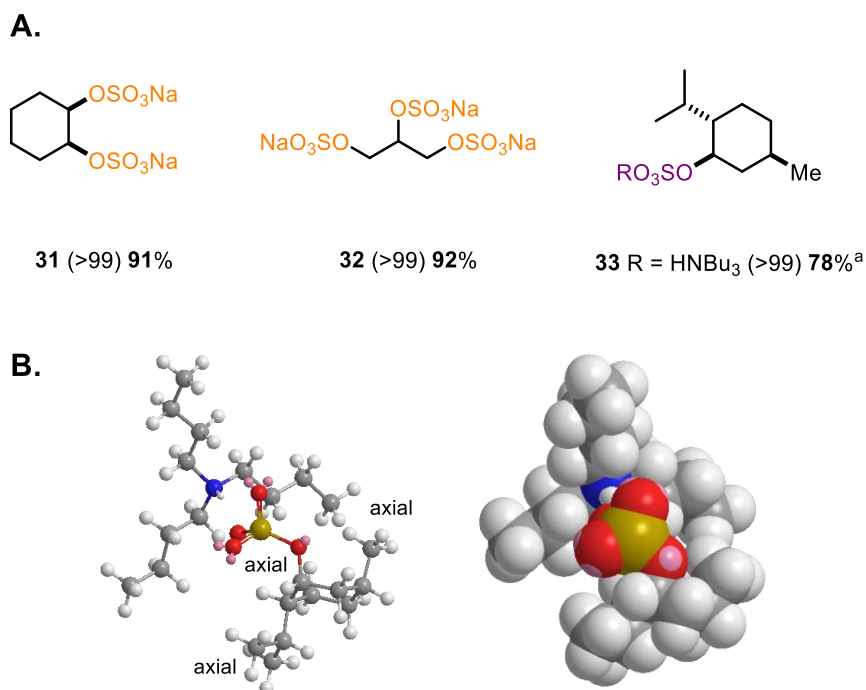


Figure 45: A) The persulfation of complex alcohols. ^aIsolated as [Bu₃NH]⁺ salt. (Parentheses indicate reaction conversion as measured by ¹H-NMR spectroscopy) **B)** Ball and stick and space filling model of **33**, demonstrating its anti-periplanar conformation and intermolecular bonding interactions from the alkyl chains of [Bu₃NH]⁺.

This was ascribed to the stability of the [Bu₃NH]⁺ in solution due to additional Van der Waals interactions between the menthol and the butyl chains. Minimum energy calculations (MM2) are in agreement with this (Figure 45, B), and proposes that all groups adopt an axial geometry where the sulfate and the *t*Pr motif reside in anti-periplanar conformation. Therefore, the ring system is highly strained and the analogous Na⁺ salt is not stabilised by additional intermolecular forces, hence no effective ion-exchange. Attempts to query this hypothesis by ¹H-NMR analysis were considered for a later investigation.

To probe the alcohol selectivity profile of $\text{Bu}_3\text{N}\bullet\text{SO}_3$, a primary alcohol was functionalised in preference to a phenol, affording sulfate **34** in 74% isolated yield (after purification by chromatography). However, adapting the reaction conditions permitted the persulfation of all (phenolic and primary) hydroxyl groups, isolated disulfate **35** in 80% yield as the Na^+ salt (Figure 46).

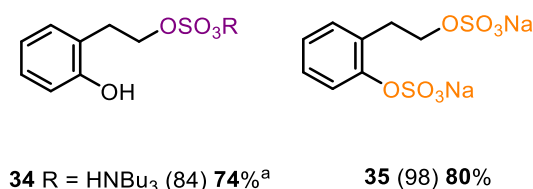


Figure 46: The chemoselective synthesis of sulfate **34** and the synthesis of persulfate **35**. ^aIsolated as $[\text{Bu}_3\text{NH}]^+$ salt. See appendix for conditions. (Parentheses indicate reaction conversion as measured by ^1H -NMR spectroscopy.)

A chemoselective sulfation of β -estradiol afforded the 17- β -estradiol sulfate **36** over the more common metabolite 3- β -estradiol,⁷⁹ in 60% isolated yield as the Na^+ salt. Notably, increasing the equivalence (5.0 per hydroxyl group) of $\text{Bu}_3\text{N}\bullet\text{SO}_3$, both the 17- and 3-positions were sulfated efficiently, affording the disulfate **37** in 84% isolated yield (Figure 47).

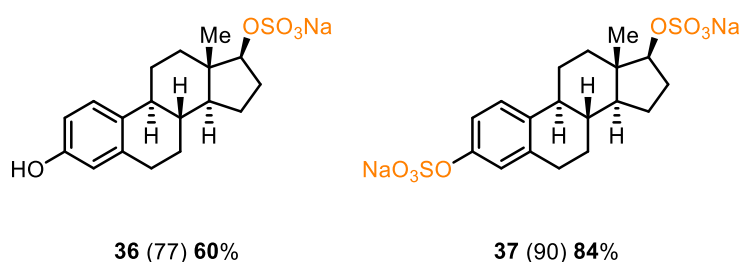
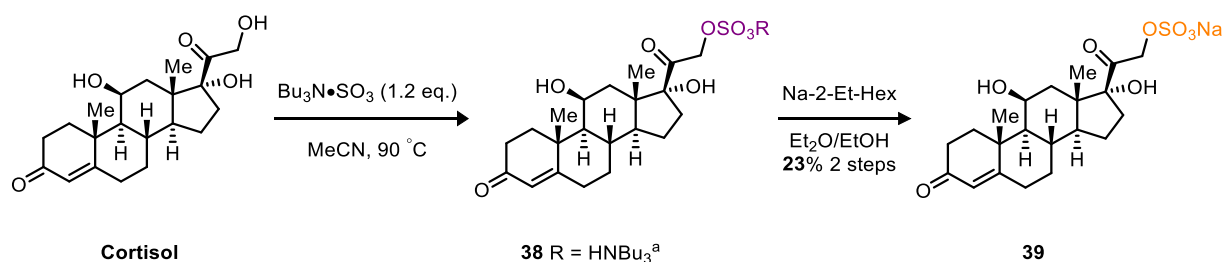


Figure 47: The chemoselective synthesis of sulfate **36** and the persulfate **37**. See appendix for conditions. (Parentheses indicate reaction conversion as measured by ^1H -NMR spectroscopy.)

A chemoselectivity profile of $\text{Bu}_3\text{N}\bullet\text{SO}_3$ was also demonstrated for the hormone Cortisol, as it has primary, secondary and tertiary hydroxyl moieties in its structure (Scheme 26). The investigation opted to sulfate only the primary position to provide a specific metabolite for a collaborative investigation.

The sulfation of Cortisol was carried out on a 30 mg scale (0.1 mmol) using 1.2 eq. of $\text{Bu}_3\text{N}\cdot\text{SO}_3$. The reaction was monitored by HPLC (Using a C18 stationary phase, MeCN/ H_2O , 3:7) and the crude reaction mixture was purified by chromatography (SiO_2) to afford 12 mg of unreacted cortisol (40%) and 24 mg of suspected intermediate **38** (not characterised). After an *in situ* ion-exchange, 8 mg (23%, based on recovered starting material) of **39** was isolated as its pure Na^+ salt (Scheme 26).



Scheme 26: The chemoselective 0.1 mmol scale synthesis of **39**. ^a**38** was not characterised (Parentheses indicate reaction conversion as measured by ¹H-NMR spectroscopy).

The synthesis of sulfate **39** demonstrates the versatility of the new sulfation methodology developed with $\text{Bu}_3\text{N}\bullet\text{SO}_3$, which is able to sulfate alcohols selectively at the 0.1 mmol scale and is advantageous for discovery-chemistry investigations.

The sulfation methodology was applied to the Fmoc protected amino acid esters, serine (**L-40**) and tyrosine (**L-41**) (Figure 48, A). The sulfation of **L-40** afforded **L-43** in excellent yield (95%) under normal conditions. Similarly, a 90% isolated yield of **L-43** was achieved using a non-denaturing temperature (30 °C) with 4.0 eq. of Bu₃N•SO₃, (See Chapter 6). HPLC analysis of the [Bu₃NH]⁺ intermediates (**L-42** and **±42**) using a chiral stationary phase verified no loss in *e.r* (>99:1) during the sulfation reaction (Figure 48, B). Furthermore, ion-exchange toward the racemic analogue afforded **±43** in 88% yield, demonstrating the reproducibility of this methodology (Figure 48).

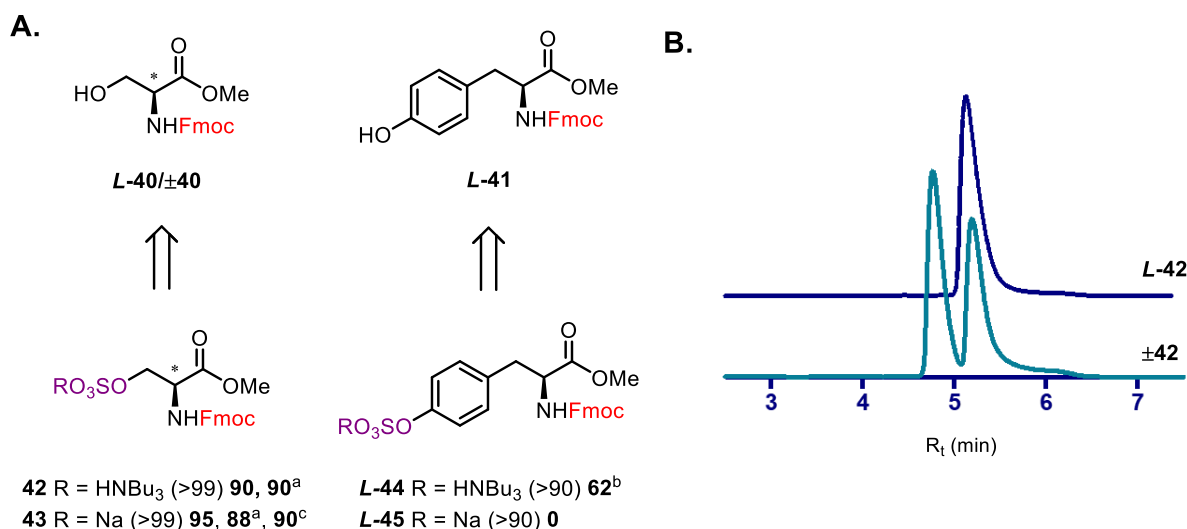


Figure 48: A) The sulfation of Fmoc protected amino esters **L-40** and **L-41**; **B)** The chiral HPLC trace (254 nm) of **L-42** and **±42**. ^ayield for the sulfation of a racemic analogue, ^bintermediate was unstable (90% pure calculated by ¹H-NMR), ^c30 °C using 5 eq. Bu₃N•SO₃. (Parentheses indicate reaction conversion as measured by ¹H-NMR spectroscopy).

The sulfation of **L-41** gave full conversion by ¹H-NMR analysis, and was afforded in 62% isolated yield. However, the intermediate [Bu₃NH]⁺ salt (**L-44**) was found to be unstable and decomposed during purification by chromatography (SiO₂, 90% pure by ¹H-NMR). Time course ¹H-NMR experiments of **L-44** (CDCl₃) confirmed that the organosulfate was also unstable in solution (See Chapter 6.6), and attempts to isolate the pure Na⁺ salt **L-45** were unsuccessful.

Finally, the new synthetic methodology was applied to the original medicinal chemistry challenge, the synthesis of the HS-glycomimetics (**1-3**) as their pure Na⁺ salts. The application of optimised conditions demonstrated full conversion of **±5** and **S-10** by ¹H-NMR. Moreover, persulfates **a-1** and **R-2** were afforded in 88% and 72% yield, respectively (Figure 49). The synthesis of **R-2** was carried out on a 400 mg (1.27 mmol) scale, establishing the benefits of the Bu₃N•SO₃ methodology in providing a scalable route to synthetically challenging, biologically relevant compounds. (The use of Bu₃N•SO₃ toward the synthesis of all remaining and novel HS-glycomimetics is discussed in Chapter 5).

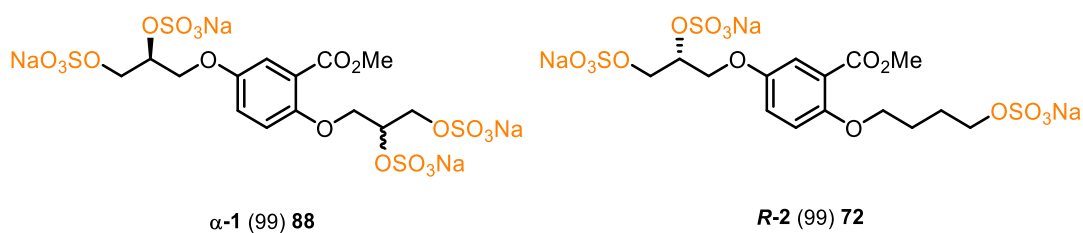
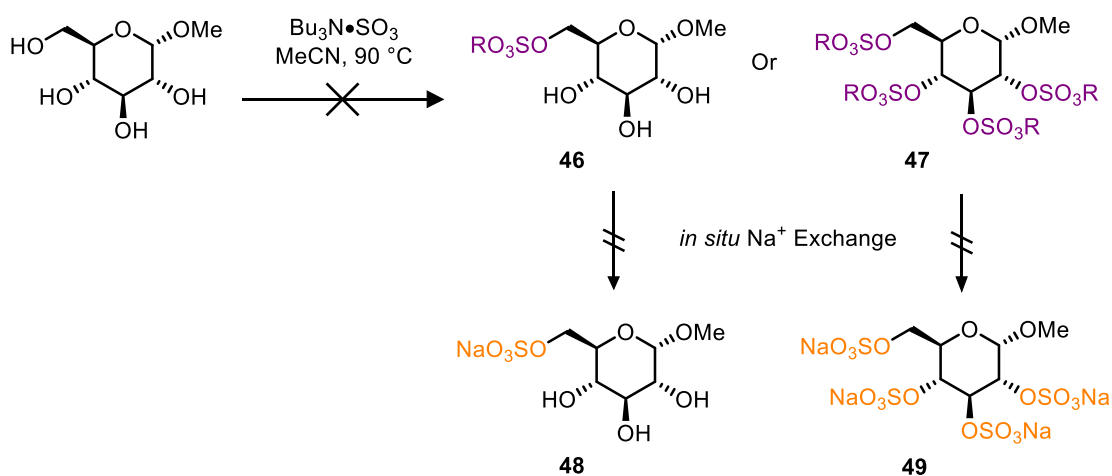


Figure 49: The synthesis of **a-1** and **R-2** using Bu₃N•SO₃. See appendix for conditions. (Parentheses indicate reaction conversion as measured by ¹H-NMR spectroscopy).

Additionally, the sulfation of α -methyl glucoside was investigated to see if the developed methodology is applicable to sugars, or sugar based molecules (Scheme 27). However, the reaction could not be monitored by ^1H -NMR due to significant peak overlap in the aliphatic proton region. Therefore, unlike previous examples, no quantitative assessment on the reaction could be performed. Attempts to isolate the monosulfate **46** and persulfate **47** were unsuccessful by chromatography. Furthermore, ion-exchange of the crude reaction mixtures was ineffective at affording the Na^+ salts **48** and **49**. This demonstrated a significant limitation to the $\text{Bu}_3\text{N}\cdot\text{SO}_3$ methodology for the sulfation of sugar molecules. This is discussed further in Chapter 4.9: Future Work.



Scheme 27: The unsuccessful sulfation of α -methyl glucoside with $\text{Bu}_3\text{N}\cdot\text{SO}_3$. $\text{R} = [\text{Bu}_3\text{NH}]^+$

4.8. Conclusion

In summary, the results of this investigation have reported the first scalable preparation of $\text{Bu}_3\text{N}\bullet\text{SO}_3$ and demonstrated its application toward the synthesis of organosulfates and persulfated structures, including the biologically important compounds **a-1** and **R-2**. The use of $\text{Bu}_3\text{N}\bullet\text{SO}_3$ is shown to circumvent the disadvantages associated to the poor solubility of organosulfates in organic solvents, and facilitates their efficient isolation as $[\text{Bu}_3\text{NH}]^+$ and Na^+ salts. Furthermore, the methodology is practical, straightforward to perform and holds promise with an ability to install up to four sulfate groups on complex, biologically relevant substrates, including phenols, steroids and amino-acids. Furthermore, $\text{Bu}_3\text{N}\bullet\text{SO}_3$ as a reagent has demonstrated chemoselectivity, which can selectively sulfate different alcohol moieties on a single molecule, however, chemoselectivity was also shown to be overcome, permitting persulfate of all possible hydroxyl sites on a substrate. Overall, the use of $\text{Bu}_3\text{N}\bullet\text{SO}_3$ for the synthesis of organosulfates has demonstrated a marked advantage over pre-existing sulfation methods and commercially available $\text{R}_3\text{N}\bullet\text{SO}_3$ complexes.

For a communication of this work see: *Sulfation Made Simple: A Strategy for Synthesising Sulfated Molecules*, D. M. Gill, L. Male, A. M. Jones, *Chem. Commun.*, 2019, **55**, 4319 – 4322 (found at the end of this chapter).

4.9. Further and Future work

4.9.1. Sulfamation Made Simple: A Continuation towards the Synthesis of *N*-Sulfamates

Following on from the success of this investigation it was proposed that the sulfation methodology (developed with $\text{Bu}_3\text{N}\bullet\text{SO}_3$) be applied to amine systems. As a result, a separate study was carried out by Ms A. M. Benedetti, to optimise the reaction conditions and demonstrate a sulfamation method towards a variety of amines,

amides, amino acid esters and peptides, with applications to structural biology (Figure 50).

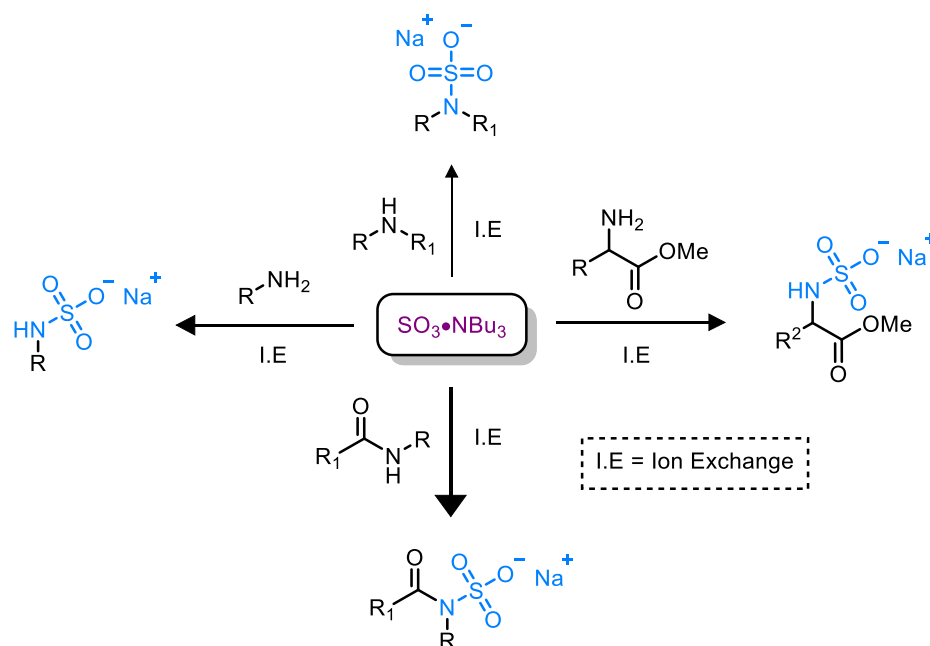


Figure 50: The general synthesis of *N*-sulfamates using $\text{Bu}_3\text{N}\cdot\text{SO}_3$. R = alkyl, aryl & benzyl; R^1 = alkyl, aryl & benzyl; R^2 = amino acid side chain.

In summary, this investigation developed a rapid, mild and operationally straightforward route to *N*-sulfamates, demonstrating a broad substrate scope and heteroatom selectivity. It was discovered that *N*-sulfamation preferentially occurs over *O*-sulfation and *S*-sulfurothiolation, and the investigation provided multiple examples of amines, amides, amino acid esters, and two examples of chemically sulfated/sulfamated peptides, glutathione and bradykinin. Notably, the method also demonstrated site-selective sulfamation of amino acid residues, with possible applications in sensing and the understanding sulfoprotein biology.⁸⁰

All results, discussions and conclusions from this investigation can be found in the communication titled: *Chemical Methods for N- and O-Sulfation of Small Molecules, Amino Acids and Peptides*, A. M. Benedetti, D. M. Gill, C. W. Tsang, A. M. Jones, *ChemBioChem*, 2020, **21**, 938 – 942 (found at the end of this chapter).

4.9.2. The Sulfation of Sugars and Polysaccharides

New methods towards the chemical sulfation of sugars are important to facilitate the growing demand from research looking at H- and HS-oligosaccharides, and HS-binding proteins (Chapter 2). However, early attempts at using $\text{Bu}_3\text{N}\bullet\text{SO}_3$ to sulfate sugars were unsuccessful and the reactions could not be evaluated by ^1H -NMR analysis. Therefore, future work will aim to develop a methodology towards the chemoselective sulfation of sugar monomers through a liquid chromatography mass spectrometry (LCMS) investigation, and apply this methodology toward the sulfation of polysaccharide frameworks, including H/HS-like precursors.

4.9.3. Factors Effecting *in situ* Ion-exchange

It was highlighted early on in the investigation that the *in situ* ion-exchange protocols were inadequate if the sulfated species are lipophilic as their Na^+ salt. This was tested by the sulfation of decanol under the standard conditions, as it is known that sodium decyl sulfate is a solid at room temperature but is highly lipophilic. Therefore, it was proposed to not precipitate out of organic solution.⁸² The synthesised $[\text{Bu}_3\text{NH}]^+$ intermediate of dodecanol sulfate was subjected to ion-exchange under all three sets of conditions (i-iii, See Chapter 6.1.9) and no precipitate formed, thus agreeing with the proposed hypothesis. The $[\text{Bu}_3\text{NH}]^+$ salts are easily isolated using chromatography, however, future work looking to address this issue will seek to identify a more general set of conditions/methodology for an efficient ion-exchange that is applicable to highly soluble organosulfate salts.

References

1. D. A. Shirley, *Organic Chemistry*, Holt, Rinehart and Winston, 1966, 253
2. D. Vaidyanathan, A. Williams, J. S. Dordick, M. A. G. Koffas, R. J. Linhardt, *Bioeng. Transl. Med.*, 2017, **2**, 12 – 30
3. P. Sondermann, E. M. Carreira, *J. Am. Chem. Soc.*, 2019, **141**, 10510 – 10519
4. T. Stachyra, P. Levasseur, M.-C. P  chereau, A.-M. Girard, M. Claudon, C. Miossec, M. T. Black, *J. Antimicrob. Chemother.*, 2009, **64**, 326 – 32
5. G. M. Pacifici, K. Allegaert, *Curr. Ther. Res.*, 2015, **77**, 24 – 30
6. J. V. Mulcahy, J. Du Bois, *J. Am. Chem. Soc.*, 2008, **130**, 12630 – 12631
7. M. P. Goldman, R. G. Bennett, *J. Am. Acad. Dermatol.*, 1987, **17**, 167 – 182
8. J. R. Bundgaard, J. F. Rehfeld, Tyrosylprotein sulfotransferases, *Handbook of Biologically Active Peptides* (2nd Edition), Academic Press, 2013, 1829 – 1834
9. Y. Wang, J. Ren, X. H. Hilda-Huang, R. Tong, J. Z. Yu, *Environmental Science & Technology*, 2017, **51**, 6791 – 6801
10. K. C. Nicolaou, P. Heretsch, T. Nakamura, A. Rudo, M. Murata, K. Konoki, *J. Am. Chem. Soc.*, 2014, **136**, 16444 – 16451
11. K. C. Nicolaou, *J. Org. Chem.*, 2009, **74**, 951 – 972
12. W. Zheng, J. A. DeMattei, J.-P. Wu, J. J.-W. Duan, L. R. Cook, H. Oinuma, Yoshito Kishi, *J. Am. Chem. Soc.*, 1996, **118**, 7946 – 7968
13. J. M. Tarbell, L. M. Cancel, *J. Intern. Med.*, 2016, **280**, 97 – 113
14. M. C. Z. Meneghetti, A. J. Hughes, T. R. Rudd, H. B. Nader, A. K. Powell, E. A. Yates, M. A. Lima, *J. R. Soc. Interface*, 2015, **12**, 20150589
15. M. W. H. Coughtrie, *Chemico-Biological Interaction*, 2016, **259**, 2 – 7
16. A. C. S. Barbosa, Y. Feng, C. Yu, M. Huang, W Xie, *Expert Opinion on Drug Metabolism & Toxicology*, 2019, **15**, 329 – 339
17. P. A. Foster, J. W. Mueller, *J. Mol. Endocrinol.*, 2018, **61**, T271 – T283
18. J. W. Mueller, L. C. Gilligan, J. Idkowiak, W. Arlt, P. A. Foster, *Endocr. Rev.*, 2015, **36**, 526 – 563
19. R. Hobkirk, *Trends Endocrinol. Metab.*, 1993, **4**, 69 – 74
20. T. S. Raju, *Sulfation of Proteins and Glycoproteins*. Co and Post-Translational Modifications of Therapeutic Antibodies and Proteins, 2019, T.S. Raju (Ed.)
21. G. D. Balderrama, E. P. Meneses, L. H. Orihuela, O. V. Hernandez, R. C. Franco, V. P. Robles, C. V. F. Batista, *Rapid Commun. Mass Spectrom.*, 2011, **25**, 1017 – 1027
22. K. F. Medzihradszky, S. Guan, D. A. Maltby, A. L. Burlingame. *J. Am. Soc. Mass Spectrom.*, 2007, **18**, 1617
23. M. Shih, S. A. McLuckey, *Int. J. Mass Spectrom.*, 2019, **444**, 116 – 181
24. W. Chen, J. Dong, S. Li, Y. Liu, Y. Wang, L. Yoon, P. Wu, K. Barry Sharpless, J. W. Kelly, *Angew. Chem. Int. Ed.*, 2016, **55**, 1835 – 1838.
25. N. Vale, R. C. Veloso, P. Gomes, *Eur. J. Org. Chem.* 2015, **2015**, 7413 – 7425
26. M. W. Duffel, *Sulfotransferases, Comprehensive Toxicology* (3rd Edition), Elsevier, 2018, 407 – 428

27. R. T. Lanišnik, *Frontiers in Pharmacology*, 2016, **7**, 30
28. Y. Ji, S. Islam, A. M. Mertens, D. F. Sauer, G. V. Dhoke, F. Jakob, U. Schwaneberg, *App. Microbiol. Biotechnol.*, 2019, **103**, 3761 – 3771
29. K. Valentová, K. Káňová, F. D. Meo, H. Pelantová, C. Chambers, L. Rydlová, L. Petrásková, A. Křenková, J. Cvačka, P. Trouillas, V. Křen, *Int. J. Mol. Sci.* 2017,**18**, 2231
30. A. F. Hartog, R. Wever, *J. Mol. Cat. B*, 2016, **129**, 43 – 46
31. I. Ayuso-Fernndez, M. A. Galms, A. Bastida, E. Garcia-Junceda, *ChemCatChem*, 2014, **6**, 1059 – 1065
32. J. Li, G. Su, J. Liu, *Angew. Chem. Int. Ed.*, 2017, **56**, 11784
33. W. Lu, C. Zong, P. Chopra, L. E. Pepi, Y. Xu, I. J. Amster, J. Liu, G.-J. Boons, *Angew. Chem. Int. Ed.*, 2018, **57**, 5340
34. G. Dado, R. Bernhardt, *Sulfonation and Sulfation*, Kirk-Othmer Encyclopedia of Chemical Technology, 2017, John Wiley & Sons Inc (Ed.)
35. L. F. Fieser, M. Fieser, T. Ho, T.-L. Ho, M. Fieser, L. Fieser, *Sulfur trioxide*, Fieser and Fieser's Reagents for Organic Synthesis, 2006
36. N. C. Deno, Melvin S. Newman, *J. Am. Chem. Soc.*, 1950, **72**, 3852 – 3856
37. R. L. Burwell, *J. Am. Chem. Soc.*, 1949, **71**, 1769 – 177
38. N. C. Deno, M. S. Newman, *J. Am. Chem. Soc.*, 1951, **73**, 1920 – 1923
39. C. P. Hoiberg, R. O. Mumma, *J. Am. Chem. Soc.*, 1969, **91**, 4273 – 4278
40. L. S. Simpson, T. S. Widlanski, *J. Am. Chem. Soc.*, 2006, **128**, 1605 – 1610
41. Y. Liu, I.-F. Lien, S. Ruttgaizer, P. Dove, S. D. Taylor, *Org. Lett.*, 2004, **6**, 209 – 212
42. A. D. Proud, J. C. Prodger, S. L. Flitsch, *Tetrahedron Lett.*, 1997, **38**, 7243 – 7246.
43. E. E. Watson, J. Ripoll-Rozada, A. C. Lee, M. C. L. Wu, C. Franck, T. Pasch, B. Premdjee, J. Sayers, M. F. Pinto, P. M. Martins, S. P. Jackson, P. J. B. Pereira, R. J. Payne. *Pro. Nat. Ac. Sci.*, 2019, **116**, 13873 – 13878
44. L. J. Ingram, A. Desoky, A. M. Ali, S. D. Taylor, *J. Org. Chem.*, 2009, **74**, 6479 – 6485
45. M. Huibers, Á. Manuzi, F. P. J. T. Rutjes, F. L. Van Delft, *J. Org. Chem.*, 2006, **71**, 7473 – 7476
46. E. E. Gilbert, *Chem. Rev.*, 1962, **62**, 549 – 589
47. H. C. Reitz, R. E. Ferrel, H.S. Olcott, H. Fraenkel-Conrat, *J. Am. Chem. Soc.*, 1946, **68**, 1031 – 1035
48. R. A. Al-Horani, U. R. Desai, *Tetrahedron*, 2010, **66**, 2907 – 2918
49. A. Raghuraman, M. Riaz, M. Hindle, U. R. Desai, *Tetrahedron Lett.*, 2007, **48**, 6754 – 6758
50. V. B. Krylov, N. E. Ustyuzhanina, A. A. Grachev, N. E. Nifantiev, *Tetrahedron Lett.*, 2008, **49**, 5877 – 5879.
51. D. Gorelik, Y. C. Lin, A. L. Briceno-Strocchia, M. S. Taylor, *J. Org. Chem.*, 2019, **84**, 900 – 908
52. J. R. Parikh, W. V. E. Doering, *J. Am. Chem. Soc.*, 1967, **89**, 5505 – 5507

53. B. R. Brummel, K. G. Lee, C. D. McMillen, J. W. Kolis, D. C. Whitehead, *Org. Lett.*, 2019, **21**, 9622 – 9627
54. S. Hemmerich, D. Verdugo, V. L. Rath, *Drug Discovery Today*, 2004, **9**, 967 – 97
55. M. Rawat, C. I. Gama, J. B. Matson, L. C. Hsieh-Wilson, *J. Am. Chem. Soc.*, 2008, **130**, 2959 – 2961
56. D. Chandler, *Nature*, 2005, **437**, 640 – 647
57. M. Ball, A. Boyd, G. J. Ensor, M. Evans, M. Golden, S. R. Linke, D. Milne, R. Murphy, A. Telford, Y. Kalyan, G. R. Lawton, S. Racha, M. Ronsheim, S. H. Zhou, *Org. Process Res. Dev.*, 2016, **20**, 1799 – 1805
58. I. K. Mangion, R. T. Ruck, N. Rivera, M. A. Huffman, M. Shevlin, *Org. Lett.*, 2011, **13**, 5480 – 5483
59. P. Érdi; J. Tóth, *Mathematical Models of Chemical Reactions: Theory and Applications of Deterministic and Stochastic Models*. Manchester University Press, 1989, 3 – 4
60. J. R. M. Bastidas, T. J. Oleskey, S. L. Miller, M. R. Smith III, Ro. E. Maleczka Jr., *J. Am. Chem. Soc.*, 2019, **141**, 15483 – 15487
61. E. A. Raiber, J. A. Wilkinson, F. Manetti, M. Botta, J. Deakin, J. Gallagher, M. Lyon, S. W. Ducki, *Bioorg. Med. Chem. Lett.*, 2007, **17**, 6321 – 6325
62. A. M. Mahmoud, F. L. Wilkinson, A. M. Jones, J. A. Wilkinson, M. Romero, J. Duarte, M. Y. Alexander, *Heart*, 2015, **101**, A41
63. F. L. Wilkinson, A. M. Mahmoud, A. M. Jones, J. A. Wilkinson, M. Romero, J. Duarte, M. Y. Alexander, *Heart*, 2016, **102**, A136
64. F. L. Wilkinson, A. M. Mahmoud, A. M. Jones, J. A. Wilkinson, M. Romero, J. Duarte, M. Y. Alexander, *Cardiovascular Research*, 2016, **101**, S65
65. A. W. W. Langford-Smith, A. Hasan, R. Weston, N. Edwards, A. M. Jones, A. J. M. Boulton, F. L. Bowling, S. T. Rashid, F. L. Wilkinson, M. Y. Alexander, *Sci. Rep.*, 2019, **9**, 2309
66. A. M. Mahmoud, F. L. Wilkinson, A. M. Jones, J. A. Wilkinson, M. Romero, J. Duarte, M. Y. Alexander, *Biochimica et Biophysica Acta (BBA) - General Subjects*, 2017, **1861**, 3311 – 3322,
67. G. P. Sidgwick, P. Walling, A. Shabbir, R. Weston, A. Schiro, F. Serracino-Inglott, A. M. Jones, M. Kamalov, M. A. Brimble, F. L. Wilkinson, M. Y. Alexander, *Heart*, 2016, **102**, A132
68. F. L. Wilkinson, G. P. Sidgwick, A. Shabbir, R. Weston, A. M. Jones, M. Y. Alexander, *Heart*, 2016, **102**, A11
69. G. P. Sidgwick, R. Weston, A. M. Jones, F. L. Wilkinson, M. Y. Alexander, *Heart*, 2017, **103**, A126
70. G. P. Sidgwick, R. Weston, A. M. Jones, F. L. Wilkinson, M. Y. Alexander, *J. Vasc. Res.*, 2017, **54**, 24
71. A. M. Mahmoud, A. M. Jones, G. P. Sidgwick, A. M. Arafat, F. L. Wilkinson, M. Y. Alexander, *Cell. Phys. Biochem.*, 2019, **53**, 323 – 336
72. R. Weston, A. W. W. Langford-Smith, A. Hasan, A. M. Jones, F. L. Wilkinson, A. Boulton, T. Rashid, M. Y. Alexander, *Diabetic Medicine*, 2017, **34**, 39 – 39

73. P. Abayakoon, R. Epa, M. Petricevic, C. Bengt, J. W.-Y. Mui, P. L. Van der Peet, Y. Zhang, J. P. Lingford, J. M. White, E. D. Goddard-Borger, S. J. Williams, *J. Org.Chem.*, 2019, **84**, 2901 – 2910
74. J. A. Moede, C. Curran, *J. Am. Chem. Soc.*, 1949, **71** , 852 – 858
75. B. Passet, V. Parshikov, *Org. React.*, 1976, **13**, 555 – 560
76. B. Parshikov, B. Passet, N. Kopeina, *Org. React.*, 1976, **13**, 310 – 314
77. J. S. Fritz, *J. Chromatogr. A.*, 2005, **1085**, 8 – 17
78. F. A. Kanda, A. J. King, *J. Am. Chem. Soc.*, 1951, **73**, 2315 – 2319
79. J. Kubas, A. C. Larson, R. R. Ryan, *J. Org. Chem.*, 1979, **44**, 3867 – 3871
80. H. Fex, K. E. Lundvall, A. Olsson, *Acta Chem. Scand.*, 1968, **22**, 254 – 264
81. T. Hunter, *Cell*, 1995, **80**, 225 – 236



Sulfation made simple: a strategy for synthesising sulfated molecules†

Daniel M. Gill,^a Louise Male^b and Alan M. Jones  [✉]Cite this: *Chem. Commun.*, 2019, 55, 4319Received 5th February 2019,
Accepted 12th March 2019

DOI: 10.1039/c9cc01057b

rsc.li/chemcomm

The study of organosulfates is a burgeoning area in biology, yet there are significant challenges with their synthesis. We report the development of a tributylsulfoammonium betaine as a high yielding route to organosulfates. The optimised reaction conditions were interrogated with a diverse range of alcohols, including natural products and amino acids.

Organosulfates play a variety of important roles in biology, from xenobiotic metabolism to the downstream signalling of steroidal sulfates in disease states.¹ Sulfate groups on glycosaminoglycans (GAGs) such as heparin, heparan sulfate and chondroitin sulfate, facilitate molecular interactions and protein ligand binding at the cellular surface,² an area of interest in drug discovery.³

Heparin (an anticoagulant),⁴ avibactam[®] (a β -lactamase inhibitor),⁵ sotradecol (a treatment for varicose veins),⁶ the sulfate metabolite of paracetamol (an analgesic),⁷ and the glycomimetic C3 (used to study atherosclerosis),⁸ contain organosulfate motifs (Fig. 1). There are many other natural sources of bioactive sulfated compounds.⁹

The incorporation of polar hydrophilic organosulfate groups onto drug-like molecules is timely to facilitate research investigating sulfated GAGs as potential new therapies.¹⁰ However, the insertion and isolation of sulfate groups into target molecules remains a challenging aspect of their synthesis,¹¹ prompting recent advances into sulfate revealing pro-drugs.¹²

The presence of one or more sulfate group makes chemical synthesis and purification of (per)sulfated compounds challenging, primarily due to their poor solubility in organic solvents.¹³ Therefore the insertion of organosulfate groups is typically the final step in a synthetic method, limiting further chemical modifications.¹⁴

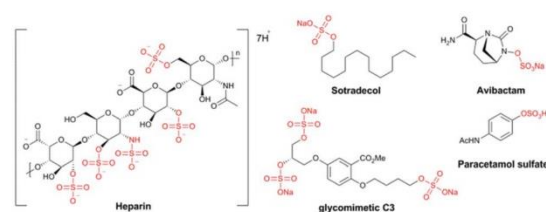


Fig. 1 Examples of drug molecules containing organosulfates: heparin, sotradecol[®] and avibactam[®]; a chemical tool compound (C3) and a metabolite of paracetamol.

A variety of methods to prepare organosulfates are shown in Chart 1.

The preparation of organosulfate esters include a microwave assisted approach to the sulfation of alcohols, using Me_3NSO_3 and PySO_3 , Chart 1(i).^{15,16} The addition of catalytic diaryl borinic acid can be used with Me_3NSO_3 to sulfate carbohydrates.¹⁷ The limitations with these routes include the need for a stoichiometric excess of the reagent per alcohol group (up to 10 eq. per hydroxyl group) and difficulties with purification. Poor solubility in organic solvents makes aqueous purification protocols and ion-exchange chromatography a standard procedure, limiting the practicality. An alkyl chlorosulfate ester with subsequent deprotection has proven a reliable method, but limitations include the need to use a strong base and a deprotection step leads to side products (Chart 1(ii)).¹⁸ A DCC/ H_2SO_4 -sulfate coupling has been demonstrated but is not amenable to acid sensitive substrates (Chart 1(iii)).¹⁹ A sulfitylation-oxidation protocol (Chart 1(iv)) involves the synthesis of a protected sulfite ester, oxidation to the protected sulfate ester and cleavage to the sodium sulfate salt.²⁰ However, the use of multiple steps and purification sequences is limiting. A process route to Avibactam²¹ (Fig. 1 and Chart 1(v)) involved sulfation of the hydroxylamine intermediate using Me_3NSO_3 , followed by cation exchange with tetrabutylammonium acetate, gave the organosulfate as its tetrabutylammonium salt. The sodium salt was obtained by precipitation in 77% yield over 2 steps on a multi-kg scale. Similarly, the use of a sulfate bis(tributylammonium) salt for the preparation for

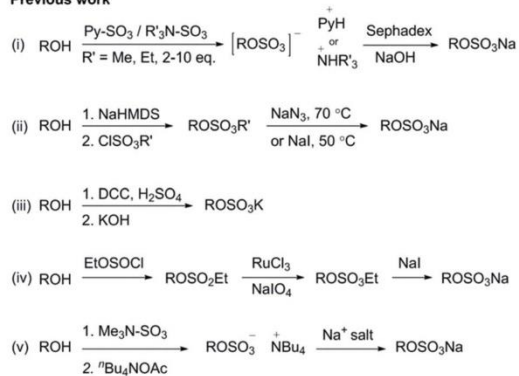
^a School of Pharmacy, University of Birmingham, Edgbaston, B15 2TT, UK.
E-mail: a.m.jones.2@bham.ac.uk; Tel: +44 (0)1214147288

^b School of Chemistry, University of Birmingham, Edgbaston, B15 2TT, UK

† Electronic supplementary information (ESI) available: Preparative routes, compound characterisation, copies of ^1H and ^{13}C spectra and the cif file for the X-ray crystal structure of 1. CCDC 1894165 (1). For ESI and crystallographic data in CIF or other electronic format see DOI: 10.1039/c9cc01057b

Communication

Previous work



This work

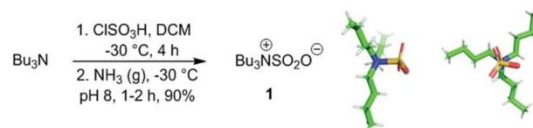


Chart 1 Previous strategies to the synthesis of sulfate esters: this work: sulfate ester formation using tributylsulfoammonium betaine gives direct access to an organic soluble organosulfate intermediate that can be readily ion exchanged.

nucleoside phosphosulfates²² highlighted that the solubility of the organosulfate ester can be modulated by increasing the lipophilicity of the corresponding cation.

During a medicinal chemistry programme we encountered difficulties using the established sulfation methods to persulfate compounds, due to the poor solubility of the organosulfate intermediates and their resulting purification. We sought to develop an all in one reagent, to improve the solubility of the intermediate organosulfate ester. Combining tributylamine (pK_a , 10.89) with SO_3 , we envisioned this would create a complex (Bu_3NSO_3 , **1**) for the persulfation of alcohols, with increased lipophilicity of the intermediate sulfate ester, improving the overall solubility of the organosulfates in organic solvents. We rationalised that **1** would retain similar activity to SO_3 complexes with Et_3N and Me_3N , due to their similar Lewis base strengths, $\text{pK}_a = 11.01$ and 10.63 , respectively. Overall, **1** may permit sequential chemical steps in organic solvents, with a simple purification method to the corresponding sodium salt, streamlining the synthesis of organosulfates.

The complexation of sulfur trioxide to nitrogen or oxygen containing molecules (such as pyridine, NMe_3 , NEt_3 , DMF, THF and dioxane) is well known,^{11,15} the use of an organic solubilising partner, tributylamine, is however not. To the best of our knowledge, the only literature report of the synthesis and physical study of **1** was by Moede in 1949.²³ It was not until 1976 that Parshikov and co-workers²⁴ studied **1** as a sulfating agent on simple aliphatic alcohols (without spectroscopic characterisation) and found that **1** reacts *via* an $\text{S}_\text{N}2$ mechanism driven by the hydrogen-bonding propensity of the alcohol under study. However, to the best of our knowledge no further use or development of this reagent has been reported.



Scheme 1 (a) Synthesis of Bu_3NSO_3 (**1**); (b) alternative views of the crystal structure of **1** obtained from small molecule single crystal X-ray diffraction.

We synthesised **1** by reaction of tributylamine with chlorosulfonic acid, affording a 90% yield on a 60 g scale (Scheme 1(a)).²⁵ For the first time both NMR spectral data and the crystal structure of **1**, obtained from small molecule single crystal X-ray diffraction, was determined (Scheme 1(b)).²⁶ Bu_3NSO_3 (**1**) adopts a *Gauche* conformation within an asymmetric unit cell caused by hydrogen bonding between the methylene hydrogen atoms α to the nitrogen and the oxygens of SO_3 . The measured N-S bond length in **1** is $1.886(3) \text{ \AA}$, a comparable bond length to a single N-S bond (typically: $1.73\text{--}1.83 \text{ \AA}$ versus 2.06 \AA for a donor-acceptor system),²⁷ suggesting that **1** exists as a betaine in the solid state which may have implications for the other unsolved amine- SO_3 complexes and their associated mechanisms.

Benzyl alcohol (**2a**) was selected for the optimisation study (Chart 2) due to a distinct down-field shift ($+0.35 \text{ ppm}$) of the benzylic signal after sulfation (by $^1\text{H-NMR}$ spectroscopy).

We examined the sulfation of **2a** with varying equivalents of **1** (entries 1 to 4). It was found that 2.0 equivalents of **1** was optimal for high conversions ($>99\%$) and isolated yields (95%, entry 3).

Entry	amine- SO_3	Eq.	T $^\circ\text{C}$	t (h)	Additive	Conversion at 0.5 h (%)	Conversion at end (%)	Isolated yield (%)
1	NBu_3	1.1	90	8.0	-	48	83	41
2	NBu_3	1.5	90	4.0	-	26	69	62
3	NBu_3	2.0	90	1.0	-	90	>99	95
4	NBu_3	4.0	90	0.5	-	>99	>99	95
5	NBu_3	2.0	70	6.0	-	22	>99	96
6	NBu_3	2.0	50	8.0	-	9	60	58
7	NBu_3	2.0	30	120	-	2	>99	96
8	NBu_3	2.0	20	18	-	1	9	*
9	Py	2.0	70	0.5	-	>99	>99	17 ^b
10	Py	2.0	70	0.5	$\text{Bu}_4\text{N}^+\text{F}^-$	>99	>99	47
11	Py	2.0	70	0.5	$\text{Bu}_4\text{N}^+\text{OAc}^-$	>99	>99	76
12	NMe_3	2.0	70	6.0	-	3	29	*
13	NMe_3	2.0	70	6.0	$\text{Bu}_4\text{N}^+\text{I}^-$	-	88	*
14	NBu_3	2.0	105 ^d	0.5	-	68	68	*
15	NBu_3	2.0	120 ^d	1.0	-	68	68	*
16	NBu_3	2.0	70	2.0	Na_2CO_3	16	57	*
17	NBu_3	2.0	70	2.0	K_2CO_3	8	8	*
18	NBu_3	2.0	70	2.0	Et_3N	15	34	*
19	NBu_3	2.0	70	6.0	Bu_2N	48	60	*

Chart 2 Optimisation of a model system. ^a Not isolated; ^b isolated as the pyridinium salt; ^c additive used during work-up; ^d microwave irradiation.

Less than 2.0 equivalents of **1** (entries 1 and 2) gave incomplete conversion to **3a**. We next surveyed the effect of temperature (entries 5–8 vs. entry 3). 90 °C and 2.0 equivalents of **1** gave complete conversion to **3a** within 2 h. Notably, reaction completion was achieved, even at 30 °C (with increased reaction time) demonstrating that **1** could be a suitable reagent for temperature sensitive substrates such as proteins.¹³

We compared the use of two commercially available amine- SO_3 complexes, namely pyridine and trimethylamine (entries 9 and 12, respectively). Py-SO_3 was more reactive than **1**, giving complete conversion to **3a** in 0.5 h but only a 17% isolated yield of the pyridinium species. As a control experiment, the sequential exchange of the pyridinium salt with different Bu_4N cations afforded the isolation of **4a** in 47% (Bu_4NI) and 76% (Bu_4NOAc) yield, respectively (entries 10 and 11). The use of $\text{Me}_3\text{N-SO}_3$ gave poor results (0% isolated yield of **4a** from a 29% conversion to **3a**). The addition of Bu_4NI to the reaction mixture significantly improved the reaction, affording an 88% conversion to **3a** (entry 13). Unfortunately, a more complex reaction mixture was detrimental to the isolation of **4a**. These results demonstrate the isolation benefits associated with the protocol developed with **1**.

We observed that **1** can achieve high conversions of **2a** to **3a/4a** without microwave irradiation (entries 1–7 vs. 14 and 15) unlike other reported sulfating agents. The addition of a hetero or homogenous base (entries 16–19) was investigated and in all cases this led to a decrease in conversion to **3a**. Most notably, the addition of tributylamine (entry 19) initially increased the rate conversion to **3a**, but reduced the overall conversion contradicting the original report.²⁴ We rationalised that the addition of Et_3N (with a higher $\text{p}K_{\text{a}}$ value than Bu_3N) competes in the reaction, forming Et_3NSO_3 *in situ*. This amine exchange has also been observed in the reaction of Et_3N with PySO_3 .²¹

We applied the optimal conditions to the synthesis of a range of sulfate esters (Chart 3). In all examples (Chart 3) we observed a near-quantitative conversion to the corresponding sulfate ester as the tributylammonium salt, independent of

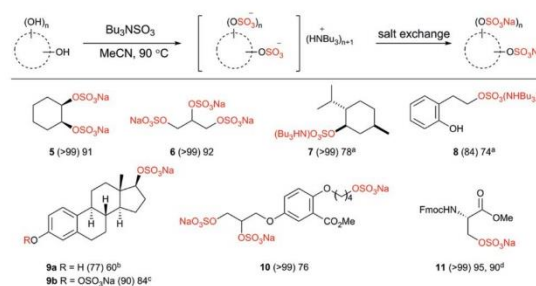


Chart 4 Reaction scope on diverse alcohols (2.0 eq. of **1** per OH group except where indicated). ^a Isolated as NBu_3H salt; ^b 1.5 eq. of **1**; ^c 5.0 eq. of **1**; ^d reaction performed at 38 °C using 4.0 eq. of **1** in DMF. (Parentheses indicate reaction conversion as measured by ^1H NMR spectroscopy.)

both electronic and steric factors. Differences occurred when converting the intermediate into a crystalline sodium salt; most likely due to the variability in precipitation of the sodium salt. Therefore differences of electron-withdrawing and electron-donating factors are difficult to draw with certainty. Steric bulk adjacent to the reacting centre was accommodated with ease (**4h**) and the reaction could also be applied to phenolic alcohols (**4i**).

Driving an organosulfate ester reaction to completion, by sulfating all possible hydroxyl sites in a structure remains a synthetic challenge. This is influenced by anionic crowding, making per-sulfation progressively more difficult.¹⁶ Therefore we applied the conditions to examples of compounds requiring two or more sulfation events, including natural products, and compounds containing different hydroxyl moieties within the same structure to probe the selectivity profile (Chart 4).

Cyclohexane-1,2-diol afforded the disulfate in high conversion and isolated yield, likewise with glycerol, the tri-sulfated analogue was prepared with ease (**5** and **6**, respectively). The reaction of **1** with menthol (**7**) delivered the NHBu_3 salt with ease.

To probe the alcohol selectivity profile, a primary alcohol was functionalised in preference to a phenol in **8**. Therefore, β -estradiol afforded 17- β -estradiol sulfate²⁸ over the more common metabolite 3- β -estradiol in 60% isolated yield (**9a**) using 1.5 eq. **1**. Using 5.0 eq. of **1** both the 17- and 3-positions were sulfated in 84% isolated yield (**9b**).

We then applied the methodology to the original medicinal chemistry challenge, the sodium salt of glycomimetic **C3** (**10**).⁸ High conversion and an isolated yield of 76% on a 500 mg scale was achieved. The methodology was applied to the Fmoc-protected amino acid, serine, resulting in excellent yields (95% under normal conditions) and 90% at a non-denaturing temperature (**11**) both using 4.0 eq. of **1**. Importantly, no loss in enantiomeric ratio was observed upon sulfation (>99:1).²⁹

In summary, we have reported the first scalable preparation and reaction scoping study of **1** as a mild, bench-stable, and chromatography-free method to access organic sulfate esters as their ammonium or sodium salts. The reaction holds promise with the ability to install up to three sulfate groups on complex scaffolds including examples where sterics would limit other

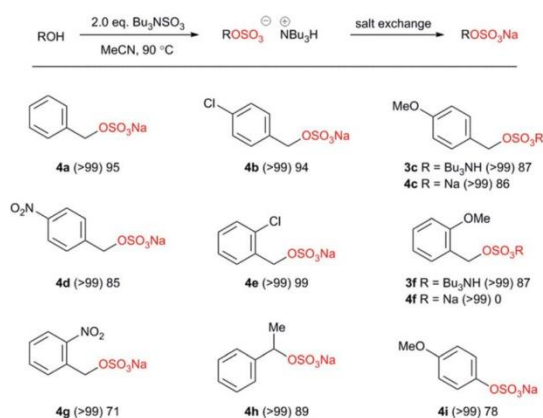


Chart 3 Application of methodology to benzylic and phenolic alcohols. (Parentheses indicates reaction conversion as measured by ^1H NMR spectroscopy.)

methods. Further work to elucidate the scope of the reaction on human sulfate metabolites is ongoing.

The authors thank Dr Chi Tsang and the Centre for Chemical and Materials Analysis in the School of Chemistry, University of Birmingham for analytical support. D. M. G. thanks the University of Birmingham for a PhD scholarship. The authors thank Dr J. W. Mueller, Dr K. A. Roper, and Ms A. M. Benedetti for helpful discussions.

Conflicts of interest

There are no conflicts to declare.

Notes and references

- (a) J. W. Mueller, L. C. Gilligan, J. Idkowiak, W. Arlt and P. A. Foster, *Endocr. Rev.*, 2015, **36**, 526–563; (b) P. A. Foster and J. W. Mueller, *J. Mol. Endocrinol.*, 2018, **61**, T271–T283.
- D. M. Tollefsen, in *Prog. Mol. Biol. Transl. Sci.*, ed. Zhang, L., Academic Press, 2010, vol. 93, pp 351–372.
- B. Ernst and J. L. Magnani, *Nat. Rev. Drug Discovery*, 2009, **8**, 661–677.
- R. J. Linhardt, *J. Med. Chem.*, 2003, **46**, 2551–2564.
- T. Stachyra, P. Levasseur, M.-C. Péchereau, A.-M. Girard, M. Claudon, C. Miossec and M. T. Black, *J. Antimicrob. Chemother.*, 2009, **64**, 326–329.
- M. P. Goldman and R. G. Bennett, *J. Am. Acad. Dermatol.*, 1987, **17**, 167–182.
- G. M. Pacifici and K. Allegaert, *Curr. Ther. Res.*, 2015, **77**, 24–30.
- A. M. Mahmoud, F. L. Wilkinson, A. M. Jones, J. A. Wilkinson, M. Romero, J. Duarte and M. Y. Alexander, *Biochim. Biophys. Acta, Gen. Subj.*, 2017, **1861**, 3311–3322.
- F. Carvalhal, M. Correia-da-Silva, E. Sousa, M. Pinto and A. Kijjoo, *J. Mol. Endocrinol.*, 2018, **61**, T211–T231.
- D. C. Blakemore, L. Castro, I. Churcher, D. C. Rees, A. W. Thomas, D. M. Wilson and A. Wood, *Nat. Chem.*, 2018, **10**, 383–394.
- R. A. Al-Horani and U. R. Desai, *Tetrahedron*, 2010, **66**, 2907–2918.
- E. M. Gordon, M. A. J. Duncton and M. A. Gallop, *J. Med. Chem.*, 2018, **61**, 10340–10344.
- S. Hemmerich, D. Verdugo and V. L. Rath, *Drug Discovery Today*, 2004, **9**, 967–975.
- M. Rawat, C. I. Gama, J. B. Matson and L. C. Hsieh-Wilson, *J. Am. Chem. Soc.*, 2008, **130**, 2959–2961.
- E. E. Gilbert, *Chem. Rev.*, 1962, **62**, 549–589.
- A. Raghuraman, M. Riaz, M. Hindle and U. R. Desai, *Tetrahedron Lett.*, 2007, **48**, 6754–6758.
- D. Gorelik, Y. C. Lin, A. L. Briceno-Strocchia and M. S. Taylor, *J. Org. Chem.*, 2019, **84**, 900–908.
- L. S. Simpson and T. S. Widlanski, *J. Am. Chem. Soc.*, 2006, **128**, 1605–1610.
- R. O. Mumma, *Lipids*, 1966, **1**, 221–223.
- M. Huibers, A. Manuzi, F. P. J. T. Rutjes and F. L. van Delft, *J. Org. Chem.*, 2006, **71**, 7473–7476.
- M. Ball, A. Boyd, G. J. Ensor, M. Evans, M. Golden, S. R. Linke, D. Milne, R. Murphy, A. Telford, Y. Kalyan, G. R. Lawton, S. Racha, M. Ronsheim and S. H. Zhou, *Org. Process Res. Dev.*, 2016, **20**, 1799–1805.
- J. Kowalska, A. Osowniak, J. Zuberek and J. Jemielity, *Bioorg. Med. Chem. Lett.*, 2012, **22**, 3661–3664.
- J. A. Moede and C. Curran, *J. Am. Chem. Soc.*, 1949, **71**, 852–858.
- (a) B. Passet and V. Parshikov, *Org. React.*, 1976, **13**, 555–560; (b) V. Parshikov, B. Passet and N. Kopeina, *Org. React.*, 1976, **13**, 310–314.
- The original report of **1**²³ used the reaction of NBU₃ with liquid SO₃ in CCl₄ but no isolated yield or characterisation data (apart from the melting point) is available.
- CCDC 1894165 (**1**) contains the supplementary crystallographic data for this paper. Crystal data for **1**: C₁₂H₂₇NO₃S (*M* = 265.40 g mol^{−1}): trigonal, space group *R*3*c* (no. 161), *a* = 14.3352(2) Å, *c* = 12.2455(2) Å, *V* = 2179.28(8) Å³, *Z* = 6, *T* = 100.01(10) K, *μ*(CuKα) = 1.969 mm^{−1}, *D*_{calc} = 1.213 g cm^{−3}, 8776 reflections measured (16.14° ≤ 2θ ≤ 147.692°), 977 unique (*R*_{int} = 0.0273, *R*_{sigma} = 0.0115) which were used in all calculations. The final *R*₁ was 0.0209 (*I* > 2σ(*I*)) and *wR*₂ was 0.0570 (all data).
- (a) F. A. Kanda and A. J. King, *J. Am. Chem. Soc.*, 1951, **73**, 2315–2319; (b) G. J. Kubas, A. C. Larson and R. R. Ryan, *J. Org. Chem.*, 1979, **44**, 3867–3871.
- The only other report to the preparation of **9a** involved a protection-deprotection cascade: H. Fex, K. E. Lundvall and A. Olsson, *Acta Chem. Scand.*, 1968, **22**, 254–264.
- We thank reviewer 2 for this suggestion and the insight it provided. Chiral HPLC traces are provided in the ESI†.

Chemical Methods for N- and O-Sulfation of Small Molecules, Amino Acids and Peptides

Anna Mary Benedetti,^[a] Daniel M. Gill,^[a] Chi W. Tsang,^[b] and Alan M. Jones^{*,[a]}

Sulfation of the amino acid residues of proteins is a significant post-translational modification, the functions of which are yet to be fully understood. Current sulfation methods are limited mainly to O-tyrosine (sY), which requires negatively charged species around the desired amino acid residue and a specific sulfotransferase enzyme. Alternatively, for solid-phase peptide synthesis, a de novo protected sY is required. Therefore, synthetic routes that go beyond O-sulfation are required. We have developed a novel route to N-sulfation and can dial-in/out O-sulfation (without S-sulfurothiolation), mimicking the initiation step of the ping-pong sulfation mechanism identified in structural biology. This rapid, low-temperature and non-racemising method is applicable to a range of amines, amides, amino acids, and peptide sequences.

The sulfate group is a ubiquitous post-translational modification that accounts for approximately 1% of all known epigenetic markers, and plays a vital role in a variety of biological processes, including protein–protein and oligosaccharide interactions.^[1–9]

Yet, sulfoproteins have been overlooked in favour of more common phosphorylated proteins, thus limiting our exploration of their function. Recent developments in ultra-high-resolution mass spectrometry have revealed a *m/z* difference of 9.5 mDa between kinase phosphorylation and sulfation.^[10–12] Therefore, many previously assigned phosphorylated proteins might have been mis-assigned. Protein sulfation might be more abundant and important than previously recognised. As with phosphorylation, proteins have been discovered to be sulfated at tyrosine (sY), serine (sS), threonine (sT) and histidine (sH).^[13] This opens up the possibility of further sulfation motifs that are yet to be discovered.

Methods to prepare sulfated proteins have focussed on the sulfated amino acid sY,^[2–5] with very limited examples of sS and sT.^[14,15] The pre-installation of a sulfate group onto Y is possible, using alternative protecting group methods,^[14,16–26] but with the added complication of the instability of sY to solid-

phase peptide cleavage. Chemical methods have various merits and drawbacks, but do allow for pinpoint accuracy in installing a sulfate group. Alternatively, the use of sulfotransferase (SULT), tyrosylprotein sulfotransferase (TPST), or aryl-sulfate sulfotransferase (ASST) with 3'-phosphoadenosine-5'-phosphosulfate (PAPS) cofactor allows selectivity between tyrosine groups, due to the ± 5 amino acids around Y and the effects of pre-existing sulfate groups (Scheme 1, previous work).^[2,27] A ping-pong mechanism discovered to operate with arylsulfotransferases, through a histidine N-sulfamate intermediate,^[28] spurred our interest in developing a general N-sulfation strategy to small molecules and peptides.

To the best of our knowledge, limited non-enzymatic methods to chemically sulfate a peptide directly have only been reported at phenolic tyrosine residues.^[29] Inspired by the role of sY, we sought to expand the sulfation epigenetic tool box to other amino acids. To address this, we detail a mild betaine-mediated method using tributyl sulfoammonium betaine (TBSAB) for the novel and rapid preparation of N-sulfamates.^[15] We demonstrate its scope on a diverse array of nitrogen-containing substrates and investigate heteroatom selectivity (N-sulfation v. O-sulfation v. S-sulfurothiolation). We surveyed the reactivity on nine canonical nucleophilic amino acid residues and demonstrate the ability to chemically modify peptide sequences (Scheme 1, this work).

There are limited reliable methods^[30] to prepare N-sulfamates: 1) direct sulfation with an SO₃–amine complex (amines used include Me₃N, Et₃N, Me₂Bz, Py, N-methylmorpholine) or an SO₃ source (chlorosulfonic acid); 2) sulfuric acid-mediated hydrosulfation of isocyanates; and 3) the reverse addition of a sulfamate through a carbonate intermediate for N-acyl sulfamates only.^[31] The limitations of these methods include the requirement for extensive chromatography and ion-exchange methods, incompatibility with acid sensitive substrates, and multistep sequences.

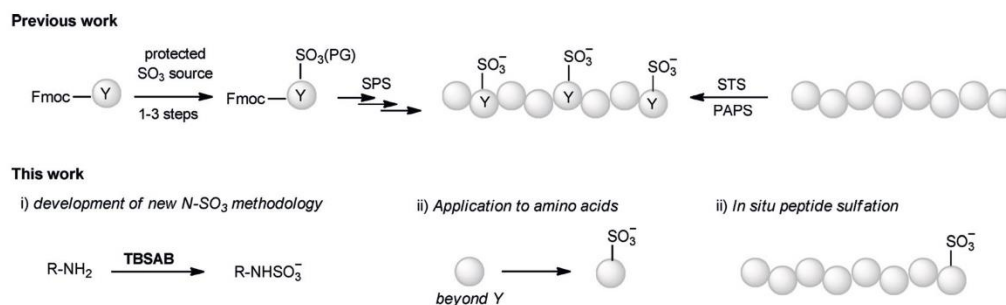
We have previously developed a new class of sulfating agent, TBSAB, that overcomes the purification challenges with sulfate esters,^[15] so considered whether TBSAB would provide a solution to the issues associated with accessing an under-exploited but important functional group. With benzylamine (1) as a model system, the progress of N-sulfation was readily monitored by ¹H NMR spectroscopy (Table 1). Subtle changes in the shielding of the benzylic methylene group gave insight into the variety of reaction pathways that could operate, including the dynamic interplay between protonation, sulfation, cation exchange and imidosulfation.

Surveying the reaction temperature (Table 1, entries 1–5) showed that 30 °C was optimal with 2.0 equivalents of TBSAB. Varying the equivalents of TBSAB (Table 1, entry 3 vs. 6–9)

[a] A. M. Benedetti, D. M. Gill, Dr. A. M. Jones
School of Pharmacy, University of Birmingham
Edgbaston, Birmingham B15 2TT (UK)
E-mail: a.m.jones.2@bham.ac.uk
Homepage: www.jonesgroupresearch.wordpress.com

[b] Dr. C. W. Tsang
School of Chemistry, University of Birmingham
Edgbaston Birmingham B15 2TT (UK)

Supporting information and the ORCID identification numbers for the authors of this article can be found under <https://doi.org/10.1002/cbic.201900673>.



Scheme 1. Previous approaches to sulfating tyrosine and sulfated peptides. This work: a new route to sulfating nitrogen, sulfation of a range of amino acids including tyrosine, and the nonenzymatic in situ sulfation of a peptide.

Table 1. Optimisation of benzylamine N-sulfamation.

	Amine-SO ₃	Equiv	T [°C]	Atmos.	Additive	Conv. [%]
1	Bu ₃ N	2.0	0	Ar	–	52 ^[a]
2	Bu ₃ N	2.0	20	Ar	–	71
3	Bu ₃ N	2.0	30	Ar	–	> 99 (98)
4	Bu ₃ N	2.0	60	Ar	–	87 ^[b]
5	Bu ₃ N	2.0	80	Ar	–	84 ^[b]
6	Bu ₃ N	0.5	30	Ar	–	> 99 ^[a]
7	Bu ₃ N	1.0	30	Ar	–	86 ^[a]
8	Bu ₃ N	1.5	30	Ar	–	86
9	Bu ₃ N	3.0	30	Ar	–	81
10	Me ₃ N	2.0	60	Ar	–	> 99 (23)
11	Py	2.0	60	Ar	–	47
12	Bu ₃ N	2.0	30	air	–	> 99 (48)
13	Bu ₃ N	2.0	30	Ar	Bu ₃ N (0.5 eq.)	> 99
14	Bu ₃ N	2.0	80	Ar	Bu ₃ NHCl (0.1 eq.)	> 99
15	Bu ₃ N	2.0	80	Ar	Bu ₃ NHCl (0.5 eq.)	78

[a] Formation of the benzylammonium salt (**2b**) observed. [b] Miscellaneous side products observed. Reaction conversions reported as measured by ¹H NMR spectroscopy. Selected isolated yields are reported in parentheses.

showed that 2.0 equivalents afforded high conversions. Unexpectedly, it was observed that the conversion for entry 6, with 0.5 equivalents of TBSAB, was quantitative. It was revealed that the tributylammonium cation can proton exchange with unreacted benzylamine in situ to afford **2b**. We found that extended reaction times increased the conversion to **2b**, with shorter reaction times (generally < 30 min, depending on substrate), avoiding this and leading to **2a** exclusively. Although **2b** is an impurity, exchange to the sodium salt delivers the identical product, **3**. The structures of **2a** and **2b** were confirmed by single-crystal X-ray crystallography.^[32]

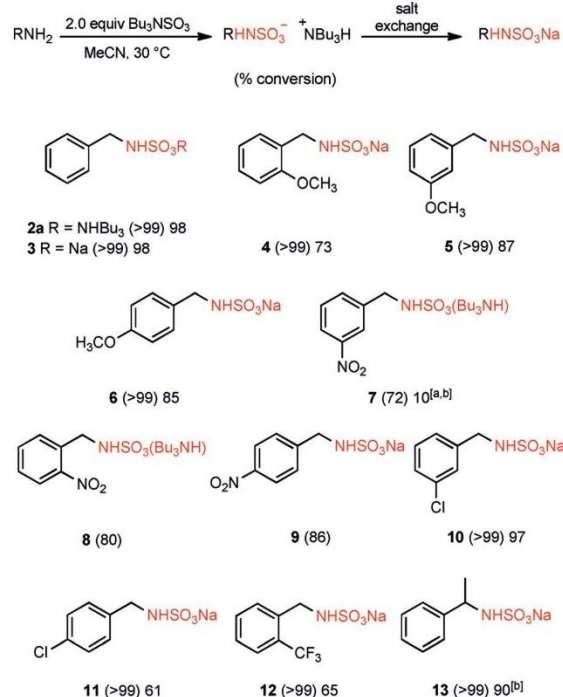
We next compared entry 3 with the commercial sulfating agents Me₃N–SO₃ and Py–SO₃ (Table 1, entries 10 and 11, respectively). The opposite reactivity trend to O-sulfation^[15] was observed with Me₃N–SO₃, affording a near-quantitative conver-

sion (> 99%) compared with Py–SO₃ (47%). An isolated yield of 23% was obtained from entry 10. It was proposed that this was due to the decreased lipophilicity of the trimethylammonium cation (cf. tributylammonium), which complicated purification. These control experiments highlighted the challenging purification cascades to obtaining analytically pure N-sulfated molecules with known strategies.

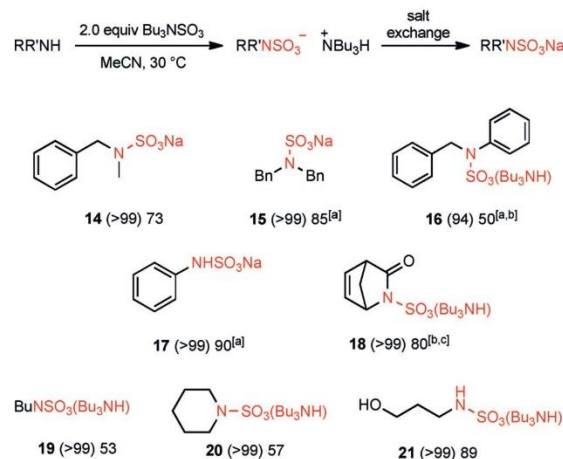
No deleterious effect of moisture was found (Table 1, entry 12). The use of additional base, such as tributylamine, was unnecessary (entry 13). The use of hydrochloride salt additives, at 10–50 mol% (entries 14 and 15), produced no observable or a modest (–21%) decrease in conversion, respectively. In summary, robust, optimised reaction conditions were identified as 2.0 equivalents of TBSAB at 30 °C, which afforded quantitative conversion and 98% isolated yield of **3** in less than 30 min. Importantly, the formation of imidosulfates was not observed under these conditions.^[33]

We then surveyed the generality of the developed conditions on a range of benzylamines with a range of stereoelectronic parameters (Scheme 2). The parent benzylamine was isolated as either the sodium (**3**) or tributylammonium salt (**2a**) in excellent isolated yields (both 98%). The incorporation of a strongly electron-donating methoxy group (**4–6**) was tolerated in all positions (quantitative conversions), except for a slight reduction in isolated yield for the *ortho* substituent (**4**); this is more likely to be due to the isolation method than the effect of intramolecular hydrogen bonding. The incorporation of a strongly electron-withdrawing nitro group (**7–9**) was tolerated, with good conversions in all cases (72–86%). Isolation as either the amine or sodium salt was complicated by the presence of the nitro group; note that with the nitro group in the *meta* position (**7**), the benzylamine was isolated as the tributylammonium salt (10%). Next, we investigated the effect of functionality relevant to medicinal chemistry, for example, with chloro (**10** and **11**) and trifluoromethyl (**12**) groups the reaction proceeded with quantitative conversion and 61–97% isolated yields. Finally, we considered whether a steric block on the α -benzylic position (**13**) would impede the reaction; however, the reaction proceeded with high conversion (> 99%) and excellent isolated yield (90%).

N-Sulfamation of secondary benzylamines with an *N*-methyl (**14**) or *N*-benzyl (**15**) group was well tolerated (Scheme 3). The



Scheme 2. Reaction scope on benzylamines. [a] $t = 60$ min; [b] isolated as NBu₃H salt. Parentheses indicate reaction conversion as measured by ¹H NMR spectroscopy.



Scheme 3. Reaction scope on diverse amines, amides and aminoalcohols. [a] $t = 60$ min; [b] isolated as NBu₃H salt; [c] $t = 24$ h. Parentheses indicate reaction conversion as measured by ¹H NMR spectroscopy.

incorporation of a *N*-phenyl (**16**) group, which changed the amine from an sp³ to a sp² centre, led to a noticeable drop in isolated yield and increased instability of the product. To investigate the *N*(sp²) effect, the sulfamation of aniline was attempted with an extended reaction time. This led to an excellent

yield of the antipyretic **17**.^[34] Finally, the sp² amide nitrogen reactivity of an Fsp³-rich scaffold (vinyl lactam) was investigated; a modest conversion to the *N*-sulfamate **18** was observed after 30 min, but this improved upon extended reaction time to afford the desired compound in an excellent 80% yield.

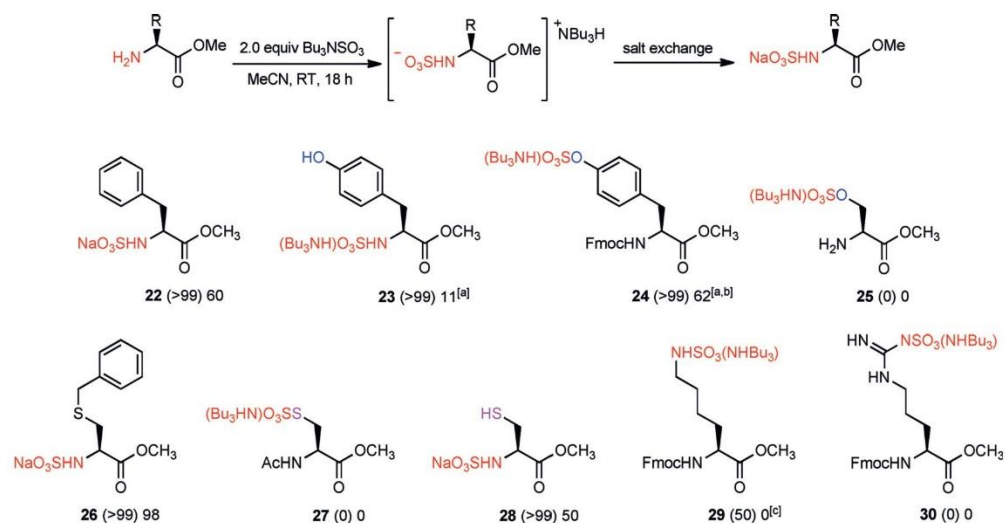
The methodology is also readily applicable to alkyl amines (linear **19**, 53% and cyclic **20**, 57%) and amino alcohols (**21**, 89%) with exclusive selectivity for *N*-sulfation over *O*-sulfation. A control experiment was performed to determine the stability of the dual-heteroatom-containing **21** for possible *N*-to-*O* sulfate transfer.^[35–37] Warming the sample led to partial conversion of the *N*-SO₃-containing **21** to the *O*-SO₃-containing molecule, presumably via a six-membered transition state, driven by the stability of the *O*-S bond over *N*-S.^[38]

We next sought to apply the methodology to amino acids (Scheme 4). If the reaction is to have wide appeal, the *N*-sulfamation chemistry needs to be performed at a non-denaturing temperature. Therefore, lower temperature (<38 °C) and longer reaction times were used. In all cases, no formation of an *N*-protonated amino acid counterion (cf. **2b**) was identified in the crude ¹H NMR spectra. We explored the generality of the optimised one-pot sulfamation methodology and the potential for heteroatom selectivity (nitrogen, oxygen and sulfur). We began with phenylalanine, which under non-denaturing reaction conditions led to quantitative conversion and a good isolated yield of **22** (60%) at the *N*-terminal position. The use of tyrosine raised the possibility of phenolic sulfation versus amine sulfamation. Under the optimised conditions, a quantitative conversion of **23** was observed at the *N*-terminal position. However, a low isolated yield of the sulfamate was obtained (11%). Importantly, no detection of phenolic sulfation in the crude ¹H NMR was observed.

It is also possible to sulfate the phenolic oxygen of tyrosine (sY) with TBSAB, but under different conditions that afforded the *N*-Fmoc-protected tyrosine *O*-sulfate **24** in 62% isolated yield. Sulfate **24** was found to be unstable in solution and desulfated to the starting material with time.^[39]

¹H NMR spectroscopy showed that serine underwent no detectable reaction at either the oxygen or nitrogen position (**25**, sulfation or sulfamation, respectively). The close proximity of an adjacent nucleophile likely shuts down the *N*-sulfamation route due to the steric bulk of TBSAB. Considering the result with tyrosine, the possibility of amino acid functional group selectivity is possible. We have shown a single example of serine *O*-sulfation is possible with TBSAB under markedly different reaction conditions (4.0 equiv of TBSAB, 38 °C for 52 h in DMF),^[15] thus demonstrating the potential to dial-in different reaction outcomes by careful selection of the conditions.

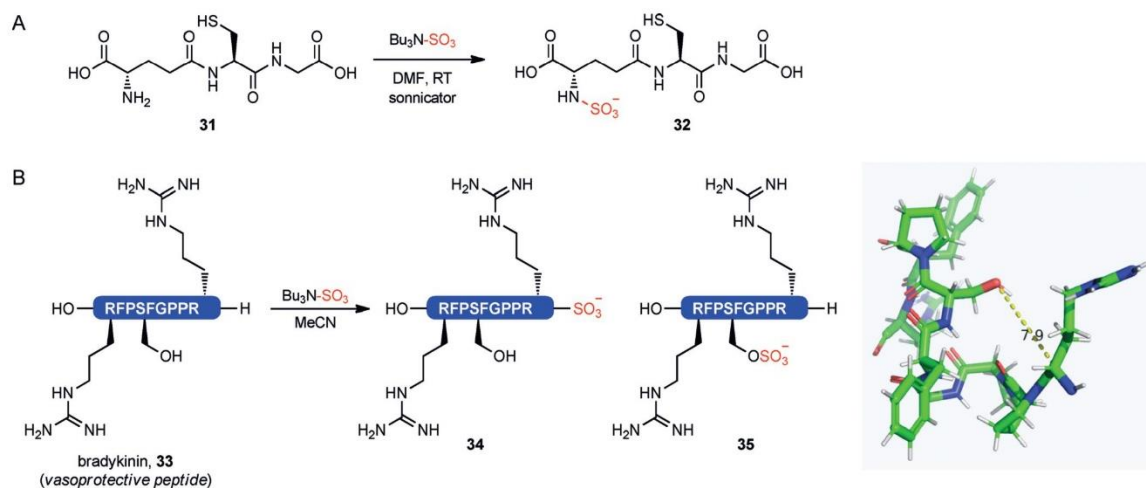
Next, we considered the ability to obtain heteroatom selectivity in cysteine analogues. The fully protected *S*-benzyl analogue gave exclusive *N*-terminal sulfamation in excellent conversion and isolated yield for **26** (98%). When the protecting group is transposed to the nitrogen (as an *N*-acyl amide), no *S*-sulfurothiolation was observed in **27** under mild conditions, thus demonstrating the *N*-selectivity profile of TBSAB under these conditions. When using a molecule with both an amine and thiol group, *N*-sulfamation was the exclusive product over



Scheme 4. Canonical amino acid reactivity survey. [a] Isolated as NBu_3H salt; [b] 4.0 equiv TBSAB, reflux, 6 h; [c] An analytically pure, stable sample could not be obtained. Parentheses indicate reaction conversion as measured by ^1H NMR spectroscopy.

S-sulfurothiolation with quantitative conversion and a modest isolated yield of **28** (50%). Next, we considered nitrogen-containing side chains in lysine and arginine. Lysine was partially sulfamated at the alkylamine position (**29**, 50% conversion), but, due to the poor N-nucleophilicity of guanidine, arginine did not react with TBSAB (**30** was not detected); again this demonstrated selectivity within the canonical amino acids. We also demonstrated that TBSAB does not racemise optically active amino acids, even under more forcing conditions.^[15] Measurement of the $[\alpha]_{\text{D}}^{25}$ of the sulfamates (**22–24**, **26**, and **28**) indicated that racemisation did not occur in these examples.

To test the hypothesis for site-selective sulfamation, a trimer (glutathione, **31**) and a nonamer (bradykinin, **33**) peptide sequence were selected (Scheme 5).^[40] In particular, bradykinin is a representative member of the vasoactive kinin class of cardioprotective peptides, and known to be secreted as sulfates in mammals.^[41] Treatment of glutathione gave rise to a single product, **32**, monosulfated at the N-terminal amine of glutamic acid. As a test of the methodology, it was envisioned that the sulfation of the nonamers, bradykinin, should lead to N-terminal sulfation (**34**). LCMS analysis revealed two monosulfated bradykinin derivatives (**34** and **35**). MS fragmentation patterns combined with a sulfation/sulfamation survey of canonical



Scheme 5. In situ sulfation of glutathione and bradykinin. Inset: crystal structure of bradykinin (PDB ID: 6F3V) with a 7.9 Å distance between Ser(OH) and Arg(NH₂).

amino acids (Scheme 4) indicated that bradykinin contains two potential nucleophilic sites. The major product (**34**) is the expected N-terminal sulfamation product; the minor product (**35**) was shown to be serine O-sulfate at serine. Analysis of the crystal structure of **33** (PDB ID: 6F3V) revealed a 7.8 Å distance between the *i* and *i*+5 residues (Arg and Ser), this is due to the presence of multiple proline residues that compress the α -helix (c. –20% per Pro). This gives further credence to the previously reported N-to-O sulfate shuttle in nature^[28] and a rationalisation for the observed sS product.

Conclusion

In summary, we have developed a rapid, mild and operationally straightforward route to the currently underexplored N-sulfamate class of molecules, a key functional group in chemical biology. We have demonstrated its wide scope and probed the heteroatom-selectivity profile and shown that, without protecting groups, N-sulfamation preferentially occurs over O-sulfation and S-sulfurothiolation without racemisation of the stereocentres. We have reported non-enzymatic examples of chemically sulfating and sulfamating a peptide in situ. This holds promise as a method to perform site-selective sulfamation of amino acid residues. The ability to modify post-translational protein sequences opens the door to future applications in structure sensing and understanding the underlying biology of sulfoprotein biology.

Acknowledgements

A.M.B. thanks the Erasmus⁺ UniPharma programme (University of Sapienza, Italy) for sponsorship. D.M.G. thanks the University of Birmingham for a PhD scholarship. The authors thank Dr. Louise Male, Dr. Cécile Le Duff, and the Centre for Chemical and Materials Analysis in the School of Chemistry, University of Birmingham for analytical support.

Conflict of Interest

The authors declare no conflict of interest.

Keywords: amino acids • sulfamation • sulfation • sulfopeptides • sulfurothiolation

- [1] S. Günl, R. Hardman, S. Kopriva, J. W. Mueller, *J. Biol. Chem.* **2019**, *294*, 12293–12312.
- [2] C. Seibert, M. Cadene, A. Sanfiz, B. T. Chait, T. P. Sakmar, *Proc. Natl. Acad. Sci. USA* **2002**, *99*, 11031–11036.
- [3] C.-C. Wang, B.-H. Chen, L.-Y. Lu, K.-S. Hung, Y.-S. Yang, *ACS Omega* **2018**, *3*, 11633–11642.
- [4] M. J. Stone, S. Chuang, X. Hou, M. Shoham, J. Z. Zhu, *New Biotechnol.* **2009**, *25*, 299–317.
- [5] J. P. Ludeman, M. J. Stone, *Br. J. Pharmacol.* **2014**, *171*, 1167–1179.
- [6] G. Loers, Y. Liao, C. Hu, W. Xue, H. Shen, W. Zhao, M. Schachner, *Sci. Rep.* **2019**, *9*, 1064.
- [7] G. Chen, X. Chen, *J. Biol. Chem.* **2003**, *278*, 36358–36364.
- [8] A. Hille, W. B. Huttner, *Eur. J. Biochem.* **1990**, *188*, 587–596.

- [9] J.-C. Lee, X.-A. Lu, S. S. Kulkarni, Y.-S. Wen, S.-C. Hung, *J. Am. Chem. Soc.* **2004**, *126*, 476–477.
- [10] D. P. Byrne, Y. Li, P. Ngamlert, K. Ramakrishnan, C. E. Evers, C. Wells, D. H. Drewry, W. J. Zuercher, N. G. Berry, D. G. Fernig, P. A. Evers, *Biochem. J.* **2018**, *475*, 2435–2455.
- [11] Y.-S. Yang, C.-C. Wang, B.-H. Chen, Y.-H. Hou, K.-S. Hung, Y.-C. Mao, *Molecules* **2015**, *20*, 2138–2164.
- [12] G. D. Balderrama, E. P. Meneses, L. H. Orihuela, O. V. Hernandez, R. C. Franco, V. P. Robles, C. V. F. Batista, *Rapid Commun. Mass Spectrom.* **2011**, *25*, 1017–1027.
- [13] T. Hunter, *Cell* **1995**, *80*, 225–236.
- [14] S. V. Campos, L. P. Miranda, M. Meldal, *J. Chem. Soc. Perkin Trans. 1* **2002**, 682–686.
- [15] D. M. Gill, L. Male, A. M. Jones, *Chem. Commun.* **2019**, *55*, 4319–4322.
- [16] A. M. Ali, S. D. Taylor, *Angew. Chem. Int. Ed.* **2009**, *48*, 2024–2026; *Angew. Chem.* **2009**, *121*, 2058–2060.
- [17] K. Kitagawa, C. Aida, H. Fujiwara, T. Yagami, S. Futaki, M. Kogire, J. Ida, K. Inoue, *J. Org. Chem.* **2001**, *66*, 1–10.
- [18] L. S. Simpson, J. Z. Zhu, T. S. Widlanski, M. J. Stone, *Chem. Biol.* **2009**, *16*, 153–161.
- [19] T. Young, L. L. Kiessling, *Angew. Chem. Int. Ed.* **2002**, *41*, 3449–3451; *Angew. Chem.* **2002**, *114*, 3599–3601.
- [20] L. S. Simpson, T. S. Widlanski, *J. Am. Chem. Soc.* **2006**, *128*, 1605–1610.
- [21] A. Y. Desoky, J. Hendel, L. Ingram, S. D. Taylor, *Tetrahedron* **2011**, *67*, 1281–1287.
- [22] D. Taleski, S. J. Butler, M. J. Stone, R. J. Payne, *Chem. Asian J.* **2011**, *6*, 1316–1320.
- [23] X. Liu, L. R. Malins, M. Roches, J. Sterjovski, R. Duncan, M. L. Garcia, N. C. Barnes, D. A. Anderson, M. J. Stone, P. R. Gorry, R. J. Payne, *ACS Chem. Biol.* **2014**, *9*, 2074–2081.
- [24] Y. S. Hsieh, L. C. Wijeyewickrema, B. L. Wilkinson, R. N. Pike, R. J. Payne, *Angew. Chem. Int. Ed.* **2014**, *53*, 3947–3951; *Angew. Chem.* **2014**, *126*, 4028–4032.
- [25] M. J. Stone, R. J. Payne, *Acc. Chem. Res.* **2015**, *48*, 2251–2261.
- [26] A. Benjdia, A. Guillot, P. Ruffie, J. Leprince, O. Berteau, *Nat. Chem.* **2017**, *9*, 698–707.
- [27] A. S. Woods, H.-Y. J. Wang, S. N. Jackson, *J. Proteome Res.* **2007**, *6*, 1176–1182.
- [28] G. Malojčić, R. L. Owen, J. P. A. Grimshaw, M. S. Brozzo, H. Dreher-Teo, R. Glockshuber, *Proc. Natl. Acad. Sci. USA* **2008**, *105*, 19217–19222.
- [29] T. Nakahara, M. Waki, H. Uchimura, M. Hirano, J. S. Kim, T. Matsumoto, K. Nakamura, K. Ishibashi, H. Hirano, A. Shirashi, *Anal. Biochem.* **1986**, *154*, 194–199.
- [30] R. A. Al-Horani, U. R. Desai, *Tetrahedron* **2010**, *66*, 2907–2918.
- [31] H. Rogers, G. Humphrey, A. Chiu, T. Pei, *Synthesis* **2008**, 2298.
- [32] CCDC 1936116 (**2a**) and 1935974 (**2b**) contain the supplementary crystallographic data for this paper. These data are provided free of charge by The Cambridge Crystallographic Data Centre.
- [33] F. Kanetani, H. Yamaguchi, *Bull. Chem. Soc. Jpn.* **1974**, *47*, 2713–2716.
- [34] L. F. Audrieth, M. Sveda, *J. Org. Chem.* **1944**, *9*, 89–101.
- [35] See the Supporting Information: additional data section **S5** for ¹H, ¹H COSY NMR spectra of the in situ N-to-O sulfate shuttle control experiment.
- [36] For a report of N-desulfation kinetics, see: K. Nagasawa, H. Yoshidome, *Chem. Pharm. Bull.* **1969**, *17*, 1316–1323.
- [37] For related examples of N-to-O sulfate shuttling, see: a) A. Hopkins, A. Williams, *J. Org. Chem.* **1982**, *47*, 1745–1750; b) A. Hopkins, R. A. Day, A. Williams, *J. Am. Chem. Soc.* **1983**, *105*, 6062–6070.
- [38] Y. Inoue, K. Nagasawa, *J. Org. Chem.* **1973**, *38*, 1810–1813.
- [39] See the Supporting Information: additional data section **S6** for tyrosine O-sulfate stability studies.
- [40] See the Supporting Information: additional data section **S7** for sulfated peptide LCMS traces.
- [41] X. Xi, B. Li, T. Chen, H. F. Kwok, *Toxins* **2015**, *7*, 951–970.

Manuscript received: November 2, 2019

Accepted manuscript online: November 6, 2019

Version of record online: ■ ■ ■ 0000

Chapter 5: The Rational Design and Synthesis of Heparin and Heparan Sulfate Glycomimetics

5.1. Synthesis of the 1st Generation HS-Glycomimetics

At the end of Chapter 2.4 the primary aims of this investigation were described:

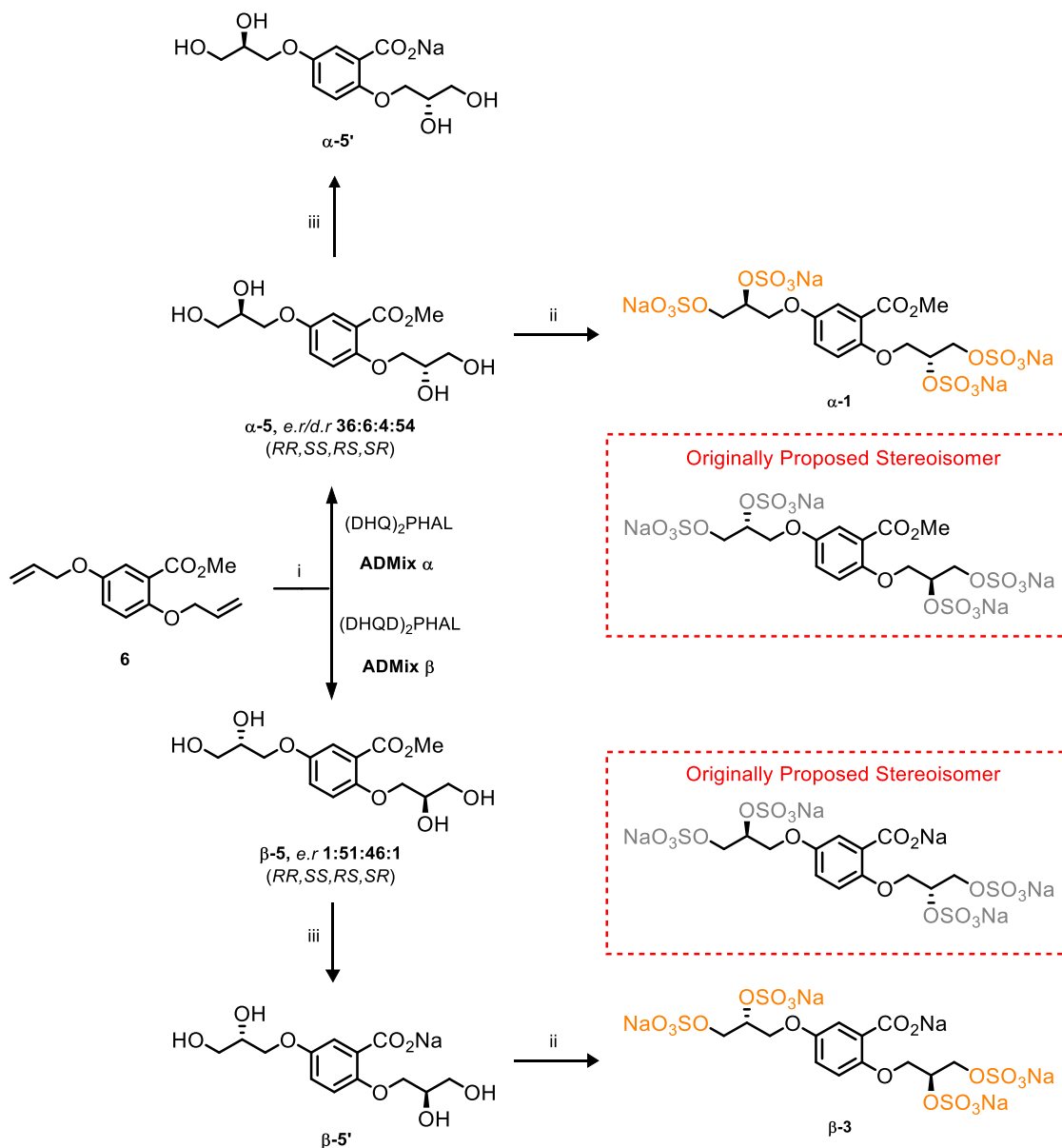
- Create a robust chemical synthesis towards the first generation of small molecule HS-glycomimetics, providing a stock of compounds for further use and biological testing
- Examine the original glycomimetics computationally and in a binding affinity assay to gain additional evidence to support or query the results of previous investigations on HGF binding/inhibition
- Design additional generations of HS-glycomimetics and computationally model their interactions in the H/HS-binding site of HGF
- Synthesise the newly designed glycomimetic structures and quantify their HGF-binding affinities in a biological assay, thus providing an SAR profile (Figure 18)

This chapter focuses on the four primary aims of this investigation, the synthesis, characterisation and computational modelling of a 1st and 2nd generation HS-glycomimetics derived from the compounds (**1-3**) originally prepared by Raiber et. al.¹

5.1.1. The Synthesis of HS-Glycomimetics *RS-1* and *SR-3*

With the results of the chPLC investigation (Chapter 3) providing new knowledge of the stereochemical outcome from a tandem AD of diene **6**, and by using the newly developed sulfation methodology (Chapter 4), the persulfation of tetraols **α -5** and **β -5** afforded the first generation HS-glycomimetics **α -1** and **β -3** in 88% and 86% yield, The chPLC results confirmed that **α -5** and **β -5** are diastereomeric mixtures in both cases, and, in comparison to the original literature, the stereochemistry of the two persulfates is reversed. Therefore, the AD conditions to access the originally assigned tetraols and subsequent glycomimetics, ***RS-1*** and ***SR-3***, are reversed (Scheme 28).

In short, this has corrected the original report¹ and subsequent reports relating to the biological activity of HS-glycomimetics **1** and **3**.²⁻¹²



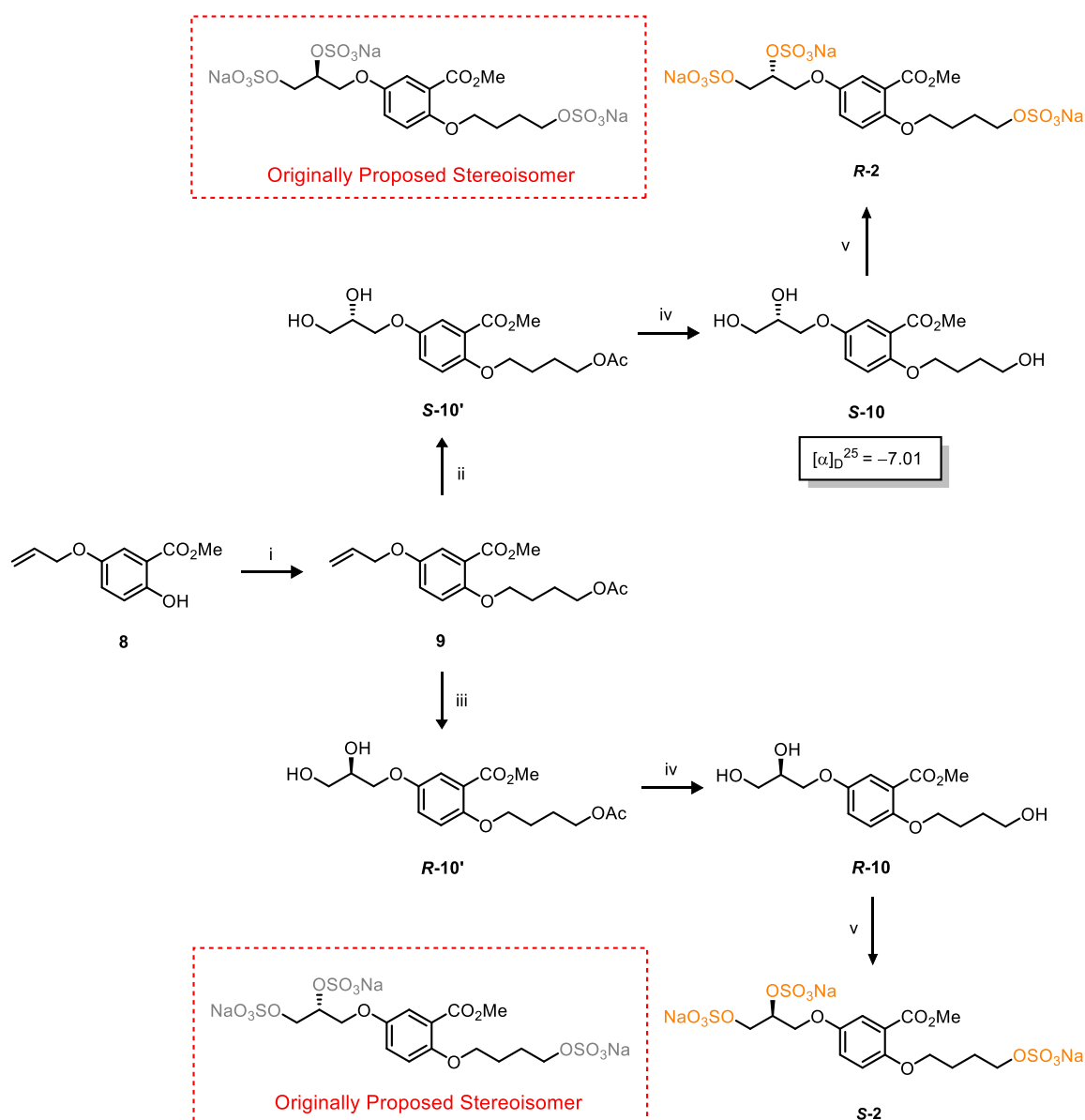
Scheme 28: The synthesis of first generation HS-glycomimetics **α-1** and **β-3**, including four biologically relevant intermediates considered in this investigation. Conditions: **i**) K₂CO₃, K₃Fe(CN)₆, K₂O₅(OH)₄, tBuOH/H₂O, 0 °C, 12 h, **99%** for both; **ii**) Bu₃N•SO₃, MeCN, 90 °C, 8 h; **iii**) NaOH, MeOH, 70 °C, 2 h **99%** for both; **ii**) Bu₃N•SO₃, MeCN, **88%** and **86%** for **α-1** and **β-3**, respectively.

It was proposed that all intermediates should be examined for biological activity, to validate the binding interactions of anionic sulfate groups to HGF. Therefore, the methyl esters **α/β-5** and hydrolysed intermediates **α/β-5'** were used as additional examples of non-sulfated species (Scheme 28). Overall, this provided a set of six

glycomimetics, 2 persulfated (the corrected **α -1** and **β -3** from the original report¹) and three non-sulfated compounds **α -5**, **α -5'** and **β -5'**.

5.1.2. The Synthesis of HS-Glycomimetics ***S*-2** and ***R*-2**

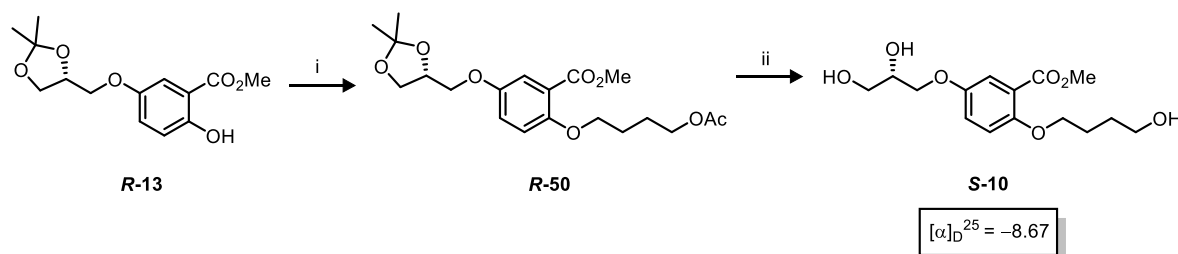
The synthesis of ***S*-2** and ***R*-2** was adapted from the original literature report, in similar accordance to the synthesis of **α -1** and **β -3**, (Scheme 29).¹ The alkylation of phenol **8** with 4-bromobutylacetate afforded alkene **9** in 90% yield.



Scheme 29: The synthesis of HS-glycomimetics ***S*-2** and ***R*-2**. Conditions: **i**) 4-Bromobutylacetate, K₂CO₃, TBAI, acetone, reflux, 12 h, **90%**, **ii**) ADmix β , ^tBuOH/H₂O, 0 °C, 12 h, **99%** for both; **iii**) ADmix α , ^tBuOH/H₂O, 0 °C, 12 h, **99%** for both; **iv**) K₂CO₃, MeOH, rt, 12 h, **99%** for both; **v**) Bu₃N•SO₃, MeCN, 90 °C, 12 h, **72%** and **97%** for ***R*-2** and ***S*-2**, respectively.

With **9** in hand, twin AD reactions were carried out under α and β conditions, affording diols **R-10'** and **S-10'** in 99% yield, for both (Scheme 29). A chemoselective hydrolysis of the acetate functionality using K_2CO_3 in MeOH afforded triols **R-10** and **S-10** in 99% yield, for both. Final sulfation of the triols using $Bu_3N \cdot SO_3$ afforded first generation HS-glycomimetics **R-2** and **S-2** in 72% and 97% yield, respectively (Scheme 29). Particularly, the sulfation of enantiomer **R-10** was carried out on a 400 mg (1.27 mmol) scale for a collaborative investigation, affording 600 mg of **S-2** as a pure Na^+ salt (76% yield).

Due to the prior results gained from the AD of alkene **17** (Chapter 3.9.5), it was proposed that the stereochemical outcome of the diols (**10'**) would be between 85:15 – 95:5 *e.r* (for the major stereoisomer) and match the stereochemical prediction of the Sharpless mnemonic device. To confirm this, the synthesis of **R-10** was also accomplished by a chiral pool method, and the optical rotation of both intermediates (**S-10**) were compared to calculate the extent of enantioselectivity in the AD of alkene **9**. The optical rotations correlated with the predicted stereochemical outcome from the Sharpless mnemonic device, and the closely matching values (-7.01 Vs -8.67 , c 1.0, $CHCl_3$) confirm that the correct enantiomer was synthesised in 91:9 *e.r* (*S/R*) (Scheme 30).



Scheme 30: A chiral pool synthesis of **S-10** for the comparison of optical rotation. Conditions: **i**) 4-Bromobutylacetate, K_2CO_3 , TBAI, acetone, reflux, 12 h, **90%**, **ii**) 1) NaOMe 2) TFA, MeOH, 12 h. **quant.**

The results of this investigation also show that the proposed stereochemistry of diols **10'** and corresponding HS-glycomimetics were incorrectly assigned in the original investigation, and in further reports of their biological activity.¹⁻¹² Therefore, this investigation has assigned the correct stereochemistry to all original HS-glycomimetics (**1-3**) previously reported by Raiber et. al.¹⁻¹²

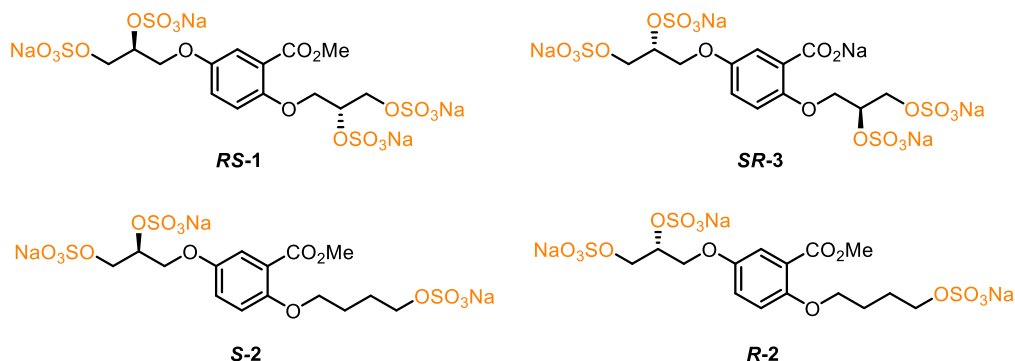
In summary, the first generation of HS-glycomimetics (**1-3**), designed to target the HGF/MET-receptor interaction, were synthesised in high yield, providing a stock of biologically relevant structures for testing and future use. Each HS-glycomimetic and their intermediates were characterised with full elucidation of stereochemistry, and the final organosulfates were afforded as their biologically relevant Na⁺ salts, thus completing the first overall aim of this investigation.

5.1.3. Computational Modelling and Docking Studies

The HS-glycomimetics (**RS-1**, **R-2**, **S-2** and **SR-3**) from the current literature were chosen for a computational docking study (Figure 51, A).¹⁻¹² Considering HS has many non-sulfated regions in its macrostructure (See Chapter 1), and non-ionic interaction can account for up to 70% of the binding free energy,¹³ it is proposed that the interactions of HS with HGF do not rely predominantly on anionic charge density from multiple sulfate functionalities. Therefore, for further comparison, three non-sulfated intermediates were also studied (**α-5**, **α-5'** & **β-5'**) to examine the significance of sulfate groups to the binding of HGF (Figure 51, B). The previously reported biological activity of HS-glycomimetics **1-3** demonstrated a similar therapeutic effect *in vitro*,²⁻¹² however, it is now known that **α-1** and **β-3** are mixtures of persulfated diastereoisomers, so to simplify the docking study only stereo-defined diastereomers were selected. Therefore, the results can be corroborated with the results of previous investigations²⁻¹² and the biological assays conducted by this investigation. Notably, a

computational investigation for each enantiomer/diastereoisomer of HS-glycomimetic **1** is discussed in Chapter 5.2.

A. Sulfated



B. Non-sulfated

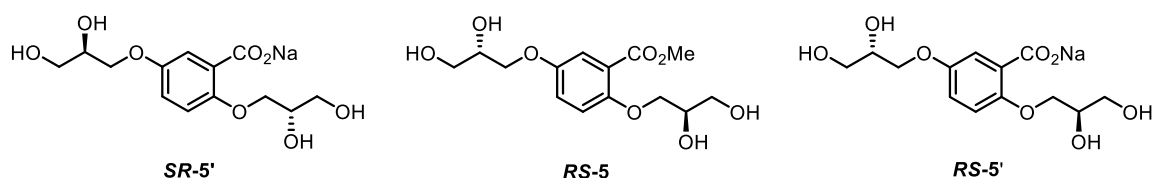


Figure 51: The selected HS-glycomimetics chosen for a computational docking study, along with relevant non-sulfated intermediates that were selected to examine the effects of sulfation to the binding interaction.

Similar to previous work by Raiber et. al.¹, the computational model was built based on the X-Ray crystal structures of NK1 (HGF) (PDB: 1BHT, 2.0 Å resolution).¹⁴ In order to check that the selected blind docking process was adequate for finding a correct binding site of the HS-glycomimetics, a H-tetrasaccharide was extracted from an H-NK1 complex¹⁵ (1GMN, 3.0 Å resolution) and docked into the higher resolution 1BHT using Autodock[®] 1.5.6 (100 runs). All docked structures were clustered at 1.0 Å (root-mean-square deviation of atomic positions, RMSD). The most negative energy cluster contained an H-tetrasaccharide conformation with a docking energy of $-580.11 \text{ kJ mol}^{-1}$, and a matching conformation to the X-ray crystal structure of H-NK1 complex.¹⁴ Each HS-glycomimetic and non-sulfated intermediate was docked individually against

1BHT under matching conditions (Table 11) and each minimum docking energy was calculated.¹⁶ All active conformations can be found in Chapter 6.7.

Table 11: The minimum docking energies, number of sulfate groups and hydrogen bonding interactions of selected HS-glycomimetics and non-sulfated intermediates. Chemical structures are given in **Figure 53**.

Entry	Compound Number	Docking Energy (kJ mol ⁻¹)	No. of SO ₃ ⁻	No. of H-bonds
1	RS-1	-60.92	4	7
2	SR-3	-64.31	4	6
3	S-2	-49.25	3	8
4	R-2	-48.91	3	4
5	RS-5'	-17.28	0	4
6	SR-5'	-15.69	0	4
7	RS-5	-12.22	0	6

The results of the docking study show that the persulfated HS-glycomimetics (Table 11, Entries 1 – 4) have a significantly greater binding energy and, therefore, a higher affinity for the HS-binding site of HGF than the non-sulfated intermediates (Table 11, Entries 5 – 7). This can be attributed to a greater interaction facilitated by the numerous anionic sulfate groups in the chemical structures. A comparison between the four sulfated compounds demonstrates a further enhancement in the binding energy by the hydrolysis of the methyl ester (Table 11, Entries 1 vs. 2). This is likely the result of the carboxylate anion of **SR-3** creating further ionic bonding interactions with the basic (cationic) residues at the protein's accessible surface. Conversely, **SR-3** is calculated to have less hydrogen bonding interactions (See Chapter 6.7), so the observed binding energy is associated with electrostatics and possible stereochemistry, which creates a better matched interaction with the HS binding-site. Although, the calculated 0.34 kJ mol⁻¹ difference in binding energy between **S-2** and **R-2** (Table 11, Entries 3 vs. 4) suggests that single point changes in point chirality are not significant

to the binding interaction. Similar trends are also observed for the non-sulfated intermediates (Table 11, Entries 5 – 6). The number of intermolecular H-bonds does not correlate with the calculated binding energy, nor the number of sulfate groups, and the overall results of the docking study show that the binding of the HS-glycomimetics to HGF is expected to be facilitated by electrostatic interactions from the anionic sulfate groups in their structures. Moreover, the non-sulfated intermediates are predicted to interact in a different area of the HS-binding site (See Chapter 6.7), so HGF binding of the non-sulfated intermediates (**5** & **5'**) is likely non-specific. Nonetheless, the intermediates are shown to bind HGF, which gives justification to the analysis of their biological activity (This is discussed further in Chapter 5.1.4).

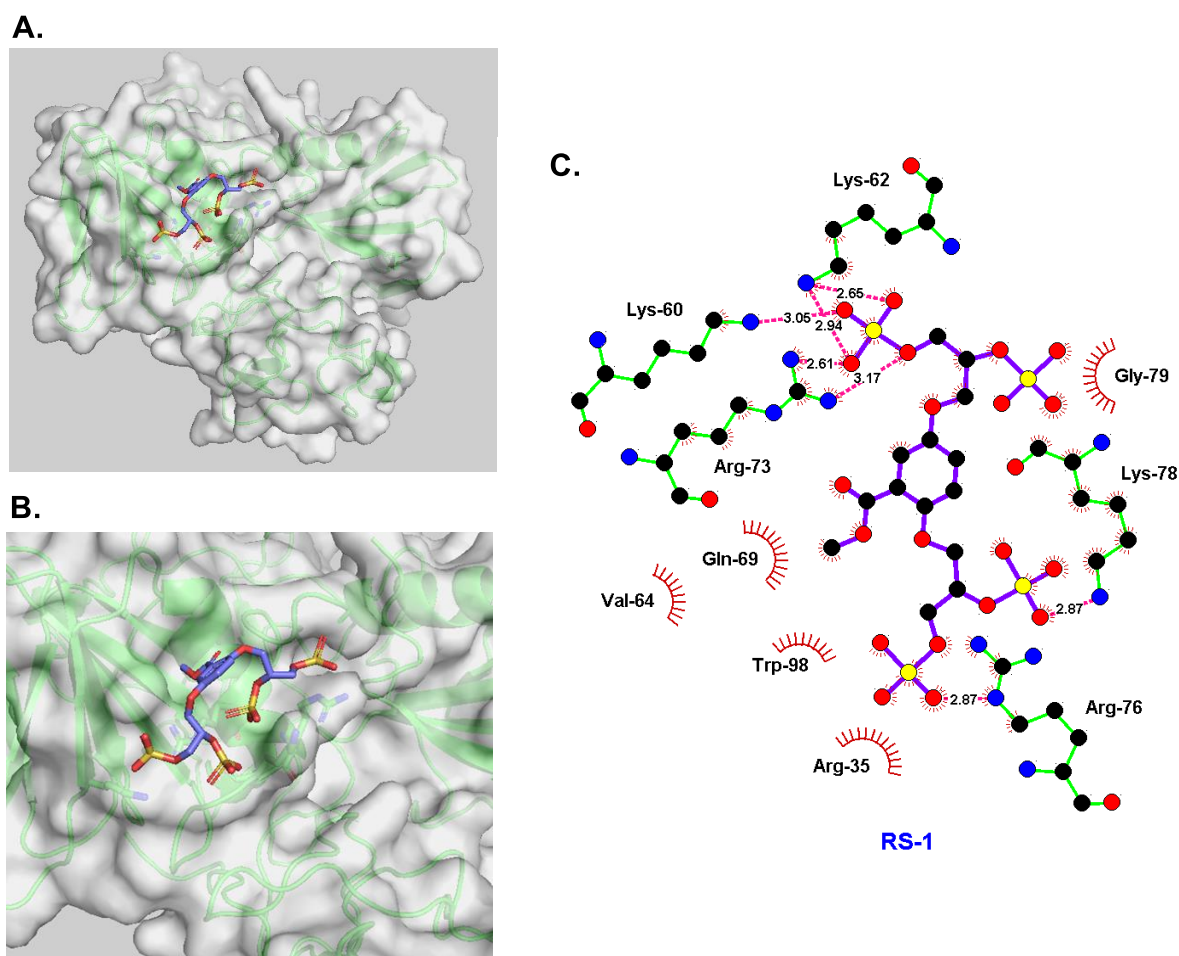


Figure 52: **A)** The minimum energy docked structure of HS-glycomimetic **RS-1** into the H/HS-binding site of NK1 (HGF), Table 11, Entry 1; **B)** Zoomed in view of the docked structure; **C)** Ligplot representation of the binding interaction, displaying the vicinal amino acid residues and the hydrogen bonding of specific amino acids to **RS-1**.

Interestingly, the docked structure of the ***RS-1***-HGF complex (Figure 52, A) shows that the methyl ester is orientated directly into a hydrophobic pocket on the protein's accessible surface (Figure 52, B). Comparing this interaction to the ***SR-3***-HGF complex (See Chapter 6.7) indicates that this mode of binding is specific to the methyl ester group (present in both HS-glycomimetics **1** & **2**), and the anionic carboxylate group (present in HS-glycomimetic **3**) is orientated differently inside the HS-binding site of HGF (Figure 52, C). This interaction is interesting, as it is not gained through further electrostatic forces and is likely driven by enhanced hydrogen bonding and Van der Waals forces. Consequently, the methyl ester is considered important to the design of a second generation of HS-glycomimetics (discussed in Chapter 5.3).

Overall, the results of the computational study propose that the HS-glycomimetics bind HGF predominantly through electrostatic interactions. However, the results also highlight the potential significance of the methyl ester and point chirality to the binding interaction of HGF.

5.1.4. Results of Biological Assays

The biological assays used in this investigation focused on the production of nitric oxide (NO) and the upregulation of nitric oxide synthase (eNOS), the production of reactive oxygen species (ROS) and the activity of nicotinamide adenine dinucleotide phosphate (NADPH) oxidase (Table 12). From the hypothesised model of HS-glycomimetic activity (Figure 17),^{2, 5} the glycomimetics are proposed to attenuate the binding of HGF to the cMET receptor. This disruption to MET-receptor activation is proposed to modulate intracellular phosphorylation leading to an upregulation of eNOS and increased output of extracellular NO. Furthermore, the mechanism of action has also been demonstrated to modulate the enzymes: superoxide dismutase (SOD), catalase (CAT) and glutathione peroxidase (GPx), which quench intracellular ROS using NADPH as

cofactor. Overall, the cross examination of NO output and reduction of ROS was used to determine the therapeutic action of the first generation glycomimetics **α -1**, **R -2**, **S -2** and **β -3**, as well as 3 non-sulfated intermediates **α -5**, **α -5'** and **β -5**, on free fatty acid (FFA) induced, oxidatively stressed endothelial cell cultures (Table 12).⁶

Table 12: Biological data for eNOS and ROS. All data are averaged % of increase (+) or decrease (–) compared to control (FFA induced oxidatively stresses endothelial cells). All biological assays were carried out by Dr. A. M. Mahmoud (Department of endocrinology, diabetes and nutrition, center for cardiovascular research, Charité - Universitätsmedizin Berlin, Berlin, Germany). (n = 3)

Entry	Compound Number	MW (Da)	NO production	eNOS phosphorylation	ROS production	NADPH oxidase activity
1	α-1	723.87	+110	+342	–28	–29
2	β-3	731.83	+62	+318	–29	–31
3	S-2	619.95	+63	+397	–39	–27
4	R-2	619.95	+52	+613	–23	–31
5	α-5'	324.08	+41	+312	–23	–21
6	β-5'	324.08	+52	+294	–19	–27
7	α-5	316.11	+46	+286	–36	–26

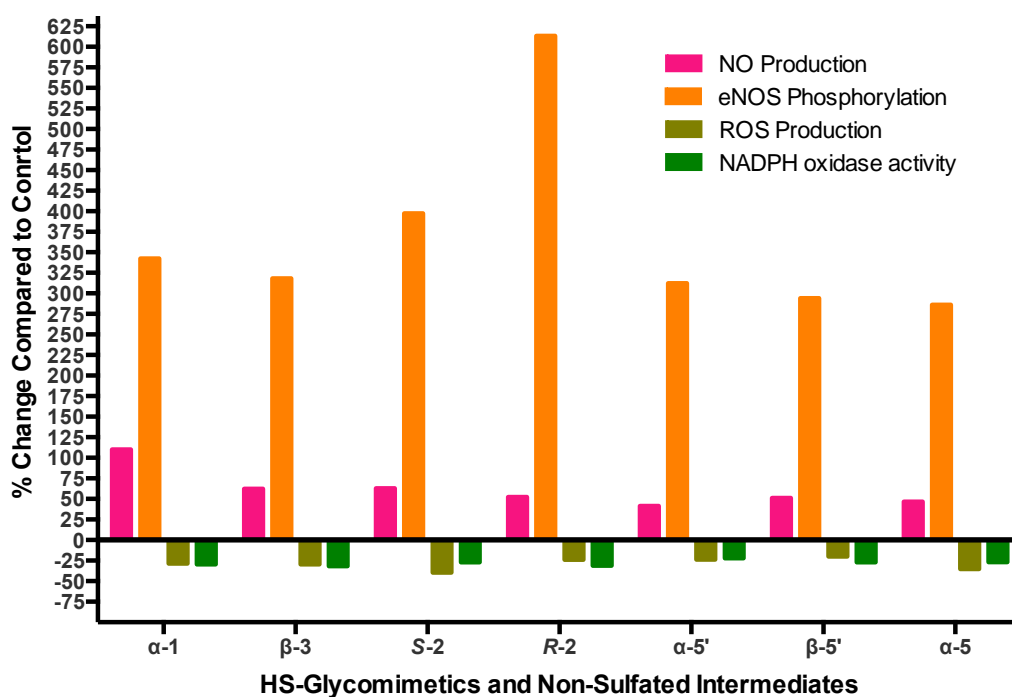


Figure 53: A graphical representation of the biological results presented in Table 12, n = 3.

The results of the biological assays demonstrate similar trends across each compound (Table 12). Administration of the HS-glycomimetics and non-sulfated intermediates generates an increase in eNOS phosphorylation with an associated output of NO. Furthermore, each compound demonstrated a correlation in the reduction of ROS and NADPH oxidase activity.

Specifically, for the HS-glycomimetic **a-1** (Table 12, Entry 1), the concentration of NO increase by +110% compared to the control. However, the increased phosphorylation of eNOS is comparable to the other compounds tested, with the exception of **R-2**, which is shown to increase eNOS phosphorylation significantly greater than all the other compounds tested (+613%, Table 12, Entry 4). However, the increased eNOS phosphorylation does not correlate with the output of NO (+52%), which could be attributed to the controlled concentrations of arginine (NO source) in the biological media.⁶ The results demonstrated by **a-1** are in conflict with this, thus the results are considered anomalous as no further evidence could be provided to rationalise this effect *in vitro*.

All the remaining compounds demonstrated similar biological activity. Therefore, no significant conclusions can be made regarding the structure activity relationships (SAR) of the HS-glycomimetic. Furthermore, the biological results do not correlate with the proposed binding interactions/energies calculated in the computational docking study, suggesting that anionic sulfate groups are not significant to the inhibition of HGF. Moreover, because the sulfated HS-glycomimetics demonstrated a similar biological activity to the non-sulfated intermediates, the overall results propose that the non-sulfated compounds have an enhanced ligand efficiency, because they have a lower molecular weight (43 – 45% less by molecular mass).

The conflicting evidence suggests that the non-sulfated intermediates (**5** and **5'**) may interact differently with HGF, which may be causing the observed enhancement of inhibitory activity. However, it may also be plausible that the sulfated HS-glycomimetics are unstable at physiological pH (7.4) or in the presence of the FFA, administered to the cell cultures to induce oxidative stress (*in vitro*). Such instability is likely to decompose the persulfates back to their corresponding polyol intermediates prior to HGF binding. Therefore, the sulfated compounds may act as a hydrophilic prodrug, and the observed therapeutic action could be the result of a previously uncovered biological activity with other cellular receptors, such as FGF and VEGF.¹⁷⁻¹⁸ Overall, the conflicting results of the computational and biological investigations highlight that all future sulfated and non-sulfated compounds need to be considered for biological activity against HGF. Furthermore, the stability of the sulfated HS-glycomimetics needs to be investigated further, to ascertain if the persulfates are unstable at a physiological pH or in the presence of FFA (This is discussed further in Chapter 5.6. Future work).

The results of this study fulfil the second overall aim of this investigation, by computationally modelling a variety of first generation HS-glycomimetics and analysing their HGF binding in relevant biological assays. However, the results have provided no evidence in favour or against the proposed mode of biological activity and the binding of HGF.

5.1.5. Conclusion

In summary, the work discussed in this chapter presents conflicting arguments for the HS-glycomimetic binding/inhibition of HGF. The computational docking studies and the *in vitro* biological assays suggest that anionic sulfate groups are not a prerequisite for the successful inhibition of MET-receptor activation. However, the results highlight a potentially different mode of HGF binding for the non-sulfated intermediates (**5** and

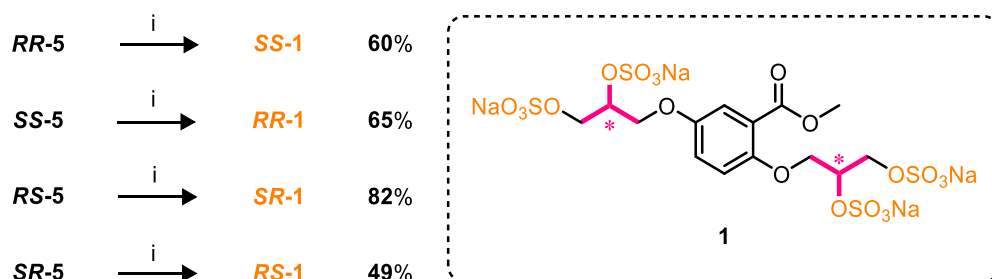
5') that generates a similar biological response to the sulfated HS-glycomimetics (**1-3**). The results query the stability of the synthesised persulfates at a physiological pH, or in the presence of free fatty acids (FFA), and changes in stereochemistry does not significantly enhance or diminish the associated biological activity. However, to investigate this further a computational docking study was performed with individual enantiomers and diastereomers of HS-glycomimetic **1**, and is discussed in the following chapter.

5.2. Is Stereochemistry Significant to the Binding of HGF?

This Chapter focuses on the last (two) overall aims of this investigation (See the beginning of Chapter 5.1).

5.2.1. The Chiral Pool Synthesis of HS-Glycomimetic ± 1

For every stereochemical combination of **1**, a chiral pool method was utilised as the precursors (tetraol **5**) had already been afforded by a previous investigation (Chapter 3). Using the newly developed sulfation methodology (Chapter 4), every stereo-defined tetraol (Scheme 31) was sulfated with $\text{Bu}_3\text{N}\cdot\text{SO}_3$, affording the corresponding persulfated glycomimetic (**1**) in 49 – 82% isolated yield (Na^+ salts). Overall, this route provided an efficient synthesis to each stereochemical combination of **1**.



Scheme 31: A chiral pool synthesis of **1**, synthesising each stereochemical combination. Conditions: **i**) 1) $\text{Bu}_3\text{N}\cdot\text{SO}_3$, MeCN, 90 °C, 2) NEH, $t\text{BuOMe/EtOH}$.

5.2.2. Computational Modelling and Docking Studies

A computational docking study was conducted for each stereochemical combination to determine if the binding interactions of the HS-glycomimetics are effected by single point changes in chirality (Table 13).

Table 13: The calculated minimum docking energies and hydrogen bonding interactions of each stereochemical combination of HS-glycomimetic **1**.

Entry	Compound Number	Docking Energy (kJ mol ⁻¹)	No. of H-bonds
1	RR-1	-58.53	7
2	SS-1	-61.42	5
3	RS-1	-60.92	7
4	SR-1	-59.25	6

The results of the computational docking study proposes that each stereochemical combination binds with similar energies (Table 13, Entries 1 – 4) and with a similar numbers of hydrogen bonding interactions. Therefore, at first appearance, the data suggests that stereochemistry is not significant to the binding interactions of **1** with HGF. The docking results calculated that the enantiomer **SS-1** to have the greatest energy binding interaction with NK1 (-61.42 kJ mol⁻¹, Table 13, Entry 2). Furthermore, the enantiomer **RR-1** is calculated to have the lowest binding energy (-58.53 kJ mol⁻¹, Table 13, Entry 1). However, an difference of ± 2.38 kJ mol⁻¹ suggests that non-electrostatic intermolecular forces, such as VdW, have minimal effects on the binding interaction.¹¹ The diastereomers **SS-1/RS-1** have closely matched energies (± 0.50 kJ mol⁻¹, Table 13, Entries 3 & 4), which is comparable to the docking energies observed from enantiomers **R-2** and **S-2** (Table 11, Entries 3 & 4). Changes in stereochemistry at the 2-positions (relative to the methyl ester) demonstrate an associated decrease in hydrogen bonding, and suggests that the presence of a vicinal methyl ester

encourages further hydrogen bonding interactions relative to the stereochemistry of the proximal organosulfate. This is in agreement with previous observations. (See Chapter 5.1.2.) For the docked structures of **RR-1** and **SS-1**, see Chapter 6.7.

5.2.3. Conclusions and Considerations

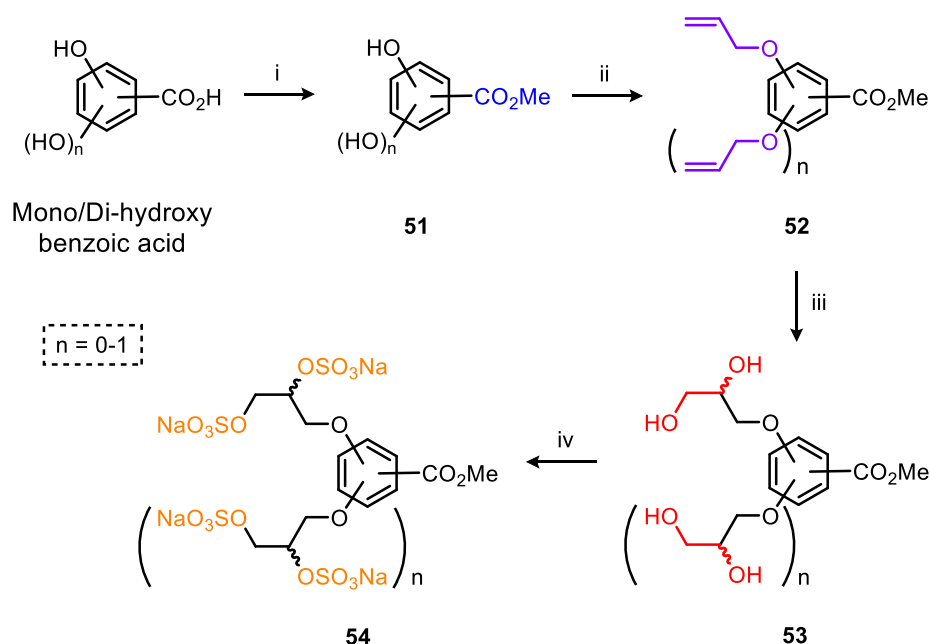
Overall, the results gained by this docking study propose that the HS-glycomimetic's binding of HGF are not effected by their inherent stereochemistry, which is in agreement with the computational and biological results gained from the first generation HS-glycomimetics (**1-3**). Therefore, stereochemistry is not imperative in the design of further generations of HS-glycomimetics designed to target HGF. Therefore, the design of a second generation of HS-glycomimetics will focus on the spatial orientation of anionic sulfate groups around an aromatic core structure, in similar accordance to the design of **1-4** by Raiber et. al (Scheme 32).¹ Moreover, the use of non-asymmetric methods will facilitate a simpler chemical synthesis and a higher throughput of compounds.

5.3. The 2nd Generation of HS-Glycomimetics

5.3.1. Glycomimetic Design and Synthesis

A design for the second generation of HS-glycomimetics was intended to utilise the existing chemistry developed throughout the investigation so far. Thus, by starting from alternate mono- or di-hydroxybenzoic acid core structures, similar to the synthesis of ester **7**, the position and spatial orientation of sulfate groups can be transformed by changing the positions of phenolic groups around the aromatic ring. Overall, this changes the spatial orientation of sulfate groups in relation to each other and in relation to a carbonyl group, which was previously observed to bind in a specific pocket at the accessible surface of HGF (Scheme 32).

In summary, the phenolic positions were efficiently substituted with allyl groups via an S_N2 reaction with allyl bromide. The allyloxy intermediates were subsequently dihydroxylated using the Upjohn methodology, affording a variety of diols and tetraol intermediate precursors. Final sulfation of the dihydroxylated intermediates with $Bu_3N\bullet SO_3$ afforded a library of novel persulfates and potential HS-glycomimetics (Scheme 32, all structures and individual yields are given in Table 14).



Scheme 32: The synthetic strategy and rational design for the second generation HS-glycomimetics, utilising previously demonstrated synthetic methods. Conditions: **i**) H_2SO_4 , MeOH, reflux; **ii**) allyl bromide, K_2CO_3 , TBAI, acetone, reflux; **iii**) $K_2OsO_2(OH)_4$, NMO, acetone/ H_2O (9:1); **iv**) $Bu_3N\bullet SO_3$, MeCN, $90^\circ C$.

5.3.2. Synthesis

The chemical synthesis of a series of second generation HS-glycomimetics was achieved directly in 3 to 4 synthetic steps using previously demonstrated methods (Scheme 32, Table 14). For all examples, each intermediate was achieved in good yield (esters **51**: 60 – 90%; for alkenes/dienes **52**: 56 – 90%; for polyols **53**: 54 – 94% and for persulfates **54**: 23 – 85%) following standard procedures (See Chapter 6.1). Notably, for the synthesis of **54b** (Table 14, Entry 2) both Fischer esterification and alkylation steps afforded the desired intermediates in only moderate comparable yields

(60 & 56% for **51b** & **52b**, respectively). For the methyl ester **52a**, the reduced yield can be attributed to the electron donating effects of the phenolic oxygen, making the carbonyl more electron rich and reducing its electrophilicity.¹⁹ For the synthesis of diene **52b**, the reaction was found to install the allyl groups in a stepwise manner. Therefore, the moderate overall yield can be deduced from an effect of sterics, but it is likely caused by an intramolecular hydrogen bonding interaction which stabilises both *o*-phenolic protons, hampering the S_N2 mechanism and leading to the observed reduction in overall yield (Figure 54).

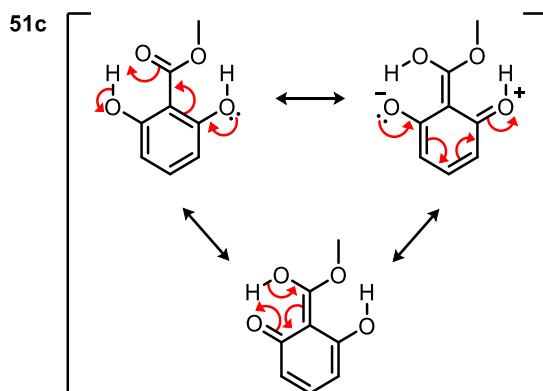


Figure 54: Resonance structures of ester **51c**, illustrating intramolecular hydrogen bonding interaction between the *o*-phenols and the methyl ester functionality.

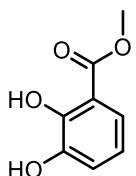
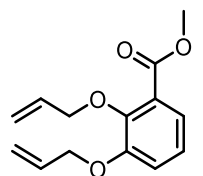
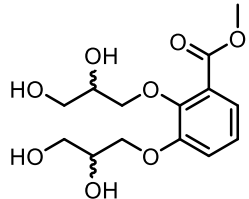
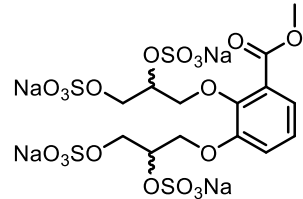
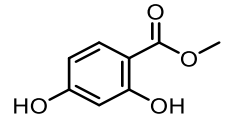
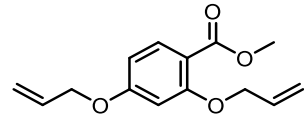
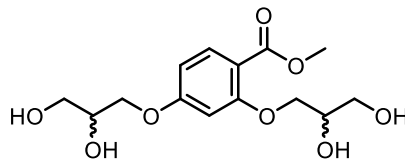
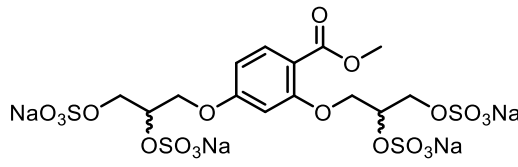
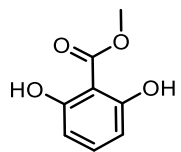
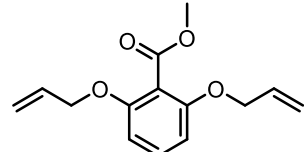
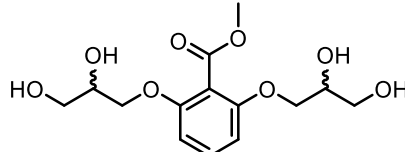
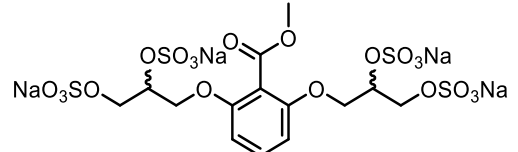
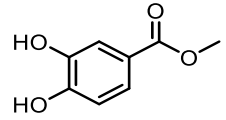
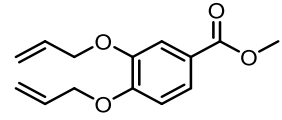
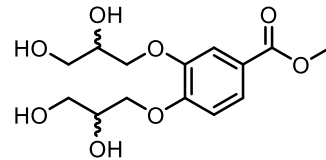
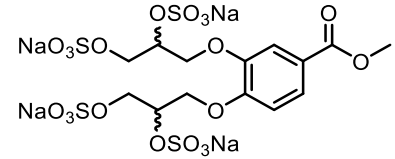
Notably, for unsymmetrical tetraols **53a**, **53b** and **53d**, no *d.r* could be confirmed by analysis of the crude ¹H-NMR and ¹³C-NMR spectra data. This is in accordance with the observed resonance signals for tetraol **5**, however, due to operating under non-symmetric reaction conditions, the *e.r/d.r* is proposed to be 1:1:1:1 (*RR,SS,RS,SR*) in each case.

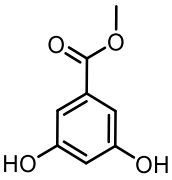
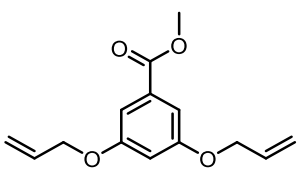
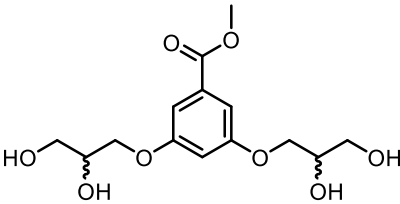
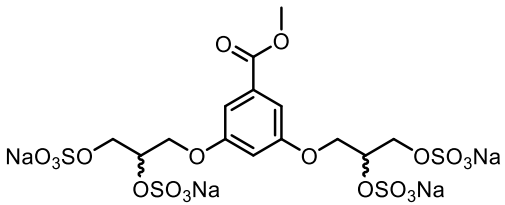
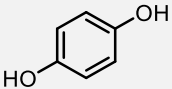
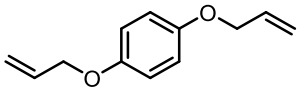
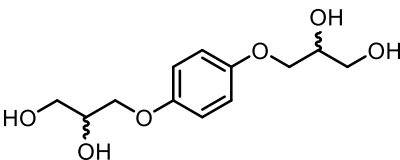
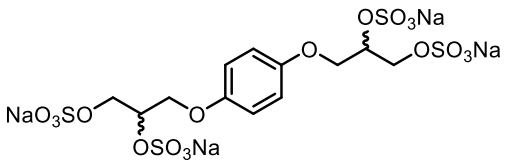
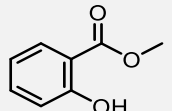
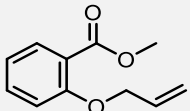
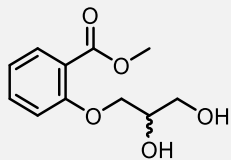
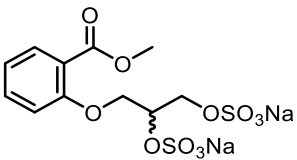
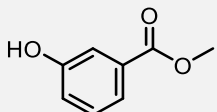
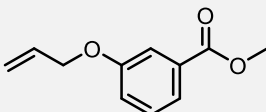
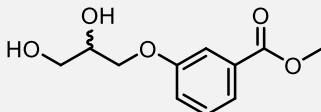
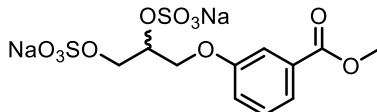
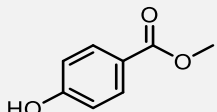
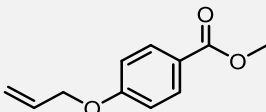
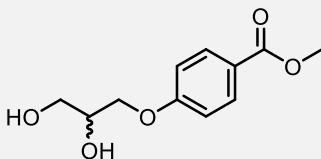
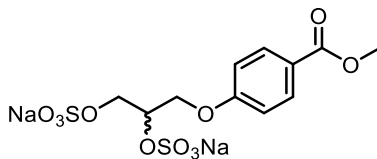
Final sulfation of the diol and tetraol intermediates **53** (Table 14) with Bu₃N•SO₃ afforded 9 novel organosulfates (**54**) designed around the structure of HS-glycomimetic **1**. Furthermore, the synthesis of racemic analogues potentially afforded 34 individual enantiomers and diastereoisomers that can be tested against HGF/MET-

receptor activation. Moreover, due to the observed similarities in biological activity of non-sulfated intermediates **5** and **5'** (Table 12), this synthetic approach actually afforded 18 novel compounds and 48 individual stereoisomers that can be tested against HGF/MET-receptor activation, exhibiting the creativity of this synthetic design.

Table 14 is located on the following page (178).

Table 14: The synthesis of a second generation HS-glycomimetics. For conditions see **Scheme 31**. All yields are given in %.

Entry	51	Yield	52	Yield	53	Yield	54	Yield
1	 51a	88	 52a	73	 53a	72	 54a	85
2	 51b	88	 52b	78	 53b	60	 54b	23
3	 51c	60	 52c	56	 53c	90	 54c	80
4	 51d	80	 52d	74	 53d	54	 54d	68

5	 51e	90	 52e	82	 53e	87	 54e	63
6	 hydroquinone	—	 52f	90	 53f	94	 54f	83
7	 3s	99	 19	91	 ±22	97	 54g	70
8	 1s	92	 17	94	 ±20	97	 54h	46
9	 2s	97	 18	80	 ±21	97	 54i	72

5.3.3. Computational Modelling and Docking Studies

Table 15: Listing the minimum docking energies, hydrogen bonding interactions and number of sulfate groups of the second generation HS-glycomimetics.

Entry	Compound Number	Docking Energy (kJ mol ⁻¹)	No. of SO ₃ ⁻	No. of H-bonds
1	54a	-58.87	4	3
2	54b	-58.41	4	8
3	54c	-59.08	4	7
4	54d	-60.92	4	7
5	54e	-61.25	4	5
6	54f	-62.72	4	6
7	54g	-42.34	2	3
8	54h	-43.68	2	1

The results from the previous computational investigation (Chapter 5.2.2) calculated the **SS-1** enantiomer to have the greatest energy binding interaction with HGF (Table 13, Entry 2). Therefore, to streamline the docking study of the second generation glycomimetics, only the *SS/S*-enantiomers were computationally docked against NK1 (HGF). The results of the computational study (Table 15) propose that changing the position and spatial orientation of anionic sulfate groups around the aromatic core has an insignificant effects on the binding interaction. Furthermore, similar to previous results, the number of hydrogen bonds do not correlate with the minimum binding energy of the tetrasulfated compounds (Table 14, Entries 1 – 6). Moreover, the absence of the methyl ester, affording persulfate **54f** (Table 15, Entry 6), demonstrates a further increase in binding energy, the greatest observed in this series (-62.72 kJ mol⁻¹), contradicting the previously demonstrated interactions of the methyl ester group (Chapter 5.1). The removal of entire sulfate groups, affording disulfates **54g** and **54h**

(Table 15, Entries 7 & 8), demonstrates a disproportionate correlation in the calculated binding energy. The structurally smaller disulfates **54g/h** have a reduced molecular weight (–40% by molecular mass), however, the average increase in binding energy is inconsistent (avg. +28.2%), suggesting the two organosulfates are likely to be more efficient at binding HGF (acting as ligands). Furthermore, this result also highlights that the persulfated glycomimetics (**54a-f**) are inefficient at binding HGF, and the binding interaction is facilitated by two anionic sulfate groups. Nonetheless, these results elucidate a valuable SAR, and recommend that simpler, smaller organosulfates should be investigated as potential HS-glycomimetics targeting the HGF/MET-receptor pathway.

Unfortunately, due to a lack of relevant biological collaborators, the investigation could not commence with biological testing of the new organosulfates (**54**) and non-sulfated intermediates (**53**). Therefore, no conclusions can be drawn on their *in vitro* biological activity at this time. However, the results of this study suggest that altering the spatial orientation of sulfate groups around an aromatic framework have little effect on the binding interactions with HGF, so no conclusions can be made regarding the SAR of the original HS-glycomimetics (**1-3**) and the potential second generation (**54**). Nonetheless, the removal of specific sulfate and methyl ester functionalities has provided a valuable SAR that is to be considered in future investigations looking at novel HGF inhibitors. This is discussed further in Chapter 5.5: Future work.

5.3.4. Conclusion

In short, the work presented in this chapter partly fulfils the third and fourth overall aims of this investigation. A variety of novel sulfated HS-glycomimetics have been synthesised and their structures have been computationally docked into the HS binding-site of HGF. The results of the *in silico* study highlighted that changing the

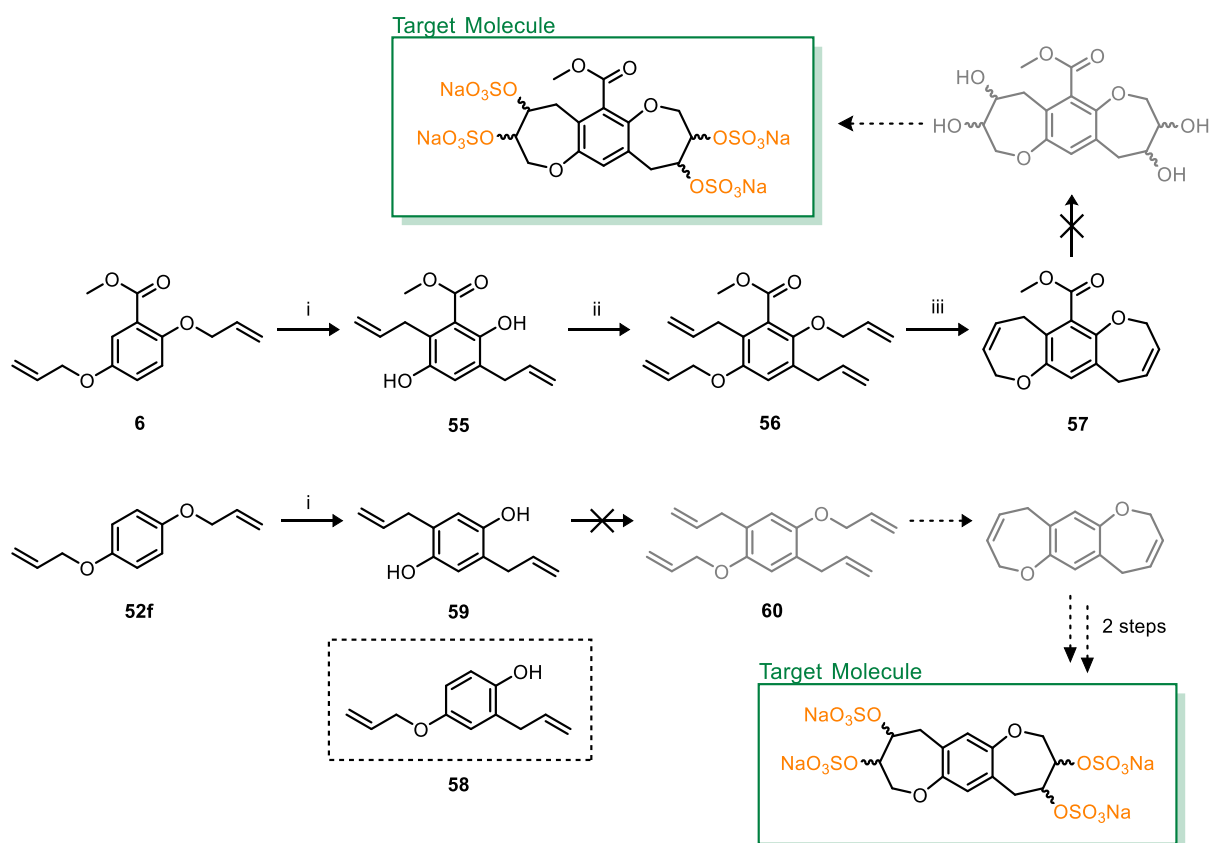
arrangement of sulfate groups around a simple aromatic core is likely to have little effect on biological activity. However, removal of specific functionalities demonstrated a relevant SAR.

5.4. Target Oriented Synthesis

5.4.1. Ring Systems and Structural Rigidity

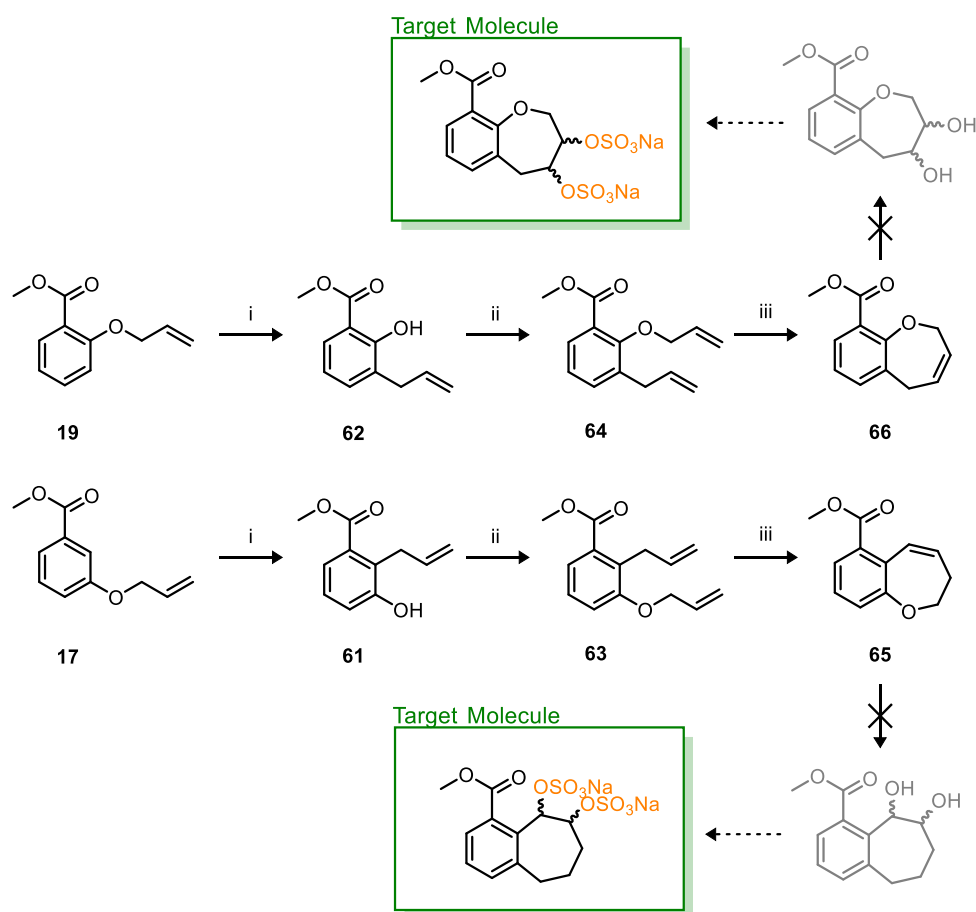
It was envisioned that the degrees of freedom within the HS-glycomimetic **1** could be removed by incorporating a tricyclic ring system into the final molecule. Therefore, a synthetic study was carried out to build such a molecule from the readily accessible diene **6**. A Claisen rearrangement²⁰ followed by a Grubbs ring closing metathesis²¹ was hypothesised to construct the desired double ring system around an aromatic core structure (Scheme 33). Furthermore, using the relevant diene **6** ensured that no intermediate compounds required synthesising, as the investigation already had a surplus of diene **6** left over from earlier investigations.

With diene **6** in hand, a double Claisen rearrangement afforded **55** in 6% yield. This was followed by alkylation with allyl bromide to afford the tetra allyl intermediate **56** in 99% yield. A tandem Grubbs ring closing metathesis of **56** afforded the bicyclic diene **57** in 99% yield (Scheme 33). A Claisen rearrangement of diene **52f** afforded the single rearrangement produce (**58**) and double rearrangement product (**59**) in 40% and 5% yield, respectively. Alkylation of **59** with allyl bromide afforded no isolatable material, and analysis of the crude ¹H-NMR could not confirm the synthesis of **60** (Scheme 33).



Scheme 33: The target oriented synthesis of tricyclic diene **57** and tetra-alkene **60**. Conditions: **i**) PhH, 200 °C, 18 h, **6%** and **5%** for **55** and **56**, respectively; **ii**) Allyl-Br, K₂CO₃, TBAI, acetone, reflux, **99%**; **iii**) Grubbs-2nd Gen., Toluene, Ar 50 °C, 1 h, **99%**.

Additionally, this synthetic approach was also envisioned on single alkenes **17** and **19** (Scheme 34). This was proposed to provide a library of structurally related analogues of **1** with single point changes to the final structure. A similar procedure was carried out on alkenes **17** and **19**, affording the Claisen rearrangement products **61** and **62** in 56% and 83% yield, respectively. Alkylation with allyl bromide afforded dienes **63** and **64** in 38% and 12% yield, respectively. Grubbs ring closing metathesis of diene **64** afforded bicyclic alkene **66** in 99% yield (Scheme 34). However, the ring closing metathesis of diene **63** afforded the unexpected cyclic isomer **65** in 74% yield. The alkene isomerisation was proposed to be caused by residual ruthenium hydrides formed under the reaction conditions,²² affording the conjugated alkene at the benzylic position.



Scheme 34: The target oriented synthesis of cyclic alkenes **65** and **66**. Conditions: **i)** PhH, 200 °C, 18 h, **56%** and **83%** for **61** and **62**, respectively; **ii)** Allyl-Br, K₂CO₃, TBAI, acetone, reflux, **38%** and **12%** for **63** and **66**, respectively; **iii)** Grubbs-2, PhMe, 50 °C, 1 h, **74%** and **99%** for **65** and **66**, respectively.

The bicyclic and tricyclic alkenes (**57**, **65** & **66**) were subjected to dihydroxylation under Upjohn conditions, but no isolated material was afforded in all cases. This was proposed to be caused by a lack of starting material and the statistical synthesis of multiple diastereoisomers, which hindered the analysis of crude ¹H-NMR spectra data and made any dihydroxylated material difficult to isolate by chromatography (SiO₂). Overall, this study demonstrates a unique way to incorporate ring systems around a biologically relevant HS-glycomimetic structure from an easy to synthesise, biologically relevant intermediate, diene **6**. However, no final product was afforded (Scheme 34).

5.4.2. The Insertion of Heteroatoms

Continuing on from the original structure of HS-glycomimetic **1**, it was proposed that the installation of a *para*-sulfate/sulfamate functionality, relative to the carbonyl, would be an interesting structure to synthesise due to a similar group being present in the structures of H and HS (Figure 55).

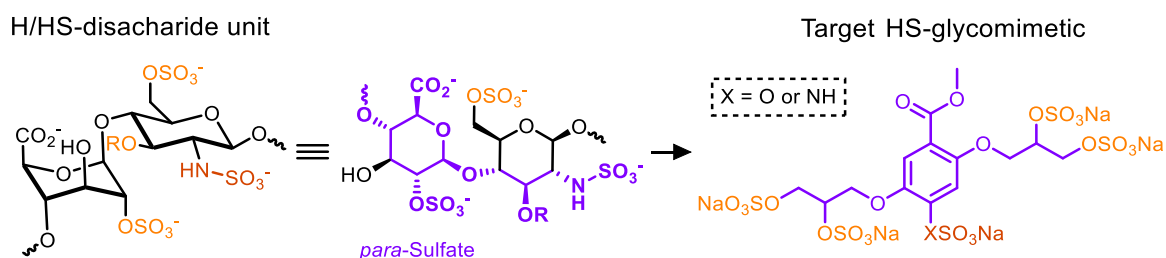
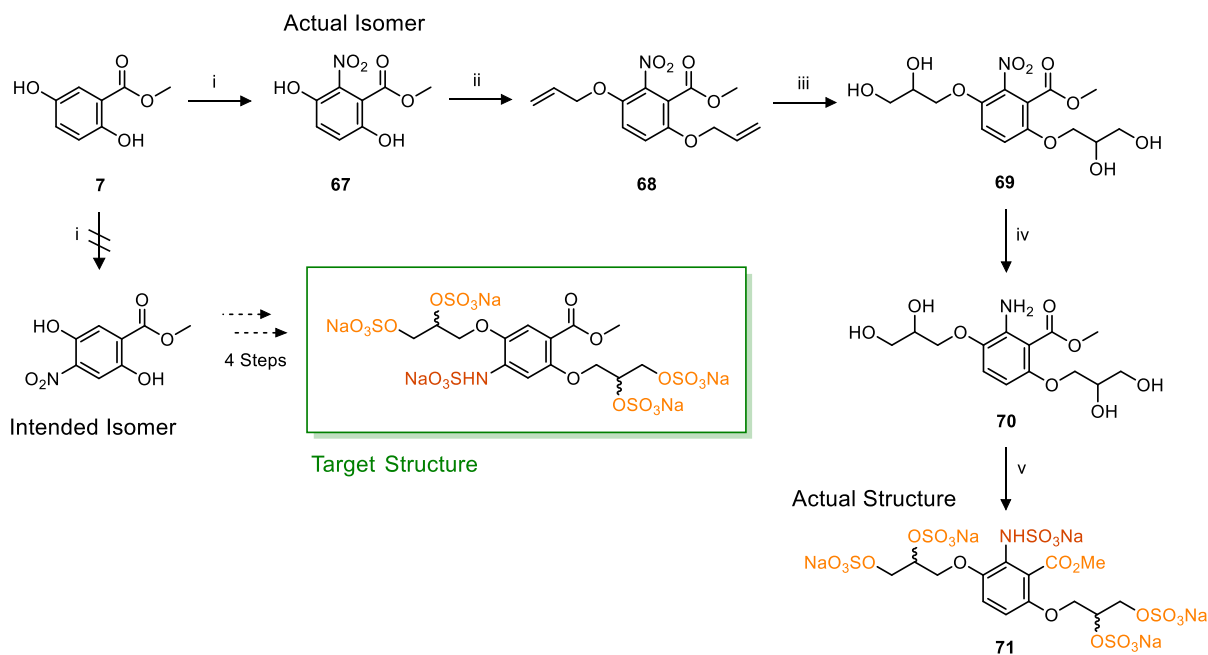


Figure 55: The rational design for a glycomimetic containing a *p*-sulfate/sulfamate functionality.

Attempts to synthesise this target structure by nitration of ester **7** (affording **67** in 14% yield) were problematic and resulted in the synthesis of the regioisomer **71**. The analysis of ^1H -NMR spectra data (of **67**) demonstrated no multiplicity for the aromatic protons, thus the intended *p*-Nitro regioisomer was considered to be present. Furthermore, no resonance signal was observed for $\underline{\text{C}}\text{-NO}_2$, although a very weak signal could be elucidated from ^1H - ^{13}C HSQC analysis (See Chapter 6: Compound Characterisation).

When the synthesis was carried forward and **67** was subsequently alkylated to afford diene **68** (in 48% yield), a multiplicity was observed for the aromatic protons (Scheme 35). However, the interactions of the aromatic protons gave no concise values for J_3 or J_4 coupling. With this in mind, the synthesis was carried forward again to afford tetraol **69** (in 61% yield) and confirmed that the desired *para*-regioisomer had not been synthesised, and the product was elucidated from ^1H -NMR data as the *o*-

regioisomer. This was later confirmed by small molecule single crystal X-ray crystallography of **67** (performed by Dr Louise Male. See appendix).



Scheme 35: The synthesis of HS-glycomimetic **71**. Conditions: **i**) HNO_3 , AcOH , Ac_2O , **15%**; **ii**) Allyl-Br, K_2CO_3 , TBAI, acetone, reflux, **48%**; **iii**) $\text{K}_2\text{OsO}_2(\text{OH})_4$, NMO, acetone/ H_2O , 9:1, 40°C , **61%**; **iv**) H_2 , Pd/C, MeOH (H-Cube), **94%**; **v**) 1) $\text{Bu}_3\text{N}\cdot\text{SO}_3$, MeCN, 90°C , 2) NEH, $t\text{BuOMe}/\text{PrOH}$, **33%**.

Repeated nitration of ester **7** gave matching results and only ester **67** was isolated from the reaction mixture. Nonetheless, the synthesis was carried forward, and the intermediate was hydrogenated to afford amine **70** in 96% yield. Sulfation of the hydroxyl and amine groups with $\text{Bu}_3\text{N}\cdot\text{SO}_3$ afforded the penta-sulfate **71** in 33% yield on a 12 mg (0.036 mmol) scale (Scheme 35). Attempts to access the *p*-regioisomer using alternate nitration methods were unsuccessful. Notably, in an attempt to access more diverse heteroatomic structures, the Sharpless aminohydroxylation was attempted on diene **6**.²³ However, this reaction gave consistently unsatisfactory results and the investigation was stopped altogether.

5.4.3. Conclusion

The work presented in this chapter demonstrates how ring systems and heteroatoms can be incorporated into biologically relevant HS-glycomimetic structures, in attempts to synthesise a variety of target molecules that contain inherent structural rigidity and greater diversity.

5.5. Overall Conclusions and Future Work

A final aim of this investigation was to test the biological activity of a series of novel organosulfates against the HGF/Met-receptor interaction. This was not fulfilled. Therefore, future work aims to test the novel organosulfates for any HS-glycomimetic (inhibitory) activity towards the binding of HGF, so this investigation can obtain a SAR based off their biological activity, and compare this with data gained through the computational docking study carried out in Chapter 5.3.

Future investigations seeking to use the original and novel HS-glycomimetics for their investigations have a stock of fully characterised, stereo defined compounds to use at their disposal. The final organosulfates were afforded through the use of a new synthetic methodology developed as part of this investigation, which permits a straightforward and efficient synthesis of small, persulfated and sulfamated compounds. The new sulfation methodology with $\text{Bu}_3\text{N}\cdot\text{SO}_3$ will facilitate future investigations looking at more diverse, target orientated organosulfates. However, this investigation discovered a valuable SAR to the existing HS-glycomimetics (**1-3**), which proposes that the structures can be designed to be smaller and more efficient. Therefore, future work will also consider testing all small, non-steroid based organosulfates synthesised in prior investigations (Chapter 4).

The stability of the relevant organosulfates at physiological pH, and in the presence of free fatty acids (FFAs), is currently ongoing.

In summary, this investigation fulfilled the majority of aims it set out to achieve, correcting the results of previous investigations, and providing new knowledge toward the synthesis, characterisation and biological activity of small molecule HS-glycomimetics.

References

1. E. A. Raiber, J. A. Wilkinson, F. Manetti, M. Botta, J. Deakin, J. Gallagher, M. Lyon, S. W. Ducki, *Bioorg. Med. Chem. Lett.*, 2007, **17**, 6321 – 6325
2. A. M. Mahmoud, F. L. Wilkinson, A. M. Jones, J. A. Wilkinson, M. Romero, J. Duarte, M. Y. Alexander, *Heart*, 2015, **101**, A41
3. F. L. Wilkinson, A. M. Mahmoud, A. M. Jones, J. A. Wilkinson, M. Romero, J. Duarte, M. Y. Alexander, *Heart*, 2016, **102**, A136.
4. F. L. Wilkinson, A. M. Mahmoud, A. M. Jones, J. A. Wilkinson, M. Romero, J. Duarte, M. Y. Alexander, *Cardiovascular Research*, 2016, **101**, S65
5. A. W. W. Langford-Smith, A. Hasan, R. Weston, N. Edwards, A. M. Jones, A. J. M. Boulton, F. L. Bowling, S. T. Rashid, F. L. Wilkinson, M. Y. Alexander, *Sci. Rep.*, 2019, **9**, 2309
6. A. M. Mahmoud, F. L. Wilkinson, A. M. Jones, J. A. Wilkinson, M. Romero, J. Duarte, M. Y. Alexander, *Biochimica et Biophysica Acta (BBA) - General Subjects*, 2017, **1861**, 3311 – 3322,
7. G. P. Sidgwick, P. Walling, A. Shabbir, R. Weston, A. Schiro, F. Serracino-Inglott, A. M. Jones, M. Kamalov, M. A. Brimble, F. L. Wilkinson, M. Y. Alexander, *Heart*, 2016, **102**, A132
8. F. L. Wilkinson, G. P. Sidgwick, A. Shabbir, R. Weston, A. M. Jones, M. Y. Alexander, *Heart*, 2016, **102**, A11
9. G. P. Sidgwick, R. Weston, A. M. Jones, F. L. Wilkinson, M. Y. Alexander, *Heart*, 2017, **103**, A126
10. G. P. Sidgwick, R. Weston, A. M. Jones, F. L. Wilkinson, M. Y. Alexander, *J. Vasc. Res.*, 2017, **54**, 24
11. A. M. Mahmoud, A. M. Jones, G. P. Sidgwick, A. M. Arafat, F. L. Wilkinson, M. Y. Alexander, *Cell. Phys. Biochem.*, 2019, **53**, 323 – 336
12. R. Weston, A. W. W. Langford-Smith, A. Hasan, A. M. Jones, F. L. Wilkinson, A. Boulton, T. Rashid, M. Y. Alexander, *Diabetic Medicine*, 2017, **34**, 39 – 3
13. L. D. Thompson, M. W. Pantoliano, B. A. Springer, *Biochem.*, 1994, **33**, 3831 – 3840
14. M. Ultsch, N. A. Lokker, P. J. Godowski, A. M. de Vos, *Structure*, 1998, **6**, 1383 – 1389
15. D. Leitha, D. Y. Chirgadze, B. Mulloy, T. L. Blundell, E. Gherardi, *Embo J.*, 2001, **20**, 5543
16. G. M. Morris, D. S. Goodsell, R. S. Halliday, R. Huey, W. E. Hart, R. K. Belew, A. J. Olson, *J. Comput. Chem.*, 1998, **19**, 1639
17. M. Maccarana, B. Casu, U. Lindahl, *J. Biol. Chem.*, 2003, **268**, 23898 – 23905
18. C. J. Robinson, B. Mulloy, J. T. Gallagher, S. E. Stringer, *J. Biol. Chem.*, 2006, **281**, 1731 – 1740
19. G. E. Dunn, T. L. Penner, *Canadian Journal of Chemistry*, 1966, **45**, 1699 – 1706
20. L. Claisen, *Chem. Ber.*, 1912, **45**, 3157 – 3166

21. R. H. Grubbs, *Handbook of Metathesis*, Wiley-VCH, Weinheim, 2003
22. S. H. Hong, D. P. Sanders, C. W. Lee & R. H. Grubbs, *J. Am. Chem. Soc.*, 2005, **127**, 17160 – 17161
23. Z. P. Demko, M. Bartsch, K. B. Sharpless, *Org. Lett.*, 2000, **2**, 2221 – 2223

Chapter 6: Appendix

CONTENTS

6.1. GENERAL METHODS -----	192
6.1.1. Procedure A: The synthesis of hydroxybenzoic acid methyl esters	194
6.1.2. Procedure B: The synthesis of allyloxy benzoic acid methyl esters	194
6.1.3. Procedure C: The Upjohn dihydroxylation of aryl-allyl ethers	195
6.1.4. Procedure D: The Sharpless AD of aryl-allyl ethers	196
6.1.5. Preparation of Stock solutions I-V	196
6.1.6. Procedure E: The chiral pool synthesis of 2,2-dimethyl-4-(aryloxymethyl)-1,3-dioxolanes	197
6.1.7. Procedure F: The acid hydrolysis of chiral solketal-derived acetals	198
6.1.8. Procedure G: The acetylation of aryloxy-1,2-propanediols	199
6.1.9. Procedure H: The preparation of organosulfates using $\text{Bu}_3\text{N}\cdot\text{SO}_3$	200
6.2. SYNTHESIS OF TRIBUTYLSULFOAMMONIUM BETAINE ($\text{Bu}_3\text{N}\cdot\text{SO}_3$) -----	202
6.3. PREPARATION OF (<i>R</i>) OR (<i>S</i>)-(2,2-DIMETHYL-1,3-DIOXOLAN-4-YL)-METHYL TRIFLUOROMETHANESULFONATE-	203
6.4. REGIOSELECTIVITY ANALYSIS OF THE SAD: SYNTHESIS OF DIOLS 23 AND 24 -----	204
6.5. HYDROLYSIS ANALYSIS OF DIOL S-21: THE EFFECTS OF HYDROLYSIS AND ACETYLATION ON STEREOCHEMISTRY	208
6.6. DESULFATION EXPERIMENT OF L-44 -----	210
6.7. RESULTS OF DOCKING STUDIES -----	211
6.8. BIOLOGICAL ASSAYS -----	220
6.8.1. Cell Viability Assessment (MTT)	220
6.8.2. Preparation of FFA-albumin complexes and cell treatments	221
6.8.3. NO release assay and Quantification of ROS production.	221
6.8.4. NADPH oxidase activity	222
6.8.5. In situ quantification of ROS species	222
6.8.6. Western blot analysis	223

COMPOUND CHARACTERISATION

(α-1) Sodium 3-(4-((<i>S</i>)-2,3-bis(sulfonatooxy)propoxy)-2-(methoxycarbonyl)phenoxy)propane-1,2-diyl bis(sulfate)	224
---	------------

(RR-1) Sodium (<i>R</i>)-3-(4-((<i>R</i>)-2,3-bis(sulfonatooxy)propoxy)-2-(methoxycarbonyl)phenoxy)propane-1,2-diyl bis(sulfate)	225
(SS-1) Sodium (<i>S</i>)-3-(4-((<i>S</i>)-2,3-bis(sulfonatooxy)propoxy)-2-(methoxycarbonyl)phenoxy)propane-1,2-diyl bis(sulfate)	226
(RS-1) Sodium (<i>R</i>)-3-(4-((<i>S</i>)-2,3-bis(sulfonatooxy)propoxy)-2-(methoxycarbonyl)phenoxy)propane-1,2-diyl bis(sulfate)	226
(SR-1) Sodium (<i>S</i>)-3-(4-((<i>R</i>)-2,3-bis(sulfonatooxy)propoxy)-2-(methoxycarbonyl)phenoxy)propane-1,2-diyl bis(sulfate)	227
(R-2) Sodium (<i>R</i>)-3-(3-(methoxycarbonyl)-4-(4-(sulfonatooxy)butoxy)phenoxy)propane-1,2-diyl bis(sulfate)	228
(S-2) Sodium (<i>S</i>)-3-(3-(methoxycarbonyl)-4-(4-(sulfonatooxy)butoxy)phenoxy)propane-1,2-diyl bis(sulfate)	229
(β-3) Sodium 5-((<i>R</i>)-2,3-bis(sulfonatooxy)propoxy)-2-(2,3-bis(sulfonatooxy)propoxy)benzoate	230
(±5) Methyl 2,5-bis(2,3-dihydroxypropoxy)benzoate	231
(RR-5) Methyl 2,5-bis((<i>R</i>)-2,3-dihydroxypropoxy)benzoate	232
(SS-5) Methyl 2,5-bis((<i>S</i>)-2,3-dihydroxypropoxy)benzoate	232
(RS-5) Methyl 2-((<i>R</i>)-2,3-dihydroxypropoxy)-5-((<i>S</i>)-2,3-dihydroxypropoxy)benzoate	233
(SR-5) Methyl 2-((<i>S</i>)-2,3-dihydroxypropoxy)-5-((<i>R</i>)-2,3-dihydroxypropoxy)benzoate	234
(α-5) Methyl 5-((<i>R</i>)-2,3-dihydroxypropoxy)-2-((±)-2,3-dihydroxypropoxy)benzoate	234
(α-5') Sodium 5-((<i>R</i>)-2,3-dihydroxypropoxy)-2-((±)-2,3-dihydroxypropoxy)benzoate	235
(β-5) Methyl 5-((<i>S</i>)-2,3-dihydroxypropoxy)-2-((±)-2,3-dihydroxypropoxy)benzoate	236
(β-5') Sodium 5-((<i>S</i>)-2,3-dihydroxypropoxy)-2-((±)-2,3-dihydroxypropoxy)benzoate	237
(6) Methyl 2,5-bis(allyloxy)benzoate	238
(7) Methyl 2,5-hydroxybenzoate	239
(8) Methyl 5-(allyloxy)-2-hydroxybenzoate	239
(9) Methyl 2-(4-acetoxybutoxy)-5-(allyloxy)benzoate	240
(R-10') Methyl (<i>R</i>)-2-(4-acetoxybutoxy)-5-(2,3-dihydroxypropoxy)benzoate	241
(S-10') Methyl (<i>S</i>)-2-(4-acetoxybutoxy)-5-(2,3-dihydroxypropoxy)benzoate	242
(R-10) Methyl (<i>R</i>)-2-(4-hydroxybutoxy)-5-(2,3-dihydroxypropoxy)benzoate	243
(S-10) Methyl (<i>S</i>)-2-(4-hydroxybutoxy)-5-(2,3-dihydroxypropoxy)benzoate	244
(±11) Methyl 2,5-bis(2,3-bis((tert-butyl)dimethylsilyl)oxy)propoxy)benzoate	245
(±12) Methyl (±)-2,5-bis(2,3-di(acetoxy)propoxy)benzoate	246
(RR-12) (2 <i>R</i> ,5 <i>R</i>)-((2-(methoxycarbonyl)-1,4-phenylene)bis(oxy))bis(propane-3,1,2-triyl) tetraacetate	247
(SS-12) (2 <i>S</i> ,5 <i>S</i>)-((2-(methoxycarbonyl)-1,4-phenylene)bis(oxy))bis(propane-3,1,2-triyl) tetraacetate	248
(RS-12) (2 <i>R</i> ,5 <i>S</i>)-((2-(methoxycarbonyl)-1,4-phenylene)bis(oxy))bis(propane-3,1,2-triyl) tetraacetate	249
(SR-12) (2 <i>S</i> ,5 <i>R</i>)-((2-(methoxycarbonyl)-1,4-phenylene)bis(oxy))bis(propane-3,1,2-triyl) tetraacetate	250
(α-12) (2 <i>R</i> ,5 <i>S</i>)-((2-(methoxycarbonyl)-1,4-phenylene)bis(oxy))bis(propane-3,1,2-triyl) tetraacetate	251
(β-12) (2±,5 <i>R</i>)-((2-(methoxycarbonyl)-1,4-phenylene)bis(oxy))bis(propane-3,1,2-triyl) tetraacetate	252
(R-13) Methyl (<i>R</i>)-5-((2,2-dimethyl-1,3-dioxolan-4-yl)methoxy)-2-hydroxybenzoate	253
(S-13) Methyl (<i>S</i>)-5-((2,2-dimethyl-1,3-dioxolan-4-yl)methoxy)-2-hydroxybenzoate	254
(RR-14) Methyl 2,5-bis(((<i>R</i>)-2,2-dimethyl-1,3-dioxolan-4-yl)methoxy)benzoate	255
(SS-14) Methyl 2,5-bis(((<i>S</i>)-2,2-dimethyl-1,3-dioxolan-4-yl)methoxy)benzoate	256
(RS-14) Methyl 2-(((<i>R</i>)-2,2-dimethyl-1,3-dioxolan-4-yl)methoxy)-5-(((<i>S</i>)-2,2-dimethyl-1,3-dioxolan-4-yl)methoxy)benzoate	257

(SR-14) Methyl 2-(((<i>S</i>)-2,2-dimethyl-1,3-dioxolan-4-yl)methoxy)-5-(((<i>R</i>)-2,2-dimethyl-1,3-dioxolan-4-yl)methoxy)benzoate	258
(15) Methyl 2-fluoro-5-hydroxybenzoate	259
(16) Methyl (<i>S</i>)-5-((2,2-dimethyl-1,3-dioxolan-4-yl)methoxy)-2-fluorobenzoate	260
(17) Methyl 3-(allyloxy)benzoate	261
(18) Methyl 4-(allyloxy)benzoate	262
(19) Methyl 2-(allyloxy)benzoate	262
(±20) Methyl (±)-3-(2,3-dihydroxypropoxy)benzoate	263
(α-20) Methyl (<i>R</i>)-3-(2,3-dihydroxypropoxy)benzoate	264
(β-20) Methyl (<i>S</i>)-3-(2,3-dihydroxypropoxy)benzoate	265
(S-20) Methyl (<i>S</i>)-3-(2,3-dihydroxypropoxy)benzoate	266
(±21) Methyl (±)-4-(2,3-dihydroxypropoxy)benzoate	266
(α-21) Methyl (<i>R</i>)-4-(2,3-dihydroxypropoxy)benzoate	267
(β-21) Methyl (<i>S</i>)-4-(2,3-dihydroxypropoxy)benzoate	268
(S-21) Methyl (<i>S</i>)-4-(2,3-dihydroxypropoxy)benzoate	269
(±22) Methyl (±)-2-(2,3-dihydroxypropoxy)benzoate	270
(α-22) Methyl (±)-2-(2,3-dihydroxypropoxy)benzoate	271
(β-22) Methyl (±)-2-(2,3-dihydroxypropoxy)benzoate	272
(S-22) Methyl (<i>S</i>)-2-(2,3-dihydroxypropoxy)benzoate	273
(R-23) Methyl (<i>R</i>)-2-(allyloxy)-5-(2,3-dihydroxypropoxy)benzoate	274
(S-23) Methyl (<i>S</i>)-2-(allyloxy)-5-(2,3-dihydroxypropoxy)benzoate	275
(R-24) Methyl (<i>R</i>)-5-(allyloxy)-2-(2,3-dihydroxypropoxy)benzoate	276
(R-25) Methyl (<i>R</i>)-2-(allyloxy)-5-((2,2-dimethyl-1,3-dioxolan-4-yl)methoxy)benzoate	277
(S-25) Methyl (<i>S</i>)-2-(allyloxy)-5-((2,2-dimethyl-1,3-dioxolan-4-yl)methoxy)benzoate	278
(S-26) Methyl (<i>S</i>)-5-(allyloxy)-2-((2,2-dimethyl-1,3-dioxolan-4-yl)methoxy)benzoate	279
(27c) Tributylammonium 4-methoxybenzyl sulfate	280
(27f) Tributylammonium 2-methoxybenzyl sulfate	280
(28) Sodium benzyl sulfate	281
(28a) Sodium 4-nitrobenzyl sulfate	282
(28b) Sodium 4-chlorobenzyl sulfate	283
(28c) Sodium 4-methoxybenzyl sulfate	283
(28d) Sodium 2-nitrobenzyl sulfate	284
(28e) Sodium 2-chlorobenzyl sulfate	284
(29) Sodium 1-phenylethyl sulfate	285
(30) Sodium 4-methoxyphenyl sulfate	285
(31) Sodium (1 <i>R</i> , 2 <i>S</i>)-cyclohexane-1,2-diyl bis(sulfate)	286
(32) Sodium propane-1,2,3-triyl tris(sulfate)	287
(33) Tributylammonium (±)-2-isopropyl-5-methylcyclohexyl sulfate	287
(34) Tributylammonium 2-hydroxyphenylethanol sulfate	288
(35) Sodium 2-(2-(sulfonatoxy)ethyl)phenyl sulfate	289
(36) Sodium (17β)-estra-1,3,5(10)-triene-3-ol,17-sulfate	290
(37) Sodium (8 <i>R</i> ,9 <i>S</i> ,13 <i>S</i> ,14 <i>S</i> ,17 <i>S</i>)-13-methyl-7,8,9,11,12,13,14,15,16,17-decahydro-6 <i>H</i> -cyclopenta[<i>a</i>]phenanthrene-3,17-diyl bis(sulfate)	291
(39) Sodium 2-((8 <i>S</i> ,9 <i>S</i> ,10 <i>R</i> ,11 <i>S</i> ,13 <i>S</i> ,14 <i>S</i> ,17 <i>R</i>)-11,17-dihydroxy-10,13-dimethyl-3-oxo-2,3,6,7,8,9,10,11,12,13,14,15,16,17-tetradecahydro-1 <i>H</i> -cyclopenta[<i>a</i>]phenanthren-17-yl)-2-oxoethyl sulfate	292
(±40) <i>N</i> -Fmoc- <i>D</i> / <i>L</i> -serine methyl ester	293
(L-40) <i>N</i> -Fmoc- <i>L</i> -serine methyl ester	294
(L-41) <i>N</i> -Fmoc- <i>L</i> -tyrosine methyl ester	295
(±42) Tributylammonium (±)-2-(((9 <i>H</i> -fluoren-9-yl)methoxy)carbonyl)amino)-3-methoxy-3-oxopropyl sulfate	296

(L-42) Tributylammonium (<i>S</i>)-2-((((9H-fluoren-9-yl)methoxy)carbonyl)amino)-3-methoxy-3-oxopropyl sulfate	297
(L-43) Sodium (<i>S</i>)-2-((((9 <i>H</i> -fluoren-9-yl)methoxy)carbonyl)amino)-3-methoxy-3-oxopropyl sulfate	298
(L-44) Tributylammonium (<i>L</i>)- <i>N</i> -Fmoc tyrosine methyl ester sulfate.....	299
(R-50) Methyl (<i>S</i>)-2-(4-acetoxybutoxy)-5-((2,2-dimethyl-1,3-dioxolan-4-yl)methoxy)benzoate	300
(51a) Methyl 2,3-dihydroxybenzoate	301
(51b) Methyl 2,4-dihydroxybenzoate	302
(51c) Methyl 2,6-dihydroxybenzoate	302
(51d) Methyl 3,4-dihydroxybenzoate	303
(51e) Methyl 3,5-dihydroxybenzoate	303
(52a) Methyl 2,3-bis(allyloxy)benzoate	304
(52b) Methyl 2,4-bis(allyloxy)benzoate.....	305
(52c) Methyl 2,6-bis(allyloxy)benzoate	305
(52d) Methyl 3,4-bis(allyloxy)benzoate.....	306
(52e) Methyl 3,5-bis(allyloxy)benzoate.....	307
(52f) 1,4-Bis(allyloxy)benzene	308
(53a) Methyl 2,3-bis(2,3-dihydroxypropoxy)benzoate.....	308
(53b) Methyl 2,4-bis(2,3-dihydroxypropoxy)benzoate.....	309
(53c) Methyl 2,6-bis(2,3-dihydroxypropoxy)benzoate	310
(53d) Methyl 3,4-bis(2,3-dihydroxypropoxy)benzoate.....	310
(53e) Methyl 3,5-bis(2,3-dihydroxypropoxy)benzoate.....	311
(53f) 1,4-Phenylenebis(oxy))bis(propane-1,2-diol	312
(54a) Sodium 3-(2-(2,3-bis(sulfonatoxy)propoxy)-3-(methoxycarbonyl)phenoxy)propane-1,2-diyl bis(sulfate).....	312
(54b) Sodium 3-(5-(2,3-bis(sulfonatoxy)propoxy)-2-(methoxycarbonyl)phenoxy)propane-1,2-diyl bis(sulfate).....	313
(54c) Sodium ((2-(methoxycarbonyl)-1,3-phenylene)bis(oxy))bis(propane-3,1,2-triyl) tetrakis(sulfate)	314
(54d) Sodium 3-(2-(2,3-bis(sulfonatoxy)propoxy)-4-(methoxycarbonyl)phenoxy)propane-1,2-diyl bis(sulfate).....	315
(54e) Sodium ((5-(methoxycarbonyl)-1,3-phenylene)bis(oxy))bis(propane-3,1,2-triyl) tetrakis(sulfate)	316
(54f) Sodium (1,4-phenylenebis(oxy))bis(propane-3,1,2-triyl) tetrakis(sulfate)	316
(54g) Sodium 3-(2-(methoxycarbonyl)phenoxy)propane-1,2-diyl bis(sulfate)	317
(54h) Sodium 3-(3-(methoxycarbonyl)phenoxy)propane-1,2-diyl bis(sulfate)	318
(54i) Sodium 4-(3-(methoxycarbonyl)phenoxy)propane-1,2-diyl bis(sulfate)	318
(55) Methyl 2,5-diallyl-3,6-dihydroxybenzoate.....	319
(56) Methyl 2,5-diallyl-3,6-bis(allyloxy)benzoate	320
(57) Methyl 2,5,8,11-tetrahydrobenzo[1,2- <i>b</i> :4,5- <i>b'</i>]bis(oxepine)-6-carboxylate	321
(58) 2-Allyl-4-(allyloxy)phenol	321
(59) 2,5-Diallylbenzene-1,4-diol	322
(61) Methyl 2-allyl-3-hydroxybenzoate.....	323
(61') Methyl 4-allyl-3-hydroxybenzoate.....	323
(62) Methyl 3-allyl-2-hydroxybenzoate.....	324
(63) Methyl 2-allyl-3-(allyloxy)benzoate	325
(64) Methyl 3-allyl-2-(allyloxy)benzoate	326
(65) Methyl 2,3-dihydrobenzo[<i>b</i>]oxepine-6-carboxylate	327
(66) Methyl 2,5-dihydrobenzo[<i>b</i>]oxepine-9-carboxylate	328
(67) Methyl 3,6-dihydroxy-2-nitrobenzoate	329
(68) Methyl 3,6-bis(allyloxy)-2-nitrobenzoate	330

(69) Methyl 3,6-bis(2,3-dihydroxypropoxy)-2-nitrobenzoate	331
(70) Methyl 2-amino-3,6-bis(2,3-dihydroxypropoxy)benzoate	332
(71) Sodium 3-(4-(2,3-bis(sulfonatooxy)propoxy)-2-(methoxycarbonyl)-3-(sulfonatoamino)phenoxy)propane-1,2-diyl bis(sulfate)	333

SUPPLEMENTARY COMPOUND CHARACTERISATION

(1s) Methyl 3-hydroxybenzoate	335
(2s) Methyl 4-hydroxybenzoate	336
(3s) Methyl salicylate	336
(±4s) Methyl (±)-3-(2,3-di(acetoxy)propoxy)benzoate	337
(R-4s) Methyl (R)-3-(2,3-di(acetoxy)propoxy)benzoate	338
(α-4s) Methyl (S)-3-(2,3-di(acetoxy)propoxy)benzoate	339
(β-4s) Methyl (R)-3-(2,3-di(acetoxy)propoxy)benzoate	340
(±5s) Methyl (±)-4-(2,3-di(acetoxy)propoxy)benzoate	341
(R-5s) Methyl (R)-4-(2,3-di(acetoxy)propoxy)benzoate	342
(α-5s) Methyl (S)-4-(2,3-di(acetoxy)propoxy)benzoate	343
(β-5s) Methyl (R)-4-(2,3-di(acetoxy)propoxy)benzoate	344
(±6s) Methyl (±)-2-(2,3-di(acetoxy)propoxy)benzoate	345
(R-6s) Methyl (R)-2-(2,3-di(acetoxy)propoxy)benzoate	346
(α-6s) Methyl (±)-2-(2,3-di(acetoxy)propoxy)benzoate	347
(β-6s) Methyl (±)-2-(2,3-di(acetoxy)propoxy)benzoate	348
(7s) Methyl (R)-3-((2,2-dimethyl-1,3-dioxolan-4-yl)methoxy)benzoate	349
(8s) Methyl (R)-4-((2,2-dimethyl-1,3-dioxolan-4-yl)methoxy)benzoate	350
(9s) Methyl (R)-2-((2,2-dimethyl-1,3-dioxolan-4-yl)methoxy)benzoate	351
(10s) Methyl 2-((S)-2,3-dihydroxypropoxy)-5-(((S)-2,2-dimethyl-1,3-dioxolan-4-yl)methoxy)benzoate	352
(11s) Methyl 2-((±)-2,3-dihydroxypropoxy)-5-(((S)-2,2-dimethyl-1,3-dioxolan-4-yl)methoxy)benzoate	353
(12s) Methyl 2-((±)-2,3-dihydroxypropoxy)-5-(((S)-2,2-dimethyl-1,3-dioxolan-4-yl)methoxy)benzoate	354
(13s) Methyl 2-((S)-2,3-dihydroxypropoxy)-5-((R)-2,3-dihydroxypropoxy)benzoate	355
(14s) Methyl 2-((±)-2,3-dihydroxypropoxy)-5-((R)-2,3-dihydroxypropoxy)benzoate	356
(15s) Methyl 5-((R)-2,3-dihydroxypropoxy)-2-((±)-2,3-dihydroxypropoxy)benzoate	357
(16s) (2R,5S)-((2-(methoxycarbonyl)-1,4-phenylene)bis(oxy))bis(propane-3,1,2-triyl)tetraacetate	357
(17s) (2±,5S)-((2-(methoxycarbonyl)-1,4-phenylene)bis(oxy))bis(propane-3,1,2-triyl)tetraacetate	358
(18s) (2±,5S)-((2-(methoxycarbonyl)-1,4-phenylene)bis(oxy))bis(propane-3,1,2-triyl)tetraacetate	359
(19s) Methyl 5-((R)-2,3-dihydroxypropoxy)-2-(((S)-2,2-dimethyl-1,3-dioxolan-4-yl)methoxy)benzoate	360
(20s) Methyl 5-((S)-2,3-dihydroxypropoxy)-2-(((S)-2,2-dimethyl-1,3-dioxolan-4-yl)methoxy)benzoate	361
(21s) Methyl 5-((±)-2,3-dihydroxypropoxy)-2-(((S)-2,2-dimethyl-1,3-dioxolan-4-yl)methoxy)benzoate	362
(22s) Methyl 2,5 bis-((R)-2,3-dihydroxypropoxy)benzoate	363
(23s) Methyl 5-((S)-2,3-dihydroxypropoxy)-2-((R)-2,3-dihydroxypropoxy)benzoate	364
(24s) Methyl 5-(2,3-dihydroxypropoxy)-2-((R)-2,3-dihydroxypropoxy)benzoate	365
(25s) (2S,5S)-((2-(methoxycarbonyl)-1,4-phenylene)bis(oxy))bis(propane-3,1,2-triyl)tetraacetate	365

(26s) (2 <i>S</i> ,5 <i>R</i>)-((2-(methoxycarbonyl)-1,4-phenylene)bis(oxy))bis(propane-3,1,2-triyl) tetraacetate	366
(27s) (2 <i>S</i> ,5±)-((2-(methoxycarbonyl)-1,4-phenylene)bis(oxy))bis(propane-3,1,2-triyl) tetraacetate	367
(28s) Methyl 5-((<i>R</i>)-2,3-dihydroxypropoxy)-2-((±)-2,3-dihydroxypropoxy)benzoate	368
(29s) Methyl 5-((<i>R</i>)-2,3-dihydroxypropoxy)-2-((±)-2,3-dihydroxypropoxy)benzoate	369
(30s) Methyl 5-((<i>R</i>)-2,3-dihydroxypropoxy)-2-((<i>S</i>)-2,3-dihydroxypropoxy)benzoate	370
(31s) (2±,5 <i>S</i>)-((2-(methoxycarbonyl)-1,4-phenylene)bis(oxy))bis(propane-3,1,2-triyl) tetraacetate	370
(32s) (2±,5 <i>S</i>)-((2-(methoxycarbonyl)-1,4-phenylene)bis(oxy))bis(propane-3,1,2-triyl) tetraacetate	371
(33s) (2 <i>R</i> ,5 <i>S</i>)-((2-(methoxycarbonyl)-1,4-phenylene)bis(oxy))bis(propane-3,1,2-triyl) tetraacetate	372
(34s) Methyl 2-((<i>R</i>)-2,3-dihydroxypropoxy)-5-((<i>R</i>)-2,3-dihydroxypropoxy)benzoate	373
(35s) Methyl 2-((<i>R</i>)-2,3-dihydroxypropoxy)-5-((<i>S</i>)-2,3-dihydroxypropoxy)benzoate	374
(36s) Methyl 2-((<i>R</i>)-2,3-dihydroxypropoxy)-5-(2,3-dihydroxypropoxy)benzoate	375
(37s) (2 <i>S</i> ,5 <i>S</i>)-((2-(methoxycarbonyl)-1,4-phenylene)bis(oxy))bis(propane-3,1,2-triyl) tetraacetate	376
(38s) (2 <i>S</i> ,5 <i>R</i>)-((2-(methoxycarbonyl)-1,4-phenylene)bis(oxy))bis(propane-3,1,2-triyl) tetraacetate	377
(39s) (2 <i>S</i> ,5±)-((2-(methoxycarbonyl)-1,4-phenylene)bis(oxy))bis(propane-3,1,2-triyl) tetraacetate	378
(40s) Methyl 2-((±)-2,3-dihydroxypropoxy)-5-(((<i>R</i>)-2,2-dimethyl-1,3-dioxolan-4-yl)methoxy)benzoate	379
(41s) Methyl 2-((<i>S</i>)-2,3-dihydroxypropoxy)-5-(((<i>R</i>)-2,2-dimethyl-1,3-dioxolan-4-yl)methoxy)benzoate	380
(42s) Methyl 2-((±)-2,3-dihydroxypropoxy)-5-((<i>S</i>)-2,3-dihydroxypropoxy)benzoate	381
(43s) Methyl 2-((<i>S</i>)-2,3-dihydroxypropoxy)-5-((<i>S</i>)-2,3-dihydroxypropoxy)benzoate	381
(44s) (2±,5 <i>R</i>)-((2-(methoxycarbonyl)-1,4-phenylene)bis(oxy))bis(propane-3,1,2-triyl) tetraacetate	382
(45s) (2 <i>R</i> ,5 <i>R</i>)-((2-(methoxycarbonyl)-1,4-phenylene)bis(oxy))bis(propane-3,1,2-triyl) tetraacetate	383
(46s) Methyl 5-((<i>S</i>)-2,3-dihydroxypropoxy)-2-((±)-2,3-dihydroxypropoxy)benzoate	384
(47s) (±2,5 <i>R</i>)-((2-(methoxycarbonyl)-1,4-phenylene)bis(oxy))bis(propane-3,1,2-triyl) tetraacetate	385

CHIRAL HPLC DATA AND ANALYSIS

±12 (1 mL min ⁻¹ , MeCN/H ₂ O, 7:18)	390
<i>RR</i> -12 (1 mL min ⁻¹ , MeCN/H ₂ O, 7:18)	391
<i>SS</i> -12 (1 mL min ⁻¹ , MeCN/H ₂ O, 7:18)	391
<i>RS</i> -12 (1 mL min ⁻¹ , MeCN/H ₂ O, 7:18)	392
<i>SR</i> -12 (1 mL min ⁻¹ , MeCN/H ₂ O, 7:18)	392
α-12 (1 mL min ⁻¹ , MeCN/H ₂ O, 7:18)	393
β-12 (1 mL min ⁻¹ , MeCN/H ₂ O, 7:18)	393
±4s (1 mL min ⁻¹ , MeCN/H ₂ O, 3:7)	394
<i>R</i> -4s (1 mL min ⁻¹ , MeCN/H ₂ O, 3:7)	394
α-4s (1 mL min ⁻¹ , MeCN/H ₂ O, 3:7)	395
β-4s (1 mL min ⁻¹ , MeCN/H ₂ O, 3:7)	395
±5s (1 mL min ⁻¹ , MeCN/H ₂ O, 3:7)	396
<i>R</i> -5s (1 mL min ⁻¹ , MeCN/H ₂ O, 3:7)	396
α-5s (1 mL min ⁻¹ , MeCN/H ₂ O, 3:7)	397

β-5s (1 mL min ⁻¹ , MeCN/H ₂ O, 3:7)	397
\pm6s (1 mL min ⁻¹ , MeCN/H ₂ O, 1:3)	398
<i>R</i>-6s (1 mL min ⁻¹ , MeCN/H ₂ O, 1:3)	398
α-6s (1 mL min ⁻¹ , MeCN/H ₂ O, 1:3)	399
β-6s (1 mL min ⁻¹ , MeCN/H ₂ O, 1:3)	399
16s (1 mL min ⁻¹ , MeCN/H ₂ O, 7:18)	400
17s (1 mL min ⁻¹ , MeCN/H ₂ O, 7:18)	400
18s (1 mL min ⁻¹ , MeCN/H ₂ O, 7:18)	401
25s (1 mL min ⁻¹ , MeCN/H ₂ O, 7:18)	401
26s (1 mL min ⁻¹ , MeCN/H ₂ O, 7:18)	402
27s (1 mL min ⁻¹ , MeCN/H ₂ O, 7:18)	402
31s (1 mL min ⁻¹ , MeCN/H ₂ O, 7:18)	403
32s (1 mL min ⁻¹ , MeCN/H ₂ O, 7:18)	403
33s (1 mL min ⁻¹ , MeCN/H ₂ O, 7:18)	404
37s (1 mL min ⁻¹ , MeCN/H ₂ O, 7:18)	404
38s (1 mL min ⁻¹ , MeCN/H ₂ O, 7:18)	405
39s (1 mL min ⁻¹ , MeCN/H ₂ O, 7:18)	405
44s (1 mL min ⁻¹ , MeCN/H ₂ O, 7:18)	406
45s (1 mL min ⁻¹ , MeCN/H ₂ O, 7:18)	406
47s (1 mL min ⁻¹ , MeCN/H ₂ O, 7:18)	407
\pm42 (1 mL min ⁻¹ , MeCN/H ₂ O, 2:3)	407
<i>L</i>-42 (1 mL min ⁻¹ , MeCN/H ₂ O, 2:3)	408

SMALL MOLECULE SINGLE CRYSTAL X-RAY DIFFRACTION DATA

EXPERIMENTAL	409
Compound Bu ₃ N•SO ₃	410
Compound <i>RR</i>-14	412
Compound <i>SS</i>-14	416
Compound <i>RS</i>-14	420
Compound <i>SR</i>-14	423
Compound 67	426

6.1. General Experimental Methods

All reactions involving moisture sensitive reagents were carried out in oven-dried reaction vessels under a nitrogen or argon atmosphere. All anhydrous solvents were directly obtained from an SPS dispensary or were dried over 4 Å molecular sieves for 24 h prior to use. Solvents used for work up procedures and column chromatography were of technical grade from Honeywell, VWR and Fischer Scientific. Unless stated otherwise, solvents were removed by rotary evaporation under a reduced pressure between 30-50 °C. All chemical reagents were used as received unless stated otherwise.

The progress of reactions was monitored by thin layer chromatography (TLC) using Merck® silica gel 60 F254 plates, which were visualized with UV light and potassium permanganate. Flash column chromatography was carried out using Geduran 60 Å silica gel and the indicated solvent systems.

¹H- and ¹³C-NMR spectra were recorded on a Bruker Avance® III (400 MHz) spectrometer at 400 and 101 MHz, respectively. Chemical shift data are reported in parts per million (ppm, δ scale) downfield from tetramethylsilane (TMS: δ 0.0), and referenced internally to the residual solvent signal. The deuterated solvents used for NMR analysis were: chloroform (CDCl₃: δ_H 7.26, δ_C 77.16), dimethyl sulfoxide ((CD₃)₂SO: δ_H 2.50, δ_C 39.52), acetone ((CD₃)₂CO: δ_H 2.05, δ_C 29.84), methanol (CD₃OD: δ_H 3.31, δ_C 49.00) and deuterium oxide (D₂O: δ_H 4.78). Coupling constants are given in hertz (Hz). All individual assignments were made using 2D NMR (¹H-¹H COSY, ¹H-¹³C HSQC, and ¹H-¹³C HMBC) spectroscopy. The spectroscopic data are presented as follows: Chemical shift, multiplicity (s = singlet, d = doublet, t = triplet, q = quartet, p = pentet (quintet), m = multiplet, br = broad, app. = apparent and combinations thereof), coupling constant, integration and structural assignment.

Mass spectra were recorded on a Waters Xevo G2-XS ToF or Synap G2-S mass spectrometer using Zspray, and a Bruker microTOF® LCMS using Electro-spray ionisation in positive (ESI+) and negative (ESI-) modes.

Infrared spectra were recorded on a Perkin Elmer Spectrum 100 FT-IR and a Varian 660-IR FTIR spectrometer, using Agilent Resolution Pro with absorption maxima 4 (Vmax) reported in cm^{-1} .

Melting points were measured using a Gallenkamp melting point apparatus and are uncorrected.

Optical rotations were measured using a Bellingham and Stanley ADP450 Series-Peltier polarimeter at 25 °C using the sodium D line (589.3 nm) with the indicated concentration and solvent.

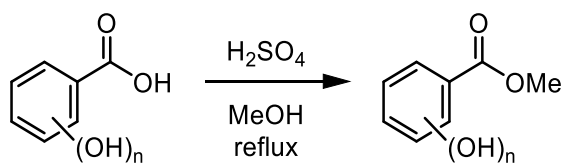
High performance liquid chromatography (HPLC) analysis was performed using an LC-20 prominence system from Shimadzu, Chromeleon client, version 6.80 SR15, Build 4656, using Phenomenex C18 and Lux® Cellulose-1 (3 μm , 250 x 4.6 mm) columns. A Shimadzu SPD-M20A diode Array Detector was used for the UV detection, monitored at either 210, 220, 254 or 280 nm with the indicated flow rate and solvent system.

All chemical experiments were carried out by the Author (Daniel Gill)

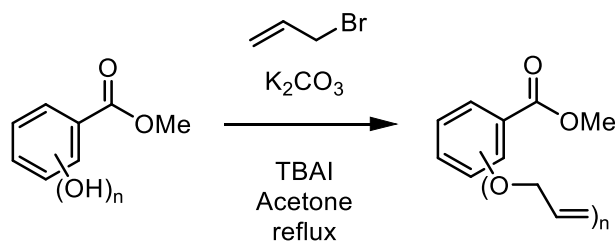
All NMR, HPLC and IR analysis was performed and analysed by the Author.

All mass spectrometry analysis was performed and analysed by either the author, Dr Chi Tsang and Dr Christopher Williams (University of Birmingham, School of Chemistry).

All small molecule single crystal X-Ray diffraction data was analysed and the structures solved by Dr Louise Male (School of Chemistry, University of Birmingham).

6.1.1. Procedure A: The synthesis of hydroxybenzoic acid methyl esters

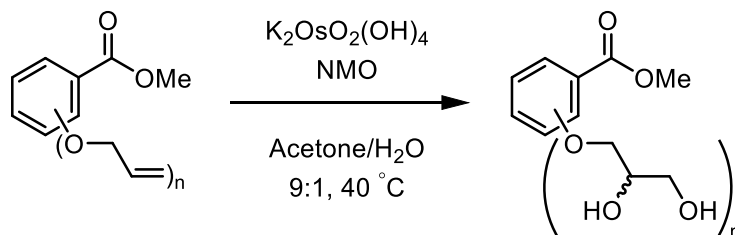
A solution of benzoic acid (10 mmol) in MeOH (20 mL) was charged with conc. H_2SO_4 (0.2 mL). The reaction mixture was heated under reflux until complete consumption of starting material was observed (TLC). The flask was cooled to an ambient temperature and the solvent removed under reduced pressure to afford a crude oil. The oil was neutralised to pH 8 – 9 with satd. NaHCO_3 (aq.) (50 mL) and extracted with EtOAc (3×30 mL). The combined organic extracts were washed with brine (30 mL) and dried (MgSO_4). Filtration of the solids and removal of solvent under reduced pressure afforded the desired benzoic acid methyl ester.

6.1.2. Procedure B: The synthesis of allyloxy benzoic acid methyl esters

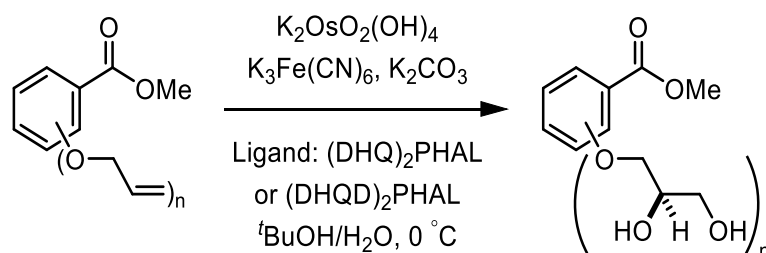
A mixture of hydroxybenzoic acid methyl ester (5.0 mmol), K_2CO_3 (1.2 eq. per OH) and tetrabutylammonium iodide (TBAI) (0.5 eq.) in acetone (25 mL) was charged dropwise with allyl bromide (1.2 eq.) at room temperature. The reaction mixture was heated under reflux until complete consumption of starting material was observed (TLC). The flask was cooled to an ambient temperature and the solvent removed under reduced pressure to afford a crude oil. The oil was charged with satd. NH_4Cl (aq.) (50 mL) and the product extracted with EtOAc (3×30 mL). The combined organic extracts

were washed with 1.0 M HCl (aq.) (2 × 30 mL), H₂O (30 mL), brine (30 mL) and dried (MgSO₄). Filtration of the solids and removal of solvent under reduced pressure afforded a crude mixture. Purification by chromatography (SiO₂, EtOAc/hexane, 1:9) afforded the desired allyloxy benzoic acid methyl ester.

6.1.3. Procedure C: The Upjohn dihydroxylation of aryl-allyl ethers



A 25 mL round bottom flask containing *N*-methylmorpholine-*N*-oxide (NMO) (1.2 eq.) was charged with acetone/H₂O (9:1, 10 mL) and stirred vigorously. Potassium osmate (0.01 eq.) was added directly and the reaction mixture was stirred at room temperature for 10 min. The flask was charged with alkene (1.0 eq.) dropwise and heated at 40 °C until complete consumption of starting material was observed (TLC, EtOAc/hexane 1:1, or EtOH/EtOAc 1:4). The reaction was quenched with Na₂SO₃ (3.0 eq) and stirred at room temperature for 1 h. The majority of solvent was removed under reduced pressure and the flask was charged with H₂O (10 mL). The aqueous mixture was extracted with CH₂Cl₂ (3 × 30 mL) and the combined organic extracts were washed with 1.0 M HCl (aq.) (2 × 30 mL), brine (30 mL) and dried (MgSO₄). Filtration of the solids and removal of solvent under reduced pressure afforded the desired 1,2-propanediol. Alternatively, for highly polar compounds, no work up procedure was required and the crude reaction mixture was purified directly by chromatography (SiO₂, EtOAc/EtOH 4:1).

6.1.4. Procedure D: The Sharpless AD of aryl-allyl ethers

A 25 mL round bottom flask was charged with stock solution **I** (3.0 eq.), **II** (3.0 eq.), **III** (0.002 eq.) and either solution **IV** (ADmix α /DHQ₂(PHAL)) or **V** (ADmix β /DHQD₂(PHAL)) (0.02 eq.) forming a biphasic homogeneous mixture. The flask was cooled to $0\text{ }^\circ\text{C}$ (ice bath) and stirred vigorously for 20 min creating a heterogeneous orange slurry to which the alkene (1.0 eq.) was added directly. The reaction mixture was stirred at $0\text{ }^\circ\text{C}$ until complete consumption of starting material was observed (TLC, EtOAc/hexane 1:1, or EtOH/EtOAc 1:4). The reaction was quenched with neat Na_2SO_3 (12.0 eq.) and warmed to room temperature over 1 h. The flask was charged with H_2O (5 mL) and extracted with CH_2Cl_2 ($3 \times 20\text{ mL}$). The combined organic extracts were washed with 1.0 M $\text{HCl}_{(\text{aq.})}$ ($2 \times 30\text{ mL}$), brine (30 mL) and dried (MgSO_4). Filtration of the solids and removal of solvent under reduced pressure afforded the desired 1,2-propanediol. Alternatively, for highly polar compounds, no work up procedure was required and the crude reaction mixture was purified directly by chromatography (SiO_2 , EtOAc/EtOH 4:1).

6.1.5. Preparation of Stock solutions I-V

Stock solution I*: A 25 mL volumetric flask was charged with $\text{K}_3\text{Fe}(\text{CN})_6$ (12.347 g, 37.5 mmol) and diluted with distilled water (25.0 mL). The flask was placed in an ultrasonic bath at $50\text{ }^\circ\text{C}$ to give a 1.5 M solution.

Stock solution II: A 25 mL volumetric flask was charged with K_2CO_3 (5.182 g, 37.5 mmol) and diluted with distilled water (25.0 mL) to give a 1.5 M solution.

Stock solution III: A 10 mL volumetric flask was charged with $\text{K}_2\text{OsO}_2(\text{OH})_4$ (7.3 mg, 0.02 mmol) and diluted with distilled water (10.0 mL) to give a 0.002 M solution.

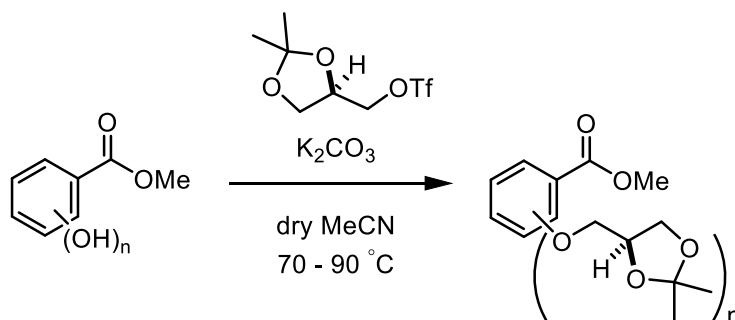
Stock solution IV*: A 25 mL volumetric flask was charged with $(\text{DHQ})_2\text{PHAL}$ (194.7 mg, 0.25 mmol) and diluted with warmed $t\text{BuOH}$ (25.0 mL) to give a 0.01 M solution.

Stock solution V*: A 25 mL volumetric flask was charged with $(\text{DHQD})_2\text{PHAL}$ (194.7 mg, 0.25 mmol) and diluted with warmed $t\text{BuOH}$ (25.0 mL) to give a 0.01 M solution.

Note: Stock solutions **II**, **IV** and **V** are stable at room temperature for greater than 2 months. Solutions **I** and **III** were found to be stable up to 3 weeks stored in a fridge at 4 – 8 °C under an inert atmosphere of argon.

*Stock solution **I** was placed in an ultrasonic bath at 50 °C for 20 min and cooled to room temperature prior to each use. Stock solution **IV** and **V** were warmed to 35 °C prior to each use.

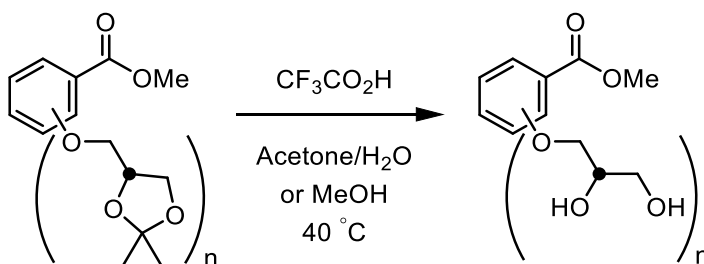
6.1.6. Procedure E: The chiral pool synthesis of 2,2-dimethyl-4-(aryloxymethyl)-1,3-dioxolanes



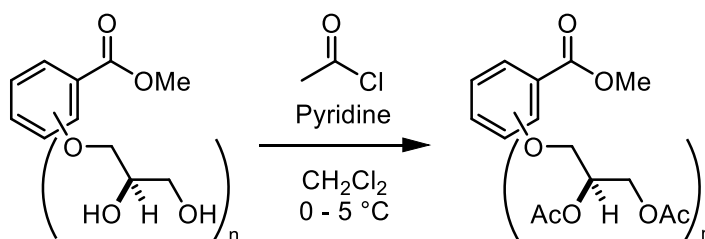
A 25 mL Schleck flask fitted with a reflux condenser was charged with the appropriate phenol (1.0 eq.) and K_2CO_3 (2.0 eq.). The flask was sealed and the internal atmosphere made inert by a pump-purge cycle with dry argon. MeCN was added (2 – 4 mL) and

the heterogeneous mixture was stirred for 10 min at room temperature. The chiral pool-derived Solketal-OTf (*R* or *S*) was added directly (1.2 – 1.5 eq.) and the reaction mixture was heated at 70 °C with monitoring (TLC). The flask was cooled to an ambient temperature and charged with H₂O (5 mL). The aqueous mixture was extracted with CH₂Cl₂ (3 × 30 mL) and the combined organic extracts were washed with brine (20 mL) and dried (MgSO₄). Filtration of the solid and removal of solvent under reduced pressure gave a crude oil. Purification by chromatography (SiO₂, EtOAc/hexane) afforded the corresponding acetal.

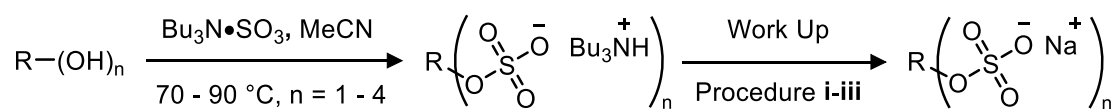
6.1.7. Procedure F: The acid hydrolysis of chiral solketal-derived acetals



A flask containing the acetal (1 – 2 eq.) was charged with acetone/H₂O or MeOH/H₂O (2.0 mL, 5:1 or 4:1, respectively) and stirred at room temperature to give a homogeneous solution. Trifluoroacetic acid (0.2 mL) was added dropwise and the reaction mixture was heated at 40 °C with monitoring (TLC, EtOAc/Hexane or EtOH/EtOAc). The solvent was removed under reduced pressure and residual TFA was removed by repeated azeotropic distillation with acetone (2 – 4 mL × 4). The final residue was dried under vacuum (1 – 5 mbar) for 2 h to afford the corresponding 1,2-propanediol.

6.1.8. Procedure G: The acetylation of aryloxy-1,2-propanediols

An oven dried 25 mL Schlenk flask was charged with the appropriate diol (1.0 eq.) and the internal environment was made inert by a pump-purge cycle with dry argon. The flask was charged with Pyridine (4.0 eq.), CH_2Cl_2 (4.0 mL) and placed in an ultrasonic bath (25 °C) for 2 min to form a clear, homogenous solution. The flask was cooled to 0 °C in an ice bath (ice/acetone) for 10 min with stirring. AcCl (4.0 eq.) was added dropwise over 2 min and the reaction mixture was stirred for a further 30 min and warmed to room temperature. The reaction mixture was quenched with H_2O (10 mL) and extracted with CH_2Cl_2 (3×20 mL). The combined organic extracts were washed successively with satd. NaHCO_3 (aq.) (2×20 mL) and 1 M HCl (aq.) (2×20 mL), brine (50 mL) and dried (MgSO_4). Filtration of the solid and removal of the solvent under reduced pressure afforded the crude esterification product. Purification by chromatography (SiO_2 , EtOAc/hexane, 1:1) afforded the pure acetylated esters.

6.1.9. Procedure H: The preparation of organosulfates using $\text{Bu}_3\text{N}\cdot\text{SO}_3$ 

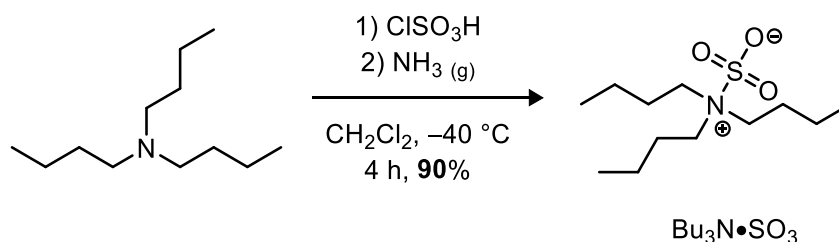
A flame dried 25 mL Schlenk flask was charged with $\text{R}-(\text{OH})_n$ (1.0 mmol) and $\text{Bu}_3\text{N}\cdot\text{SO}_3$ (2.0 eq. per OH group) and the internal environment was made inert by a pump-purge cycle with dry argon. Anhydrous MeCN was added (giving a concentration of 0.50 – 0.25 Mol dm^{-3} to the limiting reagent) and the reaction mixture heated at 90 $^\circ\text{C}$, with monitoring by TLC. The flask was cooled to room temperature and the solvent removed under reduced pressure. The flask was charged with H_2O (20 mL) and the aqueous mixture extracted with EtOAc or CH_2Cl_2 (4 \times 30 mL). The organic extracts were pooled, dried (MgSO_4), filtered and the solvent was removed under reduced pressure to afford the desired sulfate ester as its $[\text{Bu}_3\text{NH}]^+$ salt. Alternatively, the crude reaction mixture was used directly in steps **i-iii** without extraction into organic solvent.

Work-Up procedure i: The flask containing the $[\text{Bu}_3\text{NH}]^+$ salt was charged with EtOH (30 mL) and NEH (5.0 eq. per sulfate group). The reaction mixture was stirred vigorously for 1 h at room temperature. The solid was collected by filtration, washed with EtOH (3 \times 20 mL) and dried to a constant weight to afford the desired sulfate as its Na^+ salt.

Work-Up procedure ii: The flask containing the $[\text{Bu}_3\text{NH}]^+$ salt was charged with Et_2O (30 mL), EtOH (5 mL) and NEH (5.0 eq. per sulfate group). The reaction mixture was stirred vigorously for 1h at room temperature. The solid was removed by filtration, washed with a small amount of cold EtOH and dried to a constant weight to afford the desired sulfate as its Na^+ salt.

Work-Up procedure iii: The flask containing the $[\text{Bu}_3\text{NH}]^+$ salt was charged with MeCN (20 mL) and NaI (5.0 eq. per sulfate group). The reaction mixture was stirred vigorously for 1h at room temperature. The solid was removed by filtration, washed with MeCN (3×30 mL) and dried to a constant weight to afford the desired sulfate as its Na^+ salt.

6.2. Synthesis of tributylsulfoammonium betaine ($\text{Bu}_3\text{N}\bullet\text{SO}_3$)

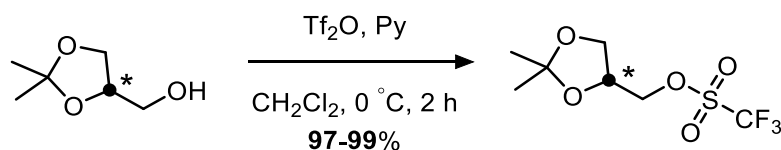


A three necked round bottom flask was fitted with a temperature probe and a pressure equalising dropping funnel. The flask under an atmosphere of argon was charged with tributylamine (59.4 mL, 0.25 mol) and anhydrous CH_2Cl_2 (200 mL). The solution was stirred vigorously and cooled to $-40\text{ }^\circ\text{C}$ (MeCN/CO_2). A solution of chlorosulfonic acid (16.75 mL, 0.253 mol) in anhydrous CH_2Cl_2 (200 mL) was added dropwise over 2 h at a rate ensuring the internal temperature did not exceed $-30\text{ }^\circ\text{C}$. After full addition of the ClSO_3H solution, and stirring for a further 1 h, $\text{NH}_3\text{ (g)}$ was gently bubbled through the reaction mixture until pH 7 – 8 was achieved. The white solid was removed by vacuum filtration, washed with CH_2Cl_2 (100 mL) and the filtrate was collected. The solvent was removed under reduced pressure and the crude product was treated with cold H_2O (500 mL). The precipitate was collected, washed with H_2O ($5 \times 100\text{ mL}$) and freeze dried. Recrystallization from CH_2Cl_2 /hexane affording $\text{Bu}_3\text{N}\bullet\text{SO}_3$ as a bright white solid (59.8 g, 0.23 mol, 90%). **M.P** $95 - 96\text{ }^\circ\text{C}$ (from $\text{CH}_2\text{Cl}_2/\text{H}_2\text{O}$). Lit. $94\text{ }^\circ\text{C}$;¹ **IR** $V_{\text{max}}\text{ cm}^{-1}$ 2962 w, 2875 w, 1473 m, 1293 m (O-S); **$^1\text{H-NMR}$** δ_{H} (400 MHz, CDCl_3) 3.32 – 3.22 (m, 6H, N- CH_2), 1.87 – 1.73 (m, 6H, CH_2), 1.37 (dt, $J = 7.4\text{ Hz}$, 6H, CH_2), 0.98 (t, $J = 7.4\text{ Hz}$, 9H, CH_3); **$^{13}\text{C-NMR}$** δ_{C} (101 MHz, CDCl_3) 57.1 (N(CH_2)₃), 25.6 (CH_2), 20.6 (CH_2), 13.7 (CH_3); **LRMS** m/z (ESI[−]) 264.1 ($[\text{M-H}]^-$, 100%), 208.1 ($[\text{M}-\text{C}_4\text{H}_{10}]^-$, 53); **HRMS** m/z (ESI[−]) $\text{C}_{12}\text{H}_{26}\text{NO}_3\text{S}$ $[\text{M-H}]^-$ requires 264.1613, Found: 264.1612 ($[\text{M-H}]^-$). Stability measurement showed that prolonged exposure to moisture in the air gave ~12% degradation of $\text{Bu}_3\text{N}\bullet\text{SO}_3$ after 15 days by $^1\text{H-NMR}$

spectroscopy. Exclusion of moisture from the storage atmosphere (e.g. N₂, Ar or vacuum atmosphere) in the vial containing Bu₃N•SO₃ gave long term stability (1 – 2 months minimum per batch).

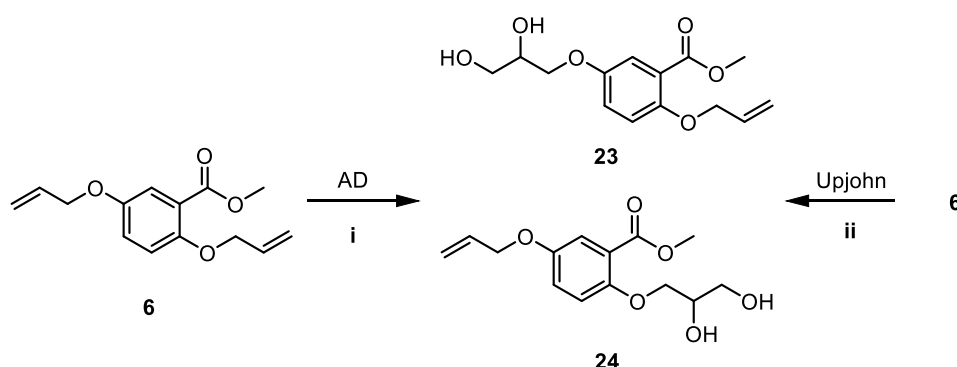
Data were in accordance with the literature.¹

6.3. Preparation of (*R*) or (*S*)-(2,2-dimethyl-1,3-dioxolan-4-yl)-methyl trifluoromethanesulfonate



An oven dried round bottom flask was sealed and the internal atmosphere made inert by a pump-purge cycle with argon. The flask was charged with anhydrous CH₂Cl₂ (30 mL), (*R* or *S*)-Solketal (1.00 mL, 8.0 mmol), pyridine (0.71 mL, 8.8 mmol) and cooled to 0 °C (ice bath) for 20 min whilst stirring. *Via* cannula, a solution of trifluoromethanesulfonic anhydride (Tf₂O, freshly distilled from P₂O₅) (1.48 mL, 8.8 mmol) in anhydrous CH₂Cl₂ (20 mL) was added dropwise over 1 h at 0 °C. After full addition of the Tf₂O solution, the reaction mixture was stirred for 1 h and slowly brought to room temperature (15 – 20 °C). The flask was charged with additional CH₂Cl₂ (20 mL) and washed with satd. NaHCO₃ (aq.) (40 mL), citric acid/sodium citrate buffer (aq.) (2 × 40 mL, 1.0 M, pH 4) brine (40 mL) and dried (MgSO₄). Filtration of the solids and removal of solvent under reduced pressure (at 20 °C) yielded the title compound as an amber oil (2.00 – 2.10 g, 97 – 99%). The trifluoromethanesulfonate was used directly without further purification and had a storage life of approximately 48 h at –20 °C. **¹H-NMR** (400 MHz, CDCl₃) δ_H 4.51 – 4.29 (m, 3H), 4.10 (dd, *J* = 9.0, 6.3 Hz, 1H), 3.83 (dd, *J* = 9.0, 4.7 Hz, 1H), 1.42 (s, 3H), 1.34 (s, 3H).

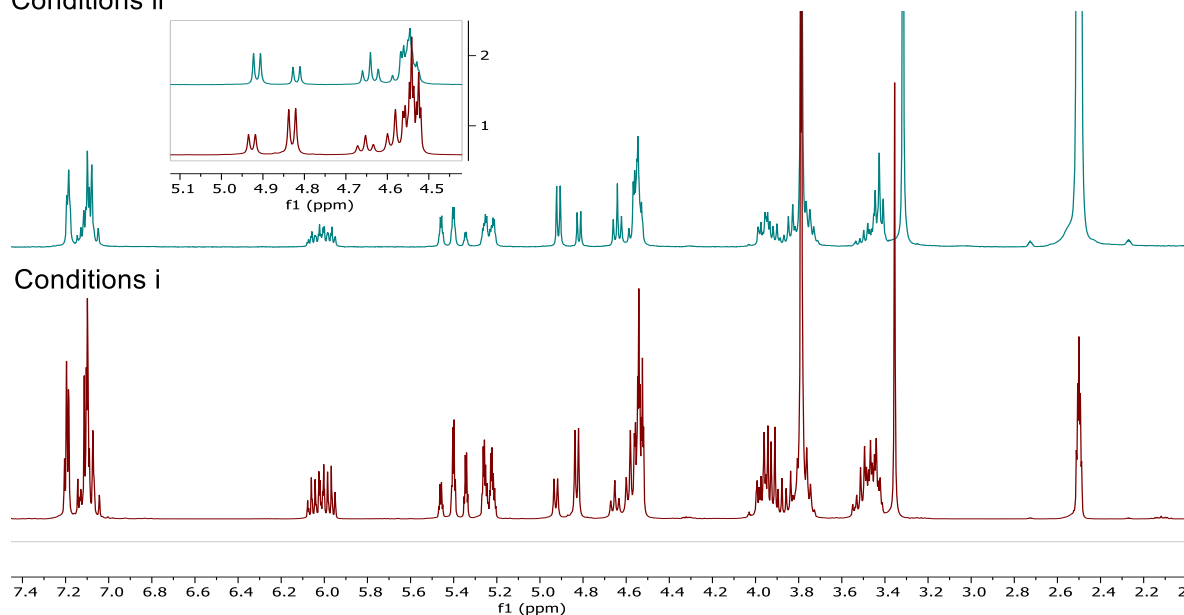
Data were in accordance with the literature.²

6.4. Regioselectivity analysis of the SAD: Synthesis of diols 23 and 24

Conditions i: Following general procedure **D** using stock solutions: **I** (2 mL, 3.0 mmol), **II** (2 mL, 3.0 mmol), **III** (1.0 mL, 2.0 μ mol) and **V** (5.0 mL, 20.0 μ mol). Methyl 2,5-bis(allyloxy)benzoate (**6**) (248 mg, 1.0 mmol, 2 eq. alkene) was added and the reaction mixture was stirred at 0 °C until complete consumption of **6** was observed (TLC), 8 h. The aqueous mixture was extracted with CH_2Cl_2 (4 \times 30 mL). The combined organic extracts washed with 1 M $\text{HCl}_{(\text{aq.})}$ (2 \times 30 mL), brine (20 mL) and dried (MgSO_4) to yield a clear oil (140 mg, 50%).

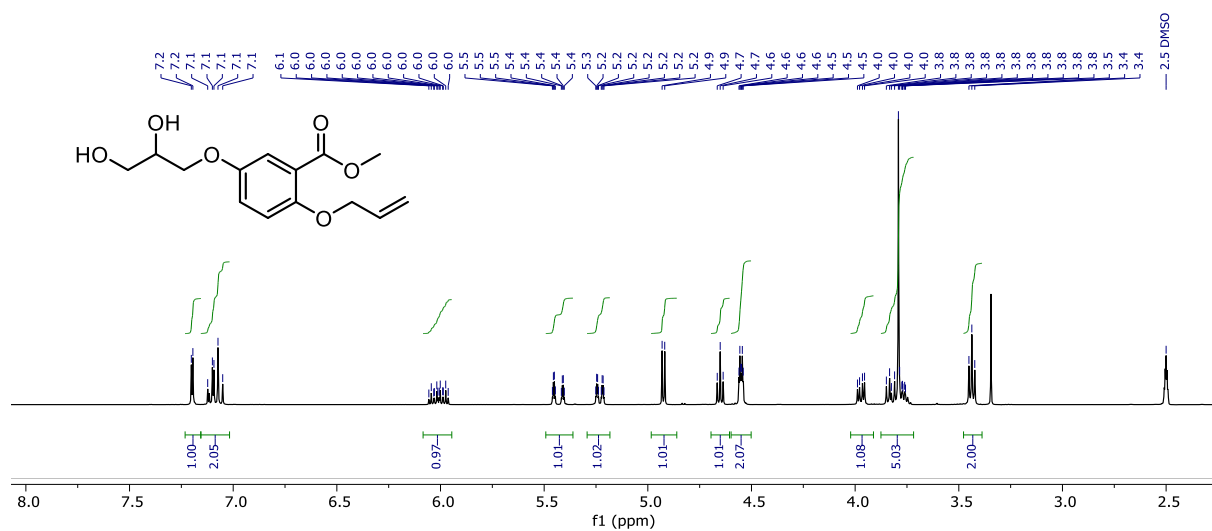
Conditions ii: Following general procedure **C**: NMO (140 mg, 1.20 mmol) was charged with acetone/ H_2O (9:1, 10 mL) and $\text{K}_2\text{OsO}_2(\text{OH})_4$ (3.7 mg, 0.01 mmol). 2,5-bis(allyloxy)benzoate (**6**) (248 mg, 1.0 mmol) was added and the reaction mixture was heated at 40 until complete consumption of **6** was observed (TLC), 8 h. The solvent was removed and charged with satd. $\text{Na}_2\text{SO}_3_{(\text{aq.})}$ (20 mL). The aqueous mixture was extracted with CH_2Cl_2 (4 \times 30 mL). The combined organic extracts washed with 1 M $\text{HCl}_{(\text{aq.})}$ (2 \times 30 mL), brine (20 mL) and dried (MgSO_4) to yield a clear oil (190 mg, 67%).

Conditions ii

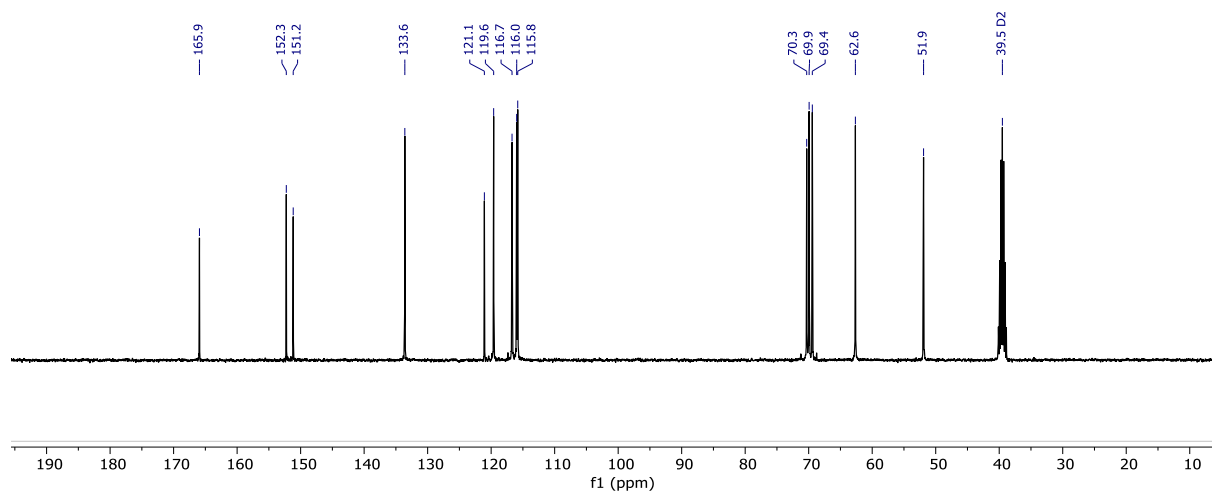


The two oils were combined and purified by column chromatography (SiO_2 , acetone/hexane, 1:19) to yield diol **23** (50 mg) and a crude mixture of diols **23** and **24**.

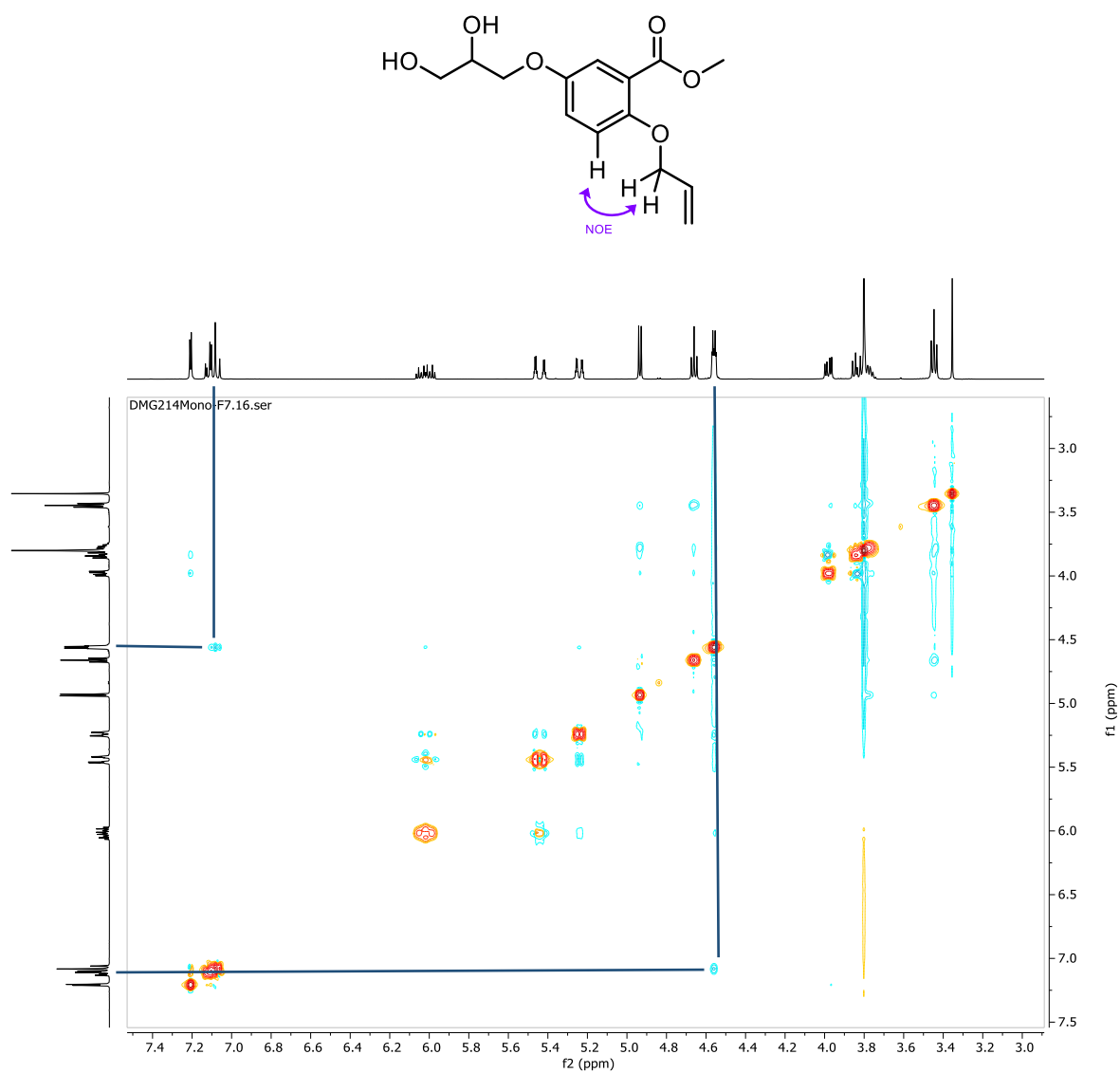
For **23**: **$^1\text{H-NMR}$** (400 MHz, $(\text{CD}_3)_2\text{SO}$) δ_{H} 7.20 (d, $J = 3.0$ Hz, 1H, C6-H), 7.15 – 6.99 (m, 2H, C3-H, C4-H), 6.01 (ddt, $J = 17.2, 10.7, 4.7$ Hz, 1H, CH=CH₂), 5.43 (dq, $J = 17.3, 1.9$ Hz, 1H, CH=CH₂), 5.23 (dq, $J = 10.6, 1.7$ Hz, 1H, CH=CH₂), 4.92 (d, $J = 5.1$ Hz, 1H, CH-OH), 4.65 (t, $J = 5.7$ Hz, 1H, CH₂-OH), 4.55 (dt, $J = 4.7, 1.7$ Hz, 2H, C2-OCH₂), 3.97 (dd, $J = 9.6, 4.0$ Hz, 1H, CH-OH), 3.88 – 3.70 (m, 5H, Me & C5-OCH₂), 3.44 (t, $J = 5.6$ Hz, 2H, CH₂-OH); **$^{13}\text{C-NMR}$** (101 MHz, $(\text{CD}_3)_2\text{SO}$) δ_{C} 165.9 (CO₂Me), 152.3 (C5), 151.2 (C2), 133.6 (CH=CH₂), 121.1 (C1), 119.6 (C4), 116.7 (CH=CH₂), 116.0 (C6), 115.8 (C3), 70.3 (CH-OH), 69.9 (C5-OCH₂), 69.4 (C2-OCH₂), 62.7 (CH₂-OH), 51.9 (Me)

¹H-NMR spectrum **23** ((CD₃)₂SO, 400 MHz)

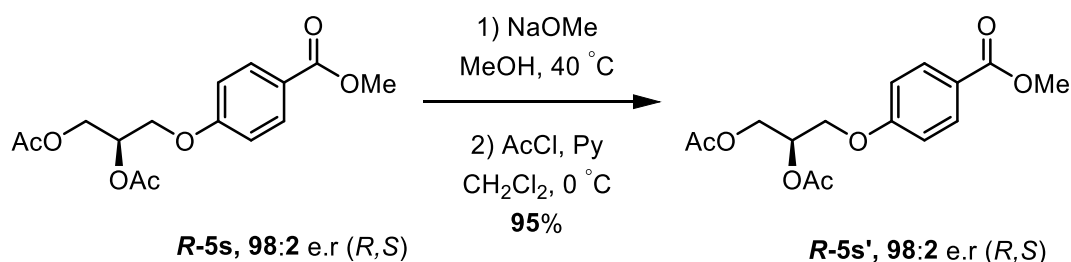
¹³C-NMR spectrum **23** ((CD₃)₂SO, 101 MHz)



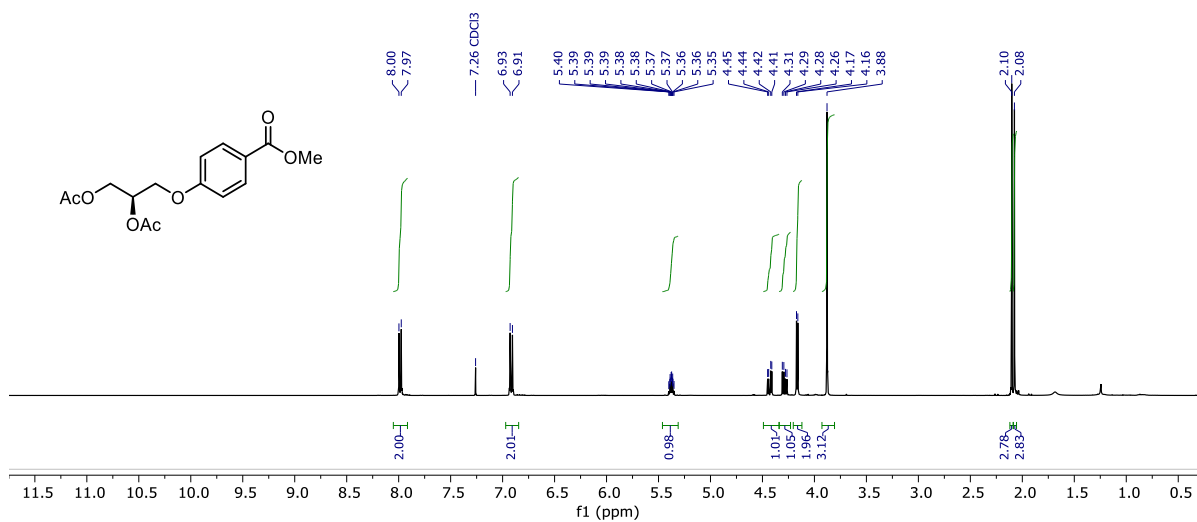
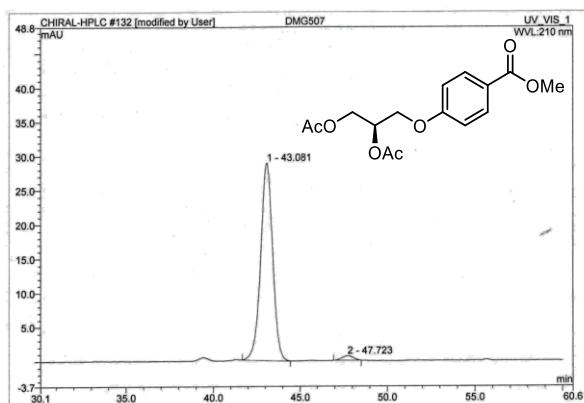
^1H -NOESY-NMR spectrum **23** ($(\text{CD}_3)_2\text{SO}$, 400 MHz)



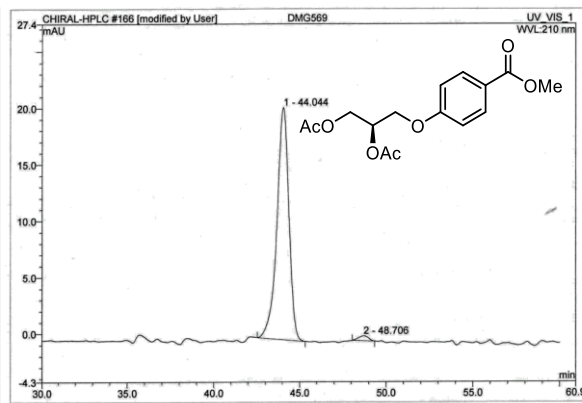
6.5. Hydrolysis analysis of diol **S-21**: The effects of hydrolysis and acetylation on stereochemistry



Part 1: Methyl (*R*)-4-(2,3-di(acetoxy)propoxy)benzoate (**R-5s**) (20 mg, 0.064 mmol) was dissolved in a solution of freshly prepared NaOMe (2 mL) and was stirred at 40 °C for 12 h. The reaction was quenched by the dropwise addition of 1 M HCl (aq.) and acidified to pH 4. The solvent was removed under reduced pressure and the residue triturated with EtOAc (10 mL). The mixture was filtered through a pad of celite, the filtrate was collected and the solvent was removed under reduced pressure to afford a clear oil. **Part 2:** Following general procedure **G**: the oil was dissolved in CH₂Cl₂ (2 mL) and charged with pyridine (20.8 µL, 0.256 mmol). The flask was cooled (ice bath) and the reaction mixture was charged dropwise with AcCl (18.2 µL, 0.256 mmol). The reaction mixture was stirred for a further 10 min. The final product was purified by chromatography (SiO₂, EtOAc/Hexane 1:1, *R_f* = 0.55) yielding methyl (*R*)-4-(2,3-di(acetoxy)propoxy)benzoate (**R-5s'**) as a clear oil (18 mg, 95%, 2 steps). **[α]_D²⁵** – 43.17 (c. 1.0, CHCl₃, 98:2 *e.r* (*R,S*)); **IR** *V*_{max} cm^{–1} 2955 w (C–H), 1740 s (C=O), 1714 s (C=O), 1606 s, 1580 w, 1510 w, 1435 w, 1370 w, 1280 s, 1217 s; **¹H-NMR** (400 MHz, CDCl₃) δ_H 8.02 – 7.96 (m, 2H, C3–H), 6.95 – 6.89 (m, 2H, C2–H), 5.38 (dtd, *J* = 5.9, 5.1, 4.0 Hz, 1H, CH–OAc), 4.44 (dd, *J* = 12.0, 4.0 Hz, 1H, CH₂–OAc), 4.29 (dd, *J* = 12.0, 5.9 Hz, 1H, CH₂–OAc), 4.17 (d, *J* = 5.1 Hz, 2H, C4–OCH₂), 3.88 (s, 3H, Me), 2.10 (s, 3H, Ac), 2.08 (s, 3H, Ac); **LRMS** *m/z* (ESI+) 333.10 (100%, [M+Na]⁺). Data were in accordance with the original starting material (**R-5s**).

¹H-NMR spectrum **R-5s'** (400 MHz, CDCl₃)chPLC analysis of **R-5s** and **R-5s'** (1 mL min⁻¹, MeCN/H₂O, 3:7)

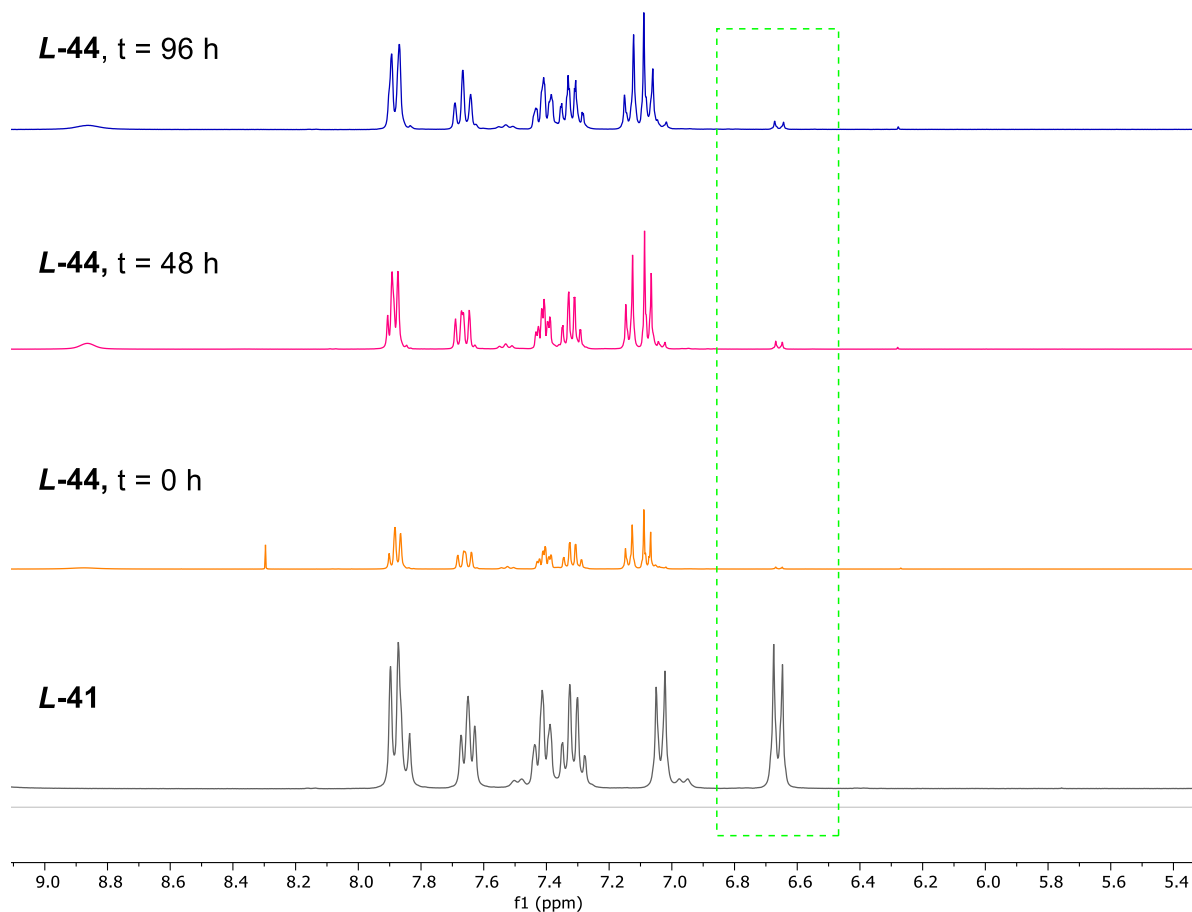
No.	Ret.Time min	Peak Name	Height mAU	Area mAU*min	Rel.Area %	Amount	Type
1	43.08	n.a.	28.861	23.151	97.92	n.a.	BMB
2	47.72	n.a.	0.654	0.491	2.08	n.a.	BMB*
Total:			29.515	23.642	100.00	0.000	



No.	Ret.Time min	Peak Name	Height mAU	Area mAU*min	Rel.Area %	Amount	Type
1	44.04	n.a.	20.567	16.651	98.34	n.a.	BMB*
2	48.71	n.a.	0.428	0.282	1.66	n.a.	BMB*
Total:			20.995	16.932	100.00	0.000	

6.6. Desulfation experiment of **L-44**

Time course ^1H -NMR (CDCl_3) of **L-44** at 0 – 96 h (^1H -NMR spectra). The green box highlights the reappearance of starting material resonances (**L-41**).

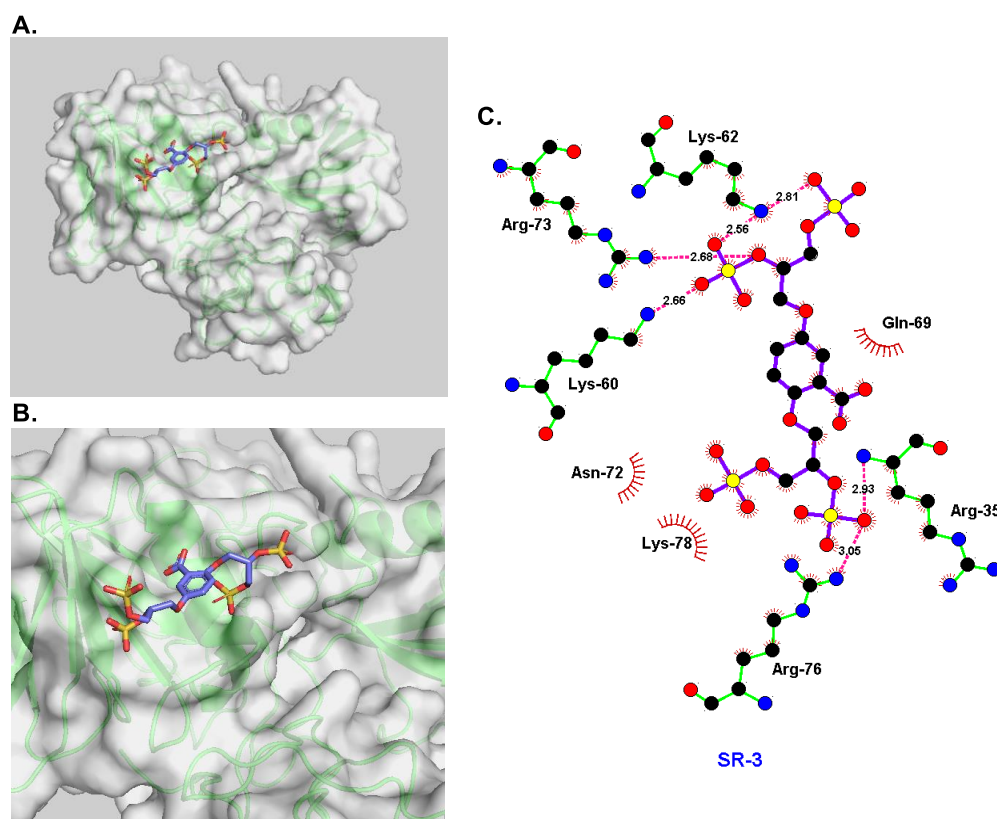


6.7. Results of Docking Studies

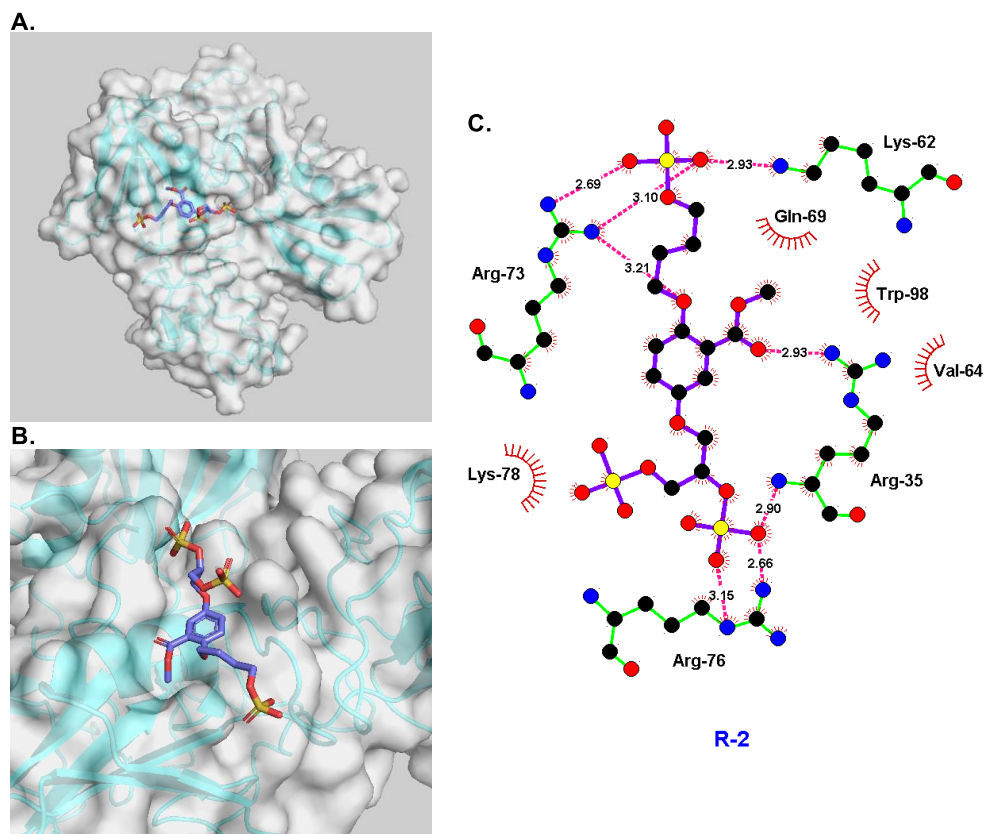
All docking studies were carried out by the Author (Daniel Gill) using Autodoc[®] V1.5.4. All molecular energies were minimized using MM2 minimum energy calculations in Chemdraw[®] 3D prior to being imported into the AutoDOC[®] software. Search parameters: NPTS = 40/40/40, spacing = 0.592, grid center = 57.496:18.131:71.217 (X,Y,Z), with a smooth factor of 0.5, operating on 100 runs.

Minimum energy interaction of **SR-3**, docked into the H/HS-binding site of NK1(HGF); For all, **A)** Full image of the binding interaction; **B)** Zoomed in view of the binding interaction; **C)** Ligplot representation of individual binding interactions displaying vicinal amino acid residues and hydrogen bonds. E.g. for **SR-3** Arg-35, Lys-60, Lys-62, Agr-73 and Arg-76 are proposed to hydrogen bond to the HS-glycomimetic.

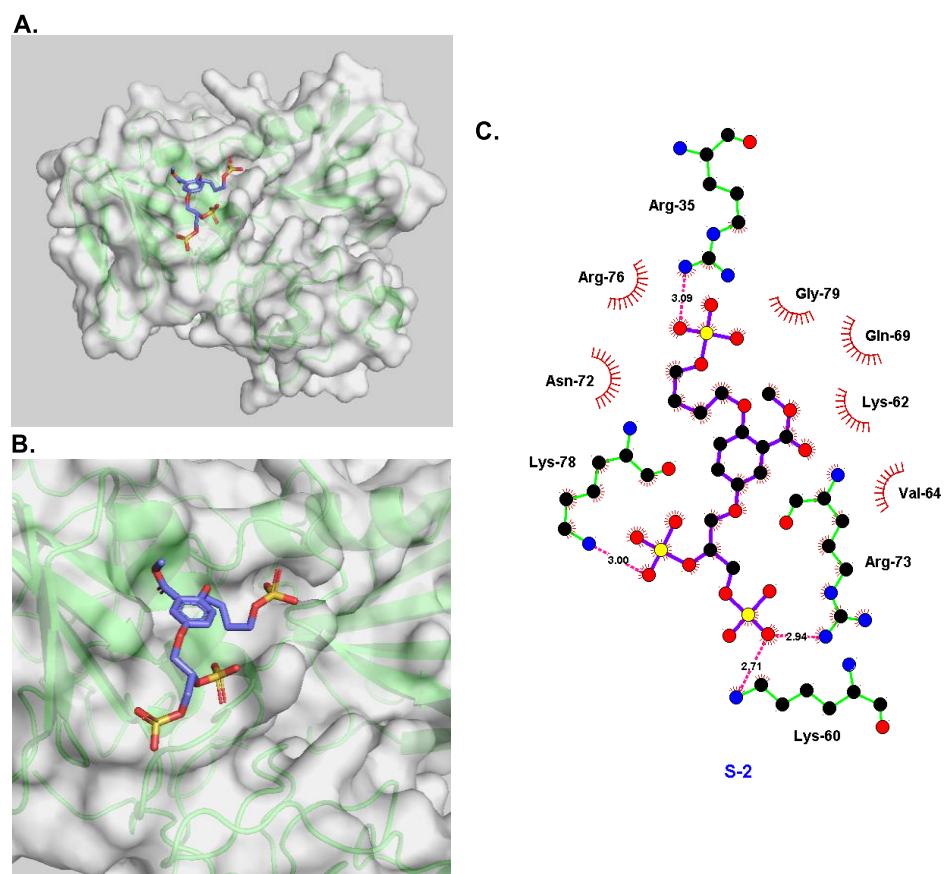
Minimum energy interaction of **SR-3**



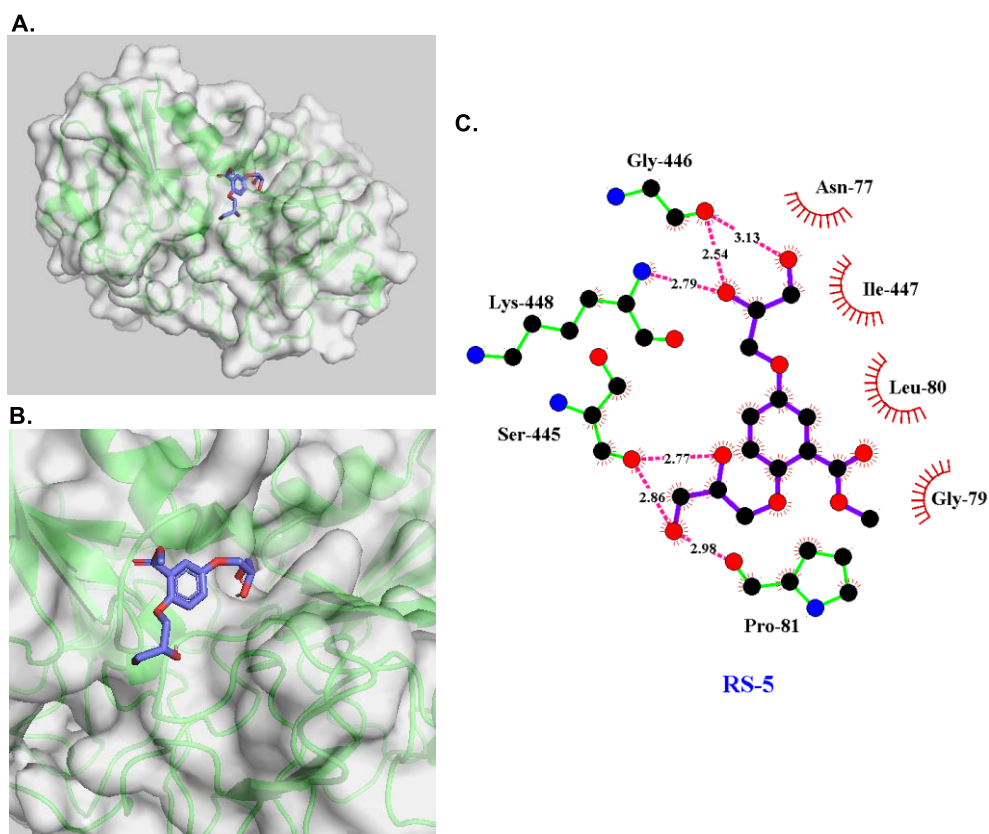
Minimum energy interaction of **R-2**



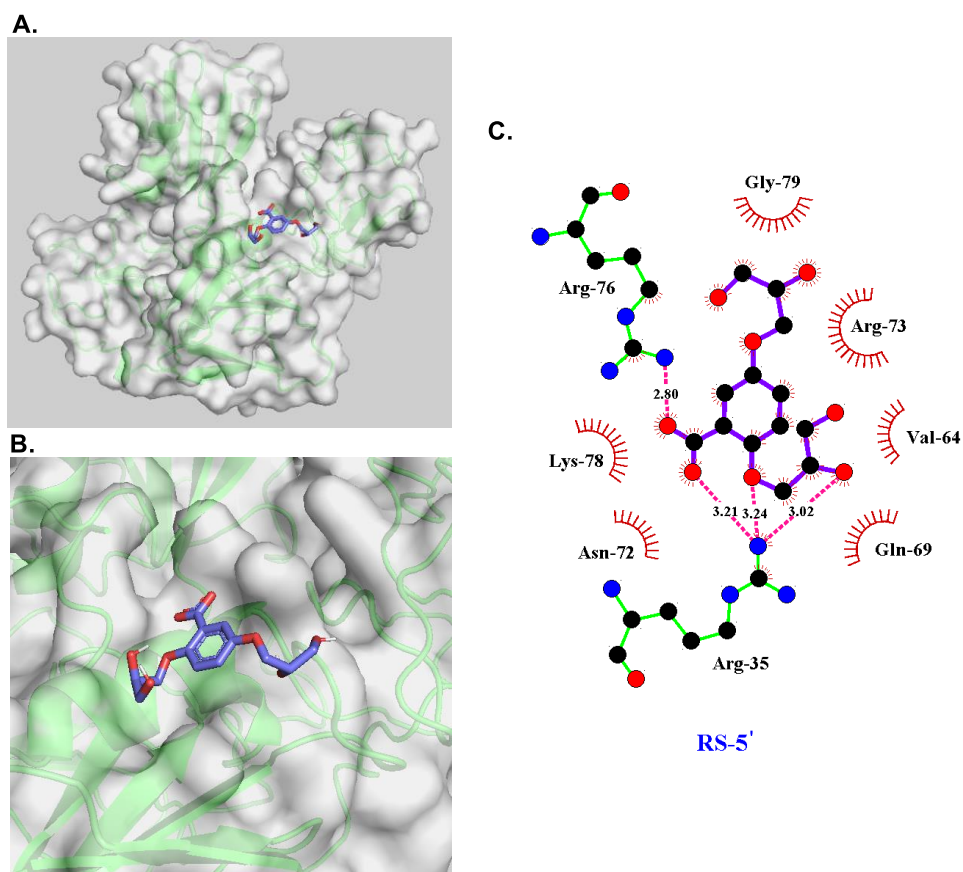
Minimum energy interaction of **S-2**



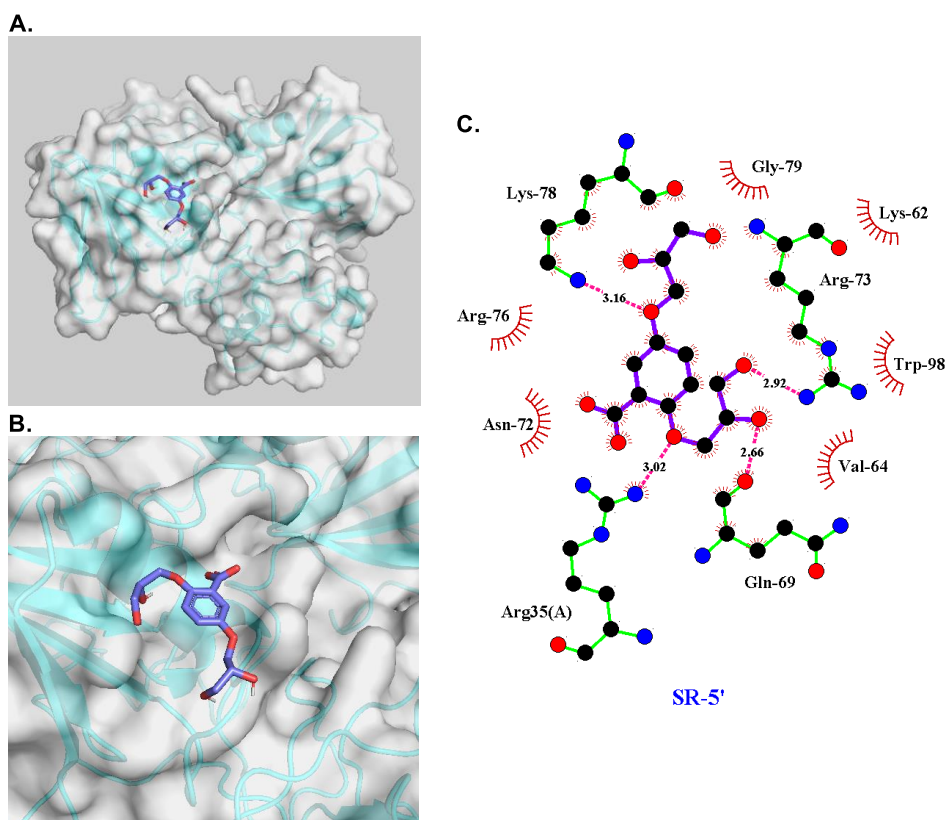
Minimum energy interaction of **RS-5**



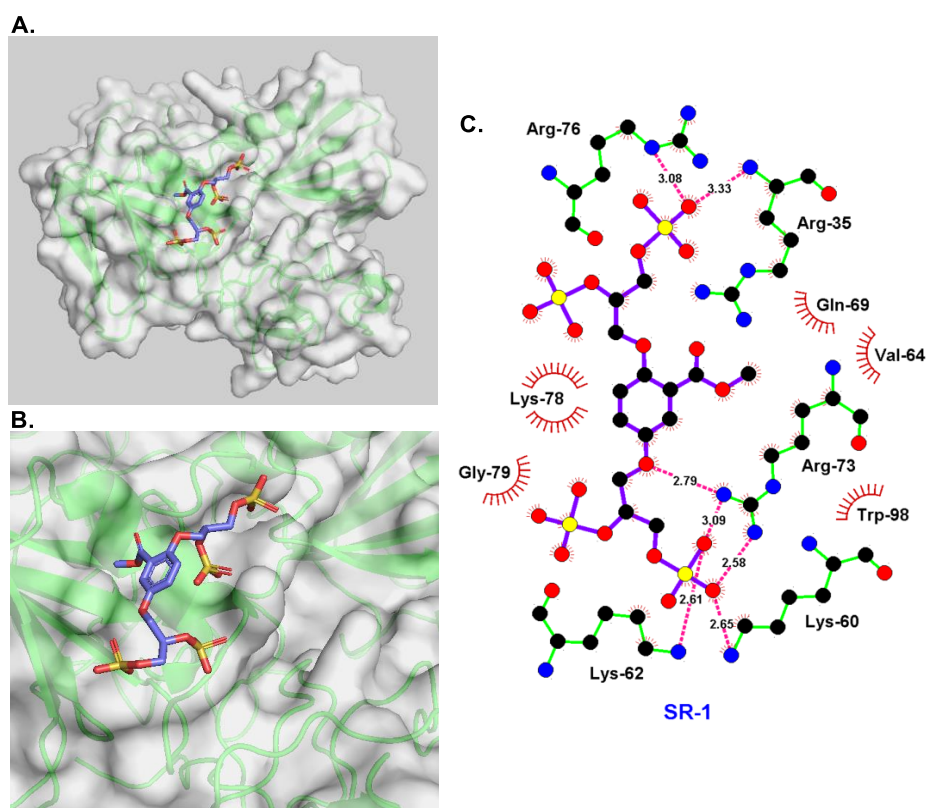
Minimum energy interaction of **RS-5'**



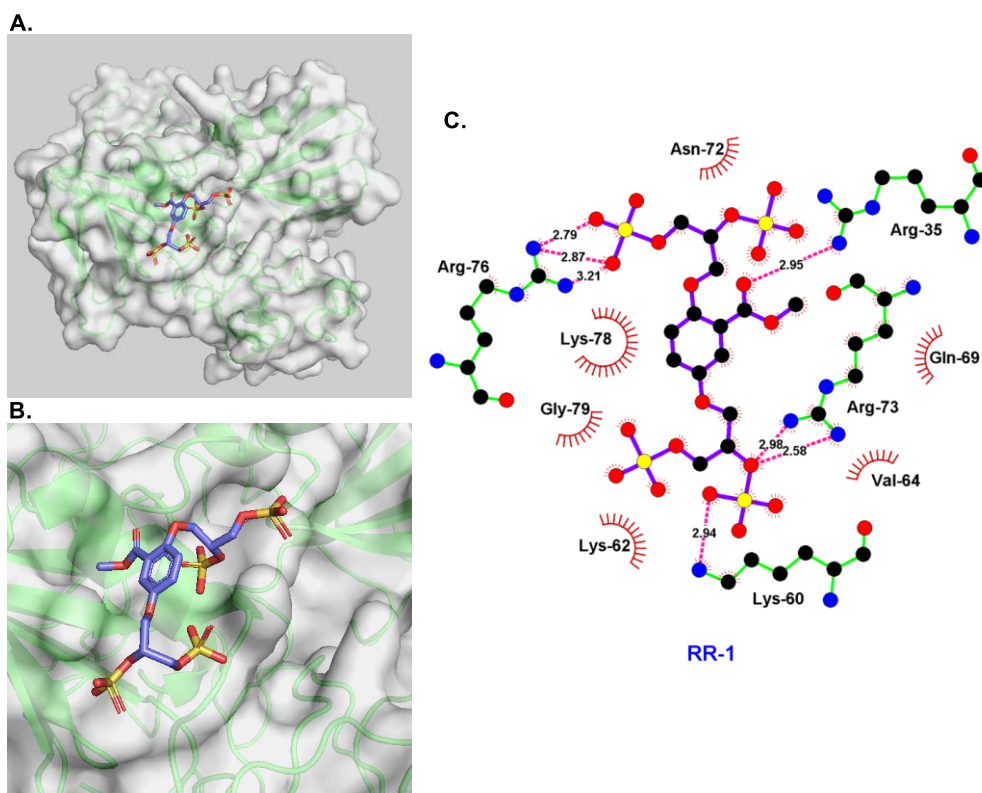
Minimum energy interaction of **SR-5'**



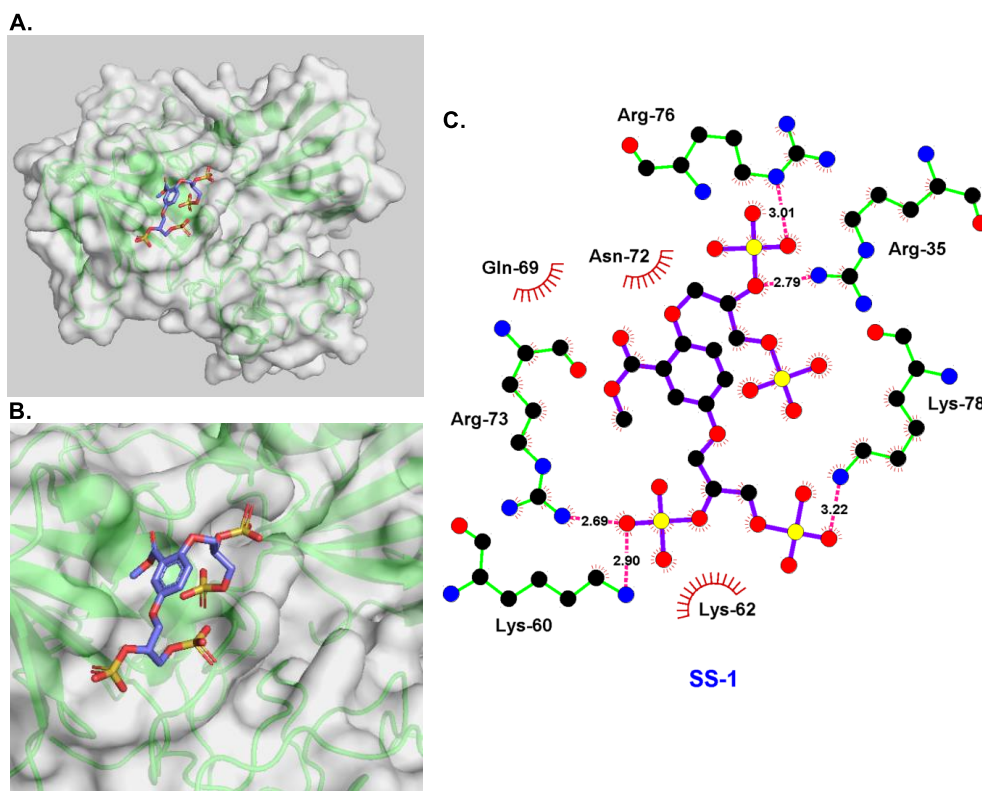
Minimum energy interaction of **SR-1**



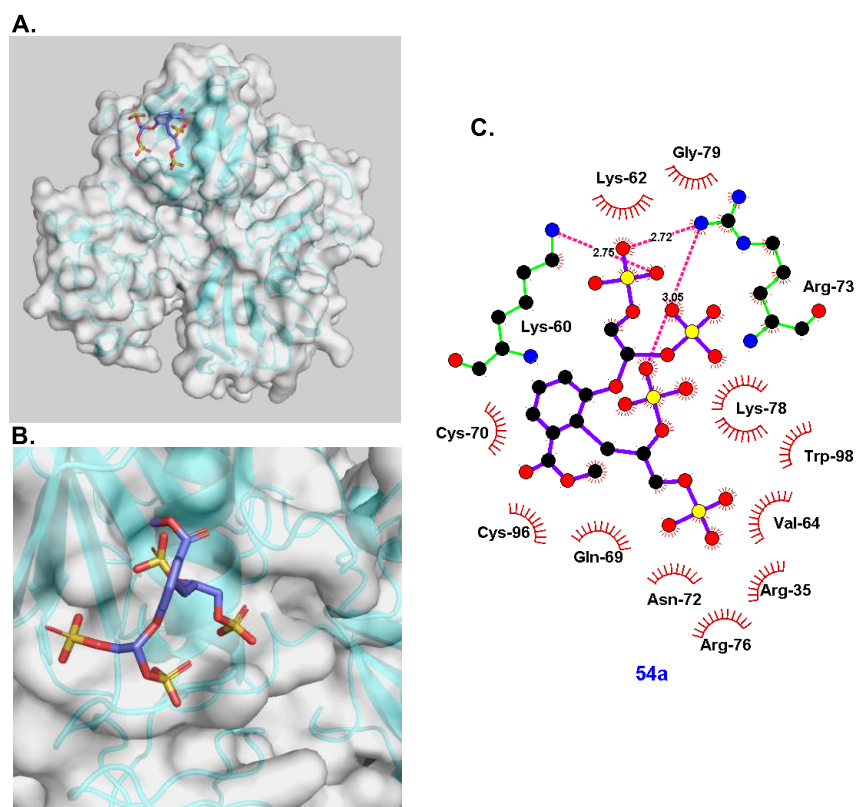
Minimum energy interaction of **RR-1**



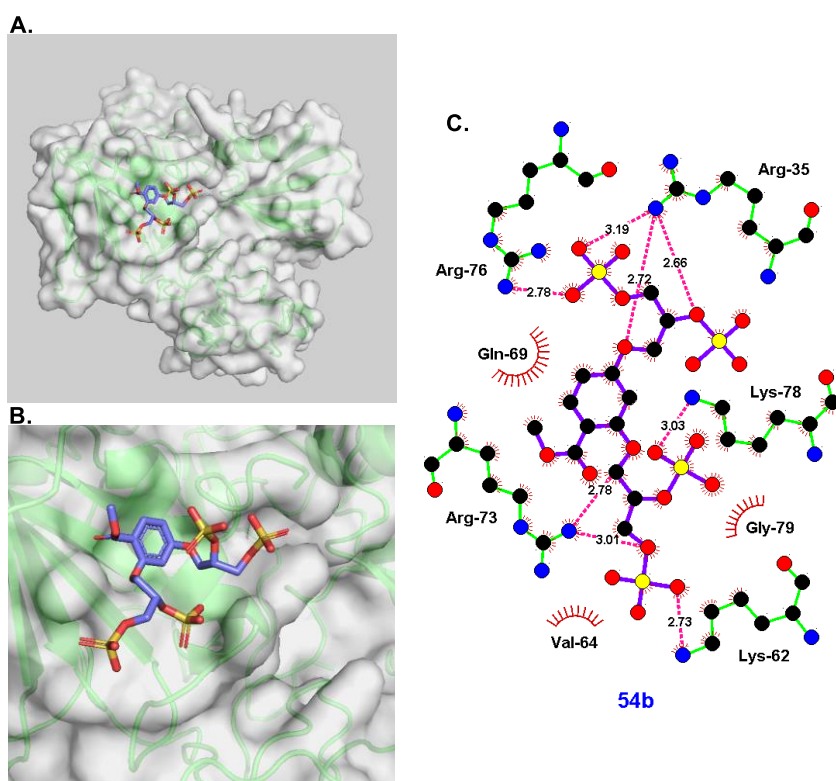
Minimum energy interaction of **SS-1**



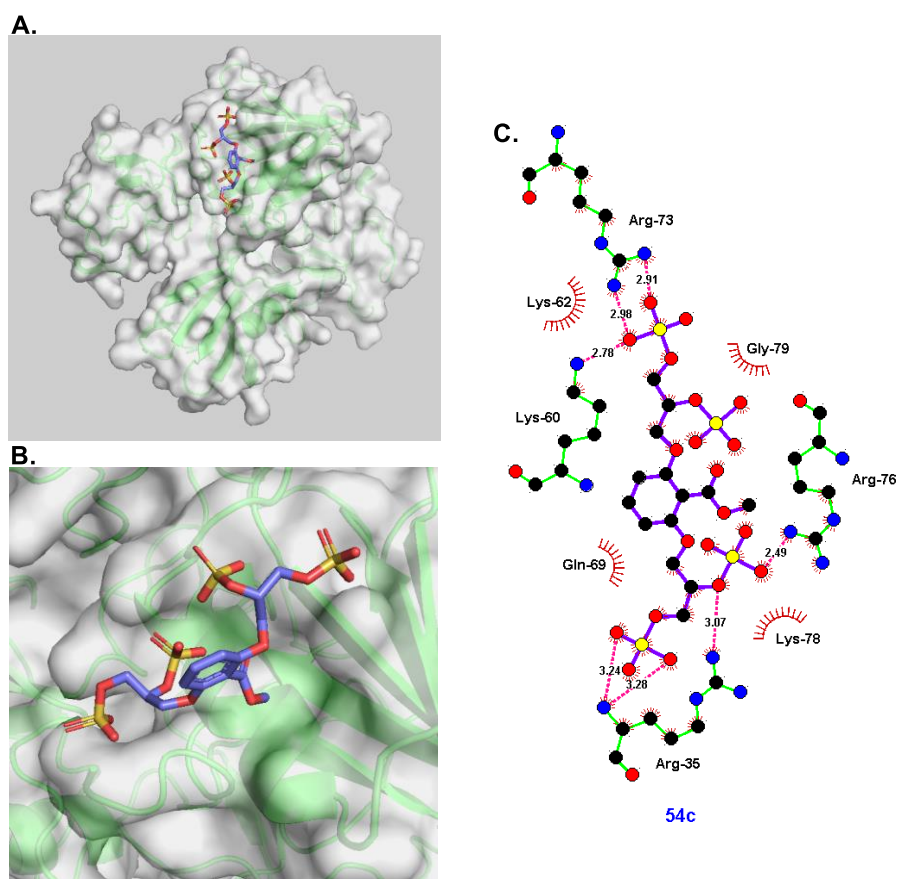
Minimum energy interaction of **54a**



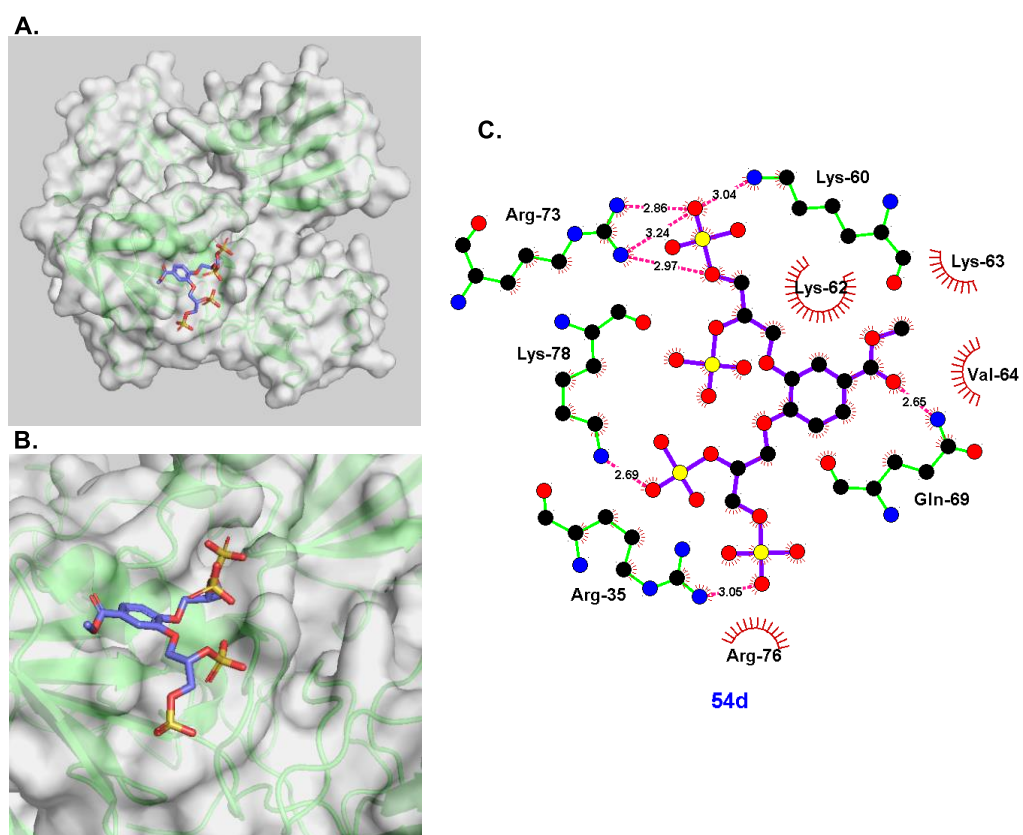
Minimum energy interaction of **54b**



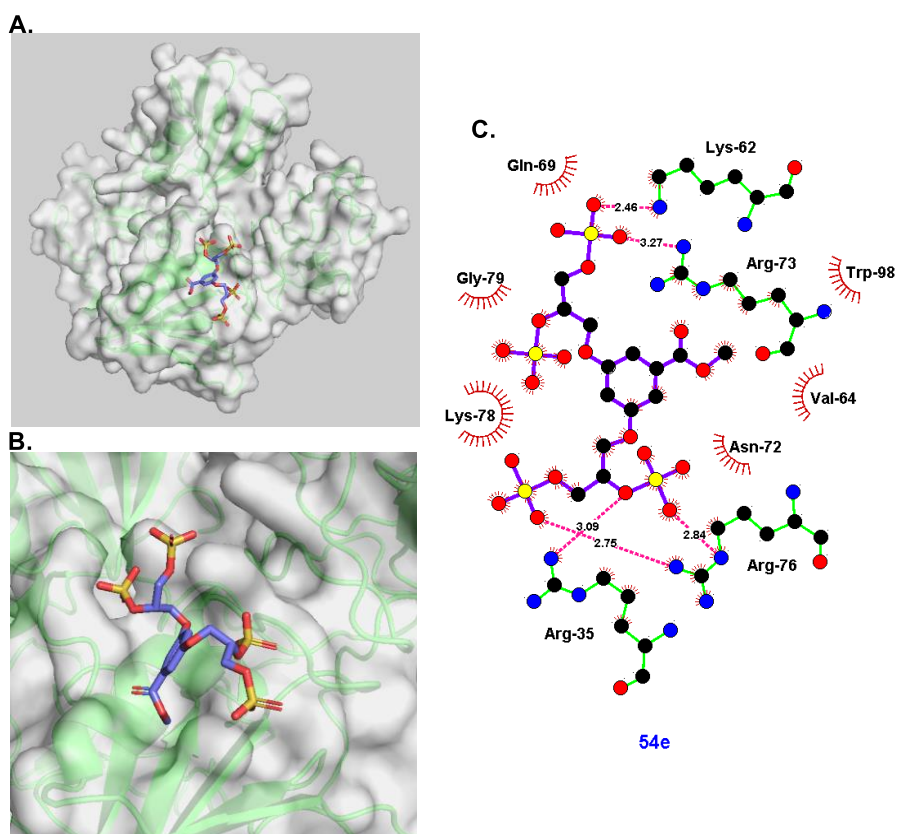
Minimum energy interaction of **54c**



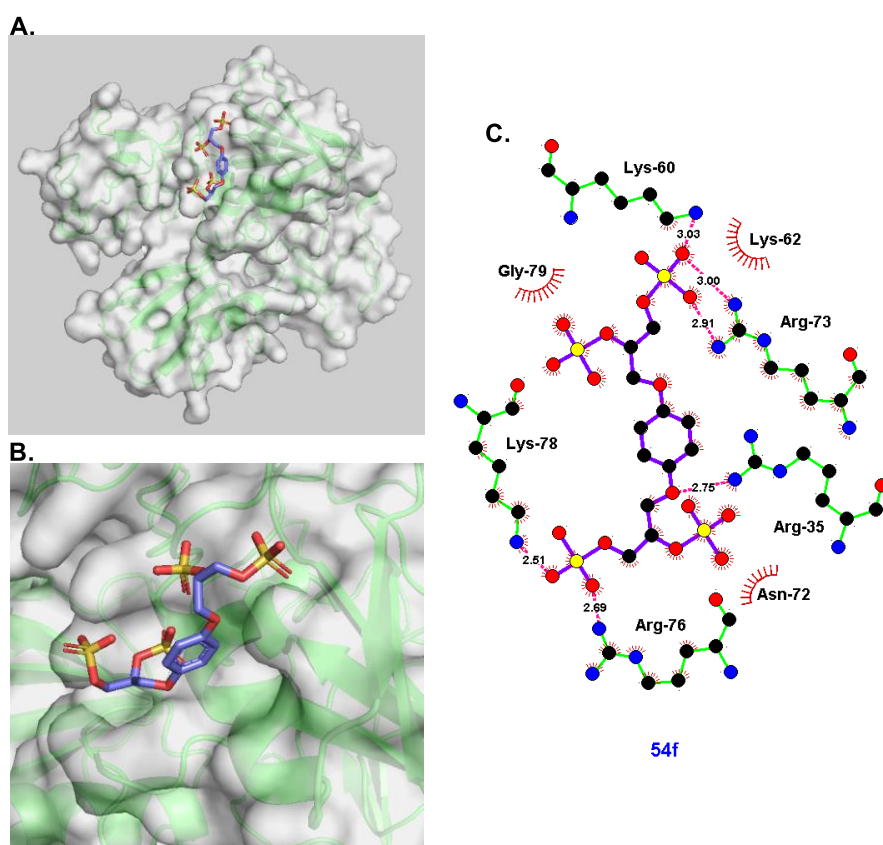
Minimum energy interaction of **54d**



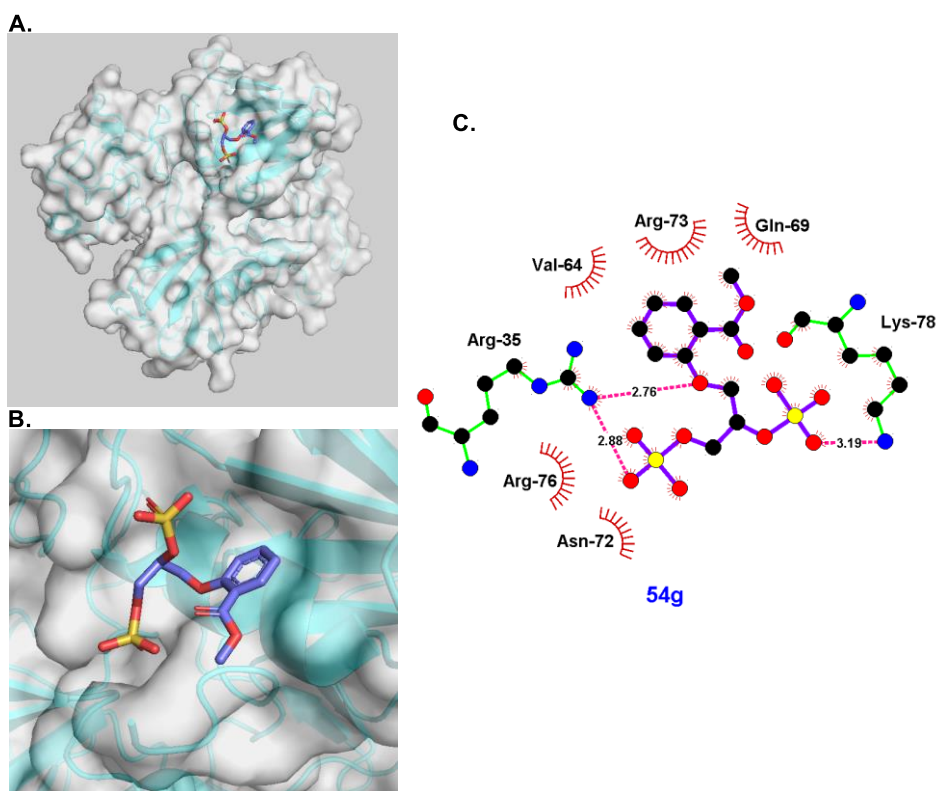
Minimum energy interaction of **54e**



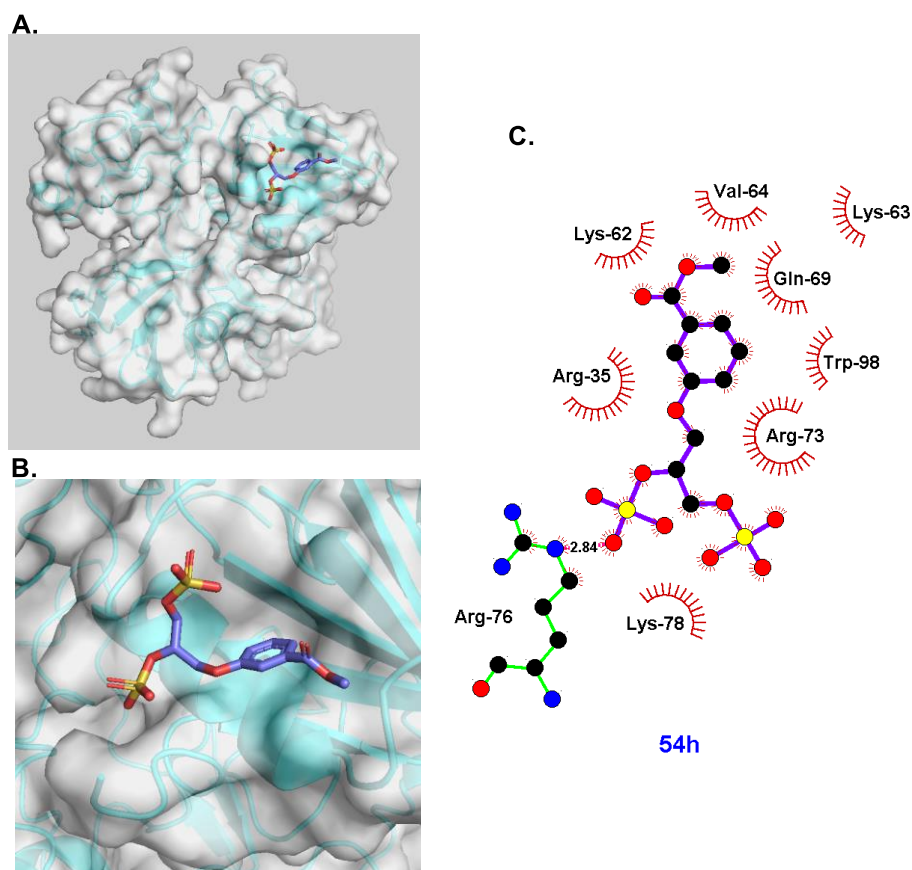
Minimum energy interaction of **54e**



Minimum energy interaction of **54g**



Minimum energy interaction of **54h**



6.8. Biological assays

All biological assays were carried out by Dr A. M. Mahmoud (Department of endocrinology, diabetes and nutrition, center for cardiovascular research, Charité - Universitätsmedizin Berlin, Berlin, Germany).

6.8.1. Cell Viability Assessment (MTT)

HepG2 human hepatocellular carcinoma cells were plated on 96-well tissue culture polystyrene plates for 24 h prior to dosing of the cells. Test compound is diluted in DMSO and serial dilutions are made in 0.5% DMSO in growth media. Test compound at 8 concentrations in triplicate is then incubated for 72 h, and appropriate controls are simultaneously used as quality controls. One hour prior to the end of the incubation period, the cells are loaded with MTT [yellow; 3-(4,5-Dimethyl-2-thiazolyl)-2,5-diphenyl-2H-tetrazolium bromide], the plates are dried and re-solubilised using DMSO. The plates are then scanned at 570 nm. The vehicle controls are used to determine the definitions of "normal" for each parameter, then software calculates the percentage of cells that are low or high responders (depending on the biological significance of a particular readout). The vehicle control wells are then used to determine significance limits for wells that have a greater than expected fraction of low or high responders. The minimum effective concentration is determined from the lowest concentration whose mean value exceeds the significance level, provided either a clear dose-response relationship is observed, or at least two consecutive concentration points are above the significance level. AC_{50} values are also determined provided a clear dose-response relationship is observed.

6.8.2. Preparation of FFA-albumin complexes and cell treatments

To generate the in vitro model of oxidative stress, sodium palmitate was conjugated to bovine serum albumin (BSA) as outlined by Chavez and Summers,³ with modifications. Sodium palmitate (FFA) was dissolved in EtOH at 60 °C and diluted 1:100 in M199 media supplemented with 2% fatty acid-free bovine serum albumin (BSA) and incubated for 1 h at 37 °C. HepG2 cells were treated with 1 µmol/L of the synthesized HS-glycomimetics in the presence of palmitate (100 µmol/L) for 3 h or pre-treated with glycomimetics for 12 h followed by 3 h palmitate (100 µmol/L). Control cells were incubated in serum free M199 containing 2% (wt/vol) fatty acid-free BSA.

6.8.3. NO release assay and Quantification of ROS production.

NO release was determined using diaminofluorescein-2 (DAF-2).⁴ The cells were washed with PBS and incubated with *L*-arginine (100 µmol/L in PBS) for 5 min at 37 °C before incubation with DAF-2 (0.1 µmol/L) for 2 min, followed by the calcium ionophore calimycin (A23187, 1 µmol L) for 30 min. L-NAME (100 µmol/L), a nitric oxide inhibitor (NOS), was also added 20 min before the addition of *L*-arginine in some experiments to determine the involvement of NOS. DAF-2 fluorescence (arbitrary units, AU) was quantified using a microplate reader (BioTek) with excitation and emission wavelengths of 485 nm and 540 nm, respectively. The auto-fluorescence was subtracted from each value. Cells were incubated with 10 µmol/L of the fluorescent probe: 2'-7'-dichlorodihydrofluorescein diacetate (CM-H2DCFDA, Sigma) for 30 min at 37 °C, and the level of fluorescence was determined (excitation 490 nm; emission 540 nm) using a microplate reader (BioTek).

6.8.4. NADPH oxidase activity

The level of NADPH-enhanced superoxide anions ($O_2^{\bullet-}$) in HepG2 homogenates was determined by lucigenin-enhanced chemiluminescence.⁵ Following the various treatment conditions, cells were homogenized in a buffer (20 mmol/L H_2KPO_4 and 1 mmol/L EDTA supplemented with aprotinin, leuprotinin, pepstatin and PMSF). The total protein quantified using the Bicinchoninic acid (BCA) assay (Pierce Biotechnology). To 50 μ g of total protein, NADPH (100 μ mol/L) was added in a total volume of 500 μ L, with lucigenin (5 μ mol/L) and was injected automatically. Activity was determined by measuring luminescence over 200 s in a scintillation counter (Lumat LB 9507, Berthold, Germany). Basal values of NADPH oxidase activity were subtracted from the experimental values and expressed as RLU/min/ μ g protein for cells.

6.8.5. In situ quantification of ROS species

Superoxide dismutase (SOD) and catalase (CAT) activity assays, and *in situ* detection of vascular ROS content. The activity of the enzymes, SOD and CAT, was determined in cell homogenates using assay kits according to the manufacturer's instructions (Cayman; Cat No 706002 and 707002 respectively). A unit of SOD was defined as the amount of enzyme required to demonstrate 50% dismutation of superoxide radical. Similarly, a unit of CAT was defined as the amount required to form 1.0 nmol of formaldehyde per min at 25 °C.⁶

HepG2 cells were incubated in serum-free DMEM containing 2% fatty acid-free BSA (control) or palmitate conjugated BSA (100 μ mol/L) in the presence of HS-glycomimetics (1 or 10 μ mol/L) for 24 h. The cells were incubated for 30 min in Hepes-buffered solution containing 10 μ mol/L dihydroethidium (DHE), which intercalates with DNA in the presence of ROS and is detectable by fluorescence. Cells were

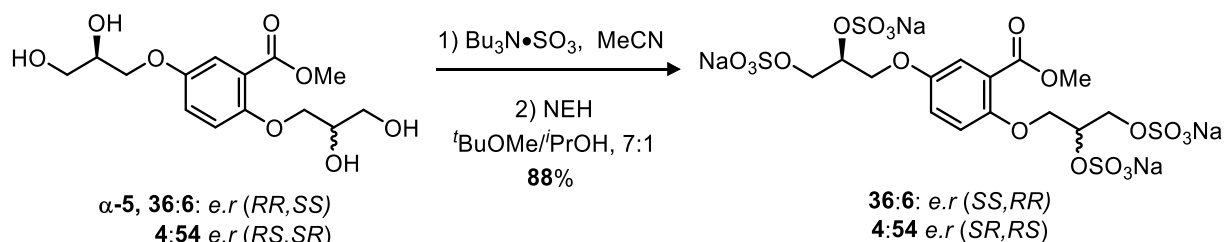
counterstained with the nuclear stain DAPI at 0.3 $\mu\text{mol/L}$. In the following 24 h, the cell cultures were examined using a fluorescence microscope (Leica DMIRB). Sections were photographed and fluorescence was quantified using ImageJ. All parameters (pinhole, contrast, gain and offset) were held constant for all sections from the same experiment. ROS production was estimated from the ratio of ethidium/DAPI fluorescence.⁷

6.8.6. Western blot analysis

HepG2 wells were lysed in RIPA buffer containing proteinase inhibitors and the total protein was quantified using BCA protein assay kit (Pierce Biotechnology). Proteins (30 $\mu\text{g/well}$) were denatured and separated by sodium dodecyl sulfate (SDS)-polyacrylamide gel electrophoresis and transferred to polyvinylidene difluoride (PVDF) membranes. Blots were blocked for 1 h in 5% semi-skimmed milk/Tris-Buffered Saline Tween-20 (TBS-T), probed with primary rabbit anti-phospho-protein kinase B (Akt), rabbit anti-Akt (Santa Cruz Biotechnology), rabbit polyclonal anti-phospho-eNOS (Cell Signaling) overnight at 4 °C followed by washing and incubation with the corresponding horse radish peroxidase-labelled secondary antibody for 1 h at room temperature. After washing with TBS-T, membranes were incubated with ECL reagent and visualized (Amersham Pharmacia Biotech). Densitometry analysis using ImageJ[®] (version 1.32j, NIH) was used to quantify the protein signal.⁸

Compound Characterisation

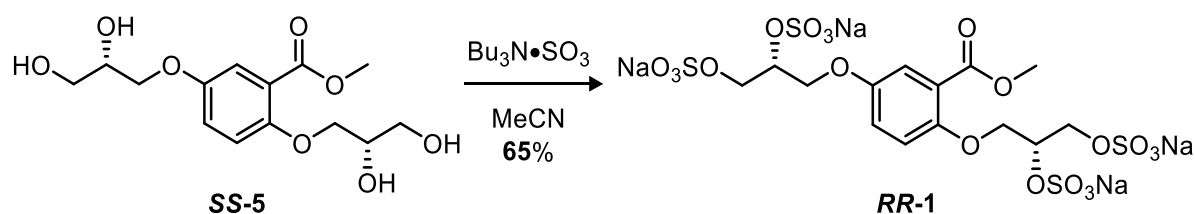
(α-1**)** Sodium 3-(4-((*S*)-2,3-bis(sulfonatooxy)propoxy)-2-(methoxycarbonyl)phenoxy)propane-1,2-diyl bis(sulfate)



Adapted from General procedure **H**: A 25 mL Schlenk tube was charged with **α-5** (81 mg, 0.25 mmol) and $\text{Bu}_3\text{N}\cdot\text{SO}_3$ (530 mg, 2.00 mmol) under Ar (g) and MeCN was added (0.5 mL). The flask was heated at 80 °C for 12 h with monitoring (TLC). The flask was cooled to room temperature and the solvent removed under reduced pressure to give a clear viscous oil. The crude oil was dissolved in $i\text{PrOH}$ (5 mL) and transferred to a flask containing $t\text{BuOMe}$ (35 mL). With vigorous stirring a solution of NEH (5.0 mL, 1.0 M) in $t\text{BuOMe}/i\text{PrOH}$ (1:7) was added dropwise over 10 min. The precipitate that formed was collected by filtration, washed with $i\text{PrOH}$ (2×10 mL) and dried under vacuum. Recrystallization from $\text{H}_2\text{O}/i\text{PrOH}$ afforded the title compound as a white solid (160 mg, 88%). [**α**]_D²⁵ −3.35 (c. 1.0, H_2O , 36:6:4:54 *e.r/d.r* (*SS,RR,SR,RS*)); **M.P** 198 – 200 °C (dec.); **IR** V_{max} cm^{-1} 2988 w, 2164 w, 1711 w (C=O), 1500 w, 1443 w, 1221 s (S=O), 1131 s (S=O); **¹H-NMR** (400 MHz, D_2O) δ_{H} 7.45 (d, J = 3.1 Hz, 1H, C6-H), 7.27 (dd, J = 9.1, 3.1 Hz, 1H, C4-H), 7.19 (d, J = 9.1 Hz, 1H, C3-H), 4.87 (td, J = 4.8,

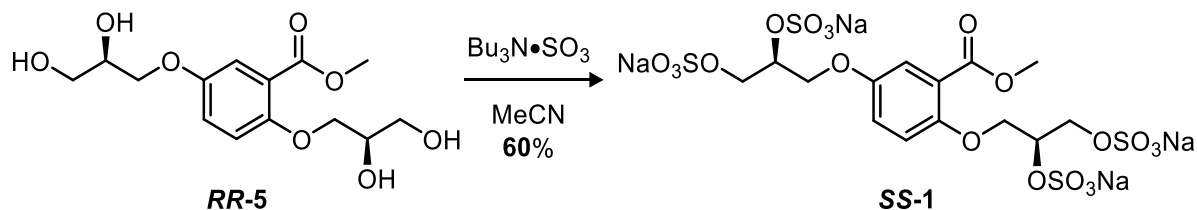
1.8 Hz, 2H, $\text{CH-OSO}_3\text{Na}$), 4.45 – 4.25 (m, 8H, Ar-OCH_2 , $\text{CH}_2\text{-OSO}_3\text{Na}$), 3.93 (s, 3H, Me); **$^{13}\text{C-NMR}$** (101 MHz, D_2O) δ 168.5 (CO_2Me), 152.2 (C2), 152.1 (C5), 121.4 (C4), 120.8 (C1), 117.4 (C6), 116.9 (C3), 75.03 ($\text{CH-OSO}_3\text{Na}$), 74.98 ($\text{CH-OSO}_3\text{Na}$), 68.2 (O-CH_2), 67.3 (O-CH_2), 66.44 ($\text{CH}_2\text{-OSO}_3\text{Na}$), 66.41 ($\text{CH}_2\text{-OSO}_3\text{Na}$), 52.8 (Me); **LRMS** m/z (ESI+) 746.86 (20%, $[\text{M}+\text{Na}]^+$); **HRMS** m/z (ESI+) $\text{C}_{14}\text{H}_{16}\text{Na}_5\text{O}_{20}\text{S}_4$ Requires: 746.8601, Found: 746.8591 ($[\text{M}+\text{Na}]^+$).

(***RR-1***) Sodium (*R*)-3-(4-((*R*)-2,3-bis(sulfonatooxy)propoxy)-2-(methoxycarbonyl)phenoxy)propane-1,2-diyl bis(sulfate)



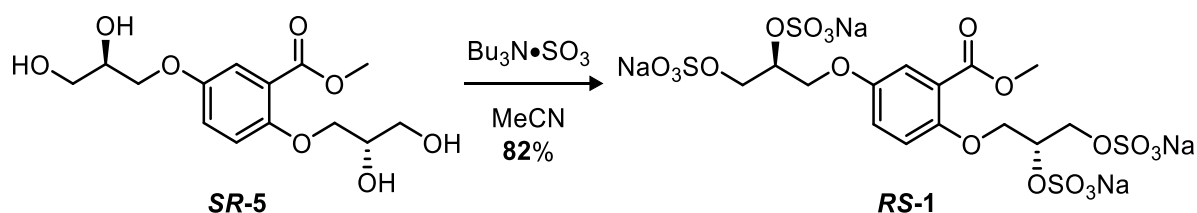
Following general procedure **H**: using ***SS-5*** (10 mg, 0.032 mmol), $\text{Bu}_3\text{N}\cdot\text{SO}_3$ (67 mg, 0.250 mmol) and work up procedure **ii** yielded the title compound as a white solid (15 mg, 65%). **IR** $V_{\text{max}} \text{ cm}^{-1}$ 2945 w, 1725 w, 1634 w, 1503 w, 1457 w, 1215 s, 1099 s; **$^1\text{H-NMR}$** (400 MHz, D_2O) δ_{H} 7.45 (d, $J = 3.2$ Hz, 1H, C6- H), 7.27 (dd, $J = 9.1, 3.2$ Hz, 1H, C4- H), 7.19 (d, $J = 9.1$ Hz, 1H, C3- H), 4.90 – 4.85 (m, 2H, $\text{CH-OSO}_3\text{Na}$), 4.52 – 4.21 (m, 8H, Ar-OCH_2 & $\text{CH}_2\text{-OSO}_3\text{Na}$), 3.93 (s, 3H, Me); **$^{13}\text{C-NMR}$** (101 MHz, D_2O) δ_{C} 168.5 (CO_2Me), 152.2 (C2), 152.1 (C5), 121.4 (C4), 120.8 (C1), 117.4 (C6), 116.9 (C3), 75.04 ($\text{CH-OSO}_3\text{Na}$), 74.99 ($\text{CH-OSO}_3\text{Na}$), 68.2 (Ar-OCH_2), 67.3 (Ar-OCH_2), 66.45 ($\text{CH}_2\text{-OSO}_3\text{Na}$), 66.42 ($\text{CH}_2\text{-OSO}_3\text{Na}$), 52.8 (Me); **LRMS** m/z (ESI+) 559.10 (100%, $[\text{M}-(\text{NaSO}_3)+\text{K}+\text{H}]^+$).

(SS-1) Sodium (*S*)-3-(4-((*S*)-2,3-bis(sulfonatooxy)propoxy)-2-(methoxycarbonyl)phenoxy)propane-1,2-diyl bis(sulfate)



Following general procedure **H**: using **RR-5** (10 mg, 0.032 mmol), $\text{Bu}_3\text{N}\cdot\text{SO}_3$ (67 mg, 0.250 mmol) and work up procedure **ii** yielded the title compound as a white solid (14 mg, 60%). **IR** $V_{\text{max}} \text{ cm}^{-1}$ 2944 w, 1725 w, 1634 w, 1505 w, 1457 w, 1210 s, 1100 s; **$^1\text{H-NMR}$** (400 MHz, D_2O) δ_{H} 7.45 (d, $J = 3.2$ Hz, 1H, C6-H), 7.27 (dd, $J = 9.1, 3.2$ Hz, 1H, C4-H), 7.19 (d, $J = 9.1$ Hz, 1H, C3-H), 4.90 – 4.85 (m, 2H, CH-OSO₃Na), 4.52 – 4.21 (m, 8H, Ar-OCH₂ & CH₂-OSO₃Na), 3.93 (s, 3H, Me); **$^{13}\text{C-NMR}$** (101 MHz, D_2O) δ_{C} 168.5 (CO₂Me), 152.2 (C2), 152.1 (C5), 121.4 (C4), 120.8 (C1), 117.4 (C6), 116.9 (C3), 75.04 (CH-OSO₃Na), 74.99 (CH-OSO₃Na), 68.2 (Ar-OCH₂), 67.3 (Ar-OCH₂), 66.45 (CH₂-OSO₃Na), 66.42 (CH₂-OSO₃Na), 52.8 (Me); **LRMS** m/z (ESI⁺) 559.10 (100%, $[\text{M}-(\text{NaSO}_3)+\text{K}+\text{H}]^+$).

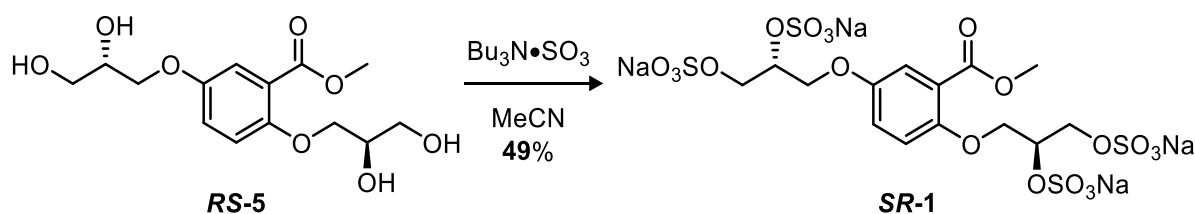
(RS-1) Sodium (*R*)-3-(4-((*S*)-2,3-bis(sulfonatooxy)propoxy)-2-(methoxycarbonyl)phenoxy)propane-1,2-diyl bis(sulfate)



Following general procedure **H**: using **SR-5** (7 mg, 0.022 mmol), $\text{Bu}_3\text{N}\cdot\text{SO}_3$ (47 mg, 0.170 mmol) and work up procedure **ii** yielded the title compound as a white solid (13 mg, 82%). **IR** $V_{\text{max}} \text{ cm}^{-1}$ 2944 w, 1726 w, 1634 w, 1503 w, 1459 w, 1215 s, 1099 s; **$^1\text{H-NMR}$** (400 MHz, D_2O) δ_{H} 7.45 (d, $J = 3.2$ Hz, 1H, C6-H), 7.27 (dd, $J = 9.1, 3.2$ Hz,

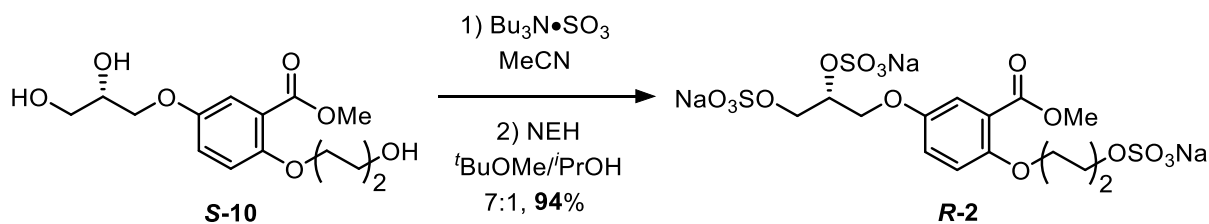
^1H , C4- $\underline{\text{H}}$), 7.19 (d, $J = 9.1$ Hz, 1H, C3- $\underline{\text{H}}$), 4.90 – 4.85 (m, 2H, $\underline{\text{CH}}$ -OSO₃Na), 4.52 – 4.21 (m, 8H, Ar-O $\underline{\text{CH}_2}$ & $\underline{\text{CH}_2}$ -OSO₃Na), 3.93 (s, 3H, Me); **^{13}C -NMR** (101 MHz, D₂O) δ_{C} 168.5 ($\underline{\text{CO}_2\text{Me}}$), 152.2 (C2), 152.1 (C5), 121.4 (C4), 120.8 (C1), 117.4 (C6), 116.9 (C3), 75.04 ($\underline{\text{CH}}$ -OSO₃Na), 74.99 ($\underline{\text{CH}}$ -OSO₃Na), 68.2 (Ar-O $\underline{\text{CH}_2}$), 67.3 (Ar-O $\underline{\text{CH}_2}$), 66.4 (2C, $\underline{\text{CH}_2}$ -OSO₃Na), 52.8 (Me); **LRMS** m/z (ESI+) 746.86 (10%, $[\text{M}+\text{Na}]^+$) 559.13 (100%, $[\text{M}-(\text{NaSO}_3)+\text{K}+\text{H}]^+$).

(**SR-1**) Sodium (*S*)-3-(4-((*R*)-2,3-bis(sulfonatooxy)propoxy)-2-(methoxycarbonyl)phenoxy)propane-1,2-diyl bis(sulfate)



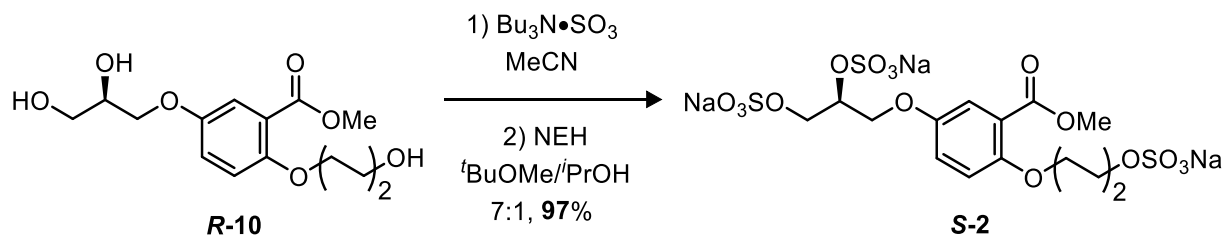
Following general procedure **H**: using **RS-5** (9 mg, 0.028 mmol), Bu₃N•SO₃ (60 mg, 0.227 mmol) and work up procedure **ii** yielded the title compound as a white solid (10 mg, 49%). **IR** V_{max} cm⁻¹ 2945 w, 1725 w, 1637 w, 1503 w, 1454 w, 1215 s, 1101 s; **^1H -NMR** (400 MHz, D₂O) δ_{H} 7.45 (d, $J = 3.2$ Hz, 1H, C6- $\underline{\text{H}}$), 7.27 (dd, $J = 9.1, 3.2$ Hz, 1H, C4- $\underline{\text{H}}$), 7.19 (d, $J = 9.1$ Hz, 1H, C3- $\underline{\text{H}}$), 4.90 – 4.85 (m, 2H, $\underline{\text{CH}}$ -OSO₃Na), 4.52 – 4.21 (m, 8H, Ar-O $\underline{\text{CH}_2}$ & $\underline{\text{CH}_2}$ -OSO₃Na), 3.93 (s, 3H, Me); **^{13}C -NMR** (101 MHz, D₂O) δ_{C} 168.5 ($\underline{\text{CO}_2\text{Me}}$), 152.2 (C2), 152.1 (C5), 121.4 (C4), 120.8 (C1), 117.4 (C6), 116.9 (C3), 75.04 ($\underline{\text{CH}}$ -OSO₃Na), 74.99 ($\underline{\text{CH}}$ -OSO₃Na), 68.2 (Ar-O $\underline{\text{CH}_2}$), 67.3 (Ar-O $\underline{\text{CH}_2}$), 66.45 ($\underline{\text{CH}_2}$ -OSO₃Na), 66.42 ($\underline{\text{CH}_2}$ -OSO₃Na), 52.8 (Me); **LRMS** m/z (ESI+) 559.10 (100%, $[\text{M}-(\text{NaSO}_3)+\text{K}+\text{H}]^+$).

(R-2) Sodium (*R*)-3-(3-(methoxycarbonyl)-4-(4-(sulfonatooxy)butoxy)phenoxy)propane-1,2-diyl bis(sulfate)



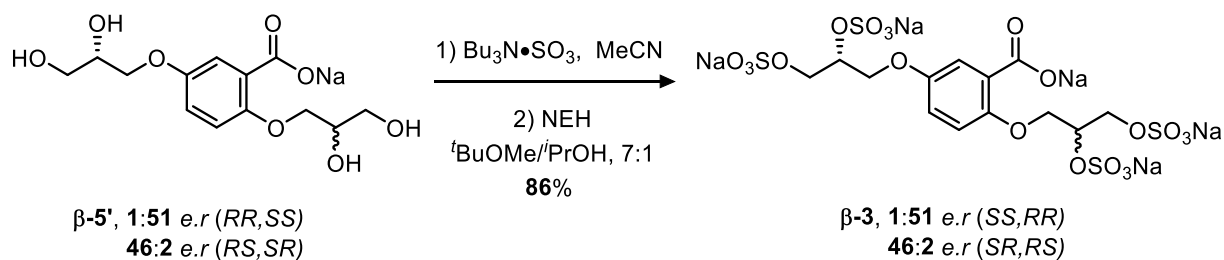
Adapted from General procedure **H**: A 25 mL Schlenk tube was charged with **S-10** (135 mg, 0.45 mmol) and $\text{Bu}_3\text{N}\bullet\text{SO}_3$ (722 mg, 2.72 mmol) under $\text{Ar}_{(\text{g})}$ and MeCN was added (1.5 mL). The flask was heated at 80 °C for 12 h with monitoring (TLC). The flask was cooled to room temperature and the solvent removed under reduced pressure to give a clear viscous oil. The crude oil was dissolved in $i\text{PrOH}$ (5 mL) and transferred to a flask containing $t\text{BuOMe}$ (35 mL). With vigorous stirring a solution of NEH (5.0 mL, 1.0 M) in $t\text{BuOMe}/i\text{PrOH}$ (1:7) was added dropwise over 10 min. The precipitate that formed was collected by filtration, washed with $i\text{PrOH}$ (2×10 mL) and dried under vacuum. Recrystallization from $\text{H}_2\text{O}/i\text{PrOH}$ afforded the title compound as a white solid (260 mg, 94%). **[α]_D²⁵** –3.11 (c. 1.0, CHCl_3); **M.P** 207 – 210 °C (dec.); **IR** V_{max} cm^{-1} 2972 w, 2166 w, 1703 w (C=O), 1500 w, 1441 w, 1103 s (S=O); **¹H-NMR** (400 MHz, D_2O) δ_{H} 7.42 (d, $J = 3.2$ Hz, 1H, C6-H), 7.25 (dd, $J = 9.2, 3.2$ Hz, 1H, C4-H), 7.14 (d, $J = 9.2$ Hz, 1H, C3-H), 4.86 (p, $J = 4.8$ Hz, 1H, CH-OSO₃Na), 4.42 – 4.29 (m, 3H), 4.26 (dd, $J = 11.0, 5.2$ Hz, 1H), 4.16 – 4.05 (m, 4H), 3.90 (s, 3H, Me), 1.86 (m, 4H, (CH₂)₂); **¹³C-NMR** (101 MHz, D_2O) δ_{C} 168.4 (CQ₂Me), 152.6 (C2), 151.7 (C5), 121.6 (C4), 120.1 (C1), 117.3 (C6), 116.4 (C3), 75.0 (CH-OSO₃Na), 69.7, 69.0, 67.3, 66.4, 52.7 (Me), 25.2 ((CH₂)₂), 24.9 ((CH₂)₂); **LRMS** m/z (ESI+) 642.94 (40%, $[\text{M}+\text{Na}]^+$); **HRMS** m/z (ESI+) $\text{C}_{15}\text{H}_{19}\text{Na}_4\text{O}_{16}\text{S}_3$ Requires: 642.9421, Found: 642.9426 ($[\text{M}+\text{Na}]^+$).

(**S-2**) Sodium (*S*)-3-(3-(methoxycarbonyl)-4-(4-(sulfonatooxy)butoxy)phenoxy)propane-1,2-diyl bis(sulfate)

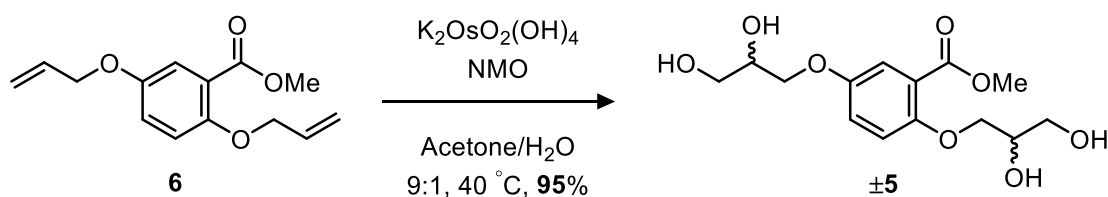


Adapted from General procedure **H**: a 25 mL Schlenk tube was charged with **R-10** (215 mg, 0.72 mmol) and $\text{Bu}_3\text{N}\cdot\text{SO}_3$ (1.145 g, 2.56 mmol) under $\text{Ar}_{(\text{g})}$ and MeCN was added (1.5 mL). The flask was heated at 80 °C for 12 h with monitoring (TLC). The flask was cooled to room temperature and the solvent removed under reduced pressure to give a clear viscous oil. The crude oil was dissolved in PrOH (5 mL) and transferred to a flask containing tBuOMe (35 mL). With vigorous stirring a solution of NEH (5.0 mL, 1.0 M) in tBuOMe/PrOH (1:7) was added dropwise over 10 min. The precipitate that formed was collected by filtration, washed with PrOH (2×10 mL) and dried under vacuum. Recrystallization from $\text{H}_2\text{O/PrOH}$ afforded the title compound as a white solid (430 mg, 97%). **[α]_D²⁵** +3.01 (c. 1.0, H_2O); **M.P** 207 – 210 °C (dec.); **IR** V_{max} cm^{-1} 2971 w, 2164 w, 1710 w (C=O), 1500 w, 1441 w, 1103 s (S=O); **¹H-NMR** (400 MHz, D_2O) δ_{H} 7.43 (d, J = 3.2 Hz, 1H, C6-H), 7.25 (dd, J = 9.2, 3.2 Hz, 1H, C4-H), 7.14 (d, J = 9.2 Hz, 1H, C3-H), 4.87 (p, J = 4.7 Hz, 1H, CH-OSO₃Na), 4.44 – 4.29 (m, 3H), 4.26 (dd, J = 11.0, 5.2 Hz, 1H), 4.12 (m, 4H), 3.90 (s, 3H, Me), 1.94 – 1.79 (m, 4H, (CH₂)₂); **¹³C-NMR** (101 MHz, D_2O) δ_{C} 168.4 (CO₂Me), 152.6 (C2), 151.7 (C5), 121.6 (C4), 120.1 (C1), 117.3 (C6), 116.4 (C3), 75.0 (CH-OSO₃Na), 69.7, 69.0, 67.4, 66.4, 52.7 (Me), 25.2 ((CH₂)₂), 24.9 ((CH₂)₂); **LRMS** m/z (ESI+) 642.94 (50%, [M+Na]⁺); **HRMS** m/z (ESI+) C₁₅H₁₉Na₄O₁₆S₃ Requires: 642.9421, Found: 642.9417 ([M+Na]⁺).

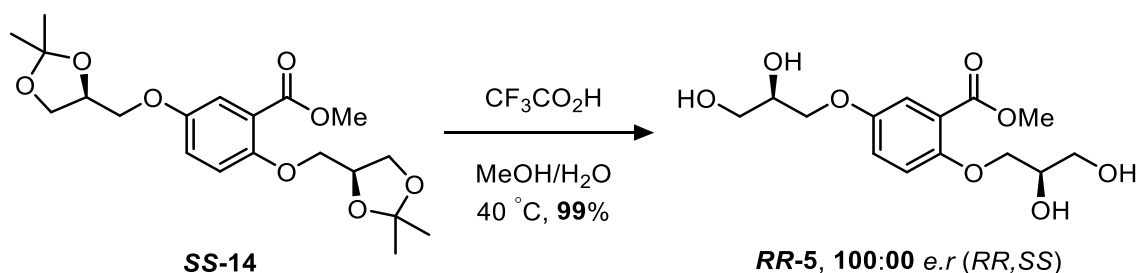
(β -3) Sodium 5-((*R*)-2,3-bis(sulfonatooxy)propoxy)-2-(2,3-bis(sulfonatooxy)propoxy)benzoate



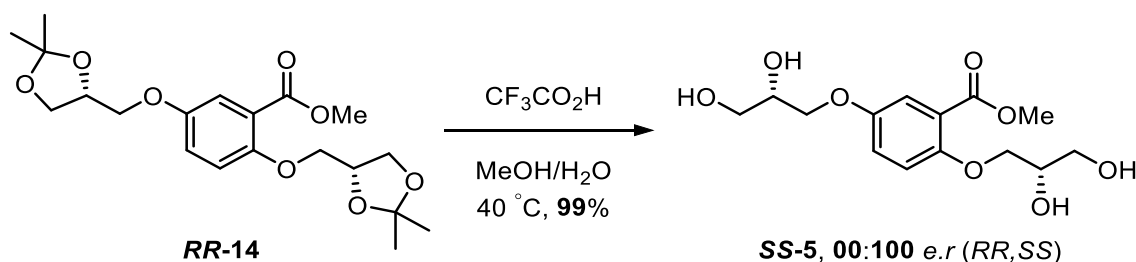
Adapted from General procedure **H**: A 25 mL Schlenk tube was charged with **β -5'** (100 mg, 0.32 mmol) and $\text{Bu}_3\text{N}\cdot\text{SO}_3$ (678 mg, 2.56 mmol) under Ar (g) and MeCN was added (0.6 mL). The flask was heated at 80 °C for 12 h and with monitoring (TLC). The flask was cooled to room temperature and the solvent removed under reduced pressure to give a clear viscous oil. The crude oil was dissolved in $i\text{PrOH}$ (5 mL) and transferred to a flask containing $^t\text{BuOMe}$ (35 mL). With vigorous stirring a solution of NEH (5.0 mL, 1.0 M) in $^t\text{BuOMe}/i\text{PrOH}$ (1:7) was added dropwise over 10 min. The precipitate that formed was collected by filtration, washed with $i\text{PrOH}$ (2×10 mL) and dried under vacuum. Recrystallization from $\text{H}_2\text{O}/i\text{PrOH}$ afforded the title compound as a white solid (200 mg, 86%). [α]_D²⁵ –1.66 (c. 1.0, H_2O , 1:51:46:2 *e.r/d.r* (*SS*,*RR*,*SR*,*RS*)); **M.P** 200 – 202 °C (dec.); **IR** V_{max} cm^{-1} 2988 w, 1712 w (C=O), 1499 w, 1435 w, 1100 s (S=O); **$^1\text{H-NMR}$** (400 MHz, D_2O) δ 7.47 – 6.94 (m, 3H), 5.00 – 4.73 (m, 2H), 4.46 – 3.99 (m, 8H); **$^{13}\text{C-NMR}$** (101 MHz, D_2O) δ 169.6 (CO_2Na), 152.3 (C-O), 151.8 (C-O), 121.5 ($\text{C-CO}_2\text{Na}$), 120.7 (C-H), 117.4 (C-H), 116.2 (C-H), 75.0 (C-H), 74.9 (C-H), 68.3 (C-H_2), 67.3 (C-H_2), 66.6 (C-H_2), 66.4 (C-H_2); **LRMS** m/z (ESI+) 732.84 (10%, $[\text{M}+\text{H}]^+$); **HRMS** m/z (ESI+) $\text{C}_{13}\text{H}_{14}\text{Na}_5\text{O}_{20}\text{S}_4$ Requires: 732.8444, Found: 732.8439 ($[\text{M}+\text{H}]^+$).

(±5) Methyl 2,5-bis(2,3-dihydroxypropoxy)benzoate

Following general procedure **C**: NMO (140 mg, 1.20 mmol) was charged with acetone/H₂O (9:1, 10 mL) and K₂OsO₂(OH)₄ (3.7 mg, 0.01 mmol). 2,5-bis(allyloxy)benzoate (**6**) (124 mg, 0.50 mmol) was added and the reaction mixture was heated at 40 °C for 12 h and monitored (TLC, EtOH/EtOAc 1:4, *R_f* = 0.20). The solvent was removed under reduced pressure and the crude mixture purified directly by chromatography (SiO₂, EtOH/EtOAc 1:4, *R_f* = 0.21) to yield the title compound as a clear viscous oil (150 mg, 95%, 4.4% MeOH from ¹H-NMR data). **IR** *V*_{max} cm⁻¹ 3340 br s (O-H), 2937 w, 1701 s (C=O), 1609 s, 1456 s, **¹H-NMR** (400 MHz, (CD₃)₂SO) δ_H 7.18 (d, *J* = 2.7 Hz, 1H, C6-H), 7.14 – 7.06 (m, 2H, C3-H & C4-H), 4.90 (br d, 2H, CH-OH), 4.66 (br s, 2H, CH₂-OH), 3.99 – 3.93 (m, 2H), 3.90 (dd, *J* = 9.7, 5.4 Hz, 1H), 3.86 – 3.79 (m, 1H), 3.79 (s, 4H, Me), 3.55 – 3.40 (m, 4H); **¹³C-NMR** (101 MHz, (CD₃)₂SO) δ_C 166.0 (C=O), 152.2 (C5), 152.0 (C2), 121.0 (C1), 119.8 (C3/C4), 115.9 (C3/C4), 115.9 (C6), 71.3 (ArO-CH₂), 70.3 (ArO-CH₂), 69.9 (2C, CH-OH), 62.7 (CH₂-OH), 62.7 (CH₂-OH), 52.0 (Me); **LRMS** (ESI+) 339.10 (100%, [M+Na]⁺), 317.10 (50%, [M+H]⁺); **HRMS** (ESI+) C₁₄H₂₁O₈ Requires: 317.1231, Found: 317.1229 ([M+H]⁺).

(RR-5) Methyl 2,5-bis((*R*)-2,3-dihydroxypropoxy)benzoate

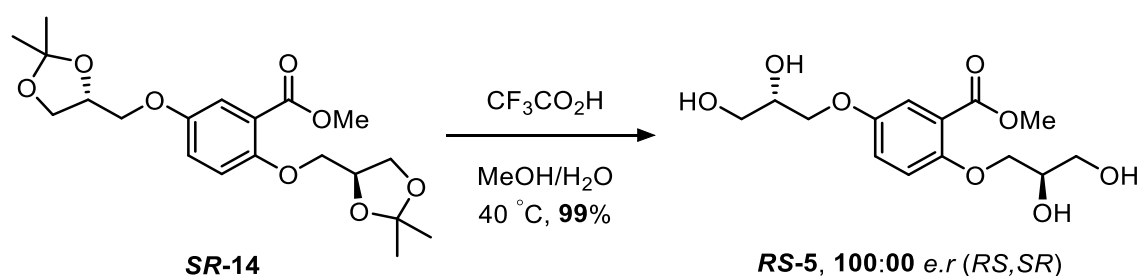
Following general procedure **F**: Methyl 2,5-bis(((*S*)-2,2-dimethyl-1,3-dioxolan-4-yl)methoxy)benzoate (**SS-14**) (30 mg, 70 μ mol) was stirred at 40 °C for 5 h. Afforded the title compound as a clear oil (22 mg, 99%). [α]_D²⁵ –16.96 (c. 1.0, MeOH, 100:00 *e.r* (2*R*5*R*, 2*S*5*S*)); **IR** V_{\max} cm^{–1} 3309 br s (O-H) 2951 w, 2885 w, 1673 s (C=O), 1499 w, 1438 w; **¹H-NMR** (400 MHz, CD₃OD) δ_{H} 7.35 (d, J = 3.1 Hz, 1H, C6-H), 7.15 (dd, J = 9.1, 3.1 Hz, 1H, C4-H), 7.09 (d, J = 9.1 Hz, 1H, C3-H), 4.13 – 3.99 (m, 3H), 3.99 – 3.89 (m, 3H), 3.88 (s, 3H, Me), 3.78 – 3.59 (m, 4H); **¹³C-NMR** (101 MHz, CD₃OD) δ_{C} 168.3 (CO₂Me), 154.3, 154.2, 121.9, 121.5, 117.8, 117.2, 72.8, 71.7, 71.5, 71.1, 64.2, 64.0, 52.7 (Me); **LRMS** m/z (ESI+) 339.11 (100%, [M+Na]⁺); **HRMS** m/z (ESI+) C₁₄H₂₀O₈Na Requires: 339.1056, Found: 339.1053 ([M+Na]⁺).

(SS-5) Methyl 2,5-bis((*S*)-2,3-dihydroxypropoxy)benzoate

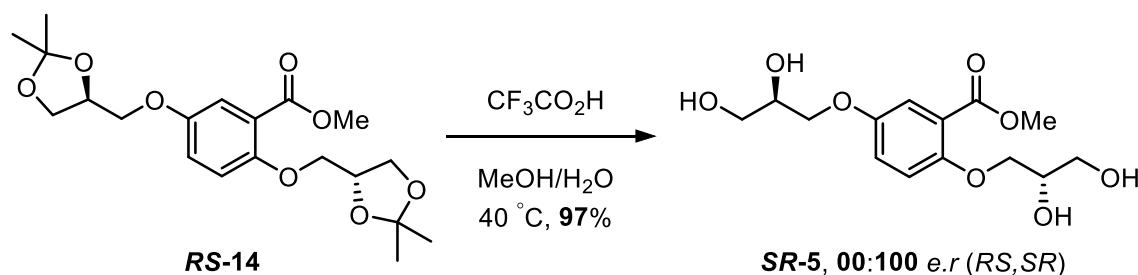
Following general procedure **F**: Methyl 2,5-bis(((*R*)-2,2-dimethyl-1,3-dioxolan-4-yl)methoxy)benzoate (**RR-14**) (30 mg, 70 μ mol) was stirred at 40 °C for 5 h. Afforded the title compound as a clear oil (22 mg, 99%). [α]_D²⁵ +13.69 (c. 1.0, MeOH, 00:100 *e.r* (2*R*5*R*, 2*S*5*S*)); **IR** V_{\max} cm^{–1} 3286 br s (O-H), 2950 w, 2882 w, 1674 s, 1500 w,

1439 w; **¹H-NMR** (400 MHz, CD₃OD) δ_{H} 7.35 (d, J = 3.1 Hz, 1H, C6-H), 7.15 (dd, J = 9.1, 3.1 Hz, 1H, C4-H), 7.09 (d, J = 9.1 Hz, 1H, C3-H), 4.13 – 3.99 (m, 3H), 3.99 – 3.89 (m, 3H), 3.87 (s, 3H, Me), 3.78 – 3.59 (m, 4H); **¹³C-NMR** (101 MHz, CD₃OD) δ_{C} 168.3 (CO₂Me), 154.3, 154.2, 121.9, 121.5, 117.8, 117.2, 72.8, 71.7, 71.5, 71.1, 64.2, 64.1, 52.7 (Me); **LRMS** m/z (ESI+) 339.11 (100%, [M+Na]⁺); **HRMS** m/z (ESI+) C₁₄H₂₀O₈Na Requires: 339.1056, Found: 339.1056 ([M+Na]⁺).

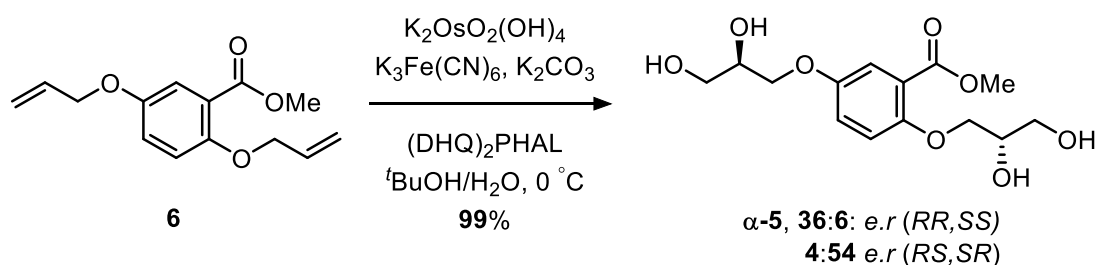
(**RS-5**) Methyl 2-((*R*)-2,3-dihydroxypropoxy)-5-((*S*)-2,3-dihydroxypropoxy)benzoate



Following general procedure **F**: Methyl 5-(((*R*)-2,2-dimethyl-1,3-dioxolan-4-yl)methoxy)-2-(((*S*)-2,2-dimethyl-1,3-dioxolan-4-yl)methoxy)benzoate (**SR-14**) (30 mg, 70 μ mol) was stirred at 40 °C for 5 h. Afforded the title compound as a clear oil (22 mg, 99%). **[α]_D²⁵** +1.39 (c. 1.0, MeOH, 100:00 *d.r* (2*R*5*S*, 2*S*5*R*)); **IR** ν_{max} cm⁻¹ 3264 br s (O-H), 2943 w, 2891 w, 1731 s, 1699 s, 1499 s, 1436 s; **¹H-NMR** (400 MHz, CD₃OD) δ_{H} 7.35 (d, J = 3.1 Hz, 1H, C6-H), 7.15 (dd, J = 9.1, 3.1 Hz, 1H, C4-H), 7.09 (d, J = 9.1 Hz, 1H, C3-H), 4.13 – 3.99 (m, 3H), 3.99 – 3.89 (m, 3H), 3.87 (s, 3H, Me), 3.78 – 3.59 (m, 4H); **¹³C-NMR** (101 MHz, CD₃OD) δ_{C} 168.2 (CO₂Me), 154.3, 154.2, 122.0, 121.5, 117.8, 117.2, 72.8, 71.7, 71.6, 71.1, 64.3, 64.1, 52.7 (Me); **LRMS** m/z (ESI+) 339.11 (100%, [M+Na]⁺); **HRMS** m/z (ESI+) C₁₄H₂₀O₈Na Requires: 339.1056, Found: 339.1057 ([M+Na]⁺).

(SR-5) Methyl 2-(((*S*)-2,3-dihydroxypropoxy)-5-(((*R*)-2,3-dihydroxypropoxy)benzoate

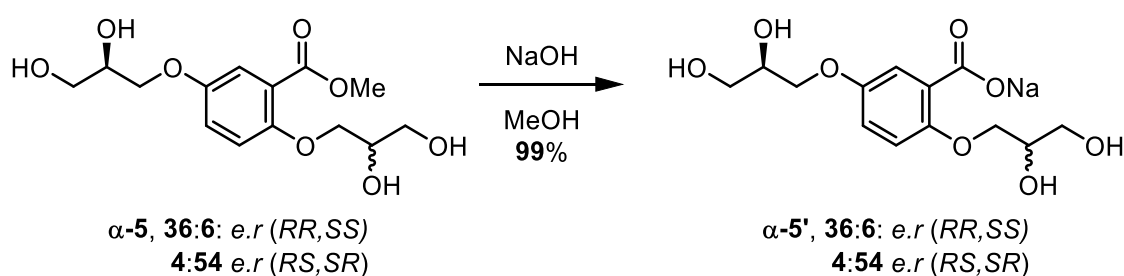
Following general procedure **F**: Methyl 2-(((*R*)-2,2-dimethyl-1,3-dioxolan-4-yl)methoxy)-5-(((*S*)-2,2-dimethyl-1,3-dioxolan-4-yl)methoxy)benzoate (**RS-14**) (30 mg, 70 μ mol) was stirred at 40 °C for 5 h. Afforded the title compound as a clear oil (21 mg, 97%). **[α]_D²⁵** –1.73 (c. 1.0, MeOH, 00:100 *d.r* (2*R*5*S*, 2*S*5*R*)); **IR** V_{\max} cm^{–1} 3254 br s (O–H) 2940 w, 2894 w, 1729 s, 1699 s, 1500 s, 1436 s; **¹H-NMR** (400 MHz, CD₃OD) δ_{H} 7.35 (d, J = 3.1 Hz, 1H, C6–H), 7.15 (dd, J = 9.1, 3.1 Hz, 1H, C4–H), 7.09 (d, J = 9.1 Hz, 1H, C3–H), 4.13 – 3.99 (m, 3H), 3.99 – 3.89 (m, 3H), 3.87 (s, 3H, Me), 3.78 – 3.59 (m, 4H); **¹³C-NMR** (101 MHz, CD₃OD) δ_{C} 168.2 (CO₂Me), 154.3, 154.2, 122.0, 121.5, 117.8, 117.2, 72.8, 71.8, 71.6, 71.1, 64.3, 64.2, 52.7 (Me); **LRMS** m/z (ESI+) 339.11 (100%, [M+Na]⁺); **HRMS** m/z (ESI+) C₁₄H₂₀O₈Na Requires: 339.1056, Found: 339.1058 ([M+Na]⁺).

(α -5) Methyl 5-(((*R*)-2,3-dihydroxypropoxy)-2-(((*S*)-2,3-dihydroxypropoxy)benzoate

Adapted from general procedure **D** using stock solutions: **I** (2 mL, 3.0 mmol), **II** (2 mL, 3.0 mmol), **III** (1.0 mL, 2.0 μ mol) and **IV** (5.0 mL, 20.0 μ mol). Methyl 2,5-bis(allyloxy)benzoate (**6**) (158 mg, 0.50 mmol) was added and the reaction mixture

was stirred at 0 °C for 6 h with monitoring (EtOH/EtOAc 1:4, R_f = 0.20). The solvent was removed under reduced pressure and the crude mixture was directly purified by chromatography (SiO₂, EtOAc/hexane 1:4) to afford the title compound as a clear oil (156 mg, 99%). **[α]_D²⁵** –13.15 (c. 1.0, MeOH, 36:6:4:54 *e.r/d.r* (2*R*5*R*, 2*S*5*S*, 2*R*5*S*, 2*S*5*R*)); **IR** V_{\max} cm^{–1} 3268 w, 2939 w, 2890 w, 1699 s (C=O), 1601 w, 1499 s, 1435 w; **¹H-NMR** (400 MHz, (CD₃)₂SO) δ_H 7.18 (d, J = 2.7 Hz, 1H, C6-H), 7.15 – 7.04 (m, 2H, C3-H & C4-H), 4.94 (d, J = 5.0 Hz, 1H, CH-OH), 4.84 (d, J = 5.0 Hz, 1H, CH-OH), 4.66 (t, J = 5.7 Hz, 1H, CH₂-OH), 4.59 (t, J = 5.7 Hz, 1H, CH₂-OH), 4.01 – 3.85 (m, 3H), 3.86 – 3.69 (m, 6H, Me), 3.55 – 3.35 (m, 4H); **¹³C-NMR** (101 MHz, (CD₃)₂SO) δ_C 166.0 (CO₂Me), 152.2 (C5), 152.0 (C2), 121.0 (C1), 119.8 (C3/C4), 115.94 (C3/C4), 115.89 (C6), 71.3 (ArO-CH₂), 70.3 (ArO-CH₂), 69.9 (2C, CH-OH), 62.72 (CH₂-OH), 62.66 (CH₂-OH), 52.0 (Me); **LRMS** m/z (ESI+) 339.12 (100%, [M+Na]⁺); **HRMS** m/z (ESI+) C₁₄H₂₀O₈Na Requires: 339.1056, Found: 339.1057 ([M+Na]⁺).

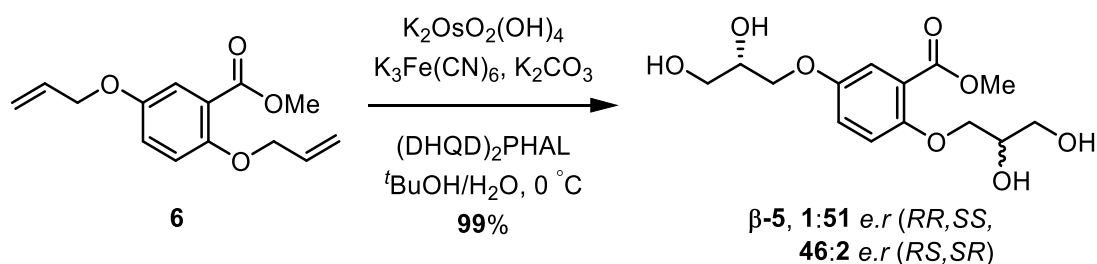
(**α-5'**) Sodium 5-((*R*)-2,3-dihydroxypropoxy)-2-((±)-2,3-dihydroxypropoxy)benzoate.



A solution of methyl 5-((*R*)-2,3-dihydroxypropoxy)-2-((±)-2,3-dihydroxypropoxy)benzoate (**α-5**) (100 mg, 0.32 mmol) in MeOH (10 mL) was charged with NaOH (13 mg, 0.32 mmol). The reaction mixture was heated under reflux for 2 h, then cooled to room temperature. The solvent was removed under reduced pressure to afford the title compound as a hygroscopic white solid (103 mg, 99%). **[α]_D²⁵** –10.48 (c. 1.0, MeOH, 36:6:4:54 *e.r/d.r* (*RR,SS,RS,SR*)); **IR** V_{\max} cm^{–1} 3246 br s (O-

H), 2934 w, 2877 w, 1559 s (C=O), 1491 s, 1455 w, 1420 s, 1374 s; **¹H-NMR** (400 MHz, CD₃OD) δ_{H} 7.36 (d, J = 3.1 Hz, 1H, C6-H), 7.15 (dd, J = 9.0, 3.1 Hz, 1H, C4-H), 7.12 – 7.05 (m, 2H, C6-H & C3-H), 6.93 (d, J = 9.0 Hz, 1H, C3-H), 6.87 (dd, J = 9.0, 3.0 Hz, 1H, C4-H), 4.16 – 3.86 (m, 2 \times 6H), 3.79 – 3.57 (m, 2 \times 4H); **¹³C-NMR** (101 MHz, CD₃OD) δ_{C} 175.9, 154.4, 154.34, 154.25, 151.7, 132.8, 122.0, 121.5, 117.8, 117.2, 116.7, 116.6, 116.2, 73.2, 72.8, 71.9, 71.8 (2C), 71.6, 71.1, 70.9, 64.3, 64.2, 64.1, 63.9; **LRMS** m/z (ESI+) 325.09 (30%, [M+H]⁺); **HRMS** m/z (ESI+) C₁₃H₁₈NaO₈ Requires: 325.0894, Found: 325.0895 ([M+H]⁺).

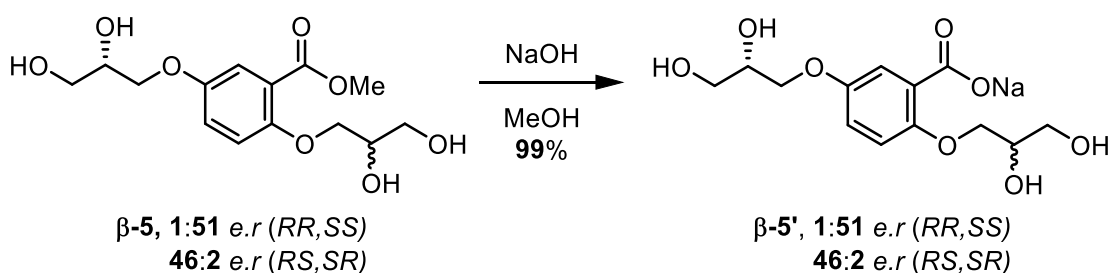
(β -5) Methyl 5-((*S*)-2,3-dihydroxypropoxy)-2-((\pm)-2,3-dihydroxypropoxy)benzoate



Adapted from general procedure **D** using stock solutions: **I** (2 mL, 3.0 mmol), **II** (2 mL, 3.0 mmol), **III** (1.0 mL, 2.0 μ mol) and **V** (5.0 mL, 20.0 μ mol). Methyl 2,5-bis(allyloxy)benzoate (**6**) (158 mg, 0.50 mmol) was added and the reaction mixture was stirred at 0 $^\circ\text{C}$ for 6 h with monitoring (EtOH/EtOAc 1:4, R_{f} = 0.20). The solvent was removed under reduced pressure and the crude mixture was directly purified by chromatography (SiO₂, EtOAc/hexane 1:4) to afford the title compound as a clear oil (156 mg, 99%). [α]_D²⁵ –7.62 (c. 1.0, MeOH, 1:51:46:2 *e.r/d.r* (2*R*5*R*, 2*S*5*S*, 2*R*5*S*, 2*S*5*R*)); **IR** ν_{max} cm^{–1} 3260 br s (O-H), 2951 w, 2874 w, 1725 (C=O), 1611 w, 1577 w, 1498 s, 1432 w; **¹H-NMR** (400 MHz, (CD₃)₂SO) δ_{H} 7.18 (d, J = 2.7 Hz, 1H, C6-H), 7.13 – 7.07 (m, 2H, C3-H & C4-H), 4.94 (d, J = 5.0 Hz, 1H, CH-OH), 4.84 (d, J = 5.0 Hz, 1H, CH-OH), 4.66 (t, J = 5.7 Hz, 1H, CH₂-OH), 4.59 (t, J = 5.7 Hz, 1H, CH₂-OH),

4.01 – 3.85 (m, 3H), 3.86 – 3.69 (m, 6H, Me), 3.55 – 3.35 (m, 4H); **¹³C-NMR** (101 MHz, (CD₃)₂SO) δ_c 166.1 (C=O₂Me), 152.2 (C5), 152.0 (C2), 121.0 (C1), 119.8 (C3/C4), 115.95 (C3/C4), 115.91 (C6), 71.3 (ArO-CH₂), 70.4 (ArO-CH₂), 69.9 (2C, CH-OH), 62.73 (CH₂-OH), 62.67 (CH₂-OH), 52.0 (Me); **LRMS** m/z (ESI+) 339.12 (100%, [M+Na]⁺); **HRMS** m/z (ESI+) C₁₄H₂₀O₈Na Requires: 339.1056, Found: 339.1057 ([M+Na]⁺).

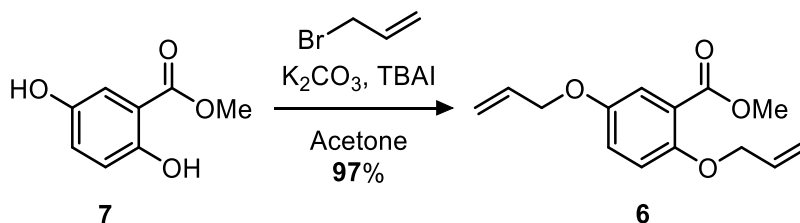
(**β -5'**) Sodium 5-((*S*)-2,3-dihydroxypropoxy)-2-((\pm)-2,3-dihydroxypropoxy)benzoate



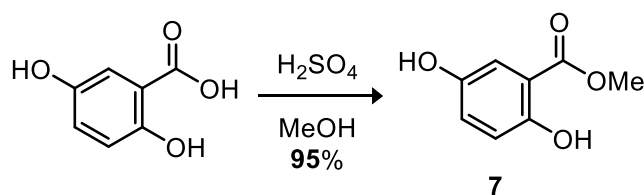
A solution of methyl 5-((*S*)-2,3-dihydroxypropoxy)-2-((\pm)-2,3-dihydroxypropoxy)benzoate (**β -5**) (100 mg, 0.32 mmol) in MeOH (10 mL) was charged with NaOH (13 mg, 0.32 mmol). The reaction mixture was heated under reflux for 2 h, then cooled to room temperature. The solvent was removed under reduced pressure to afford the title compound as a hygroscopic white solid (103 mg, 99%). [α]_D²⁵ –8.31 (c. 1.0, MeOH, 1:51:46:2 *e.r/d.r* (*RR,SS,RS,SR*)); **IR** V_{\max} cm^{–1} 3249 br s (O-H), 2934 w, 2879 w, 1559 s (C=O), 1491 s, 1455 w, 1420 s, 1374 s; **¹H-NMR** (400 MHz, CD₃OD) δ_H 7.36 (d, J = 3.1 Hz), 7.15 (dd, J = 8.9, 3.1 Hz), 7.12 – 7.07 (m, 1H, C6-H), 6.93 (d, J = 8.9 Hz, 1H, C3-H), 6.87 (dd, J = 8.9, 3.1 Hz, 1H, C4-H), 4.20 – 3.84 (m, 2 \times 6H), 3.78 – 3.55 (m, 2 \times 4H); **¹³C-NMR** (101 MHz, CD₃OD) δ_c 176.4 (C=O₂Me), 154.9, 154.9, 154.8, 152.3, 133.3, 122.0, 118.4, 117.7, 117.3, 117.12 (2C), 116.8, 116.7, 73.7, 73.3, 72.4, 72.3, 72.1, 71.6, 71.4, 64.8, 64.7, 64.6, 64.5; **LRMS** m/z (ESI+)

325.09 (30%, $[M+H]^+$); **HRMS** m/z (ESI+) $C_{13}H_{18}NaO_8$ Requires: 325.0894, Found: 325.0890 ($[M+H]^+$).

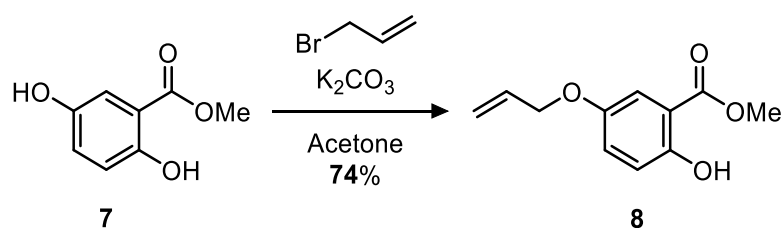
(6) Methyl 2,5-bis(allyloxy)benzoate



Following general procedure **B**: methyl 2,5-dihydroxybenzoate (**7**) (835 mg, 5.0 mmol), K₂CO₃ (1.658 g, 12.0 mmol) and TBAI (1.612 g, 5.0 mmol) in acetone (25 mL) was charged with allyl bromide (1.04 mL, 12.0 mmol) and heated under reflux for 6 h. Purification by chromatography (SiO₂, EtOAc/hexane 1:9, R_f = 0.41) yielded the title compound as a clear oil (1.201 g, 97%). **IR** ν_{\max} cm⁻¹ 3082 w, 2949 w, 2865 w, 1730 m (C=O), 1495 m, 1437 w; **¹H-NMR** (400 MHz, CDCl₃) δ_H 7.35 (d, J = 3.2 Hz, 1H, C6-H), 7.00 (dd, J = 9.0, 3.2 Hz, 1H, C4-H), 6.89 (d, J = 9.0 Hz, 1H, C3-H), 6.09 – 5.96 (m, 2H, CH=CH₂), 5.46 (dq, J = 17.3, 1.6 Hz, 1H, C5-OCH₂CH=CH₂), 5.39 (dq, J = 17.3, 1.6 Hz, 1H, C2-OCH₂CH=CH₂), 5.26 (dt, J = 10.6, 1.6 Hz, 2H, CH=CH₂), 4.54 (dt, J = 4.9, 1.6 Hz, 2H, C5-OCH₂), 4.49 (dt, J = 5.3, 1.6 Hz, 2H, C2-OCH₂), 3.88 (s, 3H, Me); **¹³C-NMR** (101 MHz, CDCl₃) δ_C 166.6 (C=O), 152.6 (C5), 152.3 (C2), 133.2 (2C, CH=CH₂), 121.3 (C1), 120.4 (C4), 117.8 (CH=CH₂), 117.30 (CH=CH₂), 117.07 (C3), 116.0 (C6), 70.7 (C5-OCH₂), 69.5 (C2-OCH₂), 52.1 (Me); **LRMS** m/z (ESI+) 248.09 (50%, $[M]^+$), 207.06 (60%, $[M-C_3H_6]^+$), 175.03 (100%, $[M-(C_3H_6)-CH_3OH]^+$); **HRMS** m/z (ESI+) $C_{14}H_{16}O_4$ Requires: 248.1049, Found: 248.1051 ($[M]^+$).

(7) Methyl 2,5-hydroxybenzoate

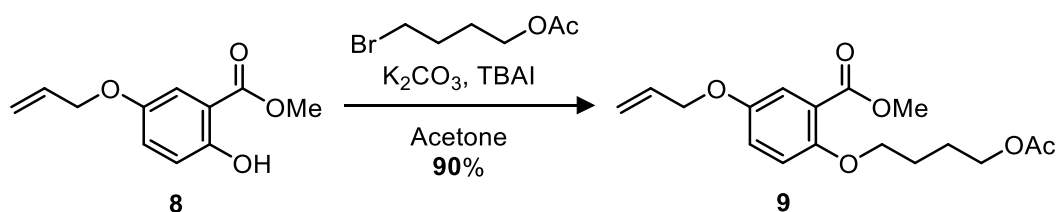
Adapted from general procedure **A**: 2,5-dihydroxybenzoic acid (15.40 g, 0.10 mol) in MeOH (200 mL) was charged with conc. H₂SO₄ (2 mL) and heated under reflux for 21 h with monitoring (EtOAc/hexane 1:3, *R_f* = 0.41). A yellow solid was afforded after work up, recrystallization (CH₂Cl₂/hexane) yielded the title compound as long yellow crystals (15.92 g, 95%). **M.P** 87 – 90 °C; **IR** *V*_{max} cm⁻¹ 3331m (O-H), 2960 w, 1683 s (C=O); **¹H-NMR** (400 MHz, CDCl₃) δ_H 10.34 (s, 1H, C2-OH), 7.28 (d, *J* = 3.1 Hz, 1H, C6-H), 7.01 (dd, *J* = 8.9, 3.1 Hz, 1H, C4-H), 6.89 (d, *J* = 8.9 Hz, 1H, C3-H), 4.66 (s, 1H, C5-OH), 3.94 (s, 3H, Me); **¹³C-NMR** (101 MHz, CDCl₃) δ_C 170.2 (C=O), 156.0 (C2), 147.8 (C5), 124.2 (C4), 118.7 (C3), 114.9 (C6), 112.3 (C1), 52.5 (Me); **LRMS** *m/z* (ESI⁻) 167.03 (100%, [M-H]⁻), 135.01 (30%, [M-CH₃OH₂]⁻); **HRMS** *m/z* (ESI⁻) C₈H₇O₄ Requires: 167.0524, Found: 167.0525 ([M-H]⁻).

(8) Methyl 5-(allyloxy)-2-hydroxybenzoate

Adapted from general procedure **B**: methyl 2,5-dihydroxybenzoate (835 mg, 5.0 mmol) and K₂CO₃ (691 mg, 5.0 mmol) in acetone (50 mL) was charged dropwise with allyl bromide (0.43 mL, 5.0 mmol) and the reaction mixture was stirred at room temperature for 48 h. Purification by chromatography (SiO₂, EtOAc/hexane, 1:9, *R_f* =

0.62) yielded the title compound as a colourless oil (770 mg, 74%). **IR** V_{\max} cm^{-1} 3222 w, 2955 w, 1677 s (C=O), 1615 w, 1486 s, 1439 s; **$^1\text{H-NMR}$** (400 MHz, CDCl_3) δ_{H} 10.39 (s, 1H, C2-OH), 7.33 (d, $J = 3.1$ Hz, 1H, C6-H), 7.12 (dd, $J = 9.0, 3.1$ Hz, 1H, C4-H), 6.93 (d, $J = 9.0$ Hz, 1H, C3-H), 6.06 (ddt, $J = 17.2, 10.5, 5.4$ Hz, 1H, $\text{CH}=\text{CH}_2$), 5.43 (dd, $J = 17.2, 1.5$ Hz, 1H, $\text{CH}=\text{CH}_2$), 5.31 (dd, $J = 10.5, 1.5$ Hz, 1H, $\text{CH}=\text{CH}_2$), 4.51 (d, $J = 5.4$ Hz, 2H, C5-OCH₂), 3.96 (s, 3H, Me); **$^{13}\text{C-NMR}$** (101 MHz, CDCl_3) δ_{C} 170.4 (CO₂Me), 156.3 (C5), 151.1 (C2), 133.3 ($\text{CH}=\text{CH}_2$), 124.9 (C4), 118.6 (C3), 117.9 ($\text{CH}=\text{CH}_2$), 113.4 (C6), 112.0 (C1), 69.7 (C5-OCH₂), 52.5 (Me); **LRMS** m/z (ESI+) 208.06 (30%, $[\text{M}]^+$), 167.02 (60%, $[\text{M}-\text{C}_3\text{H}_5]^+$), 134.99 (100%, $[\text{M}-(\text{C}_3\text{H}_5)-\text{CH}_3\text{OH}]^+$); **HRMS** m/z (ESI+) $\text{C}_{11}\text{H}_{12}\text{O}_4$ Requires: 208.0736, Found: 208.0737 ($[\text{M}]^+$).

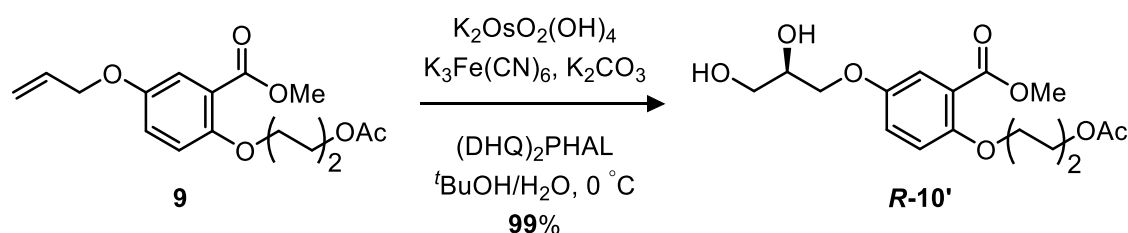
(9) Methyl 2-(4-acetoxybutoxy)-5-(allyloxy)benzoate



A flask containing methyl 5-(allyloxy)-2-hydroxybenzoate (**8**) (1.00 g, 4.8 mmol), K_2CO_3 (1.29 g, 9.6 mmol) and TBAI (0.77 g, 2.4 mmol) in acetone (20 mL) was charged with 4-bromobutyl acetate (6.1 g, 14.4 mmol) and the reaction mixture was heated under reflux for 12 h. The flask was cooled to room temperature and the solvent removed under reduced pressure. The crude residue was charged with H_2O (20 mL) and extracted with EtOAc (3×50 mL). The combined organic extracts were washed with brine, dried (MgSO_4), and filtration of the solids and removal of the solvent under reduced pressure afforded a yellow oil. Purification by chromatography (SiO_2 , EtOAc/hexane 1:5, $R_f = 0.23$) afforded the title compound as a clear oil (1.54 g, 90%). **IR** V_{\max} cm^{-1} 2946 m, 1734s (C=O), 1499 m, 1439 w; **$^1\text{H-NMR}$** (400 MHz, CDCl_3) δ_{H}

7.33 (d, $J = 3.2$ Hz, 1H, C6-H), 7.01 (dd, $J = 9.0, 3.2$ Hz, 1H, C4-H), 6.88 (d, $J = 9.0$ Hz, 1H, C3-H), 6.02 (ddt, $J = 17.2, 10.5, 5.3$ Hz, 1H, CH=CH₂), 5.39 (dd, $J = 17.2, 1.5$ Hz, 1H, CH=CH₂), 5.27 (dd, $J = 10.5, 1.5$ Hz, 1H, CH=CH₂), 4.50 (d, $J = 5.3$ Hz, 2H, C5-OCH₂), 4.16 – 4.10 (m, 2H, CH₂-OAc), 4.02 – 3.97 (m, 2H, C2-OCH₂), 3.87 (s, 3H, Me), 2.03 (s, 3H, COCH₃), 1.91 – 1.80 (m, 4H, (CH₂)₂); **¹³C-NMR** (101 MHz, CDCl₃) δ_c : 171.3 (Ac), 166.7 (CO₂Me), 153.0 (C2), 152.2 (C5), 133.2 (CH=CH₂), 121.1 (C1), 120.6 (C4), 117.9 (CH=CH₂), 117.1 (C6), 115.4 (C3), 69.6 (C5-OCH₂), 69.3 (C2-OCH₂), 64.3 (CH₂-OAc), 52.1 (Me), 26.1 (CH₂), 25.4 (CH₂), 21.1 (COCH₃); **LRMS** m/z (ESI+) 345.13 (100%, [M+Na]⁺), 323.13 (60%, [M+H]⁺); **HRMS** m/z (ESI+) C₁₇H₂₂O₆Na Requires: 345.1309, Found: 345.1309 ([M+Na]⁺).

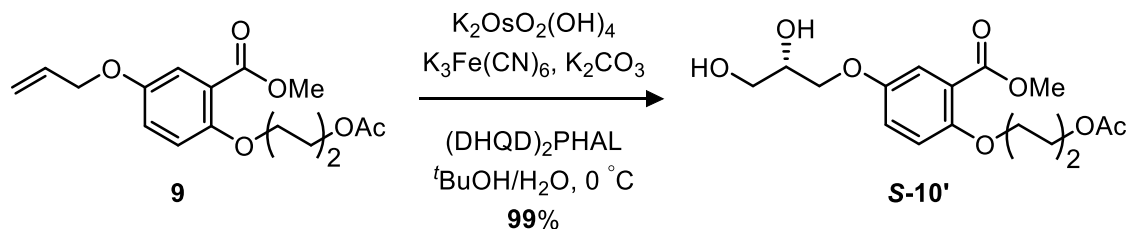
(**R-10'**) Methyl (*R*)-2-(4-acetoxybutoxy)-5-(2,3-dihydroxypropoxy)benzoate



A 25 mL round bottom flask was charged with ADmix α (1.4 g, 3.0 mmol eq.), H₂O/*t*BuOH (1:1, 10 mL) and stirred at room temperature for 2 min. The mixture was cooled to 0 °C (ice bath) for 10 min and methyl 2-(4-acetoxybutoxy)-5-(allyloxy)benzoate (**9**) (322 mg, 1.0 mmol) was added directly. The reaction mixture was stirred at 0 °C for 12 h with monitoring (EtOH/EtOAc 1:4, $R_f = 0.50$). The reaction was quenched with neat Na₂SO₃ (1.5 g) and warmed to room temperature over 1 h. The flask was charged with H₂O (10 mL) and extracted with EtOAc (4 \times 30 mL). The combined organic extracts were washed with 1M HCl (aq.) (2 \times 25 mL), brine (25 mL), and dried (MgSO₄). Filtration of the solids and removal of solvent under reduced pressure afforded the title compound as a clear oil (355 mg, 99%). [α]_D²⁵ +8.14 (c.

1.0, CHCl₃); **IR** V_{\max} cm⁻¹ 3390 br s (O-H), 2950 w, 1734 s (C=O), 1715 s (C=O), 1611 w, 1580 w, 1498 s, 1468 w, 1438 s; **¹H-NMR** (400 MHz, CDCl₃) δ_{H} 7.32 (d, J = 3.2 Hz, 1H, C6-H), 6.99 (dd, J = 9.0, 3.2 Hz, 1H, C4-H), 6.86 (d, J = 9.0 Hz, 1H, C3-H), 4.24 – 4.03 (m, 2H, CH₂-OAc), 4.09 – 4.01 (m, 1H, CH-OH), 4.01 – 3.92 (m, 4H, C2-OCH₂ & C5-OCH₂), 3.85 (s, 3H, Me), 3.83 – 3.67 (m, 2H, CH₂-OH), 3.22 (br s, 1H, OH), 2.80 (br s, 1H, OH), 2.03 (s, 3H, COCH₃), 1.90 – 1.78 (m, 4H, (CH₂)₂); **¹³C-NMR** (101 MHz, CDCl₃) δ_{C} 171.4 (Ac), 166.7 (CO₂Me), 153.2 (C2), 152.1 (C5), 121.0 (C1), 120.3 (C4), 117.0 (C6), 115.4 (C3), 70.5 (CH-OH), 69.7 (C5-OCH₂), 69.3 (C2-OCH₂), 64.3 (CH₂-OAc), 63.7 (CH₂-OH), 52.2 (Me), 26.0 (CH₂), 25.4 (CH₂), 21.1 (Ac); **LRMS** m/z (ESI+) 379.14 (100%, [M+Na]⁺); **HRMS** m/z (ESI+) C₁₇H₂₄NaO₈ Requires: 379.1363, Found: 379.1362 ([M+Na]⁺).

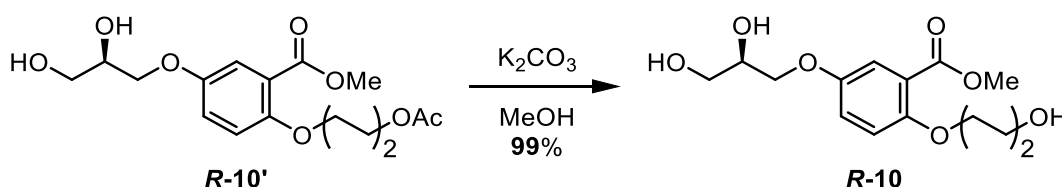
(**S-10'**) Methyl (*S*)-2-(4-acetoxymethoxy)-5-(2,3-dihydroxypropoxy)benzoate



A 25 mL round bottom flask was charged with ADmix β (1.4 g, 3.0 mmol eq.), H₂O/^tBuOH (1:1, 10 mL) and stirred at room temperature for 2 min. The mixture was cooled to 0 °C (ice bath) for 10 min and methyl 2-(4-acetoxymethoxy)-5-(allyloxy)benzoate (**9**) (322 mg, 1.0 mmol) was added directly. The reaction mixture was stirred at 0 °C for 12 h with monitoring (EtOH/EtOAc 1:4, R_f = 0.50). The reaction was quenched with neat Na₂SO₃ (1.5 g) and warmed to room temperature over 1 h. The flask was charged with H₂O (10 mL) and extracted with EtOAc (4 \times 30 mL). The combined organic extracts were washed with 1M HCl (aq.) (2 \times 25 mL), brine (25 mL), and dried (MgSO₄). Filtration of the solids and removal of solvent under reduced

pressure gave the title compound as a clear oil (355 mg, 99%). **[α]_D²⁵** –6.23 (c. 1.0, CHCl₃); **IR** V_{\max} cm^{–1} 3412 br s (O-H), 2980 s, 2901 s, 1733 s (C=O), 1716 s (C=O), 1611 w, 1580 w, 1498 s, 1470 w, 1438 s; **¹H-NMR** (400 MHz, CDCl₃) δ_{H} 7.32 (d, J = 3.2 Hz, 1H, C6-H), 6.99 (dd, J = 9.0, 3.2 Hz, 1H, C4-H), 6.86 (d, J = 9.0 Hz, 1H, C3-H), 4.24 – 4.03 (m, 2H, CH₂-OAc), 4.09 – 4.01 (m, 1H, CH-OH), 4.01 – 3.92 (m, 4H, C2-OCH₂ & C5-OCH₂), 3.85 (s, 3H, Me), 3.83 – 3.67 (m, 2H, CH₂-OH), 3.22 (br s, 1H, OH), 2.80 (br s, 1H, OH), 2.03 (s, 3H, CO₂CH₃), 1.90 – 1.78 (m, 4H, (CH₂)₂); **¹³C-NMR** (101 MHz, CDCl₃) δ_{C} 171.4 (Ac), 166.7 (CO₂CH₃), 153.2 (C2), 152.0 (C5), 121.0 (C1), 120.3 (C4), 117.0 (C6), 115.4 (C3), 70.5 (CH-OH), 70.0 (C5-OCH₂), 69.2 (C2-OCH₂), 64.3 (CH₂-OAc), 63.7 (CH₂-OH), 52.2 (Me), 26.0 (CH₂), 25.4 (CH₂), 21.1 (Ac); **LRMS** m/z (ESI+) 379.14 (100%, [M+Na]⁺); **HRMS** m/z (ESI+) C₁₇H₂₄NaO₈ Requires: 379.1363, Found: 379.1360 ([M+Na]⁺).

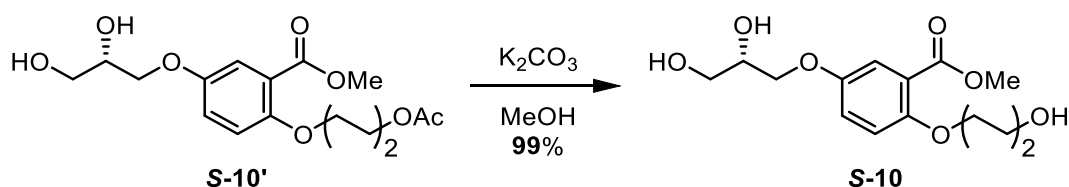
(**R-10**) Methyl (*R*)-2-(4-hydroxybutoxy)-5-(2,3-dihydroxypropoxy)benzoate



A solution of methyl (*R*)-2-(4-acetoxybutoxy)-5-(2,3-dihydroxypropoxy)benzoate (**R-10'**) (60 mg, 0.17 mmol) in MeOH (10 mL) was charged with K₂CO₃ (47 mg, 34.0 mmol). The reaction mixture was stirred at room temperature for 12 h. The reaction was slowly neutralised by the dropwise addition of conc. HCl (aq.) (pH 6) and filtered. The filtrate was collected and the solvent removed under reduced pressure to yield the title compound as a yellow oil (53 mg, 99%). **[α]_D²⁵** +8.93 (c. 1.0, CHCl₃); **IR** V_{\max} cm^{–1} 3341 br s (O-H), 2988 s, 2901 s, 1712 s (C=O), 1610 w, 1579 w, 1498 s, 1467 w, 1438 s, 1417 w; **¹H-NMR** (400 MHz, CD₃OD) δ_{H} 7.30 (d, J = 3.2 Hz, 1H, C6-H),

7.11 (dd, $J = 9.1, 3.2$ Hz, 1H, C4-H), 7.02 (d, $J = 9.1$ Hz, 1H, C3-H), 4.08 – 3.98 (m, 3H, C2-OCH₂ & CH-OH), 3.98 – 3.91 (m, 2H, C5-OCH₂), 3.85 (s, 3H, CO₂CH₃), 3.74 – 3.58 (m, 4H, CH₂CH₂-OH, CH(OH)CH₂-OH), 1.91 – 1.78 (m, 2H, CH₂), 1.78 – 1.66 (m, 2H, CH₂); **¹³C-NMR** (101 MHz, CD₃OD) δ_c 168.4 (CO₂Me), 154.2 (C2), 153.9 (C5), 122.2 (C1), 121.1 (C4), 117.7 (C6), 116.6 (C3), 71.8 (C5-OCH₂), 71.1 (CH-OH), 70.7 (C2-OCH₂), 64.1 (CH(OH)CH₂-OH), 62.6 (CH₂CH₂-OH), 52.5 (CO₂CH₃), 30.3 (CH₂), 26.9 (CH₂); **LRMS** m/z (ESI+) 337.13 (100%, [M+Na]⁺); **HRMS** m/z (ESI+) C₁₅H₂₂NaO₇ Requires: 337.1258, Found: 337.1256 ([M+Na]⁺).

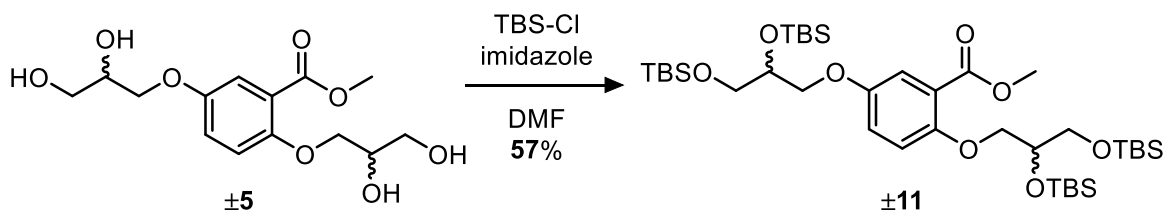
(S-10) Methyl (*S*)-2-(4-hydroxybutoxy)-5-(2,3-dihydroxypropoxy)benzoate



A solution of methyl (*S*)-2-(4-acetoxypentyloxy)-5-(2,3-dihydroxypropoxy)benzoate (**S-10'**) (71 mg, 0.19 mmol) in MeOH (10 mL) was charged with K₂CO₃ (55 mg, 0.38 mmol). The reaction mixture was stirred at room temperature for 12 h. The reaction was slowly neutralised by the dropwise addition of conc. HCl (aq.) (pH 6) and filtered. The filtrate was collected and the solvent removed under reduced pressure to yield the title compound as a yellow oil (67 mg, 99%). [α]_D²⁵ –7.01 (c. 1.0, CHCl₃); **IR** ν_{\max} cm^{–1} 3366 br s (O-H), 2942 s, 2876 s, 1712 s (C=O), 1610 w, 1579 w, 1498 s, 1467 w, 1438 s, 1417 w; **¹H-NMR** (400 MHz, CD₃OD) δ_H 7.30 (d, $J = 3.2$ Hz, 1H, C6-H), 7.11 (dd, $J = 9.1, 3.2$ Hz, 1H, C4-H), 7.02 (d, $J = 9.1$ Hz, 1H, C3-H), 4.08 – 3.98 (m, 3H, C2-OCH₂ & CH-OH), 3.98 – 3.91 (m, 2H, C5-OCH₂), 3.85 (s, 3H, CO₂CH₃), 3.74 – 3.58 (m, 4H, CH₂CH₂-OH, CH(OH)CH₂-OH), 1.91 – 1.78 (m, 2H, CH₂), 1.78 – 1.66 (m, 2H, CH₂); **¹³C-NMR** (101 MHz, CD₃OD) δ_c 168.4 (CO₂Me), 154.2 (C2), 153.9 (C5),

122.2 (C1), 121.1 (C4), 117.7 (C6), 116.5 (C3), 71.8 (C5-OCH₂), 71.1 (CH-OH), 70.7 (C2-OCH₂), 64.1 (CH(OH)CH₂-OH), 62.6 (CH₂CH₂-OH), 52.5 (Me), 30.3 (CH₂), 26.9 (CH₂); **LRMS** m/z (ESI+) 337.13 (100%, [M+Na]⁺); **HRMS** m/z (ESI+) C₁₅H₂₂NaO₇ Requires: 337.1258, Found: 337.1260 ([M+Na]⁺).

(**±11**) Methyl 2,5-bis(2,3-bis((*tert*-butyldimethylsilyl)oxy)propoxy)benzoate

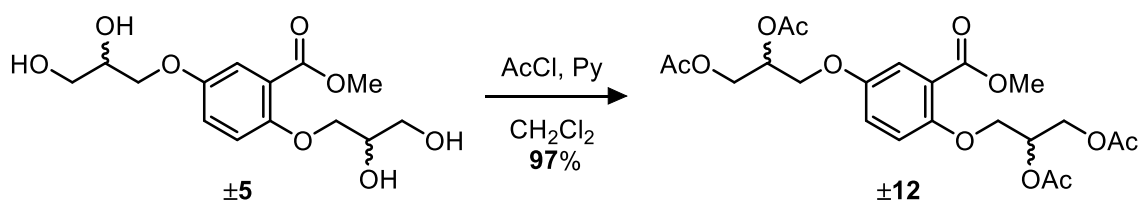


A flask containing methyl 2,5-bis(2,3-dihydroxypropoxy)benzoate (**±5**) (100 mg, 0.32 mmol) and imidazole (140 mg, 2.05 mmol) was charged with dry DMF (3 mL) and stirred under an atmosphere of N₂. The flask was charged with *tert*-butyldimethylsilyl chloride (248 mg, 1.64 mmol) as a solution in DMF (1 mL), dropwise over 5 min. The reaction mixture was stirred at RT for 4 h. The reaction was quenched with H₂O (150 mL) and extracted with CHCl₃ (2 × 50 mL). The pooled organic extracts were washed with brine (30 mL) and dried (MgSO₄). Filtration of the solids and removal of solvent under reduced pressure afforded a crude mixture. Purification by chromatography (SiO₂, EtOAc/Hexane, 1:19) afforded the title compound as a clear oil (140 mg, 57%).

¹H-NMR (400 MHz, CDCl₃) δ_{H} 7.27 (d, J = 3.1 Hz, 1H, C6-H), 6.98 (dd, J = 9.0, 3.1 Hz, 1H, C3-H), 6.92 (d, J = 9.0 Hz, 1H, C4-H), 4.10 – 3.97 (m, 4H, Ar-OCH₂), 3.97 – 3.89 (m, 1H, CH-OSi(Me)₂^tBu), 3.87 (m, 4H, Me & CH-OSi(Me)₂^tBu), 3.76 – 3.58 (m, 4H, CH₂-OSi(Me)₂^tBu), 0.91 – 0.84 (m, 36H, Si(Me)₂^tBu), 0.12 – 0.02 (m, 24H, Si(Me)₂^tBu); **¹³C-NMR** (101 MHz, CDCl₃) δ_{C} 167.0 (CO₂Me), 152.8 (C2), 152.7 (C5), 121.5 (C1), 119.9 (C3), 116.7 (C6), 115.6 (C4), 72.2 (Ar-OCH₂), 72.1 (Ar-OCH₂), 71.7 (CH-OSi(Me)₂^tBu), 70.8 (CH-OSi(Me)₂^tBu), 65.1 (CH₂-OSi(Me)₂^tBu), 65.0 (CH₂-

OSi(Me)₂^tBu), 52.1 (CO₂Me), 26.1 (^tBu), 26.0 (^tBu), 26.0 (^tBu), 18.5 (^tBu), 18.3 (^tBu), 18.2 (^tBu), -4.45 (Me), -4.50 (Me), -4.55 (Me), -4.65 (Me), -5.2 (Me), -5.3 (Me); **LRMS** *m/z* (ESI+) 795.46 (100%, [M+Na]⁺); **HRMS** *m/z* (ESI+) C₃₈H₇₆O₈NaSi₄ Requires: 795.4515, Found: 795.4513 ([M+Na]⁺).

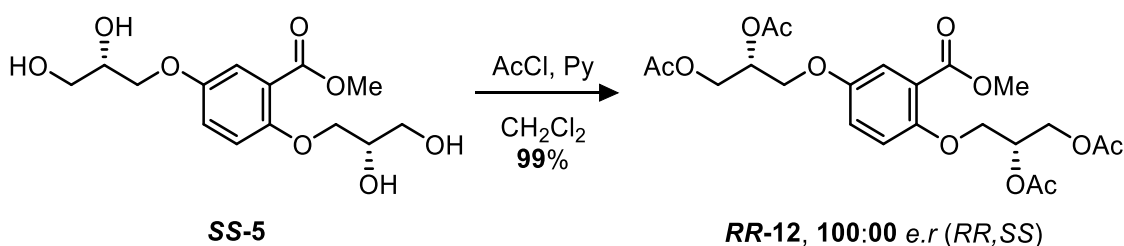
(±12) Methyl (±)-2,5-bis(2,3-di(acetoxy)propoxy)benzoate



Following general procedure **G**: Methyl (±)-2,5-bis(2,3-dihydroxypropoxy)benzoate (**±5**) (50 mg, 0.16 mmol) was charged with pyridine (103.0 µL, 1.28 mmol), CH₂Cl₂ (4.0 mL) and the AcCl (91.3 µL, 1.28 mmol) was added dropwise. The final product was purified by chromatography (SiO₂, EtOAc/Hexane 1:1, *R_f* = 0.29) yielding the title compound as a clear oil (75 mg, 97%). **IR** *V*_{max} cm⁻¹ 2925 w, 1734 s (C=O), 1488 w, 1439 w, 1370 w, 1207 s; **¹H-NMR** (400 MHz, CDCl₃) δ_H 7.34 (d, *J* = 3.3 Hz, 1H, C6-H), 7.01 (dd, *J* = 9.1, 3.3 Hz, 1H, C4-H), 6.89 (d, *J* = 9.1 Hz, 1H, C3-H), 5.36 (m, 2H, CH-OAc), 4.48 (dd, *J* = 12.0, 3.9 Hz, 1H, CH₂-OAc), 4.41 (dd, *J* = 12.0, 3.9 Hz, 1H, CH₂-OAc), 4.33 (dd, *J* = 12.0, 6.1 Hz, 1H, CH₂-OAc), 4.27 (dd, *J* = 12.0, 6.1 Hz, 1H, CH₂-OAc), 4.14 (m, 2H, ArO-CH₂), 4.09 (d, *J* = 5.2 Hz, 2H, ArO-CH₂), 3.88 (s, 3H, Me), 2.10 (obs. d, *J* = 1.0 Hz, 6H, Ac), 2.07 (obs. d, *J* = 2.5 Hz, 6H, Ac); **¹³C-NMR** (101 MHz, CDCl₃) δ_C 170.71 (Ac), 170.69 (Ac), 170.4 (Ac), 170.3 (Ac), 166.3 (CO₂Me), 152.5 (C1), 121.7 (C2 & C5), 120.5 (C4), 117.0 (C6), 116.1 (C3), 69.8 (CH-OAc), 69.7 (CH-OAc), 68.2 (ArO-CH₂), 66.9 (ArO-CH₂), 62.7 (CH₂-OAc), 62.5 (CH₂-OAc), 52.3 (Me), 21.1 (Ac), 21.0 (Ac), 20.8 (2C, Ac); **LRMS** *m/z* (ESI+) 507.15 (100%, [M+Na]⁺); **HRMS** *m/z* (ESI+) C₂₂H₂₈O₁₂Na Requires: 507.1478, Found: 507.1482 ([M+Na]⁺);

cHPLC R_{t1} = 76.39 min (*2R,5R*), area = 25.94%; R_{t2} = 83.00 min (*2S,5R*), area = 24.99%; R_{t3} = 86.59 min (*2R,5S*), area = 24.55%; R_{t4} = 116.51 min (*2S,5S*), area = 24.53%. (Phenomenex® Cellulose-1, MeCN/H₂O, 7:18, 1 mL min⁻¹, 30 °C).

(**RR-12**) (*2R,5R*)-((2-(methoxycarbonyl)-1,4-phenylene)bis(oxy))bis(propane-3,1,2-triyl) tetraacetate

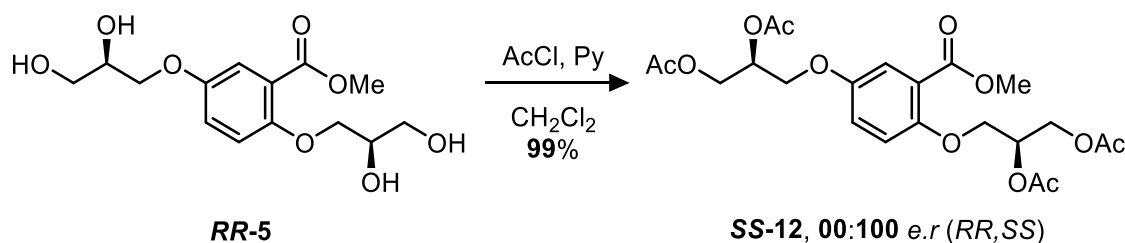


Following general procedure **G**: Using methyl 2,5-bis((*S*)-2,3-dihydroxypropoxy)benzoate (**SS-5**) (20 mg, 63 μmol). The final product was purified by chromatography (SiO₂, EtOAc/Hexane 1:1, R_f = 0.29) yielding the title compound as a clear oil (29 mg, 99%). [α]_D²⁵ –31.34 (c. 1.0, CHCl₃, 100:00 *e.r* (*2R5R*, *2S5S*)); **IR** ν_{\max} cm⁻¹ 2962 w, 1740 s (C=O), 1500 s, 1439 s; **¹H-NMR** (400 MHz, CDCl₃) δ_H 7.35 (d, J = 3.3 Hz, 1H, C6-H), 7.02 (dd, J = 9.1, 3.3 Hz, 1H, C4-H), 6.90 (d, J = 9.1 Hz, 1H, C3-H), 5.36 (m, 2H, CH-OAc), 4.48 (dd, J = 12.0, 3.9 Hz, 1H, CH₂-OAc), 4.41 (dd, J = 12.0, 3.9 Hz, 1H, CH₂-OAc), 4.34 (dd, J = 12.0, 6.1 Hz, 1H, CH₂-OAc), 4.28 (dd, J = 12.0, 3.9 Hz, 1H, CH₂-OAc), 4.15 (m, 2H, ArO-CH₂), 4.09 (d, J = 5.2 Hz, 2H, ArO-CH₂), 3.89 (s, 3H, Me), 2.11 (s, 3H, Ac), 2.11 (s, 3H, Ac), 2.08 (s, 3H, Ac), 2.07 (s, 3H, Ac); **¹³C-NMR** (101 MHz, CDCl₃) δ_C 170.77 (Ac), 170.75 (Ac), 170.5 (Ac), 170.4 (Ac), 166.3 (CO₂Me), 152.6 (C1), 121.7 (C2 & C5), 120.5 (C4), 117.1 (C6), 116.1 (C3), 69.9 (CH-OAc), 69.8 (CH-OAc), 68.3 (ArO-CH₂), 66.9 (ArO-CH₂), 62.8 (CH₂-OAc), 62.6 (CH₂-OAc), 52.4 (Me), 21.1 (br s, 2C, Ac), 20.9 (br s, 2C, Ac); **LRMS** m/z (ESI+) 507.16 (100%, [M+Na]⁺); **HRMS** m/z (ESI+) C₂₂H₂₈O₁₂Na Requires: 507.1478,

Found: 507.1476 ($[M+Na]^+$); **cHPLC** R_t = 72.87 min, area = 100.00%. (Phenomenex®

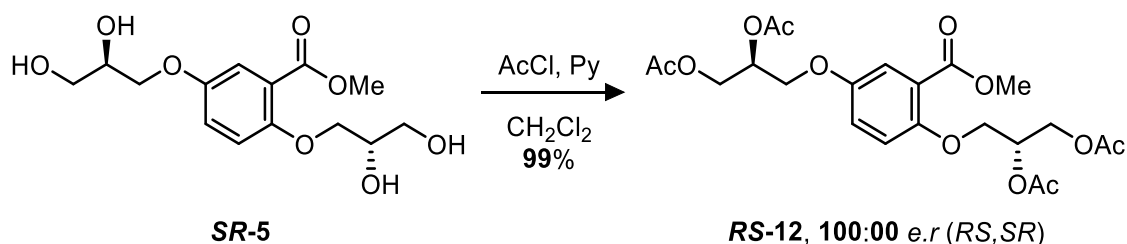
Cellulose-1, MeCN/H₂O, 7:18, 1 mL min⁻¹, 30 °C).

(**SS-12**) (2*S*,5*S*)-((2-(methoxycarbonyl)-1,4-phenylene)bis(oxy))bis(propane-3,1,2-triyl) tetraacetate



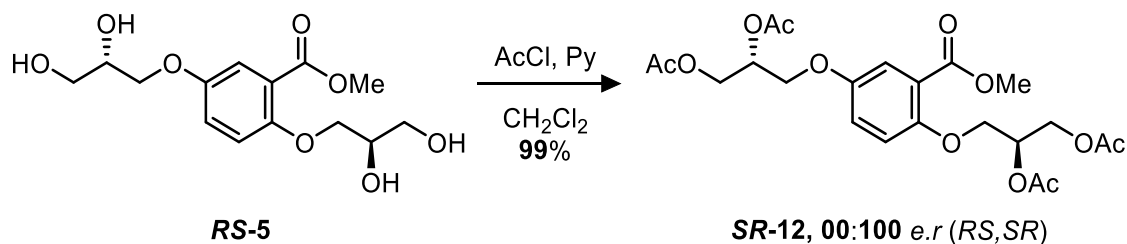
Following general procedure **G**: Using methyl 2,5-bis((*R*)-2,3-dihydroxypropoxy)benzoate (**RR-5**) (20 mg, 63 μ mol). The final product was purified by chromatography (SiO₂, EtOAc/Hexane 1:1, R_f = 0.29) yielding the title compound as a clear oil (29 mg, 99%). **[α]_D²⁵** +24.60 (c. 1.0, CHCl₃, 00:100 *e.r* (2*R*5*R*, 2*S*5*S*)); **IR** V_{max} cm⁻¹ 2957 w, 2925 s, 1737 s (C=O), 1500 s, 1439 s; **¹H-NMR** (400 MHz, CDCl₃) δ_H 7.35 (d, J = 3.3 Hz, 1H, C6-H), 7.02 (dd, J = 9.1, 3.3 Hz, 1H, C4-H), 6.89 (d, J = 9.1 Hz, 1H, C3-H), 5.36 (m, 2H, CH-OAc), 4.49 (dd, J = 12.0, 3.9 Hz, 1H, CH₂-OAc), 4.41 (dd, J = 12.0, 3.9 Hz, 1H, CH₂-OAc), 4.34 (dd, J = 12.0, 6.1 Hz, 1H, CH₂-OAc), 4.28 (dd, J = 12.0, 6.1 Hz, 1H, CH₂-OAc), 4.14 (m, 2H, ArO-CH₂), 4.10 (d, J = 5.2 Hz, 2H, ArO-CH₂), 3.89 (s, 3H, Me), 2.11 (s, 3H, Ac), 2.11 (s, 3H, Ac), 2.08 (s, 3H, Ac), 2.08 (s, 3H, Ac); **¹³C-NMR** (101 MHz, CDCl₃) δ_C 170.8 (2C, Ac) 170.5 (2C, Ac), 166.3 (C=O₂Me), 152.6 (C1), 121.7 (C2 & C5), 120.5 (C4), 117.1 (C6), 116.1 (C3), 69.9 (CH-OAc), 69.8 (CH-OAc), 68.3 (ArO-CH₂), 66.9 (ArO-CH₂), 62.8 (CH₂-OAc), 62.6 (CH₂-OAc), 52.4 (Me), 21.1 (2C, Ac), 20.9 (2C, Ac); **LRMS** m/z (ESI+) 507.16 (100%, $[M+Na]^+$); **HRMS** m/z (ESI+) C₂₂H₂₈O₁₂Na Requires: 507.1478, Found: 507.1480 ($[M+Na]^+$); **cHPLC** R_t = 111.63 min, area = 100.00%. (Phenomenex® Cellulose-1, MeCN/H₂O, 7:18, 1 mL min⁻¹, 30 °C).

(**RS-12**) (2*R*,5*S*)-((2-(methoxycarbonyl)-1,4-phenylene)bis(oxy))bis(propane-3,1,2-triyl) tetraacetate



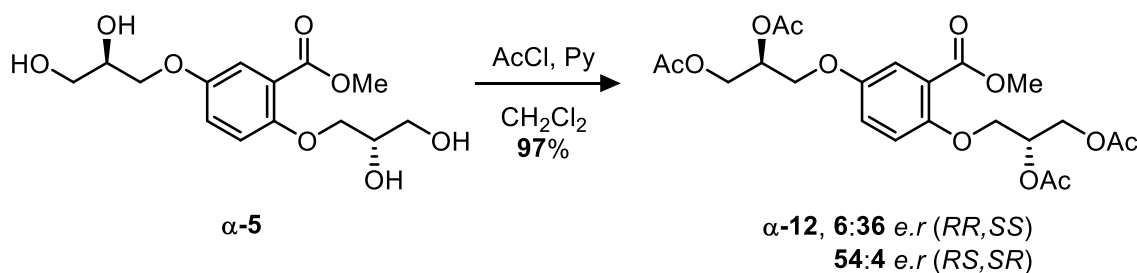
Following general procedure **G**: Using methyl 2-((*S*)-2,3-dihydroxypropoxy)-5-((*R*)-2,3-dihydroxypropoxy)benzoate (**SR-5**) (20 mg, 63 μ mol). The final product was purified by chromatography (SiO₂, EtOAc/Hexane 1:1, R_f = 0.29) yielding the title compound as a clear oil (29 mg, 99%); [α]_D²⁵ –5.44 (c. 1.0, CHCl₃, 100:00 *e.r* (2*R*5*S*, 2*S*5*R*)); **IR** V_{\max} cm^{–1} 2959 w, 2924 s, 1737 s (C=O), 1499 s, 1439 s; **¹H-NMR** (400 MHz, CDCl₃) δ_H 7.35 (d, J = 3.3 Hz, 1H, C6-H), 7.03 (dd, J = 9.1, 3.3 Hz, 1H, C4-H), 6.90 (d, J = 9.1 Hz, 1H, C3-H), 5.38 (m, 2H, CH-OAc), 4.49 (dd, J = 12.0, 3.9 Hz, 1H, CH₂-OAc), 4.42 (dd, J = 12.0, 3.9 Hz, 1H, CH₂-OAc), 4.34 (dd, J = 12.0, 6.1 Hz, 1H, CH₂-OAc), 4.28 (dd, J = 12.0, 6.1 Hz, 1H, CH₂-OAc), 4.15 (m, 2H, ArO-CH₂), 4.10 (d, J = 5.2 Hz, 2H, ArO-CH₂), 3.89 (s, 3H, Me), 2.11 (s, 3H, Ac), 2.11 (s, 3H, Ac), 2.08 (s, 3H, Ac), 2.08 (s, 3H, Ac); **¹³C-NMR** (101 MHz, CDCl₃) δ_C 170.8 (2C, Ac), 170.5 (Ac), 170.4 (Ac), 166.3 (CO₂Me), 152.6 (C1), 121.7 (C2 & C5), 120.5 (C4), 117.1 (C6), 116.1 (C3), 69.9 (CH-OAc), 69.8 (CH-OAc), 68.3 (ArO-CH₂), 66.9 (ArO-CH₂), 62.8 (CH₂-OAc), 62.6 (CH₂-OAc), 52.4 (Me), 21.1 (2C, Ac), 20.9 (2C, Ac); **LRMS** m/z (ESI⁺) 507.16 (100%, [M+Na]⁺); **HRMS** m/z (ESI⁺) C₂₂H₂₈O₁₂Na Requires: 507.1478, Found: 507.1479 ([M+Na]⁺); **chPLC** R_{t1} = 87.55 min, area = 100.00%. (Phenomenex® Cellulose-1, MeCN/H₂O, 7:18, 1 mL min^{–1}, 30 °C).

(SR-12) (2*S*,5*R*)-((2-(methoxycarbonyl)-1,4-phenylene)bis(oxy))bis(propane-3,1,2-triyl) tetraacetate



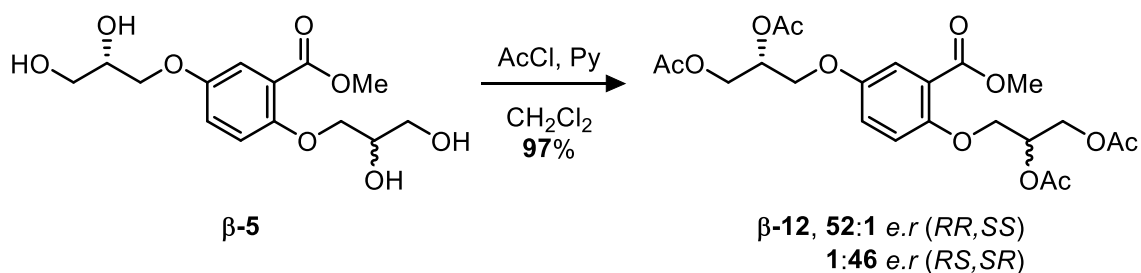
Following general procedure **G**: Using methyl 2-((*R*)-2,3-dihydroxypropoxy)-5-((*S*)-2,3-dihydroxypropoxy)benzoate (**RS-5**) (20 mg, 63 μ mol). The final product was purified by chromatography (SiO₂, EtOAc/Hexane 1:1, R_f = 0.29) yielding the title compound as a clear oil (29 mg, 99%). **[α]_D²⁵** +8.70 (c. 1.0, CHCl₃, 00:100 *e.r* (2*R*5*S*, 2*S*5*R*)); **IR** V_{\max} cm⁻¹ 2959 w, 2924 s, 1737 s (C=O), 1499 s, 1439 s; **¹H-NMR** (400 MHz, CDCl₃) δ_H 7.36 (d, J = 3.3 Hz, 1H, C6-H), 7.02 (dd, J = 9.1, 3.3 Hz, 1H, C4-H), 6.90 (d, J = 9.1 Hz, 1H, C3-H), 5.37 (m, 2H, CH-OAc), 4.49 (dd, J = 12.0, 3.9 Hz, 1H, CH₂-OAc), 4.42 (dd, J = 12.0, 3.9 Hz, 1H, CH₂-OAc), 4.33 (dd, J = 12.0, 6.1 Hz, 1H, CH₂-OAc), 4.28 (dd, J = 12.0, 6.1 Hz, 1H, CH₂-OAc), 4.15 (m, 2H, ArO-CH₂), 4.10 (d, J = 5.2 Hz, 2H, ArO-CH₂), 3.89 (s, 3H, Me), 2.11 (s, 3H, Ac), 2.11 (s, 3H, Ac), 2.08 (s, 3H, Ac), 2.07 (s, 3H, Ac); **¹³C-NMR** (101 MHz, CDCl₃) δ_C 170.78 (Ac), 170.75 (Ac), 170.5 (Ac), 170.4 (Ac), 166.3 (CO₂Me), 152.6 (C1), 121.7 (C2 & C5), 120.5 (C4), 117.1 (C6), 116.1 (C3), 69.9 (CH-OAc), 69.8 (CH-OAc), 68.3 (ArO-CH₂), 66.9 (ArO-CH₂), 62.8 (CH₂-OAc), 62.6 (CH₂-OAc), 52.4 (Me), 21.1 (2C, Ac), 20.9 (2C, Ac); **LRMS** m/z (ESI+) 507.16 (100%, [M+Na]⁺); **HRMS** m/z (ESI+) C₂₂H₂₈O₁₂Na Requires: 507.1478, Found: 507.1478 ([M+Na]⁺); **chPLC** R_t = 79.81 min, area = 100.00%. (Phenomenex® Cellulose-1, MeCN/H₂O, 7:18, 1 mL min⁻¹, 30 °C).

(α -12) (2*R*,5*S*)-((2-(methoxycarbonyl)-1,4-phenylene)bis(oxy))bis(propane-3,1,2-triyl) tetraacetate

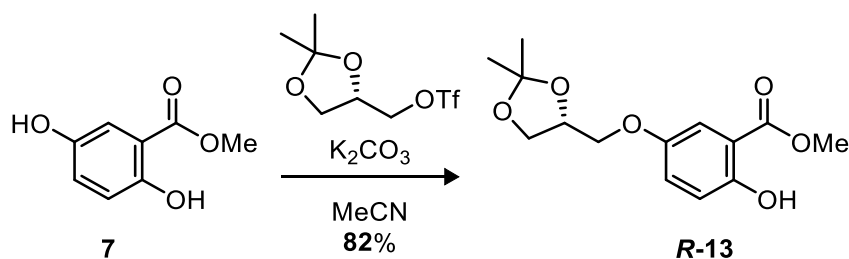


Following general procedure **G**: Methyl 5-((*R*)-2,3-dihydroxypropoxy)-2-((*S*)-2,3-dihydroxypropoxy)benzoate (**α -5**) (33 mg, 0.10 mmol) was charged with pyridine (67.0 μ L, 0.83 mmol), CH_2Cl_2 (4 mL) and the AcCl (59.0 μ L, 0.83 mmol) was added dropwise. Afforded the title compound as a clear oil (47 mg, 97%). [**α**]_D²⁵ –16.27 (c. 1.0, CHCl_3 , 6:36:54:4 *e.r/d.r* (2*R*5*R*, 2*S*5*S*, 2*R*5*S*, 2*S*5*R*)); **IR** V_{max} cm^{-1} 2959 w, 2924 w, 1737 s (C=O), 1499 s, 1440 s; **$^1\text{H-NMR}$** (400 MHz, CDCl_3) δ_{H} 7.35 (d, J = 3.3 Hz, 1H, C6-H), 7.02 (dd, J = 9.1, 3.3 Hz, 1H, C4-H), 6.89 (d, J = 9.1 Hz, 1H, C3-H), 5.37 (m, 2H, CH-OAc), 4.49 (dd, J = 12.0, 3.9 Hz, 1H, CH₂-OAc), 4.42 (dd, J = 12.0, 3.9 Hz, 1H, CH₂-OAc), 4.33 (dd, J = 12.0, 6.1 Hz, 1H, CH₂-OAc), 4.28 (dd, J = 12.0, 6.1 Hz, 1H, CH₂-OAc), 4.15 (m, 2H, ArO-CH₂), 4.10 (d, J = 5.2 Hz, 2H, ArO-CH₂), 3.89 (s, 3H, Me), 2.10 (s, 3H, Ac), 2.10 (s, 3H, Ac), 2.08 (s, 3H, Ac), 2.07 (s, 3H, Ac); **$^{13}\text{C-NMR}$** (101 MHz, CDCl_3) δ_{C} 170.8 (Ac), 170.7 (Ac), 170.44 (Ac), 170.39 (Ac), 166.3 (CO₂Me), 152.6 (C1), 121.7 (C2 & C5), 120.5 (C4), 117.0 (C6), 116.1 (C3), 69.8 (CH-OAc), 69.7 (CH-OAc), 68.3 (ArO-CH₂), 66.9 (ArO-CH₂), 62.8 (CH₂-OAc), 62.5 (CH₂-OAc), 52.3 (Me), 21.11 (Ac), 21.08 (Ac), 20.9 (2C, Ac); **LRMS** m/z (ESI+) 507.16 ([M+Na]⁺, 100%); **HRMS** m/z (ESI+) C₂₂H₂₈O₁₂Na Requires: 507.1478, Found: 507.1480 ([M+Na]⁺); **chPLC** $R_{\text{t}1}$ = 75.12 min, area = 5.71%; $R_{\text{t}2}$ = 81.73 min, area = 3.92%; $R_{\text{t}3}$ = 84.95 min, area = 54.64%; $R_{\text{t}4}$ = 114.38 min, area = 35.72%. (Phenomenex® Cellulose-1, MeCN/H₂O, 7:18, 1 mL min⁻¹, 30 °C).

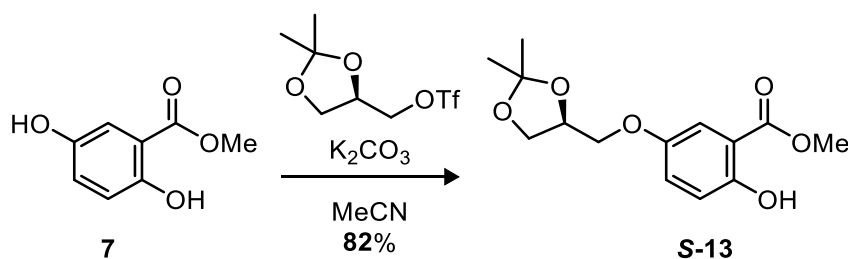
(β -12) (2 \pm ,5*R*)-((2-(methoxycarbonyl)-1,4-phenylene)bis(oxy))bis(propane-3,1,2-triyl) tetraacetate



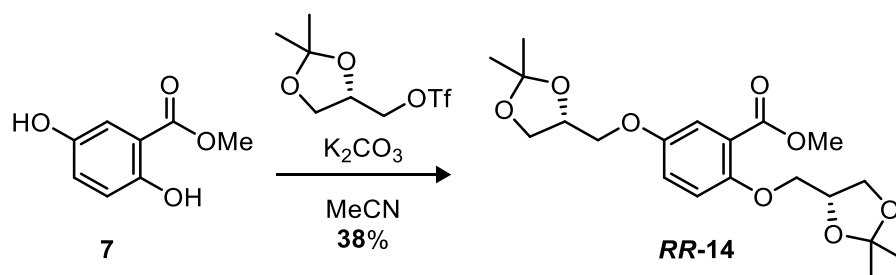
Following general procedure **G**: Methyl 5-((*S*)-2,3-dihydroxypropoxy)-2-((\pm)-2,3-dihydroxypropoxy)benzoate (**β -5**) (33 mg, 0.10 mmol) was charged with pyridine (67.0 μ L, 0.83 mmol), CH_2Cl_2 (4 mL) and the AcCl (59.0 μ L, 0.83 mmol) was added dropwise. Afforded the title compound as a clear oil (47 mg, 97%). [α]_D²⁵ –20.42 (c. 1.0, CHCl_3 , 52:1:1:46 *e.r/d.r* (*2R5R, 2S5S, 2R5S, 2S5R*)); **IR** V_{max} cm^{-1} 2959 w, 2922 w, 1736 s (C=O), 1500 s, 1439 s; **$^1\text{H-NMR}$** (400 MHz, CDCl_3) δ_{H} 7.35 (d, J = 3.3 Hz, 1H, C6-H), 7.02 (dd, J = 9.1, 3.3 Hz, 1H, C4-H), 6.90 (d, J = 9.1 Hz, 1H, C3-H), 5.38 (m, 2H, CH-OAc), 4.50 (dd, J = 12.0, 3.9 Hz, 1H, CH₂-OAc), 4.43 (dd, J = 12.0, 3.9 Hz, 1H, CH₂-OAc), 4.34 (dd, J = 12.0, 6.1 Hz, 1H, CH₂-OAc), 4.27 (dd, J = 12.0, 6.1 Hz, 1H, CH₂-OAc), 4.14 (m, 2H, ArO-CH₂), 4.10 (d, J = 5.2 Hz, 2H, ArO-CH₂), 3.88 (s, 3H, Me), 2.10 (s, 3H, Ac), 2.10 (s, 3H, Ac), 2.07 (s, 3H, Ac), 2.07 (s, 3H, Ac); **$^{13}\text{C-NMR}$** (101 MHz, CDCl_3) δ_{C} 170.74 (Ac), 170.72 (Ac), 170.5 (Ac), 170.4 (Ac), 166.3 (CO₂Me), 152.6 (C1), 121.7 (C2 & C5), 120.5 (C4), 117.0 (C6), 116.1 (C3), 69.8 (CH-OAc), 69.7 (CH-OAc), 68.3 (ArO-CH₂), 66.9 (ArO-CH₂), 62.7 (CH₂-OAc), 62.5 (CH₂-OAc), 52.3 (Me), 21.10 (Ac), 21.07 (Ac), 20.9 (2C, Ac); **LRMS** m/z (ESI+) 507.15 ($[\text{M}+\text{Na}]^+$, 100%); **HRMS** m/z (ESI+) $\text{C}_{22}\text{H}_{28}\text{O}_{12}\text{Na}$ Requires: 507.1478, Found: 507.1476 ($[\text{M}+\text{Na}]^+$); **CHPLC** $R_{\text{t}1}$ = 74.22 min, area = 51.55%; $R_{\text{t}2}$ = 80.80 min, area = 46.34%; $R_{\text{t}3}$ = 84.63 min, area = 1.14%; $R_{\text{t}4}$ = 114.59 min, area = 0.96%. (Phenomenex® Cellulose-1, MeCN/ H_2O , 7:18, 1 mL min⁻¹, 30 °C).

(R-13) Methyl (*R*)-5-((2,2-dimethyl-1,3-dioxolan-4-yl)methoxy)-2-hydroxybenzoate

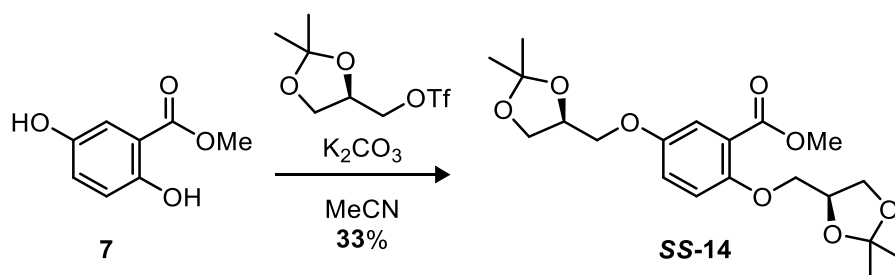
Following general procedure **E**: using methyl 2,5-dihydroxybenzoate (**7**) (169 mg, 1.0 mmol), K₂CO₃ (264 mg, 2.0 mmol) and (*S*)-(2,2-dimethyl-1,3-dioxolan-4-yl)methyl trifluoromethanesulfonate (390 mg, 1.5 mmol). The reaction mixture was heated under reflux for 12 h and monitored (EtOAc/hexane 1:9, *R_f* = 0.31). The crude oil was purified by chromatography (SiO₂, EtOAc/hexane, 1:9) to yield the title compound as a clear oil (230 mg, 82%). [α]_D²⁵ +3.46 (c. 1.0, CHCl₃); **IR** V_{max} cm⁻¹ 3217 br w (O-H), 2986 w, 2953 w, 2878 w, 1679 w (C=O), 1615 m, 1488, 1440 m; **¹H-NMR** (400 MHz, CDCl₃) δ _H 10.28 (s, 1H, C2-OH), 7.18 (d, *J* = 3.2 Hz, 1H, C6-H), 6.98 (dd, *J* = 9.0, 3.2 Hz, 1H, C4-H), 6.79 (d, *J* = 9.0 Hz, 1H, C3-H), 4.35 (p, *J* = 6.0 Hz, 1H, CH-OC(CH₃)₂), 4.05 (dd, *J* = 8.5, 6.4 Hz, 1H, CH₂-OC(CH₃)₂), 3.90 (dd, *J* = 9.5, 5.6 Hz, 1H, C5-OCH₂), 3.82 (s, 3H, Me), 3.79 (m, 2H, C5-OCH₂ & CH₂-OC(CH₃)₂), 1.37 (s, 3H, C(CH₃)₂), 1.30 (s, 3H, C(CH₃)₂); **¹³C-NMR** (101 MHz, CDCl₃) δ _C 170.0 (C=O), 156.2 (C2), 150.8 (C5), 124.3 (C4), 118.3 (C3), 112.8 (C6), 111.7 (C1), 109.5 (C(CH₃)₂), 73.9 (CH-OC(CH₃)₂), 69.5 (C5-OCH₂), 66.6 (CH₂-OC(CH₃)₂), 52.1 (Me), 26.6 (C(CH₃)₂), 25.2 (C(CH₃)₂); **LRMS** *m/z* (ESI+) 305.10 (100%, [M+Na]⁺); **HRMS** *m/z* (ESI+) C₁₄H₁₈O₆Na Requires: 305.1001, Found: 305.0998 ([M+Na]⁺).

(S-13) Methyl (*S*)-5-((2,2-dimethyl-1,3-dioxolan-4-yl)methoxy)-2-hydroxybenzoate

Following general procedure **E**: using methyl 2,5-dihydroxybenzoate (**7**) (169 mg, 1.0 mmol), K_2CO_3 (264 mg, 2.0 mmol) and (*R*)-(2,2-dimethyl-1,3-dioxolan-4-yl)methyl trifluoromethanesulfonate (390 mg, 1.5 mmol). The reaction mixture was heated under reflux for 12 h and monitored (EtOAc/hexane 1:9, $R_f = 0.31$). The crude oil was purified by chromatography (SiO_2 , EtOAc/hexane, 1:9) to yield the title compound as a clear oil (231 mg, 82%). **[α]_D²⁵** -2.77 (c. 1.0, CHCl_3); **IR** V_{max} cm^{-1} 3215 br w (O-H), 2985 w, 2953 w, 2878 w, 1680 w (C=O), 1615 m, 1486, 1440 m; **¹H-NMR** (400 MHz, CDCl_3) δ_{H} 10.37 (s, 1H, C2-OH), 7.29 (d, $J = 3.2$ Hz, 1H, C6-H), 7.10 (dd, $J = 9.0, 3.2$ Hz, 1H, C4-H), 6.90 (d, $J = 9.0$ Hz, 1H, C3-H), 4.45 (p, $J = 6.0$ Hz, 1H, CH-OC(CH₃)₂), 4.15 (dd, $J = 8.5, 6.4$ Hz, 1H, CH₂-OC(CH₃)₂), 4.01 (dd, $J = 9.5, 5.6$ Hz, 1H, C5-OCH₂), 3.92 (s, 3H, Me), 3.88 (m, 2H, C5-OCH₂ & CH₂-OC(CH₃)₂), 1.46 (s, 3H, C(CH₃)₂), 1.39 (s, 3H, C(CH₃)₂); **¹³C-NMR** (101 MHz, CDCl_3) δ_{C} 170.3 (CO₂Me), 156.5 (C2), 151.1 (C5), 124.7 (C4), 118.7 (C3), 113.1 (C6), 112.0 (C1), 109.9 (C(CH₃)₂), 74.1 (CH-OC(CH₃)₂), 69.8 (C5-OCH₂), 66.9 (CH₂-OC(CH₃)₂), 52.4 (Me), 26.9 (C(CH₃)₂), 25.4 (C(CH₃)₂); **LRMS** m/z (ESI+) 305.10 (100%, $[\text{M}+\text{Na}]^+$); **HRMS** m/z (ESI+) $\text{C}_{14}\text{H}_{18}\text{O}_6\text{Na}$ Requires: 305.1001, Found: 305.1000 ($[\text{M}+\text{Na}]^+$).

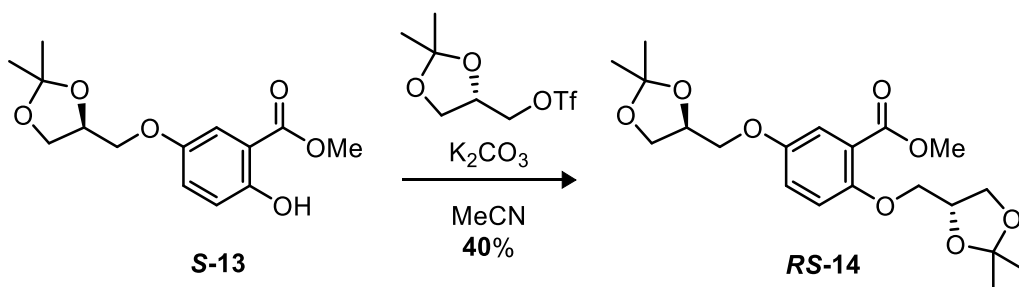
(RR-14) Methyl 2,5-bis(((*R*)-2,2-dimethyl-1,3-dioxolan-4-yl)methoxy)benzoate

Adapted from general procedure **E**: using methyl 2,5-dihydroxybenzoate (**7**) (169 mg, 1.0 mmol), K_2CO_3 (396 mg, 2.0 mmol) and (*S*)-(2,2-dimethyl-1,3-dioxolan-4-yl)methyl trifluoromethanesulfonate (792 mg, 3.0 mmol). The reaction mixture was heated under reflux for 12 h and monitored (EtOAc/hexane 1:4, $R_f = 0.53$). The crude oil was purified by chromatography (SiO_2 , EtOAc/hexane, 1:4) and recrystallized (hexane) to yield the title compound as large white crystals (150 mg, 38%). **M.P** 65 – 67 °C; $[\alpha]_D^{25} -25.27$ (c. 1.0, CHCl_3 , *er* 100:0 (*2R5R*, *2S5S*)); **IR** $\text{V}_{\text{max}} \text{ cm}^{-1}$ 2987 w, 2943 w, 2885 w, 1732 s (C=O), 1500 s, 1439 w; **$^1\text{H-NMR}$** (400 MHz, CDCl_3) δ_{H} 7.34 (d, $J = 3.2$ Hz, 1H, C6-H), 7.03 (dd, $J = 9.0, 3.2$ Hz, 1H, C4-H), 6.94 (d, $J = 9.0$ Hz, 1H, C3-H), 4.52 – 4.41 (m, 2H, $\text{CH-OC}(\text{CH}_3)_2$), 4.16 (ddd, $J = 8.7, 6.3, 2.5$ Hz, 2H, $\text{CH}_2\text{-OC}(\text{CH}_3)_2$), 4.10 (dd, $J = 9.4, 4.7$ Hz, 1H, ArO- CH_2), 4.06 – 3.99 (m, 2H, ArO- CH_2 & $\text{CH}_2\text{-OC}(\text{CH}_3)_2$), 3.99 – 3.89 (m, 2H, ArO- CH_2), 3.87 (m, 4H, Me & $\text{CH}_2\text{-OC}(\text{CH}_3)_2$), 1.45 (obsv. d, $J = 5.3$ Hz, 6H, $\text{C}(\text{CH}_3)_2$), 1.39 (obsv. d, $J = 2.9$ Hz, 6H, $\text{C}(\text{CH}_3)_2$); **$^{13}\text{C-NMR}$** (101 MHz, CDCl_3) δ_{C} 166.4 (CO_2Me), 152.8 (C2/C5), 152.7 (C2/C5), 121.6 (C1), 120.4 (C4), 116.8 (C6), 116.5 (C3), 109.9 ($\text{C}(\text{CH}_3)_2$), 109.7 ($\text{C}(\text{CH}_3)_2$), 74.1 ($\text{CH-OC}(\text{CH}_3)_2$), 74.1 ($\text{CH-OC}(\text{CH}_3)_2$), 70.9 (ArO- CH_2), 69.6 (ArO- CH_2), 67.1 ($\text{CH}_2\text{-OC}(\text{CH}_3)_2$), 66.8 ($\text{CH}_2\text{-OC}(\text{CH}_3)_2$), 52.2 (Me), 26.9 ($\text{C}(\text{CH}_3)_2$), 26.9 ($\text{C}(\text{CH}_3)_2$), 25.5 ($\text{C}(\text{CH}_3)_2$), 25.5 ($\text{C}(\text{CH}_3)_2$); **LRMS** m/z (ESI+) 419.17 (100%, $[\text{M}+\text{Na}]^+$); **HRMS** m/z (ESI+) $\text{C}_{20}\text{H}_{28}\text{O}_8\text{Na}$ Requires: 419.1682, Found: 419.1685 ($[\text{M}+\text{Na}]^+$).

(SS-14) Methyl 2,5-bis(((*S*)-2,2-dimethyl-1,3-dioxolan-4-yl)methoxy)benzoate

Adapted from general procedure **E**: using methyl 2,5-dihydroxybenzoate (**7**) (169 mg, 1.0 mmol), K_2CO_3 (396 mg, 2.0 mmol) and (*R*)-(2,2-dimethyl-1,3-dioxolan-4-yl)methyl trifluoromethanesulfonate (792 mg, 3.0 mmol). The reaction mixture was heated under reflux for 12 h and monitored (EtOAc/hexane 1:4, $R_f = 0.53$). The crude oil was purified by chromatography (SiO_2 , EtOAc/hexane, 1:4) and recrystallized (hexane) to yield the title compound as large white crystals (130 mg, 33%). **M.P** 66 – 68 °C; $[\alpha]_D^{25} +22.16$ (c. 1.0, $CHCl_3$, *er* <1:99 (*2R5R*, *2S5S*)); **IR** V_{max} cm^{-1} 2986 w, 2937 w, 2885 w, 1732 s (C=O), 1499 w, 1439 w; **1H -NMR** (400 MHz, $CDCl_3$) δ_H 7.34 (d, $J = 3.2$ Hz, 1H, C6-H), 7.03 (dd, $J = 9.0, 3.2$ Hz, 1H, C4-H), 6.94 (d, $J = 9.0$ Hz, 1H, C3-H), 4.51 – 4.41 (m, 2H, \underline{CH} -OC(CH₃)₂), 4.16 (ddd, $J = 8.7, 6.3, 2.5$ Hz, 2H, \underline{CH}_2 -OC(CH₃)₂), 4.10 (dd, $J = 9.4, 4.7$ Hz, 1H, ArO- \underline{CH}_2), 4.06 – 3.98 (m, 2H, Ar-O \underline{CH}_2 & \underline{CH}_2 -OC(CH₃)₂), 3.98 – 3.91 (m, 2H, Ar-O \underline{CH}_2), 3.91 – 3.85 (m, 4H, Me & \underline{CH}_2 -OC(CH₃)₂), 1.45 (obsv. d, $J = 5.3$ Hz, 6H, C(\underline{CH}_3)₂), 1.39 (obsv. d, $J = 2.9$ Hz, 6H, C(\underline{CH}_3)₂); **^{13}C -NMR** (101 MHz, $CDCl_3$) δ_C 166.4 (\underline{CO}_2 Me), 152.8 (C2/C5), 152.7 (C2/C5), 121.6 (C1), 120.4 (C4), 116.8 (C6), 116.5 (C3), 109.9 ($\underline{C}(\underline{CH}_3)_2$), 109.7 ($\underline{C}(\underline{CH}_3)_2$), 74.1 (\underline{CH} -OC(CH₃)₂), 74.1 (\underline{CH} -OC(CH₃)₂), 70.9 (ArO- \underline{CH}_2), 69.6 (ArO- \underline{CH}_2), 67.1 (\underline{CH}_2 -OC(CH₃)₂), 66.8 (\underline{CH}_2 -OC(CH₃)₂), 52.2 (Me), 26.9 (C(\underline{CH}_3)₂), 26.9 (C(\underline{CH}_3)₂), 25.5 (C(\underline{CH}_3)₂), 25.5 (C(\underline{CH}_3)₂); **LRMS** m/z (ESI+) 419.17 (100%, $[M+Na]^+$); **HRMS** m/z (ESI+) $C_{20}H_{28}O_8Na$ Requires: 419.1682, Found: 419.1678 ($[M+Na]^+$).

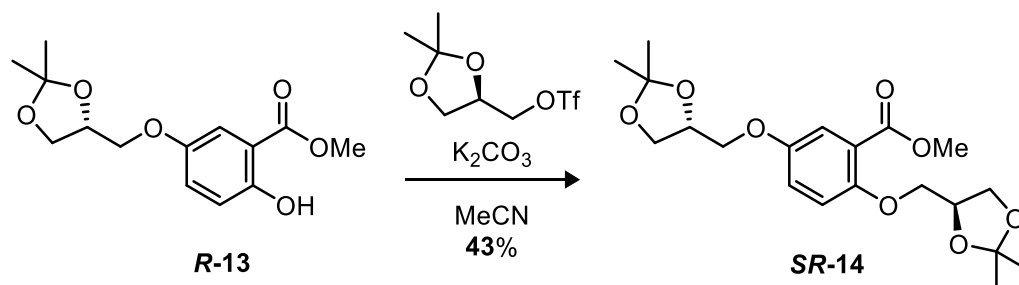
(**RS-14**) Methyl 2-(((*R*)-2,2-dimethyl-1,3-dioxolan-4-yl)methoxy)-5-(((*S*)-2,2-dimethyl-1,3-dioxolan-4-yl)methoxy)benzoate



Adapted from general procedure **E**: using methyl (*S*)-5-((2,2-dimethyl-1,3-dioxolan-4-yl)methoxy)-2-hydroxybenzoate (**S-13**) (282 mg, 1.0 mmol), K_2CO_3 (264 mg, 2.0 mmol) and (*S*)-(2,2-dimethyl-1,3-dioxolan-4-yl)methyl trifluoromethanesulfonate (390 mg, 1.5 mmol). The reaction mixture was heated under reflux for 12 h and monitored (EtOAc/hexane 1:4, $R_f = 0.53$). The crude oil was purified by chromatography (SiO_2 , EtOAc/hexane, 1:4) and recrystallized (hexane) to yield the title compound as large white crystals (160 mg, 40%). **M.P** 85 – 87 °C; $[\alpha]_D^{25} -4.54$ (c. 1.0, CHCl_3 *d.r* 100:0 (*2R5S*, *2S5R*)); **IR** ν_{max} cm^{-1} 2986 w, 2935 w, 2880 w, 1731 s (C=O), 1584 w, 1499 s; **¹H-NMR** (400 MHz, CDCl_3) δ_{H} 7.34 (d, $J = 3.2$ Hz, 1H, C6-H), 7.03 (dd, $J = 9.0, 3.2$ Hz, 1H, C4-H), 6.94 (d, $J = 9.0$ Hz, 1H, C3-H), 4.51 – 4.42 (m, 2H, CH-OC(CH₃)₂), 4.16 (ddd, $J = 8.8, 6.4, 2.7$ Hz, 2H, CH₂-OC(CH₃)₂), 4.10 (dd, $J = 9.4, 4.7$ Hz, 1H, ArO-CH₂), 4.06 – 3.98 (m, 2H, Ar-OCH₂ & CH₂-OC(CH₃)₂), 3.98 – 3.91 (m, 2H, Ar-OCH₂), 3.91 – 3.84 (m, 4H, Me & CH₂-OC(CH₃)₂), 1.45 (obsv. d, $J = 5.3$ Hz, 6H, C(CH₃)₂), 1.40 (obsv. d, $J = 2.9$ Hz, 6H, C(CH₃)₂); **¹³C-NMR** (101 MHz, CDCl_3) δ_{C} 166.4 (CO₂Me), 152.8 (C2/C5), 152.7 (C2/C5), 121.6 (C1), 120.4 (C4), 116.8 (C6), 116.5 (C3), 109.9 (C(CH₃)₂), 109.7 (C(CH₃)₂), 74.1 (CH-OC(CH₃)₂), 74.1 (CH-OC(CH₃)₂), 70.9 (ArO-CH₂), 69.6 (ArO-CH₂), 67.1 (CH₂-OC(CH₃)₂), 66.8 (CH₂-OC(CH₃)₂), 52.2 (Me), 26.9 (C(CH₃)₂), 26.9 (C(CH₃)₂), 25.5 (C(CH₃)₂), 25.5 (C(CH₃)₂); **LRMS** m/z (ESI+) 419.18 (100%,

$[M+Na]^+$); **HRMS** m/z (ESI+) $C_{20}H_{28}O_8Na$ Requires: 419.1682, Found: 419.1683 ($[M+Na]^+$).

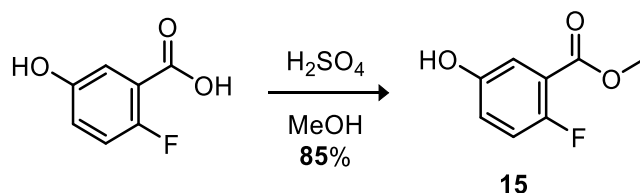
(SR-14) Methyl 2-(((*S*)-2,2-dimethyl-1,3-dioxolan-4-yl)methoxy)-5-(((*R*)-2,2-dimethyl-1,3-dioxolan-4-yl)methoxy)benzoate



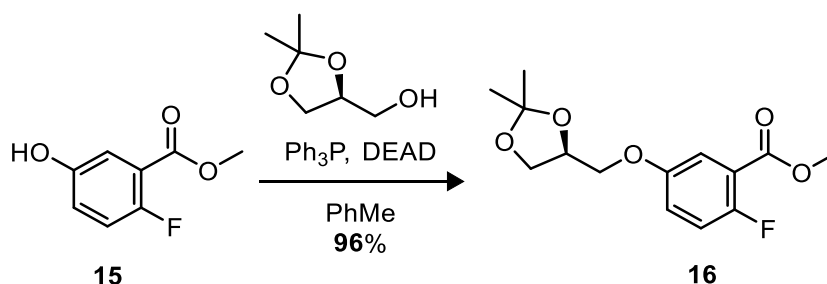
Adapted from general procedure **E**: using methyl (*R*)-5-((2,2-dimethyl-1,3-dioxolan-4-yl)methoxy)-2-hydroxybenzoate (**R-6**) (282 mg, 1.0 mmol), K_2CO_3 (264 mg, 2.0 mmol) and (*R*)-(2,2-dimethyl-1,3-dioxolan-4-yl)methyl trifluoromethanesulfonate (390 mg, 1.5 mmol). The reaction mixture was heated under reflux for 12 h and monitored (EtOAc/hexane 1:4, R_f = 0.53). The crude oil was purified by chromatography (SiO₂, EtOAc/hexane, 1:4) and recrystallized (hexane) to yield the title compound as large white crystals (172 mg, 43%). **M.P** 84 – 86 °C; $[\alpha]_D^{25} +9.69$ (c. 1.0, $CHCl_3$ *d.r* 0:100 (*2R5S*, *2S5R*)); **IR** V_{max} cm^{-1} 2986 w, 2935 w, 2880 w, 1731 s (C=O), 1584 w, 1499 w; **¹H-NMR** (400 MHz, $CDCl_3$) δ_H 7.34 (d, J = 3.2 Hz, 1H, C6-H), 7.03 (dd, J = 9.0, 3.2 Hz, 1H, C4-H), 6.94 (d, J = 9.0 Hz, 1H, C3-H), 4.51 – 4.42 (m, 2H, CH-OC(CH₃)₂), 4.16 (ddd, J = 8.8, 6.4, 2.7 Hz, 2H, CH₂-OC(CH₃)₂), 4.10 (dd, J = 9.4, 4.7 Hz, 1H, ArO-CH₂), 4.06 – 3.98 (m, 2H, Ar-OCH₂ & CH₂-OC(CH₃)₂), 3.98 – 3.91 (m, 2H, Ar-OCH₂), 3.91 – 3.84 (m, 4H, Me & CH₂-OC(CH₃)₂), 1.45 (obsv. d, J = 5.3 Hz, 6H, C(CH₃)₂), 1.40 (obsv. d, J = 2.9 Hz, 6H, C(CH₃)₂); **¹³C-NMR** (101 MHz, $CDCl_3$) δ_C 166.4 (C=O), 152.8 (C2/C5), 152.7 (C2/C5), 121.6 (C1), 120.4 (C4), 116.8 (C6), 116.5 (C3), 109.9 (C(CH₃)₂), 109.7 (C(CH₃)₂), 74.1 (CH-OC(CH₃)₂), 74.1 (CH-OC(CH₃)₂), 70.9 (ArO-CH₂), 69.6 (ArO-CH₂), 67.1 (CH₂-OC(CH₃)₂), 66.8 (CH₂-OC(CH₃)₂), 52.2 (Me), 26.9 (C(CH₃)₂).

26.9 ($\text{C}(\underline{\text{CH}_3})_2$), 25.5 ($\text{C}(\underline{\text{CH}_3})_2$), 25.5 ($\text{C}(\underline{\text{CH}_3})_2$); **LRMS** m/z (ESI+) 419.17 (100%, $[\text{M}+\text{Na}]^+$); **HRMS** m/z (ESI+) $\text{C}_{20}\text{H}_{28}\text{O}_8\text{Na}$ Requires: 419.1682, Found: 419.1685 ($[\text{M}+\text{Na}]^+$).

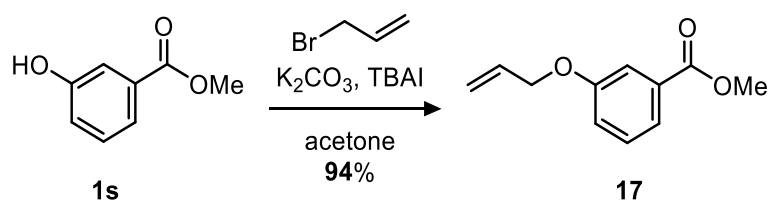
(15) Methyl 2-fluoro-5-hydroxybenzoate



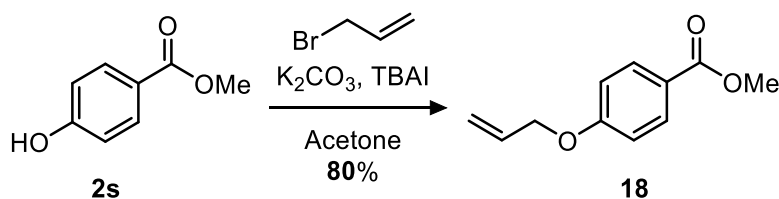
Following general procedure **A**: a solution of 2-fluoro-5-hydroxybenzoic acid (2.0 g, 12.8 mmol) in MeOH (50 mL) was charged with conc. H_2SO_4 (1 mL) and heated under reflux for 16 h. Recrystallization of the solid (CH_2Cl_2 /hexane) afforded the title compound as a long white crystals (1.85 g, 85%). **M.P** 102 – 104 °C; **IR** $\text{V}_{\text{max}} \text{ cm}^{-1}$ 3415m (O-H), 3360m (O-H), 2956w (C-H), 1700s (C=O), 1590m (C-C), 1502m (C-C), 1438s (C-H); **$^1\text{H-NMR}$** (400 MHz, CDCl_3) δ_{H} 7.50 – 7.44 (app. m, 1H, C6H), 7.07 – 7.00 (m, 2H, C3-H & C4-H), 5.89 (br s, 1H, C5OH), 3.96 (s, 3H, Me); **$^{13}\text{C-NMR}$** (101 MHz, CDCl_3) δ_{C} 165.7 (d, $J = 4.2$ Hz, $\underline{\text{CO}_2\text{Me}}$), 156.4 (d, $J = 253$ Hz, C2), 151.8 (d, $J = 2.8$ Hz, C5), 121.9 (d, $J = 8.7$ Hz, C4), 118.5 (d, $J = 12.0$ Hz, C1), 118.1 (d, $J = 24.7$ Hz, C3), 117.8 (C6), 52.8 (Me); **LRMS** m/z (ESI+) 170.03 ($[\text{M}]^+$, 75%) 139.01 ($[\text{M}-\text{CH}_3\text{OH}]^+$, 100%); **HRMS** m/z (ESI+) $\text{C}_8\text{H}_7\text{O}_3\text{F}$ Requires: 170.0379, Found: 170.0375 ($[\text{M}]^+$).

(16) Methyl (*S*)-5-((2,2-dimethyl-1,3-dioxolan-4-yl)methoxy)-2-fluorobenzoate

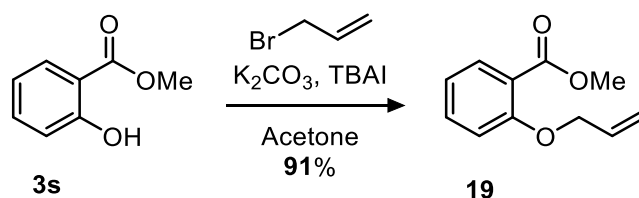
A flask containing methyl 2-fluoro-5-hydroxybenzoate (**15**) (1.0 g, 5.88 mmol), Ph_3P (1.85 g, 7.06 mmol) in anhydrous toluene (100 mL) was heated to 50 °C and charged dropwise with DEAD (1.101 mL, 7.06 mmol). The flask was stirred for 10 min at 50 °C and charged dropwise with *S*-solketal (0.88 mL, 7.06 mmol). After full addition the flask was heated at 90 °C for 16 h. The solvent was removed under reduced pressure and the Ph_3PO triturated with hexane. Filtration of the solid and removal of solvent under reduced pressure afforded a crude orange mixture. The crude mixture was purified directly by chromatography (SiO_2 , EtOAc/Hex, 1:3) afforded the title compound as clear oil (1.20 g, 96%). **IR** V_{max} cm^{-1} 2986 s (O-H), 2950 s, 1719 s (C=O), 1614 w, 1498 s, 1440 s; **$^1\text{H-NMR}$** (400 MHz, CDCl_3) δ_{H} 7.41 (m, 1H, C6-H), 7.10 – 6.99 (m, 2H, C3-H & C4-H), 4.46 (p, 5.6 Hz, 1H, CH-OC(CH₃)₂), 4.15 (dd, J = 8.5, 6.0 Hz, 1H, CH₂-OC(CH₃)₂), 4.03 (dd, J = 9.5, 6.0 Hz, 1H, C5-OCH₂), 3.94 (dd, J = 9.5, 6.0 Hz, 1H, C5-OCH₂), 3.91 (s, 3H, Me), 3.87 (dd, J = 8.5, 6.0 Hz, 1H, CH₂-OC(CH₃)₂), 1.44 (s, C(CH₃)₂), 1.39 (s, 3H, C(CH₃)₂); **$^{13}\text{C-NMR}$** (101 MHz, CDCl_3) δ_{C} 164.8 (d, J = 3.9 Hz, CO₂Me), 156.7 (d, J = 253.5 Hz, C2), 154.4 (C5), 121.5 (d, J = 8.5 Hz, C4), 118.8 (d, J = 11.6 Hz, C1), 117.9 (d, J = 24.8 Hz, C3), 116.2 (C6), 109.9 (C(CH₃)₂), 74.0 (CH-OC(CH₃)₂), 69.6 (C5-OCH₂), 66.7 (CH₂-OC(CH₃)₂), 52.5 (Me), 26.8 (C(CH₃)₂), 25.4 (C(CH₃)₂); **LRMS** m/z (ESI+) 307.09 ($[\text{M}+\text{Na}]^+$, 100%); **HRMS** m/z (ESI+) C₁₄H₁₇O₅FNa Requires: 307.0958, Found: 307.0961 ($[\text{M}+\text{Na}]^+$).

(17) Methyl 3-(allyloxy)benzoate

Following general procedure **B**: methyl 3-hydroxybenzoate (**1s**) (760 mg, 5.0 mmol), K_2CO_3 (829 mg, 6.0 mmol) and TBAI (806 mg, 2.5 mmol) in acetone (25 mL) was charged with allyl bromide (0.52 mL, 6.0 mmol) and heated under reflux for 4 h. Purification by chromatography (SiO_2 , EtOAc/hexane 1:9, R_f = 0.74) yielded the title compound as a clear oil (900 mg, 94%). **IR** V_{max} cm^{-1} 3020 w, 2950 w, 1720 s (C=O), 1586 w, 1445 w; **1H -NMR** (400 MHz, $CDCl_3$) δ_H 7.63 (dt, J = 8.0, 1.2 Hz, 1H, C6-H), 7.57 (dd, J = 2.7, 1.2 Hz, 1H, C2-H), 7.33 (app. t, J = 8.0 Hz, 1H, C5-H), 7.11 (ddd, J = 8.0, 2.7, 1.2 Hz, 1H, C4-H), 6.05 (ddt, J = 17.3, 10.5, 5.2 Hz, 1H, CH=CH₂), 5.42 (dd, J = 17.3, 1.5 Hz, 1H, CH=CH₂), 5.29 (dd, J = 10.5, 1.5 Hz, 1H, CH=CH₂), 4.57 (d, J = 5.2 Hz, 2H, C3-OCH₂), 3.90 (s, 3H, Me); **^{13}C -NMR** (101 MHz, $CDCl_3$) δ_C 167.0 (CO₂Me), 158.6 (C3), 133.0 (CH=CH₂), 131.5 (C1), 129.5 (C5), 122.3 (C6), 120.3 (C4), 118.0 (CH=CH₂), 115.0 (C2), 69.0 (C3-OCH₂), 52.3 (Me). **LRMS** m/z (ESI+) 192.06 ($[M]^+$, 100%), 177.04 (80%, $[M-CH_3]^+$), 161.05 (65%, $[M-CH_3OH]^+$), 92.02 (70%); **HRMS** m/z (ESI+) $C_{11}H_{12}O_3$ Requires: 192.0786, Found: 192.0785 ($[M]^+$).

(18) Methyl 4-(allyloxy)benzoate

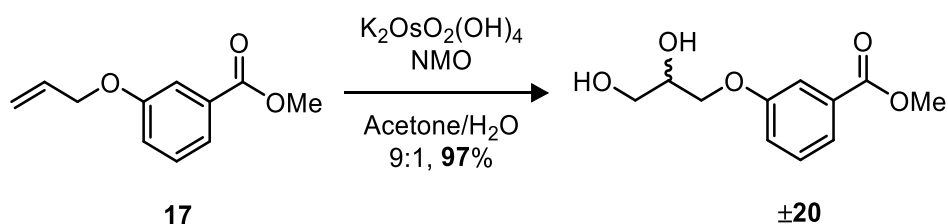
Following general procedure **B**: methyl 4-hydroxybenzoate (**2s**) (760 mg, 5.0 mmol), K₂CO₃ (829 mg, 6.0 mmol) and TBAI (806 mg, 2.5 mmol) in acetone (25 mL) was charged with allyl bromide (0.52 mL, 6.0 mmol) and heated under reflux for 4 h. Purification by chromatography (SiO₂, EtOAc/hexane 1:9, *R_f* = 0.57) yielded the title compound as a clear oil (768 mg, 80%); **IR** ν_{max} cm⁻¹ 2951 w, 1712 s (C=O), 1603 s, 1579 w, 1509 s, 1434 s; **¹H-NMR** (400 MHz, CDCl₃) δ 7.99 – 7.93 (m, 2H, C3-H), 6.93 – 6.87 (m, 2H, C2-H), 6.02 (ddt, *J* = 17.3, 10.5, 5.3 Hz, 1H, CH=CH₂), 5.40 (dq, *J* = 17.3, 1.5 Hz, 1H, CH=CH₂), 5.29 (dq, *J* = 10.5, 1.5 Hz, 1H, CH=CH₂), 4.55 (dt, *J* = 5.3, 1.6 Hz, 2H, C4-OCH₂), 3.86 (s, 3H, Me); **¹³C-NMR** (101 MHz, CDCl₃) δ 166.8 (C=O), 162.3 (C4), 132.6 (CH=CH₂), 131.6 (C3), 122.7 (C1), 118.1 (CH=CH₂), 114.3 (C2), 68.8 (C4-OCH₂), 51.9 (Me); **LRMS** *m/z* (ESI+) 192.06 (100%, [M]⁺), 161.04 (80%, [M-CH₃OH]⁺), 133.06 (70%); **HRMS** *m/z* (ESI+) C₁₁H₁₂O₃ Requires: 192.0786, Found: 192.0782 ([M]⁺).

(19) Methyl 2-(allyloxy)benzoate

Following general procedure **B**: methyl salicylate (**3s**) (760 mg, 5.0 mmol), K₂CO₃ (829 mg, 6.0 mmol) and TBAI (806 mg, 2.5 mmol) in acetone (25 mL) was charged with allyl bromide (0.52 mL, 6.0 mmol) and heated under reflux for 4 h. Purification by

chromatography (SiO₂, EtOAc/hexane 1:9, *R_f* = 0.55) yielded the title compound as a clear oil (882 mg, 91%). **IR** V_{\max} cm⁻¹ 2951 w, 1723 s (C=O), 1599 m, 1489 m, 1449; **¹H-NMR** (400 MHz, CDCl₃) δ_{H} 7.77 (dd, *J* = 7.5, 1.8 Hz, 1H, C6-H), 7.39 (ddd, *J* = 8.3, 7.5, 1.8 Hz, 1H, C5-H), 6.99 – 6.86 (m, 2H, C4-H & C3-H), 6.02 (ddt, *J* = 17.3, 10.6, 4.9 Hz, 1H, CH=CH₂), 5.49 (dq, *J* = 17.3, 1.7 Hz, 1H, CH=CH₂), 5.26 (dq, *J* = 10.6, 1.7 Hz, 1H, CH=CH₂), 4.57 (dt, *J* = 4.9, 1.7 Hz, 2H, C2-OCH₂), 3.85 (s, 3H, Me); **¹³C-NMR** (101 MHz, CDCl₃) δ_{C} 166.7 (CO₂Me), 158.0 (C2), 133.3 (C5), 132.7 (CH=CH₂), 131.6 (C6), 120.5 (C1), 120.3 (C4), 117.2 (CH=CH₂), 113.6 (C3), 69.3 (C2-OCH₂), 51.9 (Me); **LRMS** *m/z* (ESI+) 192.08 (80%, [M]⁺), 160.05 (70%, [M-CH₃OH]⁺), 132.05 (100%); **HRMS** *m/z* (ESI+) C₁₁H₁₂O₃ Requires: 192.0786, Found: 192.0784 ([M]⁺).

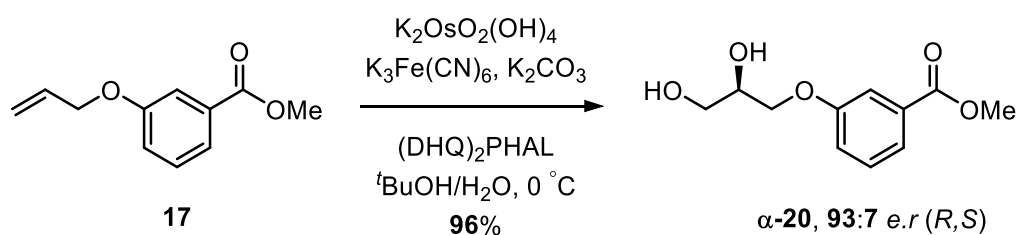
(±20) Methyl (±)-3-(2,3-dihydroxypropoxy)benzoate



Following general procedure **C**: NMO (140 mg, 1.20 mmol) was charged with acetone/H₂O (9:1, 10 mL) and K₂OsO₂(OH)₄ (3.7 mg, 0.01 mmol). Methyl 3-(allyloxy)benzoate (**17**) (192 mg, 1.00 mmol) was added, the reaction mixture was heated at 40 °C for 8 h and monitored (TLC, EtOAc/hexane 1:1, *R_f* = 0.19). Afforded the title compound as a clear oil (220 mg, 97%). **IR** V_{\max} cm⁻¹ 3408 br (O-H), 2951 w, 1706 s (C=O), 1600 w; **¹H-NMR** (400 Hz, (CD₃)₂SO) δ_{H} 7.54 (dt, *J* = 7.7, 1.2 Hz, 1H, C6-H), 7.45 (app. t, *J* = 1.2 Hz, 1H, C2-H), 7.42 (obsv. d, *J* = 7.7 Hz, 1H, C5-H), 7.23 (ddd, *J* = 8.2, 2.7, 1.2 Hz, 1H, C4-H), 5.01 (d, *J* = 5.1 Hz, 1H, CH-OH), 4.72 (t, *J* = 5.7 Hz, 1H, CH₂-OH), 4.05 (dd, *J* = 9.8, 4.0 Hz, 1H, C3-OCH₂), 3.90 (dd, *J* = 9.8,

6.0 Hz, 1H, C3-OCH₂), 3.85 (s, 3H, Me), 3.80 (pd, J = 6.0, 4.0 Hz, 1H, CH-OH), 3.52 – 3.42 (m, 2H, CH₂-OH); **¹³C-NMR** (101 MHz, (CD₃)₂SO) δ_c 166.1 (CO₂Me), 158.9 (C3), 131.0 (C1), 130.0 (C5), 121.4 (C6), 119.9 (C2), 114.4 (C4), 69.9 (C3-OCH₂), 69.9 (CH-OH), 62.6 (CH₂-OH), 52.3 (Me); **LRMS** (ESI+) 271.10 (90%, [M+2(Na)–H]⁺), 249.07 (100%, [M+Na]⁺); **HRMS** (ESI+) C₁₁H₁₄O₅Na Requires: 249.0739, Found: 249.0740 ([M+Na]⁺).

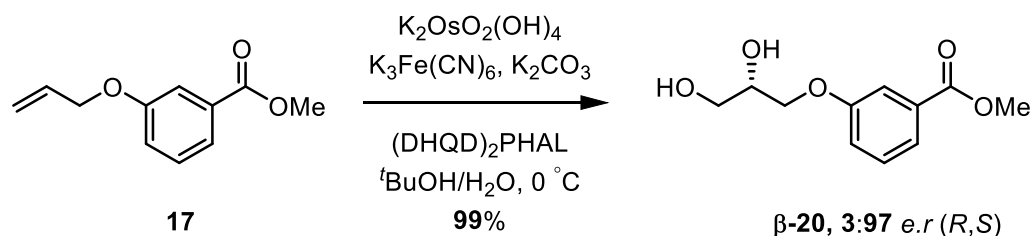
(α -20) Methyl (*R*)-3-(2,3-dihydroxypropoxy)benzoate



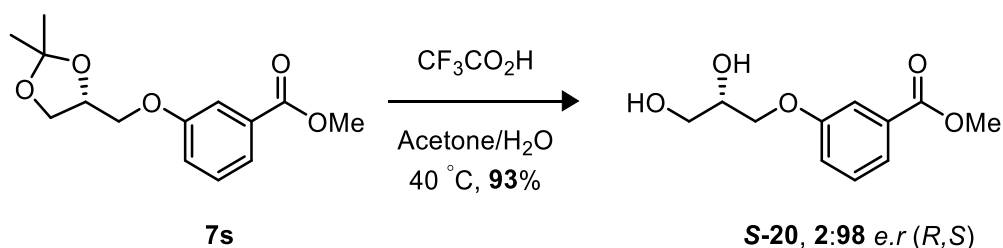
Following general procedure **D** using stock solutions: **I** (2 mL, 3.0 mmol), **II** (2 mL, 3.0 mmol), **III** (1.0 mL, 2.0 μ mol) and **IV** (5.0 mL, 20.0 μ mol). Methyl 3-(allyloxy)benzoate (**17**) (192 mg, 1.00 mmol) was added and the reaction mixture was stirred at 0 °C for 6 h with monitoring (EtOAc:hexane 1:1, R_f = 0.19). Afforded the title compound as a clear oil (218 mg, 96%). [α]_D²⁵ +4.50 (c. 1.0, CHCl₃, 93:7 *e.r* (*R,S*)); **IR** ν_{max} cm^{–1} 3241 br s (O-H), 2988 w, 2958 w, 2927 w, 2872 w, 1721 s (C=O), 1588 w, 1488 w, 1442 w; **¹H-NMR** (400 Hz, (CD₃)₂SO) δ_H 7.54 (dt, J = 7.7, 1.2 Hz, 1H, C6-H), 7.45 (app. t, J = 1.2 Hz, 1H, C2-H), 7.42 (obsv. d, J = 7.7 Hz, 1H, C5-H), 7.23 (ddd, J = 8.2, 2.7, 1.2 Hz, 1H, C4-H), 5.01 (d, J = 5.1 Hz, 1H, CH-OH), 4.72 (t, J = 5.7 Hz, 1H, CH₂-OH), 4.05 (dd, J = 9.8, 4.0 Hz, 1H, C3-OCH₂), 3.92 (dd, J = 9.8, 6.0 Hz, 1H, C3-OCH₂), 3.90 (s, 3H, Me), 3.88 – 3.76 (m, 1H, CH-OH), 3.45 (t, J = 5.7 Hz, 2H, CH₂-OH); **¹³C-NMR** (101 MHz, (CD₃)₂SO) δ_c 166.1 (CO₂Me), 158.9 (C3), 131.0 (C1), 130.0 (C5), 121.4 (C6), 119.9 (C2), 114.4 (C4), 69.9 (C3-OCH₂), 69.9 (CH-OH), 62.6 (CH₂-OH), 52.3 (Me); **LRMS** m/z (ESI+) 249.07 (100%,

$[M+Na]^+$); **HRMS** m/z (ESI+) $C_{11}H_{14}O_5Na$ Requires: 249.0739, Found: 249.0742 ($[M+Na]^+$).

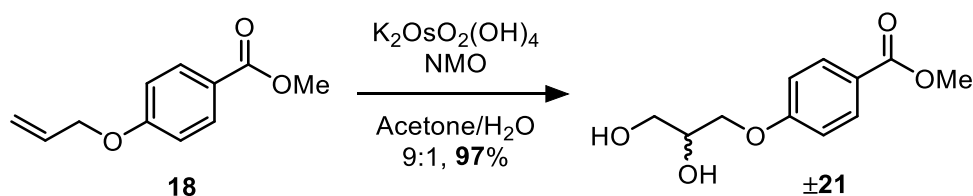
(**β -20**) Methyl (*S*)-3-(2,3-dihydroxypropoxy)benzoate



Following general procedure **D** using stock solutions: **I** (2 mL, 3.0 mmol), **II** (2 mL, 3.0 mmol), **III** (1.0 mL, 2.0 μmol) and **V** (5.0 mL, 20.0 μmol). Methyl 3-(allyloxy)benzoate (**17**) (192 mg, 1.00 mmol) was added and the reaction mixture was stirred at 0 $^\circ\text{C}$ for 6 h with monitoring (EtOAc:hexane 1:1, R_f = 0.19). Afforded the title compound as a clear oil (225 mg, 99%). **[α] $_D^{25}$** +8.65 (c. 1.0, CHCl_3 , 3:97 (*R,S*)); **IR** V_{max} cm^{-1} 3250 br s (O-H), 2988 w, 2987 w, 2956 w, 2925 w, 2872 w, 1722 s (C=O), 1587 w, 1488 w, 1443 w; **$^1\text{H-NMR}$** (400 Hz, $(\text{CD}_3)_2\text{SO}$) δ_{H} 7.54 (dt, J = 7.7, 1.2 Hz, 1H, C6-H), 7.45 (app. t, J = 1.2 Hz, 1H, C2-H), 7.42 (obsv. d, J = 7.7 Hz, 1H, C5-H), 7.23 (ddd, J = 8.2, 2.7, 1.2 Hz, 1H, C4-H), 4.99 (d, J = 5.1 Hz, 1H, CH-OH), 4.70 (t, J = 5.7 Hz, 1H, CH₂-OH), 4.05 (dd, J = 9.8, 4.0 Hz, 1H, C3-OCH₂), 3.92 (dd, J = 9.8, 6.0 Hz, 1H, C3-OCH₂), 3.90 (s, 3H, Me), 3.80 (pd, J = 6.0, 4.0 Hz, 1H, CH-OH), 3.52 – 3.33 (m, 2H, CH₂-OH); **$^{13}\text{C-NMR}$** (101 MHz, $(\text{CD}_3)_2\text{SO}$) δ_{C} 166.1 (CO₂Me), 158.9 (C3), 131.0 (C1), 130.0 (C5), 121.4 (C6), 119.9 (C2), 114.4 (C4), 69.9 (C3-OCH₂), 69.9 (CH-OH), 62.6 (CH₂-OH), 52.3 (Me); **LRMS** m/z (ESI+) 249.07 (100%, $[M+Na]^+$); **HRMS** m/z (ESI+) $C_{11}H_{14}O_5Na$ Requires: 249.0739, Found: 249.0739 ($[M+Na]^+$).

(S-20) Methyl (*S*)-3-(2,3-dihydroxypropoxy)benzoate

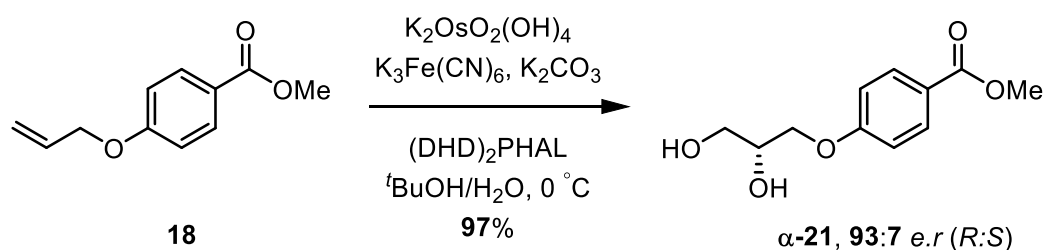
Following general procedure **F**: Methyl (*R*)-3-((2,2-dimethyl-1,3-dioxolan-4-yl)methoxy)benzoate (**7s**) (91 mg, 0.34 mmol) was stirred at 40 °C for 24 h. Afforded the title compound as a clear oil (71 mg, 93%). **[α]_D²⁵** −1.58 (c. 1.0, CHCl₃, 2:98 *e.r* (*R,S*)); **IR** Vmax cm^{−1} 3241 br s (O-H) 2988 w, 2958 w, 2927 w, 2872 w, 1721 s (C=O), 1588 w, 1488 w, 1442 w; **¹H-NMR** (400 Hz, (CD₃)₂SO) δ_H 7.54 (dt, *J* = 7.7, 1.2 Hz, 1H, C6-H), 7.45 (t, *J* = 1.2 Hz, 1H, C2-H), 7.42 (obsv. d, *J* = 7.7 Hz, 1H, C5-H), 7.23 (ddd, *J* = 8.2, 2.7, 1.2 Hz, 1H, C4-H), 4.99 (d, *J* = 5.1 Hz, 1H, CH-OH), 4.72 (t, *J* = 5.7 Hz, 1H, CH₂-OH), 4.05 (dd, *J* = 9.8, 4.0 Hz, 1H, C3-OCH₂), 3.90 (dd, *J* = 9.8, 6.0 Hz, 1H, C3-OCH₂), 3.85 (s, 3H, Me), 3.84 – 3.73 (m, 1H, CH-OH), 3.45 (t, *J* = 5.7 Hz, 2H, CH₂-OH); **¹³C-NMR** (101 MHz, (CD₃)₂SO) δ_C 166.1 (C=O), 158.9 (C3), 130.9 (C1), 130.0 (C5), 121.3 (C6), 119.9 (C2), 114.4 (C4), 69.9 (C3-OCH₂), 69.9 (CH-OH), 62.6 (CH₂-OH), 52.2 (Me); **LRMS** *m/z* (ESI+) 249.07 (100%, [M+Na]⁺); **HRMS** *m/z* (ESI+) C₁₁H₁₄O₅Na Requires: 249.0739, Found: 249.0741 ([M+Na]⁺).

(±21) Methyl (±)-4-(2,3-dihydroxypropoxy)benzoate

Following general procedure **C**: NMO (140 mg, 1.20 mmol) was charged with acetone/H₂O (9:1, 10 mL) and K₂OsO₂(OH)₄ (3.7 mg, 0.01 mmol). Methyl 4-

(allyloxy)benzoate (**18**) (192 mg, 1.00 mmol) was added and the reaction mixture was heated at 40 °C for 8 h and monitored (TLC, EtOAc/hexane 1:1, R_f = 0.14). Afforded the title compound as a white solid (220 mg, 97%). **M.P** 68 – 70 °C; **IR** V_{\max} cm^{-1} 3353 br s (O-H), 1957 br s, 2901 br s, 1718 s (C=O), 1605 s, 1509 w; **$^1\text{H-NMR}$** (400 MHz, $(\text{CD}_3)_2\text{CO}$) δ_{H} 7.98 – 7.92 (m, 2H, C3-H), 7.07 – 7.01 (m, 2H, C2-H), 4.18 (dd, J = 9.6, 4.4 Hz, 1H, C4-OCH₂), 4.14 (d, J = 5.1 Hz, 1H, CH-OH), 4.07 (dd, J = 9.6, 6.1 Hz, 1H, C4-OCH₂), 4.05 – 3.97 (m, 1H, CH-OH), 3.84 (s, 3H, Me), 3.78 (t, J = 5.8 Hz, 1H, CH₂-OH), 3.73 – 3.61 (m, 2H, CH₂-OH); **$^{13}\text{C-NMR}$** (101 MHz, $(\text{CD}_3)_2\text{CO}$) δ_{C} 166.0 (CO₂Me), 163.0 (C4), 131.3 (C3), 122.6 (C1), 114.3 (C2), 70.4 (C4-OCH₂), 69.8 (CH-OH), 63.1 (CH₂-OH), 51.1 (Me); **LRMS** (ESI+) 249.08 (100%, $[\text{M}+\text{Na}]^+$), 227.07 (90%, $[\text{M}+\text{H}]^+$), 186.16 (60%), 179.05 (90%), 177.10 (100%); **HRMS** (ESI+) $\text{C}_{11}\text{H}_{14}\text{O}_5\text{Na}$ Requires: 249.0739, Found: 249.0741 ($[\text{M}+\text{Na}]^+$)

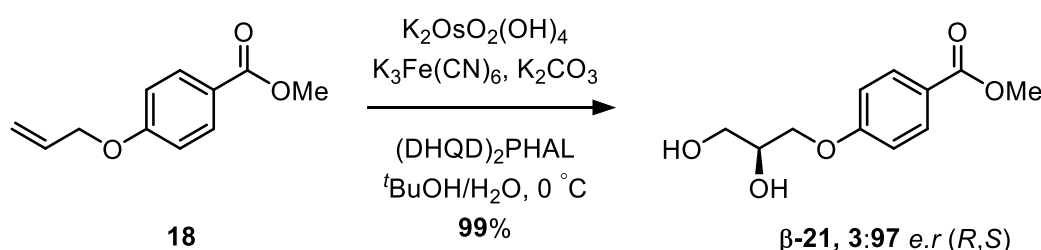
(**α -21**) Methyl (*R*)-4-(2,3-dihydroxypropoxy)benzoate



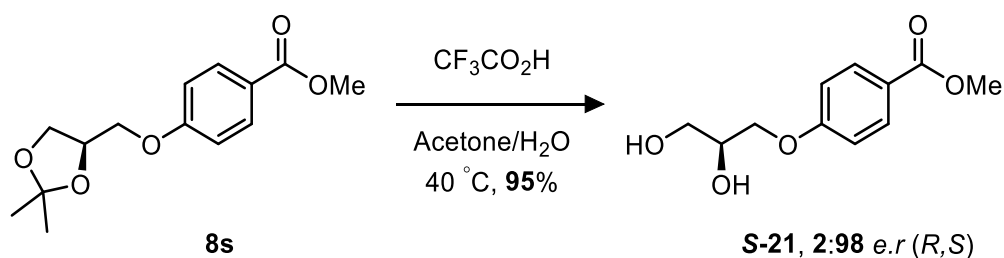
Following general procedure **D** using stock solutions: **I** (2 mL, 3.0 mmol), **II** (2 mL, 3.0 mmol), **III** (1.0 mL, 2.0 μmol) and **IV** (5.0 mL, 20.0 μmol). Methyl 3-(allyloxy)benzoate (**18**) (192 mg, 1.00 mmol) was added and the reaction mixture was stirred at 0 °C for 6 h with monitoring (EtOAc:hexane 1:1, R_f = 0.14). Afforded the title compound as a clear oil (220 mg, 97%). **M.P** 78 – 80 °C; [**α**]_D²⁵ +16.61 (c. 1.0, CHCl_3 , 93:7 *e.r* (*R,S*)); **IR** V_{\max} cm^{-1} 3340 br s, (O-H), 2956 w, 1720 s (C=O), 1606 s, 1510 w, 1434 w; **$^1\text{H-NMR}$** (400 MHz, $(\text{CD}_3)_2\text{CO}$) δ_{H} 7.98 – 7.92 (m, 2H, C3-H), 7.07 – 7.01 (m, 2H, C2-H), 4.18 (dd, J = 9.6, 4.4 Hz, 1H, C4-OCH₂), 4.14 (d, J = 5.1 Hz,

1H, CH-OH), 4.07 (dd, $J = 9.6, 6.1$ Hz, 1H, C4-OCH₂), 4.05 – 3.97 (m, 1H, CH-OH), 3.84 (s, 3H, Me), 3.78 (t, $J = 5.8$ Hz, 1H, CH₂-OH), 3.73 – 3.61 (m, 2H, CH₂-OH); **¹³C-NMR** (101 MHz, (CD₃)₂CO) δ_c 166.0 (CO₂Me), 163.0 (C4), 131.3 (C3), 122.6 (C1), 114.3 (C2), 70.4 (C4-OCH₂), 69.8 (CH-OH), 63.1 (CH₂-OH), 51.1 (Me); **LRMS** m/z (ESI+) 249.07 (30%, [M+Na]⁺), 186.22 (100%, [M-CH₃OH]⁺); **HRMS** m/z (ESI+) C₁₁H₁₄O₅Na Requires: 249.0739, Found: 249.0738 ([M+Na]⁺).

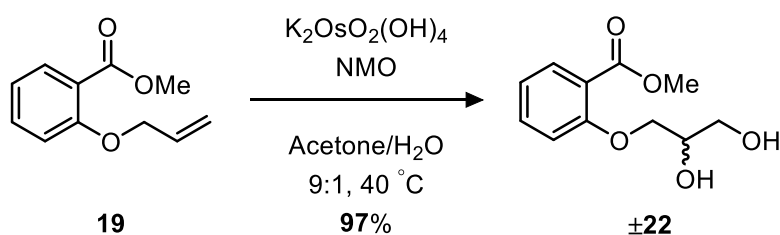
(β -21) Methyl (*S*)-4-(2,3-dihydroxypropoxy)benzoate



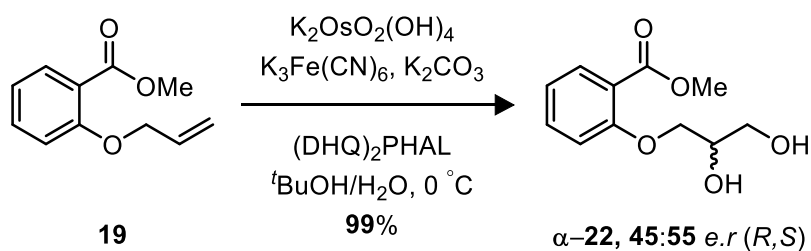
Following general procedure **D** using stock solutions: **I** (2 mL, 3.0 mmol), **II** (2 mL, 3.0 mmol), **III** (1.0 mL, 2.0 μ mol) and **V** (5.0 mL, 20.0 μ mol). Methyl 3-(allyloxy)benzoate (**18**) (192 mg, 1.00 mmol) was added and the reaction mixture was stirred at 0 °C for 6 h with monitoring (EtOAc:hexane 1:1, $R_f = 0.14$). Afforded the title compound as a clear oil (225 mg, 99%). **M.P** 78 – 80 °C; **[α]_D²⁵** –17.31 (c. 1.0, CHCl₃, 3:97 *e.r.* (*R,S*)); **IR** ν_{max} cm⁻¹ 3340 br s, (O-H), 2956 w, 1720 s (C=O), 1606 s, 1510 w, 1434 w; **¹H-NMR** (400 MHz, (CD₃)₂CO) δ_H 7.98 – 7.92 (m, 2H, C3-H), 7.07 – 7.01 (m, 2H, C2-H), 4.18 (dd, $J = 9.6, 4.4$ Hz, 1H, C4-OCH₂), 4.14 (d, $J = 5.1$ Hz, 1H, CH-OH), 4.07 (dd, $J = 9.6, 6.1$ Hz, 1H, C4-OCH₂), 4.05 – 3.97 (m, 1H, CH-OH), 3.84 (s, 3H, Me), 3.78 (t, $J = 5.8$ Hz, 1H, CH₂-OH), 3.73 – 3.61 (m, 2H, CH₂-OH); **¹³C-NMR** (101 MHz, (CD₃)₂CO) δ_c 166.0 (CO₂Me), 163.0 (C4), 131.3 (C3), 122.6 (C1), 114.3 (C2), 70.4 (C4-OCH₂), 69.8 (CH-OH), 63.1 (CH₂-OH), 51.1 (Me); **LRMS** m/z (ESI+) 249.07 (20%, [M+Na]⁺), 186.22 (100%, [M-CH₃OH]⁺); **HRMS** m/z (ESI+) C₁₁H₁₄O₅Na Requires: 249.0739, Found: 249.0741 ([M+Na]⁺).

(S-21) Methyl (*S*)-4-(2,3-dihydroxypropoxy)benzoate

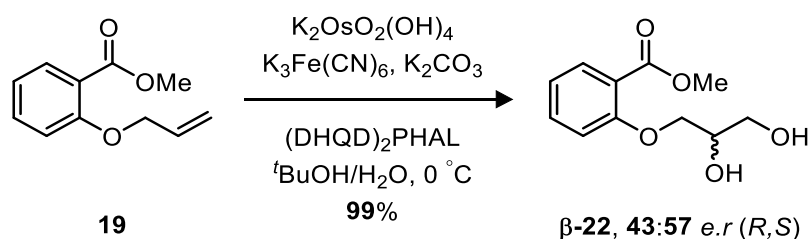
Following general procedure **F**: Methyl (*R*)-4-((2,2-dimethyl-1,3-dioxolan-4-yl)methoxy)benzoate (**8s**) (95 mg, 0.35 mmol) was stirred at 40 °C for 24 h. Afforded the title compound as a white solid (75 mg, 95%). **M.P** 78 – 80 °C; **[α]_D²⁵** –1.58 (c. 1.0, CHCl₃, 2:98 *e.r* (*R,S*)); **IR** ν_{max} cm^{–1} 3340 br s, (O-H), 2956 w, 1720 s (C=O), 1606 s, 1510 w, 1434 w; **¹H-NMR** (400 MHz, (CD₃)₂CO) δ_{H} 7.98 – 7.92 (m, 2H, C3-H), 7.07 – 7.01 (m, 2H, C2-H), 4.18 (dd, *J* = 9.6, 4.4 Hz, 1H, C4-OCH₂), 4.14 (d, *J* = 5.1 Hz, 1H, CH-OH), 4.07 (dd, *J* = 9.6, 6.1 Hz, 1H, C4-OCH₂), 4.05 – 3.97 (m, 1H, CH-OH), 3.84 (s, 3H, Me), 3.78 (t, *J* = 5.8 Hz, 1H, CH₂-OH), 3.73 – 3.61 (m, 2H, CH₂-OH); **¹³C-NMR** (101 MHz, (CD₃)₂CO) δ_{C} 165.9 (C=O₂Me), 162.9 (C4), 131.2 (C3), 122.4 (C1), 114.2 (C2), 70.2 (C4-OCH₂), 69.7 (CH-OH), 63.0 (CH₂-OH), 51.0 (Me); **LRMS** *m/z* (ESI+) 249.07 (100%, [M+Na]⁺); **HRMS** *m/z* (ESI+) C₁₁H₁₄O₅Na Requires: 249.0739, Found: 249.0737 ([M+Na]⁺).

(±22) Methyl (±)-2-(2,3-dihydroxypropoxy)benzoate

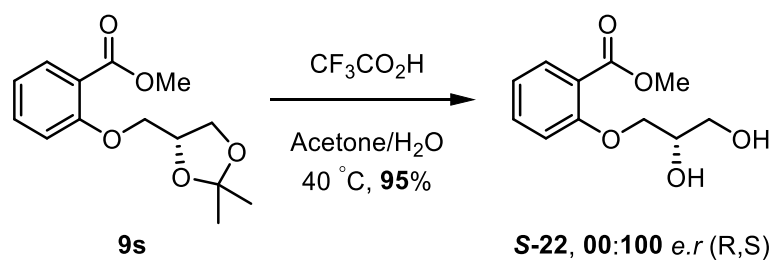
Following general procedure **C**: NMO (140 mg, 1.20 mmol) was charged with acetone/H₂O (9:1, 10 mL) and K₂OsO₂(OH)₄ (3.7 mg, 0.01 mmol). Methyl 2-(allyloxy)benzoate (**19**) (192 mg, 1.00 mmol) was added, the reaction mixture was heated at 40 °C for 8 h and monitored (TLC, EtOAc/hexane 1:1, *R_f* = 0.26). Afforded the title compound as a clear oil (220 mg, 97%). **IR** *V*_{max} cm⁻¹ 3387 br (O-H), 2951 w, 1716 s (C=O), 1586 m, 1489 m, 1444 s; **¹H-NMR** (400 Hz, (CD₃)₂SO) δ_H 7.64 (dd, *J* = 7.5, 1.8 Hz, 1H, C6-H), 7.51 (ddd, *J* = 8.5, 7.5, 1.8 Hz, 1H, C5-H), 7.15 (dd, *J* = 8.5, 1.0 Hz, 1H, C4-H), 7.01 (td, *J* = 7.5, 1.0 Hz, 1H, C3-H), 4.89 (d, *J* = 5.0 Hz, 1H, CH-OH), 4.63 (t, *J* = 5.7 Hz, 1H, CH₂-OH), 3.05 – 3.91 (m, 2H, C2-OCH₂), 3.78 (m, 4H, CH-OH & Me), 3.57 – 3.42 (m, 2H, CH₂-OH); **¹³C-NMR** (101 MHz, (CD₃)₂SO) δ_C 166.3 (C=O), 157.8 (C2), 133.6 (C5), 130.7 (C6), 120.3 (C1), 120.2 (C3), 113.8 (C4), 70.2 (C2-OCH₂), 69.8 (CH-OH), 62.7 (CH₂-OH), 51.9 (Me); **LRMS** (ESI+) 249.07 (30%, [M+Na]⁺), 226.08 (10%, [M]⁺), 195.10 (40%, [M-CH₃OH]⁺), 120.08 (100%, [C₇H₄O₂]⁺), 152.20 (50%, [**3s**]⁺); **HRMS** (ESI+) C₁₁H₁₄O₅Na Requires: 249.0739, Found: 249.0741 ([M+Na]⁺).

(α -22) Methyl (\pm)-2-(2,3-dihydroxypropoxy)benzoate

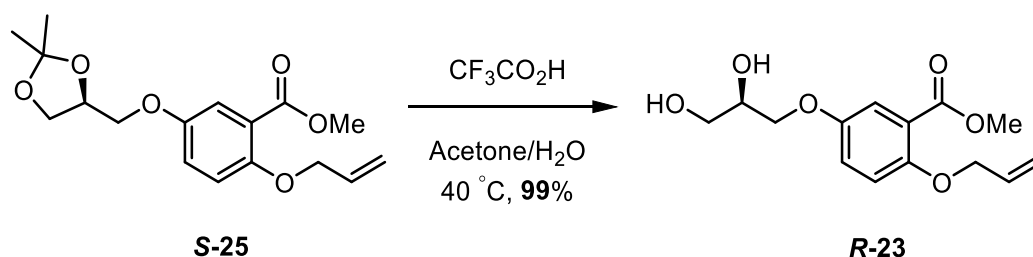
Following general procedure **D** using stock solutions: **I** (2 mL, 3.0 mmol), **II** (2 mL, 3.0 mmol), **III** (1.0 mL, 2.0 μmol) and **IV** (5.0 mL, 20.0 μmol). Methyl 2-(allyloxy)benzoate (**19**) (192 mg, 1.00 mmol) was added and the reaction mixture was stirred at 0 $^\circ\text{C}$ for 6 h with monitoring (EtOAc:hexane 1:1, R_f = 0.26). Afforded the title compound as a clear oil (224 mg, 99%). [α]_D²⁵ +9.69 (c. 1.0, CHCl_3 , 45:55 *e.r* (*R,S*)); **IR** V_{max} cm^{-1} 3420 br s (O-H) 3012 w, 2951 w, 1707 s, 1601 w, 1582 w, 1491 w, 1444 w; **$^1\text{H-NMR}$** (400 Hz, $(\text{CD}_3)_2\text{SO}$) δ_{H} 7.64 (dd, J = 7.5, 1.8 Hz, 1H, C6-H), 7.51 (ddd, J = 8.5, 7.5, 1.8 Hz, 1H, C5-H), 7.15 (dd, J = 8.5, 1.0 Hz, 1H, C4-H), 7.01 (td, J = 7.5, 1.0 Hz, 1H, C3-H), 4.90 (d, J = 5.0 Hz, 1H, CH-OH), 4.63 (t, J = 5.7 Hz, 1H, CH_2 -OH), 4.07 – 3.92 (m, 2H, C_2 -OCH₂), 3.84 – 3.74 (m, 4H, CH-OH & Me), 3.56 – 3.41 (m, 2H, CH_2 -OH); **$^{13}\text{C-NMR}$** (101 MHz, $(\text{CD}_3)_2\text{SO}$) δ_{C} 166.3 ($\text{C}=\text{O}$), 157.8 (C2), 133.6 (C5), 130.7 (C6), 120.3 (C1), 120.2 (C3), 113.8 (C4), 70.2 (C_2 -OCH₂), 69.8 (CH-OH), 62.7 (CH_2 -OH), 51.9 (Me); **LRMS** (ESI+) 249.07 (100%, $[\text{M}+\text{Na}]^+$); **HRMS** (ESI+) $\text{C}_{11}\text{H}_{14}\text{O}_5\text{Na}$ Requires: 249.0739, Found: 249.0742 ($[\text{M}+\text{Na}]^+$).

(β -22) Methyl (\pm)-2-(2,3-dihydroxypropoxy)benzoate

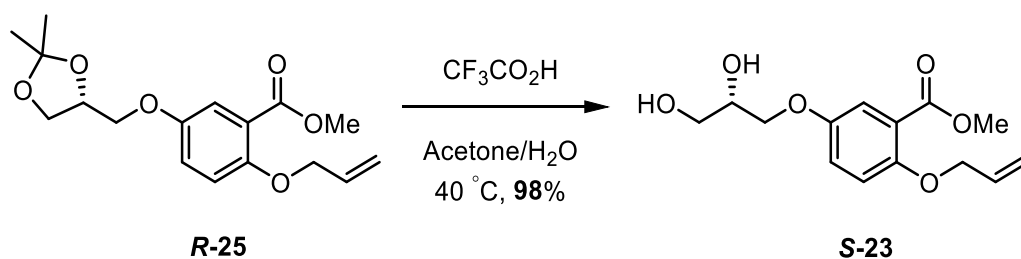
Following general procedure **D** using stock solutions: **I** (2 mL, 3.0 mmol), **II** (2 mL, 3.0 mmol), **III** (1.0 mL, 2.0 μmol) and **V** (5.0 mL, 20.0 μmol). Methyl 2-(allyloxy)benzoate (**19**) (192 mg, 1.00 mmol) was added and the reaction mixture was stirred at 0 $^\circ\text{C}$ for 6 h with monitoring (EtOAc:hexane 1:1, R_f = 0.26). Afforded the title compound as a clear oil (224 mg, 99%). [α]_D²⁵ +9.13 (c. 1.0, CHCl_3 , 43:57 *e.r* (*R,S*)); **IR** V_{max} cm^{-1} 3424 br s (O-H), 3014 w, 2951 w, 1707 s, 1600 w, 1582 w, 1491 w, 1448 w; **$^1\text{H-NMR}$** (400 Hz, $(\text{CD}_3)_2\text{SO}$) δ_{H} 7.64 (dd, J = 7.5, 1.8 Hz, 1H, C6-H), 7.51 (ddd, J = 8.5, 7.5, 1.8 Hz, 1H, C5-H), 7.15 (dd, J = 8.5, 1.0 Hz, 1H, C4-H), 7.01 (td, J = 7.5, 1.0 Hz, 1H, C3-H), 4.90 (d, J = 5.0 Hz, 1H, CH-OH), 4.63 (t, J = 5.7 Hz, 1H, CH₂-OH), 4.07 – 3.92 (m, 2H, C2-OCH₂), 3.84 – 3.74 (m, 4H, CH-OH & Me), 3.56 – 3.41 (m, 2H, CH₂-OH); **$^{13}\text{C-NMR}$** (101 MHz, $(\text{CD}_3)_2\text{SO}$) δ_{C} 166.3 (CO₂Me), 157.8 (C2), 133.6 (C5), 130.7 (C6), 120.3 (C1), 120.2 (C3), 113.8 (C4), 70.2 (C2-OCH₂), 69.8 (CH-OH), 62.7 (CH₂-OH), 51.9 (Me); **LRMS** m/z (ESI+) 249.07 ([M+Na]⁺, 100%); **HRMS** m/z (ESI+) C₁₁H₁₄O₅Na Requires: 249.0739, Found: 249.0742 ([M+Na]⁺).

(S-22) Methyl (*S*)-2-(2,3-dihydroxypropoxy)benzoate

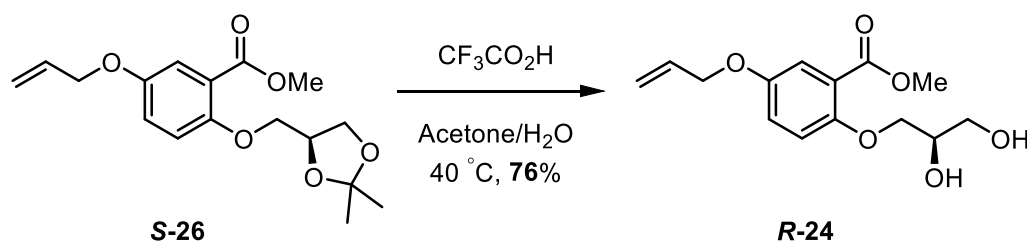
Following general procedure **F**: Methyl (*R*)-2-((2,2-dimethyl-1,3-dioxolan-4-yl)methoxy)benzoate (**9s**) (77 mg, 0.29 mmol) was stirred at 40 °C for 16 h. Afforded the title compound as a light brown oil (63 mg, 95%). **[α]_D²⁵** −1.38 (c. 1.0, CHCl₃, 0:100 *e.r* (*R,S*)); **IR** V_{max} cm^{−1} 3424 br s (O-H) 3014 w, 2951 w, 1707 s (C=O), 1600 w, 1582 w, 1491 w, 1448w; **¹H-NMR** (400 Hz, (CD₃)₂SO) δ_{H} 7.64 (dd, *J* = 7.5, 1.8 Hz, 1H, C6-H), 7.51 (ddd, *J* = 8.5, 7.5, 1.8 Hz, 1H, C5-H), 7.15 (dd, *J* = 8.5, 1.0 Hz, 1H, C4-H), 7.01 (td, *J* = 7.5, 1.0 Hz, 1H, C3-H), 4.90 (d, *J* = 5.0 Hz, 1H, CH-OH), 4.63 (t, *J* = 5.7 Hz, 1H, CH₂-OH), 4.07 – 3.92 (m, 2H, C2-OCH₂), 3.84 – 3.74 (m, 4H, CH-OH & Me), 3.56 – 3.41 (m, 2H, CH₂-OH); **¹³C-NMR** (101 MHz, (CD₃)₂SO) δ_{C} 166.3 (C=O), 157.8 (C2), 133.6 (C5), 130.7 (C6), 120.3 (C1), 120.2 (C3), 113.8 (C4), 70.2 (C2-OCH₂), 69.8 (CH-OH), 62.7 (CH₂-OH), 51.8 (Me); **LRMS** *m/z* (ESI+) 249.07 (100%, [M+Na]⁺); **HRMS** *m/z* (ESI+) C₁₁H₁₄O₅Na Requires: 249.0739, Found: 249.0740 ([M+Na]⁺).

(R-23) Methyl (*R*)-2-(allyloxy)-5-(2,3-dihydroxypropoxy)benzoate

Following general procedure **F**: Methyl (*S*)-2-(allyloxy)-5-((2,2-dimethyl-1,3-dioxolan-4-yl)methoxy)benzoate (**S-25**) (483 mg, 1.5 mmol) was stirred at 40 °C for 24 h. Afforded the title compound as a clear oil (420 mg, 99%). **[α]_D²⁵** +4.84 (c. 1.0, CHCl₃); **IR** V_{max} cm⁻¹ 3471 br s (O-H), 3018 w, 2950 w, 2885 w, 1713 s (C=O), 1611 w, 1580 w, 1496 s; **¹H-NMR** (400 MHz, CDCl₃) δ_H 7.34 (d, *J* = 3.2 Hz, 1H, C6-H), 6.99 (dd, *J* = 9.0, 3.2 Hz, 1H, C4-H), 6.88 (d, *J* = 9.0 Hz, 1H, C3-H), 6.03 (ddt, *J* = 17.3, 10.6, 5.0 Hz, 1H, CH=CH₂), 5.45 (dq, *J* = 17.3, 1.7 Hz, 1H, CH=CH₂), 5.27 (dq, *J* = 10.6, 1.7 Hz, 1H, CH=CH₂), 4.54 (dt, *J* = 5.0, 1.6 Hz, 2H, C2-OCH₂), 4.07 (ddt, *J* = 8.2, 5.8, 2.3 Hz, 1H, CH-OH), 4.01 – 3.95 (m, 2H, C5-OCH₂), 3.87 (s, 3H, Me), 3.84 – 3.66 (m, 2H, CH₂-OH), 2.84 (br s, 2H, OH); **¹³C-NMR** (101 MHz, CDCl₃) δ_C 166.6 (C=O), 152.9 (C2), 152.2 (C5), 133.1 (CH=CH₂), 121.2 (C1), 120.2 (C4), 117.5 (CH=CH₂), 117.0 (C6), 115.9 (C3), 70.6 (C2-OCH₂), 70.5 (CH-OH), 69.9 (C5-OCH₂), 63.7 (CH₂-OH), 52.3 (Me); **LRMS** (ESI+) *m/z* 283.12 (50%, [M+H]⁺), 251.09 (100%, [M+H-MeOH]⁺); **HRMS** (ESI+) *m/z* C₁₄H₁₉O₆ Requires: 283.1182, Found: 283.1183 ([M+H]⁺).

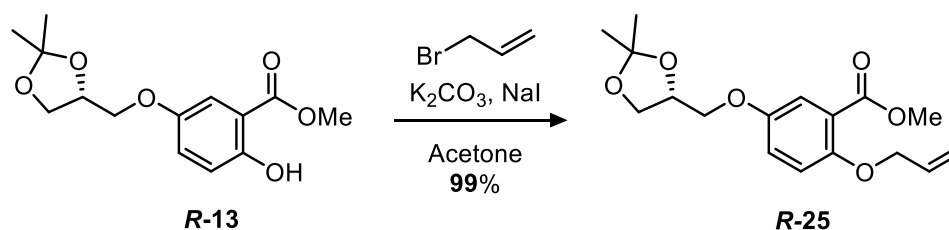
(S-23) Methyl (*S*)-2-(allyloxy)-5-(2,3-dihydroxypropoxy)benzoate

Following general procedure **F**: Methyl (*R*)-2-(allyloxy)-5-((2,2-dimethyl-1,3-dioxolan-4-yl)methoxy)benzoate (**R-25**) (200 mg, 0.62 mmol) was stirred at 40 °C for 24 h. Afforded the title compound as a clear oil (172 mg, 98%). **[α]_D²⁵** −14.97 (c. 1.0, CHCl₃); **IR** $\text{V}_{\text{max}} \text{ cm}^{-1}$ 3385 br s (O-H), 2951 w, 2874 w, 1709 s (C=O), 1612 w, 1581 w, 1496 s; **¹H-NMR** (400 MHz, CDCl₃) δ_{H} 7.32 (d, J = 3.2 Hz, 1H, C6-H), 6.97 (dd, J = 9.0, 3.2 Hz, 1H, C4-H), 6.86 (d, J = 9.0 Hz, 1H, C3-H), 6.03 (ddt, J = 17.3, 10.6, 5.0 Hz, 1H, CH=CH₂), 5.45 (dq, J = 17.3, 1.7 Hz, 1H, CH=CH₂), 5.26 (dq, J = 10.6, 1.7 Hz, 1H, CH=CH₂), 4.53 (dt, J = 5.0, 1.6 Hz, 2H, C2-OCH₂), 4.13 – 4.03 (m, 1H, CH-OH), 3.97 (d, J = 4.6 Hz, 2H, C5-OCH₂), 3.86 (s, 3H, Me), 3.84 – 3.66 (m, 2H, CH₂-OH), 3.24 (br s, 2H, O-H); **¹³C-NMR** (101 MHz, CDCl₃) δ_{C} 166.6 (CO₂Me), 152.9, (C2), 152.1 (C5), 133.1 (CH=CH₂), 121.2 (C1), 120.2 (C4), 117.4 (CH=CH₂), 117.0 (C6), 115.9 (C3), 70.6 (C2-OCH₂), 70.5 (CH-OH), 69.8 (C5-OCH₂), 63.6 (CH₂-OH), 52.3 (Me); **LRMS** (ESI+) m/z 305.10 (50%, [M+Na]⁺); **HRMS** (ESI+) m/z C₁₄H₁₈O₆Na Requires: 305.0997, Found: 305.0996 ([M+Na]⁺).

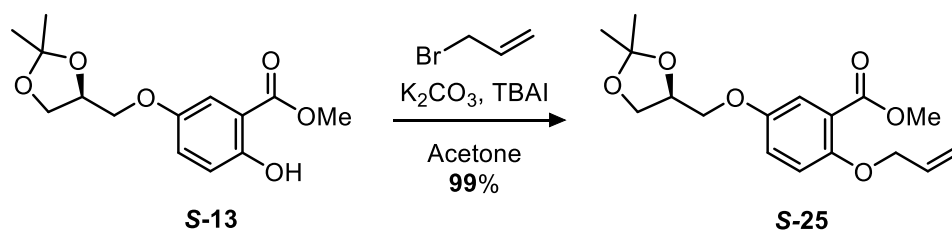
(R-24) Methyl (*R*)-5-(allyloxy)-2-(2,3-dihydroxypropoxy)benzoate

Following general procedure **F**: Methyl (*S*)-5-(allyloxy)-2-((2,2-dimethyl-1,3-dioxolan-4-yl)methoxy)benzoate (**S-26**) (300 mg, 0.93 mmol) was stirred at 40 °C for 24 h. Purification by chromatography (SiO₂, EtOAc/hexane, 1:1, *R_f* = 0.19) Afforded the title compound as a white solid (200 mg, 76%). [α]_D²⁵ –3.81 (c. 1.0, CHCl₃); **M.P** 61 – 62 °C; **IR** ν_{max} cm^{–1} 3354 br s, (O-H), 3095 w, 3039 w, 2955 w, 2881 w, 1697 s (C=O), 1607 w; **¹H-NMR** (400 MHz, CDCl₃) δ_{H} 7.41 (d, *J* = 3.2 Hz, 1H, C6-H), 7.07 (dd, *J* = 9.0, 3.2 Hz, 1H, C4-H), 6.93 (d, *J* = 9.0 Hz, 1H, C3-H), 6.03 (ddt, *J* = 17.3, 10.5, 5.3 Hz, 1H, CH=CH₂), 5.40 (dd, *J* = 17.3, 1.5 Hz, 1H, CH=CH₂), 5.29 (dd, *J* = 10.5, 1.5 Hz, 1H, CH=CH₂), 4.51 (d, *J* = 5.3 Hz, 2H, C5-OCH₂), 4.24 (dd, *J* = 9.1, 2.7 Hz, 1H, C2-OCH₂), 4.15 – 3.99 (m, 3H, C2-OCH₂, CH-OH), 3.88 (s, 3H, Me), 3.82 (dd, *J* = 6.5 3.9 Hz, 2H, CH₂OH), 3.22 (t, *J* = 6.5 Hz, 1H, CH₂OH); **¹³C-NMR** (101 MHz, CDCl₃) δ_{C} 166.3 (C=O), 153.5 (C2), 152.7 (C5), 133.0 (CH=CH₂), 121.4 (C4), 120.0 (C1), 118.0 (CH=CH₂), 117.2 (C6), 116.1 (C3), 73.5 (C2-OCH₂), 69.6 (C5-OCH₂), 69.5 (CH-OH), 63.6 (C2-OCH₂), 52.4 (Me); **LRMS** *m/z* (ESI+) 305.10 (100%, [M+Na]⁺); **HRMS** *m/z* (ESI+) C₁₄H₁₈O₆Na Requires: 305.1001, Found: 305.1003 ([M+Na]⁺).

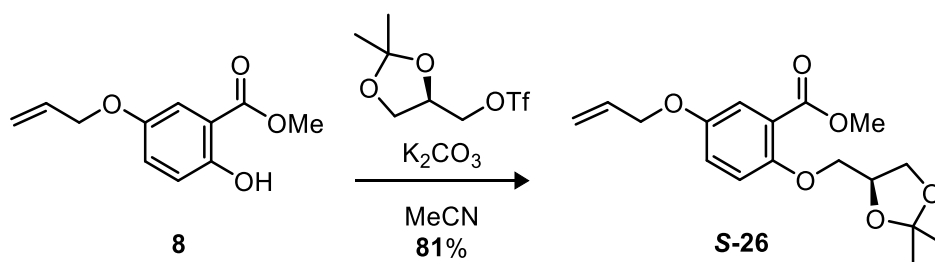
(**R-25**) Methyl (*R*)-2-(allyloxy)-5-((2,2-dimethyl-1,3-dioxolan-4-yl)methoxy)benzoate



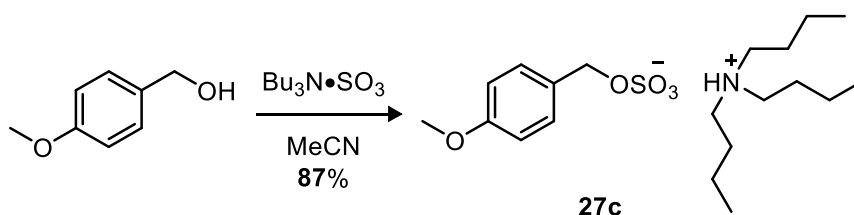
Adapted from general procedure **B**: methyl (*R*)-5-((2,2-dimethyl-1,3-dioxolan-4-yl)methoxy)-2-hydroxybenzoate (**R-13**) (1.20 g, 4.25 mmol), K_2CO_3 (885 mg, 6.40 mmol) and sodium iodide (959 mg, 6.40 mmol) in acetone (30 mL) was charged dropwise with allyl bromide (0.55 mL, 6.40 mmol) and the reaction mixture was heated under reflux for 8 h. Purification by chromatography (SiO_2 , EtOAc/Hexane, 1:9, R_f = 0.22) yielded the title compound as a colourless oil (1.36 g, 99%). $[\alpha]_D^{25} +10.42$ (c. 1.0, CHCl_3); **IR** $\text{V}_{\text{max}} \text{ cm}^{-1}$ 2987 w, 2936 w, 1730 s (C=O), 1648 w, 1610 w, 1582 w, 1496 s, 1454 w, 1438 s, 1417 w; **$^1\text{H-NMR}$** (400 MHz, CDCl_3) δ_{H} 7.35 (d, J = 3.2 Hz, 1H, C6-H), 7.01 (dd, J = 9.0, 3.2 Hz, 1H, C4-H), 6.89 (d, J = 9.0 Hz, 1H, C3-H), 6.04 (ddt, J = 17.2, 10.6, 4.9 Hz, 1H, $\text{CH}=\text{CH}_2$), 5.46 (dq, J = 17.2, 1.7 Hz, 1H, $\text{CH}=\text{CH}_2$), 5.26 (dq, J = 10.6, 1.7 Hz, 1H, $\text{CH}=\text{CH}_2$), 4.55 (dt, J = 4.9, 1.7 Hz, 2H, C2- OCH_2), 4.44 (app. p, J = 5.7 Hz, 1H, $\text{CH-OC}(\text{CH}_3)_2$), 4.14 (dd, J = 8.5, 6.4 Hz, 1H, $\text{CH}_2\text{-OC}(\text{CH}_3)_2$), 4.02 (dd, J = 9.5, 5.6 Hz, 1H, C5- OCH_2), 3.96 – 3.82 (m, 5H, Me, C5- OCH_2 & $\text{CH}_2\text{-OC}(\text{CH}_3)_2$), 1.44 (s, 3H, $\text{C}(\text{CH}_3)_2$), 1.38 (s, 3H, $\text{C}(\text{CH}_3)_2$); **$^{13}\text{C-NMR}$** (101 MHz, CDCl_3) δ_{C} 166.5 (CO_2Me), 152.8 (C2), 152.3 (C5), 133.1 ($\text{CH}=\text{CH}_2$), 121.2 (C1), 120.3 (C4), 117.4 ($\text{CH}=\text{CH}_2$), 116.8 (C6), 116.0 (C3), 109.9 ($\text{C}(\text{CH}_3)_2$), 74.1 ($\text{CH-OC}(\text{CH}_3)_2$), 70.6 (C2- OCH_2), 69.6 (C5- OCH_2), 66.8 ($\text{CH}_2\text{-OC}(\text{CH}_3)_2$), 52.2 (Me), 26.8 ($\text{C}(\text{CH}_3)_2$), 25.4 ($\text{C}(\text{CH}_3)_2$); **LRMS** m/z (ESI+) 345.08 (100%, $[\text{M}+\text{Na}]^+$), 233.03 (60%); **HRMS** m/z (ESI+) $\text{C}_{17}\text{H}_{22}\text{O}_6\text{Na}$ Requires: 345.1308, Found: 345.1309 ($[\text{M}+\text{Na}]^+$).

(S-25) Methyl (*S*)-2-(allyloxy)-5-((2,2-dimethyl-1,3-dioxolan-4-yl)methoxy)benzoate

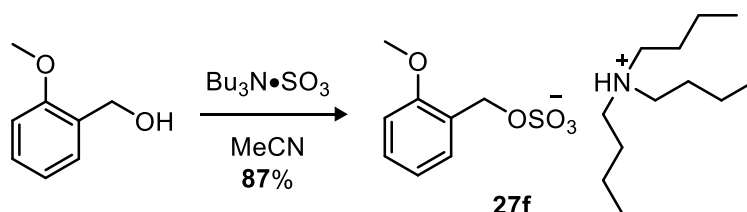
Following general procedure **B**: methyl (*S*)-5-((2,2-dimethyl-1,3-dioxolan-4-yl)methoxy)-2-hydroxybenzoate (**S-13**) (750 mg, 2.66 mmol), K_2CO_3 (691 mg, 5.00 mmol) and TBAI (806 mg, 2.50 mmol) in acetone (50 mL) was charged dropwise with allyl bromide (0.24 mL, 2.75 mmol) and the reaction mixture was heated under reflux for 4 h. Purification by chromatography (SiO_2 , EtOAc/Hexane, 1:9, $R_f = 0.22$) yielded the title compound as a colourless oil (850 mg, 99%). $[\alpha]_D^{25} +3.46$ (c. 1.0, CHCl_3); **IR** $\text{V}_{\text{max}} \text{ cm}^{-1}$ 2986 w, 2936 w, 1730 s ($\text{C}=\text{O}$), 1582 w, 1497 s, 1438 s; **$^1\text{H-NMR}$** (400 MHz, CDCl_3) δ_{H} 7.35 (d, $J = 3.2$ Hz, 1H, C6-H), 7.01 (dd, $J = 9.1, 3.2$ Hz, 1H, C4-H), 6.89 (d, $J = 9.1$ Hz, 1H, C3-H), 6.04 (ddt, $J = 17.3, 10.6, 5.0$ Hz, 1H, $\text{CH}=\text{CH}_2$), 5.46 (dq, $J = 17.3, 1.6$ Hz, 1H, $\text{CH}=\text{CH}_2$), 5.26 (dq, $J = 10.6, 1.6$ Hz, 1H, $\text{CH}=\text{CH}_2$), 4.55 (dt, $J = 5.0, 1.6$ Hz, 2H, C2-OCH_2), 4.44 (app. p, $J = 5.7$ Hz, 1H, $\text{CH-OC}(\text{CH}_3)_2$), 4.14 (dd, $J = 8.5, 6.5$ Hz, 1H, $\text{CH}_2\text{-OC}(\text{CH}_3)_2$), 4.02 (dd, $J = 9.5, 5.7$ Hz, 1H, C5-OCH_2), 3.91 (dd, $J = 9.5, 5.7$ Hz, 1H, C5-OCH_2), 3.89 – 3.84 (m, 4H, Me & $\text{CH}_2\text{-OC}(\text{CH}_3)_2$), 1.44 (s, 3H, $\text{C}(\text{CH}_3)_2$), 1.38 (s, 3H, $\text{C}(\text{CH}_3)_2$); **$^{13}\text{C-NMR}$** (101 MHz, CDCl_3) δ_{C} 166.5 (CO_2Me), 152.8 (C2), 152.3 (C5), 133.1 ($\text{CH}=\text{CH}_2$), 121.2 (C1), 120.3 (C4), 117.4 ($\text{CH}=\text{CH}_2$), 116.8 (C6), 116.0 (C3), 109.9 ($\text{C}(\text{CH}_3)_2$), 74.1 ($\text{CH-OC}(\text{CH}_3)_2$), 70.6 (C2-OCH_2), 69.6 (C5-OCH_2), 66.8 ($\text{CH}_2\text{-OC}(\text{CH}_3)_2$), 52.2 (Me), 26.9 ($\text{C}(\text{CH}_3)_2$), 25.4 ($\text{C}(\text{CH}_3)_2$); **LRMS** m/z (ESI+) 345.17 (100%, $[\text{M}+\text{Na}]^+$), 233.11 (60%); **HRMS** m/z (ESI+) $\text{C}_{17}\text{H}_{22}\text{O}_6\text{Na}$ Requires: 345.1314, Found: 345.1316 ($[\text{M}+\text{Na}]^+$).

(S-26) Methyl (*S*)-5-(allyloxy)-2-((2,2-dimethyl-1,3-dioxolan-4-yl)methoxy)benzoate

Following general procedure **G**: using methyl 5-(allyloxy)-2-hydroxybenzoate (**8**) (1.00 g, 4.80 mmol), K_2CO_3 (1.27 g, 9.6 mmol) and (*R*)-(2,2-dimethyl-1,3-dioxolan-4-yl)methyl trifluoromethanesulfonate (1.90 g, 7.3 mmol). The reaction mixture was heated under reflux for 12 h and monitored (EtOAc/hexane 1:4, $R_f = 0.56$). The crude oil was purified by chromatography (SiO_2 , EtOAc/hexane, 1:4) to yield the title compound as a clear oil (1.26 g, 81%). **[α]_D²⁵** +4.15 (c. 0.5, CHCl_3); **IR** V_{max} cm^{-1} 2986 w (C-H), 2952 w (C-H), 1730 s (C=O), 1583 w, 1498 s, 1437 w; **¹H-NMR** (400 MHz, CDCl_3) δ_{H} 7.32 (d, $J = 3.2$ Hz, 1H, C6-H), 7.01 (dd, $J = 9.0, 3.2$ Hz, 1H, C4-H), 6.92 (d, $J = 9.0$ Hz, 1H, C3-H), 6.01 (ddt, $J = 17.3, 10.5, 5.3$ Hz, 1H, $\text{CH}=\text{CH}_2$), 5.38 (dq, $J = 17.3, 1.5$ Hz, 1H, $\text{CH}=\text{CH}_2$), 5.26 (dq, $J = 10.5, 1.5$ Hz, 1H, $\text{CH}=\text{CH}_2$), 4.49 (dt, $J = 5.3, 1.5$ Hz, 2H, C5- OCH_2), 4.47 – 4.42 (m, 1H, $\text{CH}-\text{OC}(\text{CH}_3)_2$), 4.15 (dd, $J = 8.5, 6.3$ Hz, 1H, $\text{CH}_2-\text{OC}(\text{CH}_3)_2$), 4.09 (dd, $J = 9.4, 4.6$ Hz, 1H, C2- OCH_2), 3.99 (dd, $J = 8.5, 5.8$ Hz, 1H, $\text{CH}_2-\text{OC}(\text{CH}_3)_2$), 3.94 (dd, $J = 9.4, 6.6$ Hz, 1H, C2- OCH_2), 3.86 (s, 3H, Me), 1.43 (s, 3H $\text{C}(\text{CH}_3)_2$), 1.38 (s, 3H, $\text{C}(\text{CH}_3)_2$); **¹³C-NMR** (101 MHz, CDCl_3) δ_{C} 166.4 (CO_2Me), 152.7 (C5/C2), 152.6 (C5/C2), 133.1 ($\text{CH}=\text{CH}_2$), 121.5 (C1), 120.5 (C4), 117.8 ($\text{CH}=\text{CH}_2$), 117.0 (C6), 116.4 (C3), 109.6 ($\text{C}(\text{CH}_3)_2$), 74.0 ($\text{CH}-\text{OC}(\text{CH}_3)_2$), 70.8 (C2- OCH_2), 69.5 (C5- OCH_2), 67.0 ($\text{CH}_2-\text{OC}(\text{CH}_3)_2$), 52.1 (Me), 26.8 ($\text{C}(\text{CH}_3)_2$), 25.5 ($\text{C}(\text{CH}_3)_2$); **LRMS** (ESI+) m/z 345.14 (100%, $[\text{M}+\text{Na}]^+$); **HRMS** (ESI+) m/z $\text{C}_{17}\text{H}_{22}\text{O}_6\text{Na}$ Requires: 345.1314, Found: 345.1317 ($[\text{M}+\text{Na}]^+$)

(27c) Tributylammonium 4-methoxybenzyl sulfate

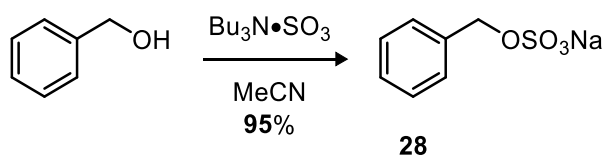
Following general procedure **H**: 4-Methoxybenzyl alcohol (138 mg, 1.0 mmol) and $\text{Bu}_3\text{N}^+\text{SO}_3^-$ (530 mg, 2.0 mmol) were dissolved in dry MeCN (2.0 mL) and heated under reflux for 2.5 h. The flask was cooled and the solvent removed under reduced pressure. The crude reaction product was purified by chromatography (SiO_2 ; $\text{CH}_2\text{Cl}_2/\text{MeOH}$, 9:1, $R_f = 0.6$) to yield the title compound as a clear oil (350 mg, 87%). **IR** ν_{max} cm^{-1} 3467 w br, 2960 m, 2874 w, 1613 w, 1514 s, 1465 m, 1247 s; **$^1\text{H-NMR}$** δ_{H} (400 MHz, CDCl_3) 9.85 (br s, 1H, NH), 7.34 – 7.28 (m, 2H, C2- H), 6.85 – 6.79 (m, 2H, C3- H), 5.00 (s, 2H, C1- CH_2), 3.77 (s, 3H, Me), 3.03 – 2.90 (m, 6H, N- CH_2), 1.73 – 1.58 (6H, m, CH_2), 1.33 (h, $J = 7.4$ Hz, 6H, CH_2), 0.91 (t, $J = 7.4$ Hz, 9H, CH_3); **$^{13}\text{C-NMR}$** δ_{C} (101 MHz, CDCl_3) 159.5 (C4), 130.1 (C2), 128.9 (C1), 113.7 (C3), 69.5 (C1- CH_2), 55.3 (Me), 52.6 (N- CH_2), 25.3 (CH_2), 20.1 (CH_2), 13.6 (CH_3); **LRMS** m/z (ESI+) 186.2 (100%, $[\text{M}-\text{OCH}_3]^2+$), 589.4 (20%, $[\text{M}+\text{Bu}_3\text{NH}]^+$); **HRMS** m/z (ESI+) $\text{C}_{32}\text{H}_{65}\text{N}_2\text{O}_5\text{S}$ Requires: 589.4614, Found: 589.4619 ($[\text{M}+\text{Bu}_3\text{NH}]^+$)

(27f) Tributylammonium 2-methoxybenzyl sulfate

Following general procedure **H**: 2-Methoxybenzyl alcohol (138 mg, 1.0 mmol) and $\text{Bu}_3\text{N}^+\text{SO}_3^-$ (530 mg, 2.0 mmol) were dissolved in dry MeCN (1.0 mL) and heated under

reflux for 2.5 h. The flask was cooled and the solvent removed under reduced pressure. The crude reaction product was purified by chromatography (SiO_2 ; $\text{CH}_2\text{Cl}_2/\text{MeOH}$, 9:1, $R_f = 0.6$) to yield the title compound as a clear oil (350 mg, 87%). **IR** V_{max} cm^{-1} 3442 br, 2960 w, 2874 w, 1604 w, 1590 w, 1494 m, 1463 m, 1243 s; **$^1\text{H-NMR}$** δ_{H} (400 MHz, CDCl_3) 9.81 (br s, 1H, NH), 7.46 (app. d, $J = 5.5$ Hz, 1H, C6- H), 7.25 – 7.20 (m, 1H, C4- H), 6.90 (app. t, $J = 7.5$ Hz, 1H, C3- H), 6.82 (app. d, $J = 8.2$ Hz, 1H, C5- H), 5.15 (s, 2H, C1- CH_2), 3.79 (s 3H, Me), 3.03 – 2.91 (m, 6H, N- CH_2), 1.67 (m, 6H, CH_2), 1.33 (h, $J = 6.8$ Hz, 6H, CH_2), 0.92 (t, $J = 6.8$ Hz, 9H, CH_3); **$^{13}\text{C-NMR}$** δ_{C} (101 MHz, CDCl_3) 157.1 (C2), 129.4 (C3), 128.9 (C6), 125.4 (C1), 120.4 (C4), 110.2 (C5), 64.8 (C1- CH_2), 55.4 (Me), 52.6 (N- CH_2), 25.3 (CH_2), 20.1 (CH_2), 13.6 (CH_3); **LRMS** m/z (ESI+) 186.2 (100%, $[\text{M}-\text{OCH}_3]^{2+}$), 589.4 (60%, $[\text{M}+\text{Bu}_3\text{NH}]^+$); **HRMS** m/z (ESI+) $\text{C}_{32}\text{H}_{65}\text{N}_2\text{O}_5\text{S}$ Requires: 589.4614, Found: 589.4617 ($[\text{M}+\text{Bu}_3\text{NH}]^+$).

(**28**) Sodium benzyl sulfate⁹

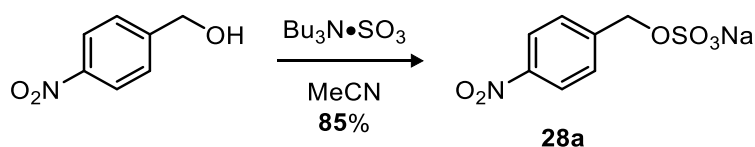


Following general procedure **H**: BnOH (108 mg, 1.0 mmol) and $\text{Bu}_3\text{N}\cdot\text{SO}_3$ (530 mg, 2.0 mmol) were dissolved in dry MeCN (2.0 mL) and heated under reflux for 2.5 h. The flask was cooled and purified by work up procedure **i** to yield the title compound as a bright white solid (200 mg, 95%). **M.P** 194 – 196 °C (lit. 194-196 °C); **IR** V_{max} cm^{-1} 3064 w, 3032 w, 1455 w, 1204 s; **$^1\text{H-NMR}$** δ_{H} (400 MHz, CD_3OD) 7.46 – 7.27 (m, 5H, CH), 5.03 (s, 2H, CH_2); **$^{13}\text{C-NMR}$** δ_{C} (101 MHz, CD_3OD) 136.4 (C1), 128.0 (C3), 127.7 (3C, C2 & C4), 69.4 (CH_2); **LRMS** m/z (ESI+) 233.0 (100%, $[\text{M}+\text{Na}]^+$). Data were consistent with the literature.⁹

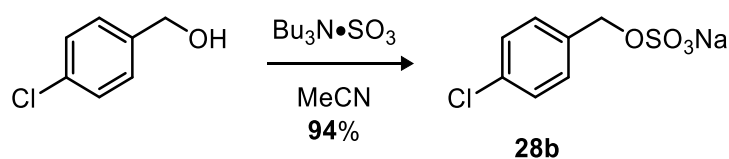
Control experiment with sequential [PyH]⁺ to [Bu₄N]⁺ exchange

Following general procedure **H**: BnOH (108 mg, 1.0 mmol) and Py•SO₃ (2.0 mmol) were dissolved in dry MeCN (2.0 mL) and heated under reflux for 2 h. The reaction was cooled to room temperature and TBAI (2.0 eq.) was added and stirred for 10 min. Solvents were removed under reduced pressure and the residue dissolved in EtOH (25 mL). NEH (5.0 eq.) was added and the mixture stirred for 1 h at room temperature. The precipitate was collected by filtration, washed with EtOH and dried under vacuum to afford **28** as a white solid (99 mg, 47%)

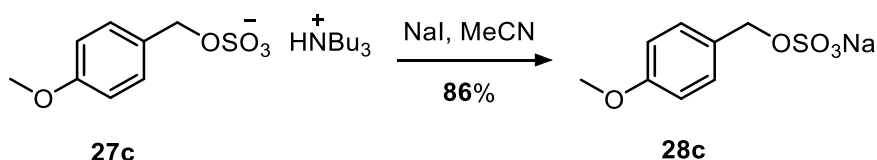
(28a) Sodium 4-nitrobenzyl sulfate



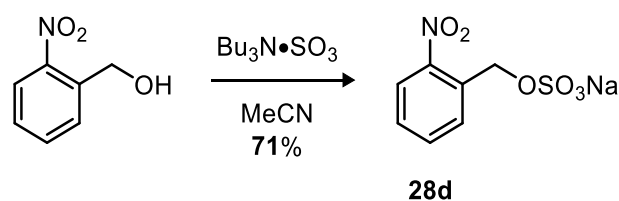
Following general procedure **H**: 4-Nitrobenzyl alcohol (153 mg, 1.0 mmol) and Bu₃N•SO₃ (530 mg, 2.0 mmol) were dissolved in dry MeCN (2.0 mL) and heated under reflux for 2.5 h. The flask was cooled and the contents purified by work up procedure **ii**. Recrystallization from hot MeOH afforded the title compound as light yellow crystals (216 mg, 85%). **M.P** 162 – 167 °C (dec.); **IR** V_{max} cm⁻¹ 2685 w, 2593 w, 1613 w, 1536 s, 1351 s, 1239 s; **¹H-NMR** δ_H (400 MHz, D₂O) 8.26 – 8.21 (m, 2H, C3-H), 7.69 – 7.55 (m, 2H, C2-H), 5.17 (s, 2H, C1-CH₂); **¹³C-NMR** δ_C (101 MHz, D₂O) 147.4 (C4), 143.2 (C1), 128.4 (C3), 123.8 (C2), 69.1 (C1-CH₂); **LRMS** *m/z* (ESI⁺) 277.9 (100%, [M+Na]⁺); **HRMS**; *m/z* (ESI⁺) C₇H₆NO₆Na₂S Requires: 277.9711, Found: 277.9712 ([M+Na]⁺).

(28b) Sodium 4-chlorobenzyl sulfate

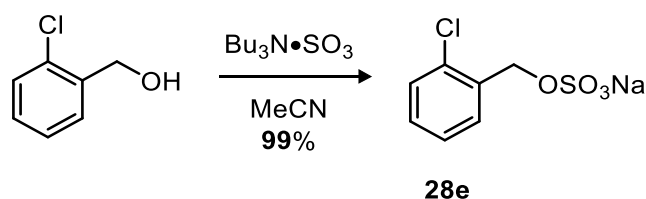
Following general procedure **H**: 4-Chlorobenzyl alcohol (142 mg, 1.0 mmol) and $\text{Bu}_3\text{N}\cdot\text{SO}_3$ (530 mg, 2.0 mmol) were dissolved in dry MeCN (2.0 mL) and heated under reflux for 2.5 h. The flask was cooled and purified by work up procedure **i** to yield the title compound as a bright white solid (229 mg, 94%). **M.P** 202 – 204 °C; **IR** V_{max} cm^{-1} 2193 w, 1205 w; **$^1\text{H-NMR}$** δ_{H} (400 MHz, CD_3OD) 7.46 – 7.28 (m, 4H, C2-H & C3-H), 4.99 (s, 2H, C1-CH₂); **$^{13}\text{C-NMR}$** δ_{C} (101 MHz, CD_3OD) 136.8 (C4), 134.8 (C1), 130.6 (CH), 129.5 (CH), 69.8 (C1-CH₂); **LRMS** m/z (ESI+) 266.9 (100%, $[\text{M}+\text{Na}]^+$); **HRMS** m/z (ESI+) $\text{C}_7\text{H}_6\text{ClNa}_2\text{O}_4\text{S}$ Requires: 266.9470, Found: 266.9471 ($[\text{M}+\text{Na}]^+$).

(28c) Sodium 4-methoxybenzyl sulfate

Tributylammonium 4-methoxybenzyl sulfate (**27c**) (161 mg, 0.4 mmol) was subjected to work up procedure **iii** to yield the title compound as a lustrous white solid (93 mg, 86%). **M.P** 100 °C (dec. pink solid); **IR** V_{max} cm^{-1} 3014 w, 2842 w, 1612 w, 1514 m, 1250 s; **$^1\text{H-NMR}$** δ_{H} (400 MHz, $(\text{CD}_3)_2\text{SO}$) 7.25 (d, $J = 8.1$ Hz, 2H, C2-H), 6.89 (d, $J = 8.1$ Hz, 2H, C3-H), 4.69 (s, 2H, C1-CH₂), 3.74 (s, 3H, Me); **$^{13}\text{C-NMR}$** δ_{C} (101 MHz, $(\text{CD}_3)_2\text{SO}$) 158.7 (C4), 129.7 (C1), 129.4 (C3), 113.6 (C2), 67.3 (C1-CH₂), 55.1 (Me); **LRMS** m/z (ESI+) 281.1 (100%, $[\text{M}+\text{Na}+\text{H}_2\text{O}]^+$), 263.0 (10%, $[\text{M}+\text{Na}]^+$); **HRMS** m/z (ESI+) $\text{C}_8\text{H}_9\text{O}_5\text{Na}_2\text{S}$ Requires: 262.9965, Found: 262.9966 ($[\text{M}+\text{Na}]^+$).

(28d) Sodium 2-nitrobenzyl sulfate¹⁰

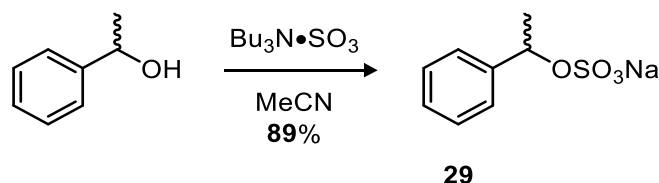
Following general procedure **H**: 2-Nitrobenzyl alcohol (153 mg, 1.0 mmol) and $\text{Bu}_3\text{N}\cdot\text{SO}_3$ (530 mg, 2.0 mmol) were dissolved in dry MeCN (2.0 mL) and heated under reflux for 2.5 h. The flask was cooled and the contents purified by work up procedure **ii**. Recrystallization from hot MeOH yielded the title compound as light yellow crystals (180 mg, 71 %). **M.P** 109 – 111 °C (dec.); **IR** $V_{\text{max}} \text{ cm}^{-1}$ 1610 w, 1526 s, 1334 s, 1225 s; **¹H-NMR** δ_{H} (400 MHz, D_2O) 8.14 – 8.08 (m, 1H), 7.78 – 7.69 (m, 2H), 7.59 – 7.52 (m, 1H), 5.41 (s, 2H, C1-CH₂); **¹³C-NMR** δ_{C} (101 MHz, D_2O) 144.2 (C2), 134.4 ($\underline{\text{C}}\text{H}$), 131.2 (C1), 129.5 ($\underline{\text{C}}\text{H}$), 129.3 ($\underline{\text{C}}\text{H}$), 125.0 ($\underline{\text{C}}\text{H}$), 67.1 (C1-CH₂); **LRMS** m/z (ESI+) 277.9 (100%, $[\text{M}+\text{Na}]^+$); **HRMS** m/z (ESI+) $\text{C}_7\text{H}_6\text{NO}_6\text{Na}_2\text{S}$ Requires: 277.9711, Found: 277.9713 ($[\text{M}+\text{Na}]^+$). Data were in accordance with literature.¹⁰

(28e) Sodium 2-chlorobenzyl sulfate

Following general procedure **H**: 2-Chlorobenzyl alcohol (142 mg, 1.0 mmol) and $\text{Bu}_3\text{N}\cdot\text{SO}_3$ (530 mg, 2.0 mmol) were dissolved in dry MeCN (2.0 mL) and heated under reflux for 2.5 h. The flask was cooled and purified by work up procedure **i** to yield the title compound as a white solid (242 mg, 99%). **M.P** 219 – 221 °C; **IR** $V_{\text{max}} \text{ cm}^{-1}$ 3580 w, 1478 w, 1252 s, 1203 s; **¹H-NMR** δ_{H} (400 MHz, D_2O) 7.52 – 7.43 (m, 2H), 7.39 – 7.31 (m, 2H), 5.15 (s, 2H, C1-CH₂); **¹³C-NMR** δ_{C} (101 MHz, D_2O) 133.5 (C2),

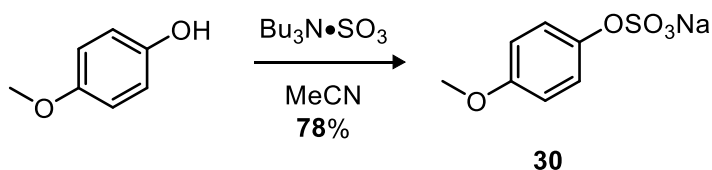
132.5 (C1), 130.8 ($\underline{\text{CH}}$), 130.4 ($\underline{\text{CH}}$), 129.5 ($\underline{\text{CH}}$), 127.3 ($\underline{\text{CH}}$), 68.1 (C1- $\underline{\text{CH}}_2$); **LRMS** m/z (ESI+) 266.9 ($[\text{M}^{35}\text{Cl}+\text{Na}]^+$, 100%), 268.9 ($[\text{M}^{37}\text{Cl}+\text{Na}]^+$, 30%); **HRMS** m/z (ESI+) $\text{C}_7\text{H}_6\text{O}_4\text{Na}_2\text{SCl}$ Requires: 266.9471, Found: 266.9475 ($[\text{M}^{35}\text{Cl}+\text{Na}]^+$).

(29) Sodium 1-phenylethyl sulfate¹¹



Following general procedure **H**: 1-Phenyl ethanol (122 mg, 1.0 mmol) and $\text{Bu}_3\text{N}\cdot\text{SO}_3$ (530 mg, 2.0 mmol) were dissolved in dry MeCN (2.0 mL) and heated under reflux for 2.5 h. The flask was cooled and purified by work up procedure **ii**. The final solid was suspended in EtOAc and filtered to yield the title compound as its sodium salt (200 mg, 89%). **M.P** 165 – 167 °C; **IR** ν_{max} cm^{-1} 1582 w, 1388w, 1148 s; **$^1\text{H-NMR}$** δ_{H} (400 MHz, CD_3OD) 7.43 – 7.38 (m, 2H, $\underline{\text{CH}}$), 7.34 – 7.28 (m, 2H, $\underline{\text{CH}}$), 7.27–7.21 (m, 1H, C4- $\underline{\text{H}}$), 5.46 (q, $J = 6.6$ Hz, 1H, C1- $\underline{\text{CH}}$), 1.60 (d, $J = 6.6$ Hz, 3H, Me); **$^{13}\text{C-NMR}$** δ_{C} (101 MHz, CD_3OD) 144.0 (C1), 129.2 ($\underline{\text{CH}}$), 128.5 (C4), 127.0 ($\underline{\text{CH}}$), 78.0 (C1- $\underline{\text{CH}}$), 23.7 (Me); **LRMS** m/z (ESI+) 695.2 (100%, $[3\text{M}+\text{Na}]^+$), 225.0 (40%, $[\text{M}+\text{H}]^+$); **HRMS**. m/z (ESI+) $\text{C}_8\text{H}_{10}\text{O}_4\text{NaS}$ Requires: 225.0198, Found: 225.0199 ($[\text{M}+\text{H}]^+$). Data were in accordance with literature.¹¹

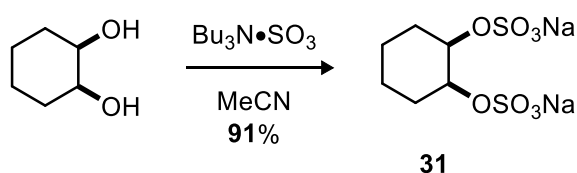
(30) Sodium 4-methoxyphenyl sulfate



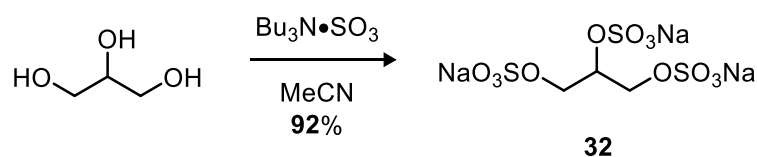
Following general procedure **H**: 4-Methoxy phenol (*p*-Guaiacol, 124 mg, 1.0 mmol) and $\text{Bu}_3\text{N}\cdot\text{SO}_3$ (530 mg, 2.0 mmol) were dissolved in dry MeCN (2.0 mL) and heated

under reflux for 5 h. The flask was cooled and purified by work up procedure **ii** to yield the title compound as its sodium salt (176 mg, 78%). **M.P** 265 °C (dec.); **IR** V_{\max} cm^{-1} 2955 w 2499 w, 1504 s; 1199 s; **$^1\text{H-NMR}$** δ_{H} (400 MHz, CD_3OD) 6.75 – 6.67 (m, 4H, CH), 3.69 (s, 3H, Me); **$^{13}\text{C-NMR}$** δ_{C} (101 MHz, CD_3OD) 154.4 (C1), 152.1 (C4), 116.7 (CH), 115.7 (CH), 56.1 (Me); **LRMS** m/z (ESI+) 331.2 (100%, $[\text{3M}+2\text{MeCN}+\text{Na}]^+$), 516.3 (10%, $[\text{2M}+\text{MeCN}+\text{Na}+\text{H}]^+$); **HRMS** m/z (ESI+) $\text{C}_9\text{H}_{10}\text{NNa}_2\text{O}_5\text{S}$ Requires: 290.0075, Found: 290.0076 ($[\text{M}+\text{MeCN}+\text{Na}]^+$).

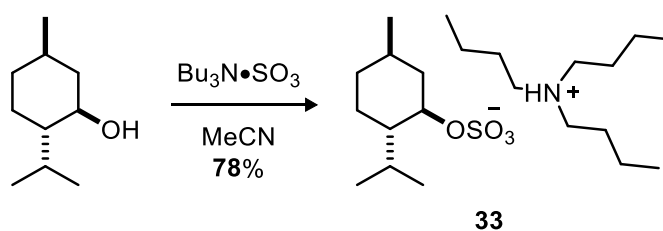
(31) Sodium (1*R*, 2*S*)-cyclohexane-1,2-diyl bis(sulfate)¹²



Following general procedure **H**: *cis*-Cyclohexanediol (116 mg, 1.0 mmol) and $\text{Bu}_3\text{N}\cdot\text{SO}_3$ (1.06 g, 4.0 mmol) were dissolved in dry MeCN (2.0 mL) and heated under reflux for 5.0 h. The flask was cooled and purified by work up procedure **i**. Recrystallization from hot EtOH yielded the title sulfate as a bright white solid (290 mg, 91%). **M.P** 203 – 205 °C (dec.); **IR** V_{\max} cm^{-1} 2946 w, 1456 w, 1328 w, 1258 w, 1232 w, 1200 w; **$^1\text{H-NMR}$** δ_{H} (400 MHz, D_2O) 4.57 – 4.52 (m, 2H, C1- H & C2- H), 1.98 – 1.95 (m, 2H, CH_2), 1.76 – 1.55 (m, 4H, CH_2), 1.49 – 1.33 (m, 2H, CH_2); **$^{13}\text{C-NMR}$** δ_{C} (101 MHz, D_2O) 77.8 (C1 & C2), 27.7 (C3 & C6), 20.8 (C4 & C5); **LRMS** m/z (ESI+) 342.9 (100%, $[\text{M}+\text{Na}]^+$), 306.85 (40%), 164.92 (32%); **HRMS** m/z (ESI+) $\text{C}_6\text{H}_{10}\text{O}_8\text{Na}_3\text{S}_2$ Requires: 342.9510, Found: 342.9514 ($[\text{M}+\text{Na}]^+$). Data were in accordance with literature.¹²

(32) Sodium propane-1,2,3-triyl tris(sulfate)¹³

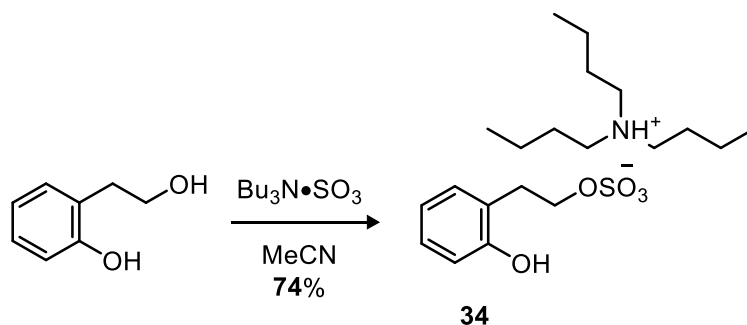
Following general procedure **H**: Glycerol (92 mg, 1.0 mmol) and $\text{Bu}_3\text{N}^+\text{SO}_3^-$ (1.59 g, 6.0 mmol) were dissolved in dry MeCN (4.0 mL) and heated under reflux for 8 h. The flask was cooled and the crude mixture was purified by work up procedure **i**. Recrystallization from hot EtOH yielded the title sulfate as a bright white solid (365 mg, 92%). **M.P** 210 °C (dec.); **IR** V_{max} cm^{-1} 1639 w, 1216 s; **$^1\text{H-NMR}$** δ_{H} (400 MHz, D_2O) 4.80 (p, $J = 4.8$ Hz, 1H, CH), 4.27 (qd, $J = 11.1, 4.8$ Hz, 4H, CH_2); **$^{13}\text{C-NMR}$** δ_{C} (101 MHz, D_2O) 74.5 (CH), 66.2 (CH_2); **LRMS** m/z (ESI+) 420.8 (100%, $[\text{M}+\text{Na}]^+$), 306.85 (50%); **HRMS** m/z (ESI+) $\text{C}_3\text{H}_5\text{O}_{12}\text{Na}_4\text{S}_3$ Requires: 420.8534, Found: 420.8538 ($[\text{M}+\text{Na}]^+$). Data were in accordance with literature.¹³

(33) Tributylammonium (\pm)-2-*isopropyl*-5-methylcyclohexyl sulfate

Following general procedure **H**: (\pm)-Menthol (156 mg, 1.0 mmol) and $\text{Bu}_3\text{N}^+\text{SO}_3^-$ (530 mg, 2.0 mmol) were dissolved in dry MeCN (2.0 mL) and heated under reflux for 3 h. The flask was cooled and the solvent was removed under reduced pressure. The crude contents were purified (SiO_2 ; $\text{CH}_2\text{Cl}_2/\text{MeOH}$, 9:1, $R_f = 0.45$) to yield the title compound as a white crystalline solid (330 mg, 78%). **M.P** 92 °C; **IR** V_{max} cm^{-1} 2957 m, 2870 m, 1458 m, 1248 s; **$^1\text{H-NMR}$** δ_{H} (400 MHz, CDCl_3) 9.95 (br s, 1H, NH), 4.16 (td, $J = 10.7, 4.4$ Hz, 1H, CH-OSO_3^-), 3.04 – 2.94 (m, 6H, N-CH_2), 2.49 – 2.43 (m, 1H, CH-Pr),

2.26 (sd, $J = 7.0, 2.5$ Hz, 1H, $\underline{\text{CH}}(\text{CH}_3)_2$), 1.74 – 1.63 (m, 6H, $\underline{\text{CH}_2}$), 1.63 – 1.57 (m, 2H, $\underline{\text{CH}_2}$), 1.35 (h, $J = 7.4$ Hz, 7H, $\underline{\text{CH}_2}$), 1.24 (tdd, $J = 10.7, 3.4, 1.7$ Hz, 1H, $\underline{\text{CH}_2}$), 1.10 – 0.96 (m, 2H, $\underline{\text{CH}_2}$), 0.93 (t, $J = 7.4$ Hz, 9H, $\underline{\text{CH}_3}$), 0.82 (dd, $J = 6.8, 4.4$ Hz, 6H, $\text{CH}(\underline{\text{CH}_3})_2$), 0.77 (d, $J = 6.8$ Hz, 4H, Me & $\underline{\text{CH}_2}$); **$^{13}\text{C-NMR}$** δ_{C} (101 MHz, CDCl_3) 78.9 ($\underline{\text{CH-OSO}_3^-}$), 52.6 (N- $\underline{\text{CH}_2}$), 48.1 ($\underline{\text{CH}}$), 42.0 ($\underline{\text{CH-Pr}}$), 34.4 ($\underline{\text{CH}_2}$), 31.6 ($\underline{\text{CH}_2}$), 25.4 ($\underline{\text{CH}}(\text{CH}_3)_2$), 25.3 ($\underline{\text{CH}_2}$), 23.2 ($\underline{\text{CH}_2}$), 22.2 ($\underline{\text{CH}_2}$), 21.2 ($\text{CH}(\underline{\text{CH}_3})_2$), 20.1 ($\underline{\text{CH}_2}$), 16.0 (Me), 13.6 ($\underline{\text{CH}_3}$); **LRMS** m/z (ESI+) 607.62 (100%, $[\text{M}+\text{NBu}_3]^+$); **HRMS** m/z (ESI+) $\text{C}_{34}\text{H}_{75}\text{N}_2\text{O}_4\text{S}$ Requires: 647.5448, Found: 647.5446 ($[\text{M}+\text{NBu}_3]^+$).

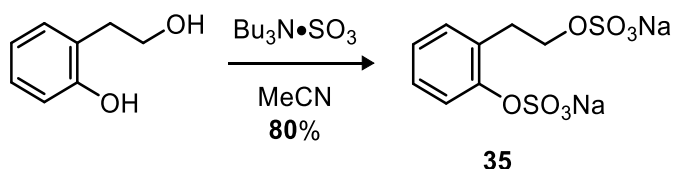
(34) Tributylammonium 2-hydroxyphenylethanol sulfate



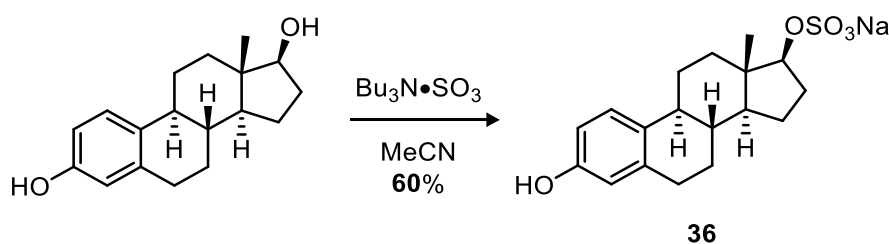
Following general procedure **H**: 2-Hydroxyphenyl ethanol (138 mg, 1.0 mmol) and $\text{Bu}_3\text{N}\cdot\text{SO}_3$ (530 mg, 2.0 mmol) were dissolved in dry MeCN (4.0 mL) and heated under reflux for 2.5 h. The flask was cooled and the solvent was removed under reduced pressure. The residue was purified by chromatography (SiO_2 , $\text{CH}_2\text{Cl}_2/\text{MeOH}$ 19:1 to 9:1) to afford the title compound as a clear oil (300 mg, 74%). **IR** V_{max} cm^{-1} 3259 br, 2962 w, 2874 w, 1596 w, 1456 m, 1245 s, 1200 s; **$^1\text{H-NMR}$** (400 MHz, CDCl_3) 7.94 (br s, 2H, $\underline{\text{NH}}$ & $\underline{\text{OH}}$), 7.08 – 6.97 (m, 2H, $\text{C3-}\underline{\text{H}}$ & $\text{C5-}\underline{\text{H}}$), 6.89 (dd, $J = 8.0, 1.3$ Hz, 1H, $\text{C6-}\underline{\text{H}}$), 6.72 (td, $J = 8.0, 1.3$ Hz, 1H, $\text{C4-}\underline{\text{H}}$), 4.26 (t, $J = 6.7$ Hz, 2H, $\underline{\text{CH}_2}\text{-OSO}_3^-$), 2.98 (t, $J = 6.7$ Hz, 2H, $\text{C1-}\underline{\text{CH}_2}$), 2.96 – 2.88 (m, 6H, N- $\underline{\text{CH}_2}$), 1.69 – 1.55 (m, 6H, $\underline{\text{CH}_2}$), 1.29 (h, $J = 7.4$ Hz, 6H, $\underline{\text{CH}_2}$), 0.88 (t, $J = 7.4$ Hz, 9H, $\underline{\text{CH}_3}$); **$^{13}\text{C-NMR}$** (101 MHz, CDCl_3) δ_{C} 155.2 (C2), 130.3 (C3), 127.5 (C5), 124.0 (C1), 119.4 (C4), 115.8 (C6), 68.2

($\text{CH}_2\text{-OSO}_3^-$), 52.4 (N- CH_2), 30.5 (C1- CH_2), 25.1 (CH_2), 19.6 (CH_2), 13.2 (CH_3); **LRMS** m/z (ESI+) 589.50 (100%, $[\text{M}+\text{NHBU}_3]^+$); **HRMS** m/z (ESI+) $\text{C}_{32}\text{H}_{65}\text{N}_2\text{O}_5\text{S}$ Requires:: 589.4614, Found: 589.4617 ($[\text{M}+\text{NHBU}_3]^+$).

(35) Sodium 2-(2-(sulfonatooxy)ethyl)phenyl sulfate

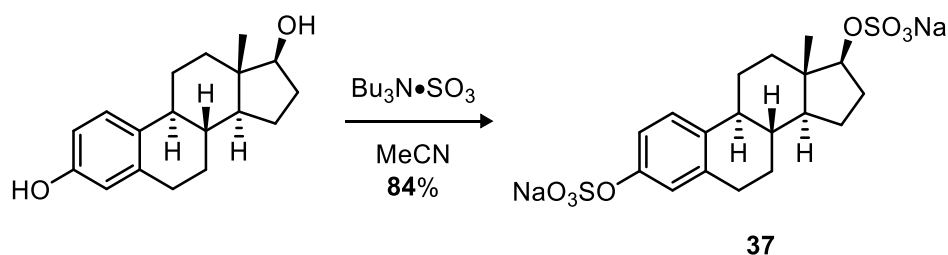


Adapted from general procedure **H**: 2-Hydroxyphenyl ethanol (69 mg, 0.5 mmol) and $\text{Bu}_3\text{N}\cdot\text{SO}_3$ (530 mg, 2.0 mmol) were dissolved in dry MeCN (1.0 mL) and heated under reflux for 4.0 h. The flask was cooled and the solvent was removed under reduced pressure. The residue was charged with H_2O (10 mL) and extracted with EtOAc (4 \times 30 mL). The pooled extracts were dried (MgSO_4) and the solvent removed under reduced pressure to afford the intermediate $[\text{Bu}_3\text{NH}]^+$ salt. The intermediate was purified by work up procedure **iii** to afford the title compound as a white solid (135 mg, 80%). **IR** ν_{max} cm^{-1} 2260 w, 1584 w, 1489 w, 1453 w, 1221 s; **$^1\text{H-NMR}$** δ_{H} (400 MHz, $(\text{CD}_3)_2\text{SO}$) 7.35 (dd, $J = 8.2, 1.3$ Hz, 1H, C6- H), 7.20 (dd, $J = 7.5, 1.8$ Hz, 1H, C3- H), 7.12 (ddd, $J = 8.2, 7.5, 1.8$ Hz, 1H, C5- H), 6.99 (td, $J = 7.5, 1.3$ Hz, 1H, C4- H), 3.89 (t, $J = 7.2$ Hz, 1H, $\text{CH}_2\text{OSO}_3\text{Na}$), 2.86 (t, $J = 7.2$ Hz, 1H, C2- CH_2); **$^{13}\text{C-NMR}$** δ_{C} (101 MHz, $(\text{CD}_3)_2\text{SO}$) 151.7 (C1- OSO_3Na), 130.6 (C2), 130.1 (C3), 126.7 (C5), 123.3 (C4), 121.3 (C6), 65.4 ($\text{CH}_2\text{OSO}_3\text{Na}$), 29.9 (C2- CH_2); **LRMS** m/z (ESI-) 318.81 (100%, $[\text{M}-\text{Na}]^-$), 660.95 (15%, $[2\text{M}-\text{Na}]^-$); **HRMS** m/z (ESI-) $\text{C}_8\text{H}_8\text{O}_8\text{NaS}_2$ Requires: 318.9558, Found: 318.9557 ($[\text{M}-\text{Na}]^-$).

(36) Sodium (17 β)-estra-1,3,5(10)-triene-3-ol,17-sulfate

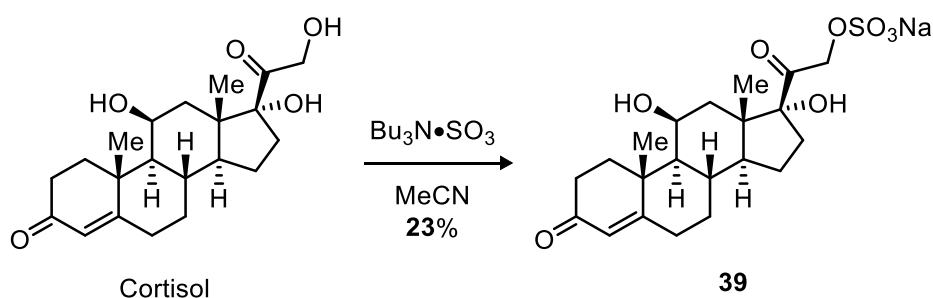
Following general procedure **H**: β -Estradiol (272 mg, 1.0 mmol) and $\text{Bu}_3\text{N}\cdot\text{SO}_3$ (398 mg, 1.5 mmol) were dissolved in dry MeCN (4.0 mL) and heated under reflux for 3 h. The flask was cooled and the solvent was removed under reduced pressure. The contents were purified (SiO_2 ; $\text{CH}_2\text{Cl}_2/\text{MeOH}$, 9:1, $R_f = 0.16$) to yield an intermediate tributylammonium sulfate as a clear oil (321 mg, 0.6 mmol). The intermediate was purified by work up procedure **iii** to yield the title compound as a bright white solid (225 mg, 60%). **M.P** 170 °C (dec. to a green solid); **IR** $\text{V}_{\text{max}} \text{ cm}^{-1}$ 3432 br, 2925 w, 2869 w, 1612 w, 1499 w, 1210 s; **$^1\text{H-NMR}$** δ_{H} (400 MHz, $(\text{CD}_3)_2\text{SO}$) 9.01 (s, 1H, OH), 7.04 (d, $J = 8.5$ Hz, 1H, C1-H), 6.50 (dd, $J = 8.5, 2.6$ Hz, 1H, C2-H), 6.42 (d, $J = 2.6$ Hz, 1H, C4-H), 4.05 (t, $J = 8.5$ Hz, 1H), 2.69 (d, $J = 6.8$ Hz, 2H), 2.29 – 2.13 (m, 1H), 2.16 – 1.83 (m, 3H), 1.84 – 1.70 (m, 1H), 1.66–1.44 (m, 2H), 1.33 – 1.06 (m, 6H), 0.68 (s, 3H, Me); **$^{13}\text{C-NMR}$** δ_{C} (101 MHz, $(\text{CD}_3)_2\text{SO}$) 154.9, 137.1, 130.4, 126.1, 114.9, 112.7, 84.1, 49.2, 43.5, 42.4, 38.5, 36.6, 29.2, 28.2, 26.9, 26.0, 22.7, 11.7; **LRMS** m/z (ESI $^-$) 351.13 (100%, $[\text{M}-\text{Na}]^-$), 725.32 (100%, $[2\text{M}-\text{Na}]^-$), 703.31 (90%, $[2\text{M}-2\text{Na}+\text{H}]^-$); **HRMS** m/z (ESI $^-$) $\text{C}_{18}\text{H}_{23}\text{O}_5\text{S}$ Requires: 351.1268, Found: 351.1268 ($[\text{M}-\text{Na}]^+$).

(37) Sodium (8*R*,9*S*,13*S*,14*S*,17*S*)-13-methyl-7,8,9,11,12,13,14,15,16,17-decahydro-6*H*-cyclopenta[*a*]phenanthrene-3,17-diyl bis(sulfate)

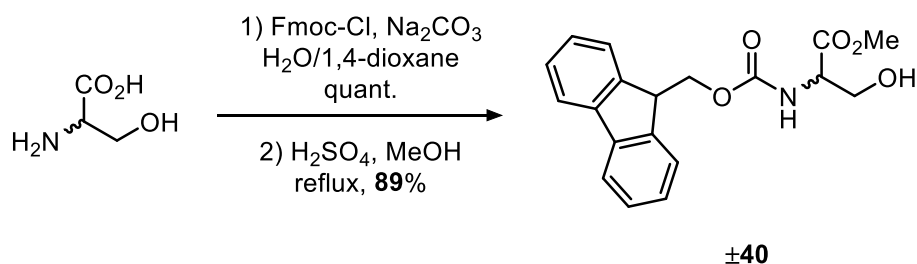


Adapted from general procedure **H**: β -Estradiol (136 mg, 0.5 mmol) and $\text{Bu}_3\text{N}\cdot\text{SO}_3$ (663 mg, 2.5 mmol) were dissolved in dry MeCN (1.0 mL) and heated under reflux for 4 h. The flask was cooled and the solvent was removed under reduced pressure. The crude product was purified by work up procedure **iii** to produce a white solid containing <4% **36** as an impurity (Calculated by $^1\text{H-NMR}$). Recrystallization from MeOH/EtOAc afforded the title compound as a bright white solid (200 mg, 84%). $[\alpha]_{\text{D}}^{25} +6.51$ (1.0, H_2O); **M.P** 137 – 140 $^\circ\text{C}$ (dec. to a red solid); **IR** $\text{V}_{\text{max}} \text{ cm}^{-1}$ 2926 w, 2868 w, 1609 w, 1499 w, 1214 s; **$^1\text{H-NMR}$** δ_{H} (400 MHz, $(\text{CD}_3)_2\text{SO}$) δ 7.15 (d, $J = 8.5$ Hz, 1H), 6.93 – 6.75 (m, 2H), 4.05 (q, $J = 10.9, 9.7$ Hz, 1H, C17-H), 2.85 – 2.67 (m, 2H), 2.31 – 2.17 (m, 1H), 2.17 – 2.09 (m, 1H), 2.09 – 1.87 (m, 2H), 1.87 – 1.70 (m, 1H), 1.69 – 1.48 (m, 2H), 1.44 – 1.05 (m, 6H), 0.70 (s, Me); **$^{13}\text{C-NMR}$** δ_{C} (101 MHz, $(\text{CD}_3)_2\text{SO}$) 151.1, 136.1, 134.8, 125.5, 120.5, 118.0, 84.1, 49.2, 43.6, 42.4, 38.3, 36.6, 29.2, 28.2, 26.8, 25.9, 22.7, 11.7; **LRMS** m/z (ESI+) 499.05 (100%, $[\text{M}+\text{Na}]^+$), 379.01 (50%), 261.01 (50%); **HRMS** m/z (ESI+) $\text{C}_{18}\text{H}_{22}\text{O}_8\text{Na}_3\text{S}_2$ Requires: 499.0449, Found: 499.0450 ($[\text{M}+\text{Na}]^+$).

(39) Sodium 2-((8*S*,9*S*,10*R*,11*S*,13*S*,14*S*,17*R*)-11,17-dihydroxy-10,13-dimethyl-3-oxo-2,3,6,7,8,9,10,11,12,13,14,15,16,17-tetradecahydro-1H-cyclopenta[*a*]phenanthren-17-yl)-2-oxoethyl sulfate



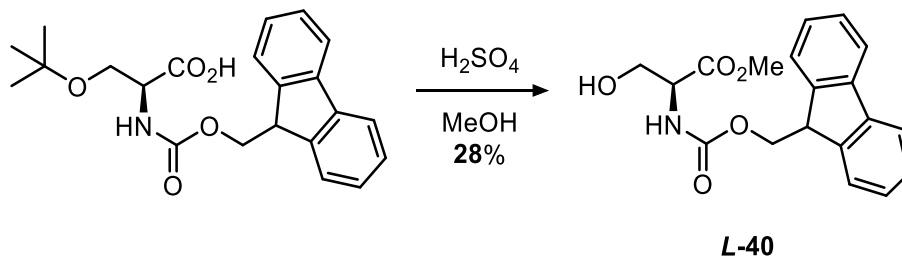
Adapted from general procedure **H**: Cortisol (36 mg, 0.1 mmol) and $\text{Bu}_3\text{N}\cdot\text{SO}_3$ (32 mg, 0.13 mmol) were dissolved in dry MeCN (0.2 mL) and heated under reflux for 2 h with monitoring by HPLC (C18 column, MeCN/ H_2O 3:7). The flask was cooled and the solvent was removed under reduced pressure. The residue was purified by chromatography (SiO_2 , EtOAc/MeOH 19:1 to 2:1) to afford 24 mg of **38** and 12mg of cortisol. The intermediate (**38**) was purified by work up procedure **i** to afford the title compound as a white solid (8 mg, 23% based on recovered starting material). **^1H -NMR** (400 MHz, $(\text{CD}_3)_2\text{SO}$) δ_{H} 5.55 (d, $J = 1.5$ Hz, 1H), 5.31 (s, 1H), 4.85 (d, $J = 18.2$ Hz, 1H), 4.43 (d, $J = 18.2$ Hz, 1H), 4.37 (d, $J = 3.4$ Hz, 1H), 4.26 (s, 1H), 2.23 – 2.12 (m, 2H), 2.08 (dd, $J = 9.4, 3.9$ Hz, 2H), 1.89 (d, $J = 9.6$ Hz, 1H), 1.84 – 1.73 (m, 2H), 1.72 – 1.62 (m, 2H), 1.60 – 1.52 (m, 3H), 1.36 (s, 3H), 1.35 – 1.21 (m, 2H), 1.07 – 0.92 (m, 3H), 0.86 (t, $J = 5.6$ Hz, 2H), 0.75 (s, 3H); **^{13}C -NMR** (101 MHz, $(\text{CD}_3)_2\text{SO}$) δ_{C} 198.1, 172.5, 165.5, 122.1, 88.7, 74.3, 71.0, 69.2, 66.4, 55.5, 51.6, 46.4, 35.5, 35.4, 34.0, 33.5, 33.0, 31.4, 31.2, 20.5, 16.9; **LRMS** m/z (ESI+) 443.17 (100%, $[\text{M}-\text{Na}+2\text{H}]^+$); **HRMS** m/z (ESI+) $\text{C}_{21}\text{H}_{31}\text{NO}_8\text{S}$ Requires: 443.1734, Found: 443.1746 ($[\text{M}-\text{Na}+2\text{H}]^+$).

(±40) *N*-Fmoc-*D/L*-serine methyl ester¹⁴

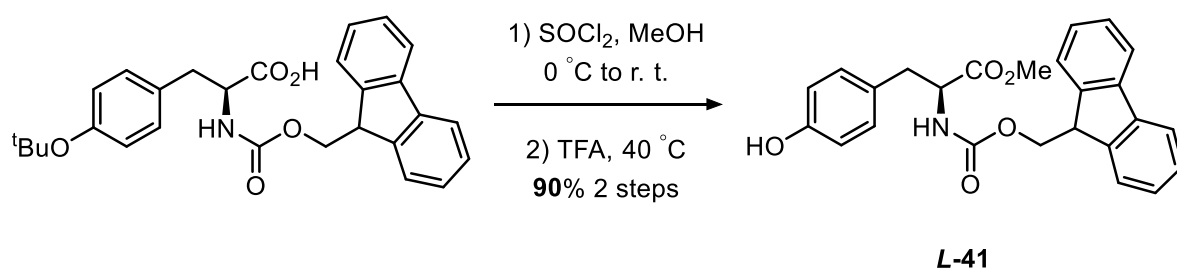
A solution of *D/L*-serine (1.03 g, 9.8 mmol) in Na_2CO_3 (aq.) (10%, 3 mL) was cooled on an ice bath. The flask was charged with a solution of 9-fluorenylmethoxycarbonyl chloride (2.45 g, 9.5 mmol) in 1,4-dioxane (3 mL) over 20 min. After full addition the flask was stirred at room temperature (20 °C) for 1 h. The aqueous mixture was washed with EtOAc (20 mL) and charged with 1 M HCl (aq.) (40 mL). The acidified solution was extracted with EtOAc (2 × 30 mL), the pooled organic extracts were washed with brine and dried (MgSO_4). Filtration of the solid and removal of solvent under reduced pressure afforded the Fmoc protected lysine as a white solid (2.90 g, 90%). The intermediate (1.0 g, 3.05 mmol) was dissolved in MeOH (20 mL) and charged with H_2SO_4 (0.1 mL). The reaction mixture was refluxed for 3 h, cool and the solvent removed under reduced pressure. The flask was charged with NaHCO_3 (aq.) (50 mL) and extracted with EtOAc (3 × 30 mL). The pooled organic extracts were washed with brined and dried (MgSO_4). Filtration of the solids and removal of the solvent under reduced pressure afforded the title compound as a white solid (2.90 g, 89%). **IR** ν_{max} cm^{-1} 3468 s, 3430 s, 2959 w, 2920 w, 2885 w, 1750 s, 1698 s, 1521 s; **$^1\text{H-NMR}$** (400 MHz, $(\text{CD}_3)_2\text{CO}$) δ_{H} 7.87 (dt, $J = 7.6, 1.0$ Hz, 2H), 7.80 – 7.67 (m, 2H), 7.42 (tt, $J = 7.6, 1.0$ Hz, 2H), 7.38 – 7.26 (m, 2H), 6.66 (d, $J = 8.5$ Hz, 1H), 4.45 – 4.14 (m, 5H), 3.99 – 3.81 (m, 2H), 3.70 (s, 3H); **$^{13}\text{C-NMR}$** (101 MHz, $(\text{CD}_3)_2\text{CO}$) δ_{C} 171.9, 157.0, 145.1, 145.0, 142.1, 128.5, 128.0, 126.21, 126.16, 120.8, 67.3, 63.0, 57.5, 52.4, 48.0;

LRMS m/z (ESI+) 364.12 (100%, $[M+Na]^+$). Data were in accordance with the literature.¹⁴

(**L-40**) *N*-Fmoc-*L*-serine methyl ester¹⁴



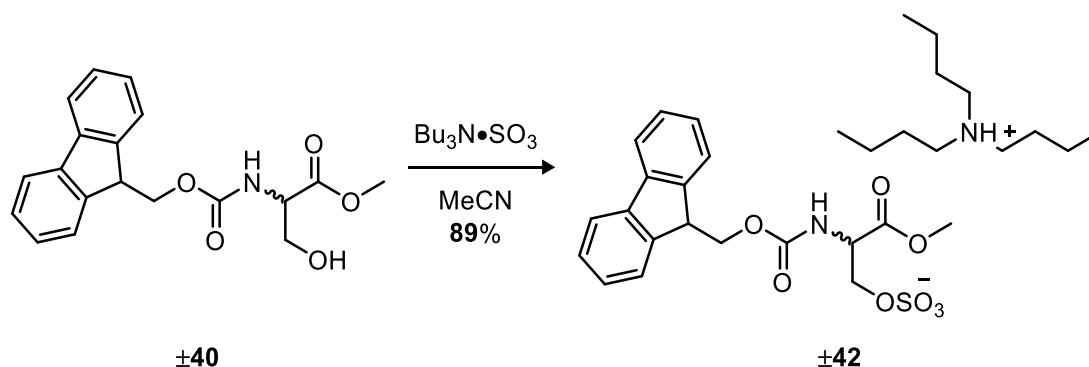
A solution of *N*-((9H-fluoren-9-yl)methoxy)carbonyl-*O*-(tert-butyl)-*L*-serine (2.0 g, 5.22 mmol) in MeOH (50 mL) was charged with H_2SO_4 (1 mL). The solution was heated under reflux for 12 h, cooled and the solvent was removed under reduced pressure. The acidic slurry was neutralised to pH 7 with $NaHCO_3$ (aq.) and extracted with EtOAc (3 × 30 mL). The pooled organic extracts were dried ($MgSO_4$) and the solvent was removed under reduced pressure. Purification by chromatography (SiO_2 , CH_2Cl_2 /Hex, 3:2 to 1:0) afforded an off white solid. Recrystallization of the solid (CH_2Cl_2) afforded the title compound as a bright white solid (500 mg, 28%). **IR** ν_{max} cm^{-1} 3468 s, 3430 s, 2959 w, 2920 w, 2885 w, 1750 s, 1698 s, 1521 s; **1H -NMR** (400 MHz, $(CD_3)_2CO$) δ_H 7.87 (dt, $J = 7.6, 1.0$ Hz, 2H), 7.80 – 7.67 (m, 2H), 7.42 (tt, $J = 7.6, 1.0$ Hz, 2H), 7.38 – 7.26 (m, 2H), 6.66 (d, $J = 8.5$ Hz, 1H), 4.45 – 4.14 (m, 5H), 3.99 – 3.81 (m, 2H), 3.70 (s, 3H); **^{13}C -NMR** (101 MHz, $(CD_3)_2CO$) δ_C 171.9, 157.0, 145.1, 145.0, 142.1, 128.5, 128.0, 126.21, 126.16, 120.8, 67.3, 63.0, 57.5, 52.4, 48.0; **LRMS** m/z (ESI+) 364.12 (100%, $[M+Na]^+$). Data were in accordance with the literature.¹⁴

(L-41) *N*-Fmoc-*L*-tyrosine methyl ester¹⁵⁻¹⁶

Esterification: A cooled (0 °C) solution of Fmoc-Tyr(^tBu)-OH (1.59 g, 3.48 mmol) in anhydrous MeOH (20 mL) was charged dropwise with freshly distilled thionyl chloride (5.05 mL, 6.96 mmol). After full addition, the flask was warmed to room temperature and the reaction mixture stirred (56 h). The solvent was removed under reduced pressure to afford a pink oil that was charged with satd. NaHCO₃ (aq.) (30 mL). The aqueous mixture was extracted with EtOAc (3 × 20 mL), and the pooled organic extract was washed with brine (20 mL), dried (MgSO₄) and filtered. Removal of solvent under reduced pressure yielded a pink solid. **^tBuOH Deprotection:** The crude solid was charged with trifluoroacetic acid (5.0 mL) and stirred at 40 °C for 2 h. The reaction mixture was neutralised to pH 8 – 9 with satd. NaHCO₃ (aq.) (50 mL). The aqueous mixture was extracted with CH₂Cl₂ (3 × 20 mL), the pooled organic extract was washed with brine (20 mL), dried (MgSO₄) and filtered. Removal of solvent under reduced pressure yielded the title compound as a white solid (1.31 g, 90% over two steps). **IR** ν_{max} cm⁻¹ 3411br w, 3319br w, 3040 w, 2953 w, 1721 w, 1693 s, 1540 w, 1515 w, 1445 w; **¹H-NMR** (400 MHz, (CD₃)₂SO) δ_{H} 9.24 (s, 1H), 7.88-7.85 (m, 3H), 7.65 (app t, J = 7.6 Hz, 2H), 7.49 – 7.37 (m, 2H), 7.31 (dtd, J = 8.8, 7.4, 1.2 Hz, 2H), 7.04 (d, J = 8.5 Hz, 2H), 6.66 (d, J = 8.5 Hz, 2H), 4.37 – 4.08 (m, 4H), 3.61 (s, 3H), 2.92 (dd, J = 13.8, 5.1 Hz, 1H), 2.78 (dd, J = 13.8, 10.0 Hz, 1H); **¹³C-NMR** (101 MHz, (CD₃)₂SO) δ_{C} 172.5, 156.0, 155.9, 143.8, 140.7, 130.0, 127.7, 127.5, 127.1, 125.3, 120.1, 115.0,

65.6, 55.9, 51.9, 46.6, 35.7; **LRMS** m/z (ESI+) 417.16 (100%, $[M]^+$), 440.15 (30%, $[M+Na]^+$). Data are consistent with literature.¹⁵⁻¹⁶

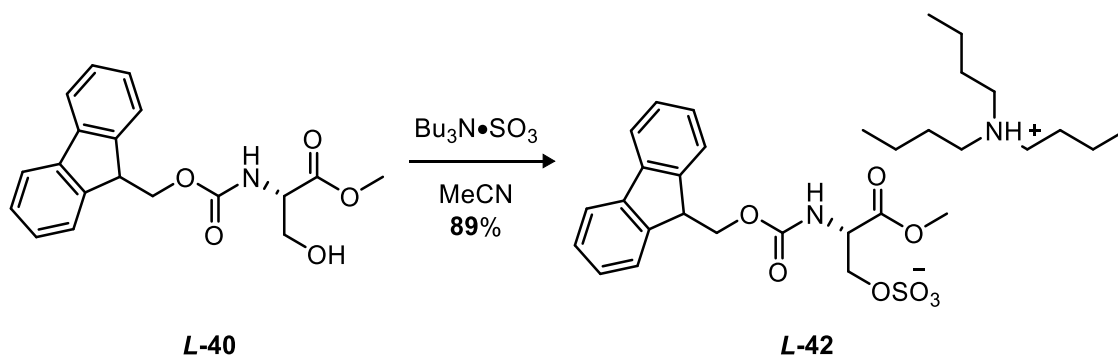
(**±42**) Tributylammonium (\pm)-2-((((9H-fluoren-9-yl)methoxy)carbonyl)amino)-3-methoxy-3-oxopropyl sulfate



Following general procedure **H**: *N*-Fmoc-*D/L*-serine methyl ester (**±40**) (341 mg, 1.0 mmol) and $\text{Bu}_3\text{N}\cdot\text{SO}_3$ (530 mg, 2.0 mmol) were dissolved in dry MeCN (2.0 mL) and heated under reflux for 2.0 h. The flask was cooled and the solvent removed under reduced pressure. Purification by chromatography (SiO_2 , CH_2Cl_2 to $\text{CH}_2\text{Cl}_2/\text{MeOH}$, 19:1) afforded the title compound as a clear oil (538 mg, 89%). **IR** ν_{max} cm^{-1} 2960 w, 2875 w, 1721 s, 1532 w, 1450 w, 1259 s, 1205 s; **$^1\text{H-NMR}$** (400 MHz, CDCl_3) δ_{H} 7.68 (dt, $J = 7.6, 1.0$ Hz, 2H, CH), 7.60 – 7.52 (m, 2H, CH), 7.37 – 7.28 (m, 2H, CH), 7.24 (tdd, $J = 7.4, 2.9, 1.2$ Hz, 2H, CH), 6.28 (d, $J = 8.2$ Hz, 1H, NH), 4.59 – 4.07 (m, 6H), 3.70 (s, 3H, Me), 2.98 – 2.90 (m, 6H, N-CH_2), 1.68 – 1.56 (m, 6H, CH_2), 1.31 (h, $J = 7.4$ Hz, 6H, CH_2), 0.89 (t, $J = 7.4$ Hz, 9H, CH_3); **$^{13}\text{C-NMR}$** (101 MHz, CDCl_3) δ_{C} 170.2 (CO_2Me), 156.3 (HNCO_2), 144.0 (Ar), 143.9 (Ar), 141.3 (CH), 141.3 (CH), 127.7 (CH), 127.19 (CH), 127.15 (CH), 125.42 (CH), 125.38 (CH), 120.0 (CH), 67.4 (CH_2), 67.3 (CH_2), 54.4 (CH), 52.7 (N-CH_2), 52.6 (Me), 47.2 (CH_2), 25.3 (CH_2), 20.0 (CH_2), 13.6 (CH_3); **LRMS** m/z (ESI+) 792.53 (60%, $[M+\text{Bu}_3\text{NH}]^+$), 186.23 (100%, $[\text{Bu}_3\text{NH}]^+$); **HRMS** m/z (ESI+) $\text{C}_{43}\text{H}_{74}\text{N}_3\text{O}_8\text{S}$ Requires: 792.5197, Found: 792.5219 ($[M+\text{Bu}_3\text{NH}]^+$).

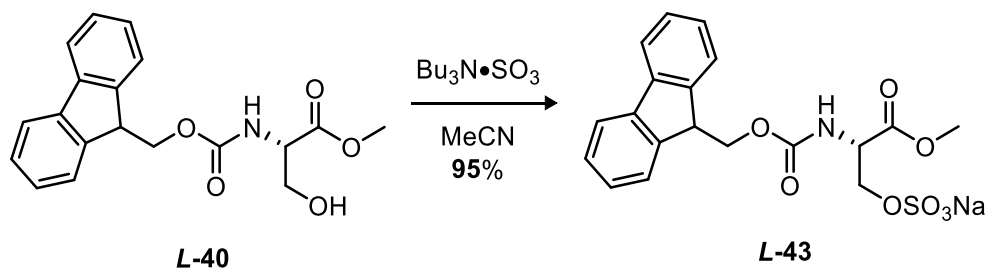
cHPLC R_{t1} = 4.77 min, area = 49.41%; R_{t2} = 5.19 min, area = 50.59%; (Phenomenex® Cellulose-1, MeCN/H₂O, 2:3, 1 mL min⁻¹, 30 °C).

(**L-42**) Tributylammonium (*S*)-2-((((9H-fluoren-9-yl)methoxy)carbonyl)amino)-3-methoxy-3-oxopropyl sulfate



Following general procedure **H**: *N*-Fmoc-*L*-serine methyl ester (341 mg, 1.0 mmol) and Bu₃N⁺SO₃⁻ (530 mg, 2.0 mmol) were dissolved in dry MeCN (2.0 mL) and heated under reflux for 2.0 h. The flask was cooled and the solvent removed under reduced pressure. Purification by chromatography (SiO₂, CH₂Cl₂ to CH₂Cl₂/MeOH, 19:1) afforded the title compound as a clear oil (540 mg, 89%). **IR** ν_{max} cm⁻¹ 2961 w, 2875 w, 1721 s, 1529 w, 1450 w, 1256 s, 1204 s; **¹H-NMR** (400 MHz, CDCl₃) δ_{H} 7.68 (dt, J = 7.6, 1.0 Hz, 2H, CH), 7.60 – 7.52 (m, 2H, CH), 7.37 – 7.28 (m, 2H, CH), 7.24 (tdd, J = 7.4, 2.9, 1.2 Hz, 2H, CH), 6.28 (d, J = 8.2 Hz, 1H, NH), 4.59 – 4.07 (m, 6H), 3.70 (s, 3H, Me), 2.98 – 2.90 (m, 6H, N-CH₂), 1.68 – 1.56 (m, 6H, CH₂), 1.31 (h, J = 7.4 Hz, 6H, CH₂), 0.89 (t, J = 7.4 Hz, 9H, CH₃); **¹³C-NMR** (101 MHz, CDCl₃) δ_{C} 170.2 (CO₂Me), 156.3 (HNCO₂), 144.0 (Ar), 143.9 (Ar), 141.3 (CH), 141.3 (CH), 127.7 (CH), 127.19 (CH), 127.15 (CH), 125.42 (CH), 125.38 (CH), 120.0 (CH), 67.4 (CH₂), 67.3 (CH₂), 54.4 (CH), 52.7 (N-CH₂), 52.6 (Me), 47.2 (CH₂), 25.3 (CH₂), 20.0 (CH₂), 13.6 (CH₃); **LRMS** m/z (ESI⁺) 792.53 (10%, [M+Bu₃NH]⁺), 186.23 (100%, [Bu₃NH]⁺); **HRMS** m/z (ESI⁺) C₄₃H₇₄N₃O₈S Requires: 792.5197, Found: 792.5217 ([M+Bu₃NH]⁺). **cHPLC** R_t = 5.08 min, area = 100.00%.

(L-43) Sodium (S)-2-((((9H-fluoren-9-yl)methoxy)carbonyl)amino)-3-methoxy-3-oxopropyl sulfate



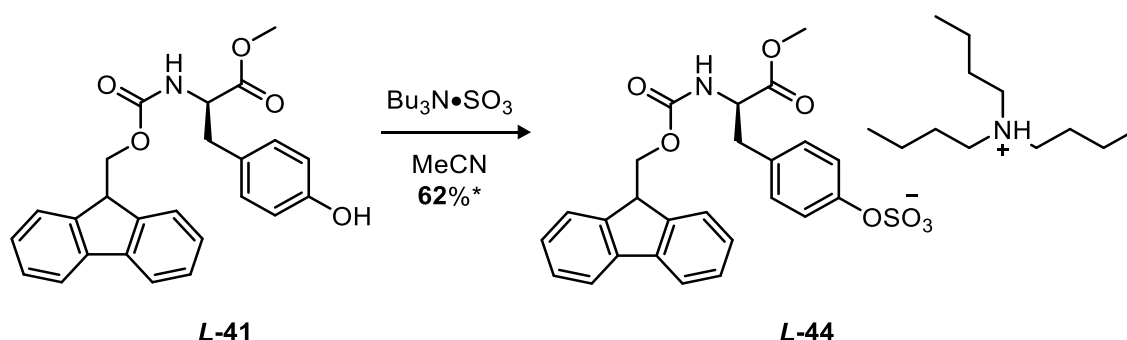
Following general procedure **H**: Methyl (((9H-fluoren-9-yl)methoxy)carbonyl)-L-serinate (**L-40**) (170 mg, 0.5 mmol) and $\text{Bu}_3\text{N}\cdot\text{SO}_3$ (530 mg, 2.0 mmol) were dissolved in 2 mL dry MeCN and heated under reflux for 6 h. The $[\text{Bu}_3\text{NH}]^+$ salt was purified by work up procedure **iii** to yield the title sulfate as a bright white solid (210 mg, 95%). **[α]_D²⁵** 4.20 (1.0, H₂O); **M.P** 179 – 182 °C (dec. 189 °C); **IR** ν_{max} cm^{-1} 3602 w, 3389 m, 3025 w, 1740 m, 1709 s, 1621 w, 1522 s; **¹H-NMR** δ_{H} (400 MHz, $(\text{CD}_3)_2\text{SO}$) 7.89 (d, $J = 7.5$ Hz, 2H), 7.83 (d, $J = 7.5$ Hz, 1H), 7.73 (d, $J = 7.5$ Hz, 2H), 7.42 (t, $J = 7.5$ Hz, 2H), 7.37 – 7.30 (m, 2H), 4.33 (td, $J = 7.0, 4.3$ Hz, 1H), 4.25 (br q, $J = 4.3$ Hz, 3H), 4.10 (dd, $J = 11.0, 4.3$ Hz, 1H), 3.97 (dd, $J = 11.0, 6.6$ Hz, 1H), 3.65 (s, 3H, Me); **¹³C-NMR** δ_{C} (101 MHz, $(\text{CD}_3)_2\text{SO}$) 170.6 ($\text{C}=\text{O}_2\text{Me}$), 155.9 ($\text{HN}\text{C}=\text{O}_2$), 143.8, 140.7, 127.7, 127.2, 125.4, 120.2, 66.0, 64.8, 54.4, 52.1 (Me), 46.6; **LRMS** m/z (ESI+) 466.06 (100%, $[\text{M}+2\text{Na}]^+$), 909.10 (50%, $[2\text{M}+3\text{Na}]^+$); **HRMS** m/z (ESI+) $\text{C}_{19}\text{H}_{18}\text{NO}_8\text{Na}_2\text{S}$ Requires: 466.0549, Found: 466.0555 ($[\text{M}+2\text{Na}]^+$).

Low Temperature Method

Methyl (((9H-fluoren-9-yl)methoxy)carbonyl)-L-serinate (**L-40**) (170 mg, 0.5 mmol) and $\text{Bu}_3\text{N}\cdot\text{SO}_3$ (530 mg, 2.0 mmol) were dissolved in 2 mL dry DMF and heated at 38 °C for 52 h. The flask was charged with H₂O (20 mL) and the aqueous mixture extracted with EtOAc (4 × 30 mL). The organic extracts were pooled and dried over

anhydrous MgSO_4 . Filtration of the solid and removal of the solvent under reduced pressure yielded the desired sulfate as its tributylammonium salt. The tributylammonium salt was purified by cation exchange procedure **iii** to yield the title sulfate as a bright white solid (200 mg, 90%).

(**L-44**) Tributylammonium (*L*)-*N*-Fmoc tyrosine methyl ester sulfate

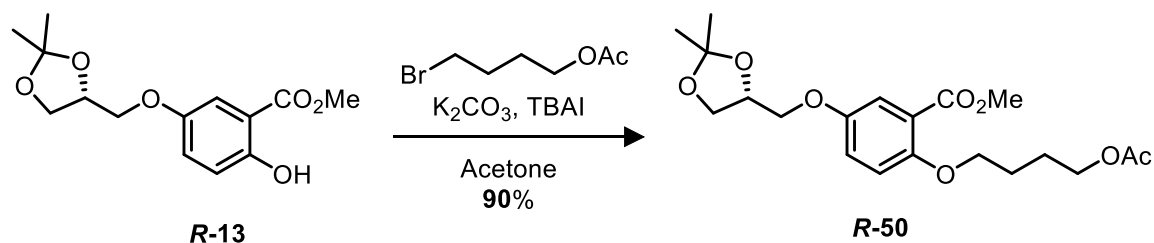


A flask was charged with (*L*)-*N*-Fmoc tyrosine methyl ester (**L-41**, 417 mg, 1.0 mmol) and $\text{Bu}_3\text{N}^+\text{SO}_3^-$ (1.06 g, 4.0 mmol). The mixture was dissolved in anhydrous MeCN (2.0 mL) and heated at reflux for 6 h. Solvent was removed under reduced pressure and the crude oil was purified by chromatography (SiO_2 , EtOAc/MeOH, 9:1, $R_f = 0.24$) to yield the title compound as a white solid (480 mg, 62%).* $[\alpha]_D^{25} + 2.35$ (c. 1.0, CDCl_3); **IR** Vmax cm^{-1} 3308 br s, 2961 w, 1717 s, 1692 s, 1615 w, 1596 w, 1541 s, 1516 s, 1445 s, 1264 s, 1216 s; **$^1\text{H-NMR}$** (400 MHz, $(\text{CD}_3)_2\text{SO}$) δ_{H} $^1\text{H-NMR}$ (400 MHz, $\text{DMSO-}d_6$) δ 8.89 (s, 1H), 7.98–7.81 (m, 3H), 7.67 (dd, $J = 10.0, 7.5$ Hz, 2H), 7.42 (tdd, $J = 7.5, 3.1, 1.1$ Hz, 2H), 7.33 (qd, $J = 7.5, 1.2$ Hz, 2H), 7.19 – 7.12 (m, 2H), 7.12 – 7.04 (m, 2H), 4.31 – 4.14 (m, 5H), 3.63 (s, 3H), 3.06 – 2.97 (m, 5H), 2.86 (dd, $J = 13.8, 10.2$ Hz, 1H), 1.64 – 1.47 (m, 5H), 1.31 (h, $J = 7.4$ Hz, 5H), 0.91 (t, $J = 7.3$ Hz, 7H); **$^{13}\text{C-NMR}$** (101 MHz, $(\text{CD}_3)_2\text{SO}$) δ_{C} 172.4, 156.0, 152.2, 143.8, 143.7, 140.7, 132.0, 129.4, 127.7, 125.3, 120.3, 120.1, 65.7, 55.7, 52.0, 51.8, 46.6, 35.7, 25.1,

19.4, 13.6; **LRMS** m/z (ESI+) 868.22 (100%, $[M+Bu_3NH]^+$); **HRMS** m/z (ESI+) $C_{49}H_{78}N_3O_8S$ Requires: 868.5507, Found: 868.5510 ($[M+Bu_3NH]^+$).

*Resonances for the $[Bu_3NH]^+$ are lower in the 1H -NMR spectrum due to the presence of starting material as an inseparable impurity from the *O*-sulfation reaction that increases with time (See Chapter: 6.6), calculated to be 9.9% (w/w) of the sample at $t = 96$ h.

(**R-50**) Methyl (*S*)-2-(4-acetoxibutoxy)-5-((2,2-dimethyl-1,3-dioxolan-4-yl)methoxy)benzoate



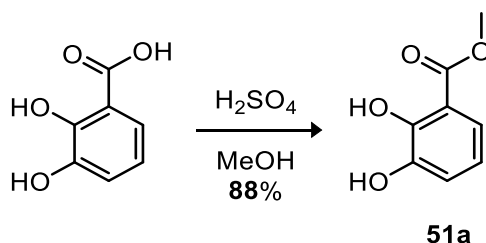
A flask containing Methyl (*S*)-5-((2,2-dimethyl-1,3-dioxolan-4-yl)methoxy)-2-hydroxybenzoate (**R-13**) (0.70 g, 2.5 mmol), K_2CO_3 (0.69 g, 4.96 mmol) and TBAI (0.40 g, 1.2 mmol) in acetone (20 mL) was charged with 4-bromobutyl acetate (0.97 g, 4.96 mmol) and the reaction mixture was heated under reflux for 12 h. The flask was cooled to room temperature and the solvent was removed under reduced pressure. The crude residue was charged with H_2O (20 mL) and extracted with EtOAc (3×50 mL). The combined organic extracts were washed with brine, dried ($MgSO_4$), and filtration of the solids and removal of the solvent under reduced pressure afforded a yellow oil. Purification by chromatography (SiO_2 , EtOAc/hexane, 1:4, $R_f = 0.20$) afforded the title compound as a clear oil (0.88 g, 90%). and were charged to a flask containing acetone (50 mL). $[\alpha]_D^{25} +7.27$ (c 1.0, $CHCl_3$); **IR** ν_{max} cm^{-1} 2942 w, 1730 s ($C=O$), 1498 m, 1439 m, 1240 s, 1212 s, 1077 s; **1H -NMR** (400 MHz, $CDCl_3$) δ_H 7.32 (d, $J = 3.2$ Hz, 1H, C6-H), 7.01 (dd, $J = 9.1, 3.2$ Hz, 1H, C4-H), 6.87 (d, $J = 9.1$ Hz,

1H, C3-H), 4.49 – 4.39 (app. m, 1H, CH-OC(CH₃)₂), 4.18 – 4.08 (m, 3H), 4.03 – 3.96 (m, 3H), 3.93 – 3.87 (m, 2H), 3.86 (s, 3H, Me), 2.02 (s, 3H, Ac), 1.90 – 1.78 (m, 4H, CH₂/CH₂), 1.44 (s, 3H, C(CH₃)₂), 1.38 (s, 3H, C(CH₃)₂); **¹³C-NMR** (101 MHz, CDCl₃) δ_C 171.2 (Ac), 166.5 (CO₂Me), 153.2 (C2), 152.2 (C5), 121.1 (C1), 120.4 (C4), 116.8 (C6), 115.4 (C3), 109.8 (CH₂), 74.1 (CH₂), 69.6, 69.3, 66.8, 64.2, 52.1 (Me), 26.9 (C(CH₃)₂), 26.0 (C(CH₃)₂), 25.4 (2C, CH₂), 21.0 (Ac); **LRMS** (ESI): C₂₀H₂₈O₈ 419.17 (100%, [M+Na]⁺); **HRMS** (ESI) *m/z* C₂₀H₂₈O₈Na Requires: 419.1682, Found: 419.1684 ([M+Na]⁺).

Acetal Deprotection step

Adapted from general procedure **F**: Hydrolysis of **R-50** in NaOMe/MeOH followed by addition of TFA afforded **S-10** in 99% yield after chromatography (SiO₂). [**a**]_D²⁵ –8.67 (*c* 1.0, CHCl₃). Data were in accordance with the known sample.

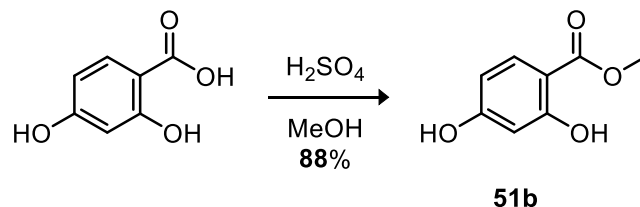
(51a) Methyl 2,3-dihydroxybenzoate¹⁷



Following the general procedure **A**: using 2,3-dihydroxybenzoic acid (5.00 g, 32.46 mmol). Recrystallization from CH₂Cl₂/hexane yielded the title compound as a pink solid (4.79 g, 88%). **M.P** 82 – 84 °C; **IR** V_{max} cm⁻¹ 3657 w (O-H), 3458 w (O-H), 2980 s, 1670 w (C=O), 1460 w; **¹H-NMR** (400 MHz, CDCl₃) δ_H 10.89 (s, 1H, C2-OH), 7.36 (dd, *J* = 8.0, 1.5 Hz, 1H, C6-H), 7.16 – 7.06 (m, 1H, C4-H), 6.80 (t, *J* = 8.0 Hz, 1H, C5-H), 5.69 (s, 1H, C3-OH), 3.95 (s, 3H, Me); **¹³C-NMR** (101 MHz, CDCl₃) δ_C 170.9 (CO₂Me), 148.9 (C2), 145.1 (C1), 120.7 (C6), 119.9 (C4), 119.3 (C5), 112.5 (C3), 52.6

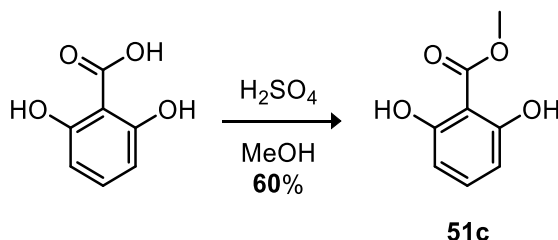
(Me); **LRMS** m/z (ESI+) 169.05 (10%, $[M+H]^+$), 186.23 (100%, $[M+H_2O]^+$) Data were in accordance with the literature.¹⁷

(51b) Methyl 2,4-dihydroxybenzoate¹⁸



Following the general procedure **A**: using 2,4-dihydroxybenzoic acid (5.00 g, 32.46 mmol). Recrystallization from CH_2Cl_2 /hexane yielded the title compound as a white solid (4.79 g, 88%). **M.P** 114 – 117 °C; **IR** V_{max} cm^{-1} 3085 w, 3019 w, 2950 w, 1720s (C=O), 1594 s; **¹H-NMR** (400 MHz, $CDCl_3$) δ_H 10.99 (s, 1H, C2-OH), 7.73 (d, J = 8.6 Hz, 1H, C6-H), 6.40 (d, J = 2.5 Hz, 1H, C3-H), 6.37 (dd, J = 8.6, 2.5 Hz, 1H, C5-H), 5.63 – 5.55 (m, 1H, C4-OH), 3.91 (s, 3H, Me); **¹³C-NMR** (101 MHz, $CDCl_3$) δ_C 170.5 ($\underline{C}O_2Me$), 163.7 (C4), 162.0 (C2), 132.1 (C6), 108.0 (C3), 106.0 (C1), 103.3 (C5), 52.2 (Me); **LRMS** m/z (ESI+) 186.23 (30%, $[M+H_2O]^+$). Data were in accordance with the literature.¹⁸

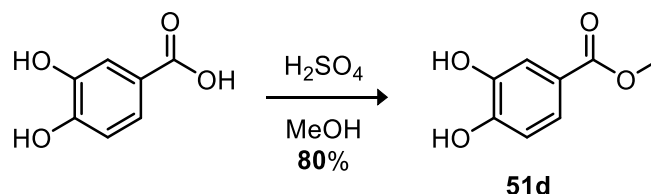
(51c) Methyl 2,6-dihydroxybenzoate¹⁹



Following the general procedure **A**: using 2,6-dihydroxybenzoic acid (5.00 g, 32.46 mmol). Recrystallization from CH_2Cl_2 /hexane yielded the title compound as large off off-white crystals (3.26 g, 60%). **M.P** 83 – 85 °C; **IR** V_{max} cm^{-1} 3412 br s (O-H), 3072 br w, 2968 w, 1667 m (C=O), 1574 s; **¹H-NMR** (400 MHz, $(CD_3)_2SO$) δ_H 9.95 (s,

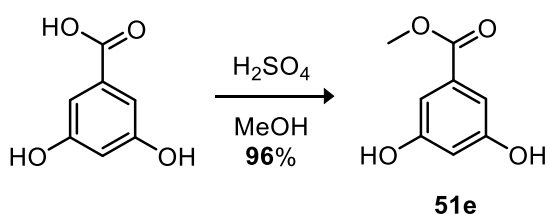
2H, C2-OH), 7.09 (t, $J = 8.2$ Hz, 1H, C4-H), 6.34 (d, $J = 8.2$ Hz, 2H, C3-H), 3.78 (s, 3H, Me); **$^{13}\text{C-NMR}$** (101 MHz, $(\text{CD}_3)_2\text{SO}$) δ_{C} 168.3 (CO_2Me), 157.4 (C2), 132.4 (C4), 107.0 (C1), 106.7 (C3), 51.9 (Me); **LRMS** m/z (ESI+) 186.22 (20%, $[\text{M}+\text{H}_2\text{O}]^+$). Data were in accordance with the literature.¹⁹

(51d) Methyl 3,4-dihydroxybenzoate²⁰



Following the general procedure **A**: using 3,4-dihydroxybenzoic acid (5.00 g, 32.46 mmol). Recrystallization from CH_2Cl_2 /hexane yielded the title compound as long fine white crystals (4.34 g, 80%). **M.P** 127 – 129 °C; **IR** V_{max} cm^{-1} 3463 br s (O-H), 3254 br s (O-H), 2969, 1680 m (C=O), 1608 s, 1442 s; **$^1\text{H-NMR}$** (400 MHz, $(\text{CD}_3)_2\text{SO}$) δ_{H} 9.56 (br s, 2H, Ar-OH), 7.35 (d, $J = 2.1$ Hz, 1H, C2-H), 7.31 (dd, $J = 8.3, 2.1$ Hz, 1H, C6-H), 6.80 (d, $J = 8.3$ Hz, 1H, C5-H), 3.76 (s, 3H, Me); **$^{13}\text{C-NMR}$** (101 MHz, $(\text{CD}_3)_2\text{SO}$) δ_{C} 166.1 (CO_2Me), 150.4 (C4), 145.0 (C3), 121.7 (C6), 120.5 (C1), 116.2 (C2), 115.3 (C5), 51.6 (Me); **LRMS** m/z (ESI+) 191.03 (90%, $[\text{M}+\text{Na}]^+$), 209.04 (60%, $[\text{M}+\text{Na}+\text{H}_2\text{O}]^+$). Data were in accordance with the literature.²⁰

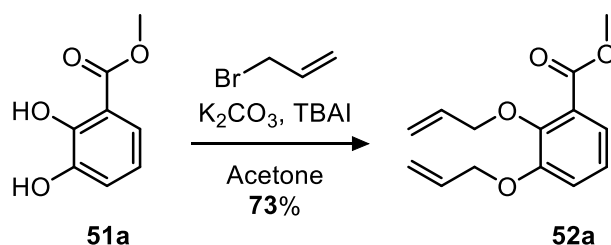
(51e) Methyl 3,5-dihydroxybenzoate²¹



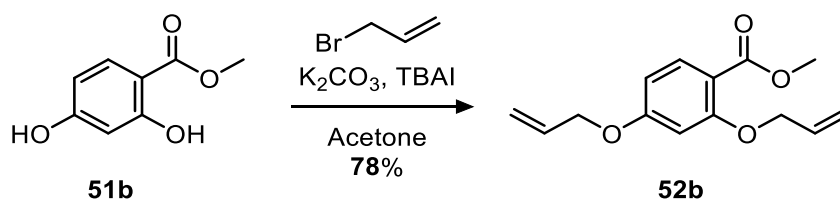
Following the general procedure **A**: using 3,5-dihydroxybenzoic acid (5.00 g, 32.46 mmol). Recrystallization from MeOH yielded the title compound as a white solid (5.21

g, 96%). **M.P** 156 – 160 °C; **IR** V_{\max} cm^{-1} 3227 s br (O-H), 2998 w, 2952 w, 1687 s (C=O), 1600 s, 1486 w; **$^1\text{H-NMR}$** (400 MHz, $(\text{CD}_3)_2\text{SO}$) δ_{H} 9.62 (s, 2H, Ar-OH), 6.81 (d, J = 2.3 Hz, 2H, C2-H), 6.44 (t, J = 2.3 Hz, 1H, C4-H), 3.78 (s, 3H, Me); **$^{13}\text{C-NMR}$** (101 MHz, $(\text{CD}_3)_2\text{SO}$) δ_{C} 166.6 (CO_2Me), 158.9 (C3), 131.7 (C1), 107.6 (C4), 107.5 (C2), 52.4 (Me); **LRMS** m/z (ESI+) 186.22 (65%, $[\text{M}+\text{Na}+\text{H}_2\text{O}]^+$), 191.03 (90%, $[\text{M}+\text{Na}]^+$), 209.04 (45%, $[\text{M}+\text{Na}+\text{H}_2\text{O}]^+$). Data were in accordance with the literature.²¹

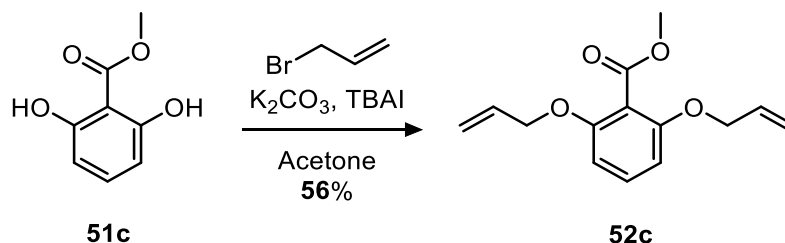
(52a) Methyl 2,3-bis(allyloxy)benzoate



Following the general procedure **B** using: methyl 2,3-dihydroxy benzoate (**51a**) (1.00 g, 5.9 mmol), K₂CO₃ (2.45 g, 17.7 mmol), TBAI (0.71 g, 2.2 mmol) and allyl bromide (1.14 mL, 13.2 mmol). The flask was heated under reflux for 8 h. Purification by silica gel chromatography (EtOAc/hexane, 1:4, R_f = 0.28) yielded the title compound as a clear oil (1.22 g, 73%). **IR** V_{\max} cm^{-1} 3080 w, 3020 w, 2949 w, 1728 m (C=O), 1580 w (C=C), 1472 m; **$^1\text{H-NMR}$** (400 MHz, CDCl_3) δ_{H} 7.31 (t, J = 4.8 Hz, 1H, C5-H), 7.02 (d, J = 4.8 Hz, 2H, C4-H/C6-H), 6.21 – 5.96 (m, 2H, $\text{CH}=\text{CH}_2$), 5.45 – 5.30 (m, 2H, $\text{CH}=\text{CH}_2$), 5.29 – 5.17 (m, 2H, $\text{CH}=\text{CH}_2$), 4.61 – 4.52 (m, 4H, Ar-OCH₂), 3.86 (s, 3H, Me); **$^{13}\text{C-NMR}$** (101 MHz, CDCl_3) δ_{C} 166.8 (CO_2Me), 152.6 (C3), 148.2 (C2), 134.2 ($\text{CH}=\text{CH}_2$), 132.9 ($\text{CH}=\text{CH}_2$), 126.6 (C1), 123.8, 122.6 (C5), 117.8, 117.6 (2C, $\text{CH}=\text{CH}_2$), 74.7 (Ar-OCH₂), 69.9 (Ar-OCH₂), 52.1 (Me); **LRMS** m/z (ESI+) 271.09 (100%, $[\text{M}+\text{Na}]^+$); **HRMS** m/z (ESI+) C₁₄H₁₆NaO₄ Requires: 271.0941, Found: 271.0949 ($[\text{M}+\text{Na}]^+$).

(52b) Methyl 2,4-bis(allyloxy)benzoate

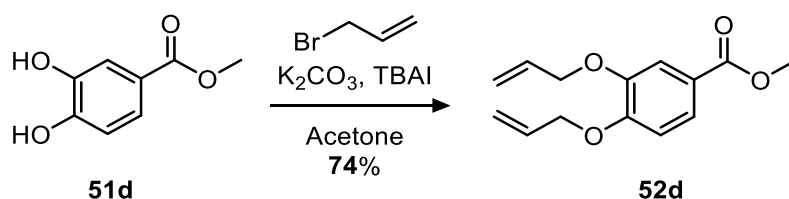
Following the general procedure **B** using: methyl 2,4-dihydroxy benzoate (**51b**) (1.00 g, 5.9 mmol), K₂CO₃ (2.45 g, 17.7 mmol), TBAI (0.71 g, 2.2 mmol) and allyl bromide (1.14 mL, 13.2 mmol). The flask was heated under reflux for 8 h. Purification by silica gel chromatography (EtOAc/hexane, 1:4, *R_f* = 0.28) yielded the title compound as a clear oil (1.30 g, 78%). **IR** V_{max} cm⁻¹ 3082 w, 2948 w, 1721 s (C=O), 1605 s (C=C); **¹H-NMR** (400 MHz, CDCl₃) δ_{H} 7.83 (m, 1H, C3-H), 6.48 (m, 2H, C5-H & C6-H), 6.03 (m, 2H, CH=CH₂), 5.53 (dd, *J* = 17.2, 1.8 Hz, 1H, CH=CH₂), 5.40 (dd, *J* = 17.2, 1.5 Hz, 1H, CH=CH₂), 5.29 (dd, *J* = 10.6, 1.5 Hz, 2H, CH=CH₂), 4.58 (dt, *J* = 4.8, 1.8 Hz, 2H, Ar-OCH₂), 4.54 (dt, *J* = 5.4, 1.5 Hz, 2H, Ar-OCH₂), 3.84 (s, 3H, Me); **¹³C-NMR** (101 MHz, CDCl₃) δ_{C} 166.1 (C=O), 163.0 (C2), 160.2 (C4), 133.8 (C3), 132.6 (CH=CH₂), 118.2 (CH=CH₂), 117.4 (CH=CH₂), 112.8 (C1), 105.7 (C6), 101.0 (C5), 69.4 (Ar-OCH₂), 68.9 (Ar-OCH₂), 51.7 (Me); **LRMS** *m/z* (ESI+) 271.10 (100%, [M+Na]⁺); **HRMS** *m/z* (ESI+) C₁₄H₁₆NaO₄ Requires: 271.0941, Found: 271.0940 ([M+Na]⁺).

(52c) Methyl 2,6-bis(allyloxy)benzoate

Following the general procedure **B** using: methyl 2,6-dihydroxy benzoate (**51c**) (1.00 g, 5.9 mmol), K₂CO₃ (2.45 g, 17.7 mmol), TBAI (0.71 g, 2.2 mmol) and allyl bromide

(1.14 mL, 13.2 mmol). The flask was heated under reflux for 8 h. Purification by silica gel chromatography (EtOAc/hexane, 1:4, R_f = 0.28) yielded the title compound as a green oil (0.94 g, 56%). **IR** V_{\max} cm^{-1} 3087 w, 3021 w, 2948 w, 1731 s (C=O), 1596 s (C=C), 1469 w; **$^1\text{H-NMR}$** (400 MHz, CDCl_3) δ_{H} 7.22 (t, 1H, J = 8.4 Hz, C4-H), 6.54 (d, J = 8.4 Hz, 2H, C3-H), 5.98 (ddt, J = 17.2, 10.6, 4.8 Hz, 2H, $\text{CH}=\text{CH}_2$), 5.37 (dd, J = 17.2, 1.6 Hz, 2H, $\text{CH}=\text{CH}_2$), 5.24 (dd, J = 10.6, 1.6 Hz, 2H, $\text{CH}=\text{CH}_2$), 4.55 (dt, J = 4.8, 1.6 Hz, 4H, C2-OCH₂), 3.90 (s, 3H, Me); **$^{13}\text{C-NMR}$** (101 MHz, CDCl_3) δ_{C} 166.8 (C=O), 156.4 (C2), 132.8 ($\text{CH}=\text{CH}_2$), 130.8 (C4), 117.2 ($\text{CH}=\text{CH}_2$), 114.0 (C1), 105.5 (C3), 69.3 (C2-OCH₂), 52.3 (Me); **LRMS** m/z (ESI+) 249.10 (5%, $[\text{M}]^+$), 271.09 (100%, $[\text{M}+\text{Na}]^+$); **HRMS** m/z (ESI+) $\text{C}_{14}\text{H}_{16}\text{NaO}_4$ Requires: 271.0941, Found: 271.0939 ($[\text{M}+\text{Na}]^+$).

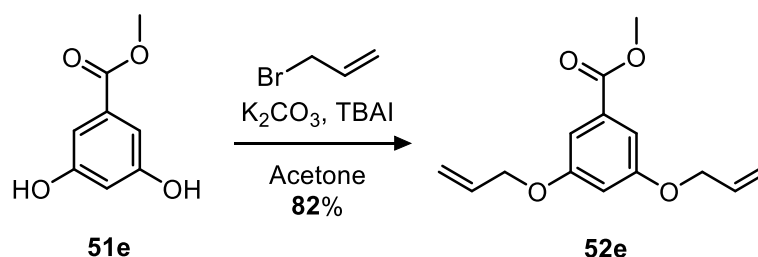
(52d) Methyl 3,4-bis(allyloxy)benzoate



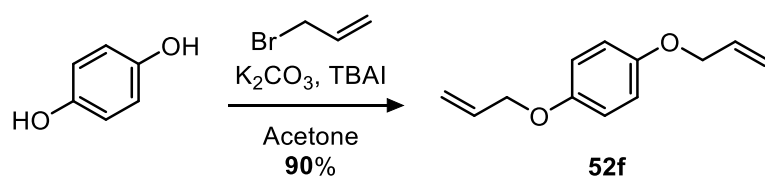
Following the general procedure **B** using: methyl 3,4-dihydroxy benzoate (**51d**) (1.00 g, 5.9 mmol), K₂CO₃ (2.45 g, 17.7 mmol), TBAI (0.71 g, 2.2 mmol) and allyl bromide (1.14 mL, 13.2 mmol). The flask was heated under reflux for 8 h. Purification by silica gel chromatography (EtOAc/hexane, 1:4, R_f = 0.28) yielded the title compound as a clear oil (1.24 g, 74%). **IR** V_{\max} cm^{-1} 3083 w, 2949 w, 2865 w, 1712 s (C=O), 1598 w (C=C); **$^1\text{H-NMR}$** (400 MHz, CDCl_3) δ_{H} 7.63 (dd, J = 8.5, 2.0 Hz, 1H, C6-H), 7.55 (d, J = 2.0 Hz, 1H, C2-H), 6.88 (d, J = 8.5 Hz, 1H, C5-H), 6.21 – 5.95 (m, 2H, $\text{CH}=\text{CH}_2$), 5.52 – 5.37 (m, 2H, $\text{CH}=\text{CH}_2$), 5.29 (qd, J = 10.5, 2.8 Hz, 2H, $\text{CH}=\text{CH}_2$), 4.74 – 4.57 (m, 4H, Ar-OCH₂), 3.87 (s, 3H, Me); **$^{13}\text{C-NMR}$** (101 MHz, CDCl_3) δ_{C} 166.8 (C=O),

152.4 (C4), 147.9 (C3), 133.0 ($\underline{\text{CH}}=\text{CH}_2$), 132.7 ($\underline{\text{CH}}=\text{CH}_2$), 123.7 (C6), 122.8 (C1), 118.1 ($\text{CH}=\underline{\text{CH}}_2$), 118.0 ($\text{CH}=\underline{\text{CH}}_2$), 114.5 (C2), 112.4 (C5), 69.8 (Ar-O $\underline{\text{CH}}_2$), 69.6 (Ar-O $\underline{\text{CH}}_2$), 52.0 (Me); **LRMS** m/z (ESI+) 249.09 (2%, $[\text{M}]^+$), 271.09 (90%, $[\text{M}+\text{Na}]^+$); **HRMS** m/z (ESI+) $\text{C}_{14}\text{H}_{16}\text{NaO}_4$ Requires: 271.0941, Found: 271.0941 ($[\text{M}+\text{Na}]^+$).

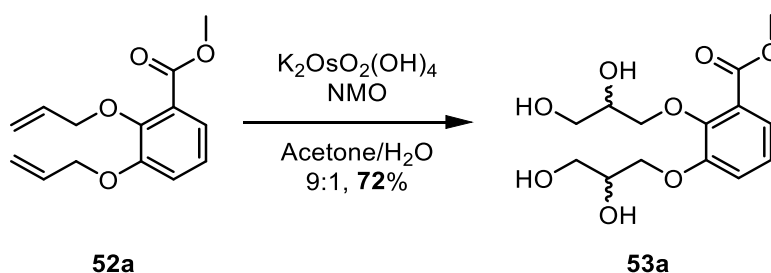
(52e) Methyl 3,5-bis(allyloxy)benzoate



Following the general procedure **B** using: methyl 3,5-dihydroxy benzoate (**51e**) (1.00 g, 5.9 mmol), K_2CO_3 (2.45 g, 17.7 mmol), TBAI (0.71 g, 2.2 mmol) and allyl bromide (1.14 mL, 13.2 mmol). The flask was heated under reflux for 8 h. Purification by silica gel chromatography (EtOAc/hexane, 1:4, $R_f = 0.28$) yielded the title compound as a transparent solid (1.38 g, 82%). **M.P** 39 °C; **IR** ν_{max} cm^{-1} 2990 w, 2951 w, 1720 s ($\text{C}=\text{O}$), 1595 s ($\text{C}=\text{C}$), 1441 s; **$^1\text{H-NMR}$** (400 MHz, $(\text{CD}_3)_2\text{CO}$) δ_{H} 7.17 (d, $J = 2.4$ Hz, 2H, C2- $\underline{\text{H}}$), 6.80 (t, $J = 2.4$ Hz, 1H, C4- $\underline{\text{H}}$), 6.09 (ddt, $J = 16.1, 10.5, 5.2$ Hz, 2H, $\underline{\text{CH}}=\text{CH}_2$), 5.45 (dd, $J = 17.3, 1.3$ Hz, 2H, $\text{CH}=\underline{\text{CH}}_2$), 5.28 (dd, $J = 10.5, 1.3$ Hz, 2H, $\text{CH}=\underline{\text{CH}}_2$), 4.64 (d, $J = 5.2$ Hz, 4H, C3-O $\underline{\text{CH}}_2$), 3.88 (s, 3H, Me); **$^{13}\text{C-NMR}$** (101 MHz, $(\text{CD}_3)_2\text{CO}$) δ_{C} 166.0 ($\underline{\text{CO}}_2\text{Me}$), 159.8 (C3), 133.4 ($\underline{\text{CH}}=\text{CH}_2$), 132.2 (C1), 116.7 ($\text{CH}=\underline{\text{CH}}_2$), 107.9 (C2), 106.3 (C4), 68.7 (C3-O $\underline{\text{CH}}_2$), 51.6 (Me); **LRMS** m/z (ESI+) 249.10 (4%, $[\text{M}]^+$), 271.09 (90%, $[\text{M}+\text{Na}]^+$); **HRMS** m/z (ESI+) $\text{C}_{14}\text{H}_{16}\text{NaO}_4$ Requires: 271.0941, Found: 271.0942 ($[\text{M}+\text{Na}]^+$).

(52f) 1,4-Bis(allyloxy)benzene²²

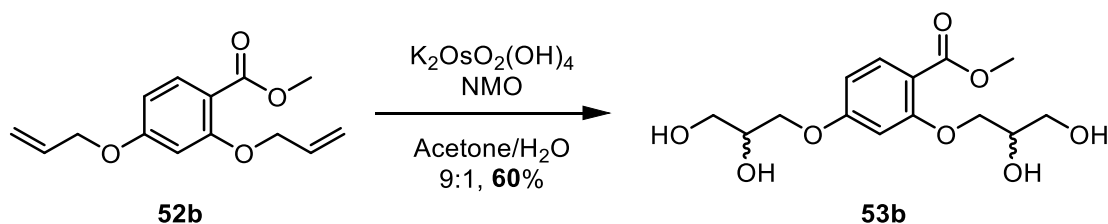
Following the general procedure **B** using: hydroquinone (0.65 g, 5.9 mmol), K_2CO_3 (2.45 g, 17.7 mmol), TBAI (0.71 g, 2.2 mmol) and allyl bromide (1.14 mL, 13.2 mmol). The flask was heated under reflux for 8 h. Purification by silica gel chromatography (EtOAc/hexane, 1:4, $R_f = 0.40$) yielded the title compound as a crystalline yellow solid (1.04 g, 90%). **M.P** 36 – 37 °C; **IR** V_{max} cm^{-1} 3020 w, 2859 w, 1506 s, 1457 w; **¹H-NMR** (400 MHz, CDCl_3) δ_{H} 6.85 (s, 4H, Ar-H), 6.05 (ddt, $J = 17.1, 10.5, 5.4$ Hz, 2H, $\text{CH}=\text{CH}_2$), 5.40 (dd, $J = 17.1, 1.5$ Hz, 2H, $\text{CH}=\text{CH}_2$), 5.27 (dd, $J = 10.5, 1.5$ Hz, 2H, $\text{CH}=\text{CH}_2$), 4.49 (d, $J = 5.4$ Hz, 4H, Ar- OCH_2); **¹³C-NMR** (101 MHz, CDCl_3) δ_{C} 153.0 (Ar- OCH_2), 133.7 ($\text{CH}=\text{CH}_2$), 117.6 ($\text{CH}=\text{CH}_2$), 115.8 (Ar-H), 69.6 (Ar- OCH_2); **LRMS** m/z (ESI+) 190.09 (90%, $[\text{M}]^+$), 149.10 (100%, $[\text{M}-\text{C}_3\text{H}_5]^+$). Data were in accordance with the literature.²²

(53a) Methyl 2,3-bis(2,3-dihydroxypropoxy)benzoate

Following the general procedure **C**: Methyl 2,3-bis(allyloxy)benzoate (**52a**) (0.25 g, 1.0 mmol) was added dropwise and the reaction mixture was stirred vigorously at RT for 24 h. Purification by silica gel chromatography (EtOH/EtOAc, 1:4, $R_f = 0.24$) afforded the title compound as a clear oil (0.19 g, 72%). **IR** V_{max} cm^{-1} 3346 s br (O-

H), 2943 w, 2891 w, 1710 s (C=O), 1477 s; **¹H-NMR** (400 MHz, CD₃OD) δ_{H} 7.32 (dd, $J = 8.0, 1.5$ Hz, 1H, C6-H), 7.24 (dd, $J = 8.0, 1.5$ Hz, 1H, C4-H), 7.12 (t, $J = 8.0$ Hz, 1H, C5-H), 4.23 (ddd, $J = 9.7, 4.2, 2.0$ Hz, 1H, C2-OCH₂), 4.17 – 3.99 (m, 4H, C2-OCH₂ & C3-OCH₂, CH-OH), 3.99 – 3.92 (m, 1H, CH-OH), 3.88 (s, 3H, Me), 3.75 – 3.61 (m, 4H, CH₂-OH); **¹³C-NMR** (101 MHz, CD₃OD) δ_{C} 168.5 (CO₂Me), 154.0 (C3), 149.5 (C2), 126.6 (C1), 125.1 (C5), 123.5 (C6), 118.7 (C4), 76.45 (C2-OCH₂), 76.42 (C2-OCH₂), 72.43 (CH-OH), 72.42 (CH-OH), 71.7 (C3-OCH₂), 71.5 (CH-OH), 64.10 (CH₂-OH), 64.07 (CH₂-OH), 52.8 (Me); **LRMS** m/z (ESI+) 281.10 (100%, [M-H₂O]⁺); **HRMS** m/z (ESI+) C₁₄H₁₈O₆Na Requires: 281.1001, Found: 281.9999 ([M-H₂O]⁺).

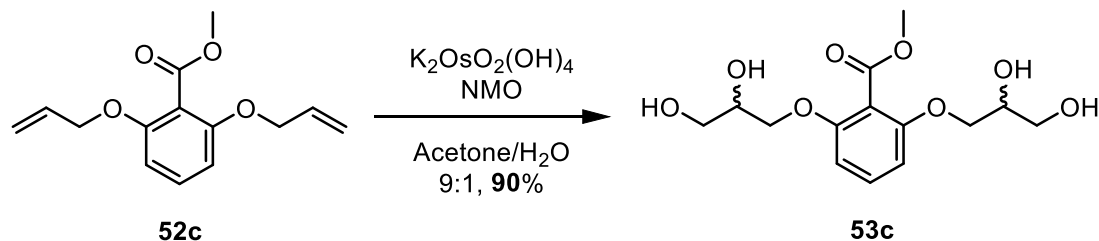
(**53b**) Methyl 2,4-bis(2,3-dihydroxypropoxy)benzoate



Following the general procedure: Methyl 2,3-bis(allyloxy)benzoate (**52b**) (0.25 g, 1.0 mmol) was added dropwise and the reaction mixture was stirred vigorously at RT for 24 h. Purification by silica gel chromatography (EtOH/EtOAc, 1:4, $R_f = 0.24$) afforded the title compound as a clear oil (0.15 g, 60%). **IR** ν_{max} cm⁻¹ 3346 br s, 2943 w, 1703 s (C=O), 1609 w, 1437 s; **¹H-NMR** (400 MHz, CD₃OD) δ_{H} 7.81 (d, $J = 8.8$ Hz, 1H, C6-H), 6.69 (d, $J = 2.3$ Hz, 1H, C3-H), 6.62 (dd, $J = 8.8, 2.3$ Hz, 1H, C5-H), 4.17 – 3.94 (m, 6H, Ar-OCH₂ & CH-OH), 3.83 (s, 3H, Me), 3.78 – 3.56 (m, 4H, CH₂-OH); **¹³C-NMR** (101 MHz, CD₃OD) δ_{C} 168.0 (CO₂Me), 165.4 (C4), 162.3 (C2), 134.7 (C6), 113.3 (C1), 107.5 (C5), 101.7 (C3), 72.0 (Ar-OCH₂), 71.6 (CH-OH), 71.4 (CH-OH), 70.7 (Ar-OCH₂), 64.3 (CH₂-OH), 64.0 (CH₂-OH), 52.2 (Me); **LRMS** m/z (ESI+) 339.10

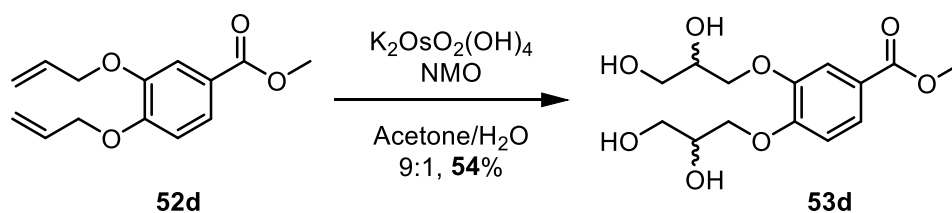
(100%, $[M+Na]^+$); **HRMS** m/z (ESI+) $C_{14}H_{20}O_8Na$ Requires: 339.1050, Found: 339.1053 ($[M+Na]^+$).

(53c) Methyl 2,6-bis(2,3-dihydroxypropoxy)benzoate



Following the general procedure **C**: Methyl 2,6-bis(allyloxy)benzoate (**52c**) (0.25 g, 1.0 mmol) was added dropwise and the reaction mixture was stirred vigorously at RT for 24 h. Purification by silica gel chromatography (EtOH/EtOAc, 1:4, R_f = 0.24) afforded the title compound as a clear oil (0.22 g, 90%). **M.P** 95 – 98 °C; **IR** V_{max} cm^{-1} 3313 w br (O-H), 2939 w, 2880 w, 1730s (C=O), 1597 s, 1455 s; **1H -NMR** (400 MHz, CD_3OD) δ_H 7.33 (t, J = 8.4 Hz, 1H, C4-H), 6.71 (d, J = 8.4 Hz, 2H, C3-H), 4.14 – 3.98 (m, 4H, C2-OCH₂), 3.91 (p, J = 5.4 Hz, 2H, CH-OH), 3.87 (s, 3H, Me), 3.71 – 3.55 (m, 4H, CH₂-OH); **^{13}C -NMR** (101 MHz, CD_3OD) δ_C 169.1 (CO₂Me), 158.1 (C2), 132.7 (C4), 114.9 (C1), 106.7 (C3), 71.6 (CH-OH), 71.2 (C2-OCH₂), 64.1 (CH₂-OH), 52.8 (Me); **LRMS** m/z (ESI+) 339.11 (100%, $[M+Na]^+$); **HRMS** m/z (ESI+) $C_{14}H_{20}O_8Na$ Requires: 339.1050, Found: 339.1052 ($[M+Na]^+$).

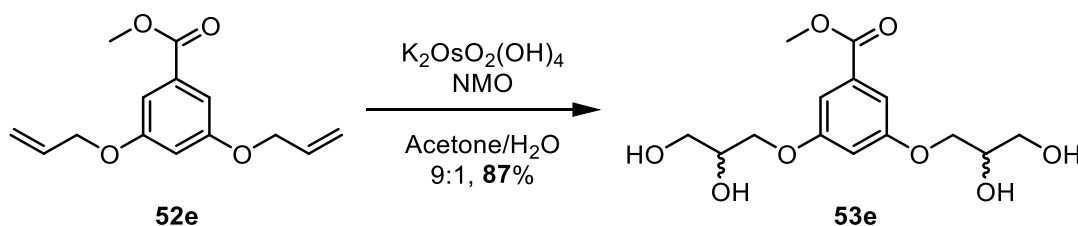
(53d) Methyl 3,4-bis(2,3-dihydroxypropoxy)benzoate



Following the general procedure **C**: Methyl 3,4-bis(allyloxy)benzoate (**52d**) (0.25 g, 1 mmol) was added dropwise and the reaction mixture was stirred vigorously at RT for

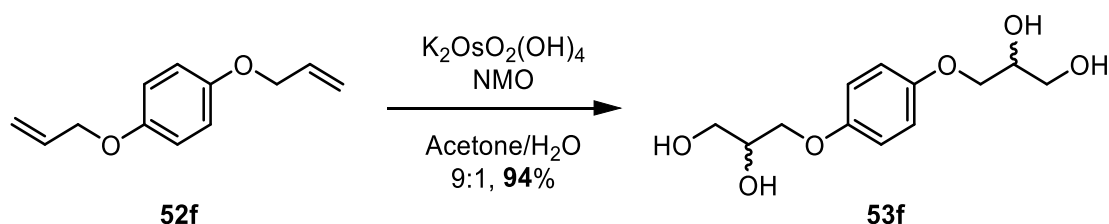
24 h. Purification by silica gel chromatography (EtOH/EtOAc, 1:4, R_f = 0.24) afforded the title compound as a clear oil (0.13 g, 54%). **M.P** 92 – 93 °C; **IR** V_{\max} cm^{-1} 3302 br s (O-H), 2942 w, 1714 s (C=O), 1596 s; **$^1\text{H-NMR}$** (400 MHz, CD_3OD) δ_{H} 7.66 (dd, J = 8.5, 2.0 Hz, 1H, C6-H), 7.60 (d, J = 2.0 Hz, 1H, C2-H), 7.06 (d, J = 8.5 Hz, 1H, C5-H), 4.29 – 3.92 (m, 6H, Ar-OCH₂ & CH-OH), 3.87 (s, 3H, Me), 3.77 – 3.63 (m, 4H, CH₂-OH); **$^{13}\text{C-NMR}$** (101 MHz, CD_3OD) δ_{C} 168.3 (CO₂Me), 154.6 (C3), 149.8 (C4), 125.2 (C6), 124.0 (C1), 115.8 (C2), 113.6 (C5), 71.9, 71.7, 71.6, 71.5, 64.1 (CH₂-OH), 64.0 (CH₂-OH), 52.5 (Me); **LRMS** m/z (ESI+) 339.11 (100%, $[\text{M}+\text{Na}]^+$); **HRMS** m/z (ESI+) $\text{C}_{14}\text{H}_{20}\text{NaO}_8$ Requires: 339.1050, Found: 339.1052 ($[\text{M}+\text{Na}]^+$).

(53e) Methyl 3,5-bis(2,3-dihydroxypropoxy)benzoate



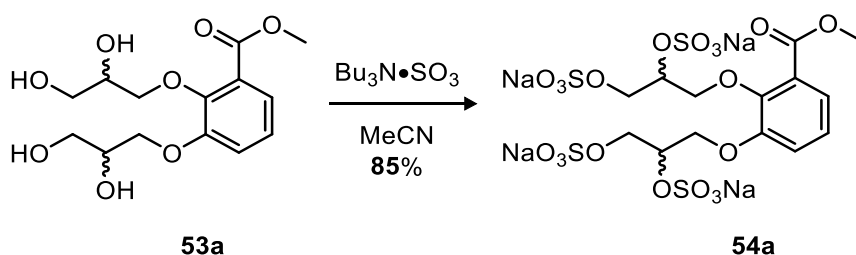
Following the general procedure **C**: Methyl 3,5-bis(allyloxy)benzoate (**52e**) (0.25 g, 1.0 mmol) was added dropwise and the reaction mixture was stirred vigorously at RT for 24 h. Purification by silica gel chromatography (EtOH/EtOAc, 1:4, R_f = 0.24) afforded the title compound as a clear oil (0.22 g, 87%). **M.P** 93 – 96 °C; **IR** V_{\max} cm^{-1} 3277 s br (O-H), 2943 w, 1711 s (C=O), 1601 m, 1446 m; **$^1\text{H-NMR}$** (400 MHz, CD_3OD) δ_{H} 7.19 (d, J = 2.3 Hz, 2H, C2-H), 6.81 (t, J = 2.3 Hz, 1H, C4-H), 4.14 – 4.04 (m, 2H, CH-OH), 4.04 – 3.92 (m, 4H, C3-OCH₂), 3.89 (s, 3H, Me), 3.74 – 3.59 (m, 4H, CH₂-OH); **$^{13}\text{C-NMR}$** (101 MHz, CD_3OD) δ_{C} 168.2 (CO₂Me), 161.5 (C3), 133.2 (C1), 109.0 (C2), 107.5 (C4), 71.7 (C3-OCH₂), 70.7 (CH-OH), 64.1 (CH₂-OH), 52.8 (Me); **LRMS** m/z (ESI+) 339.10 (100%, $[\text{M}+\text{Na}]^+$); **HRMS** m/z (ESI+) $\text{C}_{14}\text{H}_{20}\text{NaO}_8$ Requires: 339.1050, Found: 339.1047 ($[\text{M}+\text{Na}]^+$).

(53f) 1,4-Phenylenebis(oxy))bis(propane-1,2-diol



Following the general procedure **C**: 1,4-bis(allyloxy)benzene (**52f**) (0.19 g, 1.0 mmol). The reaction mixture was stirred at 40 °C for 16 h. Purification by silica gel chromatography (EtOH/EtOAc, 1:4, R_f = 0.30) afforded the title compound as a white solid (0.24 g, 94%). **M.P** 97 – 99 °C; **IR** V_{max} cm^{-1} 3232 br s (O-H), 2909 s, 2867 s; **¹H-NMR** (400 MHz, CD₃OD) δ_H 6.88 (s, 4H, Ar-H), 4.02 – 3.87 (m, 6H, Ar-OCH₂ & CH-OH), 3.65 (qd, J = 11.3, 5.2 Hz, 4H, CH₂-OH); **¹³C-NMR** (101 MHz, CD₃OD) δ_C 154.7 (Ar-O), 116.5 (Ar-H), 71.9 (CH-OH), 71.0 (Ar-OCH₂), 64.2 (CH₂-OH); **LRMS** m/z (ESI+) 281.10 (100%, [M-H₂O₂]⁺); **HRMS** m/z (ESI+) C₁₄H₁₈O₆Na Requires: 281.1001, Found: 281.9999 ([M-H₂O₂]⁺).

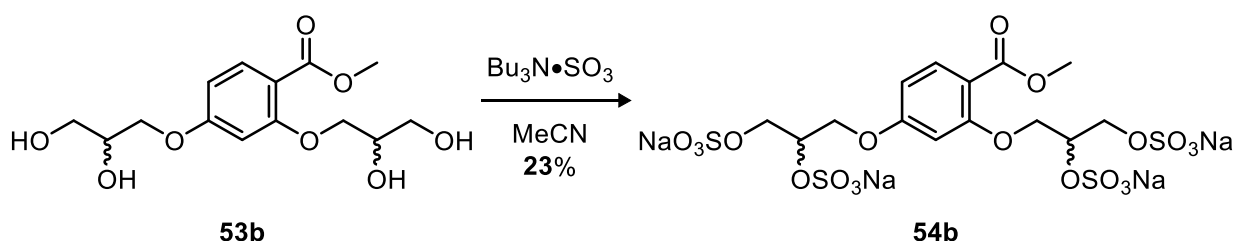
(54a) Sodium 3-(2-(2,3-bis(sulfonatooxy)propoxy)-3-(methoxycarbonyl)phenoxy)propane-1,2-diyl bis(sulfate)



Adapted from general procedure **H**: Methyl 2,3-bis(2,3-dihydroxypropoxy)benzoate (**53a**) (100 mg, 0.33 mmol) and Bu₃N•SO₃ (881 mg, 3.31 mmol) were dissolved in MeCN (2 mL) and heated at 90 °C for 24 h. The intermediate [Bu₃NH]⁺ salt was subjected to ion exchange following procedure **i**, affording the title compound as a white solid (200 mg, 85%). **IR** V_{max} cm⁻¹ 2953 w, 1711 w, 1583 w, 1480 w, 1207 w;

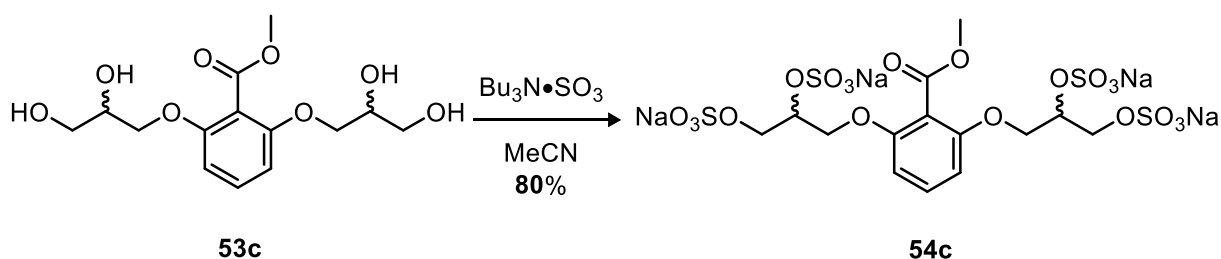
$^1\text{H-NMR}$ (400 MHz, D_2O) δ_{H} 7.32 (d, $J = 8.0$ Hz, 2H, C4-H & C6-H), 7.19 (t, $J = 8.0$ Hz, 1H, C5-H), 4.92 (p, $J = 4.8$ Hz, 1H, CH-OSO₃Na), 4.85 (p, $J = 4.8$ Hz, 1H, CH-OSO₃Na), 4.52 – 4.38 (m, 8H, Ar-OCH₂ & CH₂-OSO₃Na), 4.00 (s, 3H, Me); **$^{13}\text{C-NMR}$** (101 MHz, D_2O) δ_{C} 169.0 (CO₂Me), 151.4 (C3), 146.7 (C2), 125.5 (C5), 125.0 (C1), 122.9 (C4), 118.8 (C6), 75.93 (CH-OSO₃Na), 75.0 (CH-OSO₃Na), 72.2, 67.1, 66.8, 66.7, 53.1 (Me); **LRMS** m/z (ESI+) 888.78 (30%), 746.86 (100%, $[\text{M}+\text{Na}]^+$); **HRMS** m/z (ESI+) $\text{C}_{14}\text{H}_{16}\text{O}_{20}\text{Na}_5\text{S}_4$ Requires: 746.8606, Found: 746.8611 ($[\text{M}+\text{Na}]^+$).

(54b) Sodium 3-(5-(2,3-bis(sulfonatooxy)propoxy)-2-(methoxycarbonyl)phenoxy)propane-1,2-diyl bis(sulfate)



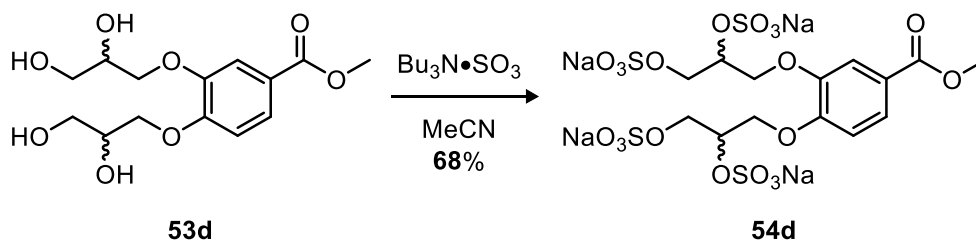
Adapted from general procedure **H**: Methyl 2,4-bis(2,3-dihydroxypropoxy)benzoate (**53b**) (30 mg, 0.09 mmol) and $\text{Bu}_3\text{N}\cdot\text{SO}_3$ (504 mg, 1.90 mmol) were dissolved in MeCN (2 mL) and heated at 90 °C for 24 h. The intermediate $[\text{Bu}_3\text{NH}]^+$ salt was subjected to ion exchange following procedure **i**, affording the title compound as a white solid (16 mg, 23%). **IR** ν_{max} cm^{-1} 2946 w, 1708 w, 158 w, 1479 w, 1210 w; **$^1\text{H-NMR}$** (400 MHz, $(\text{CD}_3)_2\text{SO}$) δ_{H} 7.68 (d, $J = 8.5$ Hz, 1H, C6-H), 6.72 – 6.52 (m, 2H C5-H & C3-H), 4.51 – 4.44 (m, 2H, CH-OSO₃Na), 4.28 – 4.02 (m, 4H), 4.06 – 3.89 (m, 3H), 3.85 (dd, $J = 10.0, 6.7$ Hz, 1H), 3.75 (s, 3H, Me); **LRMS** m/z (ESI+) 866.81 (30%), 746.86 (50%, $[\text{M}+\text{Na}]^+$), 644.93 (100%, $[\text{M}-\text{SO}_3]^+$), 542.98 (90%, $[\text{M}-\text{Na}_2\text{SO}_3]^+$); **HRMS** m/z (ESI+) $\text{C}_{14}\text{H}_{16}\text{O}_{20}\text{Na}_5\text{S}_4$ Requires: 746.8606, Found: 746.8614 ($[\text{M}+\text{Na}]^+$).

(54c) Sodium ((2-(methoxycarbonyl)-1,3-phenylene)bis(oxy))bis(propane-3,1,2-triyl) tetrakis(sulfate)



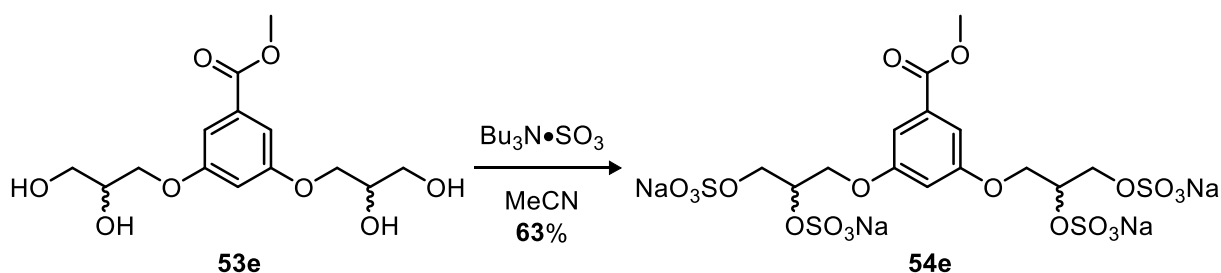
Adapted from general procedure **H**: Methyl 2,6-bis(2,3-dihydroxypropoxy)benzoate (**53c**) (100 mg, 0.32 mmol) and $\text{Bu}_3\text{N}\cdot\text{SO}_3$ (671 mg, 2.53 mmol) were dissolved in MeCN (2 mL) and heated at 90 °C for 12 h. The intermediate $[\text{Bu}_3\text{NH}]^+$ salt was subjected to ion exchange following procedure **i**, affording the title compound as a white solid (185 mg, 80%). **IR** $\text{V}_{\text{max}} \text{ cm}^{-1}$ 2953 w, 1715 w, 1475 w, 1210 w; **^1H -NMR** (400 MHz, $(\text{CD}_3)_2\text{SO}$) δ_{H} 7.29 (t, $J = 8.5$ Hz, 1H, C4-H), 6.73 (d, $J = 8.5$ Hz, 2H, C3-H), 4.47 – 4.31 (m, 2H, $\text{CH-OSO}_3\text{Na}$), 4.17 – 4.01 (m, 4H, $\text{CH}_2\text{-OSO}_3\text{Na}$), 3.95 – 3.78 (m, 4H, C2-OCH_2), 3.76 (s, 3H, Me); **^{13}C -NMR** (101 MHz, $(\text{CD}_3)_2\text{SO}$) δ_{C} 165.6 (CO_2Me), 156.0 (C2), 131.1 (C4), 113.4 (C1), 105.4 (C3), 72.2 ($\text{CH-OSO}_3\text{Na}$), 67.1 ($\text{CH}_2\text{-OSO}_3\text{Na}$), 64.2 (C2-OCH_2), 51.8 (Me); **LRMS** m/z (ESI+) 746.86 (40%, $[\text{M}+\text{Na}]^+$), 644.93 (60%, $[\text{M}-\text{SO}_3]^+$), 542.98 (100%, $[\text{M}-(\text{SO}_3)_2]^+$); **HRMS** m/z (ESI+) $\text{C}_{14}\text{H}_{16}\text{O}_{20}\text{Na}_5\text{S}_4$ Requires: 746.8606, Found: 746.8616 ($[\text{M}+\text{Na}]^+$).

(54d) Sodium 3-(2-(2,3-bis(sulfonatooxy)propoxy)-4-(methoxycarbonyl)phenoxy)propane-1,2-diyl bis(sulfate)



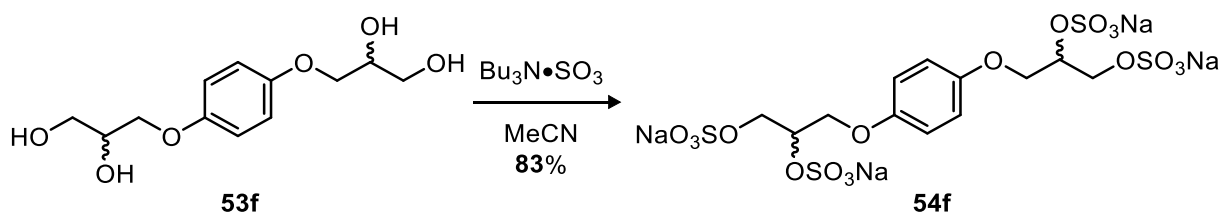
Adapted from general procedure **H**: Methyl 3,4-bis(2,3-dihydroxypropoxy)benzoate (**53d**) (100 mg, 0.32 mmol) and $\text{Bu}_3\text{N}\cdot\text{SO}_3$ (671 mg, 2.53 mmol) were dissolved in MeCN (2 mL) and heated at 90 °C for 12 h. The intermediate $[\text{Bu}_3\text{NH}]^+$ salt was subjected to ion exchange following procedure **i**, affording the title compound as a white solid (157 mg, 68%). **IR** ν_{max} cm^{-1} 2955 w, 1708 w, 1637 w, 1514 w, 1441 w, 1213 s; **$^1\text{H-NMR}$** (400 MHz, D_2O) δ_{H} 7.78 – 7.74 (m, 2H, C2-H & C6-H), 7.23 (d, J = 9.1 Hz, 1H, C5-H), 5.09 – 4.88 (m, 2H, CH- OSO_3Na), 4.59 – 4.32 (m, 8H, Ar- OCH_2 & CH- OSO_3Na), 3.94 (s, 3H, Me); **$^{13}\text{C-NMR}$** (101 MHz, D_2O) δ_{C} 168.8 ($\text{C}=\text{O}_2\text{Me}$), 152.7 (C3), 147.4 (C4), 125.1 (C6), 123.0 (C1), 116.6 (C2), 114.0 (C5), 75.1 (CH- OSO_3Na), 75.0 (CH- OSO_3Na), 74.9 (CH- OSO_3Na), 74.8 (CH- OSO_3Na), 68.04, 67.99, 67.1, 66.6, 52.6 (Me); **LRMS** m/z (ESI+) 746.86 (100%, $[\text{M}+\text{Na}]^+$); **HRMS** m/z (ESI+) $\text{C}_{14}\text{H}_{16}\text{O}_{20}\text{Na}_5\text{S}_4$ Requires: 746.8606, Found: 746.8603 ($[\text{M}+\text{Na}]^+$).

(54e) Sodium ((5-(methoxycarbonyl)-1,3-phenylene)bis(oxy))bis(propane-3,1,2-triyl) tetrakis(sulfate)



Adapted from general procedure **H**: Methyl 3,4-bis(2,3-dihydroxypropoxy)benzoate (**53e**) (50 mg, 0.16 mmol) and $\text{Bu}_3\text{N}\cdot\text{SO}_3$ (336 mg, 1.26 mmol) were dissolved in MeCN (2 mL) and heated at 90 °C for 12 h. The intermediate $[\text{Bu}_3\text{NH}]^+$ salt was subjected to ion exchange following procedure **i**, affording the title compound as a white solid (72 mg, 63%). **IR** ν_{max} cm^{-1} 1710 w, 1602 w, 1448 w, 1353 w, 1236 s; **$^1\text{H-NMR}$** (400 MHz, D_2O) δ_{H} 7.35 (d, $J = 2.3$ Hz, 2H, C2-H), 7.00 (t, $J = 2.3$ Hz, 1H, C4-H), 4.94 (p, $J = 4.7$ Hz, 2H, CH- OSO_3Na), 4.49 – 4.33 (m, 8H, C3- OCH_2 & CH₂- OSO_3Na), 3.96 (s, 3H, Me); **$^{13}\text{C-NMR}$** (101 MHz, D_2O) δ_{C} 168.6 (CO_2Me), 159.2 (C3), 131.7 (C1), 109.0 (C2), 107.6 (C4), 75.0 (CH- OSO_3Na), 66.8, 66.5, 52.8 (Me); **LRMS** m/z (ESI+) 644.93 (100%, $[\text{M}-\text{SO}_3]^+$).

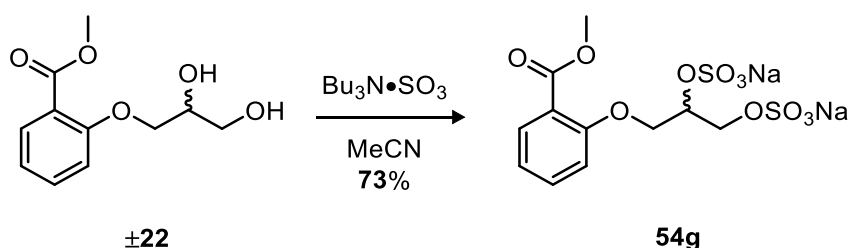
(54f) Sodium (1,4-phenylenebis(oxy))bis(propane-3,1,2-triyl) tetrakis(sulfate)



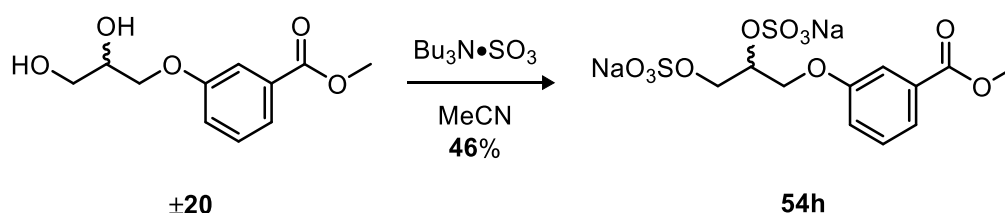
Adapted from general procedure **H**: 1,4-Phenylenebis(oxy))bis(propane-1,2-diol (**53f**) (50 mg, 0.19 mmol) and $\text{Bu}_3\text{N}\cdot\text{SO}_3$ (257 mg, 0.97 mmol) were dissolved in MeCN (1 mL) and heated at 90 °C for 5 h. The intermediate $[\text{Bu}_3\text{NH}]^+$ salt was subjected to Ion exchange following procedure **i**, affording the title compound as a white solid (91 mg,

83%). **IR** V_{\max} cm^{-1} 2947 w, 1634 w, 1509 s, 1459 w, 1208 s; **$^1\text{H-NMR}$** (400 MHz, D_2O) δ_{H} 7.02 (s, 4H, Ar-H), 4.84 (p, $J = 4.8$ Hz, 2H, CH-OSO₃Na), 4.42 – 4.28 (m, 6H ArO-CH₂ & CH₂-OSO₃Na), 4.23 (m, 2H, ArO-CH₂); **$^{13}\text{C-NMR}$** (101 MHz, D_2O) δ_{C} 152.7 (Ar-O), 116.4 (Ar-H), 75.1 (CH-OSO₃Na), 67.3 (ArO-CH₂), 66.5 (CH₂-OSO₃Na); **LRMS** m/z (ESI⁻) 642.88 (50%, [M-Na]⁻), 540.94 (50% [M-Na₂SO₃]⁻), 529.46 (100%); **HRMS** m/z (ESI⁻) C₁₂H₁₄O₁₈Na₃S₄ Requires: 642.8756, Found: 642.8760 ([M-Na]⁻).

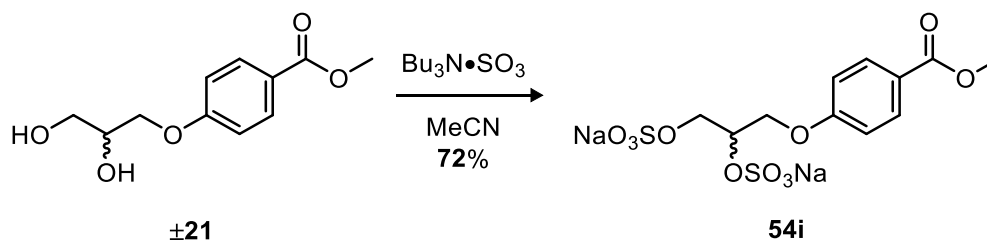
(54g) Sodium 3-(2-(methoxycarbonyl)phenoxy)propane-1,2-diyl bis(sulfate)



Adapted from general procedure **H**: Methyl (±)-2-(2,3-dihydroxypropoxy)benzoate (**±22**) (226 mg, 1.0 mmol) and Bu₃N•SO₃ (1.60 g, 4.0 mmol) were dissolved in MeCN (4 mL) and heated at 90 °C for 8 h. The intermediate [Bu₃NH]⁺ salt was subjected to ion exchange following procedure **i**, affording the title compound as a white solid (300 mg, 70%). **IR** V_{\max} cm^{-1} 1709 w, 1602 w, 1441 w, 1349 w, 1214 s; **$^1\text{H-NMR}$** (400 MHz, (CD₃)₂SO) δ_{H} 7.65 (dd, $J = 7.5, 1.9$ Hz, 1H, C6-H), 7.51 (ddd, $J = 8.6, 7.5, 1.9$ Hz, 1H, C5-H), 7.15 (d, $J = 8.6$ Hz, 1H, C4-H), 7.01 (t, $J = 7.5$ Hz, 1H, C3-H), 4.48 (p, $J = 5.3$ Hz, 1H, CH-OSO₃Na), 4.22 (dd, $J = 9.9, 5.0$ Hz, 1H, C2-OCH₂), 4.11 (dd, $J = 9.9, 3.5$ Hz, 1H, C2-OCH₂), 4.03 – 3.88 (m, 2H, CH₂-OSO₃Na), 3.80 (s, 3H, Me); **$^{13}\text{C-NMR}$** (101 MHz, (CD₃)₂SO) δ_{C} 166.5 (C=O₂Me), 157.6 (C2), 133.6 (C5), 130.8 (C6), 120.3 (C1), 120.2 (C3), 113.6 (C4), 72.3 (CH-OSO₃Na), 67.1 (C2-OCH₂), 56.0 (CH₂-OSO₃Na), 51.8 (Me); **LRMS** m/z (ESI⁺) 452.95 (90%, [M+Na]⁺), 351.01 (100%, [M-SO₃]⁺); **HRMS** m/z (ESI⁺) C₁₁H₁₂S₂O₁₁Na₃ Requires: 452.9514, Found: 452.9516 ([M+Na]⁺).

(54h) Sodium 3-(3-(methoxycarbonyl)phenoxy)propane-1,2-diyl bis(sulfate)

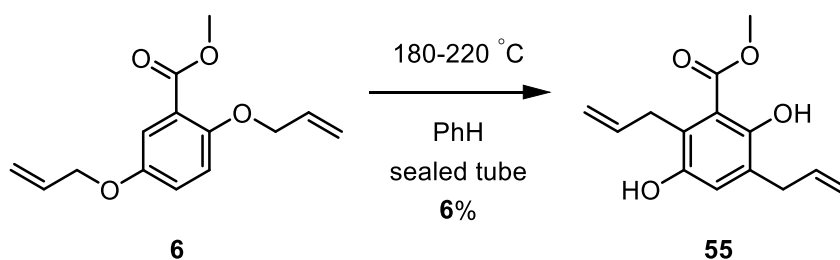
Adapted from general procedure **H**: Methyl (\pm)-3-(2,3-dihydroxypropoxy)benzoate (**±20**) (226 mg, 1.0 mmol) and $\text{Bu}_3\text{N}\cdot\text{SO}_3$ (1.60 g, 4.0 mmol) were dissolved in MeCN (4 mL) and heated at 90 °C for 8 h. The intermediate $[\text{Bu}_3\text{NH}]^+$ salt was subjected to ion exchange following procedure **i**, affording the title compound as a white solid (197 mg, 46%). **IR** V_{max} cm^{-1} 1704 w, 1606 w, 1440 w, 1353 w, 1215 s; **$^1\text{H-NMR}$** (400 MHz, $(\text{CD}_3)_2\text{SO}$) δ_{H} 7.54 (dt, $J = 8.2, 1.1$ Hz, 1H, C4-H), 7.48 – 7.38 (m, 2H, C5-H & C2-H), 7.25 (ddd, $J = 8.2, 2.8, 1.1$ Hz, 1H, C6-H), 4.47 (dq, $J = 6.8, 4.4$ Hz, 1H, CH- OSO_3Na), 4.22 – 4.05 (m, 2H, C3- OCH_2), 3.98 (dd, $J = 10.0, 5.0$ Hz, 1H, $\text{CH}_2\text{-OSO}_3\text{Na}$), 3.91 – 3.81 (m, 4H, Me & $\text{CH}_2\text{-OSO}_3\text{Na}$); **$^{13}\text{C-NMR}$** (101 MHz, $(\text{CD}_3)_2\text{SO}$) δ_{C} 166.0 (CO_2Me), 158.7 (C3), 130.9 (C1), 129.9 (C5), 121.4 (C4), 119.6 (C6), 114.6 (C2), 72.1 (CH- OSO_3Na), 66.7 (C3- OCH_2), 63.9 ($\text{CH}_2\text{-OSO}_3\text{Na}$), 52.2 (Me); **LRMS** m/z (ESI+) 452.95 (70%, $[\text{M}+\text{Na}]^+$), 351.01 (100%, $[\text{M}-\text{SO}_3]^+$), 249.07 (50%, $[\text{M}-(\text{SO}_3)_2]^+$); **HRMS** m/z (ESI+) $\text{C}_{11}\text{H}_{12}\text{S}_2\text{O}_{11}\text{Na}_3$ Requires: 452.9514, Found: 452.9529 ($[\text{M}+\text{Na}]^+$).

(54i) Sodium 4-(3-(methoxycarbonyl)phenoxy)propane-1,2-diyl bis(sulfate)

Adapted from general procedure **H**: Methyl (\pm)-3-(2,3-dihydroxypropoxy)benzoate (**±21**) (226 mg, 1.0 mmol) and $\text{Bu}_3\text{N}\cdot\text{SO}_3$ (1.60 g, 4.0 mmol) were dissolved in MeCN

(4 mL) and heated at 90 °C for 8 h. The intermediate $[\text{Bu}_3\text{NH}]^+$ salt was subjected to ion exchange following procedure **i**, affording the title compound as a white solid (310 mg, 72%). **IR** V_{max} cm^{-1} 1701 w, 1602 w, 1442 w, 1348 w, 1210 s; **$^1\text{H-NMR}$** (400 MHz, D_2O) δ_{H} 8.00 – 7.91 (m, 2H, C2-H), 7.12 – 7.04 (m, 2H, C3-H), 4.95 – 4.86 (m, 1H, CH-OSO₃Na), 4.48 – 4.31 (m, 4H, C4-OCH₂ & CH₂-OSO₃Na), 3.88 (s, 3H, Me); **$^{13}\text{C-NMR}$** (101 MHz, D_2O) δ_{C} 169.1 (CO₂Me), 162.2 (C4), 131.6 (C2), 122.3 (C1), 114.7 (C3), 74.8 (CH-OSO₃Na), 66.4 (CH₂), 66.3 (CH₂), 52.4 (Me); **LRMS** m/z (ESI+) 452.90 (100%, $[\text{M}+\text{Na}]^+$); **HRMS** m/z (ESI+) C₁₁H₁₂S₂O₁₁Na₃ Requires: 452.9515, Found: 452.9514 ($[\text{M}+\text{Na}]^+$).

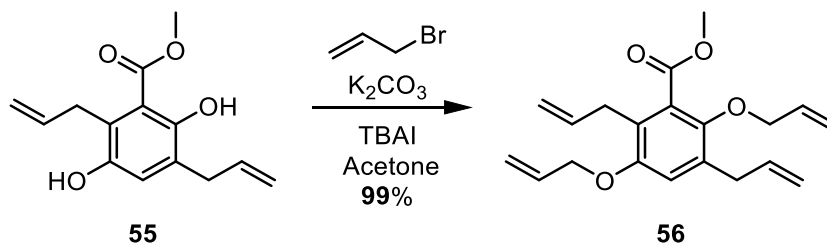
(55) Methyl 2,5-diallyl-3,6-dihydroxybenzoate



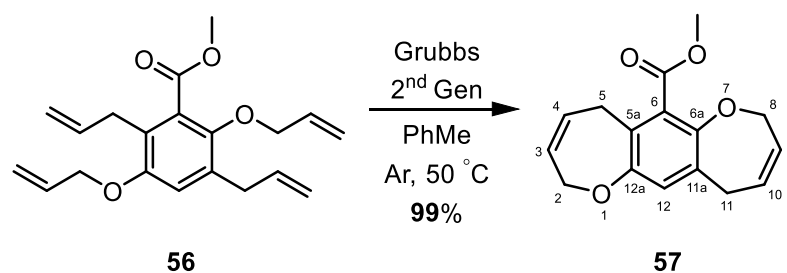
A high pressure heating tube was charged with Methyl 2,5-bis(allyloxy)benzoate (**6**) (100 mg, 0.40 mmol) and anhydrous benzene (1 mL). The flask was sealed and heated at 200 °C for 18 h. Removal of the solvent under reduced pressure afforded a black oil. Purification by chromatography (SiO_2 , EtOAc./Hexane 1:19) gave the title compound as a clear oil (6 mg, 6%) **IR** V_{max} cm^{-1} 3422 br s, 3075 w, 3012 w, 2977 w, 2959 w, 1662 s, 1434 s; **$^1\text{H-NMR}$** (400 MHz, CDCl_3) δ_{H} 10.60 (s, 1H, C6-OH), 6.89 (s, 1H, C4-H), 6.10 – 5.87 (m, 2H, CH=CH₂), 5.19 – 4.97 (m, 4H, CH=CH₂), 4.62 (s, 1H, C3-OH), 3.94 (s, 3H, Me), 3.67 (dt, $J = 5.9, 1.7$ Hz, 2H, C2-CH₂), 3.40 – 3.36 (m, 2H, C5-CH₂); **$^{13}\text{C-NMR}$** (101 MHz, CDCl_3) δ_{C} 171.8 (CO₂Me), 154.3 (C6), 146.9 (C3), 136.6 (CH=CH₂), 136.2 (CH=CH₂), 128.0 (C5), 123.9 (C1), 123.8 (C4), 116.3 (CH=CH₂), 115.5 (CH=CH₂), 112.7 (C2), 52.4 (Me), 33.9 (C5-CH₂), 32.6 (C2-CH₂);

LRMS m/z (ESI+) 271.09 (100%, $[M+Na]^+$); **HRMS** m/z (ESI+) $C_{14}H_{16}NaO_4$ Requires: 271.0941, Found: 271.0936 ($[M+Na]^+$).

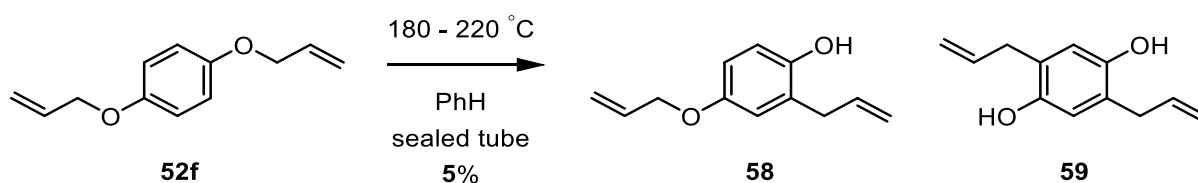
(56) Methyl 2,5-diallyl-3,6-bis(allyloxy)benzoate



Following general procedure **B**: using methyl 2,5-diallyl-3,6-dihydroxybenzoate (**55**) (6 mg, 0.024 mmol). Purification by chromatography (SiO_2 , EtOAc/hexane, 1:19) afforded the title compound as a clear oil (8 mg, 99%). **IR** V_{max} cm^{-1} 3076 w, 2919 s, 2853 w, 1732 s, 1637 w, 1603 w, 1474 s; **1H -NMR** (400 MHz, $CDCl_3$) δ_H 6.72 (s, 1H, C4-H), 6.12 – 5.80 (m, 4H, $CH=CH_2$), 5.38 (ddq, $J = 17.5, 14.3, 1.6$ Hz, 2H, $CH=CH_2$), 5.24 (ddq, $J = 17.0, 10.5, 1.5$ Hz, 2H, $CH=CH_2$), 5.11 (m, 1H, $CH=CH_2$), 5.07 (dq, $J = 8.6, 1.6$ Hz, 1H, $CH=CH_2$), 5.04 – 4.93 (m, 2H, $CH=CH_2$), 4.50 (dt, $J = 5.1, 1.6$ Hz, 2H, C3- OCH_2), 4.33 (dt, $J = 5.4, 1.5$ Hz, 2H, C6- OCH_2), 3.87 (s, 3H, Me), 3.36 (ddt, $J = 15.6, 6.4, 1.6$ Hz, 4H, C2- CH_2 & C5- CH_2); **^{13}C -NMR** (101 MHz, $CDCl_3$) δ_C 168.6 ($C=O$), 152.8 (C3), 147.4 (C6), 136.7 ($CH=CH_2$), 136.2 ($CH=CH_2$), 133.9 ($CH=CH_2$), 133.4 ($CH=CH_2$), 132.2 (C2), 130.2 (C1), 125.2 (C5), 117.3 ($CH=CH_2$), 117.2 ($CH=CH_2$), 116.5 ($CH=CH_2$), 115.4 ($CH=CH_2$), 115.0 (C4), 76.1 (C6- OCH_2), 69.6 (C3- OCH_2), 52.3 (Me), 33.9 (C2- CH_2), 31.9 (C5- CH_2); **LRMS** m/z (ESI+) 351.16 (100%, $[M+Na]^+$); **HRMS** m/z (ESI+) $C_{20}H_{24}NaO_4$ Requires: 351.1572, Found: 351.1570 ($[M+Na]^+$).

(57) Methyl 2,5,8,11-tetrahydrobenzo[1,2-b:4,5-b']bis(oxepine)-6-carboxylate

A flask containing methyl 2,5-diallyl-3,6-bis(allyloxy)benzoate (**56**) (8.0 mg, 0.024 mmol) was charged with Grubbs 2nd generation catalyst (2.3 mg, 0.003 mmol) and dry toluene (2.7 mL). The flask was heated at 80 °C for 1 h whilst being purged with Ar (g). The solvent was removed under reduced pressure and the crude mixture was purified by chromatography (SiO₂, EtOAc/Hexane, 1:19) to give the title compound as a clear oil (6.5 mg, 99%). **IR** V_{\max} cm⁻¹ 3025 w, 2953 w, 2932 w, 2853 w, 1732 s, 1473 s, 1441 w; **¹H-NMR** (400 MHz, CDCl₃) δ_{H} 6.87 (s, 1H, C12-H), 5.86 – 5.75 (m, 2H, C4-H & C10-H), 5.50 – 5.39 (m, 2H, C3-H & C9-H), 4.57 (m, 4H, C2-H₂ & C8-H₂), 3.92 (s, 3H, Me), 3.45 – 3.33 (m, 4H, C5-H₂ & C11-H₂); **¹³C-NMR** (101 MHz, CDCl₃) δ_{C} 167.9 (CO₂Me), 154.6 (C12a), 151.0 (C6a), 136.2 (C5a), 132.7 (C11a), 127.8 (C9), 127.6 (C3), 127.3 (C6), 125.1 (C10), 125.0 (C4), 123.1 (C12), 71.6 (C2), 71.4 (C8), 52.5 (Me), 31.4 (C5), 27.7 (C11); **LRMS** m/z (ESI+) 295.09 (100%, [M+Na]⁺); **HRMS** m/z (ESI+) C₁₆H₁₆NaO₄ Requires: 295.0946, Found: 295.0945 ([M+Na]⁺).

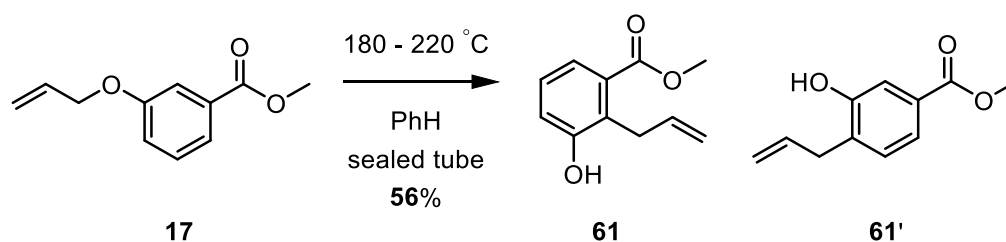
(58) 2-Allyl-4-(allyloxy)phenol

A high pressure heating tube was charged with 1,4-bis(allyloxy)benzene (**52f**) (200 mg, 1.05 mmol) and anhydrous benzene (1 mL). The flask was sealed and heated at

200 °C for 12 h. Removal of the solvent under reduced pressure afforded a black oil. Purification by chromatography (SiO₂, EtOAc/Hexane 1:19) afforded alkene **52f** (100 mg, 0.53 mmol) and the rearrangement products **58** (80 mg, 80%*) and **59** (10 mg, 10%*) as clear oils. **IR** Vmax cm⁻¹ 3398 br s, 3078 w, 2979 w, 1638 w, 1609 w, 1503 s; **¹H-NMR** (400 MHz, CDCl₃) δ_H 6.78 – 6.66 (m, 3H, Ar-H), 6.12 – 5.94 (m, 2H, CH=CH₂), 5.40 (dq, *J* = 17.2, 1.6 Hz, 1H, C4-OCH₂CH=CH₂), 5.27 (dq, *J* = 10.5, 1.4 Hz, 1H, C4-OCH₂CH=CH₂), 5.19 – 5.12 (m, 2H, C2-CH₂CH=CH₂), 4.80 (s, 1H, C1-OH), 4.48 (dt, *J* = 5.4, 1.5 Hz, 2H), 3.38 (dt, *J* = 6.4, 1.6 Hz, 2H, C2-CH₂); **¹³C-NMR** (101 MHz, CDCl₃) δ_C 152.8 (C4), 148.2 (C1), 136.3 (C2-CH₂CH=CH₂), 133.7 (C4-OCH₂CH=CH₂), 126.6 (C2), 117.6 (C4-OCH₂CH=CH₂), 117.1 (Ar-H), 116.6 (C2-CH₂CH=CH₂), 116.5 (Ar-H), 113.7 (Ar-H), 69.6 (C4-OCH₂), 35.3 (C2-CH₂); **LRMS** *m/z* (ESI+) 213.09 (100%, [M+Na]⁺); **HRMS** *m/z* (ESI+) C₁₂H₁₂NaO₂ Requires: 213.0891, Found: 213.0892 ([M+Na]⁺). *Based on recovered starting material.

(59) 2,5-Diallylbenzene-1,4-diol

M.P 122 °C; **IR** Vmax cm⁻¹ 3275 s, 2917 w, 1438 s, 1194 s, 1177 s; **¹H-NMR** (400 MHz, CDCl₃) δ_H 6.60 (s, 2H, C3-H), 5.98 (ddt, *J* = 17.8, 9.5, 6.4 Hz, 2H, CH=CH₂), 5.20 – 5.11 (m, 4H, CH=CH₂), 4.58 (s, 2H, C1-OH), 3.33 (d, *J* = 6.4 Hz, 4H, C2-CH₂); **¹³C-NMR** (101 MHz, CDCl₃) δ_C 148.0 (C1), 136.4 (CH=CH₂), 124.7 (C2), 117.7 (C3), 116.7 (CH=CH₂), 34.9 (C2-CH₂); **LRMS** *m/z* (ESI+) 213.09 (100%, [M+Na]⁺); **HRMS** *m/z* (ESI+) C₁₂H₁₂NaO₂ Requires: 213.0891, Found: 213.0892 ([M+Na]⁺).

(61) Methyl 2-allyl-3-hydroxybenzoate

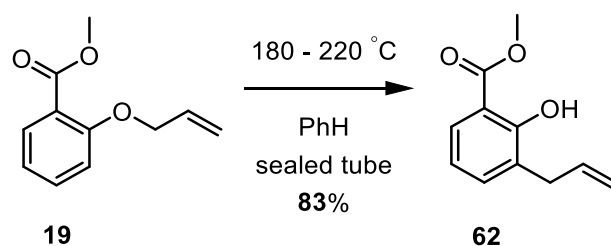
A high pressure heating tube was charged with methyl 3-(allyloxy)benzoate (**17**) (60 mg, 0.31 mmol) and anhydrous benzene (1 mL). The flask was sealed and heated at 200 °C for 12 h. Removal of the solvent under reduced pressure afforded a black oil. Purification by chromatography (SiO₂, EtOAc/Hexane 1:19) afforded **17** (15 mg, 25%) and the title compounds **61** (33 mg, 73%*) and **61'** (12 mg, 26%*) as crystalline solids. (For **61**) **M.P** 54 °C; **IR** ν_{max} cm⁻¹ 3415 br s, 3082 w, 2952 w, 1699 s, 1638 w, 1585 w; **¹H-NMR** (400 MHz, CDCl₃) δ_{H} 7.43 (dd, J = 8.0, 1.3 Hz, 1H, C6-H), 7.17 (t, J = 8.0 Hz, 1H, C5-H), 6.99 (dd, J = 8.0, 1.3 Hz, 1H, C4-H), 6.04 (ddt, J = 16.7, 10.6, 6.0 Hz, 1H, CH=CH₂), 5.36 (s, 1H, C3-OH), 5.14 – 5.11 (m, 1H, CH=CH₂), 5.09 (dq, J = 8.5, 1.7 Hz, 1H, CH=CH₂), 3.88 (s, 3H, Me), 3.76 (dt, J = 6.0, 1.7 Hz, 2H, C2-CH₂); **¹³C-NMR** (101 MHz, CDCl₃) δ_{C} 168.4 (CO₂Me), 155.1 (C3), 136.3 (CH=CH₂), 131.8 (C1), 127.4 (C6), 126.5 (C2), 123.1 (C5), 119.6 (C4), 116.0 (CH=CH₂), 52.3 (Me), 31.3 (C2-CH₂); **LRMS** m/z (ESI+) 215.06 (25%, [M+Na]⁺); **HRMS** m/z (ESI+) C₁₁H₁₂NaO₃ Requires: 215.0682, Found: 215.0678 ([M+Na]⁺). *Based on recovered starting material.

(61') Methyl 4-allyl-3-hydroxybenzoate

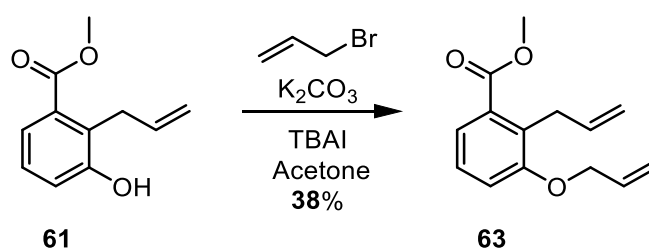
M.P 83 °C; **IR** ν_{max} cm⁻¹ 3347 br s, 3077 w, 2953 w, 2847 w, 1696 s, 1638, 1612 w, 1588 s; **¹H-NMR** (400 MHz, CDCl₃) δ_{H} 7.57 (d, J = 1.7 Hz, 1H, C2-H), 7.55 (dd, J = 7.8, 1.7 Hz, 1H, C6-H), 7.18 (d, J = 7.8 Hz, 1H, C5-H), 6.01 (ddt, J = 16.8, 10.3, 6.4 Hz, 1H, CH=CH₂), 5.84 (s, 1H, C3-OH), 5.16 (q, J = 1.6 Hz, 1H, CH=CH₂), 5.13 (dq, J

= 10.0, 1.6 Hz, 1H, CH=CH₂), 3.91 (s, 3H, Me), 3.45 (dt, J = 6.4, 1.7 Hz, 2H, C4-CH₂); **¹³C-NMR** (101 MHz, CDCl₃) δ_c 167.4 (C=O₂Me), 154.1 (C3), 135.7 (CH=CH₂), 131.7 (C4), 130.4 (C5), 129.6 (C1), 122.2 (C6), 116.9 (CH=CH₂), 116.7 (C2), 52.4 (Me), 34.9 (C4-CH₂); **LRMS** m/z (ESI+) 215.06 (80%, [M+Na]⁺); **HRMS** m/z (ESI+) C₁₁H₁₂NaO₃ Requires: 215.0682, Found: 215.0682 ([M+Na]⁺)

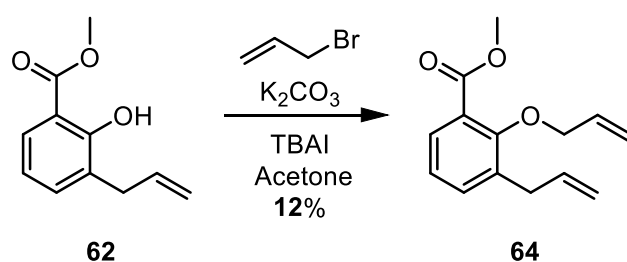
(62) Methyl 3-allyl-2-hydroxybenzoate



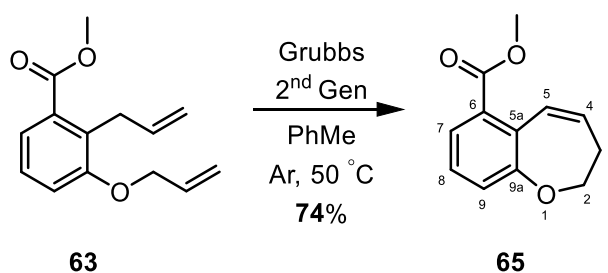
A high pressure heating tube was charged with methyl 2-(allyloxy)benzoate (**19**) (120 mg, 0.62 mmol) and anhydrous benzene (1 mL). The flask was sealed and heated at 200 °C for 12 h. Removal of the solvent under reduced pressure afforded a black oil. Purification by chromatography (SiO₂, EtOAc/Hexane 1:19) afforded the title compound as a clear oil (100 mg, 83%). **IR** ν_{max} cm⁻¹ 3141 br w, 2954 w, 1671 s, 1638 w, 1612 s, 1594 w, 1485 w, 1438 s; **¹H-NMR** (400 MHz, CDCl₃) δ_H 11.07 (d, J = 0.7, 1H, C2-OH), 7.73 (dd, J = 7.7, 1.7 Hz, 1H, C4-H), 7.33 (ddd, J = 7.7, 1.7, 0.7 Hz, 1H, C6-H), 6.83 (app. t, J = 7.7 Hz, 1H, C5-H), 6.02 (ddt, J = 17.7, 9.5, 6.5 Hz, 1H, CH=CH₂), 5.14 – 5.07 (m, 1H, CH=CH₂), 5.08 – 5.06 (m, 1H, CH=CH₂), 3.94 (s, 3H, Me), 3.44 (d, J = 6.5 Hz, 2H, C3-CH₂); **¹³C-NMR** (101 MHz, CDCl₃) δ_c 171.1 (C=O₂Me), 159.7 (C2), 136.3 (CH=CH₂), 135.9 (C6), 128.6 (C3), 128.0 (C4), 118.8 (C5), 116.0 (CH=CH₂), 112.0, 52.4 (Me), 33.8 (C3-CH₂); **LRMS** m/z (ESI+) 215.06 (100%, [M+Na]⁺); **HRMS** m/z (ESI+) C₁₁H₁₂NaO₃ Requires: 215.0679, Found: 215.0678 ([M+Na]⁺).

(63) Methyl 2-allyl-3-(allyloxy)benzoate

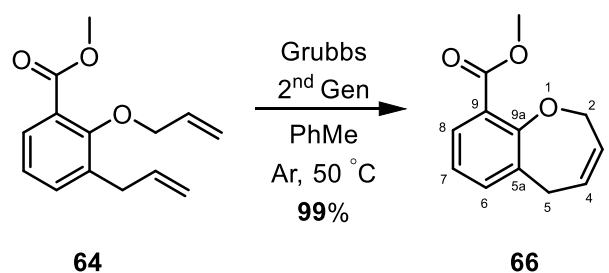
Following general procedure **B**: using methyl 2-allyl-3-hydroxybenzoate (**61**) (45 mg, 0.23 mmol). Purification by chromatography (SiO_2 , EtOAc/hexane, 1:19) afforded the title compound as a clear oil (17 mg, 38%). **IR** ν_{max} cm^{-1} 3078 w, 2951 w, 2148 w, 1722 s, 1636 w, 1581 w; **1H -NMR** (400 MHz, $CDCl_3$) δ_H 7.41 (dd, J = 8.0, 1.2 Hz, 1H, C6-H), 7.21 (t, J = 8.0 Hz, 1H, C5-H), 7.00 (dd, J = 8.0, 1.2 Hz, 1H, C4-H), 6.14 – 5.92 (m, 2H, $CH=CH_2$), 5.43 (dq, J = 17.3, 1.6 Hz, 1H, C3-OCH $_2$ CH=CH $_2$), 5.28 (dq, J = 10.6, 1.6 Hz, 1H, C3-OCH $_2$ CH=CH $_2$), 5.04 – 4.94 (m, 2H, C2-CH $_2$ CH=CH $_2$), 4.56 (dt, J = 5.0, 1.6 Hz, 2H, C3-OCH $_2$), 3.77 (dt, J = 6.3, 1.6 Hz, 2H, C2-CH $_2$); **^{13}C -NMR** (101 MHz, $CDCl_3$) δ_C 168.5 (CO $_2$ Me), 156.9 (C3), 137.0 (C2-CH $_2$ CH=CH $_2$), 133.2 (C3-OCH $_2$ CH=CH $_2$), 131.8 (C1), 130.2 (C2), 126.9 (C5), 122.5 (C6), 117.3 (C3-OCH $_2$ CH=CH $_2$), 115.3 (C4), 114.9 (C2-CH $_2$ CH=CH $_2$), 69.4 (C3-OCH $_2$), 52.1 (Me), 30.8 (C2-CH $_2$); **LRMS** m/z (ESI+) 255.10 (100%, $[M+Na]^+$); **HRMS** m/z (ESI+) $C_{14}H_{16}NaO_3$ Requires: 255.0992, Found: 255.0989 ($[M+Na]^+$).

(64) Methyl 3-allyl-2-(allyloxy)benzoate

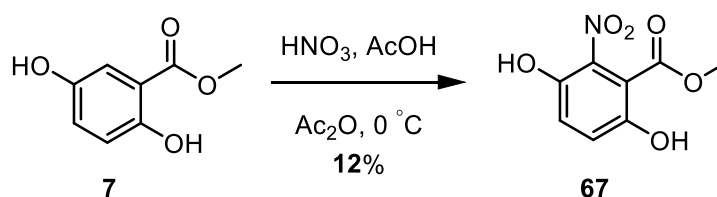
Following general procedure **B**: using methyl 3-allyl-2-hydroxybenzoate (**62**) (50 mg, 0.26 mmol). Purification by chromatography (SiO₂, EtOAc/hexane, 1:19) afforded the title compound as a clear oil (6 mg, 12%). **IR** ν_{max} cm⁻¹ 3079 w, 2950 w, 2160 w, 1728 s, 1639 w, 1592 w; **¹H-NMR** (400 MHz, CDCl₃) δ_{H} 7.68 (dd, J = 7.7, 1.8 Hz, 1H), 7.36 (dd, J = 7.7, 1.8 Hz, 1H), 7.11 (t, J = 7.7 Hz, 1H, C5-H), 6.10 (ddt, J = 17.2, 10.4, 5.7 Hz, 1H, C2-OCH₂CH=CH₂), 5.96 (ddt, J = 16.0, 10.5, 6.5 Hz, 1H, C3-CH₂CH=CH₂), 5.40 (dq, J = 17.2, 1.6 Hz, 1H, C2-OCH₂CH=CH₂), 5.26 (dq, J = 10.4, 1.3 Hz, 1H, C2-OCH₂CH=CH₂), 5.09 (dt, J = 10.5, 1.7 Hz, 1H, C3-CH₂CH=CH₂), 5.06 (dq, J = 16.0, 1.7 Hz, 1H, C3-CH₂CH=CH₂), 4.43 (dt, J = 5.7, 1.4 Hz, 2H, C2-OCH₂), 3.90 (s, 3H, Me), 3.46 (dt, J = 6.5, 1.6 Hz, 2H, C3-CH₂); **¹³C-NMR** (101 MHz, CDCl₃) δ_{C} 167.0 (C=O), 156.8 (C2), 136.8 (C3-CH₂CH=CH₂), 135.0 (C3), 134.6 (C4), 133.8 (C2-OCH₂CH=CH₂), 129.8 (C6), 125.1 (C1), 123.9 (C5), 117.7 (C2-OCH₂CH=CH₂), 116.4 (C3-CH₂CH=CH₂), 75.9 (C2-OCH₂), 52.3 (Me), 34.0 (C3-CH₂); **LRMS** m/z (ESI+) 255.10 (100%, [M+Na]⁺); **HRMS** m/z (ESI+) C₁₄H₁₆NaO₃ Requires: 255.0992, Found: 255.0995 ([M+Na]⁺).

(65) Methyl 2,3-dihydrobenzo[b]oxepine-6-carboxylate

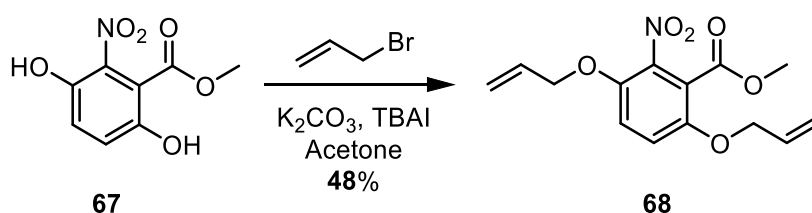
A flask containing methyl 2-allyl-3-(allyloxy)benzoate (**63**) (17 mg, 7.3×10^{-2} mmol) was charged with Grubbs 2nd generation catalyst (6 mg, 7×10^{-4} mmol) and dry toluene (7.3 mL). The flask was heated at 80 °C for 20 min whilst being purged with Ar (g). The solvent was removed under reduced pressure and the crude mixture was purified by chromatography (SiO₂, EtOAc/Hexane, 1:19) to give the title compound as a clear oil (11 mg, 74%). **IR** ν_{max} cm⁻¹ 2949 w, 2853 w, 1721 s, 1596 w, 1473 w, 1446 s, 1434 w, 1423 w; **¹H-NMR** (400 MHz, CDCl₃) δ_{H} 7.42 (dd, $J = 7.4, 1.7$ Hz, 1H, C7-H), 7.20 – 7.06 (m, 2H, C8-H & C9-H), 6.81 (dt, $J = 12.3, 1.9$ Hz, 1H, C5-H), 6.12 (dt, $J = 12.3, 4.3$ Hz, 1H, C4-H), 4.40 – 4.20 (t, $J = 5.1$ Hz, 2H, C2-H₂), 3.91 (s, 3H, Me), 2.70 (tdd, $J = 5.1, 4.3, 1.9$ Hz, 2H, C5-H₂); **¹³C-NMR** (101 MHz, CDCl₃) δ_{C} 168.9 (CO₂Me), 160.7 (C9a), 133.1 (C5a), 132.4 (C4), 127.4 (C6), 127.3 (C8), 124.69 (C7), 124.68 (C5), 123.7 (C9), 71.7 (C2), 52.5 (Me), 34.2 (C3); **LRMS** m/z (ESI+) 227.07 (100%, [M+Na]⁺); **HRMS** m/z (ESI+) C₁₂H₁₂NaO₃ Requires: 227.0684, Found: 227.0688 ([M+Na]⁺).

(66) Methyl 2,5-dihydrobenzo[b]oxepine-9-carboxylate

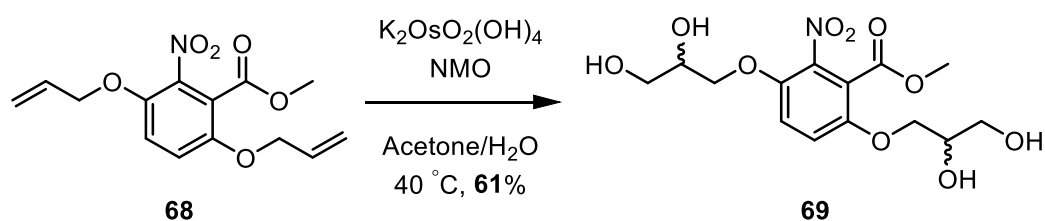
A flask containing methyl 3-allyl-2-(allyloxy)benzoate (**64**) (6 mg, 2.5×10^{-2} mmol) was charged with Grubbs 2nd generation catalyst (2 mg, 3×10^{-3} mmol) and dry toluene (2.6 mL). The flask was heated at 80 °C for 1 h whilst being purged with Ar (_g). The solvent was removed under reduced pressure and the crude mixture was purified by chromatography (SiO₂, EtOAc/Hexane, 1:19) to give the title compound as a clear oil (5 mg, 99%). **IR** ν_{max} cm⁻¹ 3024 w, 2950 w, 2860 w, 1727 s, 1598 w, 1468 s, 1433 s; **¹H-NMR** (400 MHz, CDCl₃) δ_{H} 7.64 (dd, $J = 7.7, 1.8$ Hz, 1H, C8-H), 7.27 – 7.24 (m, 1H, C6-H), 7.05 (t, $J = 7.7$ Hz, 1H, C7-H), 5.84 (dt, $J = 11.5, 5.3, 2.4$ Hz, 1H, C4-H), 5.52 – 5.43 (m, 1H, C3-H), 4.73 – 4.69 (m, 2H, C2-H₂), 3.90 (s, 3H, Me), 3.49 (dd, $J = 5.3, 2.4$ Hz, 2H, C5-H₂); **¹³C-NMR** (101 MHz, CDCl₃) δ_{C} 166.9 (C=O₂Me), 157.8 (C9a), 139.1 (C5a), 132.4 (C6), 129.3 (C8), 127.7 (C3), 125.14 (C4), 125.10 (C9), 123.8 (C7), 71.2 (C2), 52.3 (Me), 31.5 (C5); **LRMS** m/z (ESI⁺) 227.07 (100%, [M+Na]⁺); **HRMS** m/z (ESI⁺) C₁₂H₁₂NaO₃ Requires: 227.0684, Found: 227.0685 ([M+Na]⁺).

(67) Methyl 3,6-dihydroxy-2-nitrobenzoate²³

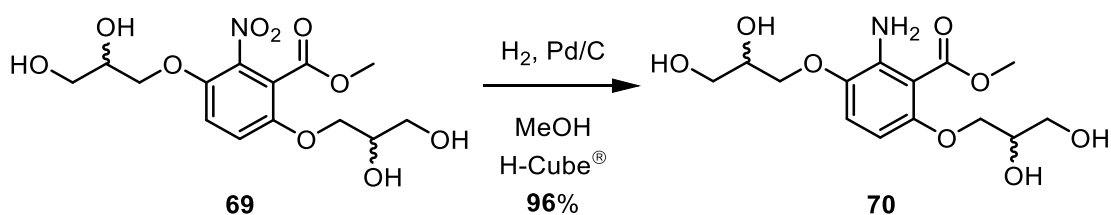
A cooled solution of HNO₃ (1.1 mL, 25.8 mmol) in AcOH (6.8 mL) was added dropwise over 5 min to a stirred solution of 2,5-dihydroxybenzoate (**7**) (2.0 g, 11.8 mmol) in AcOH (14.4 mL) and Ac₂O (7.41 mL) at 0 °C. The reaction was warmed to room temperature, stirred for 30 min and neutralised with NaHCO₃ (aq.) (250 mL). The resulting slurry was then extracted with ether (3 × 150 mL) dried (MgSO₄) and the solvent removed under reduced pressure to afford an orange oil. The crude oil was purified by column chromatography (SiO₂, 1:9 EtOAc/hexane, *R_f* = 0.08) to give an orange solid. Recrystallization (CH₂Cl₂/hexane) gave the title compound as dark orange crystals (300 mg, 12%). **M.P** 125 – 127 °C; **IR** V_{max} cm⁻¹ 3251 br, 2961 w, 1685 s, 1628 w, 1592 w, 1538 s, 1442 s; **¹H-NMR** (400 MHz, CDCl₃) δ_H 8.89 (d, 2H, OH), 7.21 (s, 2H, C3-H, C4-H), 3.90 (s, 3H, Me); **¹³C-NMR** (101 MHz, CDCl₃) δ_C 167.5 (C=O₂Me), 153.6 (C6), 146.7 (C3), 126.2 (C4), 125.4 (C5), 107.7 (C1), 53.5 (Me), C2 gave no resonance signal in ¹³C-NMR, ¹H-¹³C HSQC displayed coupling between C4 and C2; **LRMS** *m/z* (ESI+) 183.09 (100%, [M-MeOH]⁺), 213.72 (10%, [M]⁺). Data were in accordance with the literature.²³

(68) Methyl 3,6-bis(allyloxy)-2-nitrobenzoate

A flask containing methyl 3,6-dihydroxy-2-nitrobenzoate (**67**) (300 mg, 1.41 mmol), K_2CO_3 (428 mg, 3.1 mmol) and TBAI (284 mg, 0.77 mmol) was charged with acetone (10 mL) and the mixture was stirred at room temperature for 10 min. Allyl bromide (0.27 mL, 3.1 mmol) was added dropwise over 5 min and the reaction mixture was heated under reflux for 4 h. The flask was cooled, the solvent removed under reduced pressure and the flask was charged with H_2O (10 mL). The aqueous mixture was extracted with EtOAc (3×30 mL), the combined organic extracts were washed with brine (20 mL) and dried ($MgSO_4$). Removal of the solvent under reduced pressure afforded a crude oil that was purified by chromatography (SiO_2 , EtOAc/hexane 1:9, $R_f = 0.33$) to give the title compound as a yellow oil (200 mg, 48%). **IR** ν_{max} cm^{-1} 2955 w, 1731 s, 1649 w, 1578 w, 1537 s, 1485 s, 1442 s, 1423 s, 1363 s; **1H -NMR** (400 MHz, $CDCl_3$) δ_H 7.12 – 6.98 (m, 2H, C3-H & C4-H), 6.05 – 5.89 (m, 2H, CH=CH₂), 5.44 – 5.34 (m, 2H, CH=CH₂), 5.29 (ddq, $J = 10.6, 3.0, 1.4$ Hz, 2H, CH=CH₂), 4.58 (ddt, $J = 9.4, 5.0, 1.6$ Hz, 4H, O-CH₂), 3.87 (s, 3H, Me); **^{13}C -NMR** (101 MHz, $CDCl_3$) δ_C 163.5 (CO₂Me), 150.0 (C6), 144.6 (C3), 140.2 (C2, weak signal), 132.3 (CH=CH₂), 131.9 (CH=CH₂), 119.0 (C1), 118.7 (CH=CH₂), 118.2 (CH=CH₂), 117.8 (C4), 117.6 (C5), 71.2 (O-CH₂), 70.9 (O-CH₂), 53.3 (Me); **LRMS** m/z (ESI+) 316.08 (100%, $[M+Na]^+$); **HRMS** m/z (ESI+) $C_{14}H_{15}NO_6Na$ Requires: 316.0792, Found: 316.0795 ($[M+Na]^+$).

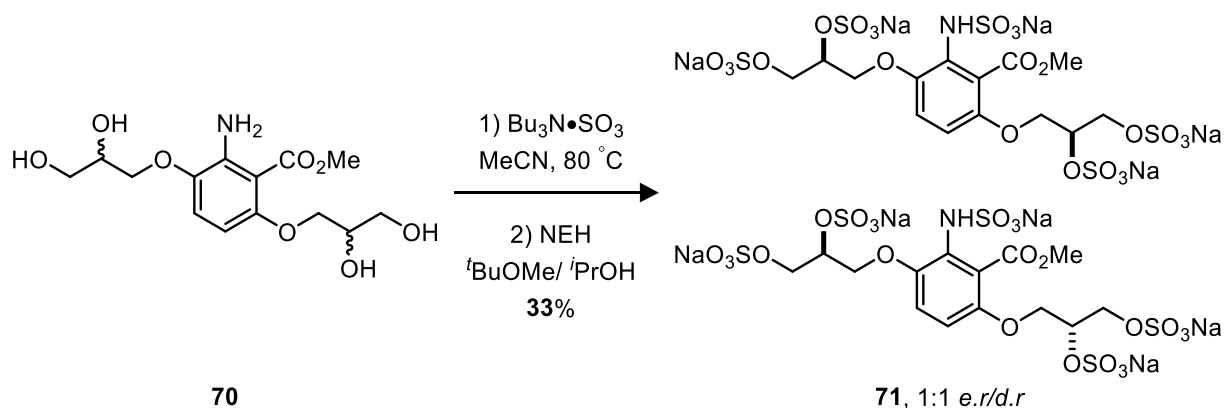
(69) Methyl 3,6-bis(2,3-dihydroxypropoxy)-2-nitrobenzoate

A flask containing methyl 3,6-bis(allyloxy)-2-nitrobenzoate (**68**) (188 mg, 0.64 mmol), was charged with NMO (208 mg, 1.54 mmol) and acetone/ H_2O (9:1, 10 mL), the mixture was stirred at room temperature for 10 min. $\text{K}_2\text{OsO}_2(\text{OH})_4$ (1 mg, 0.0027 mmol) was added and the reaction mixture was heated at 40°C for 12 h. The flask was cooled, satd. Na_2SO_3 (aq.) (10 mL) was added and the aqueous mixture was washed with EtOAc (2×20 mL). The flask was placed in liq. N_2 for 10 min and the water was removed by freeze drying for 12 h to give a light yellow solid. The solid was suspended in EtOH (50 mL) and placed in an ultrasonic bath for 10 min. The mixture was filtered through celite and the filtrate was kept, dried (MgSO_4) and filtered again. Removal of the solvent under reduced pressure afforded the title compound as a yellow oil (140 mg, 61%). **IR** $V_{\text{max}} \text{ cm}^{-1}$ 3340 br s, 2952 w, 2889 w, 1724 s, 1618 w, 1577 w, 1535 s, 1488 s, 1441 s, 1362 s; **$^1\text{H-NMR}$** (400 MHz, $(\text{CD}_3)_2\text{SO}$) δ_{H} 7.56 – 7.33 (m, 2H, C4-H, C5-H), 4.99 (d, $J = 5.1$ Hz, 1H, CH-OH), 4.94 (d, $J = 5.1$ Hz, 1H, CH-OH), 4.67 (dt, $J = 12.6, 5.7$ Hz, 2H, CH₂-OH), 4.16 – 3.92 (m, 4H, Ar-OCH₂), 3.78 (s, 3H, Me), 3.77 – 3.67 (m, 2H, CH-OH), 3.47 – 3.35 (m, 4H, CH₂-OH); **$^{13}\text{C-NMR}$** (101 MHz, $(\text{CD}_3)_2\text{SO}$) δ_{C} 163.3 (CO_2Me), 149.6 (C6), 144.3 (C3), 138.6 (C2), 118.7 (C4), 118.5 (C5), 117.2 (C1), 71.7 (Ar-OCH₂), 71.6 (Ar-OCH₂), 69.8 (CH-OH), 69.7 (CH-OH), 62.4 (CH₂-OH), 62.3 (CH₂-OH), 53.0 (Me); **LRMS** m/z (ESI+) 384.09 (60%, $[\text{M}+\text{Na}]^+$), 413.26 (100%); **HRMS** m/z (ESI+) $\text{C}_{14}\text{H}_{19}\text{NO}_{10}\text{Na}$ Requires: 384.0901, Found: 384.0902 ($[\text{M}+\text{Na}]^+$).

(70) Methyl 2-amino-3,6-bis(2,3-dihydroxypropoxy)benzoate

A solution of methyl 3,6-bis(2,3-dihydroxypropoxy)-2-nitrobenzoate (**69**) (50 mg, 0.14 mmol) in MeOH (20 mL) was placed (1 mL min⁻¹) through a Thales Nano H-Cube mini[®] using a Pd/C cartridge at 30 °C (10 – 15 bar H₂). The solution was recirculated for 80 min with monitoring (TLC, EtOAc/MeOH, 9:1, *R_f* = 0.45). The solvent was removed under reduced pressure and the crude oil was purified by chromatography (SiO₂, EtOAc/MeOH, 9:1) to afford the title compound as a light brown oil (44 mg, 96%). **IR** ν_{max} cm⁻¹ 3453 s, 3343 s, 3244 br s, 2929 s, 2878 s, 1683 s, 1615 s, 1591 s, 1566 s, 1480 s, 1447 s, 1437 s; **¹H-NMR** (400 MHz, (CD₃)₂SO) δ_{H} 6.80 (obs. d, *J* = 8.8 Hz, 1H, C4-H), 6.12 (obs. d, *J* = 8.8 Hz, 1H, C5-H), 5.53 (br s, 2H, C2-NH₂), 5.06 (d, *J* = 5.1 Hz, 1H, CH-OH), 4.78 (d, *J* = 5.1 Hz, 1H, CH-OH), 4.67 (t, *J* = 5.7 Hz, 1H, CH₂-OH), 4.56 (t, *J* = 5.7 Hz, 1H, CH₂-OH), 3.97 – 3.88 (m, 1H, CH-OH), 3.86 – 3.67 (m, 8H, Me, Ar-OCH₂ & CH-OH), 3.51 – 3.36 (m, 4H, CH₂-OH); **¹³C-NMR** (101 MHz, (CD₃)₂SO) δ_{C} 167.7 (C=O₂Me), 152.2 (C2), 140.3 (C3), 139.5 (C6), 114.4 (C4), 105.2 (C1), 98.8 (C5), 71.1 (CH-OH), 70.4 (CH-OH), 70.0 (2C, Ar-OCH₂), 62.8 (CH₂-OH), 62.5 (CH₂-OH), 51.6 (Me); **LRMS** *m/z* (ESI+) 354.10 (100%, [M+Na]⁺); **HRMS** *m/z* (ESI+) C₁₄H₂₁NO₈Na Requires: 354.1159, Found: 354.1162 ([M+Na]⁺).

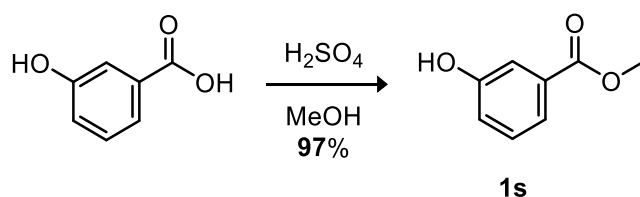
(**71**) Sodium 3-(4-(2,3-bis(sulfonatooxy)propoxy)-2-(methoxycarbonyl)-3-(sulfonatoamino)phenoxy)propane-1,2-diyl bis(sulfate)



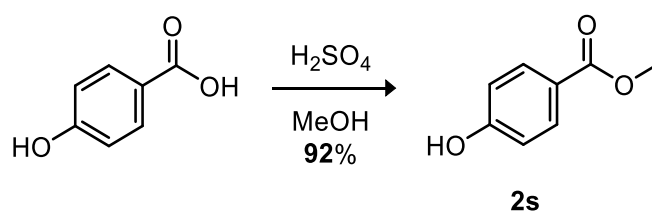
A flask containing methyl 4-amino-2,5-bis(2,3-dihydroxypropoxy)benzoate (**70**) (12 mg, 0.036 mmol) was charged with $\text{Bu}_3\text{N}\cdot\text{SO}_3$ (96 mg, 0.36 mmol) and sealed with Ar. MeCN (1 mL) was added and the reaction mixture was heated at 80 °C for 12 h. The flask was cooled and the solvent removed under reduced pressure to give an oil. The crude oil was placed on a silica plug and eluted with EtOAc/MeOH (9:1) to give a clear oil. The oil was dissolved in *i*PrOH (1 mL) and transferred to a flask containing *t*BuOMe (7 mL). With vigorous stirring a solution of NEH (1.0 mL, 1.0 M) in *t*BuOMe/*i*PrOH (1:7) was added dropwise over 2 min and the reaction mixture was stirred at room temperature for 72 h. The precipitate was collected, washed with *i*PrOH (2 × 10 mL) and dried under vacuum. Recrystallization from $\text{H}_2\text{O}/i\text{PrOH}$ afforded the title compound as a white solid (10 mg, 33%). **IR** $V_{\text{max}} \text{ cm}^{-1}$ 3472 br s, 2492 w, 1622 br s, 1437 s, 1356 s, 1220 s; **¹H-NMR** (500 MHz, D_2O) δ_{H} 7.40 (s, 2H), 7.09 (obs. d, $J = 8.8$ Hz, 1H), 6.50 (obs. d, $J = 8.9$ Hz, 1H), 5.03 – 4.82 (m, 4H), 4.60 – 4.13 (m, 16H), 4.03 (s, 3H), 3.96 (s, 3H); **¹³C-NMR** (126 MHz, D_2O) δ_{C} 168.2, 163.1, 149.2, 141.6, 141.2, 138.7, 124.0, 116.7, 113.8, 102.6, 75.7, 75.3, 75.2, 75.0, 73.8, 68.2, 67.9, 67.8, 67.5, 66.7, 66.6, 66.5, 53.3, 52.7; **LRMS** m/z (ESI+) 657.14 (100%), 863.81 (5%, $[\text{M}+\text{Na}]^+$); **HRMS** m/z (ESI+) $\text{C}_{14}\text{H}_{16}\text{NNa}_6\text{O}_{23}\text{S}_5$ Requires: 863.8097, Found: 863.8114.

Supplementary Compound Characterisation

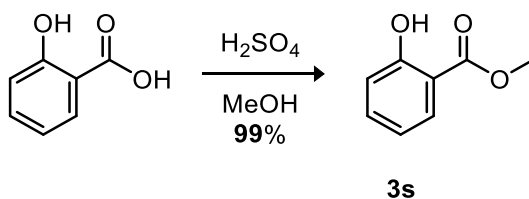
(**1s**) Methyl 3-hydroxybenzoate²⁴



Following general procedure **A**: 3-hydroxybenzoic acid (1.38g, 10.0 mmol) in MeOH was charged with conc. H₂SO₄ and heated under reflux for 7 h with monitoring (EtOAc/hexane 1:3, *R_f* = 0.41). A white solid was afforded after work up, recrystallization (CH₂Cl₂/hexane) yielded the title compound as large white crystals (1.48 g, 97%). **M.P** 85 – 86 °C; **IR** *V*_{max} cm⁻¹ 3385 br (O-H), 2953 w (C-H), 1695 m (C=O), 1454 m (C-C), 1292 s (C-O); **¹H-NMR** (400 MHz, (CD₃)₂CO) δ_H 8.66 (s, 1H, C3-OH), 7.49 (dd, *J* = 8.0, 1.5 Hz, 2H, C6-H and C2-H stack), 7.33 (app. t, *J* = 8.0 Hz, 1H, C5-H), 7.12 – 7.07 (m, 1H, C4-H), 3.86 (s, 3H, Me); **¹³C-NMR** (101 MHz, (CD₃)₂CO) δ_C 167.1 (CO₂Me), 158.3 (C3), 132.5 (C1), 130.5 (C5), 121.3 (C2), 120.9 (C4), 116.7 (C6), 52.3 (Me); **LRMS** *m/z* (ESI+) 152.0 (95%, [M]⁺), 121.0 (100%, [M-CH₃OH]⁺), 93.0 (95%, [C₆H₅OH]⁺). Data were in accordance with the literature.²⁴

(2s) Methyl 4-hydroxybenzoate²⁵

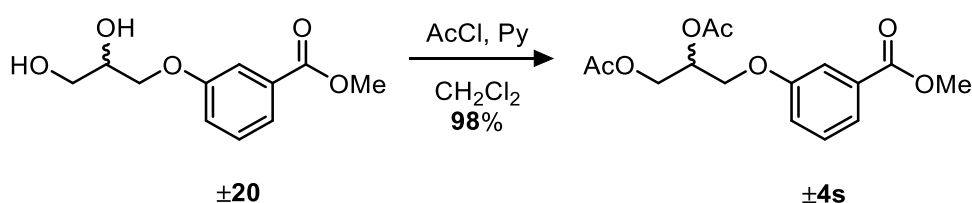
Following general procedure **A**: 4-hydroxybenzoic acid (1.38g, 10.0 mmol) in MeOH was charged with conc. H₂SO₄ and heated under reflux for 10 h with monitoring (EtOAc/Hexane 1:3, *R_f* = 0.34). A white solid was afforded after work up, recrystallization (CH₂Cl₂/hexane) yielded the title compound as large white crystals (1.40 g, 92%). **M.P** 114 – 115 °C; **R** V_{max} cm⁻¹ 3287 br (O-H), 2964 w, 1683 s (C=O), 1616 w, 1502 s, 1436 s; **¹H-NMR** (400 MHz, CDCl₃) δ_H 7.95 (d, *J* = 8.8 Hz, 2H, C3-H), 6.88 (d, *J* = 8.8 Hz, 2H, C2-H), 3.90 (s, 3H, Me); **¹³C-NMR** (101 MHz, CDCl₃) δ_C 167.5 (C=O), 160.3 (C4), 132.1 (C3), 122.5 (C1), 115.4 (C2), 52.2 (Me); **LRMS** *m/z* (ESI+) 152.04 (60%, [M]⁺), 121.0 (100%, [M-CH₃OH]⁺); **HRMS** *m/z* (ESI+) C₈H₈O₃ Requires: 152.0473, Found: 152.0472 ([M]⁺). Data were in accordance with the literature.²⁵

(3s) Methyl salicylate²⁶

Following general procedure **A**: salicylic acid (1.38 g, 10.0 mmol) in MeOH was charged with conc. H₂SO₄ and heated under reflux for 21 h with monitoring (EtOAc/hexane 1:3, *R_f* = 0.85). The title compound was afforded as a golden oil (1.50 g, 99%). **IR** V_{max} cm⁻¹ 3184 w (O-H), 2955 w, 1674 s (C=O), 1328 m, 1251 m; **¹H-NMR** (400 MHz,

CDCl₃) δ_{H} 10.77 (s, 1H, C2-OH), 7.80 (dd, J = 8.2, 1.3 Hz, 1H, C6-H), 7.47 – 7.37 (m, 1H, C4-H), 6.96 (dd, J = 8.2, 1.3 Hz, 1H, C3-H), 6.85 (ddd, J = 8.2, 7.1, 1.3 Hz, 1H, C5-H), 3.91 (s, 3H, Me); **¹³C-NMR** (101 MHz, CDCl₃) δ_{C} 170.5 (CO₂Me), 161.6 (C2), 135.6 (C4), 129.9 (C6), 119.1 (C5), 117.5 (C3), 112.3 (C1), 52.2 (Me); **LRMS** m/z (ESI+) 152.0 (50%, [M]⁺), 120.0 (100%, [M-CH₃OH]⁺), 92.1 (100%, [C₇H₈]⁺). Data were in accordance with the literature.²⁶

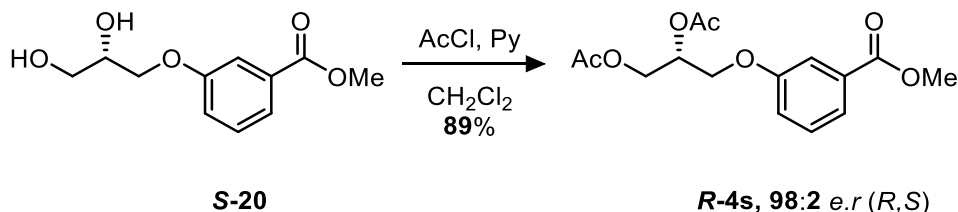
(±4s) Methyl (±)-3-(2,3-di(acetoxy)propoxy)benzoate



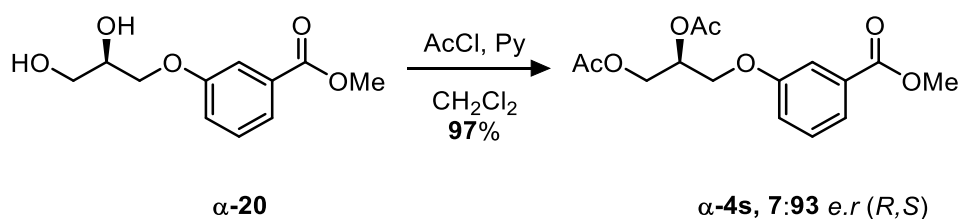
Following general procedure **G**: methyl (±)-3-(2,3-dihydroxypropoxy)benzoate (**±20**) (50 mg, 0.22 mmol) was charged with pyridine (70.8 μL , 0.88 mmol) and CH₂Cl₂ (4.0 mL). AcCl (62.7 μL , 0.88 mmol) was added dropwise. The final product was purified by chromatography (SiO₂, EtOAc/Hexane 1:1, R_f = 0.55) yielding the title compound as a clear oil (67 mg, 98%). **IR** ν_{max} cm⁻¹ 2955 w, 1740 s (C=O), 1720 s (C=O), 1586 w, 1445 w; **¹H-NMR** (400 MHz, CDCl₃) δ_{H} 7.65 (ddd, J = 7.7, 1.5, 1.0 Hz, 1H, C6-H), 7.55 (dd, J = 2.7, 1.5 Hz, 1H, C2-H), 7.34 (dd, J = 8.3, 7.7 Hz, 1H, C5-H), 7.10 (ddd, J = 8.3, 2.7, 1.0 Hz, 1H, C4-H), 5.38 (dtd, J = 5.9, 5.0, 4.0 Hz, 1H, CH-OAc), 4.43 (dd, J = 12.0, 4.0 Hz, 1H, CH₂-OAc), 4.28 (dd, J = 12.0, 5.9 Hz, 1H, CH₂-OAc), 4.16 (d, J = 5.0 Hz, 2H, C3-OCH₂), 3.90 (s, 3H, Me), 2.10 (s, 3H, Ac), 2.07 (s, 3H, Ac); **¹³C-NMR** (101 MHz, CDCl₃) δ_{C} 170.7 (Ac), 170.4 (Ac), 166.8 (CO₂Me), 158.3 (C3), 131.6 (C1), 129.6 (C5), 122.8 (C6), 120.1 (C4), 114.8 (C2), 69.7 (CH-OAc), 66.3 (ArO-CH₂), 62.5 (CH₂-OAc), 52.3 (Me), 21.0 (Ac), 20.8 (Ac); **LRMS** m/z (ESI+) 333.10 (100%, [M+Na]⁺); **HRMS** m/z (ESI+) C₁₅H₁₈O₇Na Requires: 333.0950, Found:

333.0951 ($[M+Na]^+$); **cHPLC** R_{t1} = 41.52 min (*R*), area = 50.15%; R_{t2} = 45.97 min (*S*), area = 49.85%. (Phenomenex® Cellulose-1, MeCN/H₂O, 3:7, 1 mL min⁻¹, 30 °C).

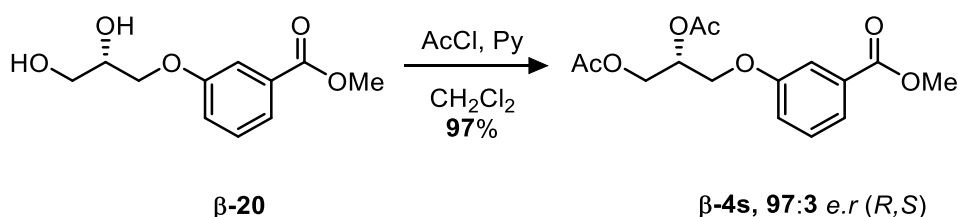
(***R*-4s**) Methyl (*R*)-3-(2,3-di(acetoxy)propoxy)benzoate



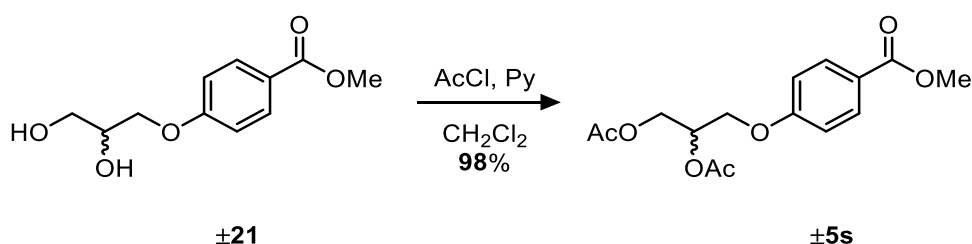
Following general procedure **G**: Methyl (*S*)-3-(2,3-dihydroxypropoxy)benzoate (**S-20**) (50 mg, 0.22 mmol) was charged with pyridine (70.8 μ L, 0.88 mmol) and CH₂Cl₂ (4 mL). AcCl (62.7 μ L, 0.88 mmol) was added dropwise. The final product was purified by chromatography (SiO₂, EtOAc/Hexane 1:1, R_f = 0.55) yielding the title compound as a clear oil (60 mg, 89%). [α]_D²⁵ –36.62 (c. 1.0, CHCl₃, 98:2 *e.r* (*R,S*)); **IR** ν_{max} cm⁻¹ 2954 w, 1742 s (C=O), 1721 s (C=O), 1587 w, 1446 w; **¹H-NMR** (400 MHz, CDCl₃) δ_H 7.66 (ddd, J = 7.7, 1.5, 1.0 Hz, 1H, C6-H), 7.56 (dd, J = 2.7, 1.5 Hz, 1H, C2-H), 7.36 (dd, J = 8.3, 7.7 Hz, 1H, C5-H), 7.11 (ddd, J = 8.3, 2.7, 1.0 Hz, 1H, C4-H), 5.39 (dtd, J = 5.9, 5.0, 4.0 Hz, 1H, CH-OAc), 4.44 (dd, J = 12.0, 4.0 Hz, 1H, CH₂-OAc), 4.29 (dd, J = 12.0, 5.9 Hz, 1H, CH₂-OAc), 4.17 (d, J = 5.0 Hz, 2H, C3-OCH₂), 3.91 (s, 3H, Me), 2.11 (s, 3H, Ac), 2.08 (s, 3H, Ac); **¹³C-NMR** (101 MHz, CDCl₃) δ_C 170.7 (Ac), 170.4 (Ac), 166.9 (CO₂Me), 158.3 (C3), 131.6 (C1), 129.7 (C5), 122.8 (C6), 120.2 (C4), 114.8 (C2), 69.7 (CH-OAc), 66.4 (ArO-CH₂), 62.5 (CH₂-OAc), 52.4 (Me), 21.1 (Ac), 20.9 (Ac); **LRMS** m/z (ESI+) 333.10 (100%, $[M+Na]^+$); **HRMS** m/z (ESI+) C₁₅H₁₈O₇Na Requires: 333.0950, Found: 333.0954 ($[M+Na]^+$); **cHPLC** R_{t1} = 41.49 min, area = 98.06%; R_{t2} = 45.91 min, area = 1.94% (Phenomenex® Cellulose-1, MeCN/H₂O, 3:7, 1 mL min⁻¹, 30 °C).

(α -4s) Methyl (*S*)-3-(2,3-di(acetoxy)propoxy)benzoate

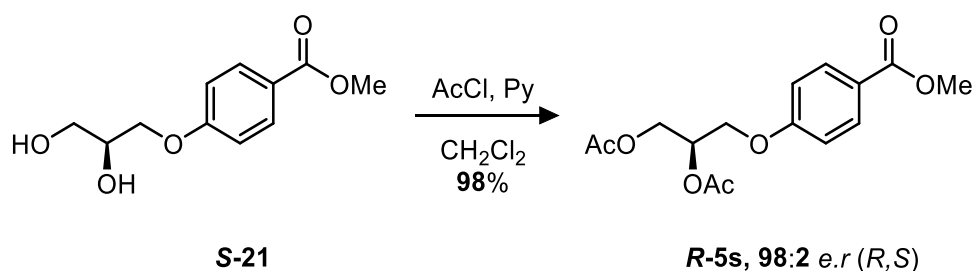
Following general procedure **G**: Methyl (*R*)-3-(2,3-dihydroxypropoxy)benzoate (**α -20**) (50 mg, 0.22 mmol) was charged with pyridine (70.8 μ L, 0.88 mmol) and CH_2Cl_2 (4 mL). AcCl (62.7 μ L, 0.88 mmol) was added dropwise. The final product was purified by chromatography (SiO_2 , EtOAc/Hexane 1:1, R_f = 0.55) yielding the title compound as a clear oil (67 mg, 97%). [α] $_D^{25}$ +29.77 (c. 1.0, CHCl_3 , 7:93 *e.r* (*R,S*)); **IR** ν_{max} cm^{-1} 2955 w, 2923 w, 2854 w, 1742 s (C=O), 1720 w, 1587 w, 1446 w; **$^1\text{H-NMR}$** (400 MHz, CDCl_3) δ_{H} 7.65 (ddd, J = 7.7, 1.5, 1.0 Hz, 1H, C6-H), 7.55 (dd, J = 2.7, 1.5 Hz, 1H, C2-H), 7.34 (dd, J = 8.3, 7.7 Hz, 1H, C5-H), 7.10 (ddd, J = 8.3, 2.7, 1.0 Hz, 1H, C4-H), 5.38 (dtd, J = 5.9, 5.0, 4.0 Hz, 1H, CH-OAc), 4.43 (dd, J = 12.0, 4.0 Hz, 1H, CH₂-OAc), 4.28 (dd, J = 12.0, 5.9 Hz, 1H, CH₂-OAc), 4.16 (d, J = 5.0 Hz, 2H, C3-OCH₂), 3.90 (s, 3H, Me), 2.10 (s, 3H, Ac), 2.07 (s, 3H, Ac); **$^{13}\text{C-NMR}$** (101 MHz, CDCl_3) δ_{C} 170.7 (Ac), 170.4 (Ac), 166.8 (CO₂Me), 158.3 (C3), 131.6 (C1), 129.6 (C5), 122.8 (C6), 120.1 (C4), 114.8 (C2), 69.7 (CH-OAc), 66.3 (ArO-CH₂), 62.5 (CH₂-OAc), 52.3 (Me), 21.0 (Ac), 20.8 (Ac); **LRMS** m/z (ESI+) 333.10 ($[\text{M}+\text{Na}]^+$, 100%); **HRMS** m/z (ESI+) $\text{C}_{15}\text{H}_{18}\text{O}_7\text{Na}$ Requires: 333.0950, Found: 333.0945 ($[\text{M}+\text{Na}]^+$); **cHPLC** R_{t1} = 41.62 min, area = 6.87%; R_{t2} = 46.00 min, area = 93.13%. (Phenomenex® Cellulose-1, MeCN/H₂O, 3:7, 1 mL min⁻¹, 30 °C).

(β -4s) Methyl (*R*)-3-(2,3-di(acetoxy)propoxy)benzoate

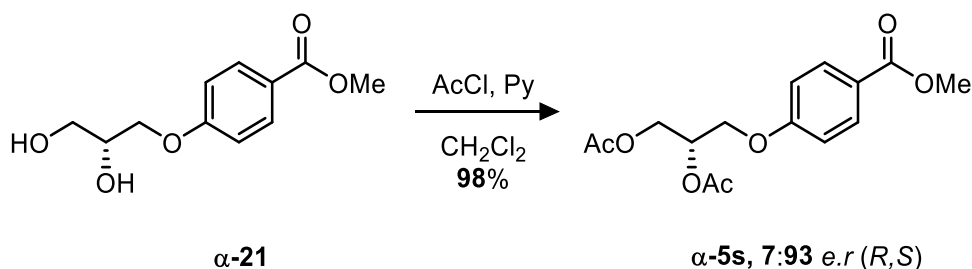
Following general procedure **G**: Methyl (*S*)-3-(2,3-dihydroxypropoxy)benzoate (**β -20**) (50 mg, 0.22 mmol) was charged with pyridine (70.8 μ L, 0.88 mmol) and CH_2Cl_2 (4 mL). AcCl (62.7 μ L, 0.88 mmol) was added dropwise. The final product was purified by chromatography (SiO_2 , EtOAc/Hexane 1:1, $R_f = 0.55$) yielding the title compound as a clear oil (66 mg, 97%). **[α] $_D^{25}$** -31.24 (c. 1.0, CHCl_3 , 97:3 *e.r* (*R,S*)); **IR** V_{max} cm^{-1} 2955 w, 2929 w, 1742 s (C=O), 1721 s (C=O), 1587 w, 1446 w; **$^1\text{H-NMR}$** (400 MHz, CDCl_3) δ_{H} 7.66 (ddd, $J = 7.7, 1.5, 1.0$ Hz, 1H, C6-H), 7.56 (dd, $J = 2.7, 1.5$ Hz, 1H, C2-H), 7.35 (dd, $J = 8.3, 7.7$ Hz, 1H, C5-H), 7.11 (ddd, $J = 8.3, 2.7, 1.0$ Hz, 1H, C4-H), 5.39 (dtd, $J = 5.9, 5.0, 4.0$ Hz, 1H, CH-OAc), 4.44 (dd, $J = 12.0, 4.0$ Hz, 1H, CH₂-OAc), 4.28 (dd, $J = 12.0, 5.9$ Hz, 1H, CH₂-OAc), 4.16 (d, $J = 5.0$ Hz, 2H, C3-OCH₂), 3.91 (s, 3H, Me), 2.10 (s, 3H, Ac), 2.08 (s, 3H, Ac); **$^{13}\text{C-NMR}$** (101 MHz, CDCl_3) δ_{C} 170.7 (Ac), 170.4 (Ac), 166.9 (CO₂Me), 158.3 (C3), 131.6 (C1), 129.6 (C5), 122.8 (C6), 120.1 (C4), 114.8 (C2), 69.7 (CH-OAc), 66.3 (ArO-CH₂), 62.5 (CH₂-OAc), 52.3 (Me), 21.1 (Ac), 20.9 (Ac); **LRMS** m/z (ESI+) 333.09 ($[\text{M}+\text{Na}]^+$, 100%); **HRMS** m/z (ESI+) $\text{C}_{15}\text{H}_{18}\text{O}_7\text{Na}$ Requires: 333.0950, Found: 333.0948 ($[\text{M}+\text{Na}]^+$); **cHPLC** $R_{\text{t}1} = 41.56$ min, area = 97.41%; $R_{\text{t}2} = 46.06$ min, area = 2.59%. (Phenomenex® Cellulose-1, $\text{MeCN/H}_2\text{O}$, 3:7, 1 mL min⁻¹, 30 °C).

(±5s) Methyl (±)-4-(2,3-di(acetoxy)propoxy)benzoate

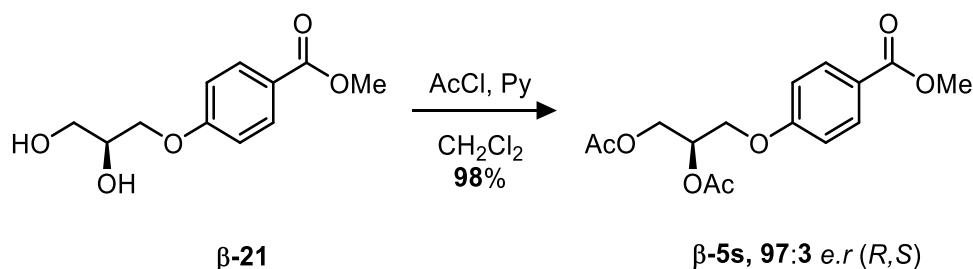
Following general procedure **G**: methyl (±)-4-(2,3-dihydroxypropoxy)benzoate (**±21**) (50 mg, 0.22 mmol) was charged with pyridine (70.8 μL , 0.88 mmol) and CH_2Cl_2 (4.0 mL). AcCl (62.7 μL , 0.88 mmol) was added dropwise. The final product was purified by chromatography (SiO_2 , EtOAc/Hexane 1:1, $R_f = 0.82$) yielding the title compound as a clear oil (67 mg, 98%). **IR** V_{max} cm^{-1} 2954 w, 1741 s (C=O), 1713 s (C=O), 1605 s, 1511 w, 1435 w; **$^1\text{H-NMR}$** (400 MHz, CDCl_3) δ_{H} 7.95 – 7.89 (m, 2H, C3-H), 6.88 – 6.82 (m, 2H, C2-H), 5.31 (dtd, $J = 5.9, 5.1, 4.0$ Hz, 1H, CH-OAc), 4.37 (dd, $J = 12.0, 4.0$ Hz, 1H, CH₂-OAc), 4.22 (dd, $J = 12.0, 5.9$ Hz, 1H, CH₂-OAc), 4.10 (d, $J = 5.1$ Hz, 2H, C4-OCH₂), 3.81 (s, 3H, Me), 2.04 (s, 3H, Ac), 2.01 (s, 3H, Ac); **$^{13}\text{C-NMR}$** (101 MHz, CDCl_3) δ_{C} 170.7 (Ac), 170.3 (Ac), 166.8 (CO₂Me), 162.0 (C4), 131.7 (C3), 123.4 (C1), 114.2 (C2), 69.6 (CH-OAc), 66.2 (O-CH₂), 62.5 (CH₂-OAc), 52.0 (Me), 21.0 (Ac), 20.8 (Ac); **LRMS** m/z (ESI+) 333.10 (100%, $[\text{M}+\text{Na}]^+$); **HRMS** m/z (ESI+) $\text{C}_{15}\text{H}_{18}\text{O}_7\text{Na}$ Requires: 333.0950, Found: 333.0952 ($[\text{M}+\text{Na}]^+$); **chPLC** $R_{t1} = 43.25$ min (*R*), area = 49.9%; $R_{t2} = 47.88$ min (*S*), area = 49.9%. (Phenomenex® Cellulose-1, MeCN/H₂O, 3:7, 1 mL min⁻¹, 30 °C).

(*R*-5s) Methyl (*R*)-4-(2,3-di(acetoxy)propoxy)benzoate

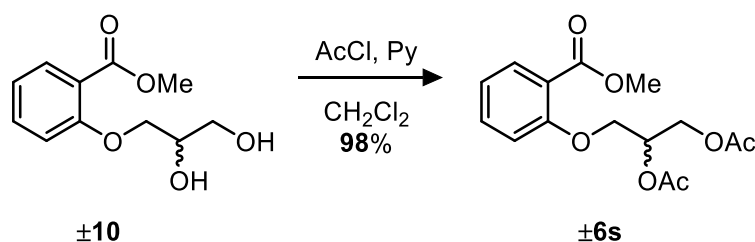
Following general procedure **G**: Methyl (*S*)-4-(2,3-dihydroxypropoxy)benzoate (**S-21**) (50 mg, 0.22 mmol) was charged with pyridine (70.8 μ L, 0.88 mmol) and CH_2Cl_2 (4 mL). AcCl (62.7 μ L, 0.88 mmol) was added dropwise. The final product was purified by chromatography (SiO_2 , EtOAc/Hexane 1:1, $R_f = 0.82$) yielding the title compound as a clear oil (67 mg, 98%). **[α]_D²⁵** -44.66 (c. 1.0, CHCl_3 , 98:2 *e.r* (*R,S*)); **IR** V_{max} cm^{-1} 2953 w (C-H), 1741 s (C=O), 1714 s (C=O), 1606 s, 1581 w, 1511 w, 1436 w, 1371 w, 1280 s, 1217 s; **¹H-NMR** (400 MHz, CDCl_3) δ_{H} 8.02 – 7.96 (m, 2H, C3-H), 6.95 – 6.89 (m, 2H, C2-H), 5.38 (dtd, $J = 5.9, 5.1, 4.0$ Hz, 1H, CH-OAc), 4.44 (dd, $J = 12.0, 4.0$ Hz, 1H, CH₂-OAc), 4.29 (dd, $J = 12.0, 5.9$ Hz, 1H, CH₂-OAc), 4.17 (d, $J = 5.1$ Hz, 2H, C4-OCH₂), 3.88 (s, 3H, Me), 2.10 (s, 3H, Ac), 2.08 (s, 3H, Ac); **¹³C-NMR** (101 MHz, CDCl_3) δ_{C} 170.7 (Ac), 170.4 (Ac), 166.8 (CO_2Me), 162.0 (C4), 131.7 (C3), 123.4 (C1), 114.2 (C2), 69.6 (CH-OAc), 66.2 (O-CH₂), 62.5 (CH₂-OAc), 52.0 (Me), 21.1 (Ac), 20.8 (Ac); **LRMS** m/z (ESI+) 333.10 (100%, $[\text{M}+\text{Na}]^+$); **HRMS** m/z (ESI+) $\text{C}_{15}\text{H}_{18}\text{O}_7\text{Na}$ Requires: 333.0950, Found: 333.0952 ($[\text{M}+\text{Na}]^+$); **cHPLC** $R_{t1} = 43.08$ min, area = 97.92%; $R_{t2} = 47.77$, area = 2.08% (Phenomenex® Cellulose-1, $\text{MeCN/H}_2\text{O}$, 3:7, 1 mL min⁻¹, 30 °C).

(α -5s) Methyl (*S*)-4-(2,3-di(acetoxy)propoxy)benzoate

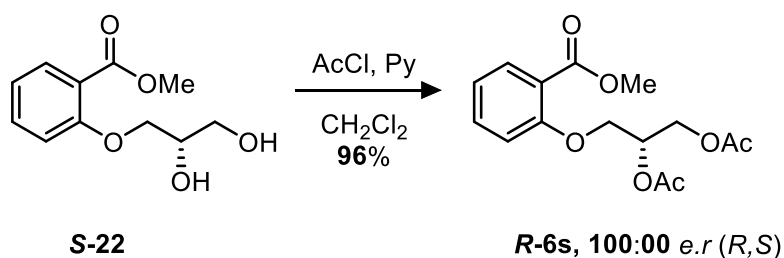
Following general procedure **G**: Methyl (*R*)-4-(2,3-dihydroxypropoxy)benzoate (**α -21**) (50 mg, 0.22 mmol) was charged with pyridine (70.8 μ L, 0.88 mmol) and CH_2Cl_2 (4 mL). AcCl (62.7 μ L, 0.88 mmol) was added dropwise. The final product was purified by chromatography (SiO_2 , EtOAc/Hexane 1:1, R_f = 0.82) yielding the title compound as a clear oil (67 mg, 98%). [α] $_D^{25}$ +23.54 (c. 1.0, CHCl_3 , 7:93 *e.r* (*R,S*)); **IR** ν_{max} cm^{-1} 2954 w, 2924 w, 2851 w, 1741 s (C=O), 1714 s (C=O), 1605 s, 1580 w, 1511 w, 1435 w; **$^1\text{H-NMR}$** (400 MHz, CDCl_3) δ_{H} 8.01 – 7.95 (m, 2H, C3-H), 6.94 – 6.88 (m, 2H, C2-H), 5.37 (dtd, J = 5.9, 5.1, 4.0 Hz, 1H, CH-OAc), 4.43 (dd, J = 12.0, 4.0 Hz, 1H, CH₂-OAc), 4.28 (dd, J = 12.0, 5.9 Hz, 1H, CH₂-OAc), 4.16 (d, J = 5.1 Hz, 2H, C4-OCH₂), 3.87 (s, 3H, Me), 2.10 (s, 3H, Ac), 2.07 (s, 3H, Ac); **$^{13}\text{C-NMR}$** (101 MHz, CDCl_3) δ_{C} 170.7 (Ac), 170.3 (Ac), 166.8 (CO₂Me), 162.0 (C4), 131.7 (C3), 123.4 (C1), 114.2 (C2), 69.6 (CH-OAc), 66.2 (O-CH₂), 62.5 (CH₂-OAc), 52.0 (Me), 21.0 (Ac), 20.8 (Ac); **LRMS** m/z (ESI+) 333.10 ($[\text{M}+\text{Na}]^+$, 100%); **HRMS** m/z (ESI+) $\text{C}_{15}\text{H}_{18}\text{O}_7\text{Na}$ Requires: 333.0950, Found: 333.0949 ($[\text{M}+\text{Na}]^+$); **chPLC** R_{t1} = 43.45 min, area = 7.28%; R_{t2} = 47.98 min, area = 92.72%. (Phenomenex® Cellulose-1, MeCN/H₂O, 3:7, 1 mL min⁻¹, 30 °C).

(β -5s) Methyl (*R*)-4-(2,3-di(acetoxy)propoxy)benzoate

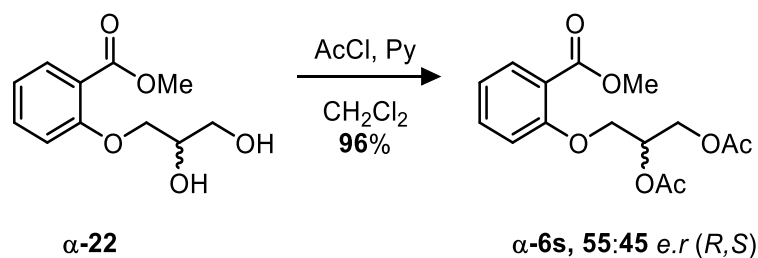
Following general procedure **G**: Methyl (*S*)-4-(2,3-dihydroxypropoxy)benzoate (β -21) (50 mg, 0.22 mmol) was charged with pyridine (70.8 μ L, 0.88 mmol) and CH_2Cl_2 (4 mL). AcCl (62.7 μ L, 0.88 mmol) was added dropwise. The final product was purified by chromatography (SiO_2 , EtOAc/Hexane 1:1, R_f = 0.82) yielding the title compound as a clear oil (67 mg, 98%). **[α]_D²⁵** –26.66 (c. 1.0, CHCl_3 , 97:3 *e.r* (*R,S*)); **IR** V_{max} cm^{-1} 2954 w, 1742 s (C=O), 1715 s (C=O), 1606 s, 1511 w, 1436 w; **¹H-NMR** (400 MHz, CDCl_3) δ_{H} 8.00 – 7.94 (m, 2H, C3-H), 6.93 – 6.88 (m, 2H, C2-H), 5.36 (dtd, J = 5.9, 5.1, 4.0 Hz, 1H, CH-OAc), 4.42 (dd, J = 12.0, 4.0 Hz, 1H, CH₂-OAc), 4.27 (dd, J = 12.0, 5.9 Hz, 1H, CH₂-OAc), 4.15 (d, J = 5.1 Hz, 2H, C4-OCH₂), 3.86 (s, 3H, Me), 2.09 (s, 3H, Ac), 2.06 (s, 3H, Ac); **¹³C-NMR** (101 MHz, CDCl_3) δ_{C} 170.6 (Ac), 170.3 (Ac), 166.7 (CO₂Me), 162.0 (C4), 131.7 (C3), 123.4 (C1), 114.2 (C2), 69.5 (CH-OAc), 66.1 (O-CH₂), 62.4 (CH₂-OAc), 52.0 (Me), 21.0 (Ac), 20.8 (Ac); **LRMS** m/z (ESI+) 333.10 ($[\text{M}+\text{Na}]^+$, 100%); **HRMS** m/z (ESI+) $\text{C}_{15}\text{H}_{18}\text{O}_7\text{Na}$ Requires: 333.0950, Found: 333.0950 ($[\text{M}+\text{Na}]^+$); **CHPLC** R_{t1} = 43.19 min, area = 96.97%; R_{t2} = 47.95 min, area = 3.03%. (Phenomenex[®] Cellulose-1, $\text{MeCN/H}_2\text{O}$, 3:7, 1 mL min⁻¹, 30 °C).

(±6s) Methyl (±)-2-(2,3-di(acetoxy)propoxy)benzoate

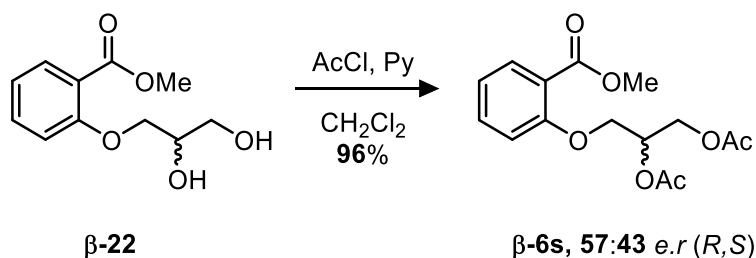
Following general procedure **G**: methyl (±)-2-(2,3-dihydroxypropoxy)benzoate (**±10**) (50 mg, 0.22 mmol) was charged with pyridine (70.8 μ L, 0.88 mmol) and CH₂Cl₂ (4.0 mL). AcCl (62.7 μ L, 0.88 mmol) was added dropwise. The final product was purified by chromatography (SiO₂, EtOAc/Hexane 1:1, R_f = 0.42) yielding the title compound as a clear oil (67 mg, 98%). **IR** V_{\max} cm⁻¹ 2955 w, 1738 s (C=O), 1583 w; **¹H-NMR** (400 MHz, CDCl₃) δ_H 7.80 (dd, J = 7.5, 1.8 Hz, 1H, C6-H), 7.44 (ddd, J = 8.4, 7.5, 1.8 Hz, 1H, C4-H), 7.01 (td, J = 7.5, 1.0 Hz, 1H, C5-H), 6.93 (dd, J = 8.4, 1.0 Hz, 1H, C3-H), 5.40 (dtd, J = 6.1, 5.1, 3.8 Hz, 1H, CH-OAc), 4.49 (dd, J = 12.0, 3.8 Hz, 1H, CH₂-OAc), 4.35 (dd, J = 12.0, 6.1 Hz, 1H, CH₂-OAc), 4.21 – 4.14 (m, 2H, C2-OCH₂), 3.88 (s, 3H, Me), 2.09 (s, 3H, Ac), 2.06 (s, 3H, Ac); **¹³C-NMR** (101 MHz, CDCl₃) δ_C 170.7 (Ac), 170.4 (Ac), 166.8 (CO₂Me), 157.7 (C2), 133.5 (C4), 132.0 (C6), 121.2 (C5), 120.9 (C1), 113.5 (C3), 69.7 (CH-OAc), 67.0 (C2-OCH₂), 62.7 (CH₂-OAc), 52.1 (Me), 21.1 (Ac), 20.9 (Ac); **LRMS** m/z (ESI+) 333.10 (100%, [M+Na]⁺); **HRMS** m/z (ESI+) C₁₅H₁₈O₇Na Requires: 333.0950, Found: 333.0953 ([M+Na]⁺); **chPLC** R_{t1} = 48.44 min (*R*), area = 50.11%; R_{t2} = 51.03 min (*S*), area = 49.89%. (Phenomenex® Cellulose-1, MeCN/H₂O, 1:3, 1 mL min⁻¹, 30 °C).

(*R*-6s) Methyl (*R*)-2-(2,3-di(acetoxy)propoxy)benzoate

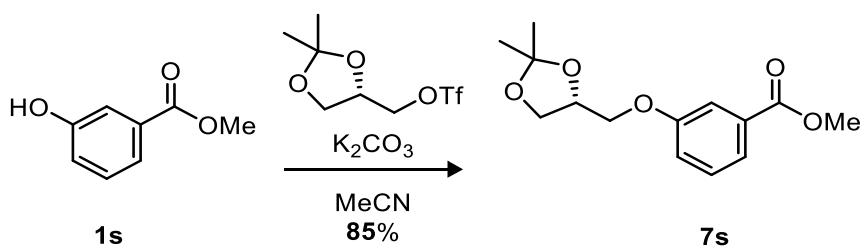
Following general procedure **G**: Methyl (*S*)-2-(2,3-dihydroxypropoxy)benzoate (**S-22**) (50 mg, 0.22 mmol) was charged with pyridine (70.8 μ L, 0.88 mmol) and CH_2Cl_2 (4 mL). AcCl (62.7 μ L, 0.88 mmol) was added dropwise. The final product was purified by chromatography (SiO_2 , EtOAc/Hexane 1:1, $R_f = 0.42$) yielding the title compound as a clear oil (65 mg, 96%). **[α] $_D^{25}$** –24.93 (c. 1.0, CHCl_3 , 100:00 *e.r* (*R,S*)); **IR** V_{max} cm^{-1} 2923 w, 1741 s (C=O), 1602 w, 1493 w, 1454 w; **$^1\text{H-NMR}$** (400 MHz, CDCl_3) δ_{H} 7.81 (dd, $J = 7.5, 1.8$ Hz, 1H, C6-H), 7.45 (ddd, $J = 8.4, 7.5, 1.8$ Hz, 1H, C4-H), 7.02 (td, $J = 7.5, 1.0$ Hz, 1H, C5-H), 6.94 (dd, $J = 8.4, 1.0$ Hz, 1H, C3-H), 5.40 (dtd, $J = 6.1, 5.1, 3.8$ Hz, 1H, CH-OAc), 4.49 (dd, $J = 12.0, 3.8$ Hz, 1H, CH₂-OAc), 4.35 (dd, $J = 12.0, 6.1$ Hz, 1H, CH₂-OAc), 4.21 – 4.14 (m, 2H, C2-OCH₂), 3.89 (s, 3H, Me), 2.11 (s, 3H, Ac), 2.07 (s, 3H, Ac); **$^{13}\text{C-NMR}$** (101 MHz, CDCl_3) δ_{C} 170.8 (Ac), 170.5 (Ac), 166.8 (CO₂Me), 157.7 (C2), 133.6 (C4), 132.1 (C6), 121.3 (C5), 120.9 (C1), 113.6 (C3), 69.7 (CH-OAc), 67.1 (C2-OCH₂), 62.7 (CH₂-OAc), 52.2 (Me), 21.1 (Ac), 20.9 (Ac); **LRMS** m/z (ESI+) 333.10 (100%, $[\text{M}+\text{Na}]^+$); **HRMS** m/z (ESI+) $\text{C}_{15}\text{H}_{18}\text{O}_7\text{Na}$ Requires: 333.0950, Found: 333.0950 ($[\text{M}+\text{Na}]^+$); **chPLC** $R_t = 48.04$ min, area = 100.00%. (Phenomenex® Cellulose-1, $\text{MeCN/H}_2\text{O}$, 1:3, 1 mL min⁻¹, 30 °C).

(α -6s) Methyl (\pm)-2-(2,3-di(acetoxy)propoxy)benzoate

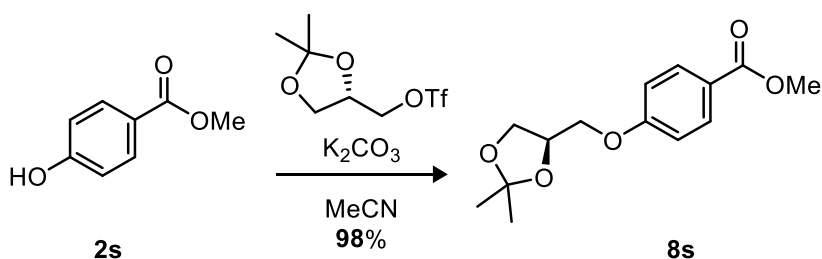
Following general procedure **G**: methyl (\pm)-3-(2,3-dihydroxypropoxy)benzoate (**α -22**) (50 mg, 0.22 mmol) was charged with pyridine (70.8 μ L, 0.88 mmol) and CH_2Cl_2 (4 mL). AcCl (62.7 μ L, 0.88 mmol) was added dropwise. The final product was purified by chromatography (SiO_2 , EtOAc/Hexane 1:1, R_f = 0.55) yielding the title compound as a clear oil (65 mg, 96%). [α]_D²⁵ –11.77 (c. 1.0, CHCl_3 , 55:45 *e.r.* (*R,S*)); **IR** V_{max} cm^{-1} 2955 w, 1737 s (C=O), 1601 w, 1583 w, 1452 w; **$^1\text{H-NMR}$** (400 MHz, CDCl_3) δ_{H} 7.80 (dd, J = 7.5, 1.8 Hz, 1H, C6-H), 7.44 (ddd, J = 8.4, 7.5, 1.8 Hz, 1H, C4-H), 7.01 (td, J = 7.5, 1.0 Hz, 1H, C5-H), 6.93 (dd, J = 8.4, 1.0 Hz, 1H, C3-H), 5.40 (dtd, J = 6.1, 5.1, 3.8 Hz, 1H, CH-OAc), 4.49 (dd, J = 12.0, 3.8 Hz, 1H, CH₂-OAc), 4.35 (dd, J = 12.0, 6.1 Hz, 1H, CH₂-OAc), 4.21 – 4.14 (m, 2H, C2-OCH₂), 3.88 (s, 3H, Me), 2.09 (s, 3H, Ac), 2.06 (s, 3H, Ac); **$^{13}\text{C-NMR}$** (101 MHz, CDCl_3) δ_{C} 170.7 (Ac), 170.4 (Ac), 166.8 (CO_2Me), 157.7 (C2), 133.5 (C4), 132.0 (C6), 121.2 (C5), 120.9 (C1), 113.5 (C3), 69.7 (CH-OAc), 67.0 (C2-OCH₂), 62.7 (CH₂-OAc), 52.1 (Me), 21.0 (Ac), 20.8 (Ac); **LRMS** m/z (ESI+) 333.10 ($[\text{M}+\text{Na}]^+$, 100%); **HRMS** m/z (ESI+) $\text{C}_{15}\text{H}_{18}\text{O}_7\text{Na}$ Requires: 333.0950, Found: 333.0954 ($[\text{M}+\text{Na}]^+$); **cHPLC** R_{t1} = 48.33 min, area = 54.55%; R_{t2} = 50.91 min, area = 45.45%. (Phenomenex® Cellulose-1, $\text{MeCN/H}_2\text{O}$, 1:3, 1 mL min^{–1}, 30 °C).

(β -6s) Methyl (\pm)-2-(2,3-di(acetoxy)propoxy)benzoate

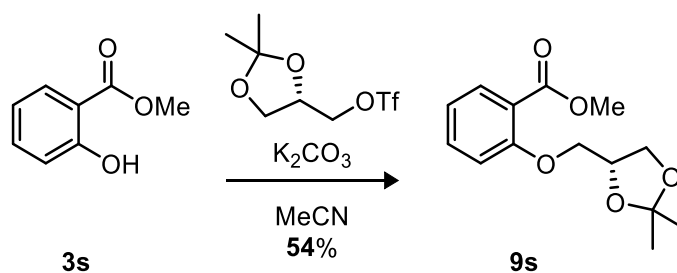
Following general procedure **G**: methyl (\pm)-3-(2,3-dihydroxypropoxy)benzoate (**β -22**) (50 mg, 0.22 mmol) was charged with pyridine (70.8 μ L, 0.88 mmol) and CH_2Cl_2 (4 mL). AcCl (62.7 μ L, 0.88 mmol) was added dropwise. The final product was purified by chromatography (SiO_2 , EtOAc/Hexane 1:1, $R_f = 0.55$) yielding the title compound as a clear oil (64 mg, 96%). [α]_D²⁵ -10.42 (c. 1.0, CHCl_3 , 57:43 *e.r.* (*R,S*)). **IR** V_{max} cm^{-1} 2953 w, 2923 w, 2853 w, 1736 s (C=O), 1601 w, 1583 w, 1453 w; **$^1\text{H-NMR}$** (400 MHz, CDCl_3) δ_{H} 7.81 (dd, $J = 7.5, 1.8$ Hz, 1H, C6-H), 7.45 (ddd, $J = 8.4, 7.5, 1.8$ Hz, 1H, C4-H), 7.02 (td, $J = 7.5, 1.0$ Hz, 1H, C5-H), 6.93 (dd, $J = 8.4, 1.0$ Hz, 1H, C3-H), 5.41 (dtd, $J = 6.1, 5.1, 3.8$ Hz, 1H, CH-OAc), 4.50 (dd, $J = 12.0, 3.8$ Hz, 1H, CH₂-OAc), 4.36 (dd, $J = 12.0, 6.1$ Hz, 1H, CH₂-OAc), 4.22 – 4.15 (m, 2H, C2-OCH₂), 3.88 (s, 3H, Me), 2.10 (s, 3H, Ac), 2.07 (s, 3H, Ac); **$^{13}\text{C-NMR}$** (101 MHz, CDCl_3) δ_{C} 170.7 (Ac), 170.4 (Ac), 166.8 (CO_2Me), 157.7 (C2), 133.6 (C4), 132.0 (C6), 121.2 (C5), 120.9 (C1), 113.5 (C3), 69.7 (CH-OAc), 67.1 (C2-OCH₂), 62.7 (CH₂-OAc), 52.2 (Me), 21.1 (Ac), 20.9 (Ac); **LRMS** m/z (ESI⁺) 333.10 ($[\text{M}+\text{Na}]^+$, 100%); **HRMS** m/z (ESI⁺) $\text{C}_{15}\text{H}_{18}\text{O}_7\text{Na}$ Requires: 333.0950, Found: 333.0954 ($[\text{M}+\text{Na}]^+$); **cHPLC** $R_{t1} = 48.30$ min, area = 56.83%; $R_{t2} = 50.88$ min, area = 43.17%. (Phenomenex[®] Cellulose-1, MeCN/ H_2O , 1:3, 1 mL min⁻¹, 30 °C).

(7s) Methyl (*R*)-3-((2,2-dimethyl-1,3-dioxolan-4-yl)methoxy)benzoate

Following general procedure **E**: using methyl 3-hydroxybenzoate (**1s**) (152 mg, 1.0 mmol), K_2CO_3 (264 mg, 2.0 mmol) and (*S*)-(2,2-dimethyl-1,3-dioxolan-4-yl)methyl trifluoromethanesulfonate (390 mg, 1.5 mmol). The reaction mixture was heated at 70 °C for 12 h and monitored (EtOAc/hexane 1:9, $R_f = 0.47$). The crude oil was purified by chromatography (SiO_2 , EtOAc/hexane, 1:9) to yield the title compound as a clear oil (225 mg, 85%). **[α]_D²⁵** –7.21 (c. 1.0, CHCl_3 *er* 98:2 (*R,S*)); **IR** V_{max} cm^{-1} 2988 w, 2951 w, 1720 s (C=O), 1587 w, 1488 w, 1445 w; **¹H-NMR** (400 MHz, CDCl_3) δ_{H} 7.62 (dt, $J = 8.0, 1.3$ Hz, 1H, C6-H), 7.54 (dd, $J = 2.7, 1.3$ Hz, 1H, C2-H), 7.31 (t, $J = 8.0$ Hz, 1H, C5-H), 7.09 (ddd, $J = 8.0, 2.7, 1.3$ Hz, 1H, C4-H), 4.46 (p, $J = 5.7$ Hz, 1H, CH-OC(CH₃)₂), 4.14 (dd, $J = 8.5, 6.4$ Hz, 1H, CH₂-OC(CH₃)₂), 4.06 (dd, $J = 9.5, 5.7$ Hz, 1H, C3-OCH₂), 3.96 (dd, $J = 9.5, 5.7$ Hz, 1H, C3-OCH₂), 3.91 – 3.83 (m, 4H, Me & CH₂-OC(CH₃)₂), 1.44 (s, 3H, C(CH₃)₂), 1.38 (s, 3H, C(CH₃)₂); **¹³C-NMR** (101 MHz, CDCl_3) δ_{C} 166.9 (CO₂Me), 158.5 (C3), 131.5 (C1), 129.5 (C5), 122.4 (C6), 120.0 (C4), 114.6 (C2), 109.9 (C(CH₃)₂), 74.0 (CH-OC(CH₃)₂), 69.0 (C3-OCH₂), 66.7 (CH₂-OC(CH₃)₂), 52.2 (Me), 26.8 (C(CH₃)₂), 25.4 (C(CH₃)₂); **LRMS** m/z (ESI+) 289.11 (100%, [M+Na]⁺); **HRMS** m/z (ESI+) C₁₄H₁₈O₅Na Requires: 289.1052, Found: 289.1053 ([M+Na]⁺).

(8s) Methyl (*R*)-4-((2,2-dimethyl-1,3-dioxolan-4-yl)methoxy)benzoate

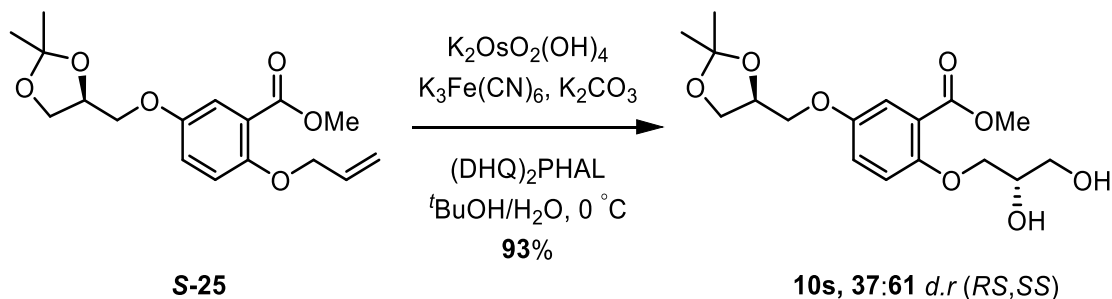
Following general procedure **E**: using methyl 4-hydroxybenzoate (**2s**) (152 mg, 1.0 mmol), K_2CO_3 (264 mg, 2.0 mmol) and (*S*)-(2,2-dimethyl-1,3-dioxolan-4-yl)methyl trifluoromethanesulfonate (390 mg, 1.5 mmol). The reaction mixture was heated at 70 °C for 12 h and monitored (EtOAc/hexane 1:9, R_f = 0.44). The crude oil was purified by chromatography (SiO_2 , EtOAc/hexane, 1:9) to yield the title compound as a clear oil (260 mg, 98%). **[α]_D²⁵** −7.21 (c. 1.0, $CHCl_3$ *er* 98:2 (*R,S*)); **IR** V_{max} cm^{-1} 2987 w, 2951 w, 1713 s (C=O), 1605 s, 1580 w, 1511 w, 1435 w; **¹H-NMR** (400 MHz, $CDCl_3$) δ_H 8.01 – 7.93 (m, 2H, C2-H), 6.95 – 6.87 (m, 2H, C3-H), 4.47 (p, J = 5.6 Hz, 1H, CH-OC(CH₃)₂), 4.16 (dd, J = 8.5, 6.4 Hz, 1H, CH₂-OC(CH₃)₂), 4.08 (dd, J = 9.6, 5.6 Hz, 1H, C4-OCH₂), 3.98 (dd, J = 9.6, 5.6 Hz, 1H, C4-OCH₂), 3.89 (dd, J = 8.5, 5.6 Hz, 1H, CH₂-OC(CH₃)₂), 3.86 (s, 3H, Me), 1.45 (s, 3H, C(CH₃)₂), 1.39 (s, 3H, C(CH₃)₂); **¹³C-NMR** (101 MHz, $CDCl_3$) δ_C 166.8 (CO₂Me), 162.3 (C4), 131.6 (C2), 123.1 (C1), 114.2 (C3), 110.0 (C(CH₃)₂), 73.9 (CH-OC(CH₃)₂), 68.9 (C4-OCH₂), 66.7 (CH₂-OC(CH₃)₂), 52.0 (Me), 26.8 (C(CH₃)₂), 25.4 (C(CH₃)₂); **LRMS** m/z (ESI+) 289.11 (100%, [M+Na]⁺); **HRMS** m/z (ESI+) C₁₄H₁₈O₅Na Requires: 289.1052, Found: 289.1049 ([M+Na]⁺).

(9s) Methyl (*R*)-2-((2,2-dimethyl-1,3-dioxolan-4-yl)methoxy)benzoate

Following general procedure **E**: using methyl salicylate (**3s**) (152 mg, 1.0 mmol), K_2CO_3 (264 mg, 2.0 mmol) and (*S*)-(2,2-dimethyl-1,3-dioxolan-4-yl)methyl trifluoromethanesulfonate (390 mg, 1.5 mmol). The reaction mixture was heated at 70 °C for 12 h and monitored (EtOAc/hexane 1:9, R_f = 0.42). The crude oil was purified by chromatography (SiO_2 , EtOAc/hexane, 1:9) to yield the title compound as a clear oil (144 mg, 54%). **[α]_D²⁵** –41.89 (c. 1.0, CHCl_3 , *er* 100:0 (*R,S*)); **IR** V_{max} cm^{-1} 2950 w, 2986 w, 1727 s (C=O), 1600 m, 1583 w, 1491 w, 1450 w; **¹H-NMR** (400 MHz, CDCl_3) δ_{H} 7.78 (dd, J = 7.6, 1.8 Hz, 1H, C6-H), 7.43 (ddd, J = 8.4, 7.6, 1.8 Hz, 1H, C5-H), 7.07 – 6.91 (m, 2H, C4-H & C3-H), 4.55 – 4.41 (m, 1H, CH-OC(CH₃)₂), 4.22 – 4.10 (m, 2H, C2-OCH₂ & CH₂-OC(CH₃)₂), 4.01 (ddd, J = 16.2, 9.0, 6.2 Hz, 2H, C2-OCH₂ & CH₂-OC(CH₃)₂), 3.86 (s, 3H, Me), 1.44 (s, 3H, C(CH₃)₂), 1.39 (s, 3H, C(CH₃)₂); **¹³C-NMR** (101 MHz, CDCl_3) δ_{C} 166.7 (CO₂Me), 158.1 (C2), 133.5 (C5), 131.8 (C6), 120.9 (C4), 120.7 (C1), 113.8 (C3), 109.7 (C(CH₃)₂), 73.9 (CH-OC(CH₃)₂), 69.4 (C2-OCH₂), 67.1 (CH₂-OC(CH₃)₂), 52.0 (Me), 26.1 (C(CH₃)₂), 25.5 (C(CH₃)₂); **LRMS** m/z (ESI+) 289.11 (100%, [M+Na]⁺); **HRMS** m/z (ESI+) C₁₄H₁₈O₅Na Requires: 289.1052, Found: 289.1055 ([M+Na]⁺).

Supplementary Compounds 10s-18s (Table 6, Entries 1-3)

(10s) Methyl 2-((*S*)-2,3-dihydroxypropoxy)-5-(((*S*)-2,2-dimethyl-1,3-dioxolan-4-yl)methoxy)benzoate

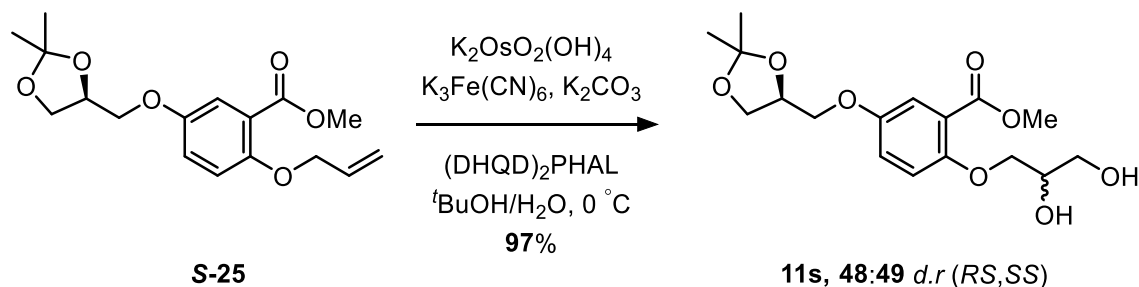


Following general procedure **D**: using stock solutions: **I** (1 mL, 1.5 mmol), **II** (1 mL, 1.5 mmol), **III** (0.5 mL, 1.0 μmol) and **IV** (2.5 mL, 10.0 μmol). Methyl (*S*)-2-(allyloxy)-5-((2,2-dimethyl-1,3-dioxolan-4-yl)methoxy)benzoate (**S-25**) (173 mg, 0.50 mmol) was added and the reaction mixture was stirred at 0 °C for 21 h with monitoring (EtOAc/hexane 1:1, R_f = 0.09). Afforded the title compound as a clear oil (170 mg, 93%). $[\alpha]_D^{25} +30.12$ (c. 1.0, MeOH, 1:61:36:2 *e.r./d.r* (2*R*5*R*, 2*S*5*S*, 2*R*5*S*, 2*S*5*R*)); **IR** $\text{V}_{\text{max}} \text{ cm}^{-1}$ 3436 br s, (O-H), 2988 w, 2933 w, 2874 w, 1710 s (C=O), 1609 s, 1499 w, 1438 w; **¹H-NMR** (400 MHz, CDCl_3) δ_c 7.41 (d, J = 3.2 Hz, 1H C6-H), 7.07 (dd, J = 9.1, 3.2 Hz, 1H, C4-H), 6.93 (d, J = 9.1 Hz, 1H, C3-H), 4.46 (p, J = 5.7 Hz, 1H, CH-OC(CH₃)₂), 4.24 (dd, J = 9.2, 2.6 Hz, 1H, C2-OCH₂), 4.16 (dd, J = 8.5, 6.4 Hz, 1H, CH₂-OC(CH₃)₂), 4.10 – 3.98 (m, 3H, C2-OCH₂ & CH-OH & C5-OCH₂), 3.95 – 3.89 (m, 1H, C5-OCH₂), 3.88 (m, 4H, Me & CH₂-OC(CH₃)₂), 3.81 (br d, J = 3.8 Hz, 2H, CH₂-OH), 3.20 (br s, 1H, O-H), 1.79 (br s, 1H, O-H), 1.46 (s, 3H, C(CH₃)₂), 1.40 (s, 3H, C(CH₃)₂); **¹³C-NMR** (101 MHz, CDCl_3) δ_c 166.2 (CO₂Me), 153.7 (C2), 152.7 (C5), 121.2 (C4), 120.0 (C1), 117.0 (C6), 116.2 (C3), 110.0 (C(CH₃)₂), 74.1 (CH-OC(CH₃)₂), 73.5 (C2-OCH₂), 69.6 (C5-OCH₂), 69.5 (CH-OH), 66.8 (CH₂-OC(CH₃)₂), 63.6 (CH₂-OH), 52.4

(Me), 26.9 (C(CH₃)₂), 25.4 (C(CH₃)₂); **LRMS** m/z (ESI+) 379.15 (100%, [M+Na]⁺);

HRMS m/z (ESI+) C₁₇H₂₄O₈Na Requires: 379.1369, Found: 379.1367 ([M+Na]⁺).

(11s) Methyl 2-((±)-2,3-dihydroxypropoxy)-5-(((*S*)-2,2-dimethyl-1,3-dioxolan-4-yl)methoxy)benzoate

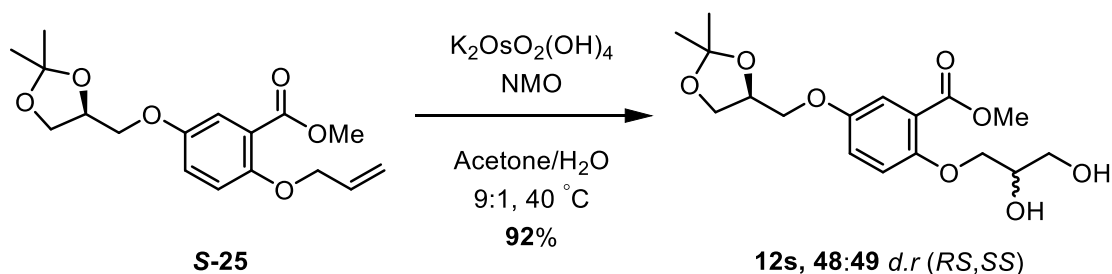


Following general procedure **D**: using stock solutions: **I** (1 mL, 1.5 mmol), **II** (1 mL, 1.5 mmol), **III** (0.5 mL, 1.0 μmol) and **V** (2.5 mL, 10.0 μmol). Methyl (*S*)-2-(allyloxy)-5-((2,2-dimethyl-1,3-dioxolan-4-yl)methoxy)benzoate (**S-25**) (173 mg, 0.50 mmol) was added and the reaction mixture was stirred at 0 °C for 21 h with monitoring (EtOAc/hexane 1:1, R_f = 0.09). Afforded the title compound as a clear oil (173 mg, 97%). $[\alpha]_D^{25} +5.19$ (c. 1.0, MeOH, 2:48:1:49, *e.r/d.r* (2*R*5*R*, 2*S*5*S*, 2*R*5*S*, 2*S*5*R*)); **IR** ν_{\max} cm⁻¹ 3436 br s, (O-H), 2986 w, 2933 w, 2874 w, 1711 s (C=O), 1609 s, 1499 w, 1438 w; **¹H-NMR** (400 MHz, CDCl₃) δ_c 7.41 (d, J = 3.2 Hz, 1H C6-H), 7.07 (dd, J = 9.1, 3.2 Hz, 1H, C4-H), 6.93 (d, J = 9.1 Hz, 1H, C3-H), 4.46 (p, J = 5.7 Hz, 1H, CH-OC(CH₃)₂), 4.24 (dd, J = 9.2, 2.6 Hz, 1H, C2-OCH₂), 4.16 (dd, J = 8.5, 6.4 Hz, 1H, CH₂-OC(CH₃)₂), 4.10 – 3.98 (m, 3H, C2-OCH₂ & CH-OH & C5-OCH₂), 3.95 – 3.89 (m, 1H, C5-OCH₂), 3.88 (m, 4H, Me & CH₂-OC(CH₃)₂), 3.81 (br d, J = 3.8 Hz, 2H, CH₂-OH), 3.20 (br s, 1H, O-H), 1.79 (br s, 1H, O-H), 1.46 (s, 3H, C(CH₃)₂), 1.40 (s, 3H, C(CH₃)₂); **¹³C-NMR** (101 MHz, CDCl₃) δ_c 166.2 (CO₂Me), 153.7 (C2), 152.7 (C5), 121.2 (C4), 120.0 (C1), 117.0 (C6), 116.2 (C3), 110.0 (C(CH₃)₂), 74.1 (CH-OC(CH₃)₂), 73.5 (C2-OCH₂), 69.6 (C5-OCH₂), 69.5 (CH-OH), 66.8 (CH₂-OC(CH₃)₂), 63.6 (CH₂-OH), 52.4

(Me), 26.9 (C(CH₃)₂), 25.4 (C(CH₃)₂); **LRMS** *m/z* (ESI+) 379.15 (100%, [M+Na]⁺);

HRMS *m/z* (ESI+) C₁₇H₂₄O₈Na Requires: 379.1369, Found: 379.1370 ([M+Na]⁺).

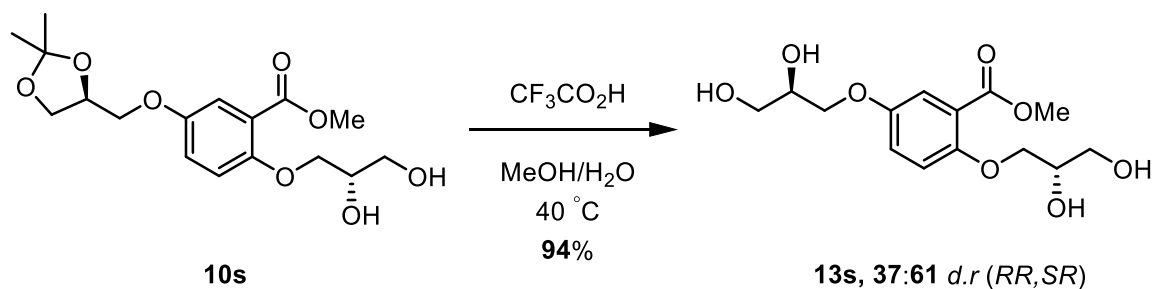
(12s) Methyl 2-((±)-2,3-dihydroxypropoxy)-5-(((*S*)-2,2-dimethyl-1,3-dioxolan-4-yl)methoxy)benzoate



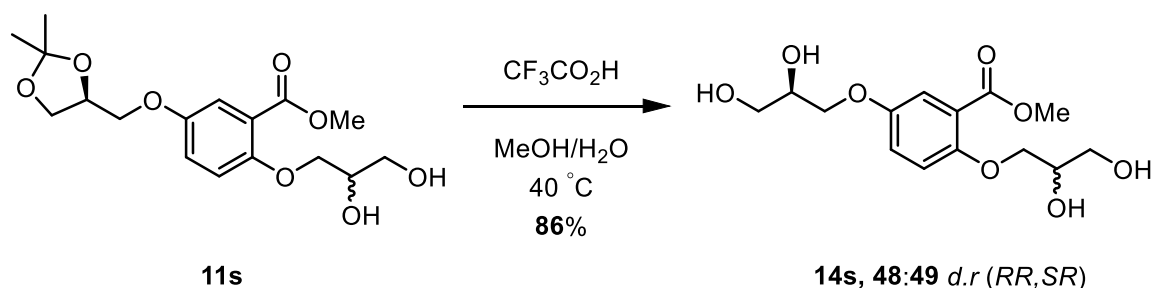
Following general procedure **C**: NMO (8.6 mg, 74.0 μmol) was charged with acetone/H₂O (9:1, 0.5 mL) and K₂OsO₂(OH)₄ (1 mg, 2.7 μmol). Methyl (*S*)-2-(allyloxy)-5-((2,2-dimethyl-1,3-dioxolan-4-yl)methoxy)benzoate (**S-25**) (20 mg, 62.0 μmol) was added and the reaction mixture was heated at 40 °C for 12 h and monitored (TLC, EtOAc/hexane 1:1, *R*_f = 0.14). The pooled organic extracts were washed with citric acid/sodium citrate buffer (aq.) (1.0 M, pH 4, 2 × 20 mL), brine (20 mL) and dried (MgSO₄). Afforded the title compound as a clear oil (20 mg, 92%). [**α**]_D²⁵ +9.34 (c. 1.0, CHCl₃, 1:2:48:49 *e.r/d.r* (2*R*5*R*, 2*S*5*R*, 2*R*5*S*, 2*S*5*S*)); **IR** *V*_{max} cm⁻¹ 3436 br s, (O-H), 2986 w, 2933 w, 2874 w, 1711 s (C=O), 1609 s, 1499 w, 1438 w; **¹H-NMR** (400 MHz, CDCl₃) δ_C 7.41 (d, *J* = 3.2 Hz, 1H C6-H), 7.07 (dd, *J* = 9.1, 3.2 Hz, 1H, C4-H), 6.93 (d, *J* = 9.1 Hz, 1H, C3-H), 4.46 (app. p, *J* = 5.7 Hz, 1H, CH-OC(CH₃)₂), 4.24 (dd, *J* = 9.2, 2.6 Hz, 1H, C2-OCH₂), 4.16 (dd, *J* = 8.5, 6.4 Hz, 1H, CH₂-OC(CH₃)₂), 4.10 – 3.98 (m, 3H, C2-OCH₂ & CH-OH & C5-OCH₂), 3.95 – 3.89 (m, 1H, C5-OCH₂), 3.88 (m, 4H, Me & CH₂-OC(CH₃)₂), 3.81 (br d, *J* = 3.8 Hz, 2H, CH₂-OH), 3.20 (br s, 1H, OH), 1.83 (br s, 1H, OH), 1.45 (s, 3H, C(CH₃)₂), 1.39 (s, 3H, C(CH₃)₂); **¹³C-NMR** (101 MHz, CDCl₃) δ_C 166.2 (CO₂Me), 153.7 (C2), 152.7 (C5), 121.2 (C4), 120.0 (C1), 117.0 (C6), 116.2 (C3), 110.0 (C(CH₃)₂), 74.1 (CH-OC(CH₃)₂), 73.5 (C2-OCH₂), 69.7 (C5-OCH₂),

69.6 ($\underline{\text{C}}\text{H-OH}$), 66.8 ($\underline{\text{C}}\text{H}_2\text{-OC}(\text{CH}_3)_2$), 63.6 ($\underline{\text{C}}\text{H}_2\text{-OH}$), 52.4 (Me), 26.9 ($\text{C}(\underline{\text{C}}\text{H}_3)_2$), 25.4 ($\text{C}(\underline{\text{C}}\text{H}_3)_2$); **LRMS** (ESI+) 379.10 (100%, $[\text{M}+\text{Na}]^+$), 357.20 (10%, $[\text{M}+\text{H}]^+$); **HRMS** (ESI+) $\text{C}_{17}\text{H}_{24}\text{O}_8\text{Na}$ Requires: 379.1369, Found: 379.1373 ($[\text{M}+\text{Na}]^+$).

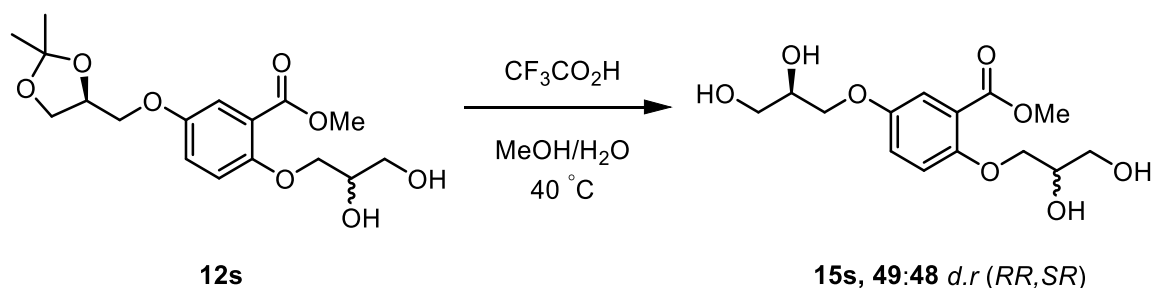
(**13s**) Methyl 2-((*S*)-2,3-dihydroxypropoxy)-5-((*R*)-2,3-dihydroxypropoxy)benzoate



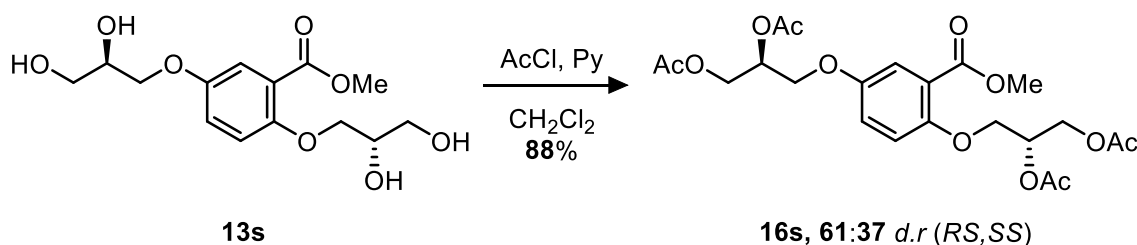
Following general procedure **F**: methyl 2-((±)-2,3-dihydroxypropoxy)-5-(((*S*)-2,2-dimethyl-1,3-dioxolan-4-yl)methoxy)benzoate (**10s**) (80 mg, 0.22 mmol) was stirred at 40 °C for 24 h. Afforded the title compound as a clear oil (65 mg, 94%). $[\alpha]_{\text{D}}^{25}$ – 30.47 (c. 1.0, MeOH, 37:1:1:61 *e.r./d.r.* (2*R*5*R*, 2*S*5*S*, 2*R*5*S*, 2*S*5*R*)); **IR** ν_{max} cm^{-1} 3315 br s (O-H) 2950 w, 2889 w, 1710 s (C=O), 1679 s, 1500 s, 1439s; **¹H-NMR** (400 MHz, $(\text{CD}_3)_2\text{SO}$) δ_{H} 7.18 (d, $J = 2.7$ Hz, 1H, C6-H), 7.13 – 7.07 (m, 2H, C3-H & C4-H), 4.94 (d, $J = 5.0$ Hz, 1H, CH-OH), 4.84 (d, $J = 5.0$ Hz, 1H, CH-OH), 4.66 (t, $J = 5.7$ Hz, 1H, CH₂-OH), 4.59 (t, $J = 5.7$ Hz, 1H, CH₂-OH), 4.01 – 3.85 (m, 3H), 3.86 – 3.69 (m, 6H, Me), 3.55 – 3.35 (m, 4H); **¹³C-NMR** (101 MHz, $(\text{CD}_3)_2\text{SO}$) δ_{C} 166.1 ($\underline{\text{C}}\text{O}_2\text{Me}$), 152.2 (C5), 152.0 (C2), 121.0 (C1), 119.8 (C3/C4), 115.9 (C3/C4), 115.9 (C6), 71.3 (O-CH₂), 70.4 (O-CH₂), 70.0 (2C, CH-OH), 62.7 (CH₂-OH), 62.7 (CH₂-OH), 52.0 (Me); **LRMS** m/z (ESI+) 339.11 (100%, $[\text{M}+\text{Na}]^+$); **HRMS** m/z (ESI+) $\text{C}_{14}\text{H}_{20}\text{O}_8\text{Na}$ Requires: 339.1056, Found: 339.1060 ($[\text{M}+\text{Na}]^+$).

(14s) Methyl 2-((±)-2,3-dihydroxypropoxy)-5-((*R*)-2,3-dihydroxypropoxy)benzoate

Following general procedure **F**: methyl 2-((±)-2,3-dihydroxypropoxy)-5-(((*S*)-2,2-dimethyl-1,3-dioxolan-4-yl)methoxy)benzoate (**11s**) (80 mg, 0.22 mmol) was stirred at 40 °C for 24 h. Afforded the title compound as a clear oil (60 mg, 86%). $[\alpha]_D^{25}$ – 8.31 (c. 1.0, MeOH, 48:1:1:49 *e.r/d.r* (*2R5R*, *2S5S*, *2R5S*, *2S5R*)); **IR** V_{\max} cm^{-1} 3330br s (O-H) 2949 w, 2882 w, 1709 s, 1678 s, 1499 s, 1439 s; **$^1\text{H-NMR}$** (400 MHz, $(\text{CD}_3)_2\text{SO}$) δ_{H} 7.18 (d, J = 2.7 Hz, 1H, C6-H), 7.13 – 7.07 (m, 2H, C3-H & C4-H), 4.94 (d, J = 5.0 Hz, 1H, CH-OH), 4.84 (d, J = 5.0 Hz, 1H, CH-OH), 4.66 (t, J = 5.7 Hz, 1H, CH₂-OH), 4.59 (t, J = 5.7 Hz, 1H, CH₂-OH), 4.01 – 3.85 (m, 3H), 3.86 – 3.69 (m, 6H, Me), 3.55 – 3.35 (m, 4H); **$^{13}\text{C-NMR}$** (101 MHz, $(\text{CD}_3)_2\text{SO}$) δ_{C} 166.0 ($\text{C}=\text{O}_2\text{Me}$), 152.2 (C5), 152.0 (C2), 121.0 (C1), 119.8 (C3/C4), 115.9 (C3/C4), 115.9 (C6), 71.3 (O-CH₂), 70.3 (O-CH₂), 69.9 (2C, CH-OH), 62.7 (CH₂-OH), 62.7 (CH₂-OH), 52.0 (Me); **LRMS** m/z (ESI+) 339.11 (100%, $[\text{M}+\text{Na}]^+$); **HRMS** m/z (ESI+) $\text{C}_{14}\text{H}_{20}\text{O}_8\text{Na}$ Requires: 339.1056, Found: 339.1060 ($[\text{M}+\text{Na}]^+$).

(15s) Methyl 5-((*R*)-2,3-dihydroxypropoxy)-2-((±)-2,3-dihydroxypropoxy)benzoate

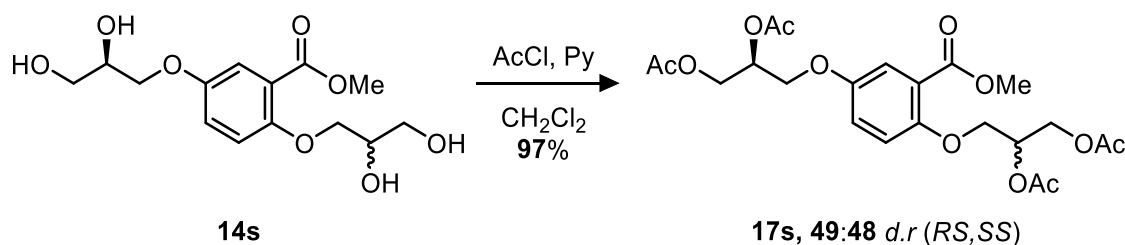
Following general procedure **F**: methyl 2-(2,3-dihydroxypropoxy)-5-(((*S*)-2,2-dimethyl-1,3-dioxolan-4-yl)methoxy)benzoate (**12s**) (10 mg, 0.14 mmol) was stirred at 40 °C for 12 h afforded the title compound that was used directly without further purification. 49:1:2:48 *e.r/d.r* (2*R*5*R*, 2*S*5*S*, 2*R*5*S*, 2*S*5*R*); **¹H-NMR** (400 MHz, CD₃OD) δ_H 7.35 (d, *J* = 3.1 Hz, 1H), 7.15 (dd, *J* = 9.0, 3.1 Hz, 1H), 7.09 (d, *J* = 9.1 Hz, 1H), 4.17 – 3.98 (m, 3H), 3.99 – 3.92 (m, 3H), 3.87 (s, 3H), 3.76 – 3.58 (m, 4H).

(16s) (2*R*,5*S*)-((2-(methoxycarbonyl)-1,4-phenylene)bis(oxy))bis(propane-3,1,2-triyl) tetraacetate

Following general procedure **G**: Methyl 5-((*R*)-2,3-dihydroxypropoxy)-2-((*S*)-2,3-dihydroxypropoxy)benzoate (**13s**) (23 mg, 0.07 mmol) was charged with pyridine (46.8 μL, 0.56 mmol), CH₂Cl₂ (4 mL) and the AcCl (39.8 μL, 0.56 mmol) was added dropwise. Afforded the title compound as a clear oil (30 mg, 88%). [**α**]_D²⁵ +7.96 (c. 1.0, CHCl₃ 1:37:61:1 *e.r/d.r* (2*R*5*R*, 2*S*5*S*, 2*R*5*S*, 2*S*5*R*)); **IR** V_{max} cm⁻¹ 2965 w, 2923 s, 1736 s (C=O), 1499 s, 1439 s; **¹H-NMR** (400 MHz, CDCl₃) δ_H 7.35 (d, *J* = 3.3 Hz, 1H, C6-H), 7.01 (dd, *J* = 9.1, 3.3 Hz, 1H, C4-H), 6.88 (d, *J* = 9.1 Hz, 1H, C3-H), 5.36

(m, 2H, $\underline{\text{CH}}$ -OAc), 4.48 (dd, $J = 12.0, 3.9$ Hz, 1H, $\underline{\text{CH}_2}$ -OAc), 4.41 (dd, $J = 12.0, 3.9$ Hz, 1H, $\underline{\text{CH}_2}$ -OAc), 4.32 (dd, $J = 12.0, 6.1$ Hz, 1H, $\underline{\text{CH}_2}$ -OAc), 4.27 (dd, $J = 12.0, 6.1$ Hz, 1H, $\underline{\text{CH}_2}$ -OAc), 4.14 (m, 2H, ArO- $\underline{\text{CH}_2}$), 4.09 (d, $J = 5.2$ Hz, 2H, ArO- $\underline{\text{CH}_2}$), 3.88 (s, 3H, Me), 2.10 (s, 3H, Ac), 2.10 (s, 3H, Ac), 2.07 (s, 3H, Ac), 2.07 (s, 3H, Ac); **^{13}C -NMR** (101 MHz, CDCl_3) δ_{C} 170.75 (Ac), 170.72 (Ac), 170.43 (Ac), 170.38 (Ac), 166.3 ($\underline{\text{CO}_2\text{Me}}$), 152.6 (C1), 121.7 (C2 & C5), 120.5 (C4), 117.0 (C6), 116.1 (C3), 69.8 ($\underline{\text{CH}}$ -OAc), 69.7 ($\underline{\text{CH}}$ -OAc), 68.3 (ArO- $\underline{\text{CH}_2}$), 66.9 (ArO- $\underline{\text{CH}_2}$), 62.7 ($\underline{\text{CH}_2}$ -OAc), 62.5 ($\underline{\text{CH}_2}$ -OAc), 52.3 (Me), 21.09 (Ac), 21.07 (Ac), 20.9 (2C, Ac); **LRMS** m/z (ESI+) 507.16 ($[\text{M}+\text{Na}]^+$, 100%); **HRMS** m/z (ESI+) $\text{C}_{22}\text{H}_{28}\text{O}_{12}\text{Na}$ Requires: 507.1478, Found: 507.1476 ($[\text{M}+\text{Na}]^+$); **CHPLC** $R_{\text{t}1} = 74.38$ min, area = 1.49%; $R_{\text{t}2} = 81.08$ min, area = 0.96%; $R_{\text{t}3} = 84.40$ min, area = 61.05%; $R_{\text{t}4} = 114.17$ min, area = 36.50%. (Phenomenex[®] Cellulose-1, MeCN/ H_2O , 7:18, 1 mL min⁻¹, 30 °C).

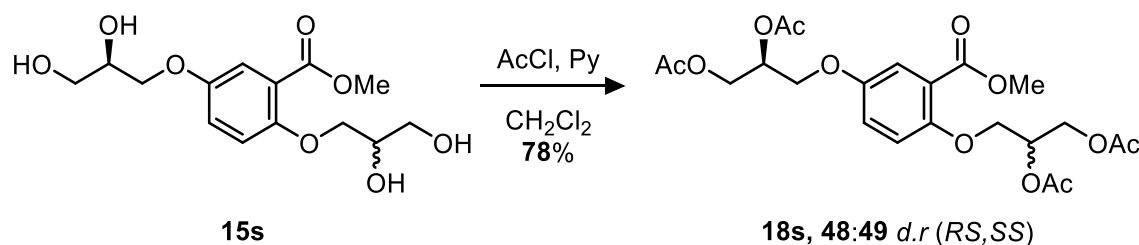
(17s) (2 \pm ,5*S*)-((2-(methoxycarbonyl)-1,4-phenylene)bis(oxy))bis(propane-3,1,2-triyl) tetraacetate



Following general procedure **G**: Methyl 5-((*R*)-2,3-dihydroxypropoxy)-2-((\pm)-2,3-dihydroxypropoxy)benzoate (**14s**) (85 mg, 0.27 mmol) was charged with pyridine (0.18 mL, 2.15 mmol), CH_2Cl_2 (4 mL) and the AcCl (0.15 mL, 2.15 mmol) was added dropwise. Afforded the title compound as a clear oil (127 mg, 97%). **$[\alpha]_{\text{D}}^{25} +22.50$** (c. 1.0, CHCl_3 , 1:48:49:1 *e.r/d.r* (2*R*5*R*, 2*S*5*S*, 2*R*5*S*, 2*S*5*R*)); **IR** ν_{max} cm⁻¹ 2924 w, 2853 w, 1735 s (C=O), 1499 s, 1439 s; **^1H -NMR** (400 MHz, CDCl_3) δ_{H} 7.34 (d, $J = 3.3$ Hz, 1H, C6- $\underline{\text{H}}$), 7.01 (dd, $J = 9.1, 3.3$ Hz, 1H, C4- $\underline{\text{H}}$), 6.88 (d, $J = 9.1$ Hz, 1H, C3- $\underline{\text{H}}$), 5.37

(m, 2H, $\underline{\text{CH}}$ -OAc), 4.48 (dd, J = 12.0, 3.9 Hz, 1H, $\underline{\text{CH}_2}$ -OAc), 4.41 (dd, J = 12.0, 3.9 Hz, 1H, $\underline{\text{CH}_2}$ -OAc), 4.32 (dd, J = 12.0, 6.1 Hz, 1H, $\underline{\text{CH}_2}$ -OAc), 4.28 (dd, J = 12.0, 6.1 Hz, 1H, $\underline{\text{CH}_2}$ -OAc), 4.14 (m, 2H, ArO- $\underline{\text{CH}_2}$), 4.10 (d, J = 5.2 Hz, 2H, ArO- $\underline{\text{CH}_2}$), 3.88 (s, 3H, Me), 2.10 (s, 3H, Ac), 2.10 (s, 3H, Ac), 2.07 (s, 3H, Ac), 2.07 (s, 3H, Ac); **^{13}C -NMR** (101 MHz, CDCl_3) δ_{C} 170.75 (Ac), 170.72 (Ac), 170.54 (Ac), 170.4 (Ac), 166.3 ($\underline{\text{CO}_2\text{Me}}$), 152.6 (C1), 121.7 (C2 & C5), 120.5 (C4), 117.0 (C6), 116.1 (C3), 69.8 ($\underline{\text{CH}}$ -OAc), 69.7 ($\underline{\text{CH}}$ -OAc), 68.3 (ArO- $\underline{\text{CH}_2}$), 66.9 (ArO- $\underline{\text{CH}_2}$), 62.7 ($\underline{\text{CH}_2}$ -OAc), 62.5 ($\underline{\text{CH}_2}$ -OAc), 52.3 (Me), 21.10 (Ac), 21.07 (Ac), 20.9 (2C, Ac); **LRMS** m/z (ESI+) 507.15 ($[\text{M}+\text{Na}]^+$, 100%); **HRMS** m/z (ESI+) $\text{C}_{22}\text{H}_{28}\text{O}_{12}\text{Na}$ Requires: 507.1478, Found: 507.1476 ($[\text{M}+\text{Na}]^+$); **chPLC** $R_{\text{t}1}$ = 74.81 min, area = 1.15%; $R_{\text{t}2}$ = 81.36 min, area = 1.17%; $R_{\text{t}3}$ = 84.63 min, area = 49.41%; $R_{\text{t}4}$ = 113.78 min, area = 48.26%. (Phenomenex[®] Cellulose-1, MeCN/ H_2O , 7:18, 1 mL min⁻¹, 30 °C).

(18s) (2 \pm ,5S)-((2-(methoxycarbonyl)-1,4-phenylene)bis(oxy))bis(propane-3,1,2-triyl) tetraacetate

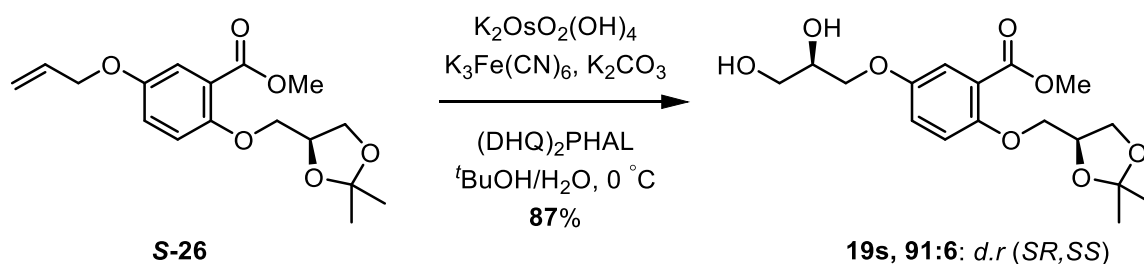


Following general procedure **G**: Methyl 5-((*R*)-2,3-dihydroxypropoxy)-2-((\pm)-2,3-dihydroxypropoxy)benzoate (**15s**) (5 mg, 0.016 mmol) was charged with pyridine (10.3 μL , 0.13 mmol), CH_2Cl_2 (4 mL) and the AcCl (9.5 μL , 0.13 mmol) was added dropwise. Afforded the title compound as a clear oil (6 mg, 78%). 1:49:48:2 *e.r/d.r* (*2R5R*, *2S5S*, *2R5S*, *2S5R*); **IR** V_{max} cm⁻¹ 2953 w, 1736 s (C=O), 1499 s, 1441 s; **^1H -NMR** (400 MHz, CDCl_3) δ_{H} 7.35 (d, J = 3.3 Hz, 1H, C6- $\underline{\text{H}}$), 7.02 (dd, J = 9.1, 3.3 Hz, 1H, C4- $\underline{\text{H}}$), 6.89 (d, J = 9.1 Hz, 1H, C3- $\underline{\text{H}}$), 5.37 (m, 2H, $\underline{\text{CH}}$ -OAc), 4.49 (dd, J = 12.0,

3.9 Hz, 1H, $\underline{\text{CH}_2\text{-OAc}}$), 4.42 (dd, $J = 12.0$, 3.9 Hz, 1H, $\underline{\text{CH}_2\text{-OAc}}$), 4.33 (dd, $J = 12.0$, 6.1 Hz, 1H, $\underline{\text{CH}_2\text{-OAc}}$), 4.28 (dd, $J = 12.0$, 6.1 Hz, 1H, $\underline{\text{CH}_2\text{-OAc}}$), 4.15 (m, 2H, ArO-CH_2), 4.10 (d, $J = 5.2$ Hz, 2H, ArO-CH_2), 3.89 (s, 3H, Me), 2.10 (s, 3H, Ac), 2.10 (s, 3H, Ac), 2.08 (s, 3H, Ac), 2.07 (s, 3H, Ac); **$^{13}\text{C-NMR}$** (101 MHz, CDCl_3) δ_{C} 170.8 (Ac), 170.7 (Ac), 170.44 (Ac), 170.39 (Ac), 166.3 (CO_2Me), 152.6 (C1), 121.7 (C2 & C5), 120.5 (C4), 117.0 (C6), 116.1 (C3), 69.84 ($\underline{\text{CH-OAc}}$), 69.75 ($\underline{\text{CH-OAc}}$), 68.3 (ArO-CH_2), 66.9 (ArO-CH_2), 62.8 ($\underline{\text{CH}_2\text{-OAc}}$), 62.5 ($\underline{\text{CH}_2\text{-OAc}}$), 52.34 (Me), 21.10 (Ac), 21.08 (Ac), 20.9 (2C, Ac); **LRMS** m/z (ESI+) 507.15 ($[\text{M}+\text{Na}]^+$, 100%); **HRMS** m/z (ESI+) $\text{C}_{22}\text{H}_{28}\text{O}_{12}\text{Na}$ Requires: 507.1478, Found: 507.1484 ($[\text{M}+\text{Na}]^+$); **cHPLC** $R_{\text{t}1} = 73.06$ min, area = 1.38%; $R_{\text{t}2} = 79.49$ min, area = 1.74%; $R_{\text{t}3} = 81.72$ min, area = 48.16%; $R_{\text{t}4} = 109.46$ min, area = 48.72%. (Phenomenex[®] Cellulose-1, MeCN/ H_2O , 7:18, 1 mL min^{-1} , 30 °C).

Supplementary Compounds 19s-27s (Table 6, Entries 4 to 6)

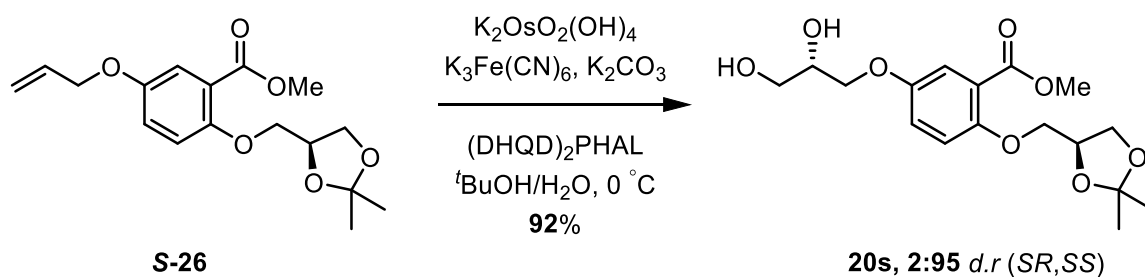
(19s) Methyl 5-((*R*)-2,3-dihydroxypropoxy)-2-(((*S*)-2,2-dimethyl-1,3-dioxolan-4-yl)methoxy)benzoate.



Following general procedure **D**: using stock solutions: **I** (0.6 mL, 0.9 mmol), **II** (0.6 mL, 0.9 mmol), **III** (0.3 mL, 0.6 μmol) and **IV** (1.5 mL, 6.0 μmol). Methyl (*S*)-5-(allyloxy)-2-((2,2-dimethyl-1,3-dioxolan-4-yl)methoxy)benzoate (**S-26**) (100 mg, 0.29 mmol) was added and the reaction mixture was stirred at 0 °C for 8 h with monitoring (EtOH/EtOAc 1:1, $R_{\text{f}} = 0.21$). Afforded the title compound as a white solid (90 mg, 87%). **M.P** 72 – 73 °C; **$[\alpha]_{\text{D}}^{25}$** –8.31 (c. 0.5, MeOH, 6:91, *d.r*(*2S5S*, *2S5R*)); **IR** V_{max}

cm⁻¹ 3431 br s, (O-H), 2993 w, 2934 w, 2885 w, 1727 s (C=O), 1499 s, 1439w; **¹H-NMR** (400 MHz, CDCl₃) δ_H 7.35 (d, *J* = 3.1 Hz, 1H, C6-H), 7.03 (dd, *J* = 9.0, 3.2 Hz, 1H, C4-H), 6.94 (d, *J* = 9.1 Hz, 1H, C3-H), 4.47 (qd, *J* = 6.3, 4.7 Hz, 1H, CH-OC(CH₃)₂), 4.16 (dd, *J* = 8.5, 6.3 Hz, 1H, Ar-OCH₂), 4.11 (dd, *J* = 9.4, 4.6 Hz, 2H, Ar-OCH₂), 4.06 – 3.99 (m, 3H, CH₂-OC(CH₃)₂ & CH-OH), 4.00 – 3.94 (m, 1H, Ar-OCH₂), 3.88 (s, 3H, Me), 3.86 – 3.70 (br m, 2H, CH₂-OH), 2.63 (d, *J* = 4.4 Hz 1H, CH-OH), 2.06 (obs s, 1H, CH₂-OH), 1.45 (s, 3H, C(CH₃)₂), 1.39 (s, 3H, C(CH₃)₂); **¹³C-NMR** (101 MHz, CDCl₃) δ_C 166.3 (CO₂Me), 153.0, 152.6, 121.6 (C1), 120.3 (C4), 116.9 (C6), 116.5 (C3), 109.7 (C(CH₃)₂), 74.1 (CH-OC(CH₃)₂), 70.8 (Ar-OCH₂), 70.4 (Ar-OCH₂), 70.0 (CH-OH), 67.0 (CH₂-OC(CH₃)₂), 63.7 (CH₂-OH), 52.3 (Me), 26.9 (C(CH₃)₂), 25.5 (C(CH₃)₂); **LRMS** *m/z* (ESI+) 379.14 (100%, [M+Na]⁺); **HRMS** *m/z* (ESI+) C₁₇H₂₄O₈Na Requires: 379.1369, Found: 379.1371 ([M+Na]⁺).

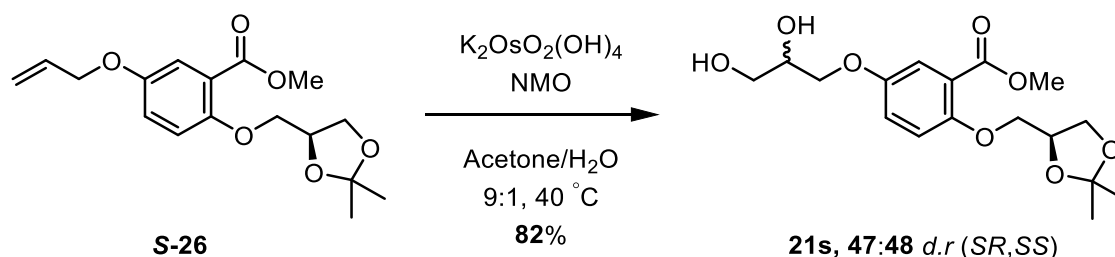
(20s) Methyl 5-((*S*)-2,3-dihydroxypropoxy)-2-(((*S*)-2,2-dimethyl-1,3-dioxolan-4-yl)methoxy)benzoate



Following general procedure **D**: using stock solutions: **I** (0.6 mL, 0.9 mmol), **II** (0.6 mL, 0.9 mmol), **III** (0.3 mL, 0.6 μmol) and **V** (1.5 mL, 6.0 μmol). Methyl (*S*)-5-(allyloxy)-2-((2,2-dimethyl-1,3-dioxolan-4-yl)methoxy)benzoate (**S-26**) (100 mg, 0.29 mmol) was added and the reaction mixture was stirred at 0 °C for 8 h with monitoring (EtOH/EtOAc 1:1, *R*_f = 0.21). Afforded the title compound as a clear oil (95 mg, 92%). **[α]_D²⁵** –16.62 (c. 0.5, MeOH, 95:2 *d.r* (2*S*5*S*, 2*S*5*R*)); **IR** Vmax cm⁻¹ 3437 br s, (O-H), 2989 w, 2937 w, 2878 w, 1727 s (C=O), 1499 s, 1439w; **¹H-NMR** (400 MHz,

CDCl₃) δ_{H} 7.35 (d, J = 3.1 Hz, 1H, C6-H), 7.03 (dd, J = 9.0, 3.2 Hz, 1H, C4-H), 6.94 (d, J = 9.1 Hz, 1H, C3-H), 4.47 (qd, J = 6.3, 4.7 Hz, 1H, CH-OC(CH₃)₂), 4.16 (dd, J = 8.5, 6.3 Hz, 1H, Ar-OCH₂), 4.11 (dd, J = 9.4, 4.6 Hz, 2H, Ar-OCH₂), 4.06 – 3.99 (m, 3H, CH₂-OC(CH₃)₂ & CH-OH), 4.00 – 3.94 (m, 1H, Ar-OCH₂), 3.88 (s, 3H, Me), 3.86 – 3.70 (br m, 2H, CH₂-OH), 2.63 (d, J = 4.4 Hz 1H, CH-OH), 2.06 (obs s, 1H, CH₂-OH), 1.45 (s, 3H, C(CH₃)₂), 1.39 (s, 3H, C(CH₃)₂); **¹³C-NMR** (101 MHz, CDCl₃) δ_{C} 166.3 (CO₂Me), 153.0, 152.6, 121.6 (C1), 120.3 (C4), 116.9 (C6), 116.5 (C3), 109.7 (C(CH₃)₂), 74.1 (CH-OC(CH₃)₂), 70.8 (Ar-OCH₂), 70.4 (Ar-OCH₂), 70.0 (CH-OH), 67.0 (CH₂-OC(CH₃)₂), 63.7 (CH₂-OH), 52.3 (Me), 26.9 (C(CH₃)₂), 25.5 (C(CH₃)₂); **LRMS** m/z (ESI+) 379.15 (100%, [M+Na]⁺); **HRMS** m/z (ESI+) C₁₇H₂₄O₈Na Requires: 379.1369, Found: 379.1370 ([M+Na]⁺).

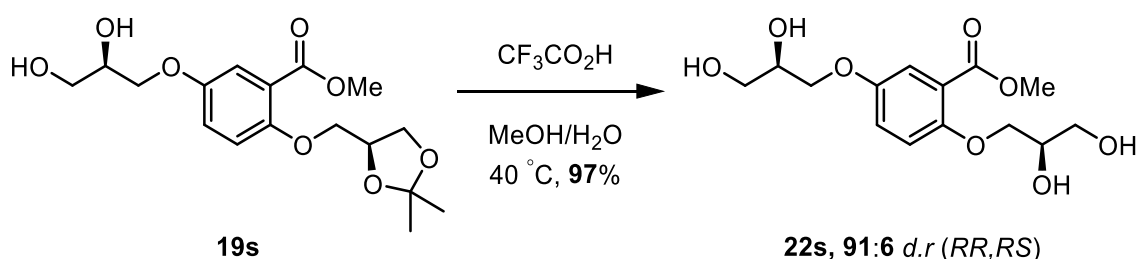
(21s) Methyl 5-((±)2,3-dihydroxypropoxy)-2-(((*S*)-2,2-dimethyl-1,3-dioxolan-4-yl)methoxy)benzoate



Following general procedure **C**: NMO (8.6 mg, 74.0 μmol) was charged with acetone/H₂O (9:1, 0.5 mL) and K₂OsO₂(OH)₄ (1 mg, 2.7 μmol). Methyl (*S*)-5-(allyloxy)-2-((2,2-dimethyl-1,3-dioxolan-4-yl)methoxy)benzoate (**S-26**) (20 mg, 62.0 μmol) was added and the reaction mixture was heated at 40 °C for 12 h and monitored (TLC, EtOAc/hexane 1:1, R_{f} = 0.14). The pooled organic extracts were washed with citric acid/sodium citrate buffer (aq.) (1.0 M, pH 4, 2 \times 20 mL), brine (20 mL) and dried (MgSO₄). Afforded the title compound as a clear oil (18 mg, 82%). [α]_D²⁵ +19.73 (c. 1.0, CHCl₃, 2:47:3:48 *e.r/d.r* (2*R*5*R*, 2*S*5*R*, 2*R*5*S*, 2*S*5*S*)); **IR** ν_{max} cm⁻¹ 3447br w (O-

H), 2987 s, 2932 s, 1712 s (C=O), 1612 w, 1583 w, 1498 s, 1438 s; **¹H-NMR** (400 MHz, CDCl₃) δ_H 7.35 (d, *J* = 3.1 Hz, 1H, C6-H), 7.03 (dd, *J* = 9.0, 3.2 Hz, 1H, C4-H), 6.95 (d, *J* = 9.0 Hz, 1H, C3-H), 4.52 – 4.43 (m, 1H, CH-OC(CH₃)₂), 4.17 (dd, *J* = 8.5, 6.3 Hz, 1H, CH₂-OC(CH₃)₂), 4.11 (dd, *J* = 9.4, 4.6 Hz, 2H, ArOC-H₂), 4.07 – 3.92 (m, 4H, CH₂-OC(CH₃)₂, CH-OH & ArOC-H₂), 3.88 (s, 3H, Me), 3.87 – 3.78 (m, 1H, CH₂-OH), 3.74 (dt, *J* = 11.1, 5.2 Hz, 1H, CH₂-OH), 2.60 (d, *J* = 4.6 Hz, 1H, CH-OH), 2.03 (t, *J* = 5.9 Hz, 1H, CH₂-OH), 1.45 (s, 3H, C(CH₃)₂), 1.39 (s, 3H, C(CH₃)₂); **¹³C-NMR** (101 MHz, CDCl₃) δ_C 166.3 (CO₂Me), 153.0, 152.6, 121.6 (C1), 120.3 (C4), 116.9 (C6), 116.5 (C3), 109.7 (C(CH₃)₂), 74.1 (CH-OC(CH₃)₂), 70.8 (ArO-CH₂), 70.4 (ArO-CH₂), 70.0 (CH-OH), 67.0 (CH₂-OC(CH₃)₂), 63.7 (CH₂-OH), 52.3 (Me), 26.9 (C(CH₃)₂), 25.5 (C(CH₃)₂); **LRMS** (ESI+) 379.12 (100%, [M+Na]⁺); **HRMS** (ESI+) C₁₇H₂₄O₈Na Requires: 379.1369, Found: 379.1372 ([M+Na]⁺).

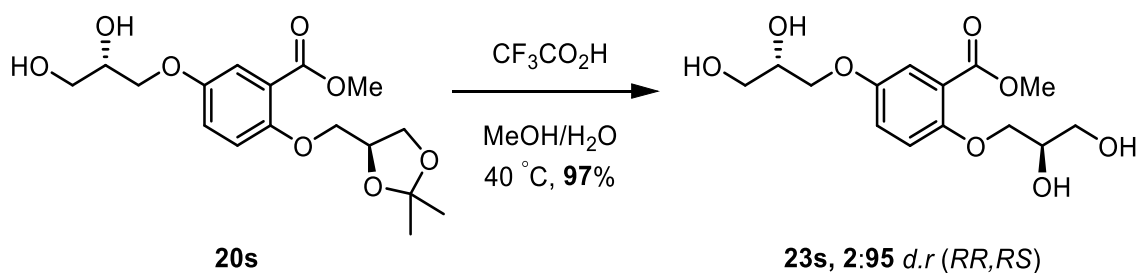
(**22s**) Methyl 2,5 bis-(*R*)-2,3-dihydroxypropoxy)benzoate



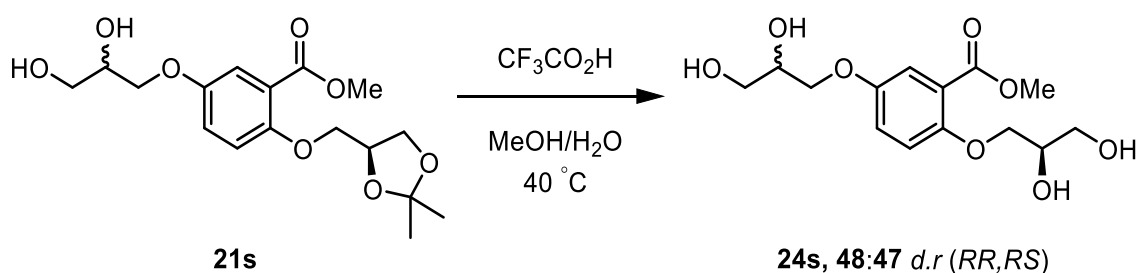
Following general procedure **F**: methyl 5-((*R*)-2,3-dihydroxypropoxy)-2-(((*S*)-2,2-dimethyl-1,3-dioxolan-4-yl)methoxy)benzoate (**19s**) (50 mg, 0.14 mmol) was stirred at 40 °C for 24 h. yielded the title compound as a clear oil (43 mg, 97%). [**α**]_D²⁵ – 10.38 (c. 1.0, MeOH, 91:6 *d.r* (2*R*5*R*, 2*R*5*S*)); **IR** V_{max} cm⁻¹ 3366br s (O-H) 2939 w, 2880 w, 1709 s (C=O), 1499 s, 1462 w, 1438 s, 1286 s, 1246 s, 1209 s; **¹H-NMR** (400 MHz, (CD₃)₂SO) δ_H 7.18 (d, *J* = 2.7 Hz, 1H, C6-H), 7.14 – 7.06 (m, 2H, C3-H & C4-H), 4.94 (d, *J* = 5.0 Hz, 1H, CH-OH), 4.84 (d, *J* = 5.0 Hz, 1H, CH-OH), 4.67 (t, *J* = 5.7 Hz, 1H, CH₂-OH), 4.59 (t, *J* = 5.7 Hz, 1H, CH₂-OH), 4.00 – 3.84 (m, 3H), 3.85 – 3.67 (m,

6H), 3.58 – 3.34 (m, 4H); **¹³C-NMR** (101 MHz, (CD₃)₂SO) δ_c 166.1 (C=O), 152.2 (C5), 152.0 (C2), 121.0 (C1), 119.8 (C3/C4), 116.0 (C3/C4), 115.9 (C6), 71.3 (O-CH₂), 70.4 (O-CH₂), 70.0 (2C, CH-OH), 62.7 (CH₂-OH), 62.7 (CH₂-OH), 52.0 (Me); **LRMS** *m/z* (ESI+) 339.11 (100%, [M+Na]⁺); **HRMS** *m/z* (ESI+) C₁₄H₂₀O₈Na Requires: 339.1056, Found: 339.1059 ([M+Na]⁺).

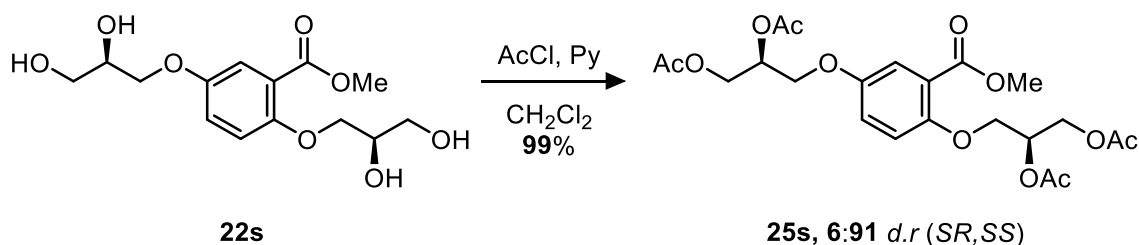
(23s) Methyl 5-((*S*)-2,3-dihydroxypropoxy)-2-((*R*)-2,3-dihydroxypropoxy)benzoate



Following general procedure **F**: methyl 5-((*S*)-2,3-dihydroxypropoxy)-2-(((*S*)-2,2-dimethyl-1,3-dioxolan-4-yl)methoxy)benzoate (**20s**) (65 mg, 0.18 mmol) was stirred at 40 °C for 24 h. yielded the title compound as a clear oil (56 mg, 97%). [**α**]_D²⁵ +11.73 (c. 1.0, MeOH, 2:95 *d.r* (*2R5R*, *2R5S*)); **IR** *V*_{max} cm⁻¹ 3254br s (O-H) 2939 w, 2894 w, 1729 s (C=O), 1699 s (C=O), 1500 s, 1462 w, 1435 w; **¹H-NMR** (400 MHz, (CD₃)₂SO) δ_H 7.18 (d, *J* = 2.7 Hz, 1H, C6-H), 7.13 – 7.07 (m, 2H, C3-H & C4-H), 4.94 (d, *J* = 5.0 Hz, 1H, CH-OH), 4.84 (d, *J* = 5.0 Hz, 1H, CH-OH), 4.66 (t, *J* = 5.7 Hz, 1H, CH₂-OH), 4.59 (t, *J* = 5.7 Hz, 1H, CH₂-OH), 4.01 – 3.85 (m, 3H), 3.86 – 3.69 (m, 5H), 3.55 – 3.35 (m, 5H); **¹³C-NMR** (101 MHz, (CD₃)₂SO) δ_c 166.1 (C=O), 152.2 (C5), 152.0 (C2), 121.0 (C1), 119.8 (C3/C4), 115.9 (C3/C4), 115.9 (C6), 71.3 (O-CH₂), 70.4 (O-CH₂), 70.0 (2C, CH-OH), 62.7 (CH₂-OH), 62.7 (CH₂-OH), 52.0 (Me); **LRMS** *m/z* (ESI+) 339.11 (100%, [M+Na]⁺); **HRMS** *m/z* (ESI+) C₁₄H₂₀O₈Na Requires: 339.1056, Found: 339.1057 ([M+Na]⁺).

(24s) Methyl 5-(2,3-dihydroxypropoxy)-2-(((*R*)-2,3-dihydroxypropoxy)benzoate

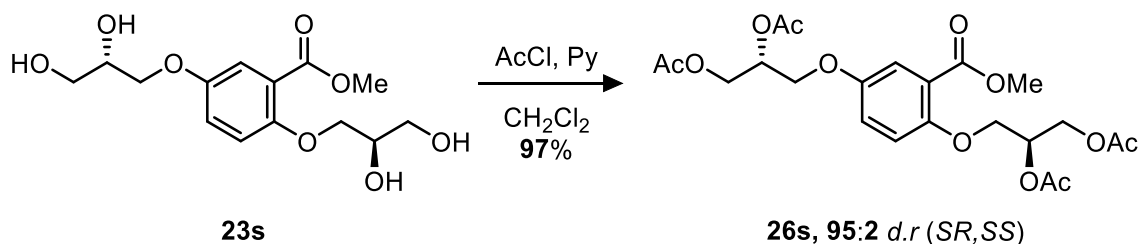
Following general procedure **F**: methyl 5-(2,3-dihydroxypropoxy)-2-(((*S*)-2,2-dimethyl-1,3-dioxolan-4-yl)methoxy)benzoate (**21s**) (10 mg, 0.22 mmol) was stirred at 40 °C for 12 h afforded the title compound that was used directly in the next reaction. 48:2:47:3 *e.r/d.r* (2*R*5*R*, 2*S*5*S*, 2*R*5*S*, 2*S*5*R*); **¹H-NMR** (400 MHz, CD₃OD) δ_H 7.35 (d, *J* = 2.9 Hz, 1H), 7.15 (dd, *J* = 9.1, 3.1 Hz, 1H), 7.09 (d, *J* = 9.1 Hz, 1H), 4.14 – 3.99 (m, 3H), 3.99 – 3.90 (m, 3H), 3.87 (s, 3H), 3.75 – 3.58 (m, 4H).

(25s) (2*S*,5*S*)-((2-(methoxycarbonyl)-1,4-phenylene)bis(oxy))bis(propane-3,1,2-triyl) tetraacetate

Following general procedure **G**: Methyl 2,5-bis((*R*)-2,3-dihydroxypropoxy)benzoate (**22s**) (25 mg, 0.08 mmol) was charged with pyridine (51.5 μL, 0.64 mmol), CH₂Cl₂ (4 mL) and the AcCl (45.7 μL, 0.64 mmol) was added dropwise. Afforded the title compound as a clear oil (38 mg, 99%). [**α**]_D²⁵ +37.39 (c. 1.0, CHCl₃, 6:91 *d.r* (2*S*5*R*, 2*S*5*S*); **IR** V_{max} cm⁻¹ 2962 w, 1740 s (C=O), 1500 s, 1439 s; **¹H-NMR** (400 MHz, CDCl₃) δ_H 7.35 (d, *J* = 3.3 Hz, 1H, C6-H), 7.02 (dd, *J* = 9.1, 3.3 Hz, 1H, C4-H), 6.89 (d, *J* = 9.1 Hz, 1H, C3-H), 5.37 (m, 2H, CH-OAc), 4.49 (dd, *J* = 12.0, 3.9 Hz, 1H, CH₂-OAc), 4.42 (dd, *J* = 12.0, 3.9 Hz, 1H, CH₂-OAc), 4.33 (dd, *J* = 12.0, 6.1 Hz, 1H, CH₂-

OAc), 4.28 (dd, $J = 12.0, 6.1$ Hz, 1H, $\underline{\text{CH}}_2\text{-OAc}$), 4.15 (m, 2H, $\text{ArO-}\underline{\text{CH}}_2$), 4.10 (d, $J = 5.2$ Hz, 2H, $\text{ArO-}\underline{\text{CH}}_2$), 3.89 (s, 3H, Me), 2.11 (s, 3H, Ac), 2.10 (s, 3H, Ac), 2.08 (s, 3H, Ac), 2.07 (s, 3H, Ac); **$^{13}\text{C-NMR}$** (101 MHz, CDCl_3) δ_{C} 170.8 (Ac), 170.7 (Ac), 170.5 (Ac), 170.4 (Ac), 166.3 ($\underline{\text{CO}}_2\text{Me}$), 152.6 (C1), 121.7 (C2 & C5), 120.5 (C4), 117.0 (C6), 116.1 (C3), 69.9 ($\underline{\text{CH}}\text{-OAc}$), 69.8 ($\underline{\text{CH}}\text{-OAc}$), 68.3 ($\text{ArO-}\underline{\text{CH}}_2$), 66.9 ($\text{ArO-}\underline{\text{CH}}_2$), 62.8 ($\underline{\text{CH}}_2\text{-OAc}$), 62.6 ($\underline{\text{CH}}_2\text{-OAc}$), 52.4 (Me), 21.1 (2C, Ac), 20.9 (2C, Ac); **LRMS** m/z (ESI+) 507.15 ($[\text{M}+\text{Na}]^+$, 100%); **HRMS** m/z (ESI+) $\text{C}_{22}\text{H}_{28}\text{O}_{12}\text{Na}$ Requires: 507.1478, Found: 507.1480 ($[\text{M}+\text{Na}]^+$); **chPLC** $R_{\text{t}1} = 80.94$ min, area = 5.95%; $R_{\text{t}2} = 84.59$ min, area = 2.78%; $R_{\text{t}3} = 113.84$ min, area = 91.27%. (Phenomenex® Cellulose-1, MeCN/ H_2O , 7:18, 1 mL min $^{-1}$, 30 °C).

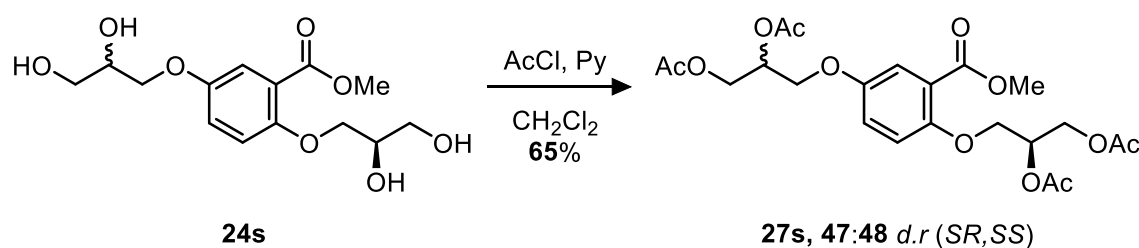
(26s) (2*S*,5*R*)-((2-(methoxycarbonyl)-1,4-phenylene)bis(oxy))bis(propane-3,1,2-triyl) tetraacetate



Following general procedure **G**: Methyl 5-((*S*)-2,3-dihydroxypropoxy)-2-((*R*)-2,3-dihydroxypropoxy)benzoate (**23s**) (25 mg, 0.08 mmol) was charged with pyridine (51.5 μL , 0.64 mmol), CH_2Cl_2 (4 mL) and the AcCl (45.7 μL , 0.64 mmol) was added dropwise. Afforded the title compound as a clear oil (36 mg, 97%). **$[\alpha]_{\text{D}}^{25}$** –13.22 (c. 1.0, CHCl_3 , 95:2 *d.r* (2*S*5*R*, 2*S*5*S*)); **IR** V_{max} cm $^{-1}$ 2957 w, 2924 w, 1737 s (C=O), 1499 s, 1439 s; **$^1\text{H-NMR}$** (400 MHz, CDCl_3) δ_{H} 7.36 (d, $J = 3.3$ Hz, 1H, C6- $\underline{\text{H}}$), 7.02 (dd, $J = 9.1, 3.3$ Hz, 1H, C4- $\underline{\text{H}}$), 6.89 (d, $J = 9.1$ Hz, 1H, C3- $\underline{\text{H}}$), 5.37 (m, 2H, $\underline{\text{CH}}\text{-OAc}$), 4.49 (dd, $J = 12.0, 3.9$ Hz, 1H, $\underline{\text{CH}}_2\text{-OAc}$), 4.42 (dd, $J = 12.0, 3.9$ Hz, 1H, $\underline{\text{CH}}_2\text{-OAc}$), 4.33 (dd, $J = 12.0, 6.1$ Hz, 1H, $\underline{\text{CH}}_2\text{-OAc}$), 4.28 (dd, $J = 12.0, 6.1$ Hz, 1H, $\underline{\text{CH}}_2\text{-OAc}$),

4.15 (m, 2H, ArO-CH₂), 4.10 (d, J = 5.2 Hz, 2H, ArO-CH₂), 3.89 (s, 3H, Me), 2.11 (s, 3H, Ac), 2.11 (s, 3H, Ac), 2.08 (s, 3H, Ac), 2.07 (s, 3H, Ac); **¹³C-NMR** (101 MHz, CDCl₃) δ_c 170.77 (Ac), 170.75 (Ac), 170.5 (Ac), 170.4 (Ac), 166.3 (CO₂Me), 152.6 (C1), 121.7 (C2 & C5), 120.5 (C4), 117.1 (C6), 116.1 (C3), 69.9 (CH-OAc), 69.8 (CH-OAc), 68.3 (ArO-CH₂), 66.9 (ArO-CH₂), 62.8 (CH₂-OAc), 62.6 (CH₂-OAc), 52.4 (Me), 21.1 (2C, Ac), 20.9 (2C, Ac); **LRMS** m/z (ESI+) 507.16 ([M+Na]⁺, 100%); **HRMS** m/z (ESI+) C₂₂H₂₈O₁₂Na Requires: 507.1478, Found: 507.1482 ([M+Na]⁺); **cHPLC** R_{t1} = 73.82 min, area = 2.49%; R_{t2} = 80.39 min, area = 95.17%; R_{t3} = 113.77 min, area = 2.34%. (Phenomenex® Cellulose-1, MeCN/H₂O, 7:18, 1 mL min⁻¹, 30 °C).

(27s) (2*S*,5±)-((2-(methoxycarbonyl)-1,4-phenylene)bis(oxy))bis(propane-3,1,2-triyl) tetraacetate

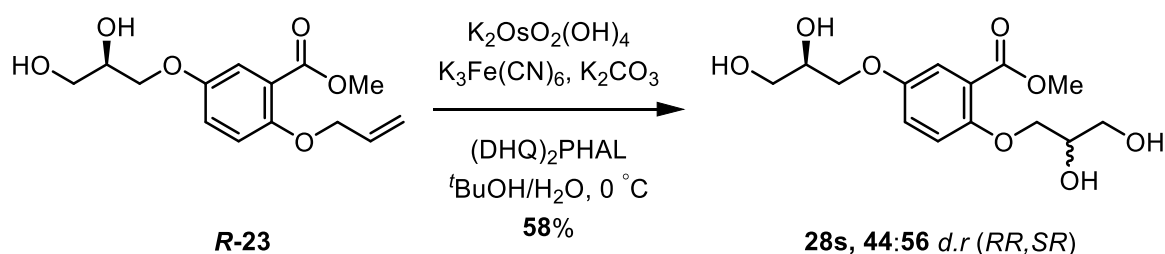


Following general procedure **G**: Methyl 5-((±)-2,3-dihydroxypropoxy)-2-((*S*)-2,3-dihydroxypropoxy)benzoate (**24s**) (5 mg, 0.016 mmol) was charged with pyridine (10.3 μ L, 0.13 mmol), CH₂Cl₂ and the AcCl (9.5 μ L, 0.13 mmol) was added dropwise. Afforded the title compound as a clear oil (5 mg, 65%). 47:48 *d.r* (2*S*5*R*, 2*S*5*S*); **IR** V_{max} cm⁻¹ 2954 w, 1736 s (C=O), 1499 s, 1439 s; **¹H-NMR** (400 MHz, CDCl₃) δ_H 7.35 (d, J = 3.3 Hz, 1H, C6-H), 7.02 (dd, J = 9.1, 3.3 Hz, 1H, C4-H), 6.89 (d, J = 9.1 Hz, 1H, C3-H), 5.37 (m, 2H, CH-OAc), 4.48 (dd, J = 12.0, 3.9 Hz, 1H, CH₂-OAc), 4.41 (dd, J = 12.0, 3.9 Hz, 1H, CH₂-OAc), 4.33 (dd, J = 12.0, 6.1 Hz, 1H, CH₂-OAc), 4.27 (dd, J = 12.0, 6.1 Hz, 1H, CH₂-OAc), 4.15 (m, 2H, ArO-CH₂), 4.10 (d, J = 5.2 Hz, 2H, ArO-CH₂), 3.89 (s, 8H, Me), 2.10 (s, 3H, Ac), 2.10 (s, 3H, Ac), 2.07 (s, 3H, Ac), 2.07 (s,

3H, Ac); **¹³C-NMR** (101 MHz, CDCl₃) δ_C 170.75 (Ac), 170.72 (Ac), 170.54 (Ac), 170.4 (Ac), 166.3 (CO₂Me), 152.6 (C1), 121.7 (C2 & C5), 120.5 (C4), 117.0 (C6), 116.1 (C3), 69.8 (CH-OAc), 69.7 (CH-OAc), 68.3 (ArO-CH₂), 66.9 (ArO-CH₂), 62.7 (CH₂-OAc), 62.5 (CH₂-OAc), 52.3 (Me), 21.10 (Ac), 21.07 (Ac), 20.9 (2C, Ac); **LRMS** *m/z* (ESI+) 507.15 ([M+Na]⁺, 100%); **HRMS** *m/z* (ESI+) C₂₂H₂₈O₁₂Na Requires: 507.1478, Found: 507.1472 ([M+Na]⁺).

Supplementary Compounds 28s-33s (Table 6, Entries 7 to 9)

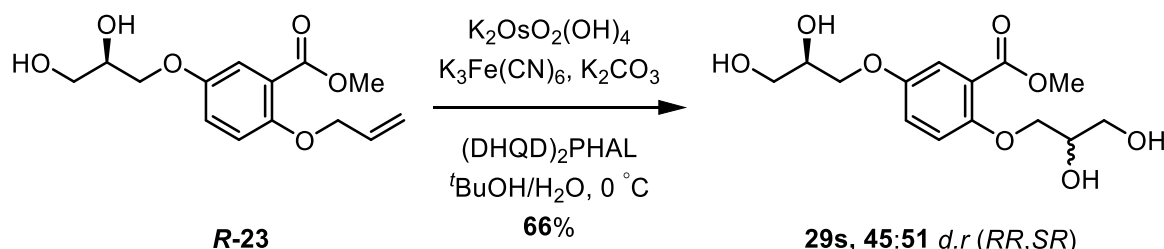
(28s) Methyl 5-((*R*)-2,3-dihydroxypropoxy)-2-((±)-2,3-dihydroxypropoxy)benzoate



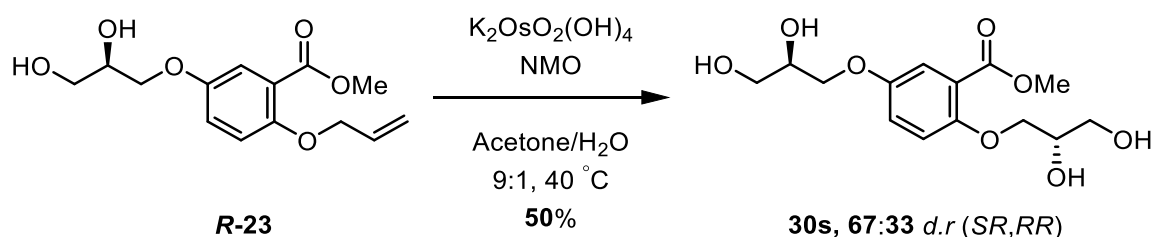
Adapted from general procedure **D**: using stock solutions: **I** (0.2 mL, 0.3 mmol), **II** (0.3 mL, 0.21 mmol), **III** (0.1 mL, 0.2 μmol) and **IV** (0.50 mL, 2.0 μmol). Methyl (*R*)-2-(allyloxy)-5-(2,3-dihydroxypropoxy)benzoate (**R-23**) (28 mg, 0.1 mmol) was added and the reaction mixture was stirred at 0 °C for 12 h with monitoring (EtOH/EtOAc 1:4, *R_f* = 0.19). The solvent was removed under reduced pressure and the crude mixture was purified directly by chromatography (SiO₂, EtOH/EtOAc 1:4) yielding the title compound as a clear oil (18 mg, 58%). [**α**]_D²⁵ +3.46 (c. 0.5, MeOH, 44:56 *d.r.* (2*R*5*R*, 2*S*5*R*)); **IR** *V*_{max} cm⁻¹ 3354 br s, (O-H), 2931 w, 2885 w, 1710 s (C=O), 1583 w, 1500 s, 1439w; **¹H-NMR** (400 MHz, CD₃OD) δ_H 7.35 (d, *J* = 3.0 Hz, 1H, C6-H), 7.18 – 7.12 (m, 1H, C4-H), 7.09 (d, *J* = 9.1 Hz, 1H, C3-H), 4.12 – 3.99 (m, 3H), 3.99 – 3.92 (m, 3H), 3.87 (s, 3H, Me), 3.76 – 3.60 (m, 4H); **¹³C-NMR** (101 MHz, CD₃OD) δ_C 168.2 (CO₂Me), 154.3, 154.2, 122.0, 121.5, 117.8, 117.2, 72.8, 71.8, 71.6, 71.1,

64.3, 64.1, 52.6 (Me); **LRMS** m/z (ESI+) 339.12 (100%, $[M+Na]^+$), 249.08 (60%, $[M-MeOH]^+$); **HRMS** m/z (ESI+) $C_{14}H_{20}O_8Na$ Requires: 339.1056, Found: 339.1060 ($[M+Na]^+$).

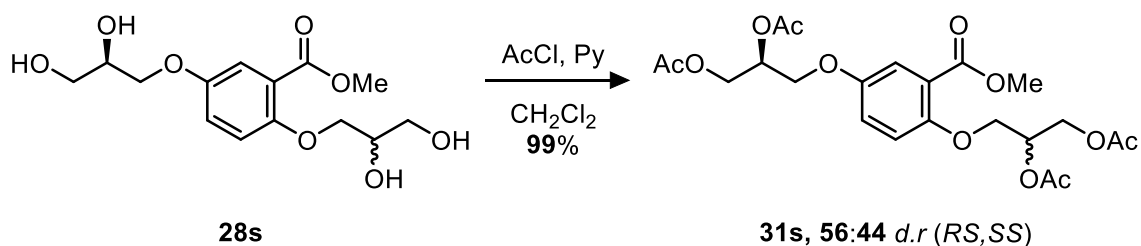
(29s) Methyl 5-((*R*)-2,3-dihydroxypropoxy)-2-((±)-2,3-dihydroxypropoxy)benzoate



Adapted from general procedure **D**: using stock solutions: **I** (0.2 mL, 0.3 mmol), **II** (0.3 mL, 0.21 mmol), **III** (0.1 mL, 0.2 μ mol) and **V** (0.50 mL, 2.0 μ mol). Methyl (*R*)-2-(allyloxy)-5-(2,3-dihydroxypropoxy)benzoate (**R-23**) (28 mg, 0.1 mmol) was added and the reaction mixture was stirred at 0 °C for 12 h with monitoring (EtOH/EtOAc 1:4, R_f = 0.19). The solvent was removed under reduced pressure and the crude mixture was purified directly by chromatography (SiO_2 , EtOH/EtOAc 1:4) yielding the title compound as a clear oil (21 mg, 66%). **[α]_D²⁵** –5.54 (c. 0.5, MeOH, 45:2:3:51 *e.r/d.r* (2*R*5*R*, 2*S*5*S*, 2*R*5*S*, 2*S*5*R*)); **IR** V_{max} cm^{-1} 3350 br s, (O-H), 2926 w, 2880 w, 1708 s (C=O), 1609 w, 1582 w, 1499 s, 1438w, 1285 s, 1245 s, 1210 s; **¹H-NMR** (400 MHz, CD_3OD) δ_H 7.35 (d, J = 3.0 Hz, 1H, C6-H), 7.18 – 7.12 (m, 1H, C4-H), 7.09 (d, J = 9.1 Hz, 1H, C3-H), 4.11 – 3.92 (m, 6H), 3.87 (s, 3H, Me), 3.76 – 3.60 (m, 4H); **¹³C-NMR** (101 MHz, CD_3OD) δ_C 168.2 (CO₂Me), 154.3, 154.2, 122.0, 121.5, 117.8, 117.2, 72.8, 71.8, 71.6, 71.1, 64.3, 64.1, 52.6 (Me); **LRMS** m/z (ESI+) 339.11 (100%, $[M+Na]^+$), 249.08 (40%, $[M-MeOH]^+$); **HRMS** m/z (ESI+) $C_{14}H_{20}O_8Na$ Requires: 339.1056, Found: 339.1059 ($[M+Na]^+$).

(30s) Methyl 5-((*R*)-2,3-dihydroxypropoxy)-2-((*S*)-2,3-dihydroxypropoxy)benzoate

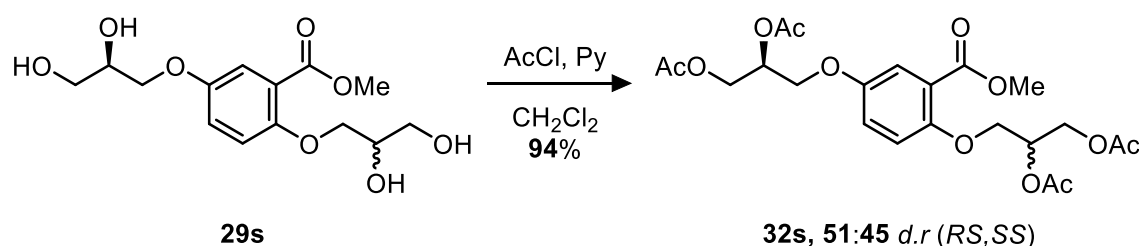
Following general procedure **C**: NMO (8.6 mg, 7.4×10^{-2} mmol) was charged with acetone/H₂O (0.5 mL, 9:1) and K₂OsO₂(OH)₄ (1 mg, 2.7×10^{-3} mmol). Methyl (*R*)-2-(allyloxy)-5-(2,3-dihydroxypropoxy)benzoate (***R*-23**) (18 mg, 6.2×10^{-2} mmol) was added and the reaction mixture was heated at 40 °C for 16 h and monitored (SiO₂, EtOH/EtOAc 1:4, *R_f* = 0.19). The solvent was removed under reduced pressure affording a crude oil that was suspended in EtOH (2 mL) and passed through a silica plug to afford the title compound as a clear oil that was used directly (10 mg, 50%). 67:33 *d.r* (2*S*5*R*, 2*S*5*S*); **¹H-NMR** (400 MHz, CD₃OD) δ_{H} 7.35 (d, *J* = 3.0 Hz, 1H), 7.15 (dd, *J* = 9.0, 3.1 Hz, 1H), 7.09 (d, *J* = 9.1 Hz, 1H), 4.15 – 3.99 (m, 3H), 3.99 – 3.90 (m, 3H), 3.87 (s, 3H), 3.79 – 3.59 (m, 4H).

(31s) (2±,5*S*)-((2-(methoxycarbonyl)-1,4-phenylene)bis(oxy))bis(propane-3,1,2-triyl) tetraacetate

Following general procedure **G** Methyl 5-((*S*)-2,3-dihydroxypropoxy)-2-((±)-2,3-dihydroxypropoxy)benzoate (**28s**) (10 mg, 0.032 mmol) was charged with pyridine (20.6 μ L, 0.26 mmol), CH₂Cl₂ (4 mL) and the AcCl (19.0 μ L, 0.26 mmol) was added dropwise. Afforded the title compound as a clear oil (15 mg, 99%). [α]_D²⁵ +7.13 (c.

1.0, CHCl₃, 56:44 *d.r* (2*R*5*S*, 2*S*5*S*)); **IR** ν_{max} cm⁻¹ 2954 w, 1737 s (C=O), 1500 s, 1440 s; **¹H-NMR** (400 MHz, CDCl₃) δ_{H} 7.36 (d, *J* = 3.3 Hz, 1H, C6-H), 7.03 (dd, *J* = 9.1, 3.3 Hz, 1H, C4-H), 6.89 (d, *J* = 9.1 Hz, 1H, C3-H), 5.37 (m, 2H, CH-OAc), 4.49 (dd, *J* = 12.0, 3.9 Hz, 1H, CH₂-OAc), 4.42 (dd, *J* = 12.0, 3.9 Hz, 1H, CH₂-OAc), 4.33 (dd, *J* = 12.0, 6.1 Hz, 1H, CH₂-OAc), 4.28 (dd, *J* = 12.0, 6.1 Hz, 1H, CH₂-OAc), 4.15 (m, 2H, ArO-CH₂), 4.10 (d, *J* = 5.2 Hz, 2H, ArO-CH₂), 3.89 (s, 3H, Me), 2.11 (s, 3H, Ac), 2.11 (s, 3H, Ac), 2.08 (s, 3H, Ac), 2.07 (s, 3H, Ac); **¹³C-NMR** (101 MHz, CDCl₃) δ_{C} 170.8 (Ac), 170.7 (Ac), 170.5 (Ac), 170.4 (Ac), 166.3 (CO₂Me), 152.6 (C1), 121.7 (C2 & C5), 120.5 (C4), 117.1 (C6), 116.1 (C3), 69.9 (CH-OAc), 69.8 (CH-OAc), 68.3 (ArO-CH₂), 66.9 (ArO-CH₂), 62.8 (CH₂-OAc), 62.6 (CH₂-OAc), 52.4 (Me), 21.1 (2C, Ac), 20.9 (2C, Ac); **LRMS** *m/z* (ESI+) 507.16 ([M+Na]⁺, 100%); **HRMS** *m/z* (ESI+) C₂₂H₂₈O₁₂Na Requires: 507.1478, Found: 507.1472 ([M+Na]⁺); **cHPLC** *R*_{t1} = 84.61 min, area = 55.70%; *R*_{t2} = 114.23 min, area = 44.30%. (Phenomenex® Cellulose-1, MeCN/H₂O, 7:18, 1 mL min⁻¹, 30 °C).

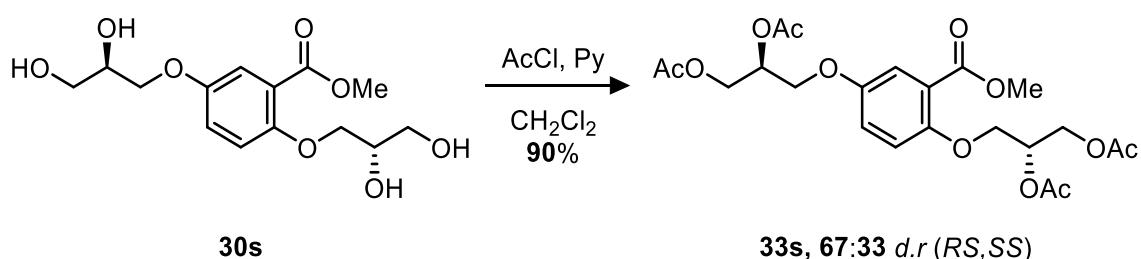
(32s) (2±,5*S*)-((2-(methoxycarbonyl)-1,4-phenylene)bis(oxy))bis(propane-3,1,2-triyl) tetraacetate



Following general procedure **G**: Methyl 5-((*S*)-2,3-dihydroxypropoxy)-2-((±)-2,3-dihydroxypropoxy)benzoate (**29s**) (10 mg, 0.032 mmol) was charged with pyridine (20.6 μ L, 0.26 mmol), CH₂Cl₂ (4 mL) and the AcCl (19.0 μ L, 0.26 mmol) was added dropwise. Afforded the title compound as a clear oil (13 mg, 94%). [α]_D²⁵ +6.83 (c. 1.0, CHCl₃, 2:51:45:2 *e.r/d.r* (2*R*5*R*, 2*R*5*S*, 2*S*5*S*, 2*S*5*R*)); **IR** ν_{max} cm⁻¹ 2954 w, 1737

s (C=O), 1500 s, 1439 s; **¹H-NMR** (400 MHz, CDCl₃) δ_H 7.36 (d, *J* = 3.3 Hz, 1H, C6-H), 7.03 (dd, *J* = 9.1, 3.3 Hz, 1H, C4-H), 6.90 (d, *J* = 9.1 Hz, 1H, C3-H), 5.38 (m, 2H, CH-OAc), 4.49 (dd, *J* = 12.0, 3.9 Hz, 1H, CH₂-OAc), 4.42 (dd, *J* = 12.0, 3.9 Hz, 1H, CH₂-OAc), 4.33 (dd, *J* = 12.0, 6.1 Hz, 1H, CH₂-OAc), 4.29 (dd, *J* = 12.0, 6.1 Hz, 1H, CH₂-OAc), 4.16 (m, 2H, ArO-CH₂), 4.10 (d, *J* = 5.2 Hz, 2H, ArO-CH₂), 3.89 (s, 3H, Me), 2.11 (s, 3H, Ac), 2.11 (s, 3H, Ac), 2.08 (s, 3H, Ac), 2.07 (s, 3H, Ac); **¹³C-NMR** (101 MHz, CDCl₃) δ_C 170.77 (Ac), 170.75 (Ac), 170.5 (Ac), 170.4 (Ac), 166.3 (CO₂Me), 152.6 (C1), 121.7 (C2 & C5), 120.5 (C4), 117.1 (C6), 116.1 (C3), 69.9 (CH-OAc), 69.8 (CH-OAc), 68.3 (ArO-CH₂), 66.9 (ArO-CH₂), 62.8 (CH₂-OAc), 62.6 (CH₂-OAc), 52.4 (Me), 21.1 (2C, Ac), 20.9 (2C, Ac); **LRMS** *m/z* (ESI+) 507.16 ([M+Na]⁺, 100%); **HRMS** *m/z* (ESI+) C₂₂H₂₈O₁₂Na Requires: 507.1478, Found: 507.1478 ([M+Na]⁺); **chPLC** *R*_{t1} = 74.40 min, area = 1.52%; *R*_{t2} = 81.26 min, area = 2.43%; *R*_{t3} = 84.83 min, area = 51.10%; *R*_{t4} = 114.77 min, area = 44.95%. (Phenomenex® Cellulose-1, MeCN/H₂O, 7:18, 1 mL min⁻¹, 30 °C).

(33s) (2*R*,5*S*)-((2-(methoxycarbonyl)-1,4-phenylene)bis(oxy))bis(propane-3,1,2-triyl) tetraacetate

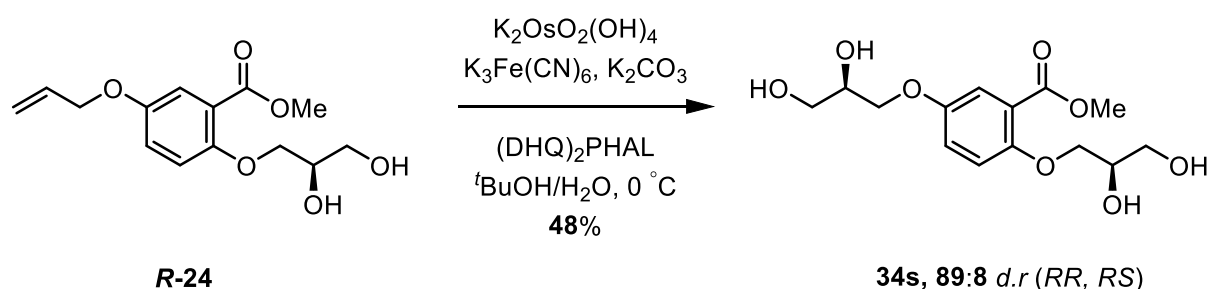


Following general procedure **G**: Methyl 5-((*R*)-2,3-dihydroxypropoxy)-2-((*S*)-2,3-dihydroxypropoxy)benzoate (**30s**) (10 mg, 0.032 mmol) was charged with pyridine (20.6 μL, 0.26 mmol), CH₂Cl₂ (4 mL) and the AcCl (19.0 μL, 0.26 mmol) was added dropwise. Afforded the title compound as a clear oil (12 mg, 90%). [**α**]_D²⁵ –3.14 (c. 1.0, CHCl₃, 67:33 *d.r* (2*R*5*S*, 2*S*5*S*)); **IR** *V*_{max} cm⁻¹ 2952 w, 1736 s (C=O), 1585 w,

1499 s, 1439 s; **¹H-NMR** (400 MHz, CDCl₃) δ_{H} 7.35 (d, J = 3.3 Hz, 1H, C6-H), 7.02 (dd, J = 9.1, 3.3 Hz, 1H, C4-H), 6.89 (d, J = 9.1 Hz, 1H, C3-H), 5.37 (m, 2H, CH-OAc), 4.49 (dd, J = 12.0, 3.9 Hz, 1H, CH₂-OAc), 4.42 (dd, J = 12.0, 3.9 Hz, 1H, CH₂-OAc), 4.33 (dd, J = 12.0, 6.1 Hz, 1H, CH₂-OAc), 4.28 (dd, J = 12.0, 6.1 Hz, 1H, CH₂-OAc), 4.15 (m, 2H, ArO-CH₂), 4.10 (d, J = 5.2 Hz, 2H, ArO-CH₂), 3.89 (s, 3H, Me), 2.10 (s, 3H, Ac), 2.10 (s, 3H, Ac), 2.08 (s, 3H, Ac), 2.07 (s, 3H, Ac); **¹³C-NMR** (101 MHz, CDCl₃) δ_{C} 170.8 (Ac), 170.7 (Ac), 170.44 (Ac), 170.39 (Ac), 166.3 (CO₂Me), 152.6 (C1), 121.8 (C2 & C5), 120.5 (C4), 117.1 (C6), 116.1 (C3), 69.9 (CH-OAc), 69.8 (CH-OAc), 68.3 (ArO-CH₂), 66.9 (ArO-CH₂), 62.8 (CH₂-OAc), 62.6 (CH₂-OAc), 52.3 (Me), 21.1 (2C, Ac), 20.9 (2C, Ac); **LRMS** m/z (ESI+) 507.16 ([M+Na]⁺, 100%); **HRMS** m/z (ESI+) C₂₂H₂₈O₁₂Na Requires: 507.1478, Found: 507.1473 ([M+Na]⁺); **cHPLC** $R_{\text{t}1}$ = 84.09 min, area = 67.09%; $R_{\text{t}2}$ = 113.52 min, area = 32.91%. (Phenomenex® Cellulose-1, MeCN/H₂O, 7:18, 1 mL min⁻¹, 30 °C).

Supplementary Compounds 34s-39s (Table 6, Entries 10 to 12)

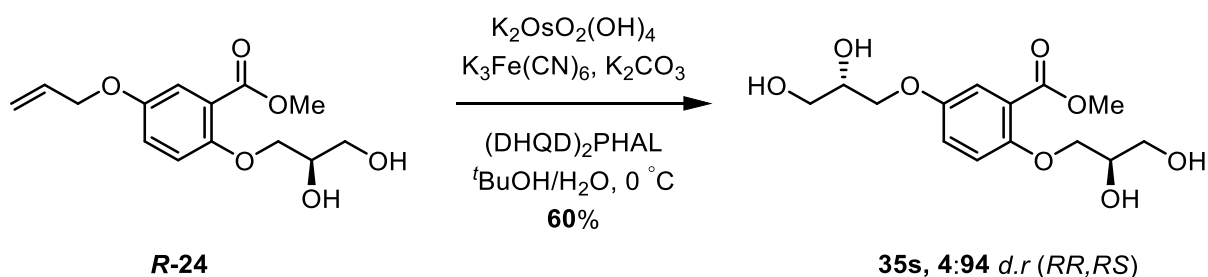
(**34s**) Methyl 2-((*R*)-2,3-dihydroxypropoxy)-5-((*R*)-2,3-dihydroxypropoxy)benzoate



Adapted from general procedure **D**: using stock solutions: **I** (0.2 mL, 0.3 mmol), **II** (0.3 mL, 0.21 mmol), **III** (0.1 mL, 0.2 μ mol) and **V** (0.50 mL, 2.0 μ mol). Methyl (*R*)-5-(allyloxy)-2-(2,3-dihydroxypropoxy)benzoate (**R-24**) (28 mg, 0.1 mmol) was added and the reaction mixture was stirred at 0 °C for 17 h with monitoring (EtOH/EtOAc 1:4, R_{f} = 0.19). The solvent was removed under reduced pressure and the crude

mixture was purified directly by chromatography (SiO₂, EtOH/EtOAc 1:4) yielding the title compound as a clear oil (15 mg, 48%). **[α]_D²⁵** –2.08 (c. 0.25, MeOH, 89:8 *d.r* (2*R*5*R*, 2*R*5*S*)); **IR** V_{max} cm^{–1} 3345 br s, (O–H), 2931 w, 2882 w, 1709 s (C=O), 1582 w, 1500 s, 1439w, 1288 s, 1247 s, 1216 s; **¹H-NMR** (400 MHz, CD₃OD) δ_H 7.35 (d, *J* = 3.1 Hz, 1H, C6–H), 7.15 (dd, *J* = 9.1, 3.1 Hz, 1H, C4–H), 7.09 (d, *J* = 9.1 Hz, 1H, C3–H), 4.13 – 3.99 (m, 3H), 3.99 – 3.89 (m, 3H), 3.87 (s, 3H, Me), 3.78 – 3.59 (m, 4H); **¹³C-NMR** (101 MHz, CD₃OD) δ_C 168.2 (C=O), 154.3, 154.2, 122.0, 121.5, 117.8, 117.2, 72.8, 71.8, 71.6, 71.1, 64.3, 64.1, 52.6 (Me); **LRMS** *m/z* (ESI+) 339.11 (100%, [M+Na]⁺), 186.22 (20%); **HRMS** *m/z* (ESI+) C₁₄H₂₀O₈Na Requires: 339.1056, Found: 339.1056 ([M+Na]⁺).

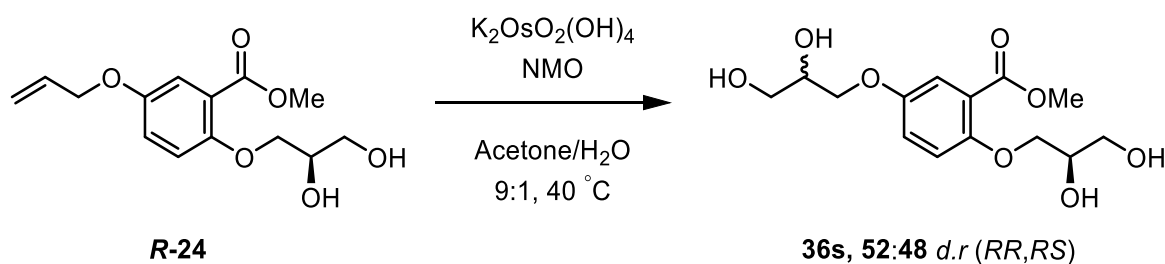
(35s) Methyl 2-((*R*)-2,3-dihydroxypropoxy)-5-((*S*)-2,3-dihydroxypropoxy)benzoate



Adapted from general procedure **D**: using stock solutions: **I** (0.2 mL, 0.3 mmol), **II** (0.3 mL, 0.21 mmol), **III** (0.1 mL, 0.2 μmol) and **IV** (0.50 mL, 2.0 μmol). Methyl (*R*)-5-(allyloxy)-2-((2,3-dihydroxypropoxy)benzoate (**R-24**) (28 mg, 0.1 mmol) was added and the reaction mixture was stirred at 0 °C for 17 h with monitoring (EtOH/EtOAc 1:4, *R_f* = 0.19). The solvent was removed under reduced pressure and the crude mixture was purified directly by chromatography (SiO₂, EtOH/EtOAc 1:4) yielding the title compound as a clear oil (16 mg, 60%). **[α]_D²⁵** –19.39 (c. 1.0, MeOH, 4:94 *d.r* (2*R*5*R*, 2*R*5*S*)); **IR** V_{max} cm^{–1} 3341 br s, (O–H), 2926 w, 1711 s (C=O), 1500 s, 1438w, 1287 s, 1247 s, 1215 s; **¹H-NMR** (400 MHz, CD₃OD) δ_H 7.35 (d, *J* = 3.0 Hz, 1H, C6–

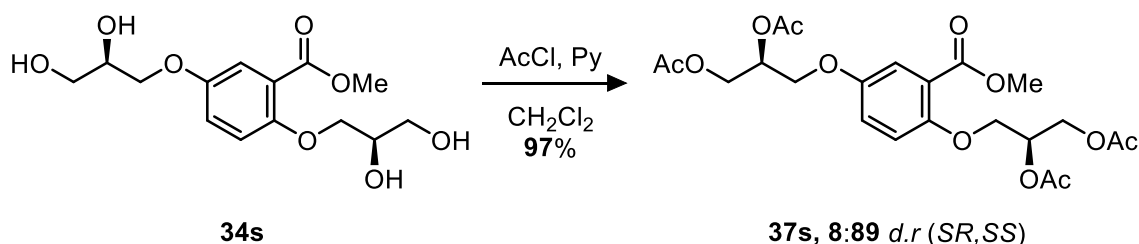
H), 7.18 – 7.12 (m, 1H, C4- H), 7.09 (d, $J = 9.1$ Hz, 1H, C3- H), 4.11 – 3.92 (m, 6H), 3.87 (s, 3H, Me), 3.76 – 3.60 (m, 4H); $^{13}\text{C-NMR}$ (101 MHz, CD_3OD) δ_{C} 168.2 (CO_2Me), 154.3, 154.2, 122.0, 121.5, 117.8, 117.2, 72.8, 71.8, 71.6, 71.1, 64.3, 64.1, 52.6 (Me); **LRMS** m/z (ESI+) 339.11 (100%, $[\text{M}+\text{Na}]^+$), 186.22 (10%); **HRMS** m/z (ESI+) $\text{C}_{14}\text{H}_{20}\text{O}_8\text{Na}$ Requires: 339.1056, Found: 339.1052 ($[\text{M}+\text{Na}]^+$).

(36s) Methyl 2-((*R*)-2,3-dihydroxypropoxy)-5-(2,3-dihydroxypropoxy)benzoate



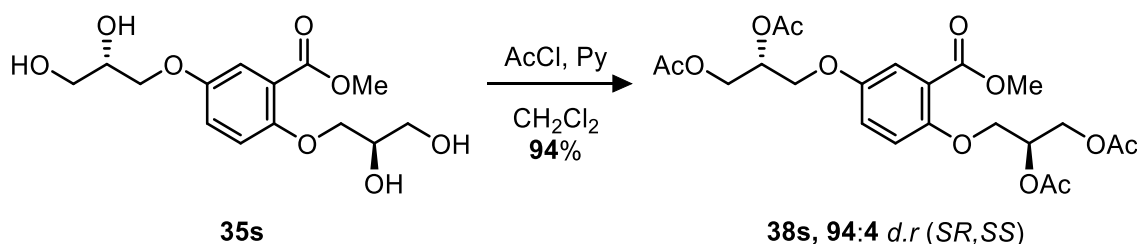
Following general procedure **C**: NMO (8.6 mg, 7.4×10^{-2} mmol) was charged with acetone/ H_2O (0.5 mL, 9:1) and $\text{K}_2\text{OsO}_2(\text{OH})_4$ (1 mg, 2.7×10^{-3} mmol). Methyl (*R*)-5-(allyloxy)-2-(2,3-dihydroxypropoxy)benzoate (**R-24**) (18 mg, 6.2×10^{-2} mmol) was added and the reaction mixture was heated at 40°C for 16 h and monitored (SiO_2 , EtOH/EtOAc 1:4, $R_f = 0.19$). The solvent was removed under reduced pressure to afford a crude oil (8 mg) that was used directly in the next reaction. 52:48 *d.r* (*2R5R*, *2R5S*); $^1\text{H-NMR}$ (400 MHz, CD_3OD) δ_{H} 7.35 (d, $J = 3.0$ Hz, 1H), 7.15 (dd, $J = 9.0, 3.1$ Hz, 1H), 7.09 (d, $J = 9.1$ Hz, 1H), 4.15 – 3.99 (m, 3H), 3.99 – 3.90 (m, 3H), 3.87 (s, 3H, Me), 3.79 – 3.59 (m, 4H).

(37s) (2*S*,5*S*)-((2-(methoxycarbonyl)-1,4-phenylene)bis(oxy))bis(propane-3,1,2-triyl) tetraacetate



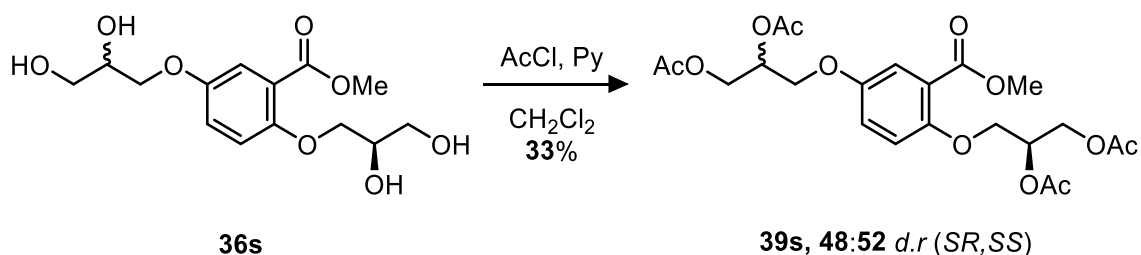
Following general procedure **G**: Methyl 2,5-bis((*R*)-2,3-dihydroxypropoxy)benzoate (**34s**) (10 mg, 0.032 mmol) was charged with pyridine (20.6 μL , 0.26 mmol), CH_2Cl_2 (4 mL) and the AcCl (19.0 μL , 0.26 mmol) was added dropwise. Afforded the title compound as a clear oil (14 mg, 97%). **[α]_D²⁵** –11.77 (c. 1.0, CHCl_3 , 8:89 *d.r.* (2*S*5*R*, 2*S*5*S*)); **IR** V_{max} cm^{-1} 2954 w, 1736 s (C=O), 1500 s, 1439 s; **¹H-NMR** (400 MHz, CDCl_3) δ_{H} 7.35 (d, J = 3.3 Hz, 1H, C6-H), 7.02 (dd, J = 9.1, 3.3 Hz, 1H, C4-H), 6.89 (d, J = 9.1 Hz, 1H, C3-H), 5.37 (m, 2H, CH-OAc), 4.49 (dd, J = 12.0, 3.9 Hz, 1H, CH₂-OAc), 4.42 (dd, J = 12.0, 3.9 Hz, 1H, CH₂-OAc), 4.33 (dd, J = 12.0, 6.1 Hz, 1H, CH₂-OAc), 4.28 (dd, J = 12.0, 6.1 Hz, 1H, CH₂-OAc), 4.15 (m, 2H, ArO-CH₂), 4.10 (d, J = 5.2 Hz, 2H, ArO-CH₂), 3.89 (s, 3H, Me), 2.10 (s, 3H, Ac), 2.10 (s, 3H, Ac), 2.08 (s, 3H, Ac), 2.07 (s, 3H, Ac); **¹³C-NMR** (101 MHz, CDCl_3) δ_{C} 170.8 (Ac), 170.7 (Ac), 170.44 (Ac), 170.39 (Ac), 166.3 (CO₂Me), 152.6 (C1), 121.7 (C2 & C5), 120.5 (C4), 117.0 (C6), 116.1 (C3), 69.9 (CH-OAc), 69.8 (CH-OAc), 68.3 (ArO-CH₂), 66.9 (ArO-CH₂), 62.8 (CH₂-OAc), 62.5 (CH₂-OAc), 52.3 (Me), 21.1 (2C, Ac), 20.9 (2C, Ac); **LRMS** m/z (ESI+) 507.15 ([M+Na]⁺, 100%); **HRMS** m/z (ESI+) C₂₂H₂₈O₁₂Na Requires: 507.1478, Found: 507.1474 ([M+Na]⁺); **chPLC** $R_{\text{t}1}$ = 80.28 min, area = 7.95%; $R_{\text{t}2}$ = 84.04 min, area = 2.91%; $R_{\text{t}3}$ = 113.62 min, area = 89.14%. (Phenomenex® Cellulose-1, MeCN/H₂O, 7:18, 1 mL min⁻¹, 30 °C)

(38s) (2*S*,5*R*)-((2-(methoxycarbonyl)-1,4-phenylene)bis(oxy))bis(propane-3,1,2-triyl) tetraacetate



Following general procedure **G**: Methyl 5-((*S*)-2,3-dihydroxypropoxy)-2-((*R*)-2,3-dihydroxypropoxy)benzoate (**35s**) (10 mg, 0.032 mmol) was charged with pyridine (20.6 μ L, 0.26 mmol), CH_2Cl_2 (4 mL) and the AcCl (19.0 μ L, 0.26 mmol) was added dropwise. Afforded the title compound as a clear oil (13 mg, 94%). **[α]_D²⁵** –12.79 (c. 1.0, CHCl_3 , 94:4 *d.r* (2*S*5*R*, 2*S*5*S*)); **IR** V_{max} cm^{-1} 2954 w, 1736 s (C=O), 1500 s, 1439 s; **¹H-NMR** (400 MHz, CDCl_3) δ_{H} 7.35 (d, J = 3.3 Hz, 1H, C6-H), 7.02 (dd, J = 9.1, 3.3 Hz, 1H, C4-H), 6.89 (d, J = 9.1 Hz, 1H, C3-H), 5.37 (m, 2H, CH-OAc), 4.49 (dd, J = 12.0, 3.9 Hz, 1H, CH₂-OAc), 4.42 (dd, J = 12.0, 3.9 Hz, 1H, CH₂-OAc), 4.33 (dd, J = 12.0, 6.1 Hz, 1H, CH₂-OAc), 4.27 (dd, J = 12.0, 6.1 Hz, 1H, CH₂-OAc), 4.14 (m, 2H, ArO-CH₂), 4.09 (d, J = 5.2 Hz, 2H, ArO-CH₂), 3.89 (s, 3H, Me), 2.10 (s, 3H, Ac), 2.10 (s, 3H, Ac), 2.08 (s, 3H, Ac), 2.07 (s, 3H, Ac); **¹³C-NMR** (101 MHz, CDCl_3) δ_{C} 170.8 (Ac), 170.7 (Ac), 170.44 (Ac), 170.39 (Ac), 166.3 (CO₂Me), 152.6 (C1), 121.7 (C2 & C5), 120.5 (C4), 117.0 (C6), 116.1 (C3), 69.84 (CH-OAc), 69.76 (CH-OAc), 68.3 (ArO-CH₂), 66.9 (ArO-CH₂), 62.8 (CH₂-OAc), 62.5 (CH₂-OAc), 52.3 (Me), 21.11 (Ac), 21.08 (Ac), 20.9 (2C, Ac); **LRMS** m/z (ESI⁺) 507.16 ($[\text{M}+\text{Na}]^+$, 100%); **HRMS** m/z (ESI⁺) C₂₂H₂₈O₁₂Na Requires: 507.1478, Found: 507.1476 ($[\text{M}+\text{Na}]^+$); **cHPLC** $R_{\text{t}1}$ = 74.39 min, area = 2.31%; $R_{\text{t}2}$ = 81.08 min, area = 94.21%; $R_{\text{t}3}$ = 114.91 min, area = 3.48%. (Phenomenex[®] Cellulose-1, MeCN/H₂O, 7:18, 1 mL min⁻¹, 30 °C).

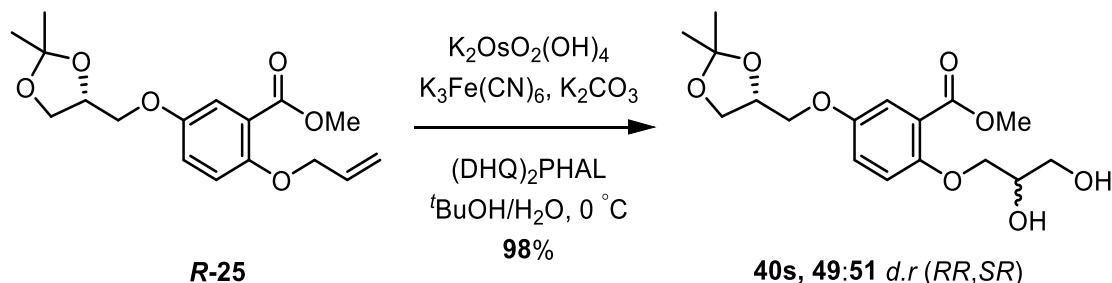
(39s) (2*S*,5*±*)-((2-(methoxycarbonyl)-1,4-phenylene)bis(oxy))bis(propane-3,1,2-triyl) tetraacetate



Following general procedure **G**: Methyl 5-((±)-2,3-dihydroxypropoxy)-2-((*S*)-2,3-dihydroxypropoxy)benzoate (**36s**) (10 mg, 0.032 mmol) was charged with pyridine (20.6 μ L, 0.26 mmol), CH_2Cl_2 (4.0 mL) and the AcCl (19.0 μ L, 0.26 mmol) was added dropwise. Afforded the title compound as a clear oil (5 mg, 33%). 48:52 *d.r* (2*S*5*R*, 2*S*5*S*); **IR** ν_{max} cm^{-1} 2952 w, 1736 s (C=O), 1584 w, 1499 s, 1439 s; **$^1\text{H-NMR}$** (400 MHz, CDCl_3) δ_{H} 7.35 (d, J = 3.3 Hz, 1H, C6-H), 7.02 (dd, J = 9.1, 3.3 Hz, 1H, C4-H), 6.89 (d, J = 9.1 Hz, 1H, C3-H), 5.37 (m, 2H, CH-OAc), 4.49 (dd, J = 12.0, 3.9 Hz, 1H, CH₂-OAc), 4.42 (dd, J = 12.0, 3.9 Hz, 1H, CH₂-OAc), 4.33 (dd, J = 12.0, 6.1 Hz, 1H, CH₂-OAc), 4.28 (dd, J = 12.0, 6.1 Hz, 1H, CH₂-OAc), 4.15 (m, 2H, ArO-CH₂), 4.10 (d, J = 5.2 Hz, 2H, ArO-CH₂), 3.89 (s, 3H, Me), 2.10 (s, 3H, Ac), 2.10 (s, 3H, Ac), 2.07 (s, 3H, Ac), 2.07 (s, 3H, Ac); **$^{13}\text{C-NMR}$** (101 MHz, CDCl_3) δ_{C} 170.75 (Ac), 170.72 (Ac), 170.4 (Ac), 170.4 (Ac), 166.3 (CO₂Me), 152.6 (C1), 121.7 (C2 & C5), 120.5 (C4), 117.0 (C6), 116.1 (C3), 69.8 (CH-OAc), 69.7 (CH-OAc), 68.3 (ArO-CH₂), 66.9 (ArO-CH₂), 62.7 (CH₂-OAc), 62.65 (CH₂-OAc), 52.3 (Me), 21.09 (Ac), 21.07 (Ac), 20.9 (2C, Ac); **LRMS** m/z (ESI+) 507.16 ([M+Na]⁺, 100%); **HRMS** m/z (ESI+) $\text{C}_{22}\text{H}_{28}\text{O}_{12}\text{Na}$ Requires: 507.1478, Found: 507.1482 ([M+Na]⁺); **chPLC** $R_{\text{t}1}$ = 80.09 min, area = 48.24%; $R_{\text{t}2}$ = 113.19 min, area = 51.76%. (Phenomenex® Cellulose-1, MeCN/H₂O, 7:18, 1 mL min⁻¹, 30 °C)

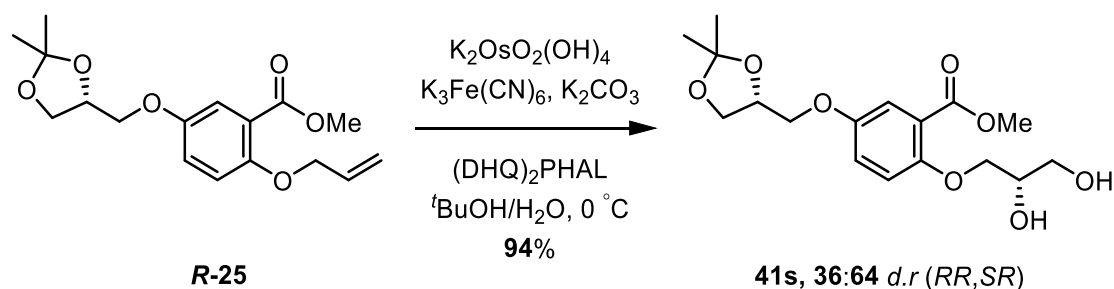
Supplementary Compounds 40s-47s (Table 6, Entries 13 to 15)

(40s) Methyl 2-((±)-2,3-dihydroxypropoxy)-5-(((*R*)-2,2-dimethyl-1,3-dioxolan-4-yl)methoxy)benzoate

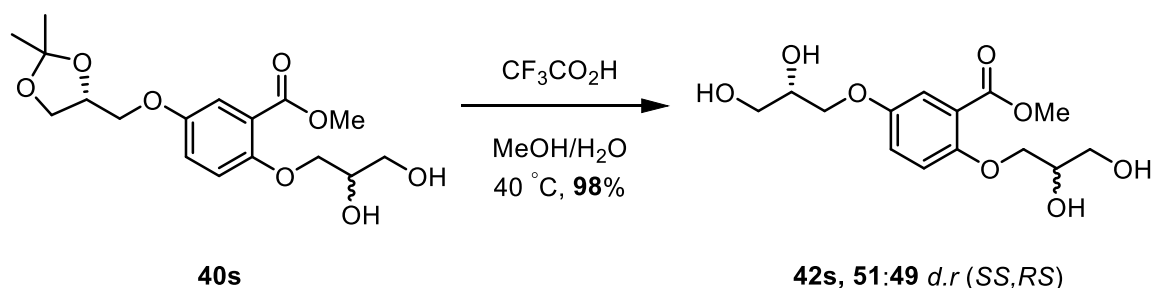


Following general procedure **D**: using stock solutions: **I** (0.5 mL, 0.75 mmol), **II** (0.5 mL, 0.75 mmol), **III** (0.25 mL, 0.5 μ mol) and **IV** (1.25 mL, 5.0 μ mol). Methyl (*S*)-2-(allyloxy)-5-((2,2-dimethyl-1,3-dioxolan-4-yl)methoxy)benzoate (**R-25**) (86 mg, 0.25 mmol) was added and the reaction mixture was stirred at 0 °C for 21 h with monitoring (EtOAc/hexane 1:1, R_f = 0.09). Afforded the title compound as a clear oil (87 mg, 98%). **[α]_D²⁵** –3.80 (c. 1.0, CHCl₃, 49:51 *d.r* (2*R*5*R*, 2*S*5*R*)); **IR** ν_{max} cm^{–1} 3426 br s, (O–H), 2987 w, 2936 w, 2885 w, 1712 s (C=O), 1614 w, 1500 w, 1439 w; **¹H-NMR** (400 MHz, CDCl₃) δ_c 7.42 (d, J = 3.2 Hz, 1H C6–H), 7.08 (dd, J = 9.1, 3.2 Hz, 1H, C4–H), 6.93 (d, J = 9.1 Hz, 1H, C3–H), 4.46 (p, J = 5.7 Hz, 1H, CH–OC(CH₃)₂), 4.26 (dd, J = 9.1, 2.7 Hz, 1H, C2–OCH₂), 4.16 (dd, J = 8.5, 6.5 Hz, 1H, CH₂–OC(CH₃)₂), 4.12 – 3.99 (m, 3H, C2–OCH₂ & CH–OH & C5–OCH₂), 3.97 – 3.85 (m, 5H, C5–OCH₂, Me & CH₂–OC(CH₃)₂), 3.82 (br d, J = 3.9 Hz, 2H, CH₂–OH), 1.46 (s, 3H, C(CH₃)₂), 1.40 (s, 3H, C(CH₃)₂); **¹³C-NMR** (101 MHz, CDCl₃) δ_c 166.2 (CO₂Me), 153.8 (C2), 152.7 (C5), 121.3 (C4), 120.0 (C1), 117.0 (C6), 116.2 (C3), 110.0 (C(CH₃)₂), 74.1 (CH–OC(CH₃)₂), 73.6 (C2–OCH₂), 69.7 (C5–OCH₂), 69.5 (CH–OH), 66.8 (CH₂–OC(CH₃)₂), 63.6 (CH₂–OH), 52.5 (Me), 26.9 (C(CH₃)₂), 25.4 (C(CH₃)₂); **LRMS** m/z (ESI+) 379.09 (100%, [M+Na]⁺); **HRMS** m/z (ESI+) C₁₇H₂₄O₈Na Requires: 379.1363, Found: 379.1364 ([M+Na]⁺).

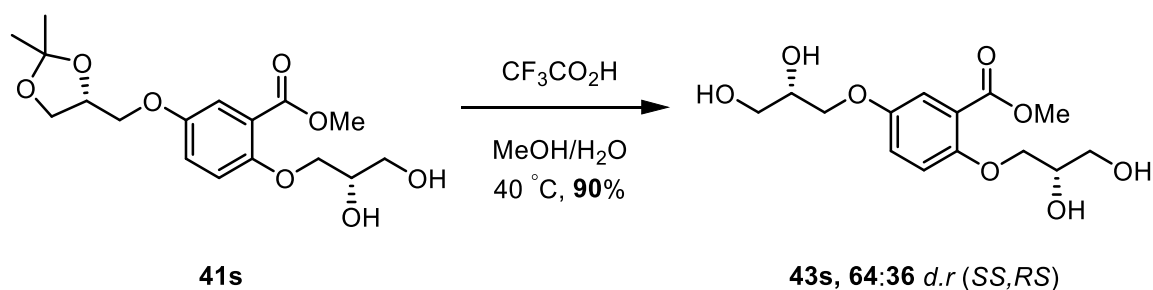
(41s) Methyl 2-((*S*)-2,3-dihydroxypropoxy)-5-(((*R*)-2,2-dimethyl-1,3-dioxolan-4-yl)methoxy)benzoate



Following general procedure **D**: using stock solutions: **I** (0.5 mL, 0.75 mmol), **II** (0.5 mL, 0.75 mmol), **III** (0.25 mL, 0.5 μ mol) and **V** (1.25 mL, 5.0 μ mol). Methyl (*S*)-2-(allyloxy)-5-((2,2-dimethyl-1,3-dioxolan-4-yl)methoxy)benzoate (**R-25**) (86 mg, 0.25 mmol) was added and the reaction mixture was stirred at 0 °C for 21 h with monitoring (EtOAc/hexane 1:1, R_f = 0.09). Afforded the title compound as a clear oil (84 mg, 94%). **[α]_D²⁵** –3.46 (c. 1.0, CHCl₃, 36:64 d.r. (2*R*5*R*, 2*S*5*R*)); **IR** V_{\max} cm^{–1} 3425 br s, (O–H), 2988 w, 2937 w, 2878 w, 1713 s (C=O), 1614 w, 1500 s, 1439 w; **¹H-NMR** (400 MHz, CDCl₃) δ_c 7.41 (d, J = 3.2 Hz, 1H C6–H), 7.07 (dd, J = 9.1, 3.2 Hz, 1H, C4–H), 6.93 (d, J = 9.1 Hz, 1H, C3–H), 4.46 (p, J = 5.7 Hz, 1H, CH–OC(CH₃)₂), 4.24 (dd, J = 9.2, 2.6 Hz, 1H, C2–OCH₂), 4.16 (dd, J = 8.5, 6.4 Hz, 1H, CH₂–OC(CH₃)₂), 4.10 – 3.98 (m, 3H, C2–OCH₂ & CH–OH & C5–OCH₂), 3.95 – 3.89 (m, 1H, C5–OCH₂), 3.88 (m, 4H, Me & CH₂–OC(CH₃)₂), 3.81 (br d, J = 3.8 Hz, 2H, CH₂–OH), 2.11 (br s, 2H, O–H), 1.46 (s, 3H, C(CH₃)₂), 1.40 (s, 3H, C(CH₃)₂); **¹³C-NMR** (101 MHz, CDCl₃) δ_c 166.2 (CO₂Me), 153.8 (C2), 152.7 (C5), 121.2 (C4), 120.0 (C1), 117.0 (C6), 116.2 (C3), 110.0 (C(CH₃)₂), 74.1 (CH–OC(CH₃)₂), 73.6 (C2–OCH₂), 69.7 (C5–OCH₂), 69.5 (CH–OH), 66.8 (CH₂–OC(CH₃)₂), 63.6 (CH₂–OH), 52.5 (Me), 26.9 (C(CH₃)₂), 25.4 (C(CH₃)₂); **LRMS** m/z (ESI+) 379.13 (100%, [M+Na]⁺); **HRMS** m/z (ESI+) C₁₇H₂₄O₈Na Requires: 379.1363, Found: 379.1364 ([M+Na]⁺)

(42s) Methyl 2-((±)-2,3-dihydroxypropoxy)-5-((*S*)-2,3-dihydroxypropoxy)benzoate

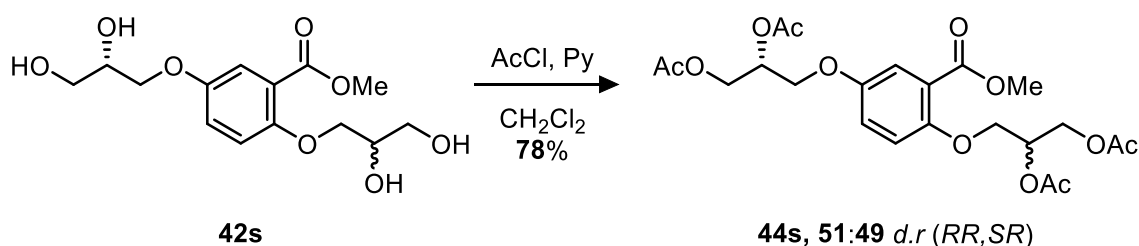
Following general procedure **F**: methyl 2-((±)-2,3-dihydroxypropoxy)-5-(((*R*)-2,2-dimethyl-1,3-dioxolan-4-yl)methoxy)benzoate (**40s**) (50 mg, 0.14 mmol) was stirred at 40 °C for 24 h. Afforded the title compound as a clear oil (43 mg, 98%). **[α]_D²⁵** +13.16 (c. 1.0, MeOH, 51:49 *d.r* (2*S*5*S*, 2*R*5*S*)); **IR** V_{\max} cm⁻¹ 3360 br s (O-H) 2935 w, 2879 w, 1708 s (C=O), 1610 w, 1581 w, 1498 s, 1438 s, 1417 w; **¹H-NMR** (400 MHz, CD₃OD) δ_H 7.35 (d, *J* = 3.1 Hz, 1H, C6-H), 7.15 (dd, *J* = 9.1, 3.1 Hz, 1H, C4-H), 7.09 (d, *J* = 9.1 Hz, 1H, C3-H), 4.13 – 3.99 (m, 3H), 3.99 – 3.89 (m, 3H), 3.87 (s, 3H, Me), 3.78 – 3.59 (m, 4H); **¹³C-NMR** (101 MHz, CD₃OD) δ_C 168.2 (C=O), 154.3, 154.2, 121.9, 121.5, 117.8, 117.2, 72.8, 71.7, 71.6, 71.1, 64.3, 64.1, 52.7 (Me); **LRMS** *m/z* (ESI+) 339.10 (100%, [M+Na]⁺); **HRMS** *m/z* (ESI+) C₁₄H₂₀O₈Na Requires: 339.1050, Found: 339.1049 ([M+Na]⁺)

(43s) Methyl 2-((*S*)-2,3-dihydroxypropoxy)-5-((*S*)-2,3-dihydroxypropoxy)benzoate

Following general procedure **F**: methyl 2-((*S*)-2,3-dihydroxypropoxy)-5-(((*R*)-2,2-dimethyl-1,3-dioxolan-4-yl)methoxy)benzoate (**41s**) (50 mg, 0.14 mmol) was stirred

at 40 °C for 24 h. Afforded the title compound as a clear oil (40 mg, 90%). **[α]_D²⁵** –7.96 (c. 1.0, MeOH, 64:36 *d.r* (2*S*5*S*, 2*R*5*S*)); **IR** V_{\max} cm^{–1} 3360 br s (O–H) 2935 w, 2879 w, 1708 s (C=O), 1610 w, 1581 w, 1498 s, 1438 s, 1417 w; **¹H-NMR** (400 MHz, CD₃OD) δ_{H} 7.35 (d, *J* = 3.1 Hz, 1H, C6-H), 7.15 (dd, *J* = 9.1, 3.1 Hz, 1H, C4-H), 7.09 (d, *J* = 9.1 Hz, 1H, C3-H), 4.13 – 3.99 (m, 3H), 3.99 – 3.89 (m, 3H), 3.87 (s, 3H, Me), 3.78 – 3.59 (m, 4H); **¹³C-NMR** (101 MHz, CD₃OD) δ_{C} 168.2 (C=O₂Me), 154.3, 154.2, 121.9, 121.5, 117.8, 117.1, 72.8, 71.7, 71.6, 71.1, 64.2, 64.1, 52.6 (Me); **LRMS** *m/z* (ESI+) 339.10 (100%, [M+Na]⁺); **HRMS** *m/z* (ESI+) C₁₄H₂₀O₈Na Requires: 339.1050, Found: 339.1049 ([M+Na]⁺).

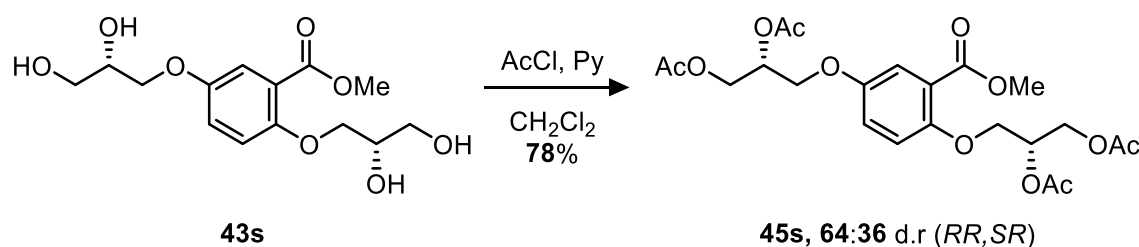
(44s) (2±,5*R*)-((2-(methoxycarbonyl)-1,4-phenylene)bis(oxy))bis(propane-3,1,2-triyl) tetraacetate



Following general procedure **G**: Methyl 5-((*S*)-2,3-dihydroxypropoxy)-2-((±)-2,3-dihydroxypropoxy)benzoate (**42s**) (5 mg, 0.016 mmol) was charged with pyridine (10.3 μL, 0.13 mmol), CH₂Cl₂ (4 mL) and the AcCl (9.5 μL, 0.13 mmol) was added dropwise. Afforded the title compound as a clear oil (6 mg, 78%). **[α]_D²⁵** –3.09 (c. 1.0, CHCl₃, 51:49 *d.r* (2*R*5*R*, 2*S*5*R*)); **IR** V_{\max} cm^{–1} 2954 w, 1740 s (C=O), 1500 w, 1439 w, 1219 s; **¹H-NMR** (400 MHz, CDCl₃) δ_{H} 7.35 (d, *J* = 3.3 Hz, 1H, C6-H), 7.02 (dd, *J* = 9.1, 3.3 Hz, 1H, C4-H), 6.89 (d, *J* = 9.1 Hz, 1H, C3-H), 5.37 (m, 2H, CH-OAc), 4.49 (dd, *J* = 12.0, 3.9 Hz, 1H, CH₂-OAc), 4.42 (dd, *J* = 12.0, 3.9 Hz, 1H, CH₂-OAc), 4.33 (dd, *J* = 12.0, 6.1 Hz, 1H, CH₂-OAc), 4.28 (dd, *J* = 12.0, 6.1 Hz, 1H, CH₂-OAc), 4.15 (m, 2H, ArO-CH₂), 4.10 (d, *J* = 5.2 Hz, 2H, ArO-CH₂), 3.89 (s, 3H, Me), 2.10 (s, 3H,

Ac), 2.10 (s, 3H, Ac), 2.08 (s, 3H, Ac), 2.07 (s, 3H, Ac); **¹³C-NMR** (101 MHz, CDCl₃) δ_c 170.8 (Ac), 170.7 (Ac), 170.5 (Ac), 170.4 (Ac), 166.3 (CO₂Me), 152.6 (C1), 121.7 (C2 & C5), 120.5 (C4), 117.0 (C6), 116.1 (C3), 69.84 (CH-OAc), 69.76 (CH-OAc), 68.3 (ArO-CH₂), 66.9 (ArO-CH₂), 62.8 (CH₂-OAc), 62.5 (CH₂-OAc), 52.4 (Me), 21.1 (2C, Ac), 20.9 (2C, Ac); **LRMS** m/z (ESI+) 507.15 ([M+Na]⁺, 100%); **HRMS** m/z (ESI+) C₂₂H₂₈O₁₂Na Requires: 507.1478, Found: 507.1484 ([M+Na]⁺); **cHPLC** R_{t1} = 72.87 min, area = 51.24%; R_{t2} = 79.26 min, area = 48.76%; (Phenomenex® Cellulose-1, MeCN/H₂O, 7:18, 1 mL min⁻¹, 30 °C).

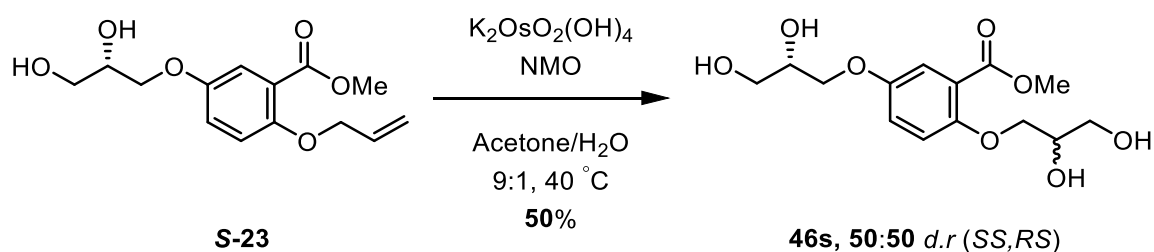
(45s) (2*R*,5*R*)-((2-(methoxycarbonyl)-1,4-phenylene)bis(oxy))bis(propane-3,1,2-triyl) tetraacetate



Following general procedure **G**: Methyl 5-((*S*)-2,3-dihydroxypropoxy)-2-((±)-2,3-dihydroxypropoxy)benzoate (**43s**) (5 mg, 0.016 mmol) was charged with pyridine (10.3 μ L, 0.13 mmol), CH₂Cl₂ (4 mL) and the AcCl (9.5 μ L, 0.13 mmol) was added dropwise. Afforded the title compound as a clear oil (6 mg, 78%). [α]_D²⁵ –6.76 (c. 1.0, CHCl₃, 64:36 *d.r* (2*R*5*R*, 2*S*5*R*)); **IR** V_{\max} cm⁻¹ 2954 w, 1740 s (C=O), 1500 w, 1439 w, 1219 s; **¹H-NMR** (400 MHz, CDCl₃) δ_H 7.35 (d, J = 3.3 Hz, 1H, C6-H), 7.02 (dd, J = 9.1, 3.3 Hz, 1H, C4-H), 6.89 (d, J = 9.1 Hz, 1H, C3-H), 5.37 (m, 2H, CH-OAc), 4.49 (dd, J = 12.0, 3.9 Hz, 1H, CH₂-OAc), 4.42 (dd, J = 12.0, 3.9 Hz, 1H, CH₂-OAc), 4.33 (dd, J = 12.0, 6.1 Hz, 1H, CH₂-OAc), 4.28 (dd, J = 12.0, 6.1 Hz, 1H, CH₂-OAc), 4.15 (m, 2H, ArO-CH₂), 4.10 (d, J = 5.2 Hz, 2H, ArO-CH₂), 3.88 (s, 3H, Me), 2.10 (s, 3H, Ac), 2.10 (s, 3H, Ac), 2.08 (s, 3H, Ac), 2.07 (s, 3H, Ac); **¹³C-NMR** (101 MHz, CDCl₃)

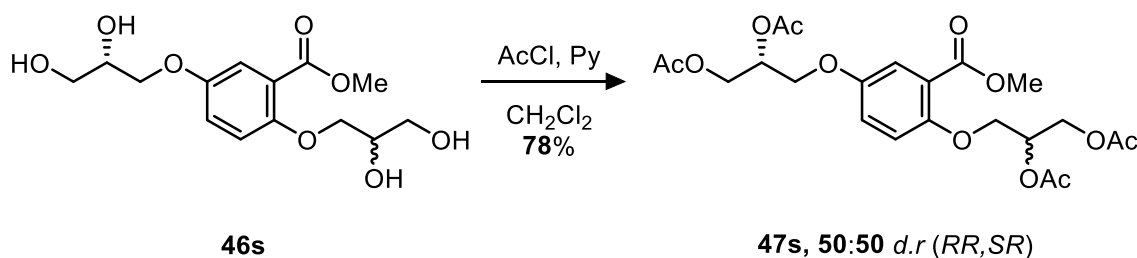
δ_c 170.8 (Ac), 170.7 (Ac), 170.44 (Ac), 170.38 (Ac), 166.3 (CO_2Me), 152.6 (C1), 121.7 (C2 & C5), 120.5 (C4), 117.0 (C6), 116.1 (C3), 69.8 (CH-OAc), 69.7 (CH-OAc), 68.3 (ArO-CH_2), 66.9 (ArO-CH_2), 62.7 ($\text{CH}_2\text{-OAc}$), 62.5 ($\text{CH}_2\text{-OAc}$), 52.3 (Me), 21.09 (Ac), 21.07 (Ac) 20.9 (2C, Ac); **LRMS** m/z (ESI+) 507.15 ($[\text{M}+\text{Na}]^+$, 100%); **HRMS** m/z (ESI+) $\text{C}_{22}\text{H}_{28}\text{O}_{12}\text{Na}$ Requires: 507.1478, Found: 507.1480 ($[\text{M}+\text{Na}]^+$); **chPLC** R_{t1} = 70.84 min, area = 63.62%; R_{t2} = 77.17 min, area = 36.38%; (Phenomenex[®] Cellulose-1, MeCN/ H_2O , 7:18, 1 mL min⁻¹, 30 °C).

(46s) Methyl 5-((*S*)-2,3-dihydroxypropoxy)-2-((\pm)-2,3-dihydroxypropoxy)benzoate

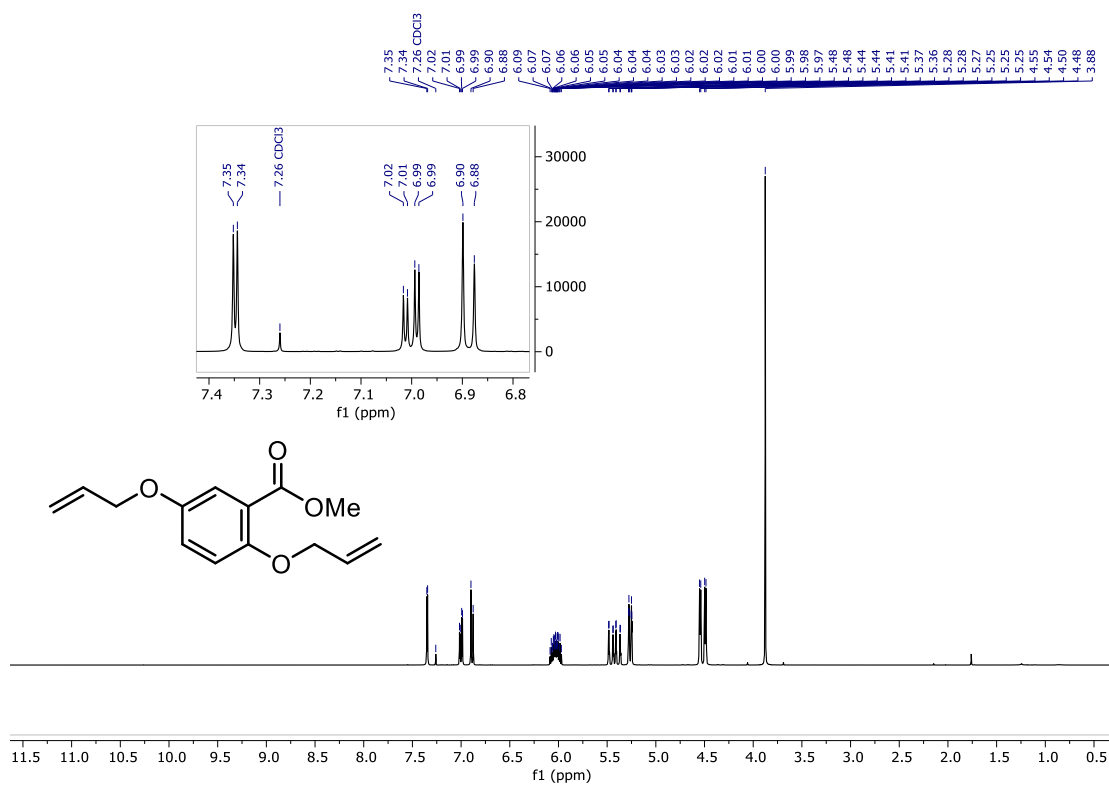
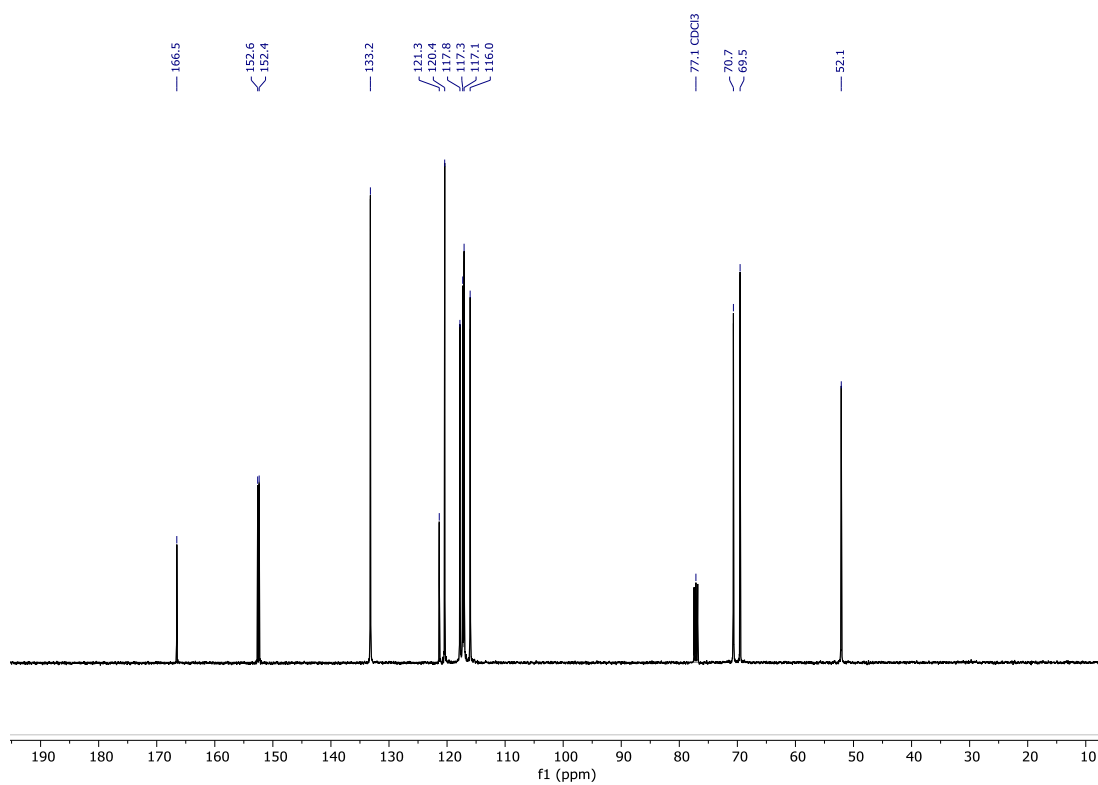


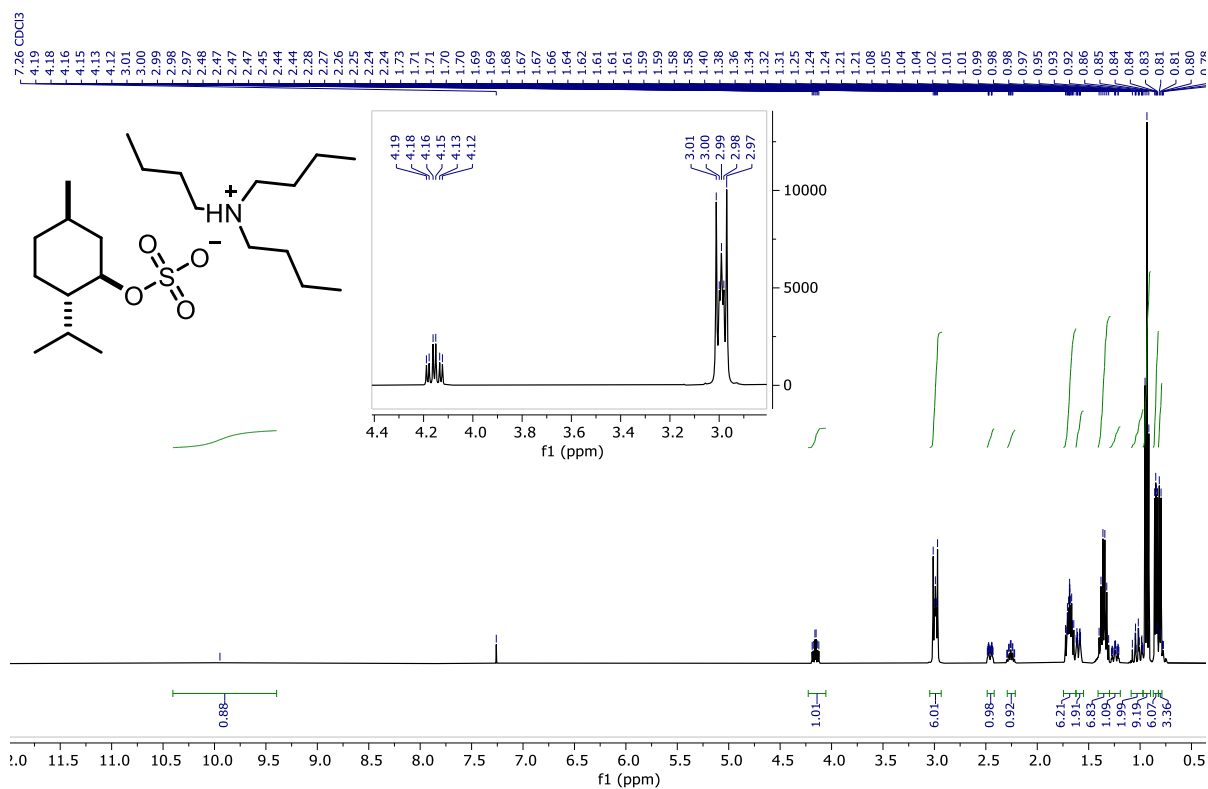
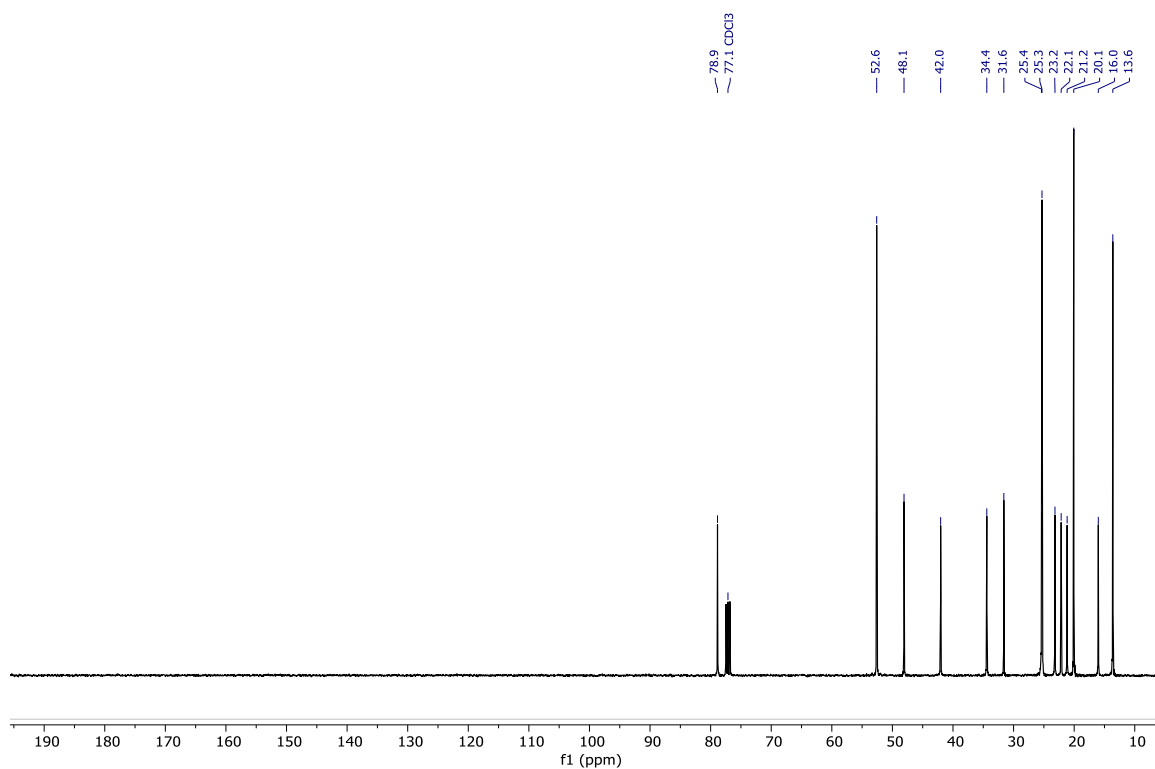
Following general procedure **C**: NMO (8.6 mg, 7.4×10^{-2} mmol) was charged with acetone/ H_2O (0.5 mL, 9:1) and $\text{K}_2\text{OsO}_2(\text{OH})_4$ (1 mg, 2.7×10^{-3} mmol). Methyl (*S*)-2-(allyloxy)-5-(2,3-dihydroxypropoxy)benzoate (**S-23**) (18 mg, 6.2×10^{-2} mmol) was added and the reaction mixture was heated at 40 °C for 16 h and monitored (SiO_2 , EtOH/EtOAc 1:4, R_f = 0.19). Afforded the title compound as a clear oil (10 mg, 50%). **[α]_D²⁵** +5.88 (c. 1.0, MeOH, 50:50 *d.r* (2*SSS*, 2*RSS*)); **IR** ν_{max} cm⁻¹ 3335 br. s (O-H), 2937 w, 1701 s (C=O), 1610 s, 1455 s; **¹H-NMR** (400 MHz, CD_3OD) δ_{H} 7.35 (d, J = 3.0 Hz, 1H), 7.15 (dd, J = 9.0, 3.1 Hz, 1H), 7.08 (d, J = 9.1 Hz, 1H), 4.12 – 4.01 (m, 3H), 3.98 – 3.91 (m, 3H), 3.87 (s, 3H, Me), 3.77 – 3.59 (m, 4H); **¹³C-NMR** (101 MHz, CD_3OD) δ_{C} 168.2, 154.3, 154.2, 122.0, 121.5, 117.8, 117.2, 72.8, 71.8, 71.6, 71.1, 64.3, 64.1, 52.7; **LRMS** (ESI+) 379.12 (100%, $[\text{M}+\text{Na}]^+$); **HRMS** (ESI+) $\text{C}_{17}\text{H}_{24}\text{O}_8\text{Na}$ Requires: 379.1369, Found: 379.1372 ($[\text{M}+\text{Na}]^+$).

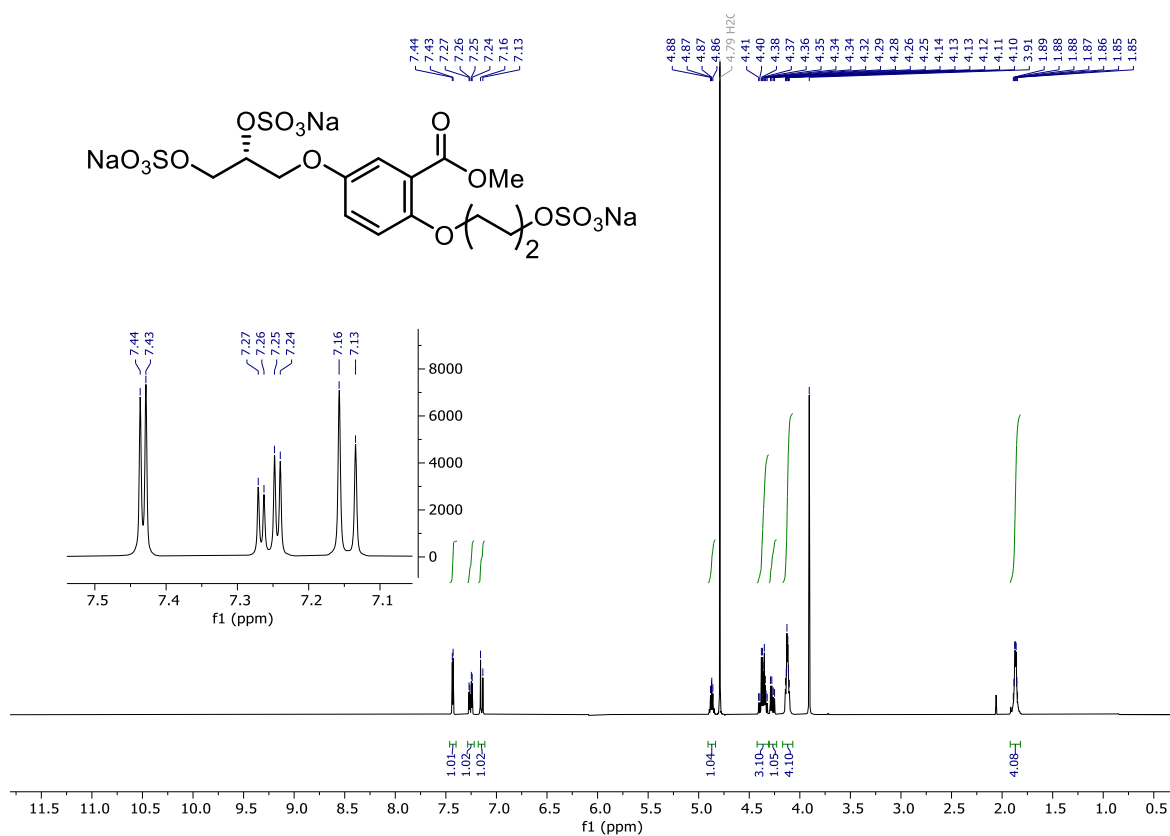
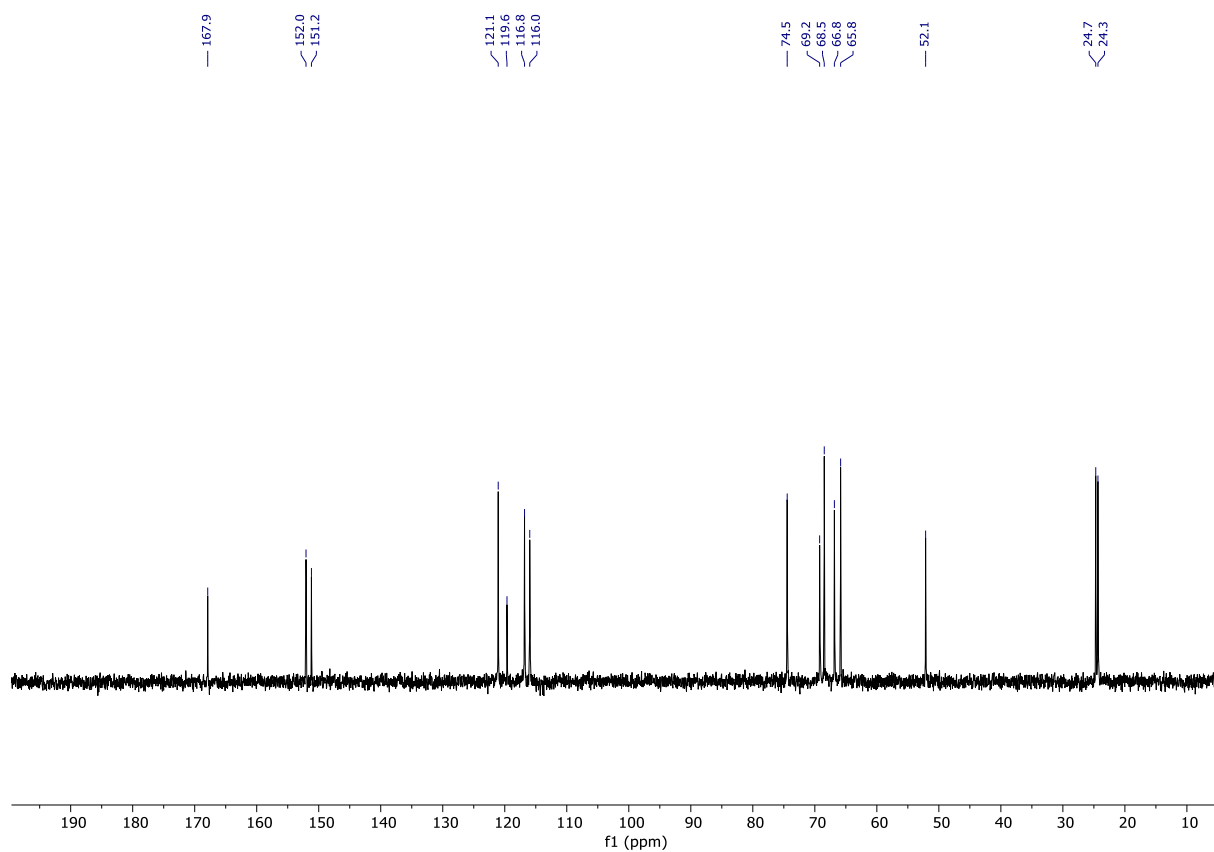
(47s) ($\pm 2,5R$)-((2-(methoxycarbonyl)-1,4-phenylene)bis(oxy))bis(propane-3,1,2-triyl) tetraacetate

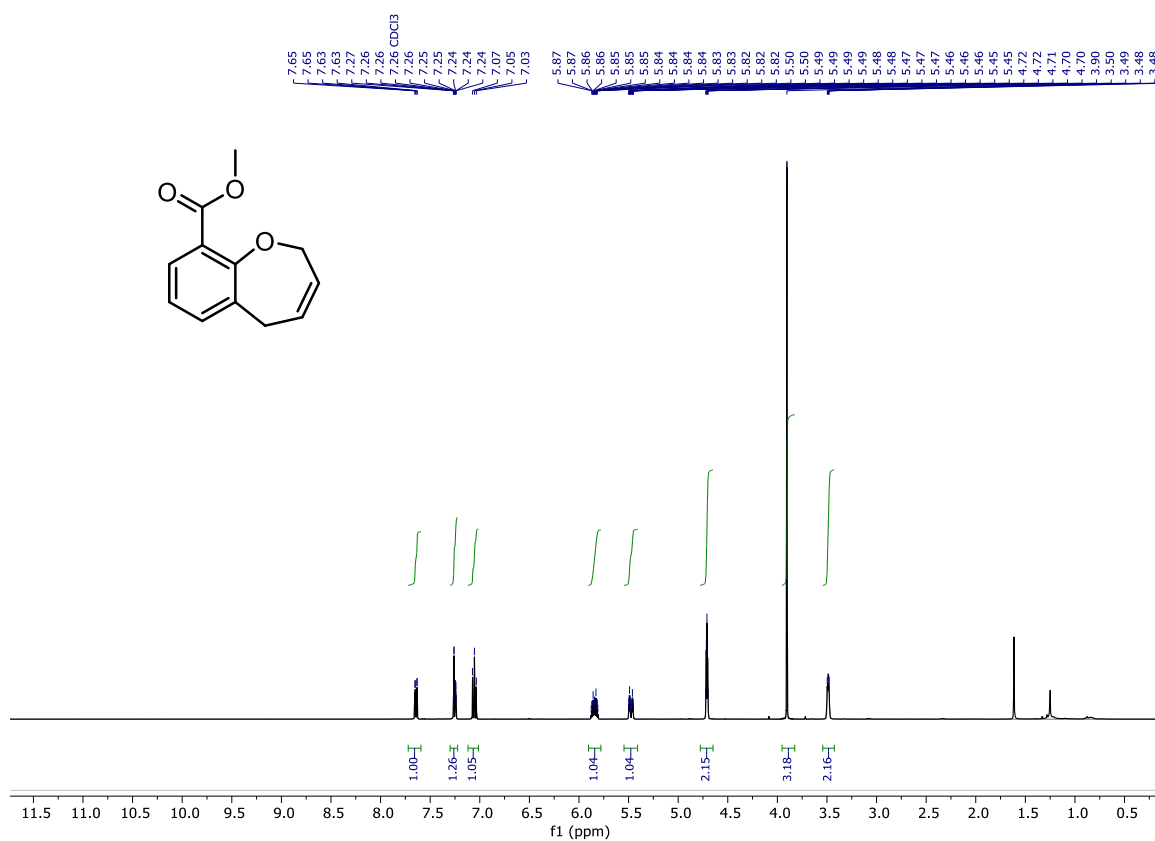
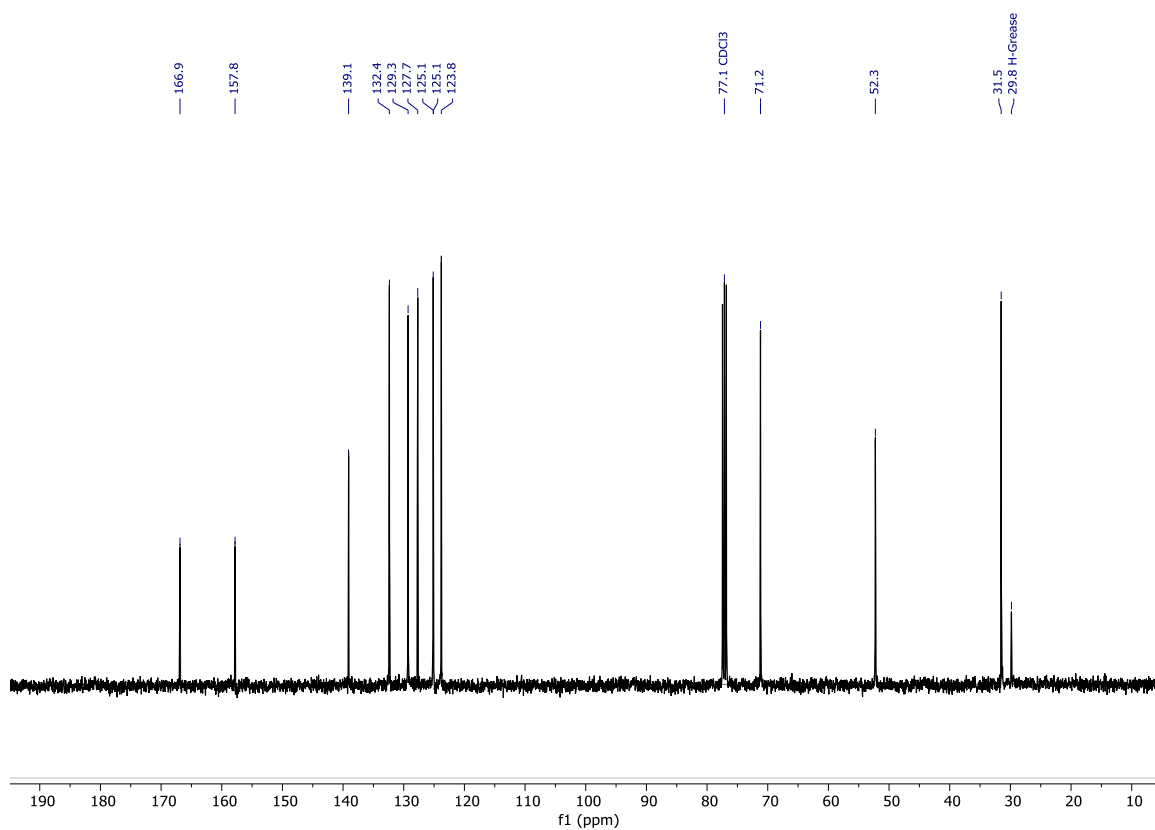


Following general procedure **G**: Methyl 5-((*S*)-2,3-dihydroxypropoxy)-2-((\pm)-2,3-dihydroxypropoxy)benzoate (**46s**) (5 mg, 0.016 mmol) was charged with pyridine (10.3 μ L, 0.13 mmol), CH_2Cl_2 (4 mL) and the AcCl (9.5 μ L, 0.13 mmol) was added dropwise. Afforded the title compound as a clear oil (6 mg, 78%). **[α]_D²⁵** –3.99 (c. 1.0, CHCl_3 , 50:50 *d.r* (*2R5R*, *2S5R*); **IR** V_{max} cm^{-1} 2954 w, 1740 s (C=O), 1500 w, 1439 w, 1219 s; **¹H-NMR** (400 MHz, CDCl_3) δ_{H} 7.35 (d, J = 3.3 Hz, 1H, C6-H), 7.02 (dd, J = 9.1, 3.3 Hz, 1H, C4-H), 6.89 (d, J = 9.1 Hz, 1H, C3-H), 5.37 (m, 2H, CH-OAc), 4.49 (dd, J = 12.0, 3.9 Hz, 1H, CH₂-OAc), 4.42 (dd, J = 12.0, 3.9 Hz, 1H, CH₂-OAc), 4.33 (dd, J = 12.0, 6.1 Hz, 1H, CH₂-OAc), 4.28 (dd, J = 12.0, 6.1 Hz, 1H, CH₂-OAc), 4.15 (m, 2H, ArO-CH₂), 4.10 (d, J = 5.2 Hz, 2H, ArO-CH₂), 3.89 (s, 3H, Me), 2.10 (s, 3H, Ac), 2.10 (s, 3H, Ac), 2.08 (s, 3H, Ac), 2.07 (s, 3H, Ac); **¹³C-NMR** (101 MHz, CDCl_3) δ_{C} 170.78 (Ac), 170.75 (Ac), 170.5 (Ac), 170.4 (Ac), 166.3 (CO₂Me), 152.6 (C1), 121.7 (C2 & C5), 120.5 (C4), 117.0 (C6), 116.1 (C3), 69.84 (CH-OAc), 69.76 (CH-OAc), 68.3 (ArO-CH₂), 66.9 (ArO-CH₂), 62.8 (CH₂-OAc), 62.5 (CH₂-OAc), 52.4 (Me), 21.11 (Ac), 21.09 (Ac), 20.9 (2C, Ac); **LRMS** m/z (ESI+) 507.15 ($[\text{M}+\text{Na}]^+$, 100%); **HRMS** m/z (ESI+) $\text{C}_{22}\text{H}_{28}\text{O}_{12}\text{Na}$ Requires: 507.1478, Found: 507.1484 ($[\text{M}+\text{Na}]^+$); **cHPLC** $R_{\text{t}1}$ = 73.77 min, area = 50.11%; $R_{\text{t}2}$ = 80.12 min, area = 49.89%; (Phenomenex® Cellulose-1, MeCN/H₂O, 7:18, 1 mL min⁻¹, 30 °C).

^1H -NMR spectrum **6** (CDCl_3 , 400 MHz). ^{13}C -NMR spectrum **6** (CDCl_3 , 101 MHz)

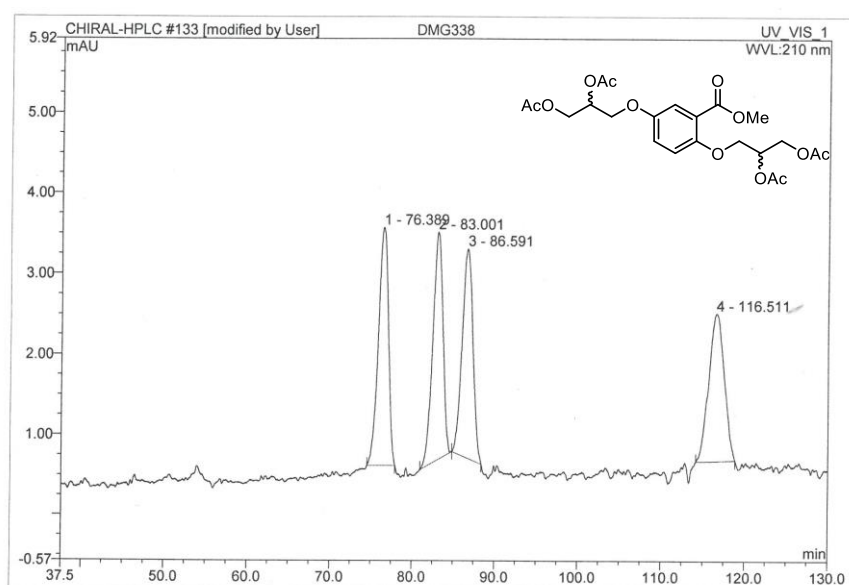
^1H -NMR spectrum **33** (CDCl_3 , 400 MHz) ^{13}C -NMR spectrum **33** (CDCl_3 , 101 MHz)

^1H -NMR spectrum **R-2** (D_2O , 400 MHz) ^{13}C -NMR spectrum **R-2** (D_2O , 101 MHz)

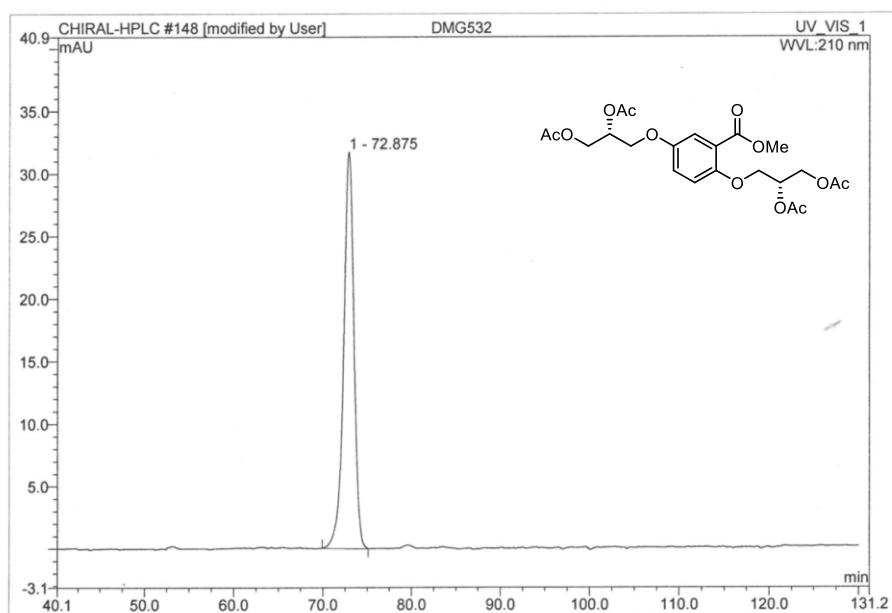
^1H -NMR spectrum **64** (CDCl_3 , 400 MHz) ^{13}C -NMR spectrum **64** (CDCl_3 , 101 MHz)

Chiral HPLC Data and Analysis

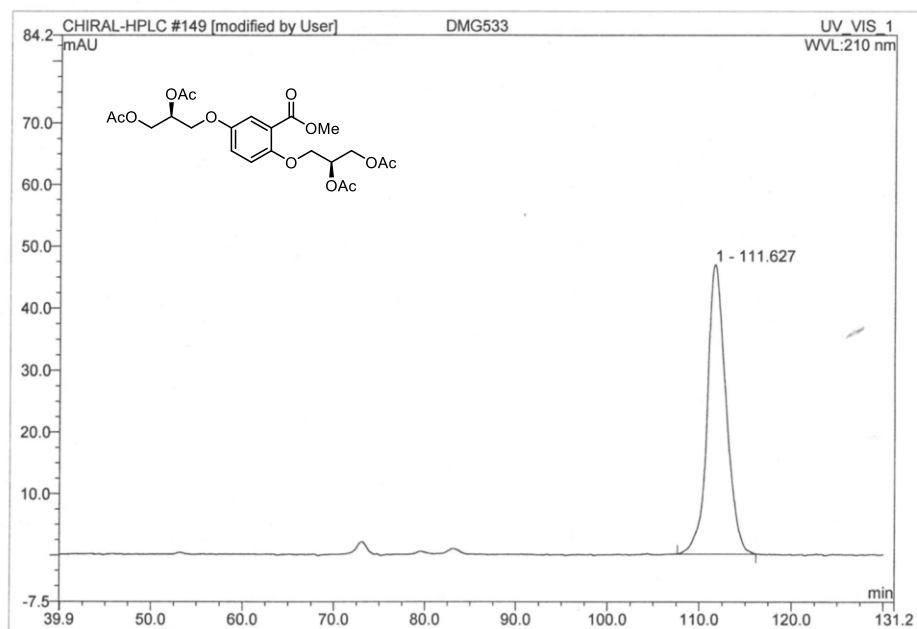
±12 (1 mL min⁻¹, MeCN/H₂O, 7:18)



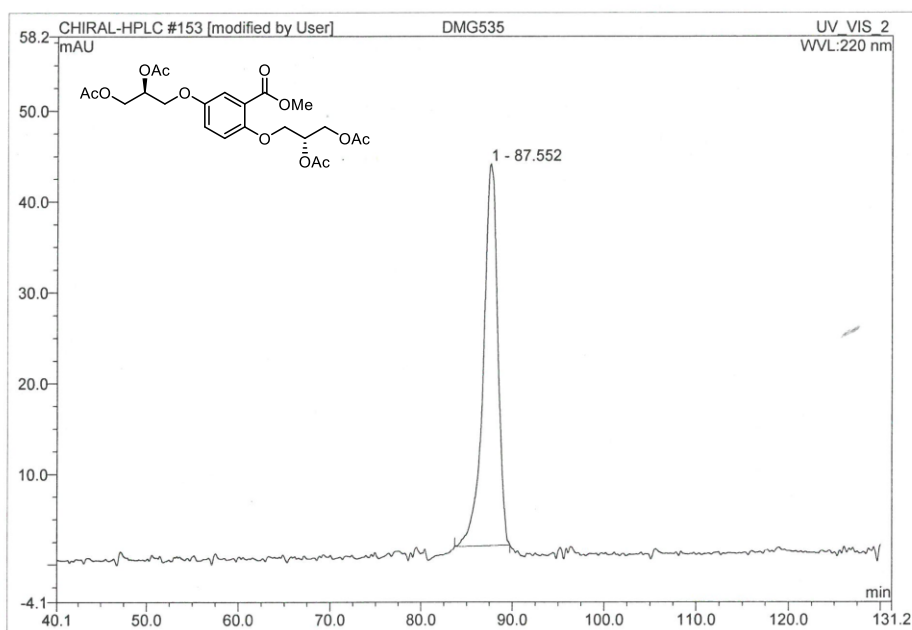
No.	Ret.Time min	Peak Name *	Height mAU	Area mAU*min	Rel.Area %	Amount	Type
1	76.39	n.a.	2.954	4.144	25.94	n.a.	BMB*
2	83.00	n.a.	2.828	3.992	24.99	n.a.	BMB*
3	86.59	n.a.	2.594	3.922	24.55	n.a.	bMB*
4	116.51	n.a.	1.834	3.919	24.53	n.a.	BMB*
Total:			10.210	15.978	100.00	0.000	

RR-12 (1 mL min⁻¹, MeCN/H₂O, 7:18)

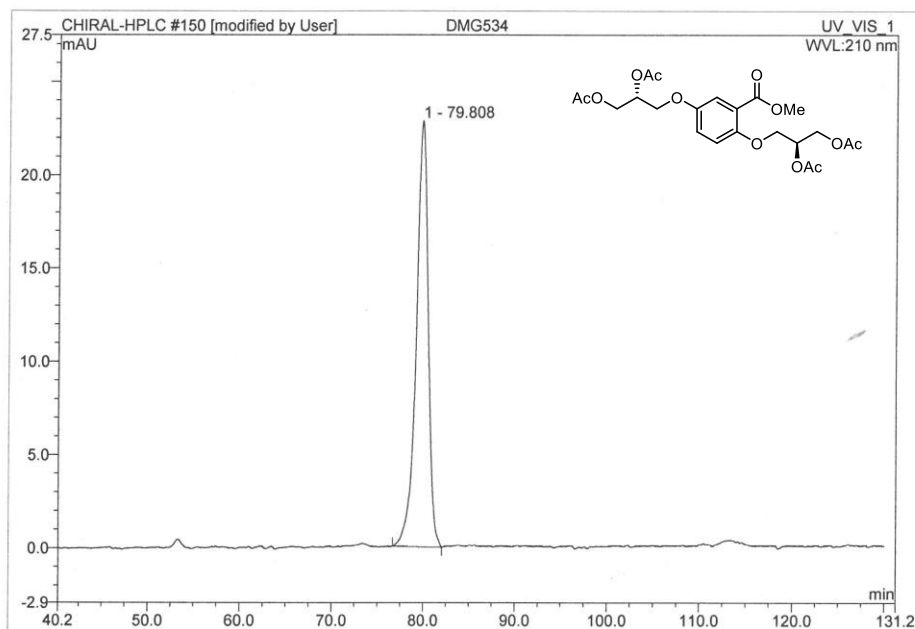
No.	Ret.Time min	Peak Name *	Height mAU	Area mAU*min	Rel.Area %	Amount	Type
1	72.87	n.a.	31.707	42.433	100.00	n.a.	BMB
Total:			31.707	42.433	100.00	0.000	

SS-12 (1 mL min⁻¹, MeCN/H₂O, 7:18)

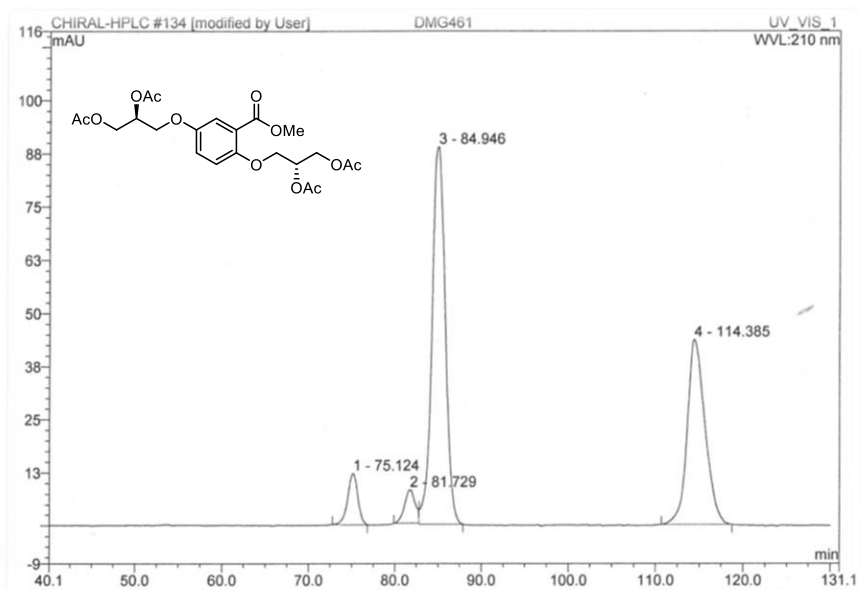
No.	Ret.Time min	Peak Name *	Height mAU	Area mAU*min	Rel.Area %	Amount	Type
1	111.63	n.a.	46.806	110.739	100.00	n.a.	BMB
Total:			46.806	110.739	100.00	0.000	

RS-12 (1 mL min⁻¹, MeCN/H₂O, 7:18)

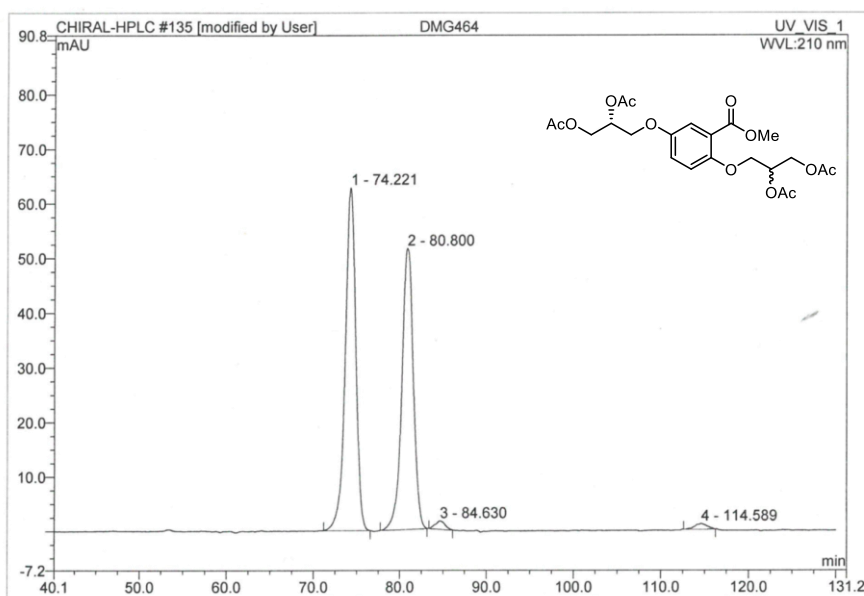
No.	Ret.Time min	Peak Name *	Height mAU	Area mAU*min	Rel.Area %	Amount	Type
1	87.55	n.a.	42.031	76.506	100.00	n.a.	BMB*
Total:			42.031	76.506	100.00	0.000	

SR-12 (1 mL min⁻¹, MeCN/H₂O, 7:18)

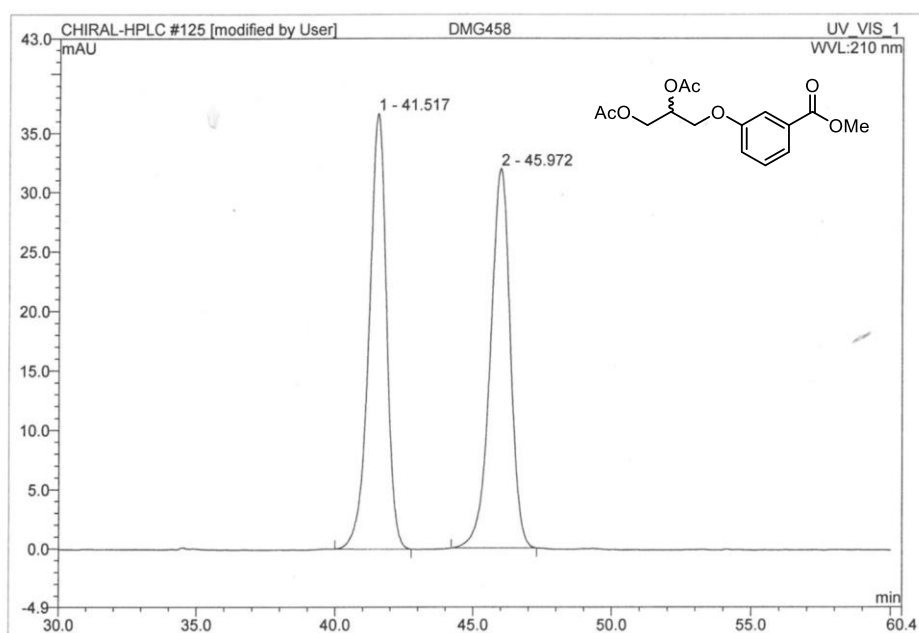
No.	Ret.Time min	Peak Name *	Height mAU	Area mAU*min	Rel.Area %	Amount	Type
1	79.81	n.a.	22.831	34.763	100.00	n.a.	BMB
Total:			22.831	34.763	100.00	0.000	

α -12 (1 mL min⁻¹, MeCN/H₂O, 7:18)

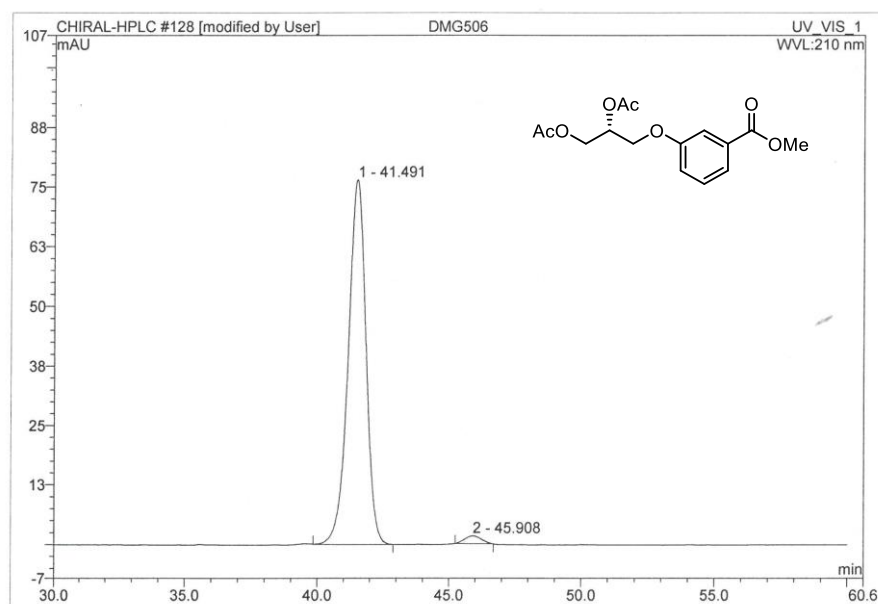
No.	Ret.Time min	Peak Name *	Height mAU	Area mAU*min	Rel.Area %	Amount	Type
1	75.12	n.a.	12.101	16.498	5.71	n.a.	BMB*
2	81.73	n.a.	7.914	11.339	3.92	n.a.	BM *
3	84.95	n.a.	88.802	157.950	54.64	n.a.	MB*
4	114.38	n.a.	43.601	103.263	35.72	n.a.	BMB
Total:			152.418	289.049	100.00	0.000	

 β -12 (1 mL min⁻¹, MeCN/H₂O, 7:18)

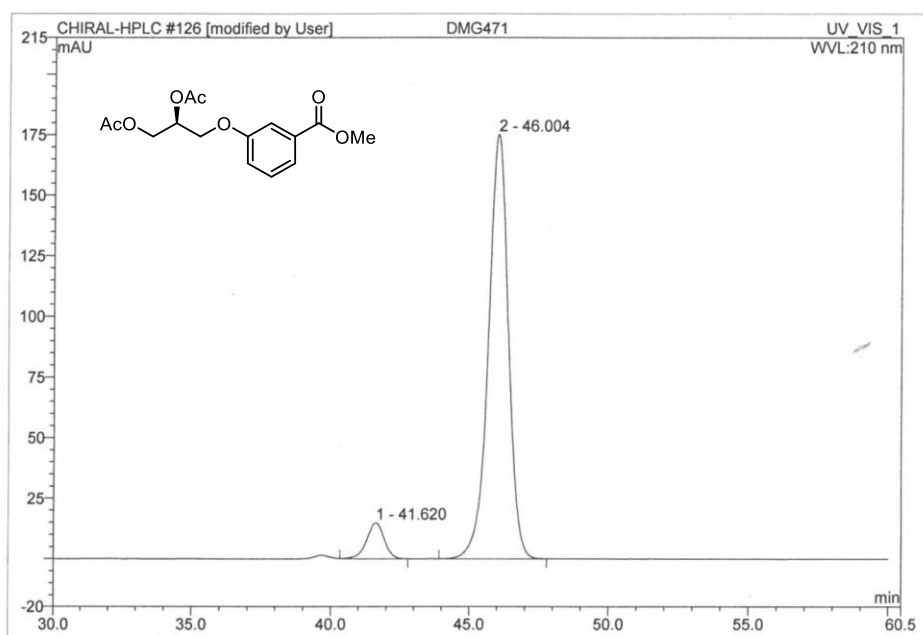
No.	Ret.Time min	Peak Name *	Height mAU	Area mAU*min	Rel.Area %	Amount	Type
1	74.22	n.a.	62.713	88.565	51.55	n.a.	BMB
2	80.80	n.a.	51.382	79.614	46.34	n.a.	BMB
3	84.63	n.a.	1.509	1.963	1.14	n.a.	BMB*
4	114.59	n.a.	1.036	1.647	0.96	n.a.	BMB*
Total:			116.640	171.789	100.00	0.000	

±4s (1 mL min⁻¹, MeCN/H₂O, 3:7)

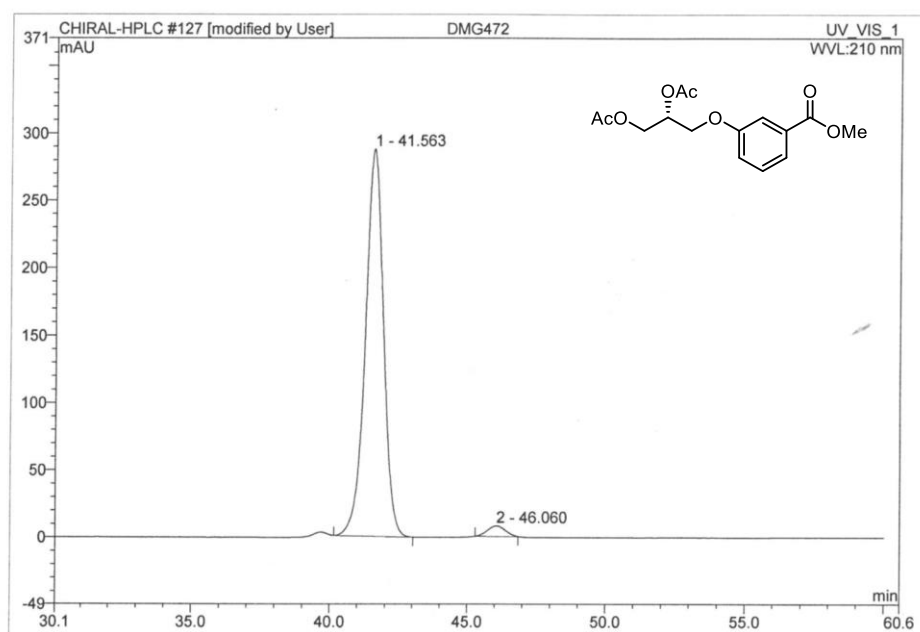
No.	Ret.Time min	Peak Name	Height mAU	Area mAU*min	Rel.Area %	Amount	Type
1	41.52	n.a.	36.698	27.034	50.15	n.a.	BMB
2	45.97	n.a.	31.944	26.870	49.85	n.a.	BMB
Total:			68.642	53.904	100.00	0.000	

R-4s (1 mL min⁻¹, MeCN/H₂O, 3:7)

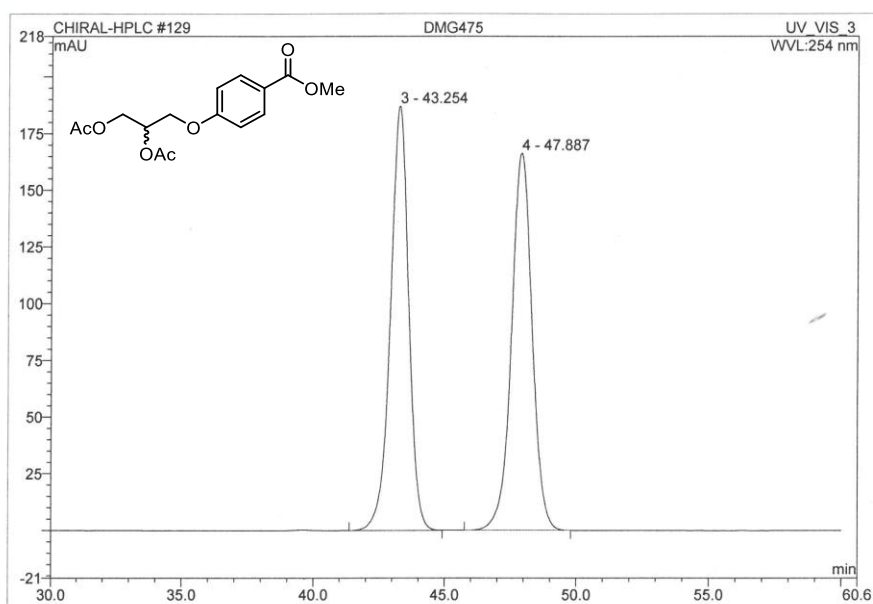
No.	Ret.Time min	Peak Name	Height mAU	Area mAU*min	Rel.Area %	Amount	Type
1	41.49	n.a.	76.415	59.645	98.06	n.a.	BMB
2	45.91	n.a.	1.611	1.182	1.94	n.a.	BMB*
Total:			78.026	60.827	100.00	0.000	

α -4s (1 mL min⁻¹, MeCN/H₂O, 3:7)

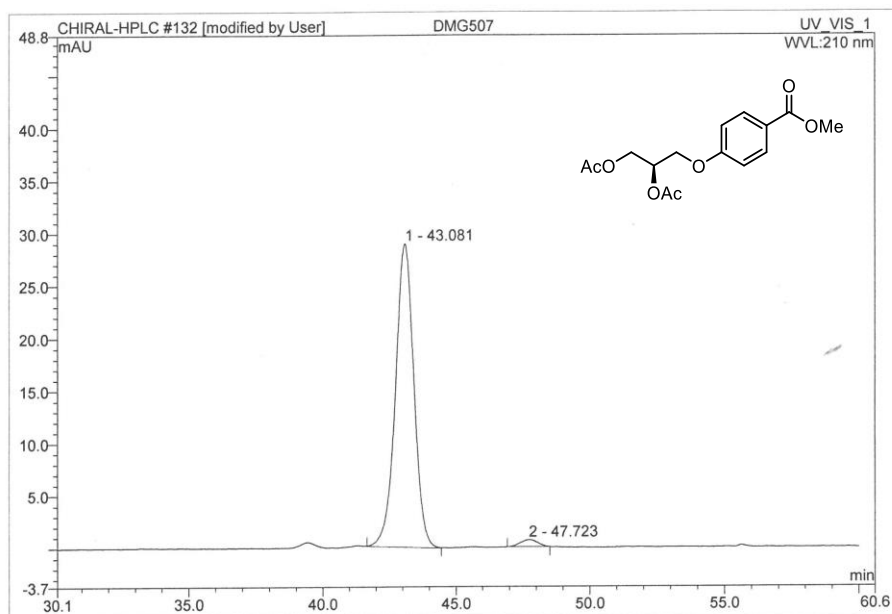
No.	Ret.Time min	Peak Name	Height mAU	Area mAU*min	Rel.Area %	Amount	Type
1	41.62	n.a.	14.801	10.779	6.87	n.a.	BMB
2	46.00	n.a.	175.150	146.155	93.13	n.a.	BMB
Total:			189.951	156.934	100.00	0.000	

 β -4s (1 mL min⁻¹, MeCN/H₂O, 3:7)

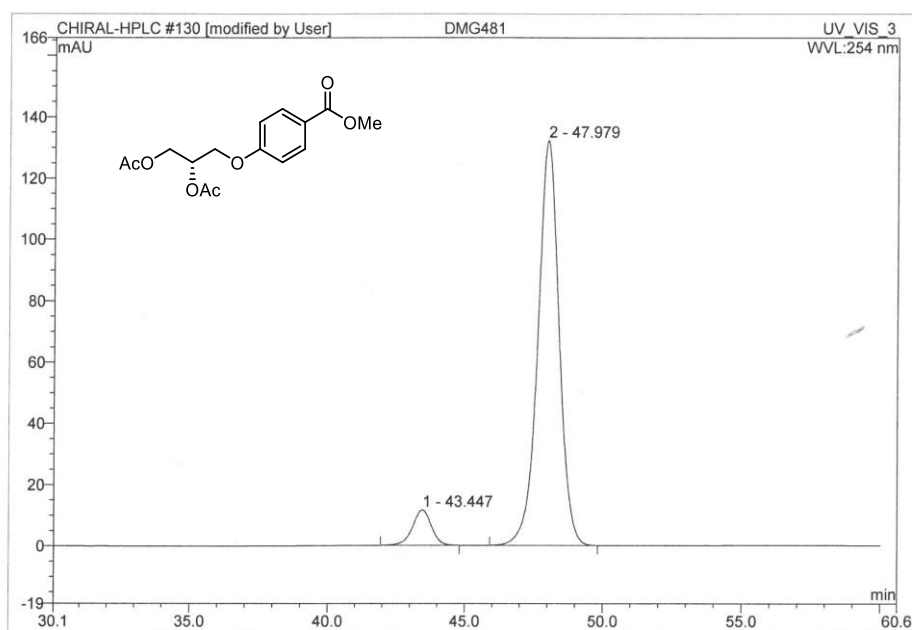
No.	Ret.Time min	Peak Name	Height mAU	Area mAU*min	Rel.Area %	Amount	Type
1	41.56	n.a.	287.379	219.168	97.41	n.a.	BMB
2	46.06	n.a.	7.772	5.824	2.59	n.a.	BMB*
Total:			295.151	224.992	100.00	0.000	

±5s (1 mL min⁻¹, MeCN/H₂O, 3:7)

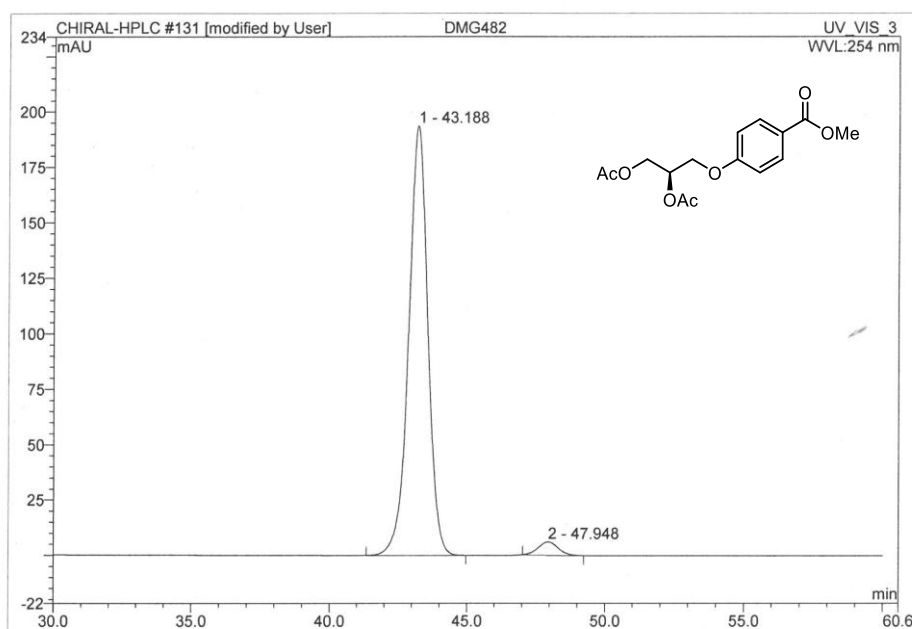
No.	Ret.Time min	Peak Name	Height mAU	Area mAU*min	Rel.Area %	Amount	Type
1	11.09	n.a.	6.153	2.255	0.73	n.a.	BM
2	11.51	n.a.	5.604	1.811	0.59	n.a.	MB
3	43.25	n.a.	186.956	151.377	49.33	n.a.	BMB
4	47.89	n.a.	166.311	151.428	49.35	n.a.	BMB
Total:			365.024	306.870	100.00	0.000	

R-5s (1 mL min⁻¹, MeCN/H₂O, 3:7)

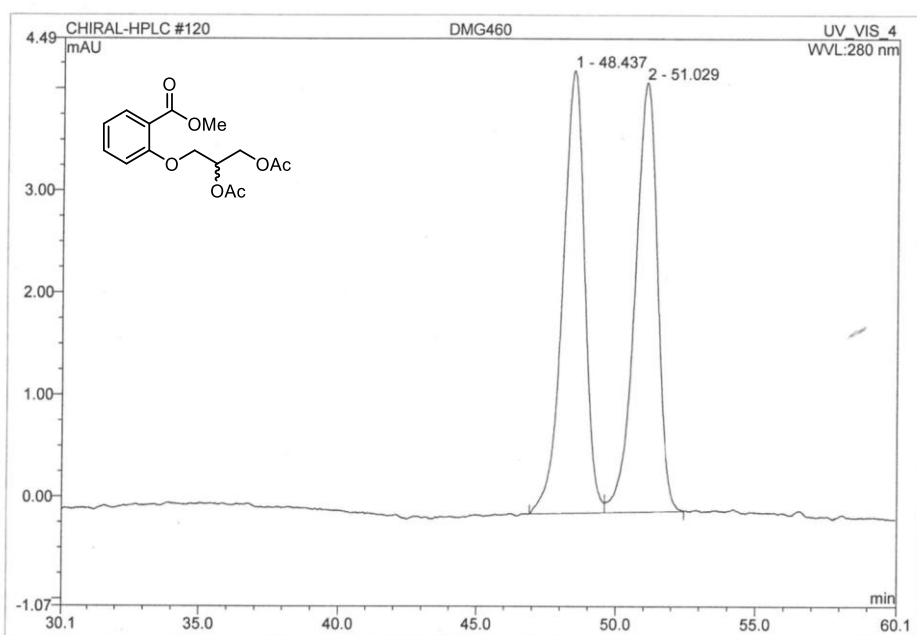
No.	Ret.Time min	Peak Name	Height mAU	Area mAU*min	Rel.Area %	Amount	Type
1	43.08	n.a.	28.861	23.151	97.92	n.a.	BMB
2	47.72	n.a.	0.654	0.491	2.08	n.a.	BMB*
Total:			29.515	23.642	100.00	0.000	

α -5s (1 mL min⁻¹, MeCN/H₂O, 3:7)

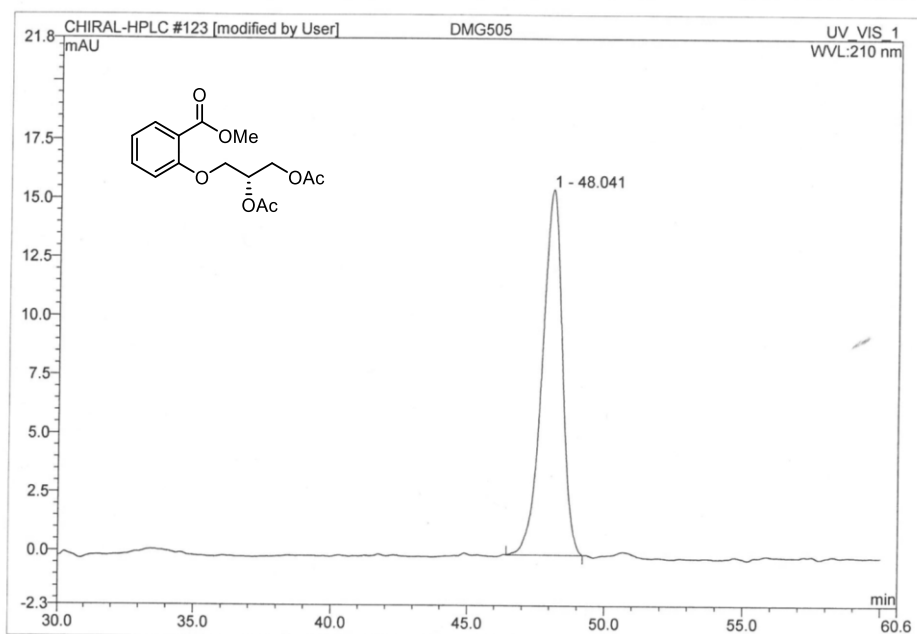
No.	Ret.Time min	Peak Name *	Height mAU	Area mAU*min	Rel.Area %	Amount	Type
1	43.45	n.a.	11.527	9.271	7.28	n.a.	BMB
2	47.98	n.a.	132.094	118.033	92.72	n.a.	BMB
Total:			143.621	127.304	100.00	0.000	

 β -5s (1 mL min⁻¹, MeCN/H₂O, 3:7)

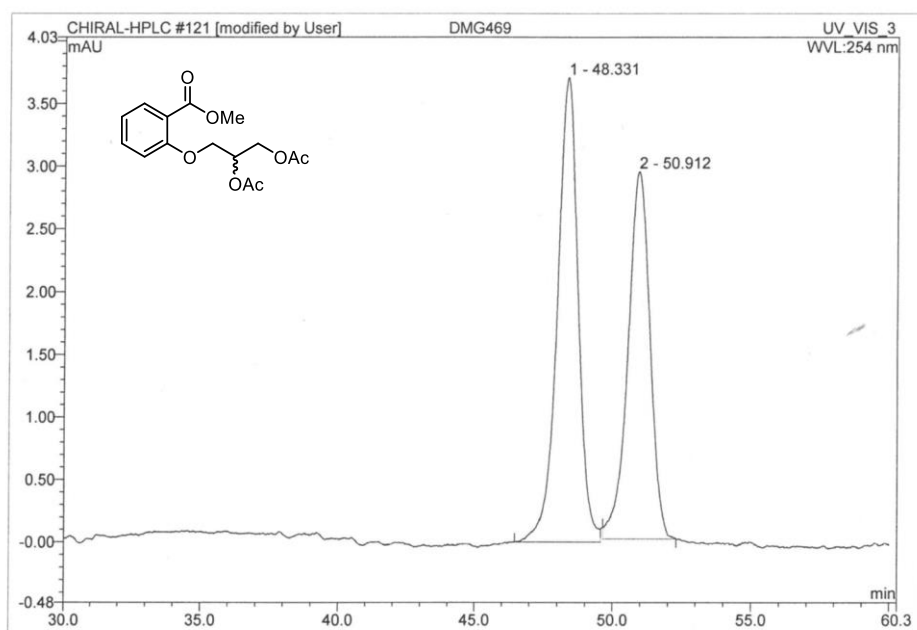
No.	Ret.Time min	Peak Name *	Height mAU	Area mAU*min	Rel.Area %	Amount	Type
1	43.19	n.a.	193.634	156.975	96.97	n.a.	BMB
2	47.95	n.a.	5.897	4.903	3.03	n.a.	BMB*
Total:			199.531	161.878	100.00	0.000	

±6s (1 mL min⁻¹, MeCN/H₂O, 1:3)

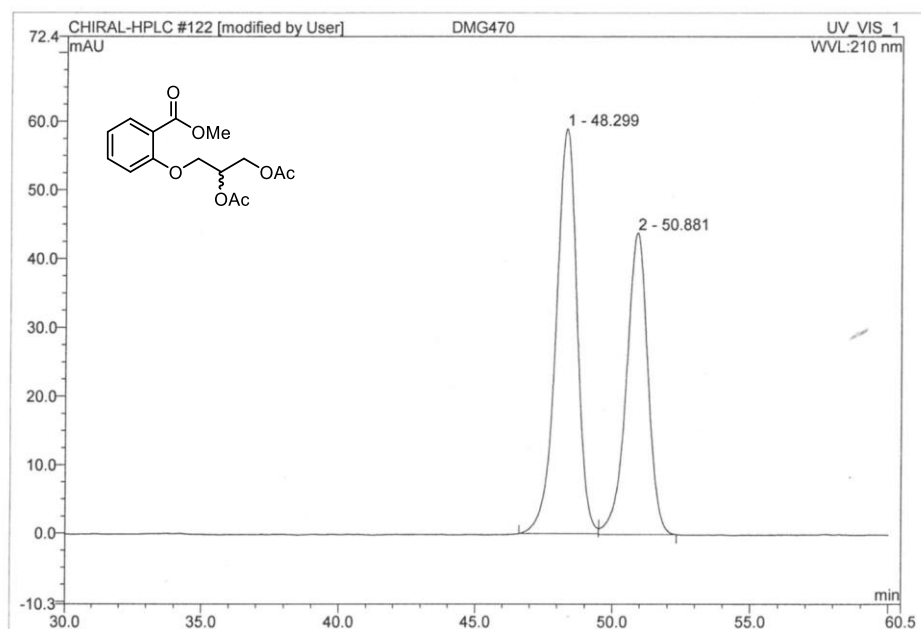
No.	Ret.Time min	Peak Name	Height mAU	Area mAU*min	Rel.Area %	Amount	Type
1	48.44	n.a.	4.334	3.965	50.11	n.a.	BM
2	51.03	n.a.	4.205	3.948	49.89	n.a.	MB
Total:			8.539	7.913	100.00	0.000	

R-6s (1 mL min⁻¹, MeCN/H₂O, 1:3)

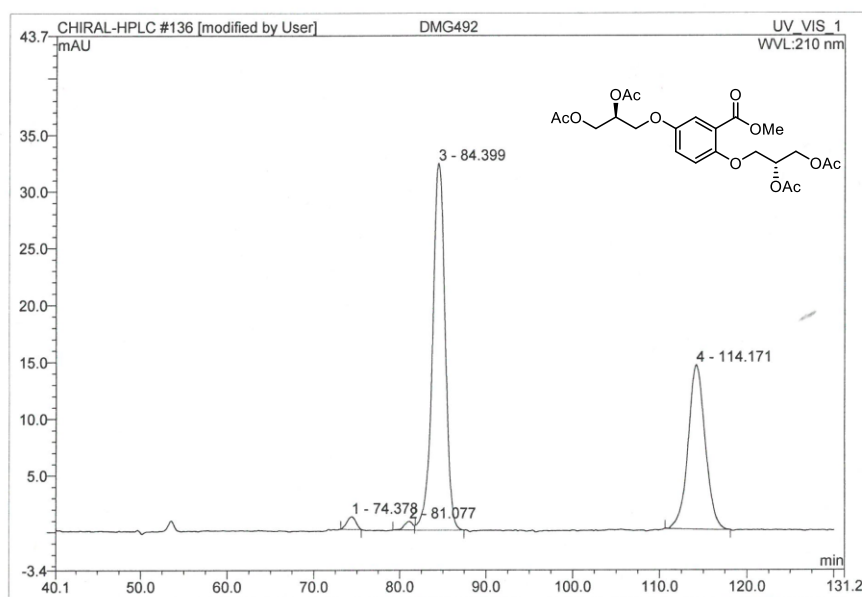
No.	Ret.Time min	Peak Name	Height mAU	Area mAU*min	Rel.Area %	Amount	Type
1	48.04	n.a.	15.534	13.247	100.00	n.a.	BMB
Total:			15.534	13.247	100.00	0.000	

α -6s (1 mL min⁻¹, MeCN/H₂O, 1:3)

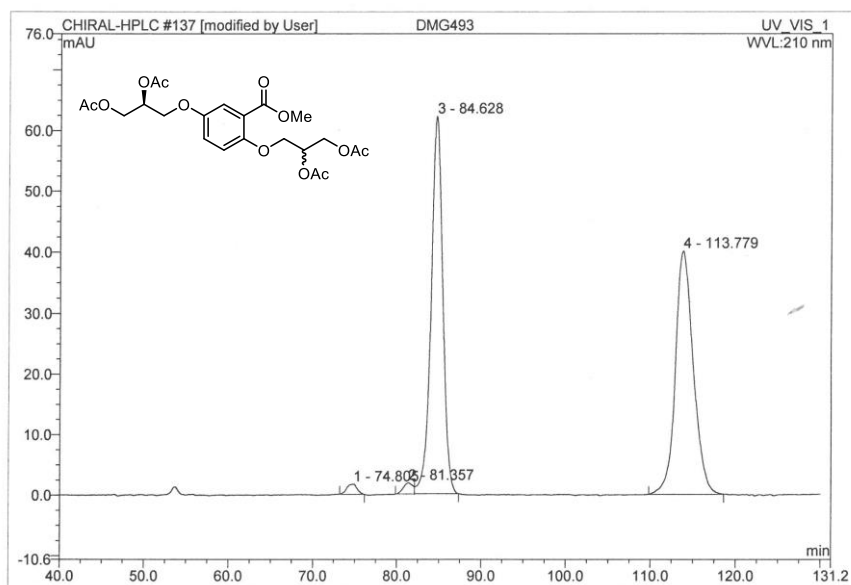
No.	Ret.Time min	Peak Name *	Height mAU	Area mAU*min	Rel.Area %	Amount	Type
1	48.33	n.a.	3.709	3.253	54.55	n.a.	BM *
2	50.91	n.a.	2.932	2.711	45.45	n.a.	MB*
Total:			6.641	5.964	100.00	0.000	

 β -6s (1 mL min⁻¹, MeCN/H₂O, 1:3)

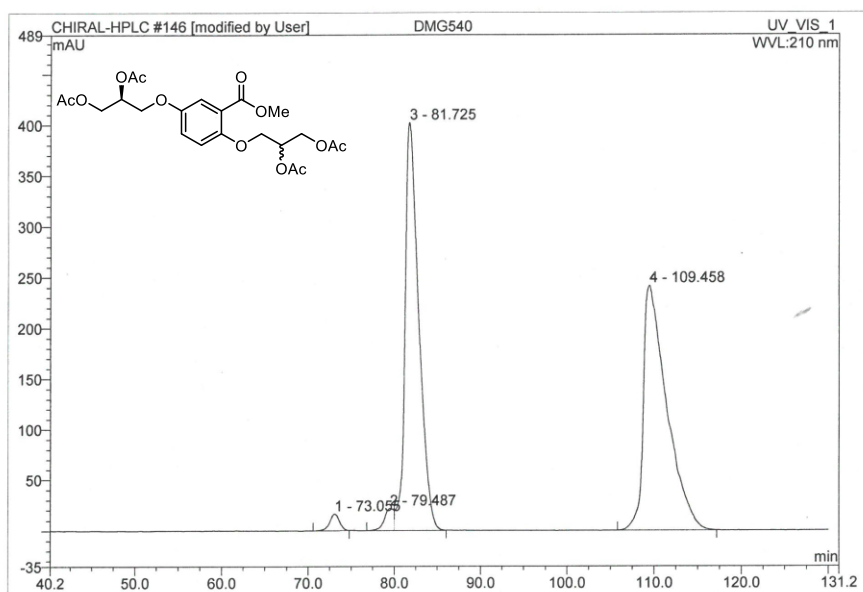
No.	Ret.Time min	Peak Name *	Height mAU	Area mAU*min	Rel.Area %	Amount	Type
1	48.30	n.a.	58.972	52.331	56.83	n.a.	BM *
2	50.88	n.a.	43.930	39.757	43.17	n.a.	MB*
Total:			102.902	92.088	100.00	0.000	

16s (1 mL min⁻¹, MeCN/H₂O, 7:18)

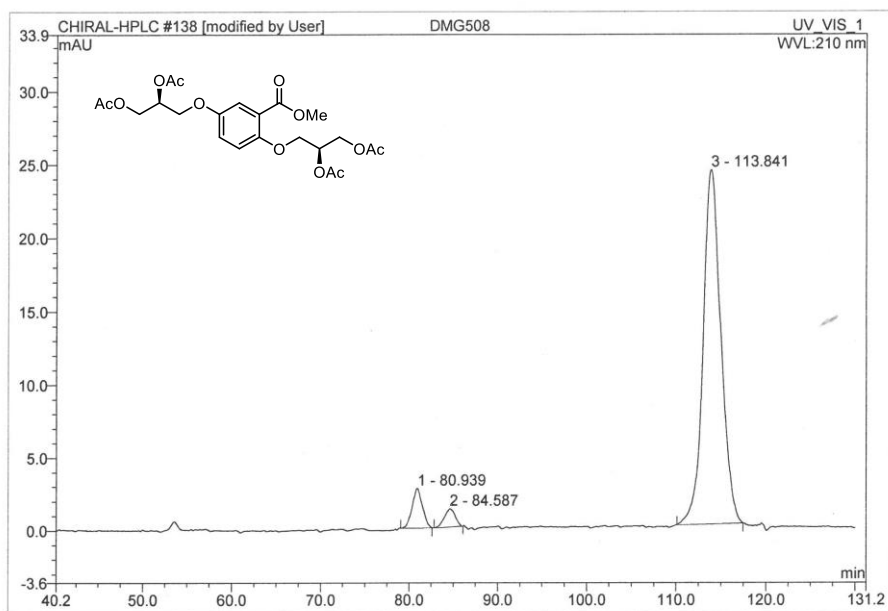
No.	Ret.Time min	Peak Name	Height mAU	Area mAU*min	Rel.Area %	Amount	Type
1	74.38	n.a.	1.116	1.339	1.49	n.a.	BMB*
2	81.08	n.a.	0.768	0.868	0.96	n.a.	BM *
3	84.40	n.a.	32.331	54.951	61.05	n.a.	MB*
4	114.17	n.a.	14.473	32.848	36.50	n.a.	BMB*
Total:			48.688	90.007	100.00	0.000	

17s (1 mL min⁻¹, MeCN/H₂O, 7:18)

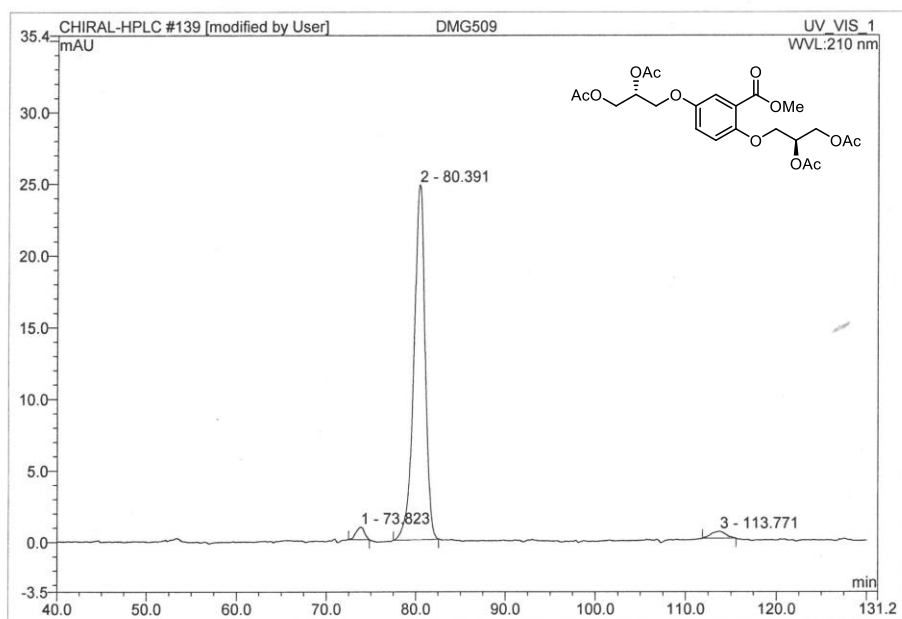
No.	Ret.Time min	Peak Name	Height mAU	Area mAU*min	Rel.Area %	Amount	Type
1	74.81	n.a.	1.647	2.338	1.15	n.a.	BMB*
2	81.36	n.a.	1.838	2.376	1.17	n.a.	BM *
3	84.63	n.a.	62.127	100.051	49.41	n.a.	MB*
4	113.78	n.a.	40.031	97.730	48.26	n.a.	BMB
Total:			105.643	202.495	100.00	0.000	

18s (1 mL min⁻¹, MeCN/H₂O, 7:18)

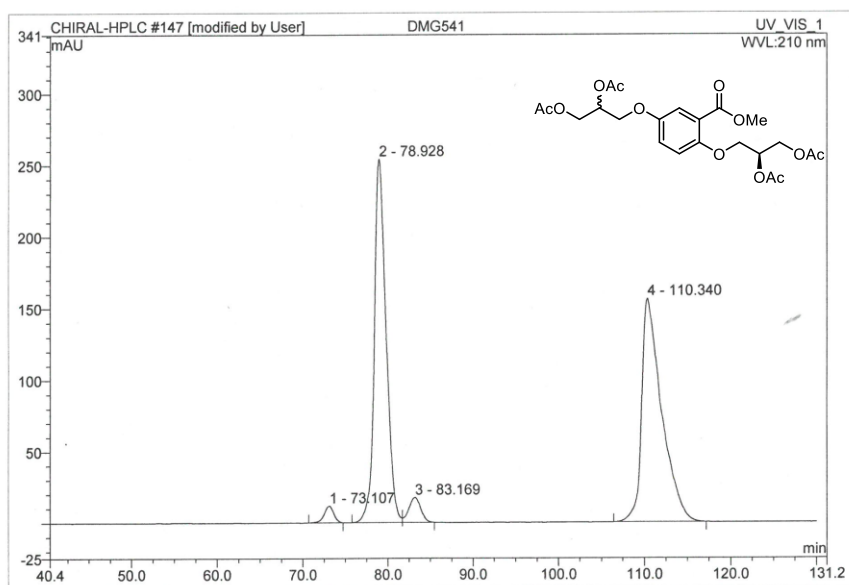
No.	Ret.Time min	Peak Name •	Height mAU	Area mAU*min	Rel.Area %	Amount	Type
1	73.06	n.a.	15.838	21.150	1.38	n.a.	BMB
2	79.49	n.a.	21.328	26.767	1.74	n.a.	BM
3	81.72	n.a.	401.751	739.591	48.16	n.a.	MB
4	109.46	n.a.	241.136	748.100	48.72	n.a.	BMB
Total:			680.053	1535.609	100.00	0.000	

25s (1 mL min⁻¹, MeCN/H₂O, 7:18)

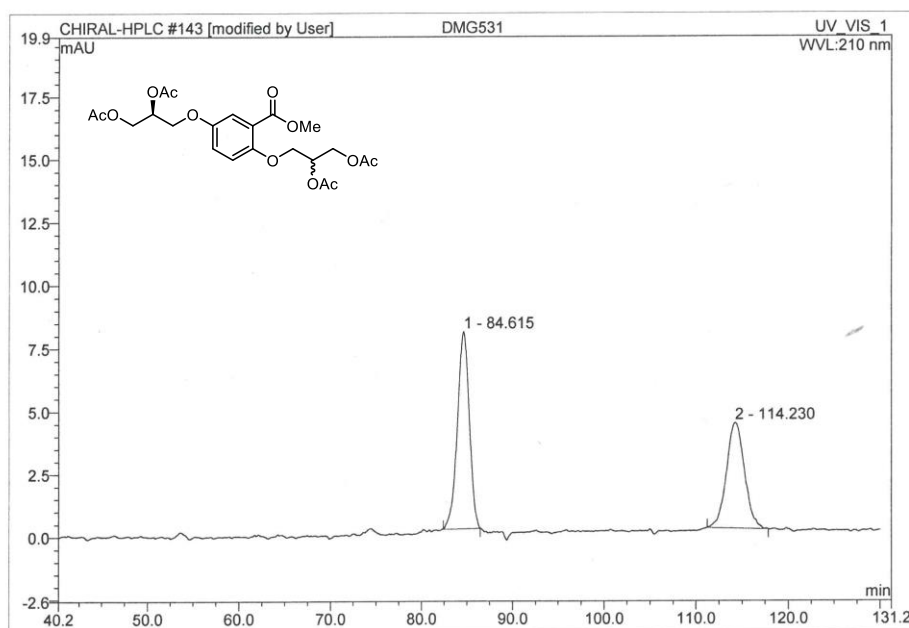
No.	Ret.Time min	Peak Name •	Height mAU	Area mAU*min	Rel.Area %	Amount	Type
1	80.94	n.a.	2.704	3.623	5.95	n.a.	BMB*
2	84.59	n.a.	1.229	1.693	2.78	n.a.	BMB*
3	113.84	n.a.	24.187	55.599	91.27	n.a.	BMB
Total:			28.120	60.916	100.00	0.000	

26s (1 mL min⁻¹, MeCN/H₂O, 7:18)

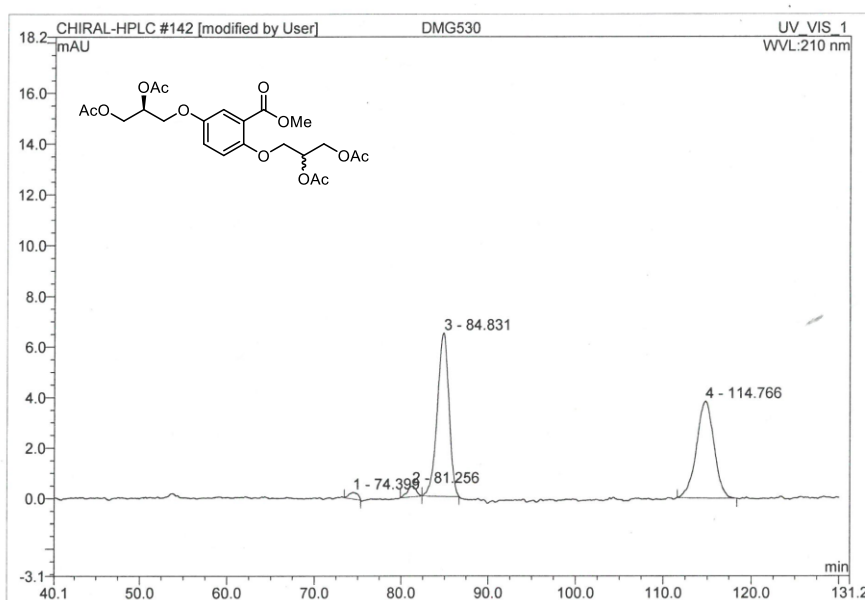
No.	Ret.Time min	Peak Name	Height mAU	Area mAU*min	Rel.Area %	Amount	Type
1	73.82	n.a.	0.876	0.951	2.49	n.a.	BMB*
2	80.39	n.a.	24.748	36.295	95.17	n.a.	BMB
3	113.77	n.a.	0.477	0.892	2.34	n.a.	BMB*
Total:			26.101	38.138	100.00	0.000	

27s (1 mL min⁻¹, MeCN/H₂O, 7:18)

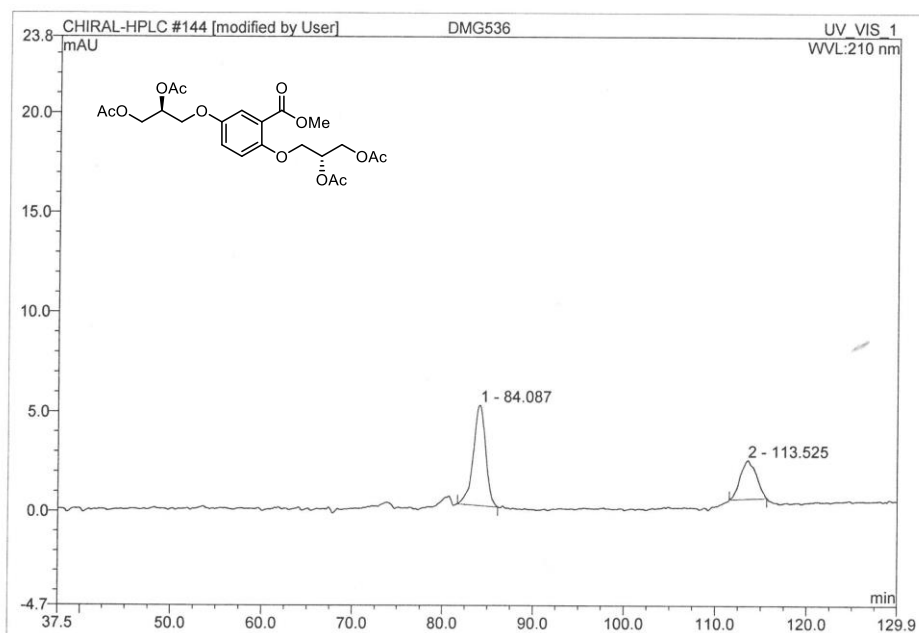
No.	Ret.Time min	Peak Name	Height mAU	Area mAU*min	Rel.Area %	Amount	Type
1	73.11	n.a.	11.687	15.341	1.77	n.a.	BMB
2	78.93	n.a.	253.936	405.428	46.68	n.a.	BM
3	83.17	n.a.	17.397	28.194	3.25	n.a.	MB
4	110.34	n.a.	156.095	419.476	48.30	n.a.	BMB
Total:			439.115	868.440	100.00	0.000	

31s (1 mL min⁻¹, MeCN/H₂O, 7:18)

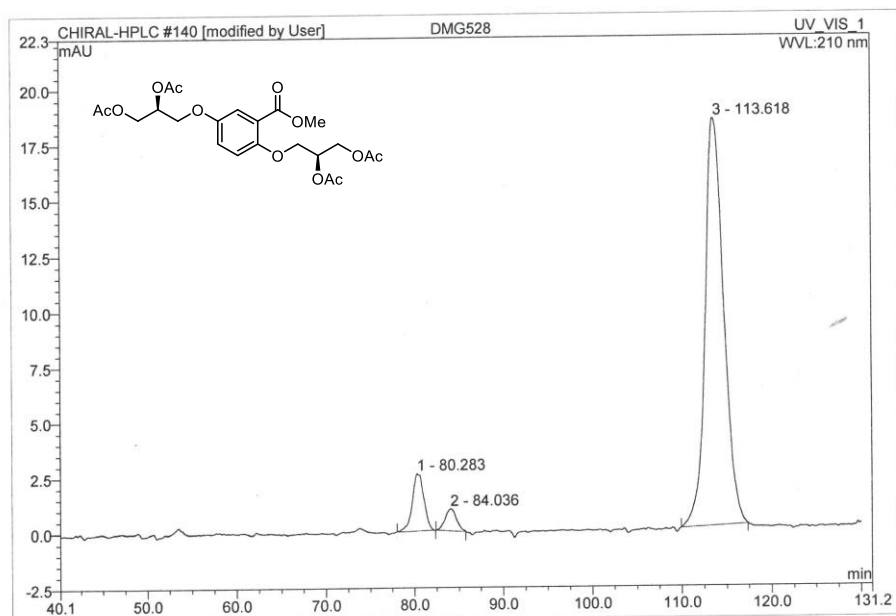
No.	Ret.Time min	Peak Name *	Height mAU	Area mAU*min	Rel.Area %	Amount	Type
1	84.61	n.a.	7.826	11.869	55.70	n.a.	BMB
2	114.23	n.a.	4.192	9.438	44.30	n.a.	BMB*
Total:			12.018	21.307	100.00	0.000	

32s (1 mL min⁻¹, MeCN/H₂O, 7:18)

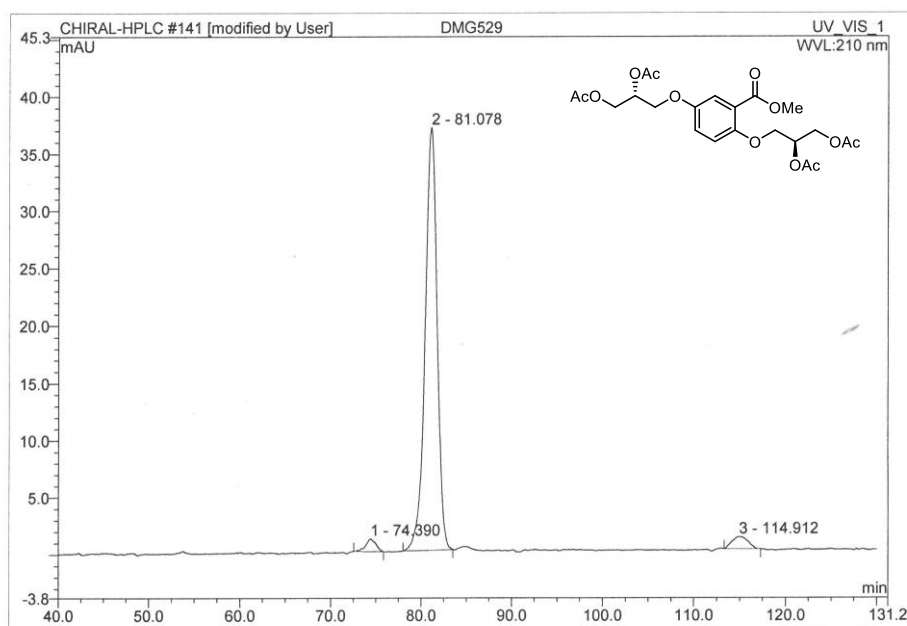
No.	Ret.Time min	Peak Name *	Height mAU	Area mAU*min	Rel.Area %	Amount	Type
1	74.40	n.a.	0.251	0.296	1.52	n.a.	BMB*
2	81.26	n.a.	0.421	0.474	2.43	n.a.	BMB*
3	84.83	n.a.	6.462	9.974	51.10	n.a.	bMB*
4	114.77	n.a.	3.831	8.774	44.95	n.a.	BMB*
Total:			10.965	19.518	100.00	0.000	

33s (1 mL min⁻¹, MeCN/H₂O, 7:18)

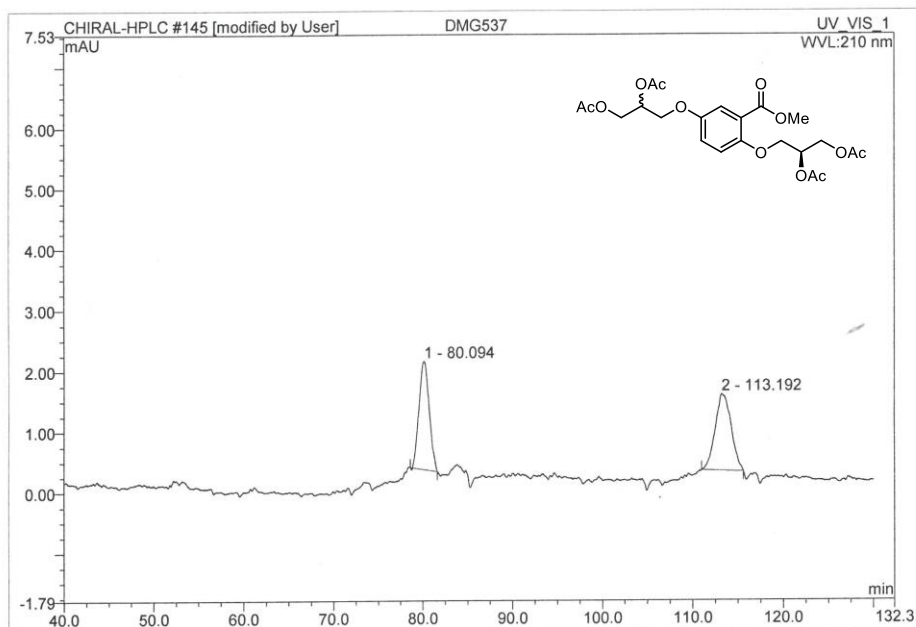
No.	Ret.Time min	Peak Name	Height mAU	Area mAU*min	Rel.Area %	Amount	Type
1	84.09	n.a.	5.037	7.991	67.09	n.a.	BMB
2	113.52	n.a.	1.938	3.920	32.91	n.a.	BMB*
Total:			6.975	11.911	100.00	0.000	

37s (1 mL min⁻¹, MeCN/H₂O, 7:18)

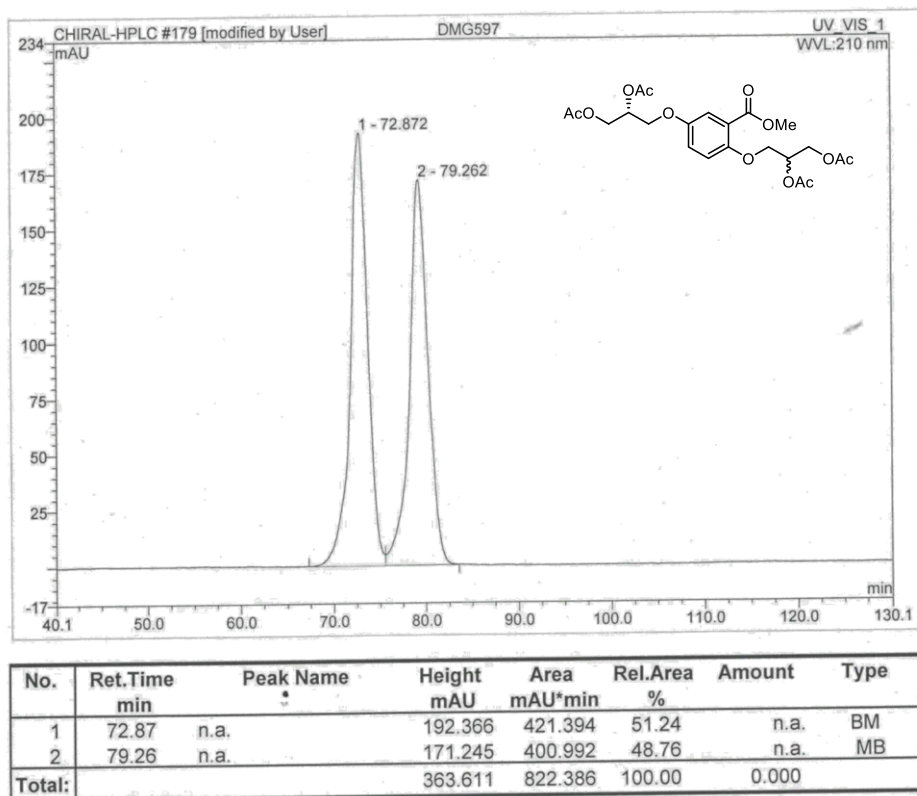
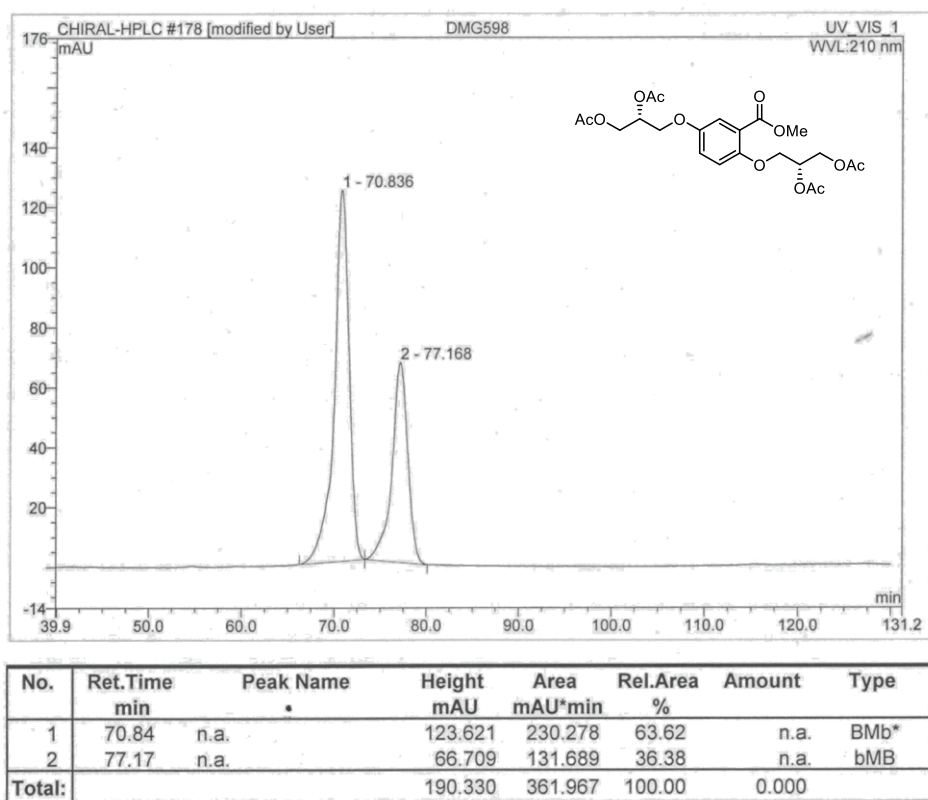
No.	Ret.Time min	Peak Name	Height mAU	Area mAU*min	Rel.Area %	Amount	Type
1	80.28	n.a.	2.594	3.932	7.95	n.a.	BMB*
2	84.04	n.a.	0.978	1.437	2.91	n.a.	BMB*
3	113.62	n.a.	18.359	44.063	89.14	n.a.	BMB
Total:			21.931	49.432	100.00	0.000	

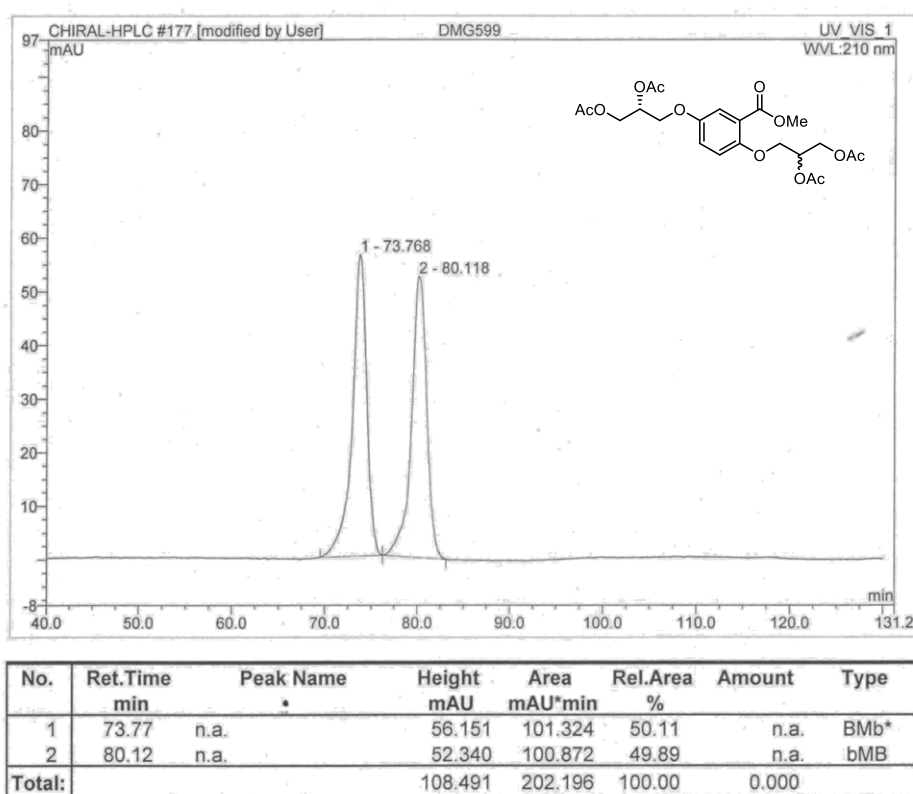
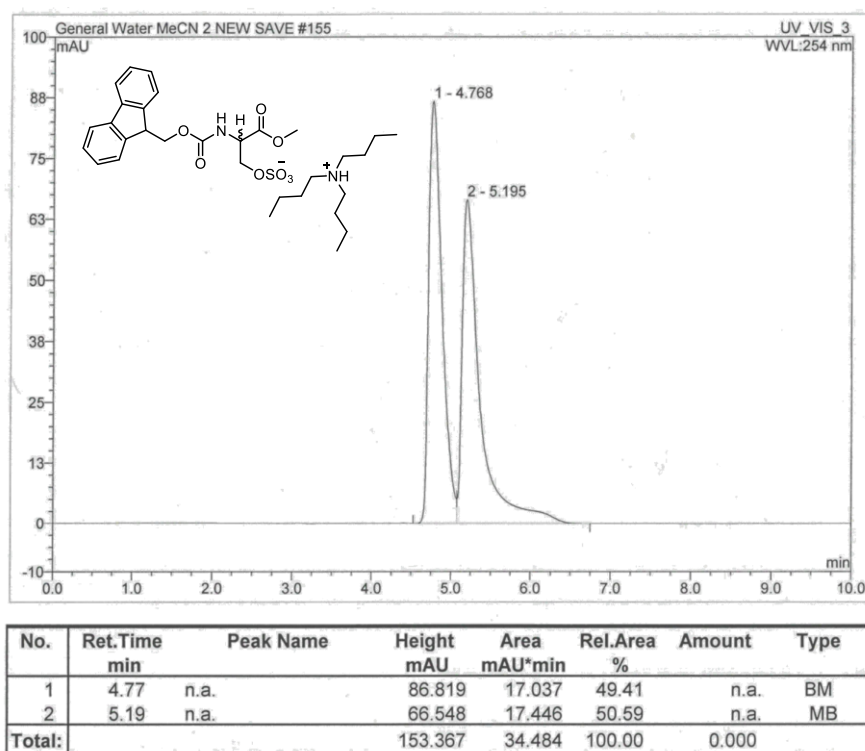
38s (1 mL min⁻¹, MeCN/H₂O, 7:18)

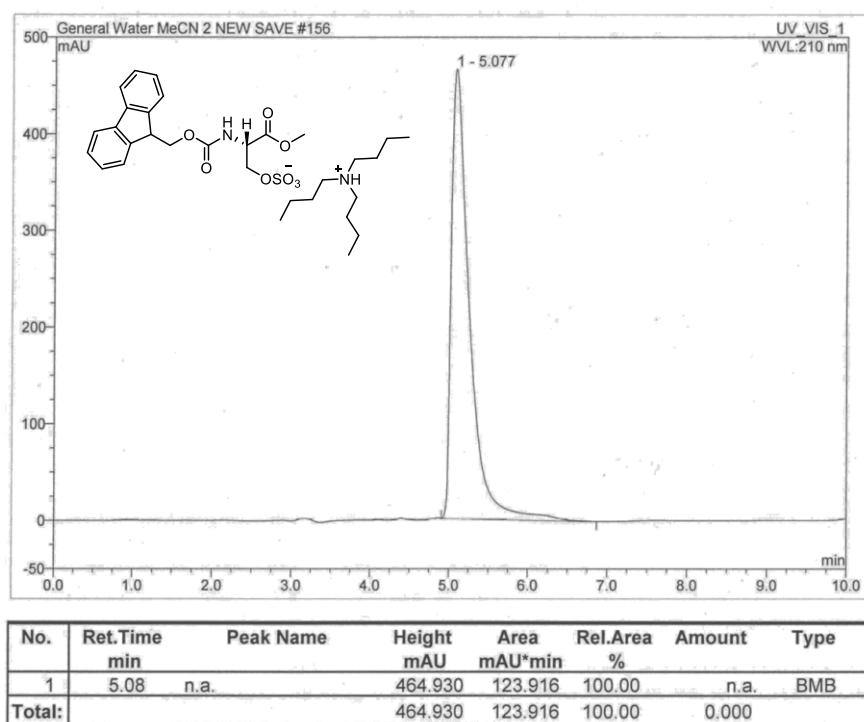
No.	Ret.Time min	Peak Name *	Height mAU	Area mAU*min	Rel.Area %	Amount	Type
1	74.39	n.a.	1.095	1.392	2.31	n.a.	BMB*
2	81.08	n.a.	36.894	56.807	94.21	n.a.	BMB*
3	114.91	n.a.	1.051	2.101	3.48	n.a.	BMB*
Total:			39.040	60.300	100.00	0.000	

39s (1 mL min⁻¹, MeCN/H₂O, 7:18)

No.	Ret.Time min	Peak Name *	Height mAU	Area mAU*min	Rel.Area %	Amount	Type
1	80.09	n.a.	1.780	2.385	48.24	n.a.	BMB*
2	113.19	n.a.	1.253	2.559	51.76	n.a.	BMB*
Total:			3.033	4.944	100.00	0.000	

44s (1 mL min⁻¹, MeCN/H₂O, 7:18)**45s** (1 mL min⁻¹, MeCN/H₂O, 7:18)

47s (1 mL min⁻¹, MeCN/H₂O, 7:18)**±42** (1 mL min⁻¹, MeCN/H₂O, 2:3)

L-42 (1 mL min⁻¹, MeCN/H₂O, 2:3)

Small Molecule Single Crystal X-Ray Diffraction Data

Experimental

The data sets for $\text{Bu}_3\text{N}\cdot\text{SO}_3$, **RR-14**, **SS-14**, **SR-14**, **RS-14** and **67** were measured on a SuperNova, Dual, Cu at home/near, Atlas diffractometer. The crystal was kept at 100.00(10) K during data collection. Using Olex2,²⁷ the structure was solved with the ShelXT²⁸ structure solution program using Intrinsic Phasing and refined with the ShelXL²⁹ refinement package using Least Squares minimization.

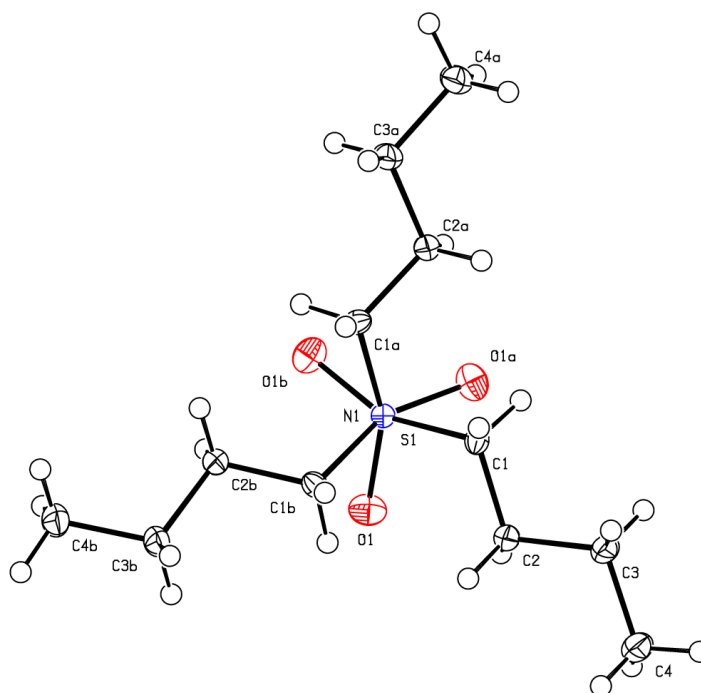
The CIF for the crystal structure of $\text{Bu}_3\text{N}\cdot\text{SO}_3$ has been deposited with the CCDC and has been given the deposition number: **CCDC 1894165**.

The CIF for the crystal structure of **RR-14** has been deposited with the CCDC and has been given the deposition number: **CCDC 1956970**.

The CIF for the crystal structure of **SS-14** has been deposited with the CCDC and has been given the deposition number: **CCDC 1956969**.

The CIF for the crystal structure of **RS-14** has been deposited with the CCDC and has been given the deposition number: **CCDC 1956968**.

The CIF for the crystal structure of **SR-14** has been deposited with the CCDC and has been given the deposition number: **CCDC 1956967**.

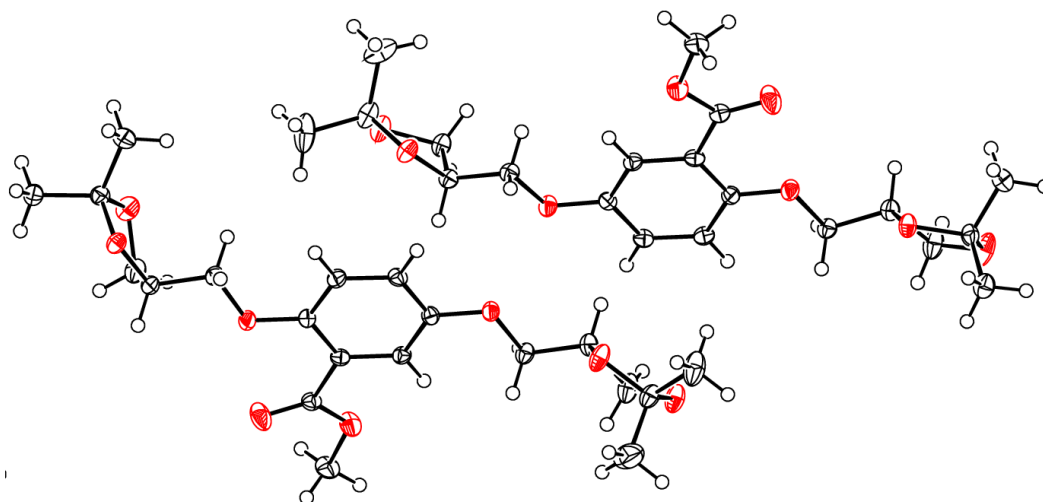
Compound **Bu₃N•SO₃****Table 1:** Crystal data and structure refinement for Compound Bu₃N•SO₃.

Identification code	DMG048
Empirical formula	C ₁₂ H ₂₇ NO ₃ S
Formula weight	265.40
Temperature/K	100.01(10)
Crystal system	trigonal
Space group	R3c
a/Å	14.3352(2)
b/Å	14.3352(2)
c/Å	12.2455(2)
α/°	90
β/°	90
γ/°	120
Volume/Å ³	2179.28(8)
Z	6
ρ _{calc} /cm ³	1.213
μ/mm ⁻¹	1.969
F(000)	876.0
Crystal size/mm ³	0.274 × 0.211 × 0.128
Radiation	CuKα (λ = 1.54184)

2 θ range for data collection/ $^{\circ}$	16.14 to 147.692
Index ranges	$-17 \leq h \leq 17, -17 \leq k \leq 17, -15 \leq l \leq 15$
Reflections collected	8776
Independent reflections	977 [$R_{\text{int}} = 0.0273, R_{\text{sigma}} = 0.0115$]
Data/restraints/parameters	977/1/53
Goodness-of-fit on F^2	1.116
Final R indexes [$I \geq 2\sigma(I)$]	$R_1 = 0.0209, wR_2 = 0.0569$
Final R indexes [all data]	$R_1 = 0.0210, wR_2 = 0.0570$
Largest diff. peak/hole / $e \text{ \AA}^{-3}$	0.18/-0.22
Flack parameter	-0.007(8)

Table 2: Fractional Atomic Coordinates ($\times 10^4$) and Equivalent Isotropic Displacement Parameters ($\text{\AA}^2 \times 10^3$) for $\text{Bu}_3\text{N} \cdot \text{SO}_3$. U_{eq} is defined as 1/3 of the trace of the orthogonalised U_{ij} tensor.

Atom	<i>x</i>	<i>y</i>	<i>z</i>	U(eq)
C1	3779.4(14)	5970.4(14)	4524.7(13)	15.2(4)
C2	3073.0(13)	4764.2(13)	4340.8(14)	16.8(4)
C3	3673.7(15)	4189.6(14)	4700.2(16)	22.4(4)
C4	2980.4(15)	2967.0(15)	4584.8(18)	26.3(4)
N1	3333.33	6666.67	4106(2)	12.6(5)
O1	2334.4(10)	5707.4(10)	2318.8(11)	23.6(3)
S1	3333.33	6666.67	2565.6(6)	16.87(19)

Compound **RR-14****Table 1:** Crystal data and structure refinement for Compound **RR-14**.

Identification code	(DMG)511
Empirical formula	C ₂₀ H ₂₈ O ₈
Formula weight	396.42
Temperature/K	100.00(10)
Crystal system	monoclinic
Space group	P2 ₁
a/Å	5.59080(10)
b/Å	32.5903(5)
c/Å	11.0624(2)
α/°	90
β/°	98.340(2)
γ/°	90
Volume/Å ³	1994.32(6)
Z	4
ρ _{calc} /cm ³	1.320
μ/mm ⁻¹	0.852
F(000)	848.0
Crystal size/mm ³	0.228 × 0.14 × 0.042

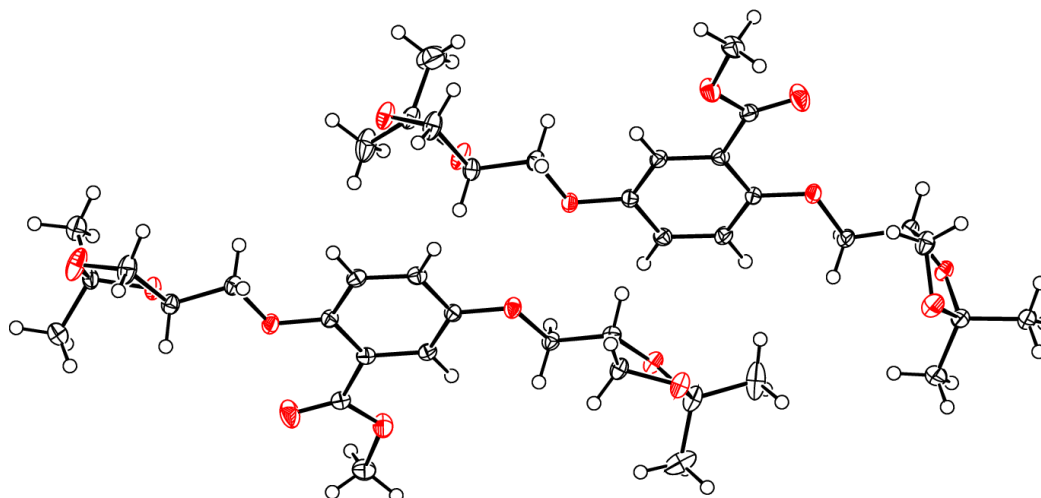
Radiation	CuK α ($\lambda = 1.54184$)
2 θ range for data collection/ $^{\circ}$	8.078 to 149.42
Index ranges	$-6 \leq h \leq 6$, $-40 \leq k \leq 40$, $-13 \leq l \leq 13$
Reflections collected	38176
Independent reflections	7983 [$R_{\text{int}} = 0.0370$, $R_{\text{sigma}} = 0.0257$]
Data/restraints/parameters	7983/1/515
Goodness-of-fit on F^2	1.040
Final R indexes [$I \geq 2\sigma(I)$]	$R_1 = 0.0319$, $wR_2 = 0.0777$
Final R indexes [all data]	$R_1 = 0.0340$, $wR_2 = 0.0798$
Largest diff. peak/hole / $e \text{ \AA}^{-3}$	0.19/-0.18
Flack parameter	-0.06(5)

Table 2: Fractional Atomic Coordinates ($\times 10^4$) and Equivalent Isotropic Displacement Parameters ($\text{\AA}^2 \times 10^3$) for Compound **RR-14**. U_{eq} is defined as 1/3 of the trace of the orthogonalised U_{ij} tensor.

Atom	x	y	z	$U(\text{eq})$
C1	3885(4)	4425.6(6)	2466(2)	16.9(4)
C2	5941(4)	4188.1(6)	2855(2)	17.5(4)
C3	7404(4)	4288.3(7)	3957(2)	19.7(4)
C4	6832(4)	4616.7(7)	4656.5(19)	18.1(4)
C5	4793(4)	4851.7(6)	4273.5(19)	17.1(4)
C6	3322(4)	4756.1(6)	3188.3(19)	17.1(4)
C7	2266(4)	4339.6(7)	1294(2)	18.8(4)
C8	-1560(5)	4479.6(8)	147(2)	27.0(5)
C9	8349(4)	3595.0(6)	2634(2)	19.5(4)
C10	8374(4)	3247.6(7)	1727(2)	19.2(4)
C11	6228(4)	2961.8(7)	1672(2)	25.0(5)
C12	9489(4)	2629.7(7)	2720(2)	20.4(4)
C13	10014(5)	2255.8(7)	1985(2)	25.0(5)
C14	10645(6)	2604.3(8)	4037(2)	34.4(6)
C15	2391(4)	5435.7(7)	4599(2)	19.6(4)

C16	2340(4)	5783.1(7)	5487(2)	19.9(4)
C17	247(4)	6074.2(7)	5092(3)	29.1(5)
C18	3704(4)	6458.4(7)	5405(2)	23.3(5)
C19	5017(5)	6692.4(9)	6464(3)	41.1(7)
C20	4157(6)	6615.9(10)	4175(3)	46.9(8)
O1	2730(4)	4125.8(7)	474.1(17)	38.8(5)
O2	164(3)	4541.3(6)	1244.0(15)	27.7(4)
O3	6427(3)	3864.0(5)	2151.5(14)	21.5(3)
O4	10380(3)	2988.8(5)	2155.8(15)	20.1(3)
O5	6964(3)	2693.9(5)	2679.4(17)	27.2(4)
O6	4390(3)	5173.6(5)	5026.2(14)	19.9(3)
O7	4430(3)	6035.1(5)	5509.9(17)	25.9(4)
O8	1187(3)	6462.4(5)	5516.9(17)	28.0(4)
C101	1921(4)	5597.1(6)	9849(2)	17.4(4)
C102	-111(4)	5848.0(6)	9526(2)	17.9(4)
C103	-1672(4)	5761.7(7)	8443(2)	19.4(4)
C104	-1250(4)	5432.2(6)	7718(2)	18.1(4)
C105	754(4)	5181.6(6)	8043.7(19)	17.0(4)
C106	2347(4)	5266.9(6)	9091.2(19)	17.4(4)
C107	3637(4)	5665.9(7)	10994(2)	18.8(4)
C108	7392(5)	5464.0(8)	12111(2)	27.2(5)
C109	-2516(4)	6424.2(7)	9954(2)	19.2(4)
C110	-2640(4)	6718.9(7)	10991(2)	20.4(4)
C111	-4882(5)	6987.3(8)	10788(3)	30.4(5)
C112	-1551(4)	7379.3(7)	11560(2)	21.1(4)
C113	-738(7)	7391.3(9)	12917(2)	43.1(7)
C114	-615(5)	7740.7(7)	10919(2)	27.2(5)
C115	3180(4)	4617.9(7)	7518(2)	18.6(4)
C116	2774(4)	4248.6(6)	6684(2)	18.0(4)
C117	953(4)	3946.0(6)	7064(2)	20.6(4)
C118	4399(4)	3587.3(7)	6911(2)	23.9(5)
C119	5385(5)	3344.8(9)	5926(3)	42.7(7)
C120	5396(5)	3452.5(8)	8192(3)	36.3(6)

O101	3371(4)	5900.0(7)	11802.5(17)	40.5(5)
O102	5588(3)	5424.5(6)	11040.2(16)	28.4(4)
O103	-471(3)	6162.7(5)	10286.0(15)	22.3(3)
O104	-734(3)	7011.2(5)	11039.8(15)	21.0(3)
O105	-4133(3)	7365.0(5)	11329(2)	36.2(4)
O106	1002(3)	4855.7(5)	7277.3(14)	20.6(3)
O107	4962(3)	4017.2(5)	6793.7(15)	21.3(3)
O108	1825(3)	3561.9(5)	6681.6(16)	24.0(4)

Compound **SS-14****Table 1:** Crystal data and structure refinement for Compound **SS-14**.

Identification code	(DMG)515
Empirical formula	C ₂₀ H ₂₈ O ₈
Formula weight	396.42
Temperature/K	100.00(10)
Crystal system	monoclinic
Space group	P2 ₁
a/Å	5.58780(10)
b/Å	32.5894(3)
c/Å	11.05540(10)
α/°	90
β/°	98.3200(10)
γ/°	90
Volume/Å ³	1992.03(4)
Z	4
ρ _{calc} /cm ³	1.322
μ/mm ⁻¹	0.853
F(000)	848.0

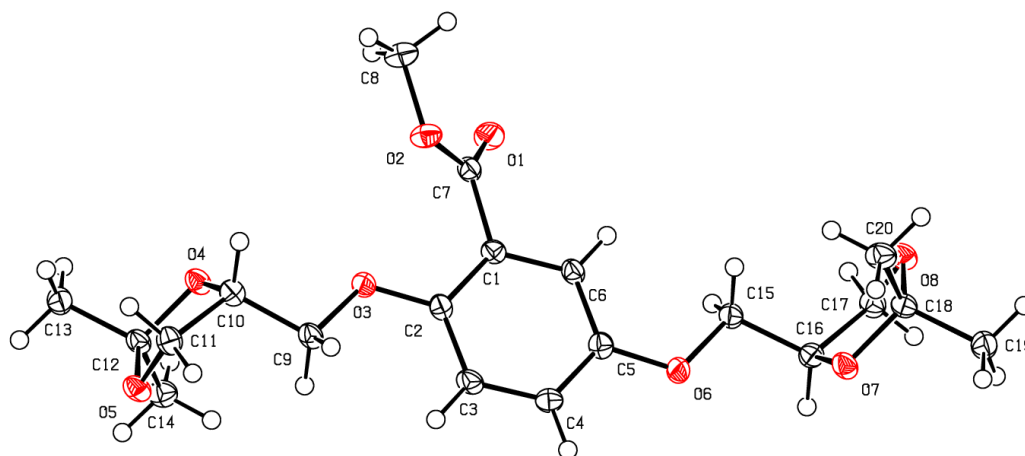
Crystal size/mm ³	0.192 × 0.125 × 0.054
Radiation	CuKα (λ = 1.54184)
2θ range for data collection/°	8.082 to 149.082
Index ranges	-6 ≤ h ≤ 6, -40 ≤ k ≤ 40, -13 ≤ l ≤ 13
Reflections collected	38501
Independent reflections	8033 [R _{int} = 0.0337, R _{sigma} = 0.0227]
Data/restraints/parameters	8033/1/515
Goodness-of-fit on F ²	1.035
Final R indexes [I >= 2σ (I)]	R ₁ = 0.0284, wR ₂ = 0.0716
Final R indexes [all data]	R ₁ = 0.0294, wR ₂ = 0.0726
Largest diff. peak/hole / e Å ⁻³	0.17/-0.17
Flack parameter	0.01(4)

Table 2: Fractional Atomic Coordinates (×10⁴) and Equivalent Isotropic Displacement Parameters (Å²×10³) for Compound **SS-14**. U_{eq} is defined as 1/3 of the trace of the orthogonalised U_{ij} tensor.

Atom	x	y	z	U(eq)
C1	6118(3)	5573.4(5)	7537.5(16)	16.2(3)
C2	4060(4)	5811.3(5)	7146.6(17)	16.4(3)
C3	2603(4)	5710.8(6)	6045.2(17)	18.6(4)
C4	3167(3)	5382.6(6)	5344.2(16)	17.5(3)
C5	5208(3)	5146.6(5)	5728.5(16)	15.9(3)
C6	6681(3)	5243.1(5)	6813.5(16)	16.1(3)
C7	7732(4)	5658.9(6)	8707.5(17)	17.6(4)
C8	11559(4)	5519.4(7)	9851.5(18)	25.4(4)
C9	1656(4)	6403.8(5)	7369.0(17)	18.4(4)
C10	1627(3)	6751.1(6)	8277.0(17)	18.2(4)
C11	3780(4)	7037.7(6)	8331.1(19)	23.7(4)
C12	513(4)	7368.8(6)	7282.9(17)	19.5(4)
C13	-7(4)	7743.2(6)	8017.8(18)	23.3(4)
C14	-636(5)	7394.7(7)	5966.5(19)	33.3(5)

C15	7611(3)	4563.5(5)	5402.7(17)	18.4(4)
C16	7655(3)	4215.6(6)	4511.0(17)	18.8(4)
C17	9753(4)	3923.6(6)	4912(2)	26.6(4)
C18	6300(4)	3540.3(6)	4595.0(18)	21.3(4)
C19	4975(5)	3305.9(7)	3535(3)	38.1(6)
C20	5844(5)	3382.8(9)	5828(3)	43.7(6)
O1	7268(3)	5872.7(6)	9528.3(14)	36.4(4)
O2	9833(3)	5458.0(5)	8757.3(13)	26.2(3)
O3	3575(3)	6134.5(4)	7851.5(12)	20.4(3)
O4	-375(2)	7010.6(4)	7847.8(12)	18.7(3)
O5	3043(3)	7305.2(4)	7324.6(14)	26.1(3)
O6	5614(2)	4825.4(4)	4975.7(12)	18.8(3)
O7	5568(2)	3963.6(4)	4488.3(14)	24.1(3)
O8	8810(3)	3535.8(4)	4481.3(14)	25.5(3)
C101	8079(3)	4402.0(5)	148.8(17)	16.6(4)
C102	10115(3)	4150.0(5)	473.3(17)	16.8(3)
C103	11674(3)	4236.3(6)	1557.8(17)	18.4(4)
C104	11252(3)	4566.4(5)	2281.7(16)	17.2(3)
C105	9245(3)	4817.5(5)	1956.8(16)	16.3(3)
C106	7653(3)	4731.4(5)	910.9(16)	16.4(3)
C107	6364(4)	4333.1(5)	-996.6(17)	17.5(4)
C108	2612(4)	4535.5(7)	-2110.7(18)	25.8(4)
C109	12516(3)	3574.7(6)	45.4(17)	17.7(4)
C110	12635(3)	3280.0(6)	-995.3(17)	18.8(4)
C111	14879(4)	3010.8(7)	-789(2)	28.5(4)
C112	11552(3)	2619.9(6)	-1560.5(17)	19.4(4)
C113	10740(6)	2607.9(8)	-2922(2)	40.8(6)
C114	10609(4)	2258.4(6)	-922(2)	25.6(4)
C115	6822(3)	5380.5(5)	2484.0(16)	17.0(3)
C116	7230(3)	5750.2(5)	3317.2(16)	16.7(4)
C117	9051(3)	6052.7(5)	2938.6(18)	19.2(4)
C118	5606(4)	6410.9(6)	3094(2)	22.1(4)
C119	4622(4)	6654.0(8)	4078(3)	40.0(6)

C120	4609(4)	6546.5(7)	1809(2)	34.3(5)
O101	6629(3)	4098.8(6)	-1803.0(14)	37.8(4)
O102	4412(3)	4574.5(5)	-1040.6(13)	26.7(3)
O103	10471(3)	3835.5(4)	-287.8(12)	20.7(3)
O104	10735(2)	2988.2(4)	-1042.6(12)	19.2(3)
O105	14131(3)	2633.8(5)	-1333.7(17)	33.6(4)
O106	8999(2)	5142.8(4)	2724.2(12)	19.7(3)
O107	5043(2)	5981.5(4)	3210.7(13)	19.6(3)
O108	8183(2)	6436.9(4)	3320.7(14)	22.1(3)

Compound **RS-14****Table 1:** Crystal data and structure refinement for Compound **RS-14**.

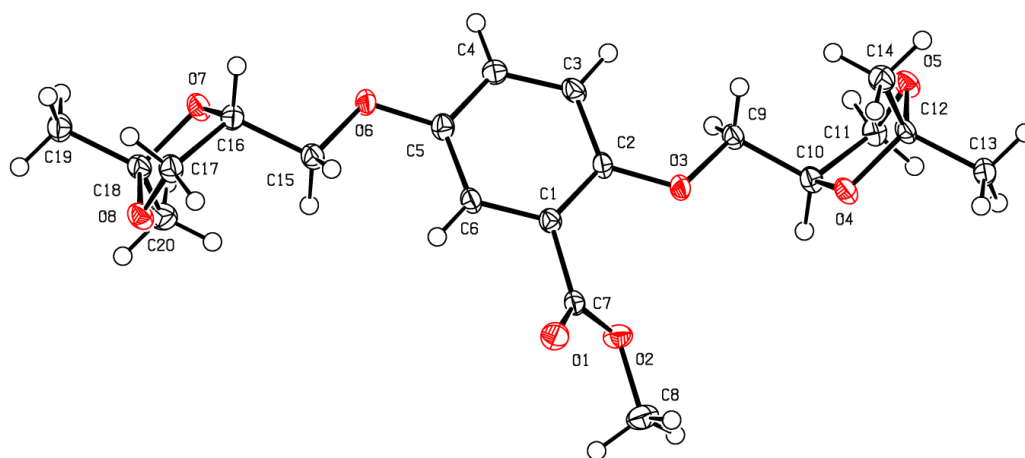
Identification code	(DMG)517
Empirical formula	C ₂₀ H ₂₈ O ₈
Formula weight	396.42
Temperature/K	100.00(10)
Crystal system	triclinic
Space group	P1
a/Å	5.8279(2)
b/Å	8.6225(2)
c/Å	9.7578(2)
α/°	102.553(2)
β/°	92.606(2)
γ/°	94.367(2)
Volume/Å ³	476.26(2)
Z	1
ρ _{calc} /cm ³	1.382
μ/mm ⁻¹	0.892
F(000)	212.0

Crystal size/mm ³	0.329 × 0.193 × 0.059
Radiation	CuKα (λ = 1.54184)
2θ range for data collection/°	9.304 to 150.142
Index ranges	-7 ≤ h ≤ 7, -10 ≤ k ≤ 10, -12 ≤ l ≤ 12
Reflections collected	16513
Independent reflections	3544 [R _{int} = 0.0205, R _{sigma} = 0.0147]
Data/restraints/parameters	3544/3/258
Goodness-of-fit on F ²	1.084
Final R indexes [I >= 2σ (I)]	R ₁ = 0.0312, wR ₂ = 0.0810
Final R indexes [all data]	R ₁ = 0.0320, wR ₂ = 0.0817
Largest diff. peak/hole / e Å ⁻³	0.34/-0.23
Flack parameter	-0.05(6)

Table 2: Fractional Atomic Coordinates (×10⁴) and Equivalent Isotropic Displacement Parameters (Å²×10³) for Compound **RS-14**. U_{eq} is defined as 1/3 of the trace of the orthogonalised U_{ij} tensor.

Atom	x	y	z	U(eq)
C1	5550(4)	6170(3)	5025(2)	17.0(5)
C2	6858(4)	5400(3)	5871(2)	18.2(5)
C3	6227(4)	3793(3)	5844(2)	20.1(5)
C4	4350(4)	2983(3)	4994(2)	20.6(5)
C5	3033(4)	3760(3)	4170(2)	19.1(5)
C6	3607(4)	5360(3)	4204(2)	18.4(5)
C7	6128(4)	7865(3)	4936(2)	18.6(4)
C8	9109(5)	9761(3)	4645(3)	27.4(5)
C9	10170(4)	5507(3)	7445(2)	18.9(5)
C10	12082(4)	6750(3)	8153(2)	19.5(5)
C11	13866(4)	6069(3)	8990(2)	21.2(5)
C12	11712(4)	7624(3)	10571(2)	18.2(5)
C13	13232(4)	9022(3)	11464(2)	21.9(5)
C14	9470(4)	7303(3)	11222(3)	23.0(5)

C15	-260(4)	3666(3)	2589(2)	19.4(5)
C16	-2170(4)	2457(3)	1823(2)	19.2(5)
C17	-3876(4)	3190(3)	973(2)	21.3(5)
C18	-1759(4)	1598(3)	-594(2)	20.2(5)
C19	-3357(4)	243(3)	-1482(2)	22.7(5)
C20	492(4)	1850(3)	-1261(3)	24.2(5)
O1	4732(3)	8824(2)	4938.8(18)	25.5(4)
O2	8376(3)	8159(2)	4780.2(18)	22.8(3)
O3	8625(3)	6303(2)	6708.2(17)	21.8(4)
O4	11232(3)	7959.9(19)	9203.4(15)	20.0(4)
O5	12882(3)	6198(2)	10324.5(17)	21.1(4)
O6	1183(3)	2853(2)	3378.9(17)	22.0(4)
O7	-1295(3)	1260.3(19)	771.4(17)	21.7(4)
O8	-2838(3)	3062(2)	-342.2(18)	21.6(4)

Compound **SR-14****Table 1:** Crystal data and structure refinement for Compound **SR-14**.

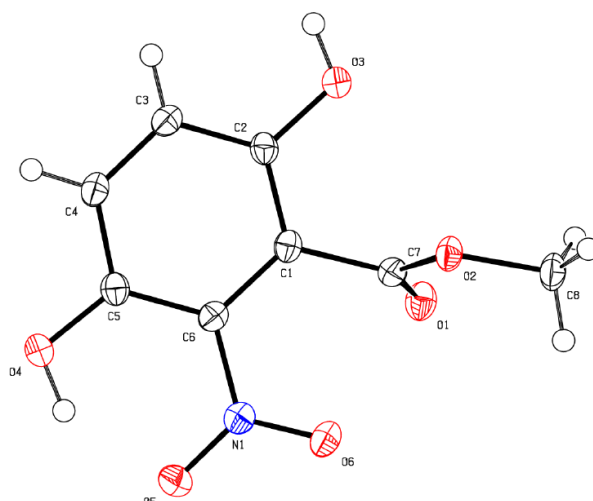
Identification code	(DMG)516
Empirical formula	C ₂₀ H ₂₈ O ₈
Formula weight	396.42
Temperature/K	99.99(10)
Crystal system	triclinic
Space group	P1
a/Å	5.8128(2)
b/Å	8.6209(2)
c/Å	9.7475(3)
α/°	102.475(3)
β/°	92.516(3)
γ/°	94.418(3)
Volume/Å ³	474.59(3)
Z	1
ρ _{calc} /cm ³	1.387
μ/mm ⁻¹	0.895
F(000)	212.0

Crystal size/mm ³	0.257 × 0.111 × 0.056
Radiation	CuKα (λ = 1.54184)
2θ range for data collection/°	9.31 to 149.352
Index ranges	-6 ≤ h ≤ 7, -10 ≤ k ≤ 10, -12 ≤ l ≤ 12
Reflections collected	16508
Independent reflections	3510 [R _{int} = 0.0185, R _{sigma} = 0.0145]
Data/restraints/parameters	3510/3/258
Goodness-of-fit on F ²	1.088
Final R indexes [I >= 2σ (I)]	R ₁ = 0.0279, wR ₂ = 0.0727
Final R indexes [all data]	R ₁ = 0.0287, wR ₂ = 0.0735
Largest diff. peak/hole / e Å ⁻³	0.21/-0.22
Flack parameter	0.00(6)

Table 2: Fractional Atomic Coordinates (×10⁴) and Equivalent Isotropic Displacement Parameters (Å²×10³) for Compound **SR-14**. U_{eq} is defined as 1/3 of the trace of the orthogonalised U_{ij} tensor.

Atom	x	y	z	U(eq)
C1	3887(4)	889(2)	8176(2)	16.2(5)
C2	2579(4)	1655(2)	7330(2)	16.7(4)
C3	3208(4)	3263(2)	7355(2)	18.8(5)
C4	5081(4)	4074(2)	8208(2)	19.3(5)
C5	6403(4)	3299(2)	9031(2)	18.0(5)
C6	5827(4)	1699(3)	8995(2)	17.4(4)
C7	3309(4)	-807(2)	8263.8(19)	17.2(4)
C8	332(4)	-2707(3)	8558(2)	26.4(5)
C9	-738(4)	1543(2)	5756(2)	17.4(4)
C10	-2649(4)	301(2)	5047(2)	18.1(5)
C11	-4440(4)	977(3)	4212(2)	20.1(5)
C12	-2280(4)	-573(2)	2628(2)	16.7(4)
C13	-3803(4)	-1969(3)	1736(2)	20.7(5)
C14	-37(4)	-246(3)	1973(2)	21.8(5)

C15	9699(4)	3398(2)	10616(2)	19.4(5)
C16	11611(4)	4604(2)	11382(2)	18.6(5)
C17	13318(4)	3873(3)	12234(2)	20.6(5)
C18	11183(4)	5459(2)	13806(2)	19.3(5)
C19	12786(4)	6812(3)	14687(2)	22.0(5)
C20	8936(4)	5203(3)	14469(2)	24.4(5)
O1	4712(3)	-1762.5(17)	8260.9(16)	24.3(3)
O2	1061(3)	-1106.1(17)	8419.5(16)	21.7(3)
O3	812(3)	753.2(17)	6490.5(16)	20.3(3)
O4	-1798(3)	-908.2(16)	3995.4(14)	19.0(3)
O5	-3455(3)	853.7(18)	2876.1(16)	20.2(3)
O6	8250(3)	4203.8(17)	9823.4(16)	20.7(3)
O7	10721(3)	5795.5(17)	12435.3(15)	21.2(4)
O8	12271(3)	3996.8(18)	13550.5(16)	20.8(3)

Compound **67****Table 1:** Crystal data and structure refinement for **67**.

Identification code	DMG 621
Empirical formula	C ₈ H ₇ NO ₆
Formula weight	213.15
Temperature/K	100.00(10)
Crystal system	monoclinic
Space group	P2 ₁ /c
a/Å	8.9555(7)
b/Å	10.1597(6)
c/Å	9.9607(8)
α/°	90
β/°	110.056(9)
γ/°	90
Volume/Å ³	851.32(12)
Z	4
ρ _{calc} /cm ³	1.663
μ/mm ⁻¹	1.278
F(000)	440.0
Crystal size/mm ³	0.149 × 0.146 × 0.119
Radiation	CuKα (λ = 1.54184)
2θ range for data collection/°	10.516 to 149.958

Index ranges	-10 ≤ h ≤ 7, -11 ≤ k ≤ 12, -12 ≤ l ≤ 12
Reflections collected	3177
Independent reflections	1687 [R _{int} = 0.0197, R _{sigma} = 0.0263]
Data/restraints/parameters	1687/0/145
Goodness-of-fit on F ²	1.045
Final R indexes [I ≥ 2σ (I)]	R ₁ = 0.0356, wR ₂ = 0.0884
Final R indexes [all data]	R ₁ = 0.0427, wR ₂ = 0.0944
Largest diff. peak/hole / e Å ⁻³	0.30/-0.23

Table 2: Fractional Atomic Coordinates ($\times 10^4$) and Equivalent Isotropic Displacement Parameters ($\text{\AA}^2 \times 10^3$) for **67**. U_{eq} is defined as 1/3 of the trace of the orthogonalised U_{ij} tensor.

Atom	x	y	z	U(eq)
C1	2905.8(17)	5107.3(15)	6228.1(15)	16.8(3)
C2	3874.7(18)	6144.2(15)	6151.9(15)	17.7(3)
C3	3936.8(18)	6536.9(15)	4817.5(16)	18.9(3)
C4	3096.0(18)	5863.7(16)	3600.0(16)	19.7(3)
C5	2162.8(18)	4766.4(15)	3636.4(16)	18.3(3)
C6	2048.4(17)	4421.7(15)	4966.0(15)	17.2(3)
C7	2926.9(17)	4697.7(15)	7686.9(15)	17.4(3)
C8	2214(2)	5295.7(17)	9672.1(16)	22.7(4)
N1	927.2(15)	3420.8(13)	5029.9(13)	18.5(3)
O1	3606.4(13)	3723.0(11)	8308.4(11)	22.6(3)
O2	2200.2(13)	5565.8(11)	8231.1(11)	19.4(3)
O3	4771.4(14)	6730.9(12)	7396.1(11)	22.0(3)
O4	1409.1(14)	4165.0(12)	2385.6(11)	23.1(3)
O5	370.3(13)	2663.3(12)	4003.0(11)	24.0(3)
O6	536.6(13)	3374.3(11)	6103.0(11)	22.6(3)

References

1. J. A. Moede, C. Curran, *J. Am. Chem. Soc.*, 1949, **71**, 852 – 858
2. S. Cassel, C. Debaig, T. Benvegny, P. Chaimbault, M. Lafosse, D. Plusquellec, P. Rollin, *Eur. J. Org. Chem.*, 2001, **5**, 875 – 896
3. J. A. Chavez, S. A. Summers, *Arch. Biochem. Biophys.*, 2003, **419**, 101 – 109
4. A. M. Quitela, R. Jimenez, L. Piqueras, M. Gomex-Guzman, J. Haro, M. J. Zarzuelo, A. Cogolludo, M. J. Sanz, M. Toral, M. Romero, F. Perez-Vizcaino, J. Duarte, *Br. J. Pharmacol.*, 2014, **171**, 3089 – 3102
5. M. Romero, R. Jimenez, M. Sanchez, R. Lopez-Sepulveda, M. J. Zarzuelo, F. O'Valle, A. Zarzuelo, F. Perez-Viscaino, J. Duarte, *Atherosclerosis*, 2010, **212**, 58 – 67
6. A. M. Mahmoud, F. L. Wilkinson, A. M. Jones, J. A. Wilkinson, M. Romero, J. Duarte, M. Y. Alexander, *Biochimica et Biophysica Acta (BBA) - General Subjects*, 2017, **1861**, 3311 – 3322,
7. M. Romero, R. Jimenez, M. Sanchez, R. Lopez-Sepulveda, A. Zarzuelo, J. Tarmargo, F. Perez-Viscaino, J. Duarte, *Atherosclerosis*, 2010, **212**, 78 – 85
8. Adapted from the procedure found in reference **7**
9. G. R. Banks, D. Cohen, *J. Chem. Soc.*, 1965, **00**, 6209 – 6212
10. J. E. T. Corrie, B. C. Gilbert, V. R. N. Munasinghe, A. C. Whitwood, *J. Chem. Soc., Perkin Trans. 2*, 2000, **00**, 2483 – 2491
11. M. Schober, T. Knaus, M. Toesch, P. Macheroux, U. Wagner, K. Faber, *Adv. Synth. Catal.*, 2012, **354**, 1737 – 1742
12. M. Huibers, Á. Manuzi, F. P. J. T. Rutjes, F. L. van Delft, *J. Org. Chem.*, 2006, **71**, 7473 – 7476
13. R. Kisilevsky, W. Szarek, D. Weaver, PCT WO 96/28187, 1996
14. T. Ghosh, A. Mukherji, P. K. Kancharla, *Org. Lett.*, 2019, **21**, 3490 – 3495
15. J. Gao, H. Wang, L. Wang, J. Wang, D. Kong, Z. Yang; *J. Am. Chem. Soc.*, 2009, **131**, 11286 – 11287
16. S. Jabar, L. A. Adams, Y. Wang, L. Aurelio, B. Graham, G. Otting, *Chem. Eur. J.*, 2017, **23**, 13033 – 13036
17. E. Baco, F. Hoegy, I. J. Schalk, G. L. A. Mislin, *Org. Biomol. Chem.*, 2014, **12**, 749 – 757
18. K. Schuenemann, D. P. Furkert, E. C. Choi, S. Connelly, J. D. Fraser, J. Sperry, M. A. Brimble, *Org. Biomol. Chem.*, 2014, **12**, 905 – 912
19. F. Carta, D. Vullo, A. Maresca, A. Scozzafava, C. T. Suparan, *Biorgan. Med. Chem.*, 2013, **35**, 1650 – 1662
20. R. K. Pandey, G. G. Jarvis, P. S. Low, *Tetrahedron Lett.*, 2012, **53**, 1627 – 1629
21. C. C. Nawrat, L. I. Palmer, A. J. Blake, C. J. Moody, *J. Org. Chem.*, 2013, **78**, 5587 – 5603
22. Z.-M. Wang, M. Shen, *J. Org. Chem.*, 1998, **63**, 1414 – 1418
23. M. H. Prudhomme, G. Dauphin, G. Jeminet, *J. Antibiotics*, 1986, **39**, 922 – 933
24. H.-L. C. Diaz, E. C. Polo, *J. Org. Chem.*, 2017, **82**, 4072 – 4112

25. R. Epple, M. Azimioara, R. Russo, Y. Xie, X. Wang, C. Cow, J. Wityak, D. Karanewsky, B. Bursulaya, A. Kreusch, T. Tuntland, A. Gerken, M. Iskandar, E. Saez, H. M. Seidel, S.-S. Tian, *Bioorg. Med. Chem. Lett.*, 2006, **16**, 5488 – 5492
26. Y. Zhang, J. Bao, X.-X. Deng, W. He, J.-J. Fan, F.-Q. Jiang, L. Fu, *Bioorg. Med. Chem. Lett.*, 2016, **26**, 4081 – 4085
27. H. O. V. Dolomanov, L. J. Bourhis, R. J. Gildea, J. A. K. Howard, H. Puschmann, *J. Appl. Cryst.*, 2009, **42**, 339 – 341
28. G. M. Sheldrick, *Acta Cryst. A*, 2015, **71**, 3 – 8
29. G. M. Sheldrick, *Acta Cryst. C*, 2015, **71**, 3 – 8